Tensile and Compressive Creep of Early Age Concrete: Testing and Modelling

Dawood S. Atrushi

Doctoral Thesis

Department of Civil Engineering
The Norwegian University of Science and Technology
Trondheim, Norway

March 2003

URN:NBN:no-3377

URN:NBN:no-3377

Acknowledgment

The Norwegian Research Council (NFR) supported this dr.ing.project financially through the project "Selmer FoU plan 1996-2000 (112102/210)". The experimental programme was in addition partly financed by the comprehensive Brite/EuRam research project IPACS (Improved Production of Advanced Concrete Structures), and by the research programme NOR-CRACK which was funded by the Norwegian Research Council (NFR (2001-2004 14398/210)). The Norwegian industrial partners in the two latter projects were: Selmer Skanska AS, Elkem ASA Materials, Norcem AS, Fesil AS and the Directorate of Public Roads.

I would like to express my deep gratitude and sincere appreciation to my supervisor Professor Terje Kanstad and co-supervisor Professor Erik Johan Sellevold for giving me the opportunity to perform this research and for their professional supervising, continuous support, fruitful discussions and constructive suggestions throughout the course of this research. Their patient guidance, advice and criticism have been a great stimulation.

My gratitude is extended to my colleague Dr. Ing. Øyvind Bjøntegaard for his helpful suggestions and our valuable discussions during the research work. I am also grateful to Professor Erik Thorenfelt for interesting discussions during the research work.

I am grateful to all my colleagues in the Group of Concrete at the Department of Structural Engineering for the pleasant and friendly environment which I had the privilege to be part of. I wish to express my most hearty appreciation to research technician Helge Rødsjø for his wonderful and substantial assistance with great skill and care during the experimental work. I would also like to thank others in the laboratory team; Kjell Kristiansen, Trygve Meltzer, Svein Aage Lorentzen, Johan Jørgen Sandnes for their contribution in the experimental work. Special thanks to Engineer John Troset who provided drawings of the testing equipment.

Further, I would like to thank the company Scandiaconsult SCC, which gave me the opportunity to take a leave of absence from the consulting work at the company in order to do this research.

Finally, I would like to express gratitude and sincere thanks to my wife Halat for her unlimited patience, understanding, encouragement, and love during the three and half years of research in Trondheim. Without her continuous support this work would not have been completed. I am deeply indebted to my kids Hevin and Lana for giving me exclusive time to fulfil this thesis. Special thanks to my mother and family members in Trondheim, Stockholm and Kurdistan for their support and encouragement.

Trondheim, March 2003

Dawood Atrushi

URN:NBN:no-3377

Abstract

The thesis deals with experimental and numerical modelling to characterize early age tensile and compressive creep and its associated stress relaxation - which are very important properties in stress simulation of early age concrete. For this purpose a comprehensive work was carried out involving construction of a new tensile creep test equipment and development of test procedures to generate basic experimental data.

The experimental program is subdivided into four series. Each of the series involves one varying parameter, which is relevant to the time-dependent behaviour of early age HPC. Most of the tests are repeated to check the reproducibility of the test results. The reproducibility of the test results for the BASE concretes confirmed that the experimental setup is reliable, and that it can be used to determine tensile creep of concrete at early ages.

An extensive test program has been performed on HPC, with w/b = 0.40. The primary parameters studied were concrete ages at loading (1, 2, 3, 4, 6 and 8 days), stress/strength levels (20-80%), and temperature levels (20, 34, 40, 57 and 60 ^{o}C) in addition to the effect of silica fume (0-15%) on tensile creep. The testing apparatus was new and significant efforts were devoted to develop reliable procedures in terms of accuracy and reproducibility. In parallel, compressive creep tests were conducted on a separate testing apparatus, and the results are compared to tensile creep behaviour.

It was found that the instantaneous deformation under tension is smaller than under compression, and that the corresponding creep curves also are different. Creep in tension is found to be lower initially, but an almost linear rate is soon established which is much higher than in compression. The consequence is greater creep magnitude and thus greater creep coefficient in tension than in compression. The tests on non-linearity showed that the proportionality limit between stress and sealed tensile creep strain is about 60% of the strength. Creep tests under isothermal temperatures showed that, as for compressive creep, the sealed tensile creep accelerates for temperatures higher than 20 ^{o}C. In addition, the maturity principle describes this effect reasonably well, for the tested loading ages of about 3 days.

The relatively large amount of experimental data, available in this study, has been used to investigate mathematical models. Comprehensive test results from the TSTM apparatus are analyzed with respect to creep and relaxation, where the effect of temperature on creep and relaxation is emphasized. Simulations of self-induced stresses are performed using the creep model denoted the Double Power Law (DPL). As solution method, the theory of linear viscoelasticity with aging is used. The model (M-DPL) is modified to take into account the effect of irrecoverable creep.

For increasing temperatures during the hardening phase, the transient creep, which takes place during heating is taken into account by an additional creep term. Its contribution to stress relaxation was found to be up to 10%. This transient creep term is considered to be irrecoverable during the subsequent temperature decrease. The modified model captures the

various characteristics of sealed creep and describes the tensile behaviour at early ages more accurately than the original Double Power Law.

The effect of relaxation is found to be relatively large and significant in development of self-induced stresses. Under isothermal temperature of 20 ^{o}C, the relaxation increases to about 40% of the fictive elastic stresses after 3 days and remains about constant after that. On the other hand, presentation of relaxation under realistic temperature histories is much more complicated, because the stresses change from compression to tension. This might also lead to increased tensile stresses because compressive creep reduces compressive stresses, but increases the subsequent tensile stresses. Underestimation of creep in this early period will lead to underestimation of the cracking risk.

Creep development at very early ages has an important effect in determination of the creep model parameters. After an evaluation of the test results using six loading ages (1, 2, 3, 4, 6 and 8 days) it was concluded that an optimal test program should include at least 3 loading ages, in which the loading ages 1 and 2 must be included.

Furthermore, the test results indicate that partial replacement of cement with silica fume (5-15%) increases the sealed tensile creep. However, the reference concrete without silica fume dose not fit to this systematic pattern.

Table of Content

Symbols and Abbreviations

1 Symbols

α	degree of hydration
α'	model parameter for long-term creep (Eq. 3.13)
$\beta_{H,T}$	temperature dependent coefficient
Δ	increment
ε	total strain
ε^{o}	stress-independent strain (shrinkage and thermal dilation)
ε_{AD}	strain due to autogenous shrinkage
ε_{cr}	creep strain
ε_{d}	non-reversal permanent deformation in Figure 3.22
ε_{e}	elastic deformation in Figure 3.22
$\boldsymbol{\varepsilon}_{el}$	elastic strain
$\varepsilon_{el,d}$	delayed elastic strain
$\boldsymbol{\varepsilon}_{free}$	free deformation in Dilation Rig
ε_{nel}	instantaneous inelastic strain
$\varepsilon_{nel,d}$	delayed inelastic strains
ε_{T}	thermal strain
ε_{TD}	strain due to thermal dilation
$\boldsymbol{\varepsilon}_{trcr}$	transient creep
$\boldsymbol{\varepsilon}_{ve}$	visco-elastic strain with transient creep,
$\boldsymbol{\varepsilon}_{ve'}$	visco-elastic strain without transient creep,
ε_{V}	delayed elastic deformation in Figure 3.22
φ_{0}	creep model parameter in (Eq. 3.13)
φ_{oe}	model parameter representing viscoelastic part of deformation
φ_{op}	model parameter representing viscoplastic part of deformation

φ_1 and φ_2	constants (Eq. 3.12)
$\varphi_c(T)$	temperature dependent coefficient in compression
$\varphi_{RH,T}$	temperature dependent creep coefficient
$\varphi_t(T)$	temperature dependent coefficient in tension
ρ	model parameter (Eq. 3.20)
σ_0	initial stress
σ'	stress increased in proportion to the increase of strength
σ_c	compressive stress
σ_{DPL}	calculated stress by DPL
σ_{fe}	fictive elastic stress
$\sigma_{M\text{-}DPL}$	calculated stress by modified DPL
σ_{test}	stresses measured in TSTM
σ_{ve}	calculated stress with transient creep
$\sigma_{ve'}$	calculated stress without transient creep
A_r	constant (Eq. 3.18)
B_r	constant (Eq. 3.18)
C_r	creep component in Figure 3.3
CTE	coefficient of thermal expansion
d	creep model parameter in (Eq. 3.13)
Dev	deviation in creep model between using one test combination and all tests
$d\varepsilon(t')$	strain increment
$d\varepsilon^o(t')$	stress-independent strain increment introduced at time t'
$d\sigma(t')$	stress increment applied at time t'
E(t')	modulus of elasticity at loading age t' (Eq. 3.11)
E(t'')	modulus of elasticity at the unloading time t'' (Eq. 6.10)
E_0	asymptotic modulus of elasticity (larger than the usual modulus of elasticity)
E_1	compressive E-modulus determined from the 3rd unloading part in Figure (5.4)
E_2	compressive E-modulus determined from the 1st loading part in Figure (5.4)
E_c	modulus of elasticity in compression
$E_c(t)$	modulus of elasticity at time t
$E_c(t')$	modulus of elasticity at loading time t'
$E_c(t_e)$	modulus of elasticity at equivalent time t_e
E_{c28}	modulus of elasticity (28 days value)
E_{cc}	Compressive modulus of elasticity (Eq. 3.9)
E_{eff}	effective modulus of elasticity which take the creep effect for the time interval from $t_{j-1/2}$ to t_j into account.
E_l	elastic strain in Figure 3.3
E_r	activation energy divided by the gas constant R=8.314, unit ^oK.

E_t	modulus elasticity in tension
f(t')	function which expresses the effect of loading age in (Eq. 3.11)
f_2(t-t')	function which describes the development of the delayed elastic creep component
f_c'	uniaxial compressive strength at reference temperature
f_c	cylinder compressive strength
f_{c28}	compressive strength at the age of 28 days
f_{cck}	characteristic compressive strength (Eq. 3.9)
f_{cm}	mean compressive strength (Eq. 3.9)
f_t	tensile strength
f_t'	tensile strength at reference temperature
f_{t28}	tensile strength (28 days value)
G(t')	exponential function which models the strong age-dependence of the instantaneous deformation (load duration 1.4 min.)
g(t-t')	function which expresses the development of creep with time under load in (Eq. 3.11)
g_2 (t)	function which describes the development of flow with time *t*
H(t,t')	exponential function which models the increase of early age creep when the load has been applied
J(t,t'), J(t,t'')	compliance functions (or creep functions) for loading ages *t′ & t″*
K_r	stiffness of the restraining concrete member
K_s	stiffness of shrinking concrete member
M	Maturity
m	number of tests in a combination
n	number of total tests
n_t & n_E	model parameters to be determined from tensile strength and modulus of elasticity tests (Eq. 3.8)
p	creep model parameter in (Eq. 3.13)
r	number of recorded strain points on creep curve in each test
r′	model parameter (Eq. 3.22)
R	relaxation in percent
R(t,t')	relaxation function of time *t* for a strain induced at time t'
RD	degree of restraint
R_j	quadratic sum of creep deviation between model and test for one test (Eq. 6.13)
s	coefficient dependent on the cement type (Eq. 3.7)
s_{CTE}, n_{CTE}	curve-fitting parameters (Eq. 2.2)
S_{new}	sum of R_j for the tests in a test combination
S_{old}	sum of *Rj* for all the tests
STD	standard deviation

t_0	time "zero"; the time when strength and stiffness of concrete is defined to be zero
t	current concrete age, measured from casting of concrete
t'	concrete age at loading
t''	concrete age at unloading
t_e	equivalent time
t-t'	load duration
$t_{j-1/2}$	middle of the time increment
T	Temperature
T_{crack}	concrete temperature where failure occurs
T_{max}	maximum temperature
w/b	water-binder ratio

2 Abbreviations

ACI	American Concrete Institute
AD	Autogenous Deformation
CEB	Comité Euro-International du Béton
CTE	Coefficient of Thermal Expansion
DPL	Double Power Law
FIP	Fédération Internationale de la Précontrainte
fib	fédération internationale du béton (the international federation for structural concrete, created from merger of CEB and FIP)
HPC	High Performance Concrete
LVDT	Linear Variable Differential Transformer
MC90	CEB-FIB Model Code 1990
M-DPL	Modified Double Power Law
NS	Norwegian Standard
NSC	Normal Strength Concrete
RILEM	The International Union of Testing and Research Laboratories for Materials and Structures
SF	Silica Fume
TD	Thermal Dilation
TSTM	Thermal Stress Testing Machine

Chapter 1
Introduction

1.1 Background

Concrete is a structural material with time-dependent properties, such as shrinkage as well as creep and its associated stress relaxation, which significantly affect the structural behaviour. On one hand, their effects are unfavourable when the time dependent deformations cause loss of prestress and increase of deformations and deflections, which may impair the serviceability of a structure. On the other hand, they can be beneficial in form of redistribution of stresses caused by imposed deformations or loads and also in form of reduction of undesirable stresses, particularly in early age concrete.

The simulation of concrete behaviour and especially simulation of its deformation and crack sensitivity has become an important field in structural analyses. Numerical simulations of the stress development may be performed in the design phase in order to evaluate the crack risk. To obtain a reliable and economical design of concrete structures, such simulations require generalized models for early age development of the relevant concrete properties. All aspects that influence the structural behaviour with time have to be included. In addition to mechanical properties such as modulus of elasticity, tensile and compressive strength, the time dependent properties of concrete, must be considered.

In the last two or three decades the development and utilization of new concretes such as high performance concrete (HPC) in tall buildings, offshore structures, bridges and other prestressed structures has been in focus. The new concretes provide superior mechanical properties and durability, high erection speed and good workability at site, but the increased use of such concretes is accompanied by concern regarding their early age cracking sensitivity. In order to get a high benefit of using these concretes there is a need for a

comprehensive understanding and treatment of the concrete in order to avoid early age cracking.

Early age concrete is a continuously changing material with transient material properties. It undergoes hydration processes during the hardening, leading to temperature increase. It undergoes rapid volume changes due to shrinkage and hydration temperatures that lead to rapid build-up of stresses if the concrete is restrained. The concrete in a structure is nearly always restrained to some degree, either internally by gradients of moisture and temperature across the component section, or externally by adjoining structure elements. Internal and external restraint nearly always coexists in all structural concrete elements. Low w/b-ratio in concrete leads to more pronounced volume instability, earlier build-up of internal tensile stresses and greater sensitivity to early cracking. An understanding of the mechanisms involved and the factors influencing the risk of cracking, such as volume change, creep/relaxation and the type of restraint, is of utmost importance.

During the hardening process, the temperature increases due to heat of hydration is accompanied by volume increase, which, if restrained, leads to compressive stresses in the concrete. The occurrence of shrinkage (normally autogenous shrinkage due to self-desiccation), which works in opposite direction to the thermal expansion in the beginning, leads to lower compressive stresses. Due to the viscoelastic behaviour of young concrete, these compressive stresses reduce to low magnitudes. Of much more significance is the volume reduction, which occurs as soon as the concrete temperature decreases. The volume reduction is then the sum of the shrinkage and the thermal contraction. If the concrete member is restrained, significant tensile stresses will be generated and they may result in severe cracks. The issue of primary interest is whether or not these induced stresses will lead to cracking.

The problem regarding cracking has always been a major concern for concrete technologist and engineers, especially in flat structures such as bridge decks, pavements and parking garage slabs. The traditional method to handle this problem has been construction of joint spacing, application of proper curing procedures such as sealing and water pounding. However, imposing joint spacing is normally not economic and it cannot be done without compromising serviceability, durability and structural capacity of the structure due to cracking. Therefore it is needed to find better solutions.

The role of the concrete properties such as tensile creep and its associated relaxation is of great important in reduction of self-induced stresses and in the assessment of the risk of cracking, particularly during the first days after placement. Tensile creep, shrinkage and thermal deformation are major factors to be considered in the assessment of cracking and performance. Shrinkage and thermal deformation in restrained concrete components causes stresses in the material whereas tensile creep counteracts these deformations as a relaxing mechanism and relieves a part of the induced stresses. Thus both creep, shrinkage and thermal deformations are to be considered for accurate stress analysis and crack prediction. In addition, restraint conditions of the element, E-modulus of elasticity and concrete strengths must be considered.

Although the assessment of cracking involves creep properties in tension, the traditional focus has been exclusively limited to creep in compression. The relation between the creep in

tension and compression has not been investigated enough, and thus similar creep behaviour in tension and compression is normally assumed in creep models. Moreover, though the knowledge of compressive creep prediction at early ages has progressed significantly, the theoretical creep modelling is still not very reliable, and the uncertainty in creep prediction is still considerable.

Recent advances in development of modern high strength concrete with low w/b-ratio and using mineral addition and admixtures have renewed the concern about volumetric instability and early age cracking. The importance of this issue and concern about cracking have become a pressing factor in introducing analysis of early age stress development in national codes of structural engineering in countries like Sweden, and it is expected that soon such analysis will be introduced in national codes in Norway and other countries in EU.

This investigation focuses on properties of early age concrete such as stress relaxation, tensile creep, compressive creep, shrinkage, with some attention also to the development of mechanical properties.

1.2 Objective and Scope of Research

The primary objective of this investigation is to provide new and extend the existing knowledge about early age creep and its associated stress relaxation in engineering practice, particularly in tension. It is intended that this knowledge should contribute to better characterization of the creep properties, which is needed to make accurate assessment of cracking risk. This investigation focuses on testing and modelling of tensile creep behaviour of concrete subjected to loading at early ages and the influence of creep behaviour on self-induced stress development.

Evaluation of the role of creep and its associated relaxation on self-induced stresses depend strongly on the temperature history in addition to the shrinkage. During the hardening process under realistic temperature history, relative small compressive stresses and then significant tensile stresses will be generated in a restrained concrete element, accompanied by both compressive relaxation and then tensile relaxation. The relaxation of stresses will occur during the whole process, but a question, which have to be answered is whether the viscoelastic behaviour of concrete is the same under both tension and compression. The research put special emphasis on tensile creep behaviour and its comparison to the compressive creep. Assessment of such comparison should be related to development of modulus of elasticity concrete at early ages in tension and compression, an issue, which is treated in the present work.

The early age creep has often a beneficial effect in reduction of self-induced stresses in the beginning of hardening phase, but one should be aware that creep might also have a detrimental effect in the process of further stress build-up. This characteristic of creep reflected in relaxation is another focus of this research.

Models for the prediction of self-induced stresses and for risk of cracking suffer from serious lack of experimental data about the viscoelastic behaviour of hardening concrete. Moreover, there is a need for a creep model, which can fit to different concrete types and under different conditions. Since experimental testing of viscoelastic properties at early ages is very complicated and time consuming, the necessary number of creep tests to find creep/relaxation parameters of the creep/relaxation model has to be limited.

Whether cracking will develop due to evolution of stresses depends on numerous parameters and processes. For prediction of self-induced stresses and cracking tendency in hardening concrete structures, the properties of early age concrete such as development of mechanical properties (strengths, E-modulus), viscoelastic behaviour (creep and relaxation), thermal dilation, shrinkage and restraining and environmental conditions must be known.

1.3 Organization of the Thesis

The doctoral thesis is organized in seven chapters. A short literature review of existing knowledge about the material properties of high performance concrete at early ages is given in Chapter 2. It provides also a brief review on time-dependent deformations, development of stress and restraint conditions.

Chapter 3 presents a review on creep in concrete and the factor influencing creep. State-of-the-Art on tensile creep and relaxation at early ages is provided and the existing mathematical models and theories for creep in concrete are explored. A suitable model for early age concrete was chosen and described.

The description of the new developed experimental equipment (Tensile creep rig) and the other used test apparatus (compressive creep rig, TSTM and Dilation rig) are given in Chapter 4. I addition, concrete compositions, concrete specimens, measuring devices, testing procedure and the experimental program are described.

Chapter 5 presents the result of a comprehensive experimental work conducted on creep of concrete in both tension and compression at early ages. With regard to various parameters, the analysis of the results is divided into five parts; the mechanical properties of concrete with particular focus on relation between tensile and compressive modulus of elasticity of different concrete mixes, comparison between creep behaviour in tension and compression, the influence of the stress level on tensile creep, the influence of isothermal temperatures on tensile creep and finally the influence of silica fume content in concrete mixes is studied and some conclusions are made. To characterize the creep occurring under sealed condition, the notion *Sealed Creep* has been introduced in the present investigation

In Chapter 6 test results from the TSTM apparatus on early age concrete are analyzed with respect to creep and relaxation, where the effect of temperature on creep and relaxation is emphasized. The effect of silica fume on self-induced stresses are also evaluated and considered in conjunction with the creep behaviour of the concrete. Stress simulations are

performed using a model based on the theory of linear viscoelasticity, where creep is separated into sealed creep and transient creep. The model parameters are calibrated against the creep tests performed in the former chapter, and the results are evaluated. Moreover, a short overview on the test program conducted on TSTM and Dilation rig is given.

Finally, in Chapter 7 the summary and main conclusions of the study are presented along with recommendations for future work.

Chapter 2

Properties of Early Age Concrete

2.1 Introduction

Concrete is a continuously changing material with transient material properties. It changes from a nearly liquid state to a viscoplastic material within a few hours, which is followed by further development into a hardened material with almost elastic properties. Limitation in the available knowledge concerning the properties of concrete at early age also limit the possibilities available to us for dealing with concrete structures and crack predictions.

Development and utilization of high performance concrete (HPC) in tall buildings, offshore structures, bridges and other prestressed structures has been in focus in the last two or three decades. The main reasons to use HPC are its high strength, high durability, high erection speed and good workability at site. Apart from these advantages, a number of new aspects have been discovered and estimated, leading to new concepts and ideas, described in Walraven (1993), such us:

- high early strength
- high plasticity of the concrete mixture
- resistance against abrasion, wear and tear
- large resistance against the penetration of chemicals
- revival of old structural concepts
- invention of new structural concepts

The new concretes provide superior mechanical properties and durability, but the increased use of such concretes is accompanied by concern regarding their early age cracking sensitivity. In order to get a high benefit of using these concretes there is a need for a comprehensive understanding and treatment of early age cracking. An understanding of the mechanisms involved and the factors influencing the risk of cracking, such as the driving forces to volume change and the type of restraint, is of utmost importance.

The research on early age concrete has shown that low w/b-ratio lead to more pronounced volume reduction, earlier build-up of internal tensile stresses and greater sensitivity to early cracking, see Proceedings of the International RILEM Symposium on Thermal Cracking in Concrete at Early Ages (1994), [e.g. Sellevold *et al.*, Tazawa *et al.*, Schöppel & Springenschmid and Schrage & Summer]. This is not only a consequence of the hydration heat, but also of autogenous shrinkage due to self-desiccation. In other words, the concrete at early ages undergoes rapid volume changes due to phenomena such as autogenous shrinkage and thermal dilation that lead to rapid build up of stresses if the concrete is restrained.

Whether cracking will develop due to evolution of stresses depends on numerous other parameters and process which control it. For prediction of stresses and cracking tendency in hardening concrete structures, the properties of early age concrete such as development of mechanical properties (strengths, E-modulus), viscoelastic behaviour, thermal dilation, autogenous shrinkage and restraining conditions must be known.

Early age cracking-tendency is a well-known phenomenon also for normal concrete qualities and is associated with early drying (plastic) shrinkage and temperature.

The primary purpose of this chapter is to give a short review of some of the existing knowledge about the material properties of high performance concrete at early ages.

2.2 Early Age High Performance Concrete

The term *early age* can be used to express the first hours, the first days or even sometimes the first weeks of the concrete life depending on the situation in question. In our investigation the term embrace the time duration, which the formwork must remain in position so as to avoid both surface cracking and through cracking. This means a period of up to 10 days after casting. No water loss from the concrete is assumed in the whole period, i.e. early plastic shrinkage cracking due to evaporation and drying shrinkage after setting are both conditions not considered in the present investigation.

High performance concrete (HPC) means concrete with high strength and low permeability, and is a logical development of normal concrete containing silica fume and super-plasticizer. The two properties are linked to one another because high strength requires also a low volume of capillary pores. A low volume of capillary pores in a mix is achieved by the use of silica fume and a low water-to-cement ratio. To achieve a sufficient workable mix the super-plasticizer is a very effective means to use with the given Portland cement.

In the present investigation, HPC denotes the concretes with water-to-binder ratio of 0.40 or less. The particular proportions of the ingredients of high performance concrete, namely, the relatively high cement content, the low water content, use of silica fume and the dosage of super-plasticizer, influence the properties of the fresh concrete in some respect in a manner different from the usual mixes.

2.2.1 Hardening concrete

The aspects of importance for cracking risk in early age concrete are; 1) the development of mechanical properties, 2) the shrinkage and thermal deformations, and 3) the degree of restraint. Concrete properties develop rapidly in the beginning, and after a time period of 1-3 days the hardening progress will proceed at a considerably reduced rate. The mechanisms that can cause cracking in this phase are thermal dilation, autogenous shrinkage and drying shrinkage.

The concrete properties develop through different phases. The life-cycle of the concrete can be divided in three phases:

- fresh phase
- hardening phase
- utility phase

The concrete is regarded as fresh right after casting and until it reaches the setting stage. Fresh concrete behaves as a plastic material and can easily be formed. Due to the hydration process and evolution of hydration products it becomes self-bearing, but still without significant mechanical strength. After the setting stage the deformability of concrete is considerably reduced, and the hardening process starts. This phase is associated with a considerable strength building and a huge release of heat due to the chemical reactions. This causes thermal deformations and reduction of volume due to shrinkage. The maximum temperature will occur during 1-2 days and then it cools for a few days, depending on the thickness of the structure.

The characteristics of early age concrete are the development of heat, the consumption of water and the development of the properties. The chemical reactions between water and cement particles are simply called hydration. During the hydration process the material properties of concrete such as strength and modulus of elasticity are developed.

Figure 2.1 shows four sketches of the development of the hydration process in cement paste, i.e. without aggregates. *Plastic phase*: the cement particles are distributed in the water and formations of hydrated products have started on the surface of the cement particles, seen as the small needles in the figure. *Setting stage*: the hydration products start to grow in between each other, and this is illustrated with the longer needles. Setting occurs normally between 5-15 hrs after mixing depending on, among other factors, additives. *Basic skeleton*: more cement particles react with water and a basic skeleton form and the material properties increase relative rapidly. *Stable skeleton*: upon increased hydration the structure of the reaction products becomes denser and the development of material properties slows down.

The progress of hydration is usually described by using the term of degree of hydration, α, and is defined as the ratio between of the amount of cement that have reacted and the amount of cement present in the concrete initially. Another way to characterize the progress of hydration is the equivalent concrete age or maturity. The maturity expresses the equivalent hydration period, normally at 20 ^{o}C, which gives the current value of a material property, e.g. the modulus of elasticity.

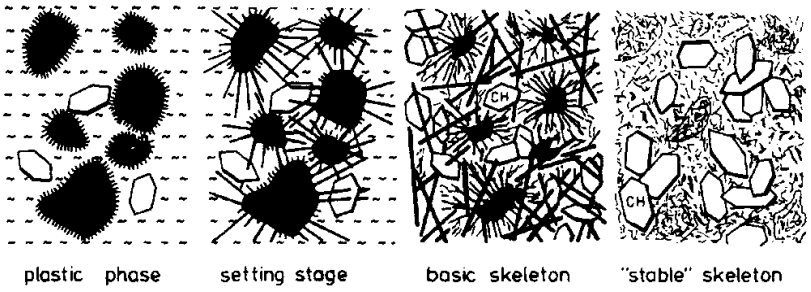

Figure 2.1 Sketch of hydration process [after van Breugel (1992)].

2.2.2 Early age volume changes

Volume changes due to shrinkage and temperature variation are of considerable important because, in practice, these movements are usually partly or wholly restrained, and therefore they induce stresses. They are defined as the time dependent volume change or strains of a concrete specimen not subjected to any external stress at a constant temperature. Early age volume changes may be categorized as stress independent and stress dependent deformations, in which they represent the driving forces and the viscoelastic response, see Figure 2.2.

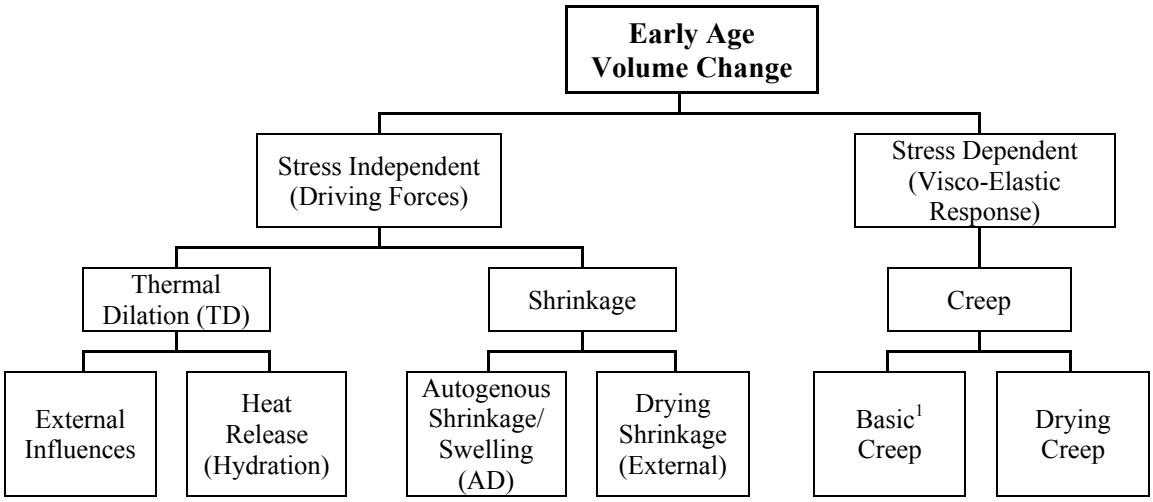

Figure 2.2 Phenomenological summary of early age volume change.

[1] The term Basic Creep is usually used for sealed NSC where neither internal nor external drying occur in concrete. For sealed HPC internal drying occurs and therefore the term Sealed Creep is introduced later on in the present investigation.

2.2.2.1 Shrinkage and swelling

Concrete exhibits changes in strain with time when no external stress is acting. Shrinkage and swelling are such stress-independent deformations, which occur with time primarily due to movement of moisture from or to the concrete or internal consumption of water by cement hydration. There exists various types of shrinkage deformations, and they are considered briefly in the following.

Plastic Shrinkage

Plastic shrinkage occurs when water in concrete is lost by evaporation from the surface of the concrete while it is in the plastic phase, before setting. Its magnitude is affected by the amount of water lost from the surface of the concrete, which is influenced by temperature, ambient relative humidity and wind velocity. Plastic shrinkage is greater the greater the cement content, the finer the cement and the lower the w/c-ratio. Silica fume is very fine and thus increases the plastic shrinkage.

Autogenous Shrinkage

During the hydration process, shrinkage will occur even when no moisture movement to or from the concrete is permitted, i.e. under sealed conditions. Autogenous shrinkage is the consequence of a process known as self-desiccation, which is a result of withdrawal of water from the capillary pores by the hydration of unhydrated cement. It results from the volume reduction during the hydration of cement, i.e. the volume of the hardened cement paste is less than the sum of the volume of water and the volume of cement prior to the chemical reaction. Among others, Bjøntegaard (1999) has investigated autogenous shrinkage in a detailed manner.

The magnitude of autogenous shrinkage for normal strength concrete (NSC) is relatively small, but increases significantly for high performance concrete (HPC), which has low w/c-ratios. Low w/b-ratios generally give very rapid autogenous shrinkage early and also the largest final autogenous shrinkage. The significance of autogenous shrinkage in HPC becomes apparent in Figure 2.3, which shows the development of the shrinkage components with time both for NSC and for HPC. Hence, it is evident that autogenous shrinkage is significant in terms of producing tensile stresses in the concrete, and, thus, must be considered when evaluating the crack risk. For given cases, it is also evident that autogenous shrinkage may actually contribute more than thermal dilation in terms of stress generation, especially in the case when the temperature increase is moderate - which may be the case for floors, slender columns etc.

The fact that autogenous shrinkage may be also seen as expansion [Bjøntegaard (1999)], the term autogenous deformation (AD) is used in the present work.

HPCs are characterized by high cracking sensitivity, which partly is a consequence of increased autogenous shrinkage. To overcome the problem, traditional curing methods using pre-soaked lightweight aggregates as internal water reservoirs has been an effective method. The application of the concept of internal curing by means of saturated lightweight aggregate was applied by Van Breugel (2001), Zhutovsky *et al.* (2001) and Bentur (2001), and showed to be effective in eliminating the autogenous shrinkage. In the recent years, there has been a great interest in autogenous shrinkage, and its mechanism as well as the effect of the mix proportion on autogenous shrinkage has been experimentally investigated [e.g. Tazawa *et al.* (1995), Persson (1997) and Bjøntegaard (1999)]. These references confirm among the others that the shrinkage is enhanced with reduction in w/b ratio, is very sensitive to temperature and the addition of silica fume generally leads to increase.

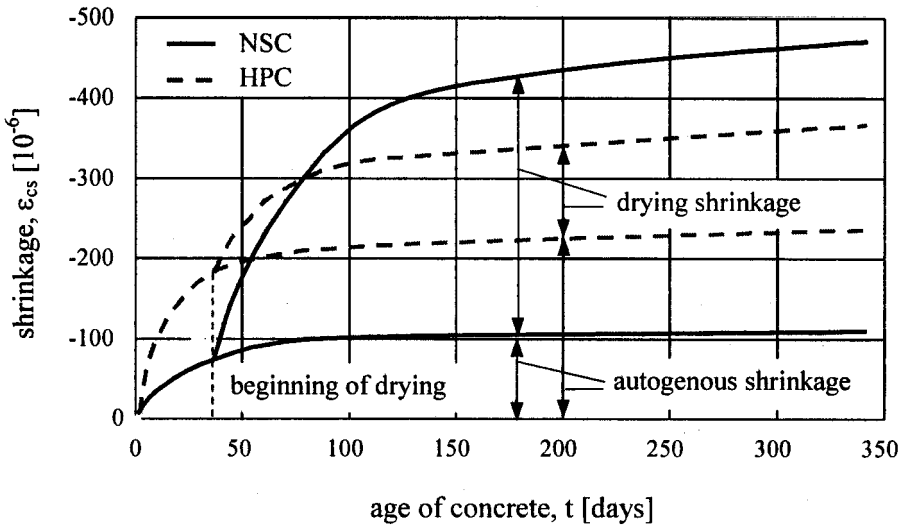

Figure 2.3 Time Dependent of autogenous shrinkage and drying shrinkage in normal strength concrete and in high-performance concrete, [after ***fib*** (1999)].

Drying Shrinkage

Drying shrinkage is consequence of evaporation of water from concrete stored in unsaturated air. When concrete is exposed to drying it exhibits drying shrinkage ranging up to $1^{o}/_{oo}$. In the present investigation, no water loss from the concrete is assumed in the whole period, i.e. neither early plastic shrinkage cracking due to evaporation nor drying shrinkage after setting is considered.

2.2.2.2 Thermal dilation (TD)

The temperature dependent volume change, called Thermal Dilation (TD) is of major importance in the stress analysis at early ages. TD is caused by the temperature change due to

heat of hydration and environmental conditions. The exothermic nature of the hydration reaction results in build up of heat within the concrete mass. The result is thermal dilation as the mass being heated at the first stages of hydration, and cooling down to ambient temperature at later stages. This state of events in any concrete structure also causes thermal gradients, which depend on the size of the concrete member and the external conditions.

The key parameter that converts the temperature change into strain in concrete is the coefficient of thermal expansion, CTE. Information about the CTE of concrete is required to estimate thermal strains. Many studies on CTE have reported a linear relation between temperature (increase and decrease) and thermal dilation/strain (expansion and contraction):

$$\varepsilon_T = CTE \cdot \Delta T \tag{2. 1}$$

in which ε_T is the thermal strain and ΔT is the temperature change. According to *fib* (1999), the linearity relation holds only for temperatures in the range of about 0 - 60 ^{o}C. Particularly for higher temperatures the coefficient of thermal expansion increase with increasing temperature. CTE is greatly affected by:

1) The type of aggregate used in the mix. The general experience is that quartz-rich aggregate has a high CTE, while limestone-rich aggregate has a low CTE - something that is reflected also in the concrete. In this regard, it is notable that the CTE of aggregates varies considerably within each mineralogical group. Consequently, general CTE-values taken from the literature will be very inaccurate.

2) The moisture state of the binder phase. Water saturated (RH = 100%) cement paste has a CTE of around 10 x 10^{-6}/^{o}C, while the CTE of "half-dry" (RH ≈ 70%) cement paste is about twice as high. The strong moisture dependence of the paste also gives a clear effect in the concrete. Hence, for concrete that self-desiccates through the hydration phase - which is particularly the case for concretes with low water-to-binder ratios - an increase of the CTE over time is expected. The CTE of concrete varies in the range of 5-15·10^{-6} /^{o}C.

CTE consequently varies with the age of concrete. This effect is illustrated by the test results by Bjøntegaard (1999) in Figure 2.4. The dots in the figure represent the calculated CTE form the measured free strain and the temperature change. The figure shows that: the CTE is very high, up to 20·10^{-6}/^{o}C, before and during setting. It drops rapidly to minimum value of around 7.5·10^{-6}/^{o}C after 12-14 hours at t_0. Beyond this minimum point, the CTE increase gradually with a rate, which depends on the concrete age. Bjøntegaard and Sellevold (2002) expressed the development of CTE by the formula:

$$CTE(t_e) = CTE(0) + \left[CTE(28) - CTE(0)\right] \cdot \left\{ \exp\left[s_{CTE} \cdot \left(1 - \sqrt{\frac{28}{t_e - t_0}} \right) \right] \right\}^{n_{CTE}} \tag{2. 2}$$

where t_e is the equivalent time, CTE(0) is the start-value at t_0 (found to be $7.5 \cdot 10^{-6}$ by a number of tests by Bjøntegaard (1999)), CTE(28) is the CTE-value at 28 days, s_{CTE} and n_{CTE} - are curve-fitting parameters by least square root iteration in the period from t_0 =10.5 to 170 hours. An activation energy of 25000 J/mole is used to transform time to maturity (the same as found from compressive tests by Kanstad *et al.* (2002a, 2002b)). Expression (2. 2) will be used in analysis of stresses in the present investigation.

A sensitivity analysis by Emborg (1998) showed that concrete with low CTE is less prone to early age thermal cracking. Differences between the CTE in expansion (heating phase) and contraction (cooling phase) are reported by few investigators. In contrast to findings by Gutsch (1998) who reported higher CTE in contraction than in expansion, Löfqvist (1946) and Emborg (1998) reported greater CTE in expansion than in contraction. The latter authors suggested constant values for CTE shown in Table 2.1:

Table 2.1 Values for CTE in expansion and contraction

Author	Heating Phase [10^{-6}/°C]	Cooling Phase [10^{-6}/°C]
Emborg (1998)	10.0 - 12.0	7.0 - 9.0
Löfqvist (1946)	12.3 - 12.4	6.3 - 7.0

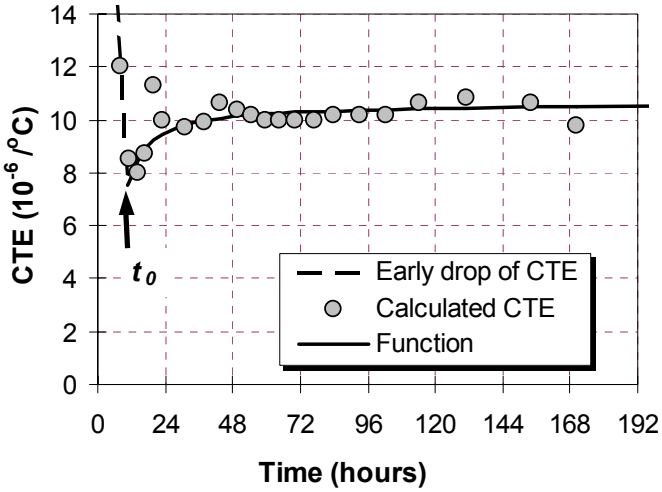

Figure 2.4 Measured and calculated coefficient of thermal expansion (CTE) for a "stepwise" test on HPC with 5% silica fume [after Bjøntegaard *et al.* (2002)].

Some other investigators have reported a different behaviour of CTE. Mitchell *et al.* tested CTE of normal strength, medium strength and high strength concretes in the first 36 hours. Their results indicated that CTE values are relatively independent of age and typically in the order of 9.5×10^{-6}/ °C. Similar conclusions were reported by other researchers; e.g. Miao (1993) and LaPlante (1994). Values of CTE that increase with time [Wittmann (1974)] and

decrease with time [Emborg (1989)] have been reported with no systematic relation to curing conditions or concrete quality. However, it should be conclude that for accurate calculations it is necessary to test CTE for the given concrete, and to take into account the CTE-increase during self-desiccation using Eq. (2. 2). In the RILEM State-of-the-Art report, a survey of research on this subject is given [Lange and Altoubat (2002)].

It should be stressed that it is well established that CTE does increase with decreasing moisture content from a saturated state, thus any results contradicting this principle are not trustworthy.

2.3 Development of Mechanical Properties at Early Ages

The early days of concrete life are characterized by complex interactions of evolution of mechanical properties, time-dependent deformations such as creep and shrinkage and thermal effects. Several studies have dealt with experimental and modelling of the development of strength and modulus of elasticity at early ages, both in compression and tension [e.g. Gutsch (2001), Kanstad *et al.* (1999), Byfors (1980), de Schutter *et al.* (1996, 1997)].

The development of mechanical properties is a necessary input to predict and model early age stress development and risk of cracking. A frequently used approach is to use standard compressive strength tests as a basis for estimating the E-modulus and tensile strength, which are directly used in the calculations. The mechanical properties (compressive strength, tensile strength and modulus of elasticity) all increase as a function of hydration time, equivalent time or degree of hydration, but they do so at different rates.

Generally, regarding modelling of mechanical properties the type of equation is not a major point, but the equations 2.3-2.5, which are based on the expressions in the CEB-FIP MC 1990, are quite convenient for practical use [Kanstad *et al.* (1999)]. A modification is introduction of the parameter t_0 which is the time when the strength and stiffness are defined to be zero. Time "zero" (t_0) is discussed by e.g. Kanstad *et al.* (1999) and Lura *et al.* (2000). Because this parameter is common for all the mechanical property expressions, (2. 3) - (2. 5) it is possible to make the experimental programs more efficient. When using degree of hydration (α) to describe the progress of hydration, the equivalent parameter to t_0 is α_0. The "t_0-concept" expresses that a certain hydration must take place before the concrete start to achieve "measurable" mechanical properties. Tests on HPC with w/b ratios of around 0.4 and with different cement types and variable silica contents have shown that t_0 varies typically between 9 to 12 hours at 20 ^{o}C [Kanstad *et al.* (1999), Krauss *et al.* (2001)]. This corresponds to a degree of hydration of 15 - 20% (i.e. $\alpha = 0.15 - 0.20$).

Compressive strength:

$$f_c(t_e) = f_{c28} \cdot \left\{ \exp\left[s \cdot \left(1 - \sqrt{\frac{28}{t_e - t_0}} \right) \right] \right\} \qquad (2.\ 3)$$

Tensile strength:

$$f_t(t_e) = f_{t28} \cdot \left\{ \exp\left[s \cdot \left(1 - \sqrt{\frac{28}{t_e - t_0}} \right) \right] \right\}^{nt} \tag{2. 4}$$

Modulus of elasticity:

$$E_c(t_e) = E_{c28} \cdot \left\{ \exp\left[s \cdot \left(1 - \sqrt{\frac{28}{t_e - t_0}} \right) \right] \right\}^{n_E} \tag{2. 5}$$

E_{c28}, f_{c28} and f_{t28} are the 28 days values of the modulus of elasticity, compressive strength and tensile strength respectively. The model parameters s and t_0 are common for all the three equations, and may determined from compressive tests, and the model parameters n_t and n_E are to be determined from tensile strength and modulus of elasticity tests, respectively. t_e represents the equivalent concrete age. These expressions are used in the present study, and the model parameters are given in Table 5.1.

2.3.1 Compressive strength

The compressive strength is the mechanical property which has been most studied for both mature and young concrete. There are many reasons for this: The primary purpose of concrete material in structures is to resist compressive stresses. The compressive strength is easy to determine and provides a good picture of the general quality of concrete. In addition, there is, for a particular concrete, a correlation to other properties, such as tensile strength, modulus of elasticity, deformation properties and durability.

Maturity laws and degree of hydration are two of the most important concepts for the description of the development of strength with time, and various mathematical models based on these concepts are available in the literature. Other concepts used to describe the growth of the compressive strength with time are [van Breugel (1991)]: the porosity concept, the gel-space ratio concept and the chemistry-oriented strength laws. Various expressions for the compressive strength based on these concepts are given in Emborg (1998). Other investigators include; Kanstad *et al.* (1999), Laube (1990), Jonasson (1984), Byfors (1980), etc.

Note that for the same concrete different strength values may be obtained, depending on the test conditions, such as size and shape of specimen, rate of loading, humidity conditions at

tests and at curing, temperature at test. In the present work these parameters are kept constant as far as possible, and in general comply with Norwegian Standard (NS) 3676.

2.3.2 Tensile strength

The properties of concrete in tension have not been studied to the same extent as those of concrete in compression, due to the facts that tensile tests are complicated to carry out and that the interest has been concentrated on the compressive capacity of the concrete. However, information on the tensile strength of the concrete is necessary in prediction of the risk of early age cracking.

The tensile strength of concrete may be determined either directly in a uniaxial tensile test or indirectly by tensile splitting. Tensile splitting tests have been widely used because of the difficulties experienced with direct tensile methods. In the splitting test, the specimen, usually a cylinder is loaded along two opposite generatrices. Ring test and flexural test are other testing methods used for testing of tensile strength.

The growth of tensile strength is mainly influenced by the same factors as those, which influences the compressive strength. Thus, depending on the same testing conditions as in compressive strength testing, different tensile strength values may be achieved for the same concrete mixture. Several authors report test results and theoretical models on tensile strength, e.g. Kanstad *et al.* (1999), Hellman (1969), Kasai *et al.* (1971), Bellander (1976), Laube (1990) and Byfors (1980). The result presented by Kanstad showed that the tensile strength grows faster than the compressive strength, as also reported by e.g. Kasai *et al.* (1974) and Khan *et al.* (1996).

2.3.3 Modulus of elasticity

The modulus of elasticity of the very strong hardened cement paste and of the aggregate in HPC differ less from one another than in medium strength concrete, and therefore the behaviour of HPC is more monolithic and the strength of the aggregate-matrix interface is higher. There is, therefore, less bond microcracking, and the linear part of the stress-strain curve extend to a stress, which may be as high as 85% of the failure stress, or even higher in HPC.

The E-modulus can be determined from compressive or tensile tests. While a Norwegian investigation [Kanstad *et al.* (1999)] showed no significant difference between results obtained by the two approaches, Onken and Rostasy (1995) concludes that the E-modulus determined in tension after 28 days is approximately 15% higher than in compression probably due to less non-linearities in tension. Hagihara *et al.* (2002) reported test results on modulus elasticity in tension (E_t) and compression (E_c), and found that E_t/E_c-ratio lies in the range of 1.07-1.18, shown in Figure 2.5. The different experience might be explained by the different standard test procedures used by the authors. This issue is discussed more in Chapter 5.

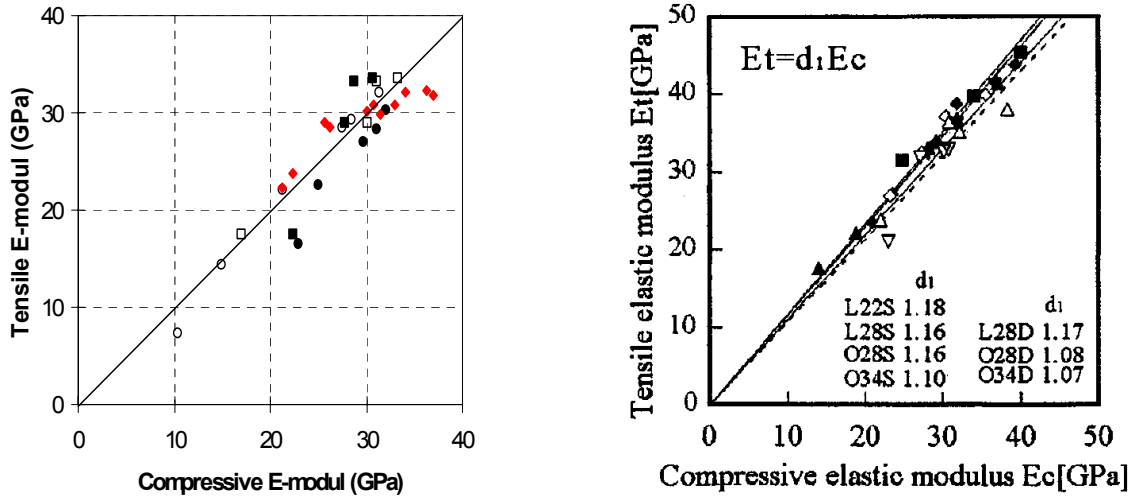

a) b)

Figure 2.5 Relation between various modulus of elasticity in tension and compression, a) [after Kanstad (1999)], b) [after Hagihara *et al.* (2002)].

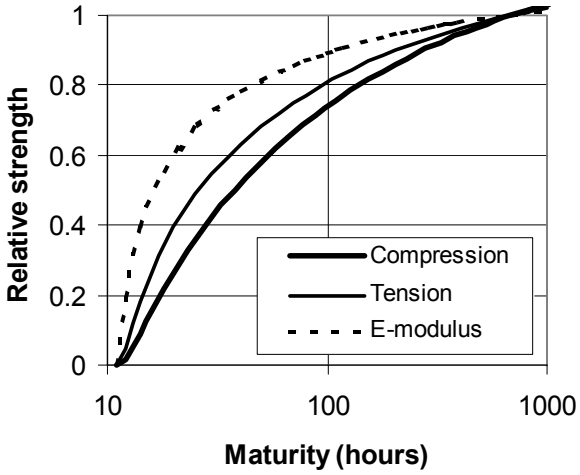

Figure 2.6 Relative strength and stiffness development for high performance concrete with 5% silica fume, according to the materials models [after Kanstad *et al.* (1999)].

Similarly to tensile strength, the growth of the modulus of elasticity is not proportional to that for compressive strength. Relative strength and stiffness development for a HPC called BASE-5, used in the present investigation, according to the materials models expressed by, equations (2. 3) - (2. 5) are shown in Figure 2.6. As is seen, and also demonstrated by other investigators, the relative rate of development of the modulus of elasticity is much higher than the relative rate of development of compressive and tensile strength, [Byfors (1980),

Laube (1990), De Schutter and Taerwe (1996) and Kanstad *et al.* (1999)]. This difference in rate is negative with respect of early age cracking sensitivity, since the stress generated will depend on the modulus of elasticity whereas the resistance to cracking will depend on the tensile strength.

2.3.4 Influence of temperature on mechanical properties

The rate of hydration of cement increases with increasing temperature. Consequently, the temperature of the concrete also influences the mechanical properties, and their development with time. Maturity concepts generally are applied to quantify this dependence; i.e. the concrete age may be adjusted to the *equivalent concrete age* (t_e in Eq. 2.3-2.5) in order to take temperature effects into account.

It is well known that higher curing temperature leads to a lower final strength (see Figure 2.7). Van Breugel (1995) explained the reason to be denser packing of hydration products, which give an increase of the capillary porosity at high temperatures. This leads also to increase cracking risk and reduction of durability. This issue was recently also studied by Kanstad *et al.* (1999), Jonasson (1994), Laube (1990) and Emborg (1989).

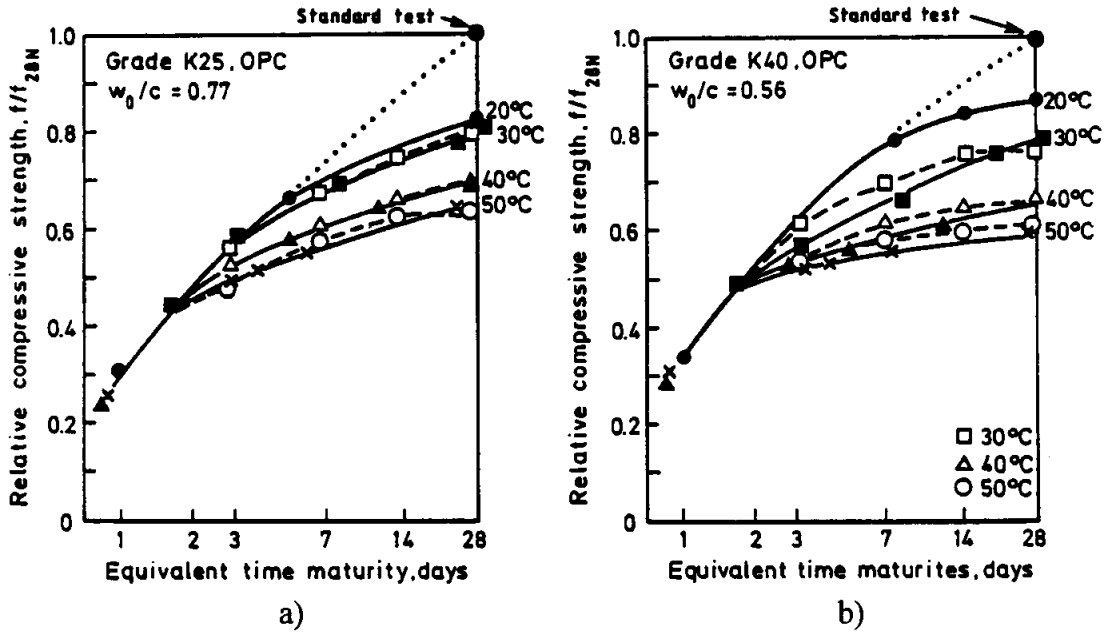

Figure 2.7 Measured strength for concrete of: a) grade K25 and b) grade K40, at different curing temperature, 150 mm cubes, tested wet and warm Type I Cement (Slite) [after Jonasson (1994)].

The influence of temperature on strength growth, important for the estimation of cracking risks, is discussed in many investigations. A comprehensive survey of references dealing with the phenomenon is given in e.g. Emborg (1998), van Breugel (1991) and Byfors (1980). The extent to which elevated temperatures influence the mechanical properties of concrete depends on the concrete composition, on the moisture state and on the drying conditions of the concrete. In particular, it has been found that HPC is less sensitive to the negative effects of effects of elevated curing temperatures than normal strength concrete [Lindgaard and Sellevold (1993)].

Kanstad *et al.* (2002a and 2002b) presents results of several test series on mechanical properties of young concrete. Five different mixes were tested, and the authors concluded that the effect of elevated temperature curing on E-modulus of elasticity was generally less than 8%.

2.3.5 Influence of silica fume

Silica fume generally improves the mechanical and durability properties of concrete, [*fip* - Rapport (1998)].

The extreme fineness of silica fume contributes to the progress of hydration, and thus early strength development is improved. The modulus of elasticity of concrete containing silica fume is also somewhat higher than is the case with concrete without silica fume and of similar strength [e.g. Kanstad *et al.* (2000) and *fip* -Rapport (1998)]. Neville (1996) suggested that use of 5-10% of the total mass of cementitious material content of silica fume is reasonable to achieve the purposes mentioned above.

Kanstad *et al.* (2000) reported test results on the development of tensile strength and E-modulus over time measured for concretes with 0-10% silica fume dosage under realistic temperature (reaching 55 - 58 ^{o}C after one day and then gradually cooling to 20 ^{o}C) conditions, shown in Figure 2.8. The figure reveals the positive effect of silica fumes on both tensile strength and E-modulus. Thus, the increased tensile strength amplified by the greater robustness to elevated temperatures with silica fume are beneficial in terms of crack risk, while the increased E-modulus is detrimental since a given restrained deformation (TD+AD) will produce a higher stress. The net result was slightly reduced crack risk with silica fume.

2.4 Cracking Tendency in Concrete

Early age cracking of mass concrete structures has been a well-known phenomenon since the beginning of the last century. A major source of the harmful cracking already in the construction stage is the proneness of the hardening concrete to crack because of restrained volume change related to hydration temperatures and shrinkage phenomenon.

Earlier it was a common practice to limit cracking by restrictions with respect to temperature differences within the cast section or in relation to older adjoining concrete members.

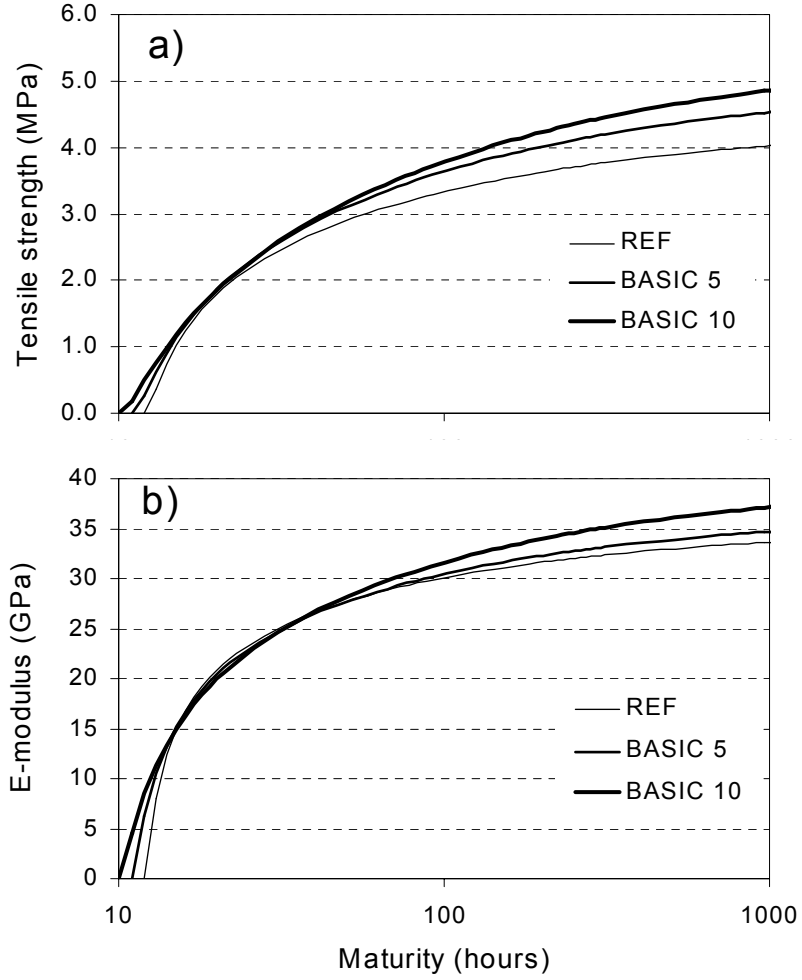

Figure 2.8 Influence of silica fume (REF: 0%, BASIC-5: 5% and BASIC-5: 10%) on development of mechanical properties, a) Tensile strength and b) E-modulus vs. maturity [after Kanstad *et al.* (2000)].

Nowadays, researchers have become more aware of the fact that temperature is not only the factor involved in the phenomena of stress build-up in young concrete. Factors also involved in cracking are shrinkage in the concrete members as well as changing mechanical properties when local or/and global restraint conditions are present.

Figure 2.9 illustrates how cracks in a symmetrical case may originate from either the heating or the cooling phase of the hydration temperature cycle. Two types of cracks, which may appear in both the heating and the cooling phases, are shown in the figure; *surface cracks* and *though cracks*. These cracks may appear shortly after pouring and tend to close at the end of cooling phase. Temperature differentials within a foundation slab or between a new cast wall and an older adjoining wall, as in the figure, may generate through cracking. The traditional method to handle this problem has been the application of proper curing procedures like sealing and water pounding, and construction of joints in slabs and pavements.

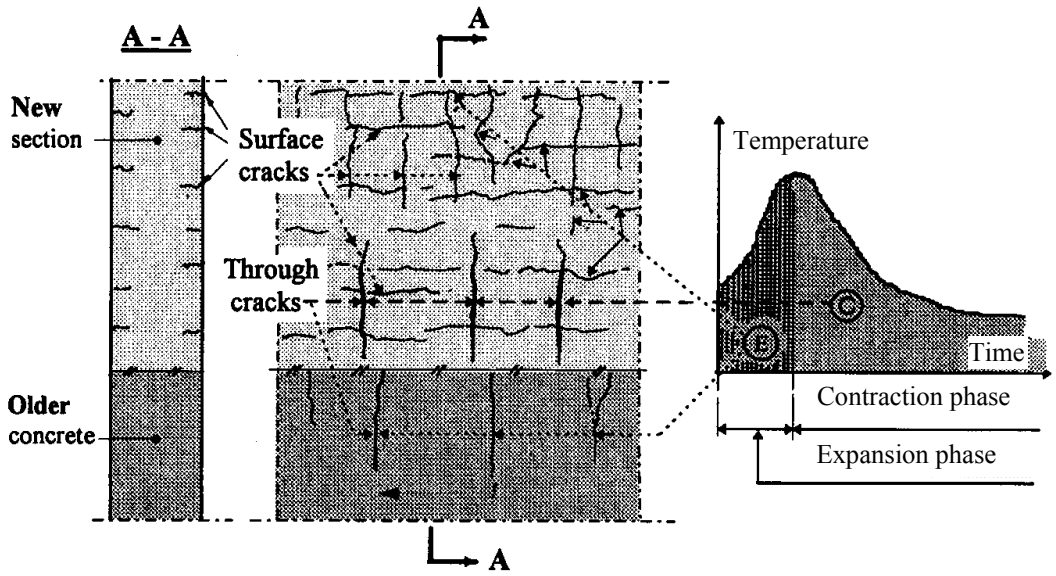

Figure 2.9 Exemplification of early age expansion cracks and contraction through cracks in a symmetrical wall cast on alder concrete [after Bernander (1998)].

2.4.1 Restrained conditions

The concrete in a structure is nearly always restrained to some degree, either *internally* by gradients of moisture and temperature across the component section, or *externally* by adjoining structure elements. Internal restraint alone appears in the totally unrestrained concrete member. However, all structural concrete elements are more or less externally restrained. Hence, internal and external restraint nearly always coexists.

The principle cause for internal restraint stresses is the variation of material properties and volume change within the young concrete element. If the free movement of the hardening concrete element is prevented externally by adjoining elements external restraint will occur. The junction of a wall with an older slab or foundation strip (Figure 2.9) is the most common type of restraint. In this case the free dilatation of the wall is impeded by the foundation, and cracks in the wall may arise because the stiffness of the foundation will exceed the stiffness of the wall. External restraint may arise at the *end* and at inner support of beams, slabs, frames, etc. It can also appears *continuous* a long to the slab or foundation cats directly on to the subsoil. In practice the combinations of end and continuous restraint occur.

The restraint is usually described by a restraint factor (or restraint degree), which varies depending on several parameters. To explain this factor, we refer to Bentur (2002). In a longitudinal Thermal Stress Testing Machine (TSTM) with external restraining rods the level of restrain is a function of the ratio between the rigidity of the rods and the concrete. This concrete rigidity is changing over time due to the hardening of the concrete. The restraint can be expressed in terms of the ratio of the stiffness of the restraining member, K_r, and the shrinking element, K_s. When the two are equal the degree of restrain is defined as 50%; in

such conditions the shrinkage of the restrained shrinking component is 50% of its free shrinkage. The degree of restrain (RD) in % values is defined as:

$$RD = \left(\frac{K_r}{K_r + K_s} \right) \cdot 100 \qquad (2.\ 6)$$

It should be pointed out that most modern TSTMs are equipped with strain measurement devices and feed back systems allowing any degree of restraint to be imposed on the concrete. According to ACI Committee 207 (1973) the strain is equal to the product of the degree of restraint existing at the point in the question and the strain which would occur if the restraining were not occur. The restraint in a structure is not uniform, but varies with the location. It also changes during the hardening period.

Restraint of thermal and autogenous shrinkage strains leads to stress generation in the concrete, possibly with cracking as a consequence. In the literature different stress-terms are used for these stresses, depending on the source of the stresses, such as: shrinkage-induced stresses, thermal stresses or restrained stresses. Shrinkage-induced stresses were used when concrete undergoes only shrinkage strains under isothermal conditions, while the term thermal stresses was used for conditions under variable temperature, before the phenomenon of autogenous shrinkage was "discovered". Restraint stresses correspond to the total induced stresses in concrete due to external restraining, i. e. without internal restraining. Recently, the term of ***self-induced stresses***, which takes all above-mentioned cases into account, has been used and this is also used in the present work.

2.4.2 Diving forces and self-induced stresses

Research worldwide has revealed that autogenous deformation (AD) and thermal dilation (TD) are the two main active mechanisms of self-induced stress generation for early age concrete. The sum of the two deformations can accurately be measured in the laboratory for a given temperature history. The total deformation is then the driving force to self-induced stress generation in restrained concrete. However, from a calculation point of view and in order to minimize the need for laboratory testing, it is necessary to “decouple” the two mechanisms and to construct engineering models of general validity for AD and TD separately. These models can then be applied to any of the many temperature developments that occur in a given structure. A common procedure to calculate the TD is based on use of coefficient of thermal expansion (CTE) discussed earlier in section.

The temperature increases due to heat of hydration is accompanied by volume increase, which, if restrained, leads to compressive stresses in the concrete. The occurrence of autogenous shrinkage simultaneously, which work in opposite direction to the thermal dilation in the beginning, leads to lower compressive stresses. Due to the viscoelastic behaviour of young concrete, these compressive stresses reduce to very low magnitudes. Of much more significance is the volume reduction, which occurs as soon as the concrete

temperature decreases. The volume reduction is then the sum of the autogenous shrinkage and the thermal contraction. If the concrete member is restrained, significant tensile stresses will be generated and they may result in severe cracks.

A typical development of temperature, restrained stress, free-strains (AD+TD) and E-modulus for concrete containing 5% silica-fume (BASE-5 concrete) is shown in Figure 2.10. The parameter t_0 in the figure denotes the time when concrete starts getting enough stiffness to generate measurable stresses, and it is found to be 11 hours for this concrete type. The maximum temperature T_{max} in the concrete is about 61 ^{o}C, and crack occurs when self-induced stress gains 3.02 MPa at concrete age of 56 hours. The free strain is zeroed at t_0. T_{crack} denotes the concrete temperature where failure occurs.

In the first hours of hardening the strength and stiffness of the concrete is very low, but increasing as hydration proceeds with time. The time has a two-fold effect here; the tensile strength increases, thus it reduces the danger of cracking, on the other hand, the modulus of elasticity increases even faster than the strength, so that the stress induced by a given deformation becomes larger. Thus, there is a competition inside the material between the development of self-induced tensile stresses and the development of strength. During the evolution of stresses the concrete will undergo relaxation, but the self-induced stresses may lead to cracks across the entire concrete section as soon as the tensile strength of the young concrete is exceeded.

In the late sixties, the first attempts were made to estimate the magnitude of stresses due to restrained shrinkage strains and thermal dilation and compare them with the increasing tensile strength of the concrete at early ages. In different research centers worldwide different experimental apparatus has been developed to measure the stresses. In 1969 the first laboratory equipment, the cracking frame, was developed by Springenschmid (1973) in order to perform model tests. Later on, in the 1980s, the Temperature Stress Testing Machine (TSTM) was developed in Munich by Springenschmid *et al.* (1985) and in Paris by Paillère *et al.* (1989). With similar machines in several other research institutes today, stress measurement may be performed for any degree of restraint and under any chosen temperature development. Using the free shrinkage as a basis for the calculations, these systems can give not only the stresses developed under restraint, but also the relaxation capacity of the concrete. Mangold (1998) has given a survey on the experimental apparatus and the experimental methods used in determination of self-induced stresses.

The development of self-induced stresses may also be estimated analytically. However, for such an analysis to be accurate a number of input data are required, which are difficult and expensive to determine experimentally for young concrete, such as the development of the creep and relaxation properties.

In the late sixties, the first attempts were made to estimate the magnitude of stresses due to restrained shrinkage strains and thermal dilation and compare them with the increasing tensile strength of the concrete at early ages. In different research centers worldwide different experimental apparatus has been developed to measure the stresses. In 1969 the first laboratory equipment, the cracking frame, was developed by Springenschmid (1973) in order to perform model tests. Later on, in the 1980s, the Temperature Stress Testing Machine (TSTM) was developed in Munich by Springenschmid *et al.* (1985) and in Paris by Paillère *et*

al. (1989). With similar machines in several other research institutes today, stress measurement may be performed for any degree of restraint and under any chosen temperature development. Using the free shrinkage as a basis for the calculations, these systems can give not only the stresses developed under restraint, but also the relaxation capacity of the concrete. Mangold (1998) has given a survey on the experimental apparatus and the experimental methods used in determination of self-induced stresses. The development of self-induced stresses may also be estimated analytically. However, for such an analysis to be accurate a number of input data are required, which are difficult and expensive to determine experimentally for young concrete, such as the development of the creep and relaxation properties.

The viscoelastic behaviour of young concrete is important for an accurate stress analysis, which, in addition require knowledge on how the other earlier mentioned parameters are described for early ages. Schematic pattern of stress development when relaxation relieves shrinkage-induced stresses is illustrated in Figure 2.11. Cracking is delayed by influence of stress relaxation, and cracking is avoided as long as the stress is smaller than the concrete strength.

The estimation and role of relaxation in self-induced stresses is one of the main issues treated in the present work, mainly in Chapter 6.

The amount of stress generated by AD and TD in a given time interval depends on the degree of restraint of the concrete element, the E-modulus and finally the creep/relaxation properties of the concrete which will reduce a given stress increment over time. Figure 2.12 illustrates the interplay of the factors; each of which changes with time. The assessment of crack risk at a given time/position then involves comparing the calculated stress in the actual concrete structural element to the concrete tensile strength at the time.

Based on the experimental results models for numerical calculations of the self-induced stresses can be deduced. A RILEM Committee TC-181 EAS, Early Age Cracking in Cementitous Systems, was established to develop a comprehensive approach for treatment of this issue. The review of this approach is presented in Bentur (2001).

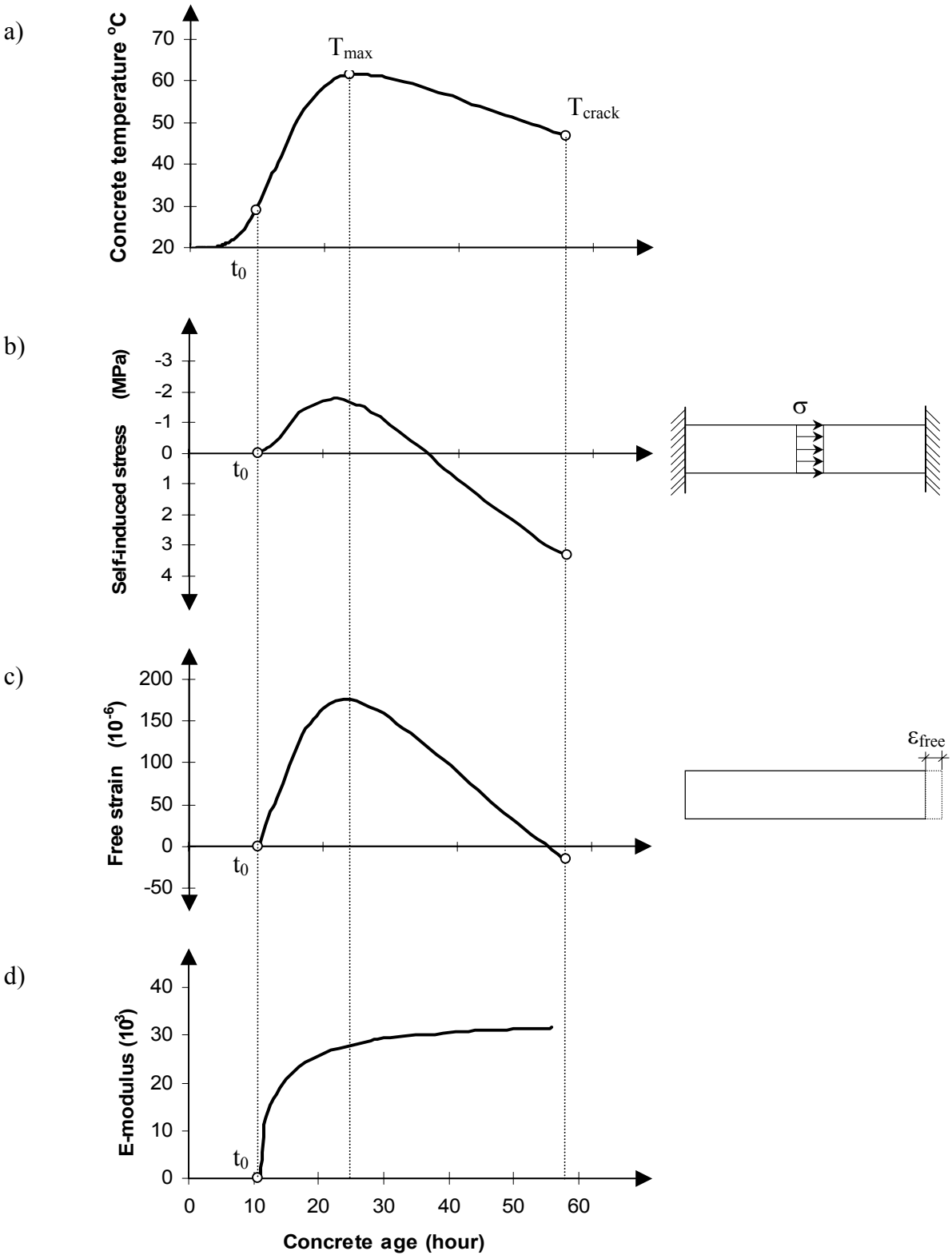

Figure 2.10 Measurements in BASE-5 concrete: a) Temperature history; b) Self-induced stress in fully restrained concrete at a TSTM; c) Free def. in a unrestrained parallel concrete and d) Development of modulus of elasticity according to expression (2.5).

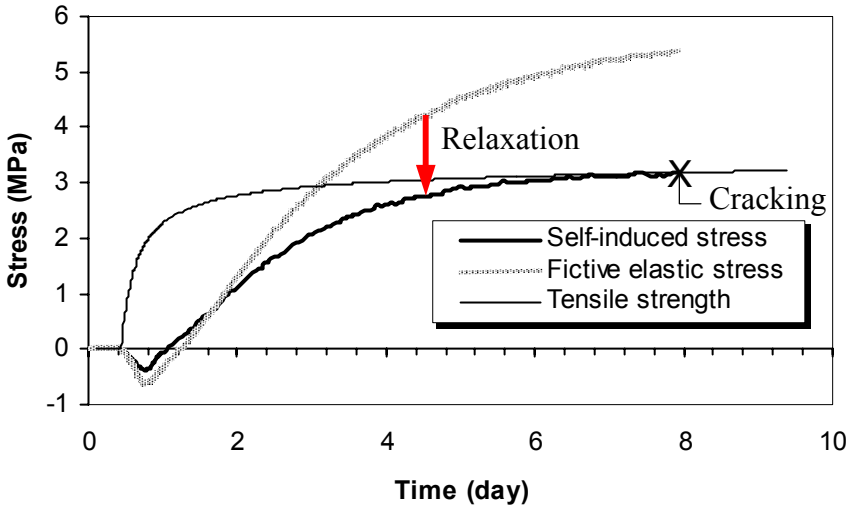

Figure 2.11 Schematic pattern of crack development when the self-induced stresses due to restrained strains are relieved by relaxation, (HPC with w/b = 0.40, 5% silica fume and T_{max}= 40 ^{o}C).

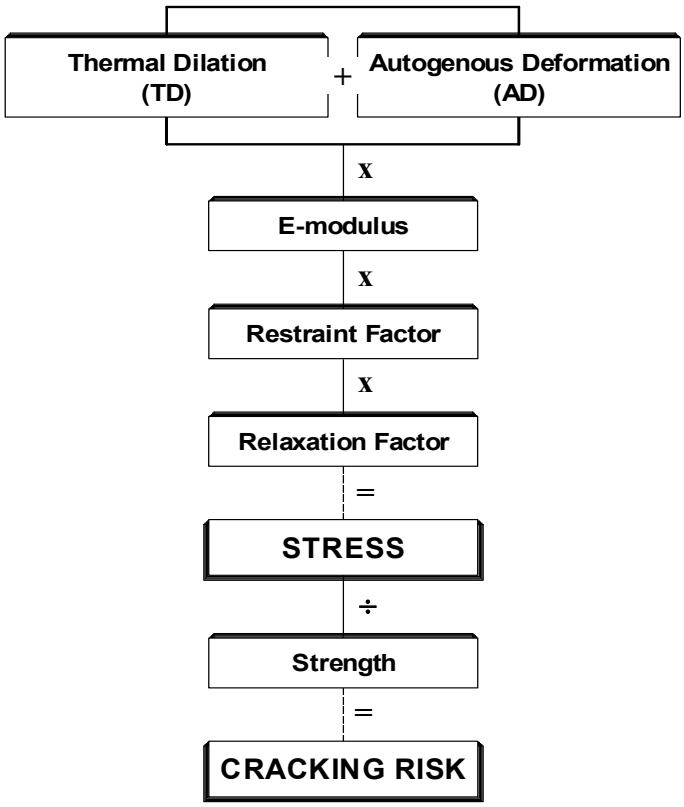

Figure 2.12 Principle of stress and crack-risk calculation

Chapter 3
Creep and Relaxation of Early Age Concrete

3.1 Introduction

When concrete is subjected to sustained loads, the instantaneous deformation at the time of stress application is followed by further deformations, which continuously develop with time. This phenomenon, of viscoelastic nature, was discovered in 1907 by Hatt, and is now referred to as creep. Moreover, as mentioned in Chapter 2, concrete undergoes stress-independent deformations which in addition to thermal dilation include shrinkage deformation, i.e. volumetric deformation due to change in water content and hydration process.

The role of the concrete properties such as creep and its associated relaxation is very important in the reduction of build-up of self-induced stresses and in the assessment of the risk of cracking, particularly during the first days after placement. During the hardening process under realistic temperature history, relative small compressive stresses and then significant tensile stresses will be generated in the restrained concrete, accompanied by both the compressive relaxation and then tensile relaxation. In other words, relaxation of stresses will occur during the whole process, but a question, which have to be answered is whether the viscoelastic behaviour of concrete is the same under both tension and compression.

The enhanced interest in the time-dependent effects in early age concrete is reflected by increased research work on this subject during the last decade. For instance, at the RILEM International Conference on "Early Age Cracking in Cementitious Systems" (2001, Haifa), several authors presented test results on visco-elastic behaviour of concrete, considering the thermal dilation and autogenous shrinkage as driving forces in building up the stresses, see [e.g. Bjøntegaard and Sellevold, van Breugel and Lokhorst, Gutsch, De Shutter, Altoubat and Lange, Hammer *et al.* and Pan and Hansen (2001), etc].

Although the knowledge of creep prediction at early ages has progressed significantly, the theoretical creep modelling is still not very reliable, and the uncertainty in creep prediction is still considerable, se Takács (2002) and Bosnjak (2001).

Generally, the creep behaviour in concrete structures may have both negative and positive effects on structures from the time where concrete casts and during their service life. Evaluation of the role of creep and its associated relaxation on self-induced stresses depend strongly on the temperature history. In the RILEM State-of-the-Art report, Hansen (2002), it is stated that: "Early age creep is beneficial and important in stress analysis", but in this context one should be aware that creep at early ages may also have a detrimental effect in the process of further stress build-up. This issue is treated in detail in this investigation.

As mentioned earlier, in addition to creep, there are also other important parameters, which of course have to be considered for an accurate stress analysis; Temperature development in the concrete element, coefficient of thermal expansion, autogenous shrinkage, restraint conditions of the element, E-modulus of elasticity and concrete strengths.

The primary purpose of this investigation is to increase our knowledge and to improve the understanding of the creep properties of concrete at early ages. It is intended that this knowledge should contribute to better characterization of the creep properties, which is needed to make accurate assessment of cracking risk.

3.2 Viscoelastic Behaviour of Concrete

Concrete structures are subjected to a wide range of external loads during their service life; self-weight, live load, wind, earthquake and changes in environmental conditions like temperature and relative humidity. Another type of loads are the internal loads, generated by imposed deformations such as shrinkage, temperature or differential settlement, and they are very important in early age concrete.

The response of concrete structures to the loads is complex and results in three fundamental types of deformations: elastic, plastic and viscous as well as their combinations, such as elasto-plastic or viscoelastic. The deformations can be classified into two categories with respect to time: *time-independent* and *time-dependent* deformations, and two categories with respect to stress: *stress-dependent* and *stress-independent* deformations (se Figure 2.2). Instantaneous deformations (defined at a certain very short time, i.e. seconds or at most minutes) refer to the time-independent deformation, and it represents the immediate reaction when the load is imposed on the concrete structure. Creep refers to the time-dependent deformations, i.e. those taking place after the immediate. It is apparent that the separation of the two deformations is something arbitrary.

Another classification of the deformation is the separation of the stress-dependent deformations into *reversible* or *irreversible* components. The reversible deformations are then the instantaneous elastic (ε_{el}) and the delayed elastic ($\varepsilon_{el,d}$); the irreversible strains are the

instantaneous inelastic (ε_{nel}) of a plastic nature, and the delayed inelastic strains ($\varepsilon_{nel,d}$) of a viscous nature. These fundamental types of deformations involved under sustained loading are tabulated in Table 3.1 and presented in Figure 3.1. Both the deformations in the time-dependent column represent creep, and the figure shows that the rate of both creep components decreases with time.

Table 3.1 Classification of strains.

Strain	Load-dependent		Load-independent
	Instantaneous	Time-dependent	
Reversible	Elastic (ε_{el})	Delayed elastic ($\varepsilon_{el,d}$)	Thermal dilation* & Shrinkage or swelling*
Irreversible	Inelastic (ε_{nel}) (*Plastic flow*)	Delayed inelastic ($\varepsilon_{nel,d}$) (*Viscous flow*)	

* *Both thermal dilation and shrinkage (or swelling) have reversible and irrecoverable components.*

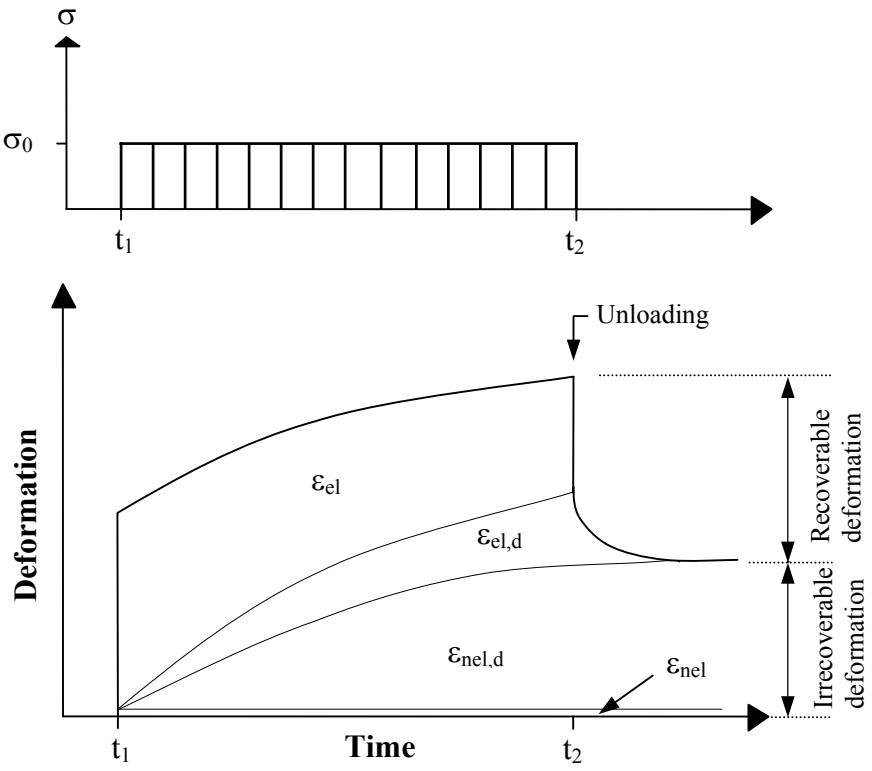

Figure 3.1 Typical strain-time development due to loading and unloading of concrete, showing fundamental types of deformations. (The notations are given in Table 3.1)

3.2.1 Creep and its nature in concrete

Creep is the time- and stress dependent deformation, which occurs on prolonged application of load. To define creep one can consider two identical specimens subjected to exactly the same environmental histories; one specimen being loaded and the other (companion specimen) load-free. Creep is commonly defined as the strain difference between a loaded and a companion load-free specimen.

Depending on the ambient humidity, one can distinguish between two types of creep, namely basic creep and drying creep. Basic creep is defined as creep occurring under no moisture exchange between the concrete and the environment. Under the condition of drying, i.e. moisture exchange with the environment, there is an additional creep component referred to as drying creep or Pickett effect. Drying creep (after subtracting the strain in the unloaded dummy) is much greater than basic creep in a moisture condition roughly corresponding to a midrange during drying. Drying creep is related to, or influenced by, the tensile stress induced in the outer part of a concrete specimen with resultant cracking, but this effect is by no means a full explanation.

Creep of concrete at young ages in sealed condition (the normal case in this work) is a special case. It is basic creep since no moisture exchange with the environment takes place, but it is also drying creep because of internal, probably uniform drying. Thus, the common definition used for mature concrete is not very relevant and rather confuses the situation in early age concrete. However, in line with common practice we define creep under sealed condition as total measured strain minus unloaded dummy. Most of the available data in the literature were obtained based on this convention, something that makes the treatment and comparison of data possible.

The deformation components stated above are presented in a strain-time diagram in Figure 3.2.

3.2.2 Instantaneous deformation

Like any other structural materials, concrete exhibits, to a certain degree, an elastic behaviour when a stress is first applied. The strain at loading is mainly elastic strain with a small inelastic component, and corresponds to the static modulus of elasticity at the age at which the load is applied. However, it should be noted that in a stress-strain experiment a certain time is used to carry out the loading processes. The loading time will increase the strain due to the creep of concrete. This means that the response will also include a certain creep deformation depending on the rate of application of load. This deformation is usually named the instantaneous deformation. The time duration for application of load in determination of the elastic modulus is not defined in all the practical codes, something that makes it difficult to compare test data published in literature. In other words - what we call instantaneous depends on our definition - or rather the available equipment and the chosen procedure. The instantaneous deformation defines the modulus of elasticity of the concrete.

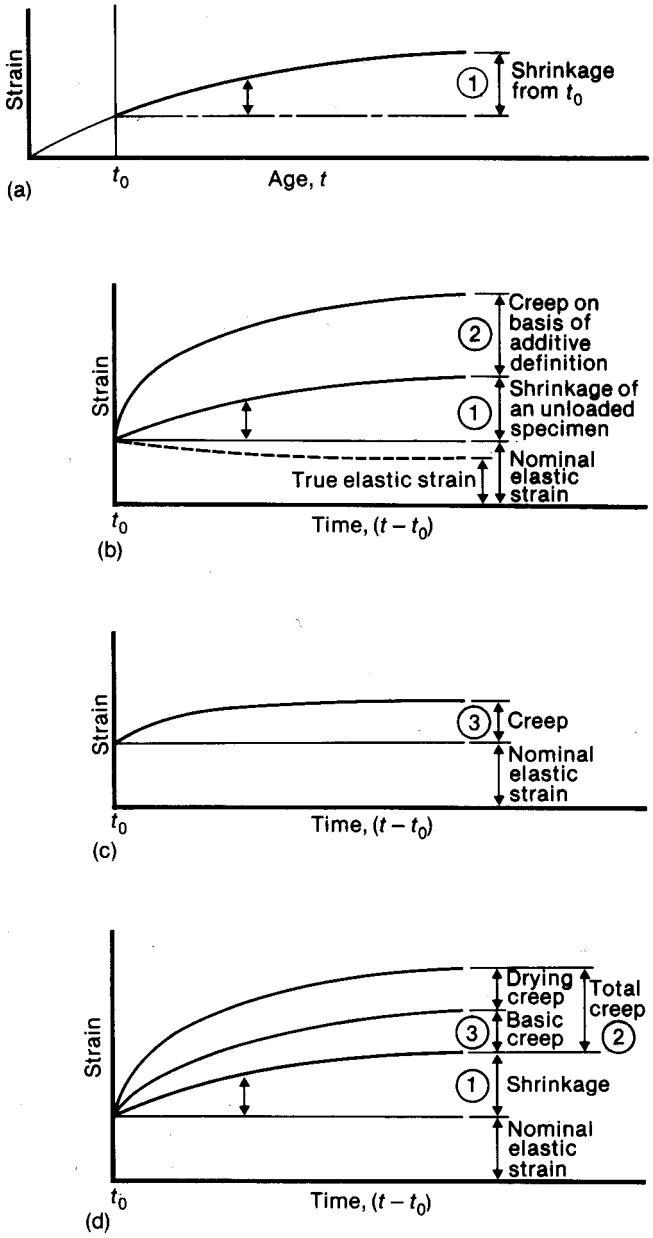

Figure 3.2 Time-dependent deformations in concrete subjected to a sustained load, in which t_0 is concrete age at loading [after Neville (1995)].

As stated earlier, the elastic deformation at application of load and subsequent creep are not easily separated from the other, see Figure 3.3. The instantaneous deformation represents a point on an almost vertical part of the response curve, point A in the figure. Therefore the subdivision into a creep component, C_r, and an elastic component, E_l, is difficult. However, for practical purposes and for interpretation of test data, the deformation occurring during loading time (second or minutes) is considered elastic, and the subsequent increase in strain is regarded as time dependent (creep).

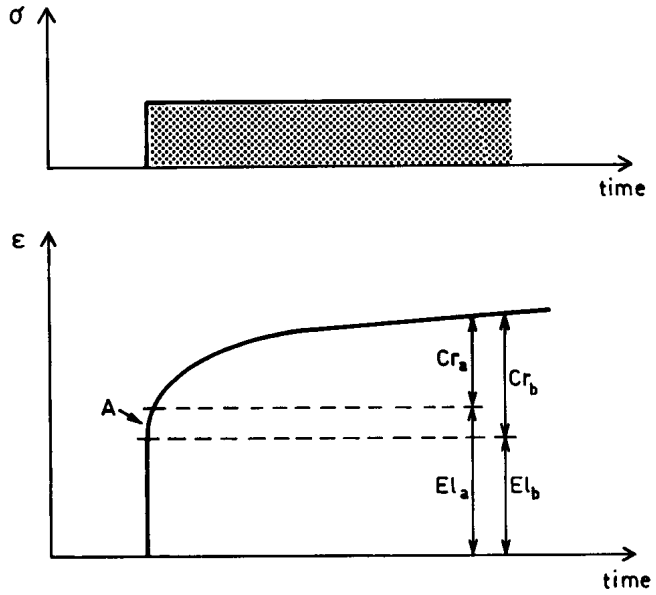

Figure 3.3 Inaccuracies related to separation of elastic and creep deformations [after Bažant and Kim (1979)].

3.2.3 Creep recovery (Delayed elastic)

If the sustained stress is removed, the strain decreases immediately by an amount defined to be the elastic deformation at the time concerned. This immediate reduction is called initial recovery or instantaneous recovery. Since the E-modulus at the given time is higher than its value at the loading age, and due to possible non-elastic deformations (irreversible) at loading, the instantaneous recovery is less than the elastic deformation was on loading. The instantaneous recovery is followed by gradual decrease in strain, called creep recovery, shown in Figure 3.4 for an early age concrete. Initial recovery corresponds to instantaneous elastic deformation at the unloading time, and creep recovery corresponds to delayed elastic deformation shown in Figure 3.1. The development of recoverable creep exhibits an initial rapid increase with time but reaches a constant value in contrast to creep which continuos indefinitely.

Figure 3.4 illustrates that creep is partly reversible. The irreversible deformation (residual deformation) in the diagram is relatively large. Creep recovery is smaller, but important in prediction of deformation in the concrete under variable stress, and it will be taken into account in calculation of self-induced stress calculation later in the present work.

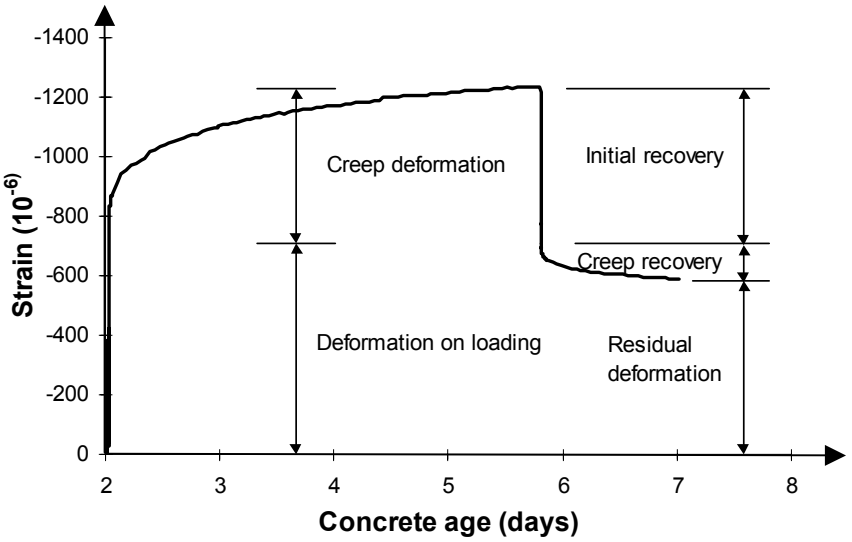

Figure 3.4 Measured compressive creep and creep recovery of a HPC specimen (BASE-5) subjected to 17.6 MPa at 2-days age, and then unloaded after 90 hours, T = 20 ^{o}C.

3.2.4 Theory of linear visco-elasticity for aging materials

Though various non-linear effects are observed for the creep of concrete, the common basis for most of the proposed creep models in the literature is the assumption of creep linearity, i.e. creep strains under constant stresses are assumed to be linearly related to the stress level. In the range of service stresses, concrete might be considered as an aging linear viscoelastic material. In consistence with the assumption of linearity, the principle of superposition may be applied to creep of concrete under constant and variable stresses.

The Boltzmann's principal of superposition of strains, which first was modified by Maslov (1940) and McHenry (1943) to include the effect of aging of concrete, states that: the strains produced in concrete at any time t by a (tensile or compressive) stress increment applied at time t' are independent of the effect of any stress applied either earlier or later than time t', but does depend on t'. It has been used in research and practical design as a convenient working assumption, and implies that creep is a delayed elastic phenomenon in which full recovery only is impeded by the progressive hydration of cement. This is not true as already pointed out, and the irreversible effects will be treated later.

Thus, summing the strain history due to all small stress increments before time t, one may write the creep law for uniaxial stress in the a form as:

$$\varepsilon(t) = \int_0^t J(t,t')d\sigma(t') + \varepsilon^o(t) \qquad (3.1)$$

where

t : current time (measured from casting of concrete)
t' : concrete age at loading
$d\sigma(t')$: stress increment applied at t'
$\varepsilon(t)$: total strain
$\varepsilon^o(t)$: stress-independent strain (shrinkage and thermal dilation)
$J(t,t')$: creep compliance

In the same way it is possible to calculate the stress history caused by an arbitrary strain history:

$$\sigma(t) = \int_0^t R(t,t')\left[d\varepsilon(t') - d\varepsilon^o(t')\right] \qquad (3.2)$$

where R is the relaxation function of time t for a strain induced at time t', $d\varepsilon(t')$ is the strain increment and $d\varepsilon^o(t')$ is the stress-independent strain increment introduced at time t'. It is worth to mention that with the superposition principle, the whole previous strain (stress) history must be used for the calculation at each new time interval. McHenry (1943) obtained experimental verification of the principle of superposition for sealed mature concrete. However, according to many authors; e.g. Bažant and Kim (1979), Ross (1958) and Polivka *et al.* (1964) the principle overestimates recovery. Figure 3.5 shows that the principle overestimates prediction of the creep recovery at unloading and the creep strain at further loading.

Neville reports recovery tests performed in both compression and tension, and the conclusion was also that the predicted recovery overestimated the real one in both cases. This is important in the present work and will be taken into account. According to Bažant and Wittman (1982) several restrictions should be fulfilled to use the principle of superposition on concrete. Generally, the principle is applicable under the following conditions:

(1) The stress level has to be below the proportionality limit, otherwise high-stress nonlinearity (microcracking) may occur.
(2) The rate of strains must not decrease markedly in magnitude (but the stresses may).
(3) A large increase in the stress magnitude late after initial loading must not occur otherwise low-stress nonlinearity (plastic flow) may occur.
(4) Significant drying of the specimen cannot take place.

The principle is of considerable practical value in simplifying the calculation of strain under sustained and varying stress, but the above restrictions do seldom hold for the stress analysis of young concrete. For early age cracking problems condition (1) is obviously not fulfilled when the cracking risk is high, as tensile stresses build may reaches the concrete strength. Neither is condition (2) fulfilled because young concrete always expands in the heating phase and then contracts in the cooling phase, which means that the stresses change from

compression to tension in most cases. Condition (3) is fulfilled. Considering condition (4), the effect of external drying is probably not significant, but the self-desiccation may have a similar effect, because of the coupling effect between creep and the autogenous shrinkage. In the literature, several approaches, which account for some of these deviations from the conditions of linearity, have been used. The main problem, however, is to identify the effects from experiments in a reliable way, so they can be expressed as general materials models. At the Munich RILEM Conference (1994) such approaches were presented by e.g. Pederson, Torrenti *et al.*, Matsui *et al.*, Onken and Rostásy, Maatjes *et al.*, Nagy & Thelandersson and Paulini *et al.*

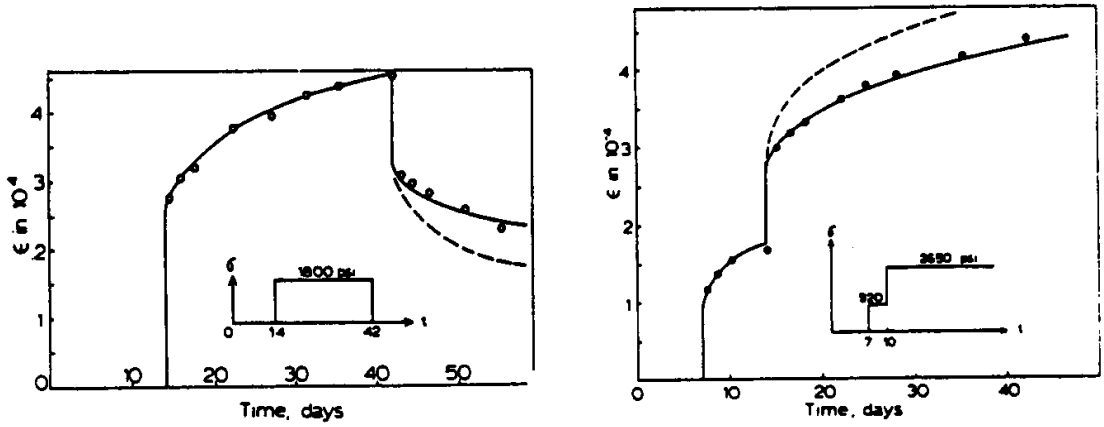

a) **b)**

Figure 3.5 Deviation from the superposition principle when a loaded concrete is: a) unloaded (creep recovery), b) further loaded (stepwise loading) [after Bažant and Kim (1979)].

3.2.5 Mechanism of creep

The physical nature and mechanism of creep has been a subject for research for several decades, but they are still not fully understood. There is a general agreement that creep of concrete has its source in hydrated cement paste and, at high stress, also in failure of the paste-aggregate bound. Creep is believed to be related to internal movement of adsorbed or inter-crystalline water, i.e. to internal seepage. A basic observation is that basic creep decreases strongly with decreasing moisture content.

There are a number of theories of creep mechanism proposed over the years, and presented in Neville *et al.* (1983). They are: mechanical deformation theory, plastic theory, viscous and visco-elastic theory, elastic after-effect theory, solid solution theory, seepage theory and micro-cracking theory. In the field of research on creep it is generally agreed that none of the proposed theories is capable to account for all the observed phenomena. None of them can explain in a unified way the behaviour of concrete under various environmental conditions

and under various states of stress. It is likely that several mechanisms are involved in the actual creep. According to American Concrete Institute, referred in Neville (1983), the main mechanism, which describes creep, are:

- Viscous-flow of the cement paste caused by sliding or shear of the gel particles.
- Consolidation due to seepage and redistribution of pore water under stress.
- Delayed elasticity due to the cement paste acting as a restraint on the elastic deformation of the skeleton formed by the aggregate and gel crystals.

As stated earlier, the essential feature of basic creep is that it takes place without loss of water from the concrete. According to Ali and Kesler (1963) the mechanism of basic creep is probably due to delayed elasticity or viscous flow of the gel and the associated gel water. An important issue regarding the mechanism of creep from our present point of view is whether it is different in tension and compression. This will be discussed later.

3.2.6 Factors effecting creep

Creep of concrete is strongly affected by a large number of factors. In most investigations, creep has been studied empirically in order to determine how it is affected by the various factors. Regarding the nature of the factors they may be subdivided into intrinsic factors and extensive factors. According to Bažant and Wittman (1982), the intrinsic factors represent those material characteristics, which are fixed to the material during whole concrete's service life, such as: the concrete's strength, characteristics of the cement paste binder, modulus of elasticity of aggregate, fraction of aggregate in concrete and maximum aggregate size. If any of these factors increase the creep as well as shrinkage will decrease. Extensive factors are those, which can vary after the casting. Most of these factors are those which can be treated as a point property of a continuum, like: temperature, age of loading, load duration, type of loading (tension or compression). In addition, specimen size and environmental humidity are important factors affecting creep.

The creep behaviour of concrete is strongly affected by microstructural changes of the hardened cement paste matrix. According to Sellevold (1969), for well-cured specimens the main variables influencing the physical properties (strength, modulus, creep, shrinkage, etc.) are the porosity and the pore size distribution in concrete. The microstructure of HPC differs considerably from that of NSC above all by having a much lower porosity and finer pore structure (lower capillary porosity), a more uniform hardened cement paste matrix and a different structure of the aggregate paste interface, Müller and Rübner (1995). Primarily due to the low porosity of the hardened cement paste matrix of high performance concrete, which is associated with a high stiffness, the magnitude of the creep deformation is reduced compared to normal strength concrete. As an example, some experimental results of compressive creep tests obtained by Schrage (1994) is shown in Figure 3.6.The figure also illustrates clearly the very large effect of drying on creep.

Factors affecting creep are described in detail by Byfors (1980), Bažant & Wittman (1982) and Neville *et al.* (1983). The influence of some of these factors is illustrated in Figure 3.7,

and they are described briefly in the following. Their particular influence on creep at *early ages* is further discussed in section 3.3.1.

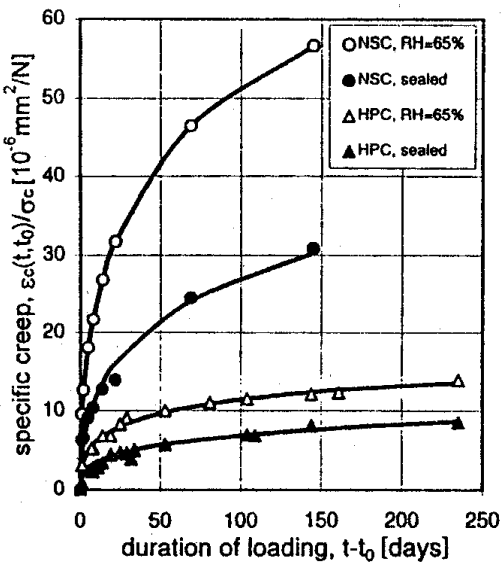

Figure 3.6 Time development of compressive creep of NSC and HPC, where loading age is 28 days, relative ambient humidity 65%, compressive strength values of the NSC and HPC is 48.7 and 97.0 MPa, respectively [after Schrage 1994].

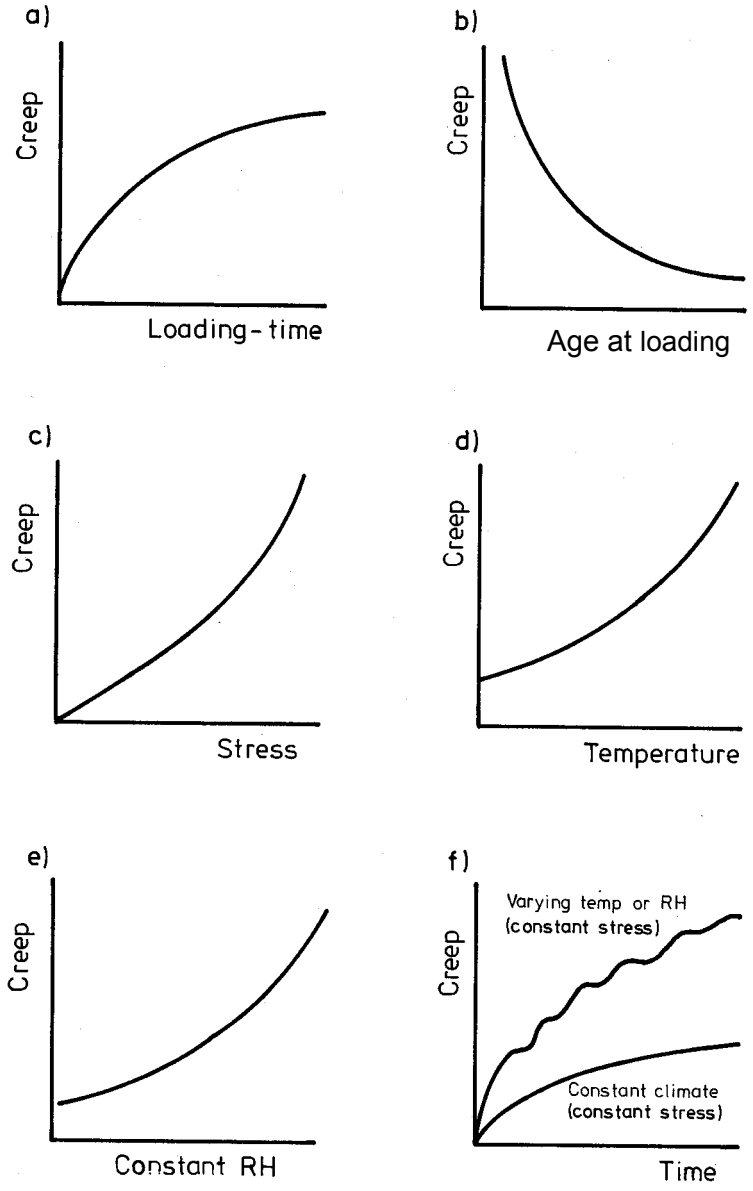

Figure 3.7 Relation between creep and various factors, which influences creep deformations [after Byfors 1980].

3.2.6.1 Influence of age of concrete

Concrete age at application of load is one of the most important extensive factors, which influence the visco-elastic behaviour of concrete. This effect at early ages is of high interest in connection with thermal stress analysis and prestressing. The general pattern of influence of the age at application of load on creep is shown in Figure 3.7b.

Already at 1933 Glanville and then Davis *et al.* (1934) studied this factor, where they noted that the rate of creep during the first weeks under load is much greater for concrete loaded at an early age than for older concrete. The former found also that the subsequent rate of creep, after about a month under load, is independent of the age at application of load.

Parrott (1978) compiled the results of compressive creep tests from many investigators and presented in Figure 3.8. The loading age varied from 12 hours to more than 3 years. The creep is given as a relative ratio to creep deformations at an age of loading of 28 days. The figure illustrates a clear dependency on age, particularly at early ages. It can be seen that, after a rapid decrease in creep, the influence of age decreases. This age effect is certainly related to the degree of hydration. The considerable spread at early ages, showed by dotted ellipse in the figure, may also mainly be caused by the differences in degree of hydration, which is more marked at an early age.

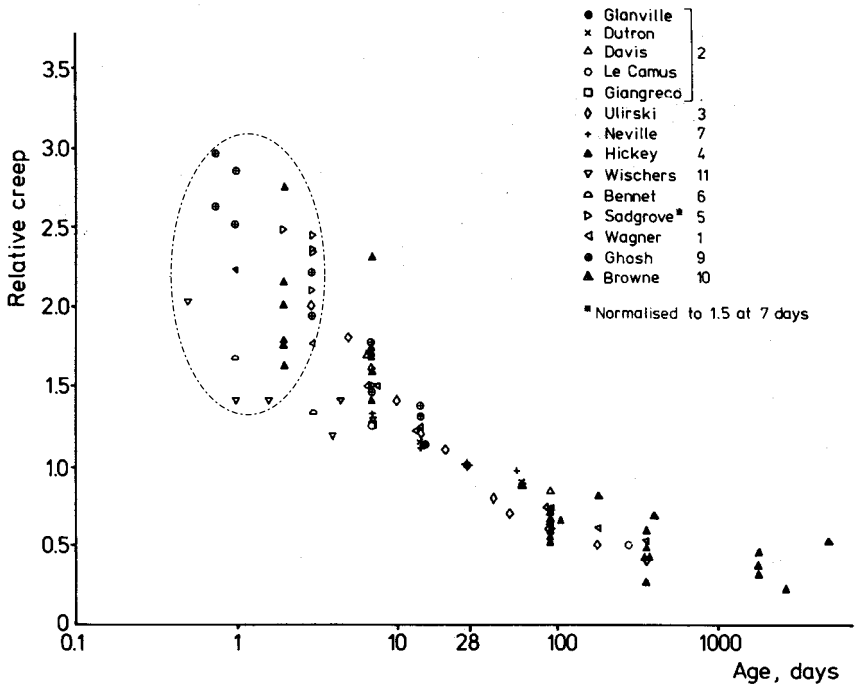

Figure 3.8 Relative creep at different loading ages, compiled by Parrott (1978) [quoted from Byfors (1980)].

3.2.6.2 Influence of stress level

From the review of the literature, it seems to be generally accepted that creep is proportional to the applied stress until a certain stress level and is inversely proportional to the stiffness of concrete at the time of application of the load, i.e. the magnitude of creep is related to the instantaneous deformation. The stress level is generally expressed by stress as a fraction of strength, and the ratio stress/strength is considered as a practical approach to express the relation between creep and stress level for different concrete qualities. There is a direct proportionality between creep and the stress/strength ratio with a possible exception of specimens loaded at an age of less than 24 hours.

The upper limit of proportionality, which is reached when severe microcracking develops in concrete, may vary between 0.3 and 0.75 of the concrete strength in compression, [Smadi and Slate (1989)]. In practical applications, the linearity assumption in compression is acceptable, because under service conditions, the stress from the load varies around 35% of the concrete strength. Only in special cases, such as in the cases of local stress caused by concentrated load, will the ratio be higher. Above the limit of proportionality, creep increases with an increase in stress/stress ratio at an increasing rate due to non-linear effects, Figure 3.9. For early age concrete the case is different in that there is a need to data up to fracture.

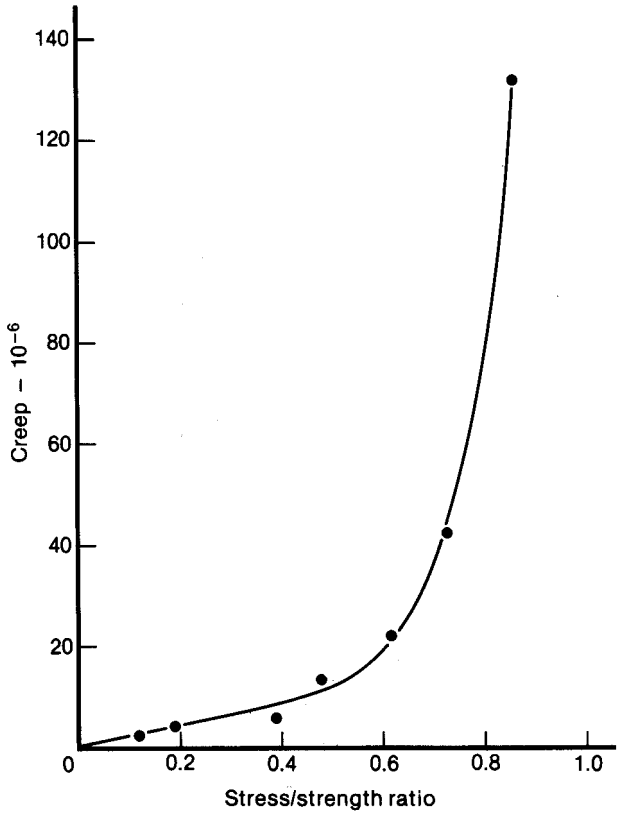

Figure 3.9 Relation between compressive creep after one minute under load to the stress/strength ratio for five days old concrete on results according to Jones and Richard (1936), [quoted from Neville *et al.* 1983].

The non-linearity of creep may appear in:

- High stress ranges, with its physical source in progressive micro-cracking, which mainly initiates in the interface between aggregate and cement mortar matrix.
- The drying conditions and moisture state of the concrete obviously has major effects on linearity or nonlinearity (see Figure 3.6). Thus these factors must be known for any discussion to be meaningful.
- Creep recovery, taking place without drying whenever load is decreasing or reversed.

The validity of the principle of proportionality (linearity) in the case of uniaxial tension has not been sufficiently investigated until now, and the limit may be different. According to Skudra (1956), (quoted from Šerda and Křístek 1988), some of the results, however, indicate that the strain versus stress relationship is linear even when the ratio of tensile stress/tensile strength of concrete approaches unity. However, certain investigators found that tensile creep as for creep in compression is proportional to the applied stress up to approximately 50-60% of strength, Illston (1965) and Neville (1983). The problem is of interest at early age concrete cracking, in which the stresses may reach failure level, and it is investigated in the present work. Note also that the compensation for the creep measured by the unloaded dummy is particularly important for tension. This will be discussed in detail in Chapter 5 and 6.

It is necessary to make some general comments about differences in the effect of stress/strength ratio on creep reported by various researchers. As mentioned earlier, the strength of concrete increases at a relative high rate under sustained load at early age concrete. This means that the stress/strength ratio decreases with time if the applied stress remains constant during the sustained load. We have to distinguish between two stress/strength ratios when the results of creep tests are discussed. In case of *constant stress/strength ratio* the applied stress must be increased in proportion to the increase of strength throughout the period under load. An earlier increase in stress leads to a higher creep. In case of *constant initial stress value* the stress/strength ratio decreases with time due to increased strength during the course of the experiment. In most of the investigations on creep behaviour reported in literature the stresses are normally kept constant during creep experiments, i.e. the creep tests are conducted with constant initial stress (not constant stress/strength ratio).

Both cases are illustrated in Figure 3.10. t' is the loading time, σ_0 is the applied constant initial stress, σ' is the applied stress increased in proportion to the increase of strength and f_c is the development of concrete strength from the time of loading.

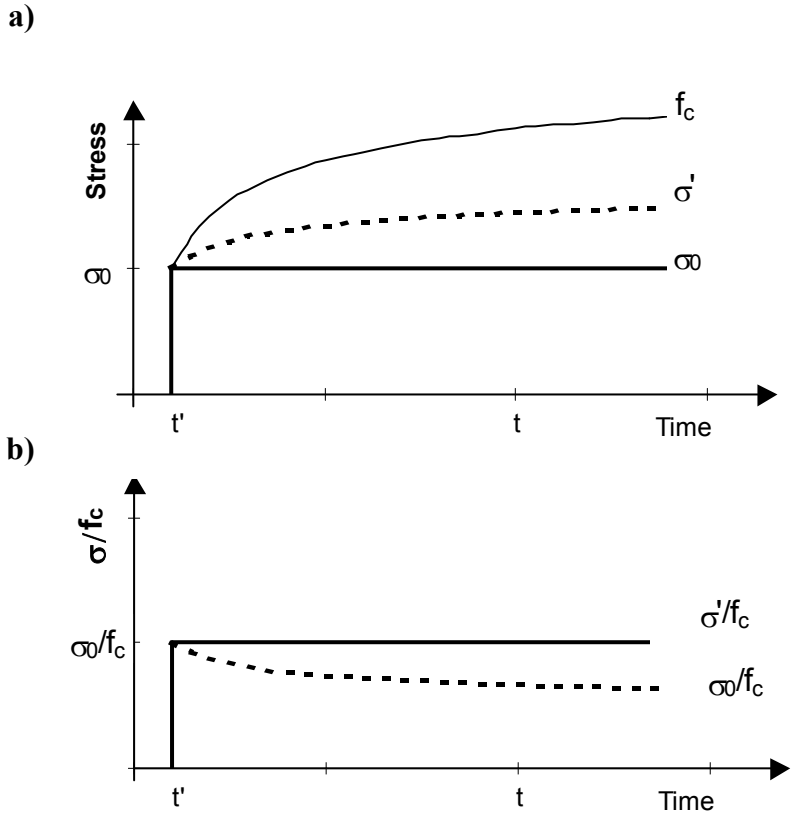

Figure 3.10 Applied stress level and development of strength of concrete:
a) Development of strength of a HPC with 10% silica fume.
b) Stress/strength ratios.

3.2.6.3 Influence of elevated temperature

Temperature is one of the main environmental factors, which influence the time-dependent deformation, see Figure 3.7d. A wide range of investigations on elevated temperatures has shown that the creep deformation increases significantly with increasing temperature, see Figure 3.11. The influence of temperature on time-dependent deformations has been of high interest especially in building of the prestressed concrete pressure vessels in nuclear reactors since the service conditions involve quite high temperatures. This is due to the fact that the prestressed concrete structures undergo more creep in hot weather than in cool air.

The influence of temperature is even larger at early ages (since any increase of temperature means faster hydration) and thus it is important in thermal stress analysis. Creep increases with increasing temperature, but the effect is offset by the fact that a temperature increase also accelerates hydration, which in turn reduces creep. Consequently, a higher temperature tends to increase the creep rate, but will also indirectly reduce the creep. Dependent on the concrete age, the former effect is usually higher than the latter one.

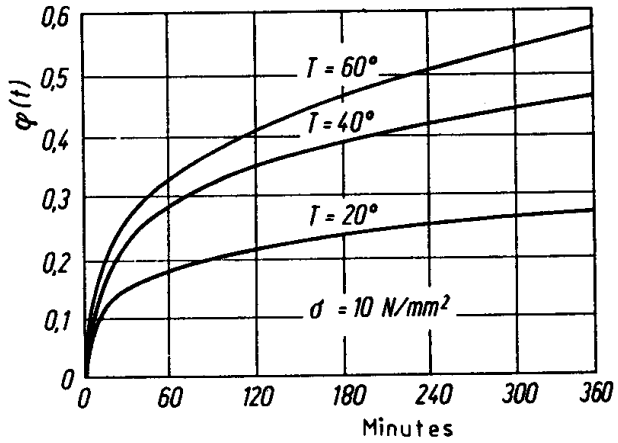

Figure 3.11 Creep development for various temperatures, for 2 months old concrete subjected to a constant stress 10 MPa [after Shkoukani (1993)].

In the literature it is reported that the strength and modulus of elasticity are affected by elevated temperature during the period of creep testing, and this will certainly affect the creep. At normal constant temperature the modulus of elasticity of sealed concrete increases slightly with age, while the E-modulus of drying concrete decreases due to the loss of load-bearing water, see section 3.4.3.

To get an overall picture of how the temperature influences creep deformations it has be to ensure that all the necessary considerations are carried out in any study carried out on temperature influence. The most important factors concerning influence of elevated temperature on creep development by time are:

- Temperature prior to loading
- Temperature during loading
- Temperature variation during loading

We have to distinguish between the temperature during the period of curing preceding the application of load and the temperature while the concrete is under load. Increase of temperature prior to loading for a long time will accelerate hydration process in concrete, and in consequence the concrete gain a higher degree of maturity. According to Neville (1983), for any elevated temperature, the creep is significantly less for concrete stored continuously at the higher temperature than when the temperature is raised a short time before loading. These statements are valid for both hardened concrete and for young concrete.

Already in the first tests carried on the influence of temperature on creep by Theuer (1937) it was determined that basic creep was enhanced by elevated temperature in a certain range of temperature, and then decreases. Depending on the curing conditions it may become greatest at a certain temperature. The majority of the experimental results show that basic creep

reaches its maximum in the region of 70 °C when the ratio of stress/strength remains constant and when the concrete is cured at the test temperature for a long period before the application of load.

When concrete undergoes creep deformations under varying temperature no thermal equilibrium is obtained. If the temperature changes during the period of sustained loading the creep rate will increase and influence the rate of aging of the concrete. Even more important is probably the fact that temperature change leads to redistribution of inherent moisture in the cement paste as well as structural change - both of clear importance for creep. Illston and Sanders (1973) describe the rapid increase in creep, due to a positive change of temperature, as transitional thermal creep which is approximately independent of maturity, and is zero when the temperature decreases or when the temperature is raised to the given level for a second time. This means also that drop of temperature does not give any creep recovery. That a positive change in temperature of mature concrete increases creep is also confirmed by Arthanari and Yu (1967). He also observed that increasing of the temperature by several steps gives a higher creep than a steady temperature after a certain period of loading.

3.2.6.4 Influence of water/cement ratio

According to Lorman (1940) creep is approximately proportional to the square of the water/cement ratio when other factors remain constant. Any change in water/cement ratio will affect the E-modulus and the strength of the concrete. For the same initial applied stress, a mix with a low water/cement ratio has a greater E-modulus and strength than a mix with a high water/cement ratio; both factors imply reduced creep.

3.2.6.5 Influence of cement and silica fume

The type of cement affects the strength development at early ages and thus influences creep deformation when loading takes place at early ages. Different types of cements have, in contact with water, different hydration rates, and as the result, at the same age, the cement paste gain different strengths.

It should be also mentioned that various cementitious materials like fly ash and silica fume have different rates of hydration and therefore of gain of strength while the concrete is under load. The mature HPC with silica fume exhibits smaller creep deformations than the concrete without silica fume. According to Igarashi *et al.* (2002), this lower creep potential in silica fumes concrete results from the higher strength and the dense microstructure at the time of loading. However, the effect of silica fume on creep at early age concrete might be different, and it will be discussed later in the present work.

3.2.6.6 Influence of ambient relative humidity

Generally, for a given unsealed concrete, creep is higher the lower relative humidity. This is mainly due to shrinkage occurring in specimen during the early stages after the application of the sustained load. Thus, the enhanced creep of concrete due to drying is due to the additional drying creep or called Pickett effect (Figure 3.6). Under drying conditions, creep develops at a higher rate in the initial period after loading than under more humid conditions. Reduced relative humidity leads to reduced creep for specimens in moisture equilibrium with the environment before loading (basic creep).

3.2.6.7 Influence of size of specimen

It is generally noticed that drying creep decreases with an increase in size of specimen. This is due to the fact that drying of course is much slower in large specimens and therefore that the core of specimen has conditions approximate to mass curing. In sealed concrete, no size effects are present. In the literature the size effect is normally expressed in terms of the volume/surface ratio of concrete member. The main point regarding this issue is that the structure size determines the drying rate, which determines the creep rate.

3.2.6.8 Influence of aggregate

As stated earlier, it is really the hydrated cement paste, which undergoes creep, and thus the primary role of aggregate in concrete is restraining of creep and shrinkage. The creep is, therefore, a function of the volumetric content of cement paste in concrete and thus volumetric content of aggregate. An increase in the aggregate contents decreases creep.

There are a certain physical properties of aggregate, which influence the creep of concrete. The modulus of elasticity of concrete is probably the most important factor. The higher the modulus the greater the restraint offered by the aggregate to the creep of the hydrated cement paste. According to Neville (1983), the higher creep of concretes made with lightweight aggregates reflects only the lower modulus of elasticity of the aggregate, but of course water in the lightweight will play a role also.

3.2.7 Relaxation

Although the term creep is often denote both the phenomenon of creep deformation and that of relaxation of stress, they are of course not the same, but different manifestations of the same fundamental viscoelastic properties. If a structural concrete member can freely deform under a permanent constant stress, its deformation increase due to *creep*. If free development of creep deformation is prevented, then the original stress is reduced over time, i.e. *relaxation* takes place.

The relaxation in concrete specimens subjected to equal initial strains at different ages of concrete is illustrated in Figure 3.12. It shows that the stress decreases at a higher rate in younger concrete analogous to the creep behaviour. The difference in relaxation of the initial stresses has relation to the increase of the modulus of elasticity with time. Comparing the stress relaxation magnitudes $\Delta\sigma_1$, $\Delta\sigma_2$ and $\Delta\sigma_3$ after a time increment Δt from the loading time t_i it is clear that the relaxation is very high at early ages and it reduces with time, just as creep reduces with age at loading.

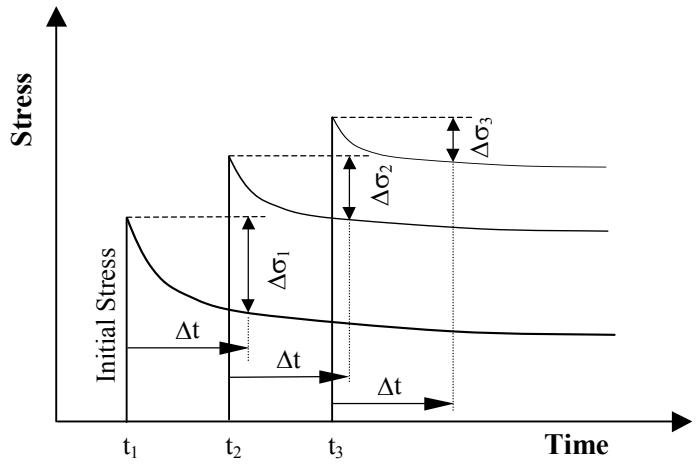

Figure 3.12 Effect of loading age on relaxation in concrete specimens subjected to equal initial strains.

The development of the relaxation process at different levels of the initial stress is plotted in Figure 3.13. It shows that the relaxation process develops more rapidly (compared to creep) at the beginning and approaches its final value asymptotically. It shows also that the relative increase of relaxation is higher than the relative increase of stresses above 11.8 MPa, i.e. nonlinearity of relaxation appears.

Due to the lack of data on stress relaxation at early ages, the findings concerning the development of creep are used in most of the theoretical studies of stress analysis for the modelling. Among the few researchers who have investigated this issue at early ages are Morimoto and Koyanagi (1994) and Rostásy *et al.* (1993). Their results are outlined in the next section. The linear viscoelastic theories allow calculation of relaxation based on creep data, see later.

Bažant and Wittman (1982) has summarized the effect creep and relaxation on concrete as follows:

- Reduction of self-induced stresses;
- Redistribution of stresses caused by imposed deformations;

- Redistribution of the stresses caused by external loads;
- Reduction of strength due to deformations;
- Increase of deformation of a concrete structure.

The effect of creep on time-dependent redistribution and reduction of the stress resultant are most pronounced:

- *where stresses develops due to imposed deformations*. Example could be a restrained early age concrete member exposed to volume change due to thermal dilation and shrinkage. This issue is discussed in detail in section 3.4.
- *in concrete members composed of materials with significantly different creep properties*; like in reinforced, prestressed, steel-concrete and concrete-concrete composite members.
- *in structures in which the creep properties vary throughout the thickness of the members*. Good examples are nuclear rectors and pressure vessels where differences in the thermal and hygral conditions may generate different creep properties within the thickness of a member.

According to Bažant and Wittman (1982), time-dependent deformations may affect the strength of the structural concrete member, in case where creep deformations results in an increase of the stress resultants. One example is slender concrete columns, where the creep deformations increase the 2. order effects.

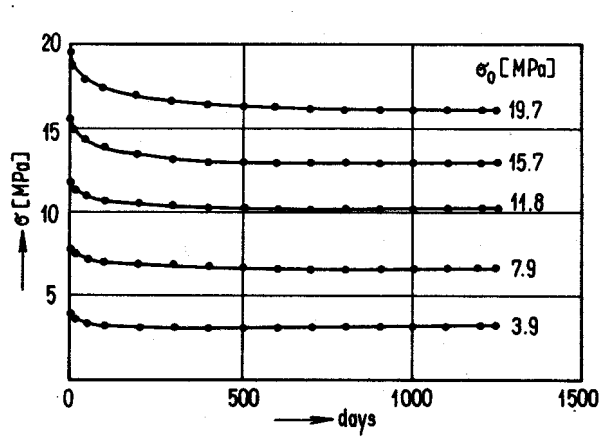

Figure 3.13 Effect of magnitude of the initial stress on the relaxation process, [Šerda and Křístek 1988].

3.3 Properties of Creep Deformation at Early ages

3.3.1 Creep deformation

Creep in practice is mainly a long-term effect, and much research conducted on the this phenomena in hardened concrete has been reported in the literature. Comprehensive summaries may be found in Bažant and Wittmann (1982), Neville *et al.* (1983), ACI committee 209 (1992) and Bažant *et al.* (1993). On the other hand, although the effect is also a very important phenomenon for early age concrete, the available data on creep of hardening concrete at early ages less than 7 days and particular at very early ages less than 2 days is limited. The reason why so little attention has been paid to creep behaviour at early age so far is probably the complexity of the material at early ages and the difficulty in performance of creep tests at this stage.

In the last two decades, the use of higher concrete qualities increased the interest for early age concrete. Several international conferences where behaviour of early age concrete was a major topic, were held, for instance in (1982, Paris), (1986, Illinois), (1987, Houston), 1992, Barcelona), (1994, Munich), (1995, London), (1999, Hiroshima), (2000, Paris), (2001, Haifa) and (2001, Boston). Most of the reports presented at these conferences have pointed out creep as an important, but uncertain property at early ages. Regarding modelling of the visco-elastic behaviour of concrete at early ages, several approaches have been suggested.

Westman (1995) reported results of compressive creep tests on young concretes with w/b-ratio of 0.3 and 0.4 with silica fume, at ages from 13 hrs to 7 days. His results indicated high creep at early age for both concretes, which rapidly developed into a stiffer response. De Shutter and Taerwe (1996) reported compressive creep data for a concrete mix with w/b-ratio of 0.5 at ages from 12 hrs to 14 days at stress/strength ratio of 20 and 40%. Their experimental results indicated a high nonlinearity of creep at early ages. This work was extended in De Shutter and Taerwe (1997) to develop a model describing early age creep as a function of degree of hydration. Their work demonstrated the close relation between basic creep at early age and the hydration process and the microstructural development.

In contrary to creep in compression, little attention has been paid to the viscoelastic behaviour of concrete in tension and thus the available experimental data on tensile creep in the literature are limited. The capacity of concrete to deform in tension, especially its creep potential could help to prevent shrinkage or/and thermal induced cracking, and thus improves the durability of concrete. The main problem regarding performance of tests on tensile creep is connected with the low degree of maturity of the young concrete. The applied load should be relatively small, and as a result the strain to be measured is small too. The theoretical problem, however, is that the recorded strains always are the sum of creep and autogenous deformation, and these deformations are in opposite directions. In tensile creep tests at high performance concretes the latter one is usually largest, a matter, which is a large challenge for the accuracy of the measurements. A short overview of the few studies found in the literature on viscoelastic behaviour of concrete in tension at early ages is given in the following:

Gutsch and Rostásy (1995) reported several test results on tensile creep of early age concrete. In the tests the *age at loading* varied between 1 and 7 days and *the initial stress/strength ratio* varied between 0.5 and 0.7. His results showed that the initial stress/strength ratio did not

exert a very significant influence on creep. In other words, in contrast to findings by many investigators, e.g. Hauggaard-Nielsen (1997a), non-linearity in tensile creep was observed in the tested range 60-80%. In Gutsch (1995, 2001), the viscoelastic behaviour of early age concrete in creep and relaxation tests, under isothermal and anisothermal conditions, in tension and compression was investigated. The results of the axial tensile creep tests, shown in Figure 3.14, confirmed that creep increases with the decrease of the equivalent age (t_e) at loading for different concrete mixes. They also confirmed that creep and relaxation of early age concrete were accelerated at temperature higher than 20 ^{o}C under loading. Furthermore the results showed that the creep in compression was in the same range as in tension. The results are shown in Figure 3.15, in which the shaded band represents the tensile creep functions of 25 tensile creep tests.

Umehara *et al.* (1994) compared the creep behaviour of concrete in both tension and compression. The *stress level*, *loading time* and *temperature* were selected as test parameters. The creep tests are divided in 4 series as shown in Table 3.2. The first series is intended to investigate the compressive stress a three different temperatures 20, 40 and 80 ^{o}C with compressive load of 1.0 MPa at the age of 1 day. Other 3 series intended to deal with the tensile creep. The specimens were first exposed to compression and then unloaded after different loading periods, followed by loading in tension to represent thermal stress development in massive concrete structures (i.e. compression and then tension stresses). The initial applied stresses 1.5 MPa and 0.2 MPa (given in the table) on concrete are 25% of the strength at that time of loading in compression and tension, respectively. The results made it clear that the higher the temperature rises, the higher the compressive creep as well as the tensile creep are, see Figure 3.16*a* and *d*. Furthermore, the results indicated that the higher compressive stresses was the higher tensile creep was, Figure 3.16b, and the longer the period of compressive loading was the lower the tensile creep was, Figure 3.16c.

By applying a viscoelastic rheological model, represented by combination of Maxwell model and Voigt model, to the results of the creep tests, two different creep models were developed; a 4-element model and a 5-element model for compressive and tensile creep, respectively. The effect of temperature was modelled by a separate temperature coefficient, multiplying the creep formula. The solid lines in Figure 3.16 represent the creep models.

Hauggaard-Nielsen (1997a) carried out an experimental study on the *non-linearities* of tensile creep at high stress level. Experiments of creep in tension were carried out at the effective stress/strength ratios 0.4, 0.6 and 0.8, at the age of loading 1 day, see Figure 3.17. The term effective stress/strength ratio means that the loads were adjusted (every 24 hours here) to the desired fraction of the tensile strength, compensating for the progress of hydration. The steps in the figure denote the stress adjustments. The result of the experiments indicated a linear response up to 60% of the stress level, while a non-linear creep appeared in the interval 0.6 to 0.8 times the tensile strength. This corresponds with results from the literature on compressive creep of hardened concrete.

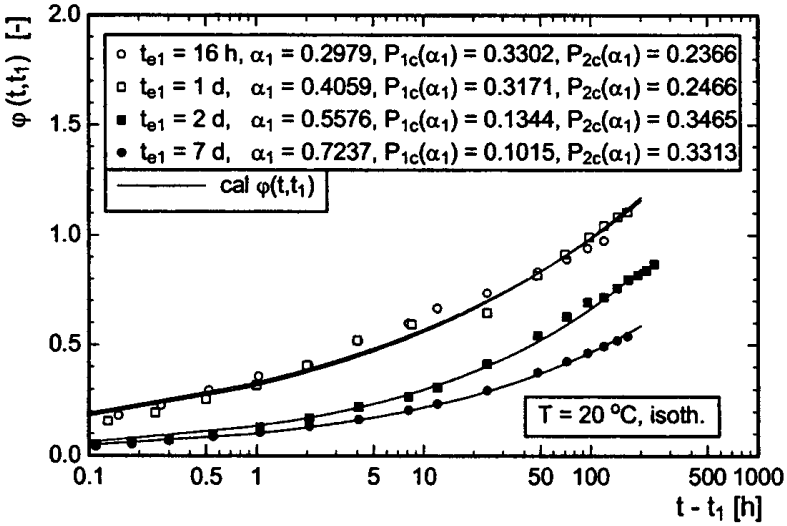

Figure 3.14 Creep function vs. time under load; test results and linear-viscoelastic model, T=20 oC [after Gutsch (2001)].

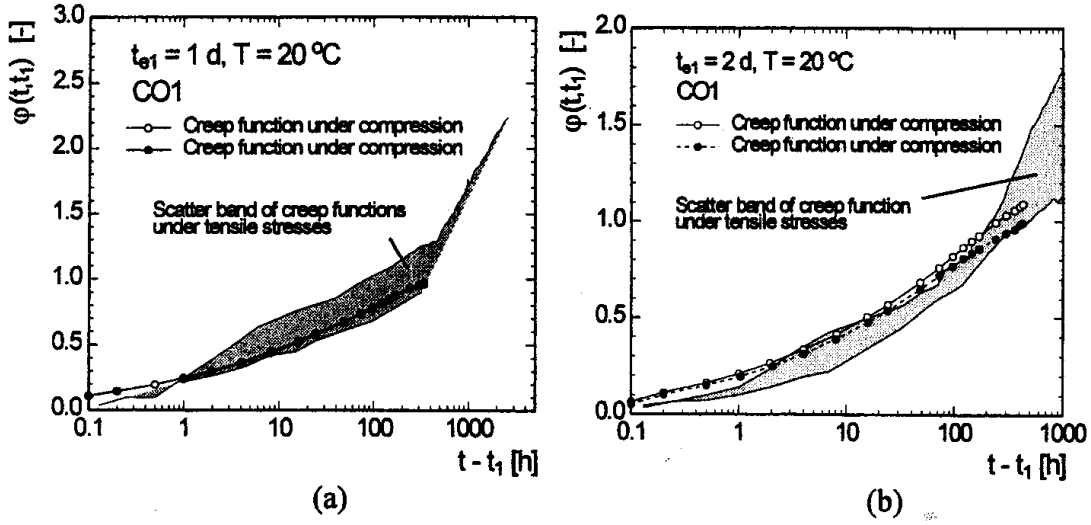

Figure 3.15 Scatter of Creep function under tensile stresses and creep function under compression vs. time under load; a) t_e = 1 d and b) t_e = s d, T=20 oC, [after Gutsch (2001)].

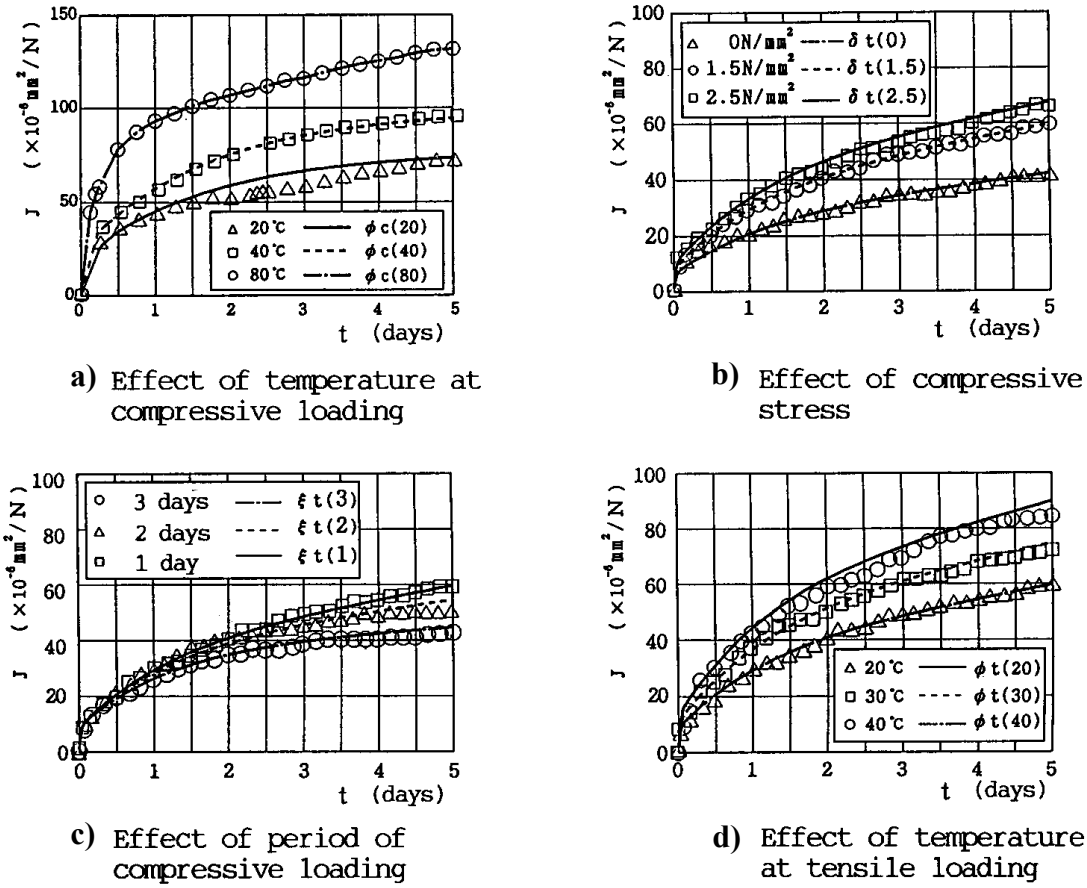

a) Effect of temperature at compressive loading

b) Effect of compressive stress

c) Effect of period of compressive loading

d) Effect of temperature at tensile loading

Figure 3.16 Result of creep tests on a concrete with w/c-ratio of 0.56, with initial compressive loading at age of 1 day, according to Table 3.2, [Umehara *et al.* (1994)];

a) Effect of temperature at compressive loading,
b) Effect of compressive stress on tensile creep,
c) Effect of time period of compressive loading on tensile creep,
d) Effect of temperature at tensile loading.

Table 3.2 Variables for creep tests in Figure 3.16.

Figure 3.20	Compression			Tension			Temperature (^{o}C)
	Stress (MPa)	A	B	Stress (MPa)	A	B	
a)	1.0	1	5	-	-	-	20, 40, 80
b)	0, 1.5, 2.5	1	1	0.2	3	5	20
c)	1.5	1	1, 2, 3	0.2	3, 4, 5	5	20
d)	1.5	1	1	0.2	3	5	20, 30, 40

A: Age of loading (day), B: Load period (day)

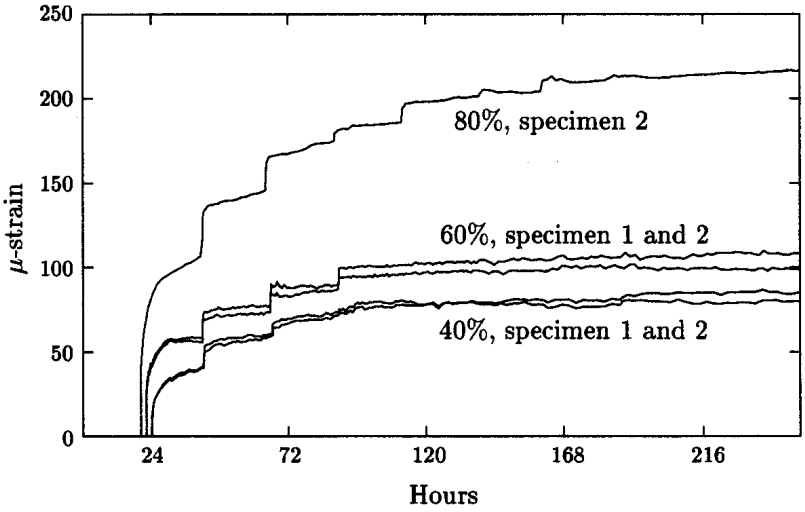

Figure 3.17 Measured creep in tension, compensated for shrinkage and thermal deformations, under different effective stress/strength ratios. Temperature range is 23.5 ~ 25.5 ^{o}C [after Haugaard-Nielsen (1997a)].

Bissonnette and Pigeon (1995) carried out a research program, to investigate the viscoelastic behaviour of repair concretes in tension. Since drying cracking is one of the major causes of the premature deterioration of thin bonded concrete repairs, both total creep tests and basic creep tests were carried out. Among the main variables, which were selected for the experimental program were the *w/c-ratio* (0.35 and 0.55) and the *age at loading* (1 and 7 d). The results of the tests can be summarized as follows: The tensile creep is a very significant phenomenon that play an important role in reducing the stresses due to restrained shrinkage in thin repair layers. The tensile creep increases significantly with the w/c-ratio, decreases with the age at loading and is little influenced by the use of silica fume. He suggested that the phenomena involved probably are similar in tensile creep and in compressive creep.

This investigation continued in Pigeon and Bissonnette (1999). In addition to the earlier parameters, the *stress level* was investigated. The results showed that: As in compression, creep in tension is significantly larger under drying condition. Thus, for tensile stresses, such behaviour is incompatible with the water migration or seepage theory, since shrinkage is acting in the opposite direction to the load. Moreover, it was found that, after a little more than a week, tensile creep under drying conditions and shrinkage are generally quite proportional to one another, Figure 3.18. This is interesting, because the value of specific creep/shrinkage ratio is a good significant indication of the relaxation capacity of the material under restrained shrinkage. From a repair perspective this could eventually be used as viscoelasticity index. Furthermore, as in compressive creep, it was observed proportionality between total creep and the level of stress applied up to 50% of the ultimate strength.

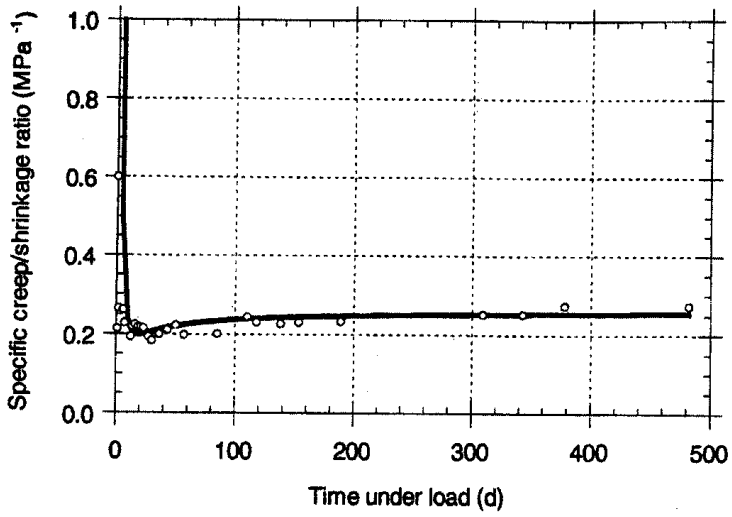

Figure 3.18 Typical evolution of the specific tensile creep to drying shrinkage ratio of concrete under drying conditions at 50% RH, w/c=0.55, water cured for 7 days before loading [after Pigeon and Bissonnette (1999)].

Kovler *et al.* (1999) reported the influence of silica fume on early age tensile creep of high strength concrete (max. aggregate size of 7 mm) with w/b-ratio of 0.33. The sealed specimen were loaded at the age of 1 day, and showed that the tensile creep of the silica fume concrete was larger than of the plain concrete with similar w/b-ratio.

Pan and Hansen (2002) obtained tensile creep compliance of different mixes performing tensile creep tests at loading ages 1, 3, 5 and 14 days. The duration of each age of loading was the same as the interval between the ages of loading. The results confirmed the fact that tensile creep increases when loading age reduces, and higher tensile creep in silica fume concrete than in silica-free concrete. He suggested an aging log power equation to predict the creep compliance.

Altoubat (2002) performed experimental and numerical analysis to characterize the early age tensile creep and shrinkage behaviour of normal and high performance concrete. Tensile creep of concrete at early ages was found to reduce shrinkage stresses in a restrained concrete by 50%. He developed a method to separated drying creep mechanism into stress-induced shrinkage and microcracking. He measured creep and shrinkage under moist, sealed and drying curing conditions. The concrete under moist curing condition gave basic creep; under sealed condition provided data on basic creep and stress-induced shrinkage, and under drying conditions provided data on basic creep, stress-induced shrinkage and microcracking. He concluded, among others, that stress-induced shrinkage is a major mechanism of drying creep.

Østergaard *et al.* (2001) studied the early-age basic tensile creep behaviour of concrete, and his experiment dealt with the influence of *concrete age at loading* (0.67, 1, 3 and 5 days), *initial stress/strength ratio* (20% and 45%) and *w/c ratio* (0.45, 0.30 and 0.19). The study showed that concrete exhibits high tensile creep strain when it is loaded at an age less than or

equal to 1 day. The strong aging of the material in the first few days results in a far stiffer response than the earlier ages. The experiments indicated that the rate of creep after a short initial time after loading is constant regardless of age at loading, given constant initial stress/strength ratio. His investigations furthermore indicated that the creep strain is not proportional to the stress when loading occurs at 1 day, Figure 3.19. Finally, the results confirmed the known dependency of magnitude of creep on w/c-ratio.

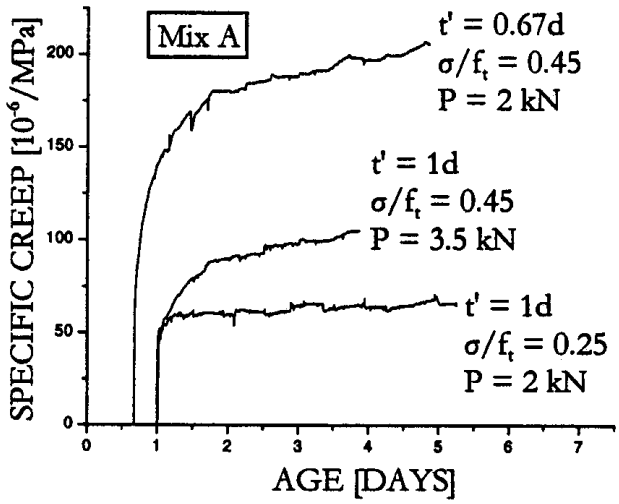

Figure 3.19 Result from tensile creep tests, w/c-ratio is 0.50, constant T = 23 ^{o}C and RH = 50% [after Østergaard (2001)].

Hagihara *et al.* (2002) conducted a comprehensive comparative study on early age compressive and tensile creep properties of HPC with different proportioning and curing conditions. The creep tests were conducted at *loading ages* 1, 3 and 7 days, with *stress/strength-ratio* 30, 40 and 75%, for concrete mixtures with *w/b-ratio* 22, 28 and 34%. The authors reported that both under sealed and dry conditions, the tensile specific creep strain was about 65-90% of the compressive specific creep strain regardless of the initial loading age. Moreover, they indicated that both under compressive and tensile loading, the specific creep strain was approximately 1.1-1.6 times greater under drying conditions than under sealed conditions.

The early age creep may be expressed in terms of specific creep curves, [Igarashi *et al.* (1999), Kovler *et al.* (1999) and Bissonnette and Pigeon (1995)], creep coefficient [Lura *et al.* (2000), Gutsch *et al.* (1998) and Gutsch *et al.* (2001)] and creep compliance [Pan and Hansen (2001)].

Concluding remarks:

Comparing the findings mentioned above, it is interesting to note that research results on tensile creep are not consistent, and thus they do not clarify the tensile creep at HPC at early ages. It is therefore evident that tensile creep, particularly at early age is a very complicated property, which need more research. The following concluding remarks can be made:

- *Viscoelasticity:*
  The entire data on tensile creep tests presented over showed a high viscoelasticity when the load was applied at early age, particularly at the ages less than 3 days.

- *Loading age:*
  The tensile creep-coefficient is shown to be very sensitive to the age of loading, increasing with decrease of age. The tensile creep strains are particularly high when it is loaded at an age less than or equal to 1 day.

- *Rate of creep:*
  Rate of specific creep after a short initial time after loading is approximately constant regardless of age at loading, given constant initial stress/strength ratio.

- *w/b-ratio:*
  The tensile creep increases significantly with the w/c-ratio.

- *Temperature:*
  Tensile creep accelerates under temperature higher than 20 ^{o}C during the time under loading and thus the higher the temperature rise the higher the tensile creep and is.

- *Non-linearity:*
  The proportionality between the tensile creep strain and the stress holds is valid up to 50-60% of the concrete strength. This corresponds with results from the literature on compressive creep of concrete. In contrast to this, Gutsh and Rostásy (1995) showed that the initial stress/strength-ratio do not have a large influence on the tensile specific creep at early ages up to 70%. According to Emborg (1998) the phenomena with non-linear behaviour of creep recovery at high tensile stresses are present in concrete subjected to early age thermal loading and should be considered in an accurate thermal stress analysis.

- *Silica fume:*
  The specific tensile creep of silica fume concrete was found to be lager than for the concrete without silica fume. This behaviour seems to be typical for loading at early ages [Igarashi *et al.* (1999), Kovler *et al.* (1999) and Igarashi *et al.* (2002)], but it is different from the trend reported in the literature for mature silica fume systems. Other found that that the tensile creep at early ages is little influenced by the use of silica fume.

It is of interest to compare compressive creep to tensile creep. The discussion above shows that investigators have observed both similarities and differences in viscoelastic behaviour of early age concrete under tensile and compressive stresses. The creep data, to

a large extent, indicates similarities in the trend of the creep under both stress conditions, but proportionality, rate and magnitude of creep in tension and compression are still questionable.

Umehara and his co-author suggested two different creep models to the two cases, and the results by Hagihara *et al.* found that the ratio of tensile creep to the compressive creep was about 65-90% in dry and sealed conditions. Contrary to these results, several researchers reported that the mature concrete creep under uniaxial tension at different ages has been found to be higher than under uniaxial compression [Illston (1965), Brooks & Neville (1977) and Brooks *et al.* (1991)]. This issue is one of the main subjects investigated in the present work.

3.3.2 Relaxation

The process how the self-induced stresses build up (including relaxation) at early age concretes and what parameters should be considered in any stress calculation were discussed in Chapter 2. Some of the available data on tensile relaxation is presented and discussed in this section. Considerable creep and its associated relaxation occur and play a significant role in reducing self-induced stresses in any restrained early age concrete member [Springenschmid *et al.* (1994), De Schutter (1996), Kanstad *et al.* (2000), Atrushi *et al.* (2001) and Igarashi *et al.* (1999)]. Altoubat and Lange (2001) reported stress relaxation in hardening concrete to be about 50%.

As mentioned earlier, due to the lack of experimental data on stress relaxation at early ages, most of the theoretical studies on self-induced stresses use creep properties for modeling. However, stress relaxation (and not creep) is involved directly in reduction of self-induced stresses in hardening concrete. Thus, it should be more appropriate to employ relaxation function directly which has been obtained from relaxation tests. Among the few experimental studies on this issue one can mention Morimoto and Koyanagi (1994) and Rostásy *et al.* (1993), where the latter work continued in Gutsch and Rostásy (1995).

Gutsch and Rostásy (1995) and Gutsch (2001) reported several test results on relaxation of early age concrete. The results of the axial tension relaxation tests, shown in Figure 3.20, revealed that relaxation increases with the decrease of the equivalent age (t_e) at loading time, respectively the degree of hydration (α_1) for different concrete mixes. Furthermore, his results showed that the initial stress/strength ratio up to 0.9 did not exert a very significant influence on relaxation. The results also confirmed that creep and relaxation of early age concrete were accelerated at temperature higher than 20 ^{o}C under loading. Furthermore, he showed that linear viscoelasticity could be assumed for modelling creep and relaxation.

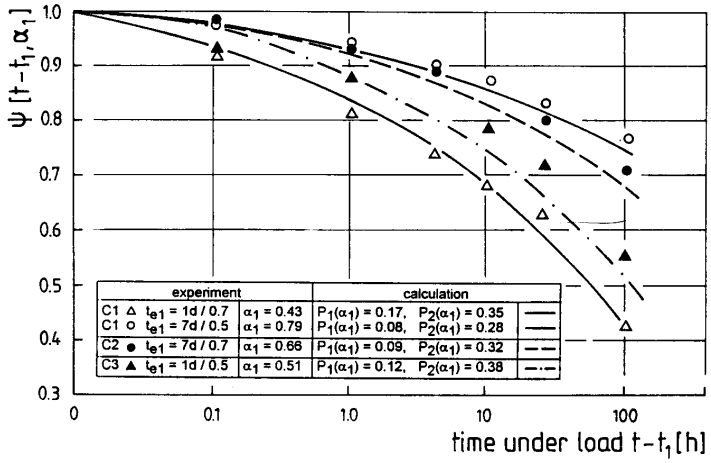

Figure 3.20 Relaxation function vs. time under load; tensile test results and linear-viscoelastic model, age at loading varied between 1 and 7 days and the initial stress/strength ratio varied between 0.5 and 0.7, T=20 oC [after Gutsch and Rustásy (1995)].

Morimoto and Koyanagi (1994) reported results of a comparative study on stress relaxation in both compression and tension. Concrete specimen where loaded at 1, 3, 7 and 14 days at 20, 40 and 60 ^{o}C. The specimens were cured until testing at their respective testing temperature. The results indicated that the tensile- and compressive relaxation are proportional to the initial stress up to 80%, and they depend on the loading age. Furthermore the test results demonstrated that tensile relaxation is much smaller and terminates in a shorter period than compressive relaxation, see Figure 3.21. Finally, the effects of testing temperature on relaxation were found to be marginal in the range under 60 ^{o}C – in contrast to the findings by Gutsch (1995) and the results of tensile creep tests sated earlier.

The author believe that, at least two of the above mentioned findings (by Morimoto and his co-authors) on the tensile relaxation are strongly doubtful; the low tensile relaxation and the marginal effect of temperature on tensile relaxation. The author means that both the initial rate and the magnitude of the tensile relaxation should be higher, and the influence of temperature on tensile relaxation should be much higher.

To illustrate the importance of creep/relaxation properties of a concrete mix, analyses of test results on self-induced stresses is useful. In Bosnjak (2001) a sensitivity analysis regarding the importance of creep at different ages of a structure was performed. She divided the hardening period into two parts where the point, which separates these periods, was the time where the stress increments change sign. The creep coefficient in the different periods of hardening was varied, and the calculated stresses compared. The conclusion from the study was that creep in the early period has negative effect on the cracking risk in externally restrained structure: compressive creep reduces compressive stresses, but increase the subsequent tensile stresses, thus increasing cracking risk. Underestimation of creep in this early period will lead to underestimation of the cracking risk. The opposite is true for internally restrained structures. Westman (1999) studied the influence of viscoelastic

behaviour on development of self-induced stresses by dividing the creep into short-term creep and long-term creep. He treated both surface cracking and through cracking, and his results demonstrated, as expected, that the stresses could not be accurately evaluated without a correct consideration of viscoelastic behaviour. He concluded that the short-term creep (the creep response during the three first days after load application) is the most important part of the creep spectra. Furthermore, his results showed that the short-term creep affects strongly both the development of compressive stresses in restraint situation and the development of tensile stresses in a structure with no external restraint. The long-term creep (load duration>3 days) had almost no influence at all on the studied typical cases for early age cracking.

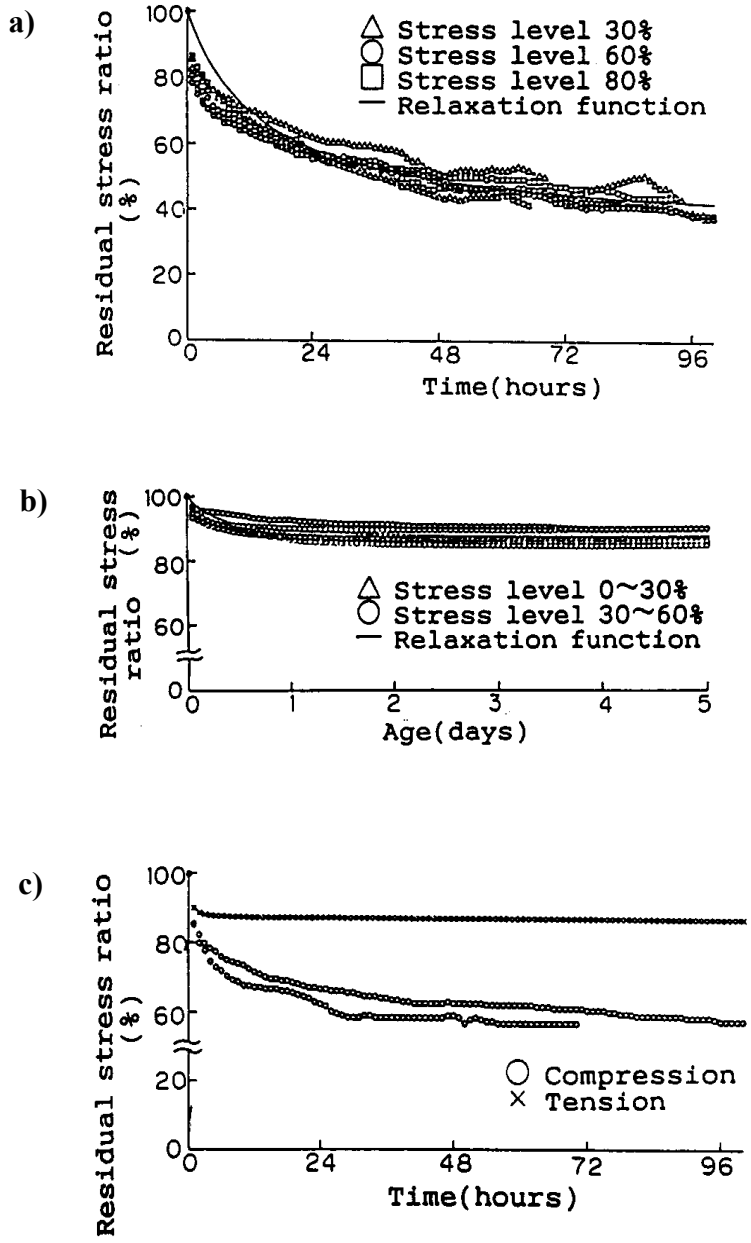

Figure 3.21 Test results on relaxation: a) Compressive relaxation curves, b) Tensile relaxation curves, c) Comparison of compressive and tensile relaxation [after Morimoto and Koyangi (1994].

3.4 Calculation Methods and Material Models for Prediction of Creep/Relaxation

From the engineering standpoint, the main interest in knowledge about creep of concrete lies in the development and the use of models, which take account for creep in design calculations. Development of material models is necessary to avoid expensive tests in the laboratory. Only knowledge of composition of mix, mechanical properties of concrete and the operating conditions are then required if appropriate models are available. To obtain a full benefit from the large number finite element programs now in existence for early ages, realistic material models must be provided as the input. The accuracy of stress analysis depends mainly on how the thermal properties, shrinkage, viscoelastic behaviour, restrained conditions and the mechanical properties are described for early ages.

A state-of-the-Art on the existing models and methods for computation of thermal stresses in early age concrete is given in Emborg (1998).

3.4.1 Calculation methods

Calculation of strain from stress and of stress from strain, and the solution of the particular case of relaxation of stress can be accomplished by various methods, such as: Effective modulus method (EM), Rate of Creep method (RC), Rate of flow method (RF), Improved Dischinger method (ID), Method of superposition, Trost-Bažant method (TB) and Rheological models (RM). The latter method may be considered as a method as well as it may represent a material model.

Most of these methods are either simplifications or modifications of the principle of linear superposition. Many of them are suitable for computing directly under varying stress or vice versa. Detailed review of these methods is given in e.g. Dilger (1982) and Neville *et al.* (1983).

3.4.1.1 Rheological models (RM method)

The subject of time dependent relations between stress and strains is called rheology. A number of rheological models have been developed to simulate the time-deformation relationship of concrete. They consist of elements, each of which represents a specific deformational characteristic. The idealized deformations, which are used to build up real behaviour of concrete, are elastic, viscous or plastic, and are represented by basic mechanical devices like a spring, a dashpot and a friction element, respectively. By use of different combination of these rheological models many equations of differential types may be expressed.

The main basic models are known as the Kelvin-Voigt model and the Maxwell model, see Figure 3.23a-b. The Kelvin-Voigt model consists of a spring and a dashpot in parallel, and it represents the phenomenon of delayed elasticity. The Maxwell model consists of the same elements as in the Kelvin-Voigt model, but they are in series. Rheological models based on Kelvin-Voigt elements have been used in the computation of thermal stresses by for instance

Haugaard-Nielsen *et al.* (1997c) and Dahlblom (1992). The Kelvin model and the Maxwell-Voigt model together can be used to build up more complex models. The most basic built-up model is the Burgers model, shown in Figure 3.23c, which is a series combination of a Kelvin-Voigt model and a Maxwell model.

The behaviour of a Burgers model is qualitatively similar to that of concrete. The deformational response of the model is a sum of responses of its Kelvin and Maxwell components; i.e. it contains elastic, delayed elastic and viscous parts.

The Burgers model, in which the coefficients of elements may *change over time* to quantitatively describe early age creep, was utilized by several investigators; Haugaard-Nielsen *et al.* (1997c), Bosnjak (2001) and Hagihara *et al.* (2002). The model is outlined in Figure 3.22. The spring elements of the Maxwell model represent reversible momentary elastic deformation $\varepsilon_e(t)$, whereas the dashpot element represents non-reversal permanent deformation $\varepsilon_d(t)$. Also, the Kelvin model represents reversible delayed elastic deformation $\varepsilon_V(t)$. Suffixes M and V denotes Maxwell and Kelvin-Voigt model, respectively. The expressions for the element strains are given in the reference.

Rheological models can in principle achieve any desired accuracy in fitting experimental curves by adding more of the basic elements in a chain. The chain models are usually utilized in finite element programs for stress analysis; Roelfstra *et al.* (1994), Bernander & Emborg (1994) and Emborg & Bernander (1994) used an aging Maxwell Chain model in a FEM-program, while Dahlblom (1992) used a differential model with a numerical procedure similar to the one of the Kelvin Chain model for the same purpose in a 2D FEM-program.

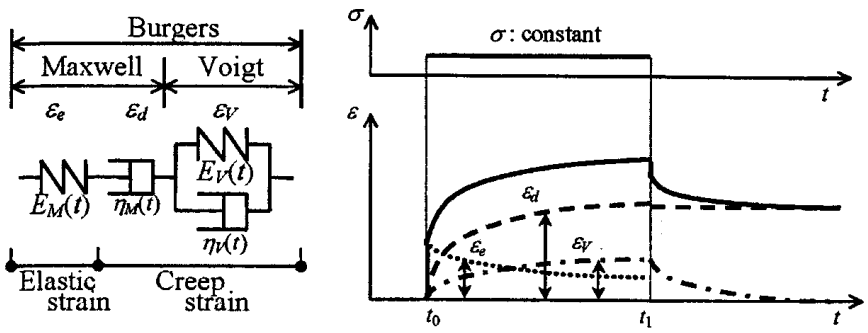

Figure 3.22 Outline of the rheological analysis method and the model for one-dimensional case [after Hagihara *et al.* (2002)].

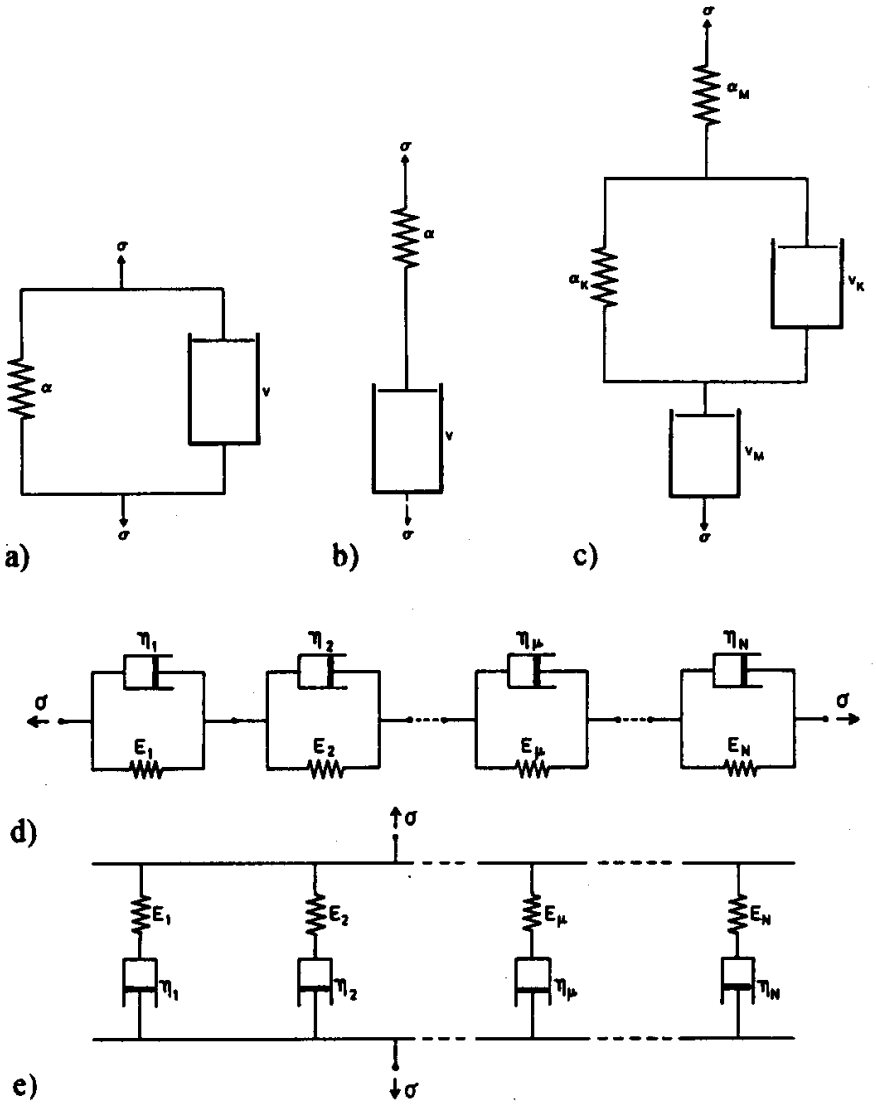

Figure 3.23 Rheological models: a) Kelvin-Voigt model, b) Maxwell model, c) Burger model, d) Kelvin Chain Model and Maxwell Chain Model [after Emborg (1998)].

3.4.1.2 Rate of flow method (RF method)

The basis of this method is a subdivision of the creep function into three parts: the elastic strain ($1/E(t')$), the recoverable delayed elastic strain ($\phi_d(t-t')/E(t')$) and the irrecoverable flow ($(\phi_f(t)- \phi_f(t'))/ E(t')$), shown in Figure 3.24. The delayed elastic strain is independent of the age of loading and reaches a final value much faster than the flow. The flow represents the irrecoverable component of creep. The compliance function may be written as:

$$J(t,t') = \frac{1}{E(t')}\left[1 + \phi_{el,d}(t,t') + \phi_{nel,d}(t) - \phi_{nel,d}(t')\right] \qquad (3.3)$$

England and Illston (1965), who proposed the method, used a step-by-step numerical procedure for the solution of practical creep problems. A similar formulation has been adopted in the present wok for self-induced stresses.

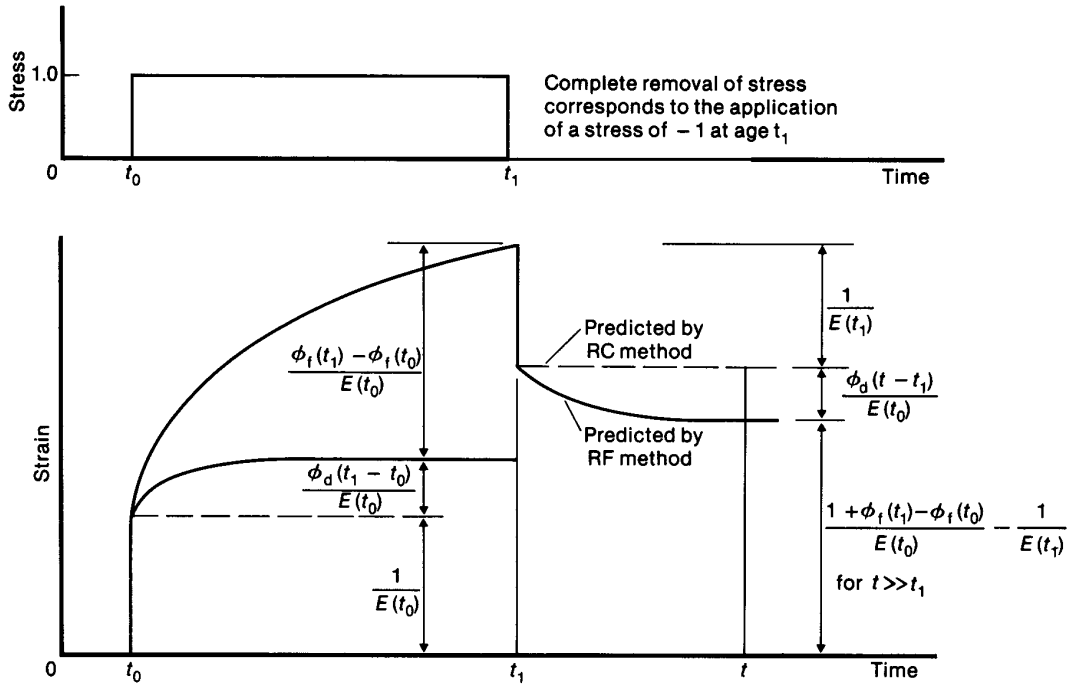

Figure 3.24 Strains due to unit stress acting between t_0 and t_1 according to the Rate of Flow method (RF) [after Dilger (1982)].

3.4.2 Models to predict modulus of elasticity

Hardened concrete:

The modulus of elasticity is more completely discussed in Chapter 2 and in the beginning of this chapter where the general development and its effect on deformability of the material are considered. In the literature a number of empirical relations have been proposed to estimate the modulus of elasticity. A survey over some of models is given for instance in Emborg (1998) and Kanstad (1990). In most relations, the E-modulus is expressed as a function of the compressive strength, and some typical examples for mature concrete are:

$$E_c = 4730\,(f_c')^{1/2} \qquad \textit{(ACI-1991)} \qquad (3.\,4)$$

$$E_c = 10000\,(f_{cm})^{1/3} \qquad \textit{(CEB-1990)} \qquad (3.\,5)$$

$$E_c = 9500\,(f_{cck})^{0.3} \qquad \textit{(Norwegian Code NS3473)} \qquad (3.\,6)$$

where:

E_c: Modulus of elasticity of concrete (MPa)
f_c': Cylinder compressive strength (MPa)
f_{cm}: Mean compressive strength (MPa)
f_{cck}: Characteristic compressive strength (MPa)

Models for young concrete:

Various expressions can be found in the literature which can be used to describe the development of the modulus of elasticity with time for early age concrete. Information on E-modulus of concrete at early age, many of them related to compressive strength for a given mix, has been presented by: e.g. Kanstad *et al.* (1999), Emborg (1998), Umehara *et al.* (1994), Laube (1990), Byfors (1980). Evaluation of the E-modulus formula has shown a large scatter between the expressions, [Emborg (1998)].

The modulus of elasticity of concrete is controlled by the modulus of elasticity of its components, i.e. the hydrated cement paste and the aggregates. The prediction of the modulus of elasticity can be considerably improved if the influence of a particular type of aggregate is taken into account, and thus CEB-FIB 1990 Model Code has introduced an empirical coefficient in the expressions for E_c. For ages at loading different than 28 d, CEB-FIB uses the following expression:

$$E_c(t) = E_{c28} \cdot \left\{ \exp\left[s\left(1 - \sqrt{\frac{28}{t/t_1}} \right) \right] \right\}^{0.5} \qquad (3.\,7)$$

where:

E_c(t): tangent modulus of elasticity at concrete age t (days)
E_{c28} : tangent modulus of elasticity at a concrete age of 28 days
s : coefficient dependent on the cement type
t : concrete age (days)
t_1 : 1 day

Kanstad *et al.* (1999) has modified the model in Eq. (3. 7) by introducing a parameter t_0 at which the strength and stiffness is defined to be zero. The parameter is also used in strength development:

$$E_c(t_e) = E_{c28} \cdot \left\{ \exp\left[s\left(1 - \sqrt{\frac{28}{t_e - t_0}} \right) \right] \right\}^{n_E} \tag{3. 8}$$

E_{c28} is the 28 days value of the modulus of elasticity. The model parameters s and t_0 may be determined from compressive tests, while the model parameter n_E should be determined from modulus of elasticity tests. This expression is used in the present study.

A model, in which the E-modulus is a function of the compressive strength, the model developed by Byfors (1980) can be mentioned. It consists of two expressions representing the modulus of elasticity for low and high strength concretes, respectively:

$$E_{cc} = 9.93 \cdot 10^3 \cdot f_{cc}^{2.675} \qquad \text{low strength concrete} \tag{3. 9}$$

$$E_{cc} = \frac{9.93 \cdot 10^3 \cdot f_{cc}^{2.675}}{1 + 1.370 \cdot f_{cc}^{2.204}} \qquad \text{high strength concrete} \tag{3. 10}$$

In which f_{cc} is the compressive cylinder strength and E_{cc} is the compressive nodulus of elasticity of concrete.

3.4.3 Models to predict creep deformations

A great number of creep functions for concrete are proposed in the literature, and most of them, in terms of the constitutive modelling, belong to the two main types of creep formulations. In the first one, the creep function is formulated as a *product* of the age at loading and the load duration functions. The general form of the resulting creep function is then:

$$\varphi(t,t') = \frac{1}{E(t')}\left[1 + \varphi_0 f_1(t') g_1(t-t')\right] \tag{3. 11}$$

where $E(t')$ is the modulus of elasticity at loading age t', φ_0 is a constant creep parameter, $f(t')$ is a function which express the effect of loading age (aging effect) and $g(t-t')$ represents the development of creep with time under load. The aging is taken into consideration via $E(t')$ and $f_1(t')$. This type of creep formulation is adapted in the BP-model [Bažant and Panula (1978)], British Concrete Society [Neville *et al.* (1983)], CEB-FIB Model Code1990 [CEB-FIP (1993)], European concrete standard EC2 [Eurocode 2 (1991)] and ACI [ACI 209 (1992)].

The other type of formulation is based on the *sum* of two (or more) components, namely a recoverable (delayed elastic) component and an irrecoverable flow component:

$$\varphi(t,t') = \frac{1}{E(t')} + \varphi_1 f_2(t-t') + \varphi_2\left[g_2(t) - g_2(t')\right] \tag{3. 12}$$

where φ_1 and φ_2 are constants, $f_2(t-t')$ describes the development of the delayed elastic creep component, and g_2 describes the development of flow with time. This type of creep formulation was f.i. used in the CEB-FIB Model Code 1978 [CEB-FIB (1984)].

The particular characteristics of both approaches and their advantages and disadvantages are discussed in Hilsdorf and Müller (1987) and Han (1996). I addition to these two formulations there are also other types of creep functions which have been used for modelling of hardened concrete, see e.g. Neville *et al.* (1983).

There are a number of creep models listed and described in e.g. Neville (1980), Bažant and Osman (1975), Bažant and Wittman (1982), Kanstad (1990), Emborg (1998) and Westman (1999). Some of these creep models are tested, modified and suggested in e.g. ACI (1987), Bažant and Panula (1978), Bažant and Chern (1985), Emborg (1989), Westman (1994, 1995), Laube (1990), Gutsch (1998), CEB-FIP Model Code 1990 (1993), Le Roy (1996), Persson (1997) and Byfors (1980). The review on these creep models in these references illustrates the variety of ideas that exists on how to model creep in concrete.

Double Power Law (DPL):

Several practical models for predicting creep and shrinkage properties for a particular concrete and environmental conditions have been developed. They differ in their degree of accuracy and simplicity, and usually one of these must be traded for the other. An analyst can among others choose from one of the following comprehensive models:

- Model of ACI Committee 209 (1992)
- Model of CEB-FIB Model Code 90 (1993)
- Bažant-Panula's Model, BP-model (1978)
- B3-Model, either its complete version or its simplified version, [Bažant and Baweja (1995)].

A simplified version of the Bažant-Panula model denoted the Double Power Law [Bažant and Panula (1978)] is used to calculate the stress development in the present work, and thus a brief review on the model will be given here. The BP-model follows the principle of linear superposition, and it does not distinguish between the usual short-time deformations and creep as for instance the CEB and the ACI models do. The basic creep of concrete expressed by the creep function (or the so-called compliance function), which gives the strain per unit stress, proposed by Bažant and Panula (1978) is:

$$J(t,t') = \frac{1}{E_0} + \frac{\varphi_0}{E_0}(\alpha' + t'^{-d})(t-t')^p \qquad (3.\ 13)$$

where:

t:	Concrete age
t':	Concrete age at loading
$J(t,t')$:	Compliance function
E_0:	Asymptotic modulus of elasticity
α':	Model parameter for long-term creep
φ_o, d and p:	Creep model parameters

This expression, which perhaps is the most known compliance function, is denoted Double Power Law (DPL) since both the aging function and the time function are power functions. E_0 is a material parameter, called asymptotic modulus of elasticity, which is considerably larger than the usual modulus of elasticity. The parameters φ_0, d and p are creep model parameters characterizing the basic creep at reference temperature (23 ^{o}C). These coefficients can be relatively simply determined from test data by optimization techniques. Times t' and t are expressed in days.

Regarding the contribution of the term $(t')^{-d}$ in estimation of the basic creep in DPL one should note the following: Since the time unit in the expression of DPL is in *days*, the parameter d has no effect on calculations of creep when the loading age is 1 day. For other

loading ages; the creep is a power function of $(t')^{-d}$ - increasing with d for loading ages lower than 1 day while it is decreasing with d for the loading ages higher than 1 day. The term is illustrated in Figure 3.25-a by choosing two values of d: 0.2 and 0.6. As can be seen, the effect is largest for loading at very early ages lower than 1 day, and the aging effect is approximately linear after 5 days.

Figure 3.25-b illustrates the effect of parameter p in the term $(t-t')^p$. The influence of the parameter p and the term for loading duration higher than 1 day is apparent in the figure. The effect is opposite for loading duration lower than 1 day. The curves in both figures show the trend of the increase of the parameters d and p on development of creep.

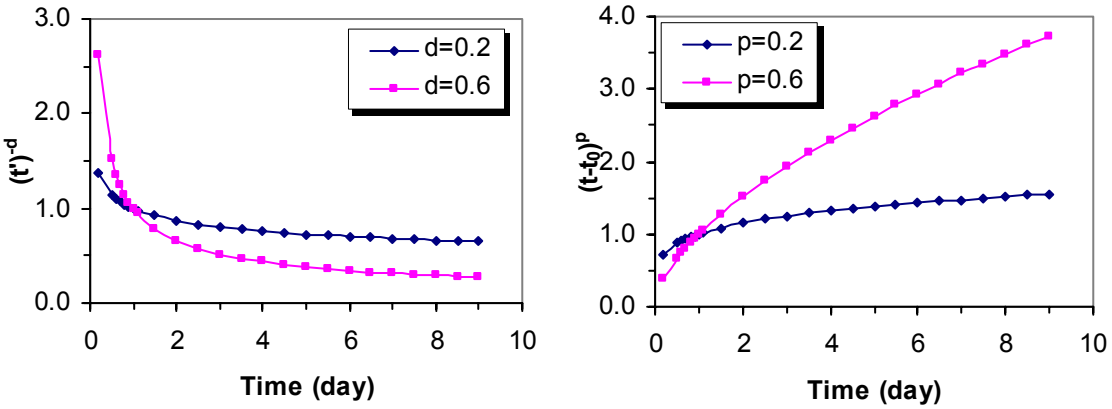

a) b)

Figure 3.25 Contribution of the terms in estimation of creep by DPL: a) effect of loading age, i.e. aging effect, b) effect of load duration.

The DPL describes creep of concrete $\varepsilon_{cr}(t)$ as a product of a function dealing with the effect of age (t') at the application of the load and a function dealing with the development of creep with the load duration $(t-t')$.

Eq. (3. 13) is best suited for long-term creep. The modified version, which is simpler and more convenient to use for young concrete, and which is further developed in this work, is:

$$J(t,t') = \frac{1}{E_c(t')}\left[1 + \varphi_o \cdot (t')^{-d}(t'-t')^p\right] \qquad (3.\ 14)$$

where:

$E_c(t')$: Modulus of elasticity at loading time, given in Eq. (3. 8)

Many investigators have previously used this expression, among them: De Borst (1994), Kanstad (1994), Bernander and Emborg (1994), Bosnjak and Kanstad (1997), Atrushi *et al.* (2001) and Bosnjak (2000).

The originally proposed DPL, expressed in Eq. (3. 13), has been criticized to overestimate creep strains after long duration. An improvement of this was achieved by replacing the DPL for basic creep by new versions of the creep laws such as the Triple Power Law or the log-double power law, aiming to take account for some other aspects of the concrete. These models are not considered in the present investigation, but the Triple Power Law is briefly presented in the following because this model is adapted to young concrete by researchers at the Technical University in Luleå.

- ***Triple Power Law (TPL):***

$$J(t,t') = \frac{1}{E_0} + \frac{\varphi_0}{E_0}(t'^{-d} + \alpha)\left[(t-t')^p - B(t,t';p)\right] \tag{3. 15}$$

Where φ_0 is a constant and α denotes infinity of the creep. The other model parameters are the same as before. In general, the model improves prediction of long-time creep. The binomial function B(t,t';p) is included to reduce the long-term creep rate, and is given by:

$$B(t,t';p) = p\int_{\xi=0}^{t-t'}\left[1-(\frac{t'}{t'-\xi})^p\right]\xi^{p-1}d\xi \tag{3. 16}$$

In which ξ=t-t'. The creep law exhibits a gradual transition from a Double Power Law for short creep duration to a logarithmic creep law for very long creep duration (Bažant and Chern 1985). According to the authors, compared to the previous DPL-Log, the present formulation has an advantage of continuity in curvature and a greater range of applicability involving also very short creep duration, including the dynamic range.

Because the TPL in general is not valid for creep at early ages (less than 2 days), Emborg (1989) included the additional functions G(t') and H(t,t') of exponential type:

$$J(t,t') = \frac{1}{E_0} + \frac{\varphi_0}{E_0}(t'^{-d} + \alpha)\left[(t-t')^p - B(t,t';p)\right] + \frac{G(t')}{E_0} + \frac{H(t,t')}{E_0} \tag{3. 17}$$

G(t') models the strong age-dependence of the instantaneous deformation (load duration 1.4 min.) and H(t,t') models the increase of early age creep when the load has been applied. The introduction of these additional functions gave better agreement with creep tests on young normal strength concretes.

Westman (1999) has further refined Eq. (3. 17) to consider creep at very early ages of high performance concrete by conversion of functions G(t') and H(t, t') into $\psi_1(t')$ and $\psi_2(t, t')$. For the details about the new terms and the model parameters in Eq. (3. 17), see the references.

3.4.4 Temperature effects

Excluding the effect of temperature on maturity and degree of hydration, respectively, there is a general trend that with increasing temperature at the time of loading both strength and the modulus of elasticity of concrete decrease. The decrease may be explained by chemical modification of bond between cement paste and aggregates.

Generally, maturity concepts are applied to quantify the concrete properties' dependence on the temperature history, i.e. the concrete age may be adjusted in order to take temperature history effects into account. For this purpose different models for the equivalent concrete age have been proposed in the literature. The concept of the Arrhenius function has given reasonable agreement with test results in several investigations, e.g. Pedersen (1997) and Byfors (1980). Kanstad (1999) applied the Eq. (3. 18) in the Norwegian investigation of mechanical properties, where the maturity (M) or the equivalent time (t_e) is expressed as:

$$t_e = M = \sum_t \exp(E_r(\frac{1}{293} - \frac{1}{273 + T_i})) \times \Delta t_i \qquad (3.\ 18)$$

Where:

$E_r = A_r$ for T > 20

$E_r = A_r + B_r \times (20 - T)$ for T < 20

In which E_r (the activation energy divided by the gas constant R=8.314, unit ^oK) is the temperature sensitivity parameter. The constants A_r and B_r were determined from the isothermal test results and the results from realistic temperature histories. Parameter Δt is the time increment and given in days.

As stated earlier, the temperature has a major influence on creep. Any temperature change will affect both *creep rate* (direct effect) and *rate of aging* (indirect effect) which again affect the creep magnitude. The temperature effect on aging of concrete in the creep model is usually taken into account by introducing the maturity concept, e.g. Eq. (3. 18), i.e by replacing concrete age t with equivalent concrete age t_e, [e.g. Kanstad (1990), Bosnjak (2000), CEB-FIP MC 90 (1992), Gutsch (2002)]. Consequently, all the parameters, which are functions of concrete age at loading, become functions of equivalent age.

3.4.4.1 Creep at constant temperature

For isothermal and sealed conditions, while the concrete is subjected to a constant sustained stress, an increase in temperature accelerates basic creep. The effect of constant temperature on rate of creep is usually modeled by introducing various empirical factors in the creep formulas. In CEB-FIP MC 90 (1993), the effect of temperature is taken into account using temperature dependent coefficients $\beta_{H,T}$ and $\varphi_{RH,T}$. Bažant and Panula (1978, 1979) generalized the Eq. (3. 14) to describe creep curves at various constant temperatures by replacing the model parameters φ_o and n by new parameters φ_θ and n_θ respectively, which are functions of curing temperatures.

Umehara *et al.* (1994) proposed expressions for a temperature dependent coefficient, which should be different for tensile and compressive creep at early ages. The coefficients are linear functions of the temperature and should be multiplied to the compliance function:

$$\begin{aligned} &\varphi_t(T) = 0.0257T + 0.487, \quad = 1.0 \text{ for } T = 20\ ^oC \qquad \text{(Tensile creep)} \\ &\varphi_c(T) = 0.0112T + 0.552, \quad = 0.776 \text{ for } T = 20\ ^oC \qquad \text{(Compressive creep)} \end{aligned} \tag{3. 19}$$

Where T: Temperature (^oC)
$\varphi_t(T)$: temperature dependent coefficient in tension
$\varphi_c(T)$: temperature dependent coefficient in compression

3.4.4.2 Creep at variable temperature

For changing temperature conditions while the concrete is under load (and still sealed), an additional creep component, the so-called transient thermal creep, which develops at the time of a temperature increase should be considered. A comprehensive historical review, of the phenomenon transient creep, is given by Khoury (1985). According to Thelanderson (1987), who investigated concrete at elevated temperatures, the term "creep" is confusing, since transient creep is a quasi-instantaneous response to temperature change, similar to that of free thermal strain. He interpreted it as an interdependence between temperature response and mechanical response, and suggested that the thermal strain rate should be made dependent on the current stress state:

$$\Delta\varepsilon_T = CTE \cdot \Delta T \cdot \left[1 + \rho \cdot \frac{\sigma_c}{f_c'}\right] \tag{3. 20}$$

where

$\Delta\varepsilon_T$: Thermal strain increment
σ_c: Compressive stress
f_c': Uniaxial compressive strength at reference temperature
ΔT: Temperature change
ρ: Model parameter
CTE: Coefficient of thermal expansion

Considering the theory of microdiffusion, which is driven by humidity- and temperature gradients [Bažant and Chern (1985)], and application of this theory to young concrete [Jonasson (1994)], Bosnjak (2002) described a modification of Eq. (3. 20). Thermal and shrinkage strain are then described as:

$$\Delta\varepsilon_T = CTE \cdot \Delta T \cdot \left[1 + \rho \cdot \frac{\sigma_c}{f_t'} . sign(\Delta H)\right] \tag{3. 21}$$

$$\Delta\varepsilon_h = k\Delta h \cdot \left[1 + r' \cdot \frac{\sigma_c}{f_t'} . sign(\Delta H)\right] \tag{3. 22}$$

$$\Delta H = \Delta h + c\Delta T \qquad \text{(c is a positive constant)} \tag{3. 23}$$

$$sign(\Delta H) = \frac{\Delta H}{|\Delta H|} \tag{3. 24}$$

Among others, Jonasson (1994a) applied this theory to young concrete, assuming that for young concrete the temperature change dominates, i.e *sign(ΔH) = sign(ΔT)*. Model parameter r' varies between 0.1 and 0.6. The transient thermal creep (or stress-induced thermal strain) due to a constant temperature increment ΔT in a time domain is defined and modeled as follows, [Jonasson (1994a), Hedlund (1996), Westman (1999) and Bosnjak (2000)]:

$$\Delta\varepsilon_{trcr} = \Delta\varepsilon_T - CTE \cdot \Delta T \tag{3. 25}$$

$$\Delta\varepsilon_{trcr} = CTE \cdot \Delta T \cdot \rho \cdot \frac{\sigma_c}{f_t'} \cdot sign\Delta T \tag{3. 26}$$

In which $\Delta\varepsilon_{trcr}$ is the transient creep strain component taking into account the change in creep during changes in temperature. The parameter f_t' is the tensile strength at reference temperature. As it is seen, the expression of transient creep depends on the current stress state, i.e. the stress applied and the tensile strength at time t', where the latter is maturity-dependent.

Bosnjak (2000) used five TSTM tests, from Bjøntegaard (1999), with different temperature histories in the calibration of the transient creep term $\Delta\varepsilon_{trcr}$ for a specific concrete mixture. She reported that the best value for ρ fitted to the test results was 0.27. Further, she noticed that transient creep resulted in reduction of self-induced stresses (stresses due to temperature, shrinkage and restraint conditions) and in increasing creep rate. Hedlund (1996) also reported values for ρ to be varied for different concrete mixtures between 0.1 and 0.7.

Generally, in restrained hardening concrete, parallel to temperature rise the stresses will be built up, and any temperature increases prior and during any stress increment will affect the creep rate. Neville (1980) states that: "the influence of temperature on creep was shown to be greater when concrete is heated soon before application of load than when it has been at the higher temperature since demolding. Application of temperature to concrete already under load causes an increase in the rate of creep." Hansen and Almudaiham (1960) observed that if the temperature is lowered after a period at a higher temperature the "excess" creep is not recovered. Illstone and Sanders (1973) confirmed that there is no sign of any creep recovery during or following a drop in temperature. However, Wallo *et al.* (1965) reported that a change of temperature increase creep deformation regardless of whether the change is positive or negative.

Based on the foregoing discussion the predicted transient creep is assumed to be constant during the decrease of temperature in stress-analysis. This means that for a temperature decrease ΔT, the $\Delta\varepsilon_{trcr}$ is assumed to be zero.

Chapter 4

Description of Experimental Equipment and Test Program

4.1 Introduction

In order to understand creep behaviour of concrete, creep tests have to be conducted, and thus different loading systems have been developed and described in the literature. Creep is a major fact of mechanical behaviour of the material, depends on many factors, and is very sensitive to the conditions of preservation. Therefore the creep tests must be standardized. According to the draft of subcommittee RILEM TC 107-CSP [Acker (1993)] for creep tests the most important point concerns the slenderness of the samples in order to measure the strains only in the central part of the sample, to eliminate the edge effects. The utility of being able to perform quasi-instantaneous loading and the possibility of reconstituting the behaviour of massive part from the experimental data are other basic ideas a creep test is based on.

The main common requirements for all the apparatus for creep tests on concrete are their capability to: maintain a constant known stress during testing period, ensure uniform stress distribution over the cross-section of the specimen, apply the load very quickly, and operate in a room with controlled temperature and humidity. The creep tests are usually performed on concrete specimen of shape of prisms and cylinders, subjected to uniaxial stress.

For the purpose of performing uniaxial tensile creep tests a new testing apparatus was developed and build at NTNU. Together with an already existing testing apparatus for compressive creep tests, parallel creep tests on both of the testing machines where conducted. Sealed concrete specimens of cylindrical shape are used in both apparatuses, but their dimensions were different. Both apparatuses are described in the following sections.

The creep tests are divided into four series, each series studying the influence of a particular parameter on tensile creep. Some of the series are repeated to check the reproducibility of the test results. The tests are performed in a climate room at nearly constant relative humidity.

Series I compares tensile creep and compressive creep at early ages. The tests are conducted under isothermal conditions at about 20 ^{o}C. In series II, different levels of tensile stresses are applied to investigate non-linearity under direct tension. The influence of isothermal temperature on tensile creep is studied in series III, and finally the effect of silica fume is studied in series IV.

In addition to the two apparatuses for creep tests in both tension and compression, a TSTM (Thermal Stress Testing Machine) equipment, is described briefly in this chapter. Test results from TSTM are analyzed in Chapter 6.

Before description of the test apparatuses we have to make clear what we mean by the basic creep, which the main interest has been devoted to in the present work. In hardened concrete, the basic creep is defined as creep occurring under no moisture exchange between the concrete and the ambient medium, or under the so-called sealed condition. Under the condition of drying process, i.e. moisture exchange with the ambient medium, there is an additional creep component referred to as drying creep. As mentioned in Chapter 3, creep of concrete at young ages in sealed condition is a special case. It is basic creep since no moisture exchange with the environment takes place, but it is also drying creep because of internal, probably uniform drying. Thus, the common definition used for mature concrete is not very relevant and rather confuses the situation. To characterize the creep occurring under sealed condition, the author introduces the notion ***Sealed Creep*** in the present investigation.

4.4 Tensile Creep Rig

Tensile creep tests are difficult to perform with high accuracy, to a large extent because it is not easy to apply a uniformly distributed tensile stress. To solve the problem, specially designed anchors are embedded in the ends of the specimen, using solid plates screwed to the anchors to prevent introduction any load eccentricity to the specimen.

A new Tensile Creep Rig, a loading system for tensile creep tests, was developed and built, shown in Figure 4.1. It is based on earlier creep systems described in Neville (1983), and consists of two parts: the creep frame, which is a vertical steel frame, and a horizontal loading frame. The load is applied by a lever arm system, and the specimens are placed inside of the two cylindrical chambers, shown in the figure. The chambers provide the temperature control of the concrete specimen, where the chamber in the right hand is loose, measuring load-independent deformations, while the chamber on the left hand is fastened to the creep frame measuring deformations under load.

The load is applied to the specimen by dead weight via a lever arm. By changing the position of the dead weight (100 kg) on the arm, the required load on the specimen is achieved. At both ends of the specimen the load transmits via a hinge and then via the specially designed steel anchorage, which is embedded in the ends of the specimen. A load cell positioned on the top of the rig records the actual load on the specimen.

Figure 4.2 shows the concrete specimen ready for testing in the Tensile Creep Rig where the upper cover of the temperature control chamber is lifted. Comprehensive drawings of the apparatus are shown in Figure 4.3 and Figure 4.4.

The loading process in the apparatus is manual, and thus the loading time takes at least 45 seconds and up to 2 minutes. The logging of data was made automatically by using an Orion-logger of type Solatorn SI 3531D. Temperature histories can also be imposed automatically by programming a temperature control machine (Julabo), where water with the desired temperature is used to control the temperature in the cylinders. Both systems are shown in Figure 4.10.

It is important to ensure axial loading when placing the test specimens in the creep frame. To achieve such requirement, two semi-universal joints are used to connect the specimen to the load bars at both ends. In addition, the load from the loading frame transfers to the load bar by a spherical hinge in the button, and the hinge was covered by Teflon to eliminate friction between the two frames during the loading.

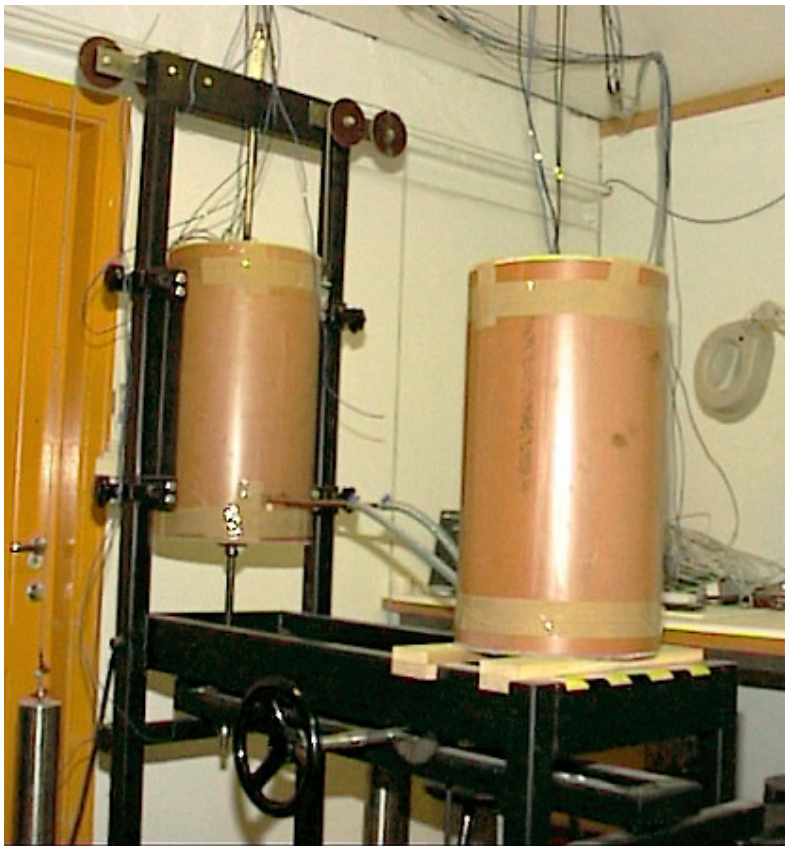

Figure 4.1 Tensile Creep Rig, an apparatus for measurement of tensile creep, consisting of a creep frame and a loading frame.

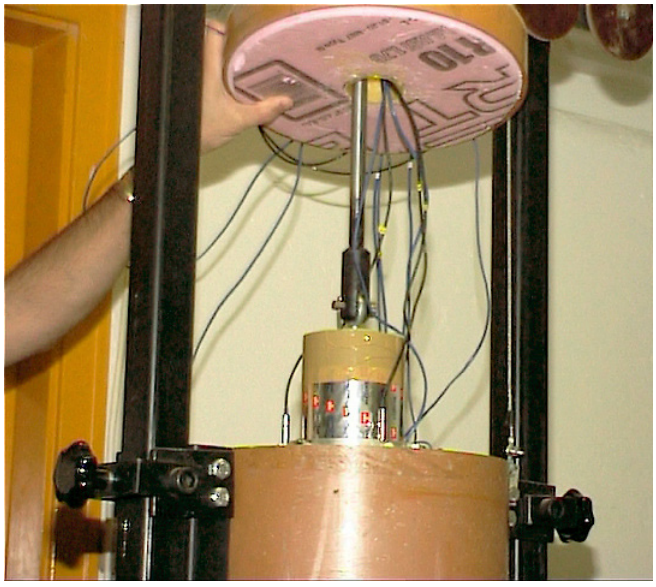

Figure 4.2 Concrete specimen inside temperature control chamber, ready for testing.

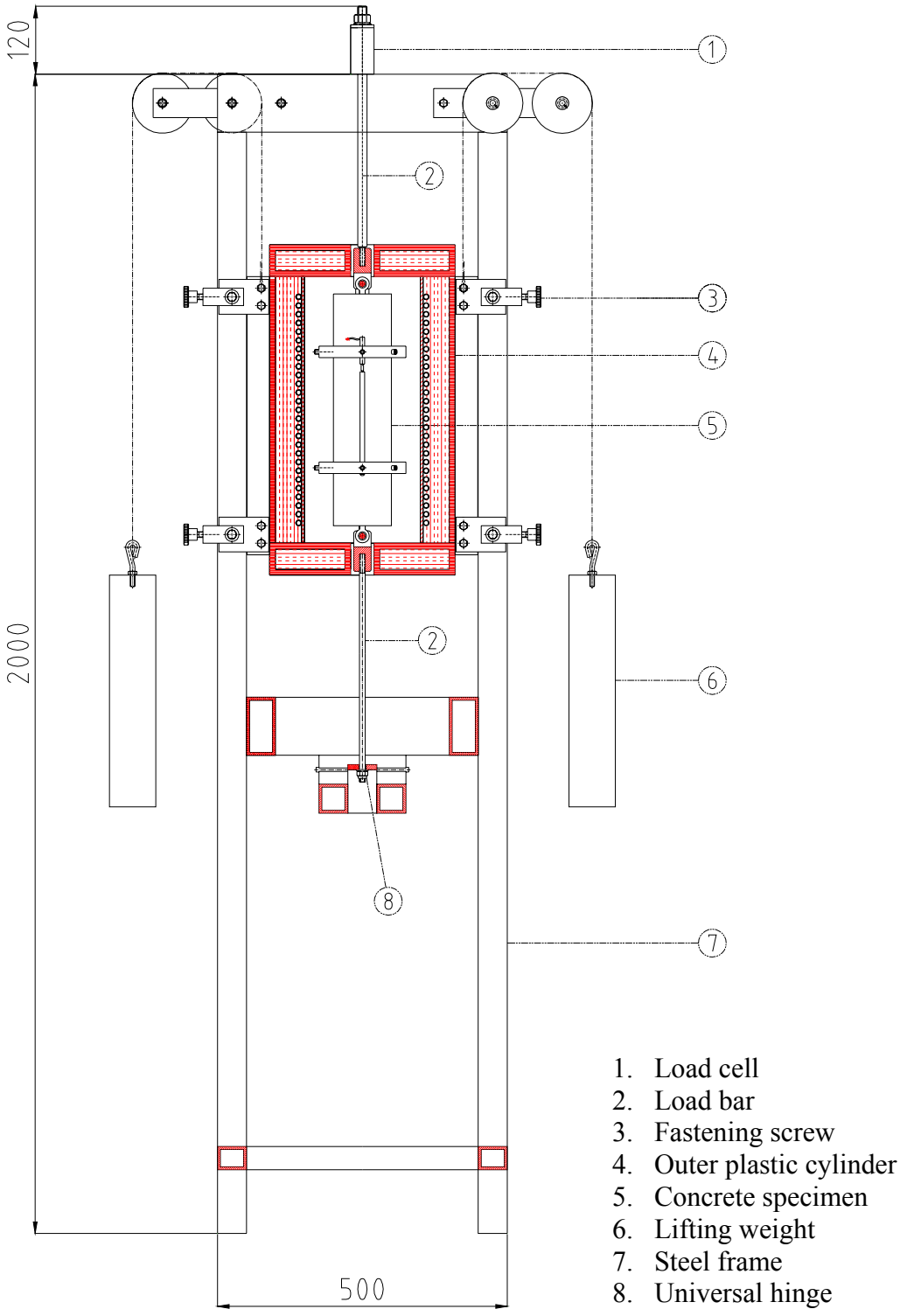

Figure 4.3 Tensile Creep Rig with the dead-load lever arm system of loading the concrete in direct tension, seen from the front. Dimensions are in *mm*.

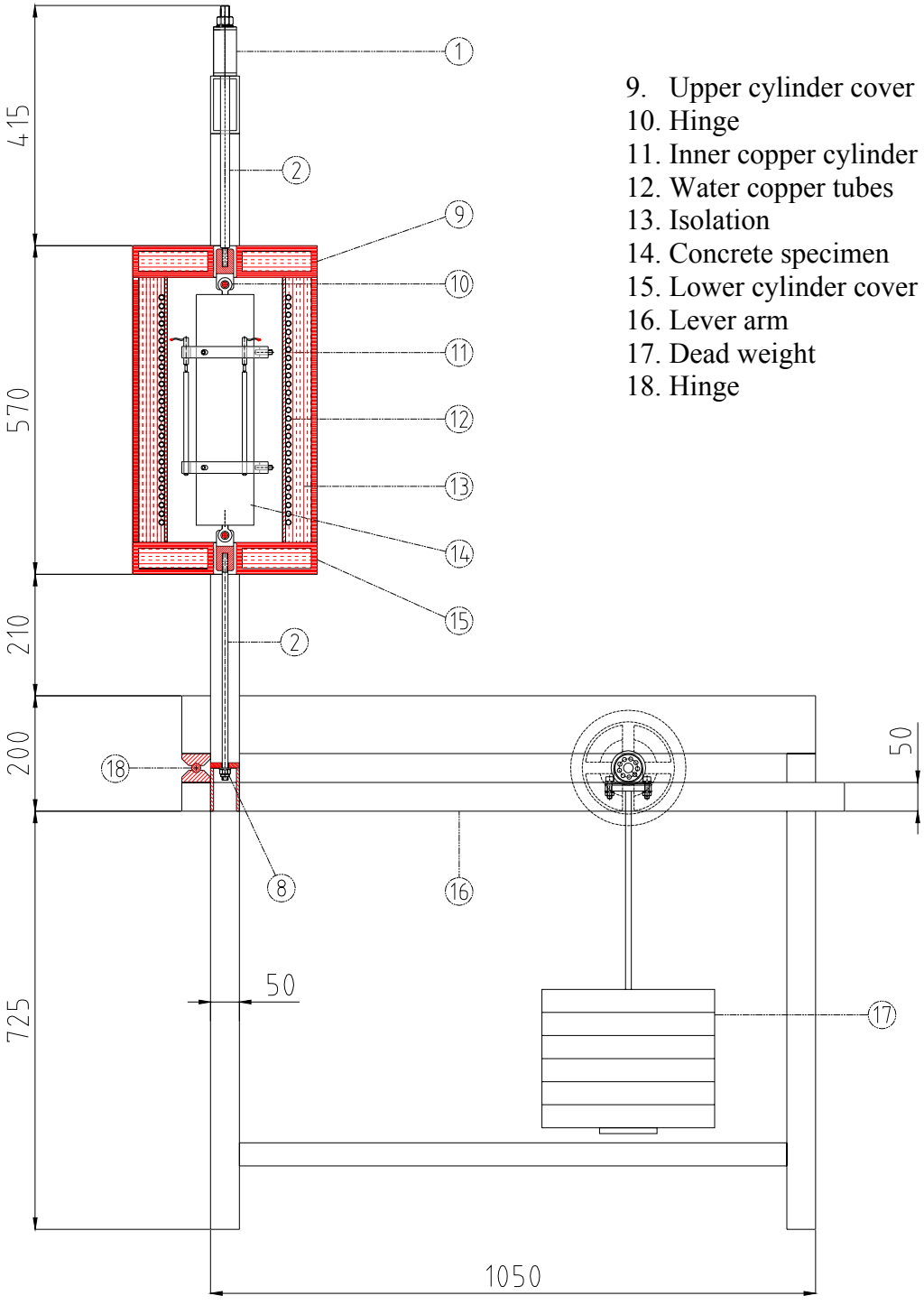

Figure 4.4 Tensile Creep Rig with the dead-load lever arm system of loading the concrete in direct tension, seen from the side. Dimensions are in *mm*.

4.4.1 Concrete specimen

Concrete cylinders with dimensions of 103x425 mm were cast vertically in plastic tubes, and they were used in the tensile creep tests. During the casting the specially designed steel anchors, shown in Figure 4.5, are embedded in the ends of the specimen. The anchors were placed vertically and aligned very carefully in the centre of the specimen mould, in the ends, during the casting. They are 125 mm long and threaded externally to establish a better bond to the concrete. At the position where the anchors end in the specimen, there is no bond between the concrete and the anchors. To reduce this area the anchors are conical. The chosen design of the anchors make the transmission of the imposed external load and the distribution of the tensile stresses in the specimen as uniform as possible. The diameter of the anchors is respectively 22 mm and 9 mm at the two ends.

To ensure an axial loading to the specimen, it was important to cast the anchors vertically and centric in both ends of the test specimens. Two provisional solid plates, which fitted to the ends of the moulds, were screwed to the anchors to prevent or at least to limit introduction of any load eccentricity to the specimen. Figure 4.5b shows the hinge, screwed into the embedded steel anchor, which transfer the imposed load.

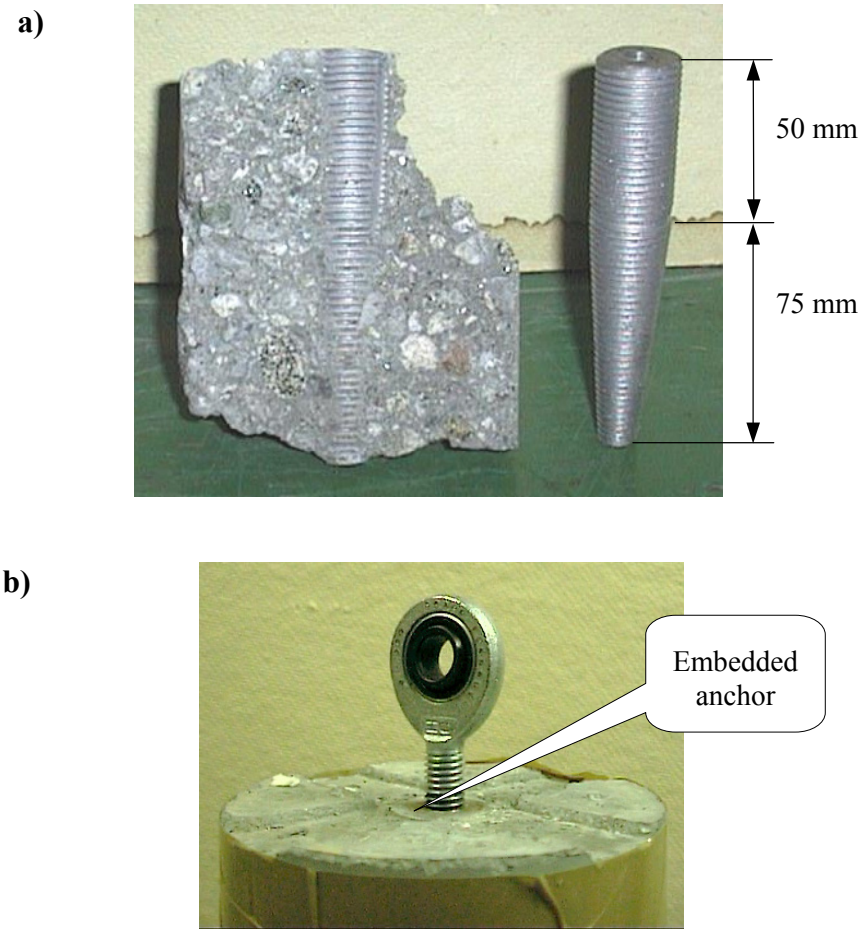

Figure 4.5 The ends of a concrete specimen. a) Anchor embedded in the end of the specimen, b) Hinge for transmission of load.

19. Embedded anchor
20. LVDT
21. Aluminium frame ring
22. Invar bar
23. Invar steel mounted to upper frame ring
24. Invar steel mounted to lower frame ring
25. Space between frame ring and specimen
26. Fastening bolt

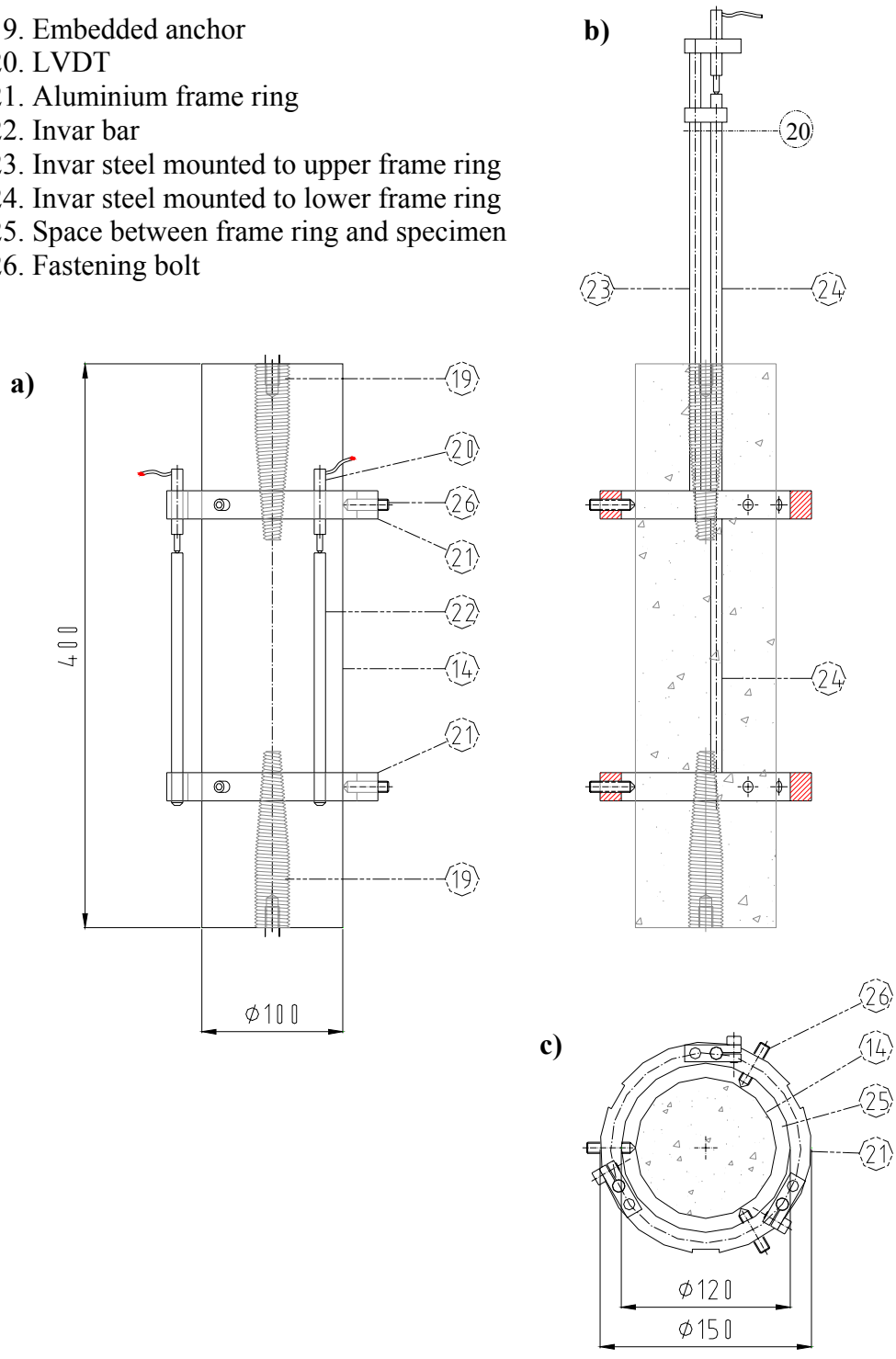

Figure 4.6 Detailed sketch of the measurement components: (Dimensions are in *mm*)
a) Specimen and measuring devices for testing under isothermal temperature,
b) Specimen and measuring devices for testing under variable temperature,
c) Aluminium frame ring.

The specimens were sealed by watertight aluminium/plastic foil, to prevent moisture exchange with the environment.

4.4.2 Strain Measurement Devices

Measurement devices of various types can be used to measure the change in deformation with time. Experience from this investigation has shown that when selecting the devices for creep measurements, a careful consideration has to be given to the *stability* of the devices over time, for the:

- working environment
- convenience and time required for measurements
- accuracy required
- preparation time

In addition to these, the expense is obviously important.

In the present investigation, the time dependent deformations of the concrete specimen are measured using displacement transducer of the type Linear Variable Differential Transformer (LVDT, D5/40G8), shown in Figure 4.7. The main advantage of the LVDT transducer over other types of displacement transducer is their high degree of robustness.

Linear Variable Differential Transformer (LVDT)

The LVDT displacement transducer is an electrical device that produces an electrical voltage proportional to the displacement of a movable Magnetic Core. It is a position-sensing device that provides an AC output voltage proportional to the displacement of its core passing through its windings. LVDTs provide linear output for small displacements where the core remains within the primary coils.

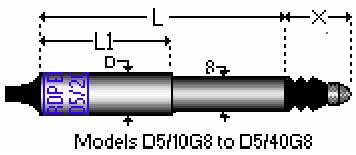

Figure 4.7 LVDT Displacement Transducer. Dimension "x" is at electrical zero position.

The LVDT is composed of these basic components:

- A Coil Winding Assembly consisting of a Primary Coil and two Secondary Coils symmetrically spaced on a tubular centre.
- A Cylindrical Case, which encloses and protects the Coil Winding Assembly.
- A Magnetic Core which is free to move axially within the Coil Winding Assembly.

Each of the two secondary coils is half the length of the primary coil wound over it, and the two halves are connected differentially (back to back) to each other. When the magnetic core is in the centre of the hollow core, the same voltage is induced in both the secondary coils and as they are connected back to back the output is zero. At any other position the signal from one half secondary will be greater than the other, and the amplitude of the combined signal will be proportional to the distance from the centre. Its phase in relation to the primary will then depend on which side of the centre the core is.

Thus, by phase sensitive demodulation one gets a voltage that is almost linearly proportional to the displacement from the centre and a polarity that depends on which side of the centre the core is. They are normally characterized by their maximum deviation from the centre and the maximum deviation of the linearity from a straight line e.g. +/- 1 mm, 0.07%.

Four tests were conducted to find how a variation in temperature would affect the measurement. The test results showed that temperature induced errors could easily grow and exceed the influence of other parameters and that the measurements also could become unstable. This is discussed later.

Measuring frame

The strain measurement device (LVDT) mounted to the specimen body by a so-called measuring frame is shown in Figure 4.8. The measuring frame is a circular aluminium frame, which consists of two aluminium rings and three Invar steel vertical rods attached to the 200 mm middle part, which is the measuring length on the concrete specimen. The thermal expansion coefficient of Invar steel is $1{,}6 \times 10^{-6}$ /^{o}C. The frame is fastened to the concrete body by six bolts, three on each ring of the frame. Three strain devices (LVDTs) are mounted with 120 ^{o}C distance on the test specimen and three on the dummy. The advantage of using three devices is that it captures any eccentricity of loading.

4.4.3 Temperature Control System

The temperature control system used in the creep tests consists of a temperature control chamber and a temperature provider apparatus. The chamber surrounds the concrete specimen in the rig. It is cylinder shaped with inner diameter 200 mm and outer diameter 315 mm, and it consists of a 5 mm thick inner copper cylinder and an outer plastic cylinder with insulation in between. Temperature control is provided by water circulation in copper tubes

fixed to the inner copper cylinder. The tubes have outer diameter of 10 mm, and are shown in Figure 4.9 during the construction process before the insulation was applied.

The Julabo apparatus, which is used to provide the water with a desired temperature to the temperature chamber, is shown in Figure 4.10. The temperature control system can be operated by an integrated temperature/time programmer, or by a computer. The first option is used in the investigation. Insulated plastic tubes provide the connection between the Julabo water bath and the chambers.

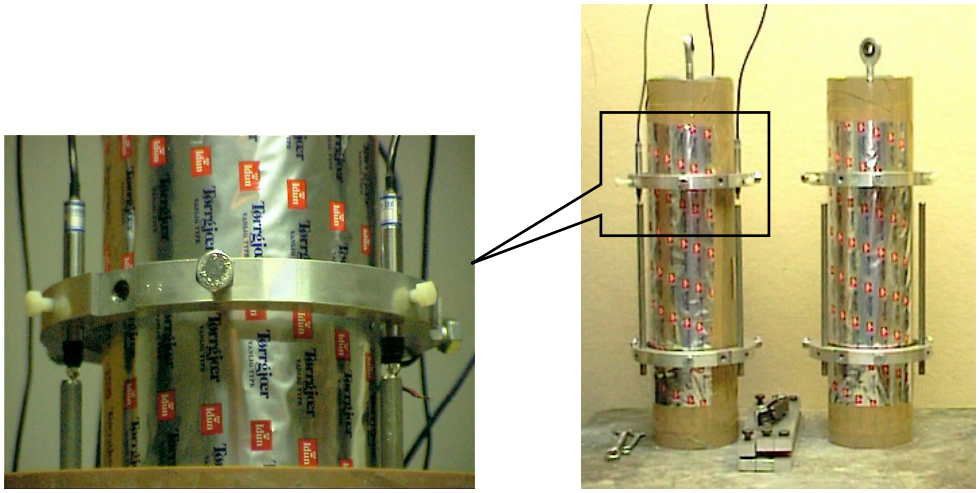

a) **b)**

Figure 4.8 Concrete specimens equipped with aluminium frame, Invar steel bars and strain measurement devices LVDT.

Figure 4.9 Temperature control chambers under construction, consisting of 5 mm copper-cylinder, water copper tubes and plastic mould.

All the creep tests where performed under the temperature imposed by the temperature control system. The temperature was measured inside the system in three places: the inside of the inner copper cylinder, the surface of the concrete specimen and the free air space in between. The function of the system is illustrated in Figure 4.11. The initial temperatures inside the chamber were:

Copper cylinder:	21.60 ^{o}C
Air space:	22.05 ^{o}C
Concrete specimen surface:	22.33 ^{o}C

The figure shows that the temperatures, in the air space and on the specimen surface, follow the temperature of the copper cylinder, but it lies 0.2-0.3 ^{o}C back. The temperatures are stabilized after about 2 days.

Figure 4.10 Temperature provider apparatus Julabo on the left side and the data-logger system Solatorn on the right hand.

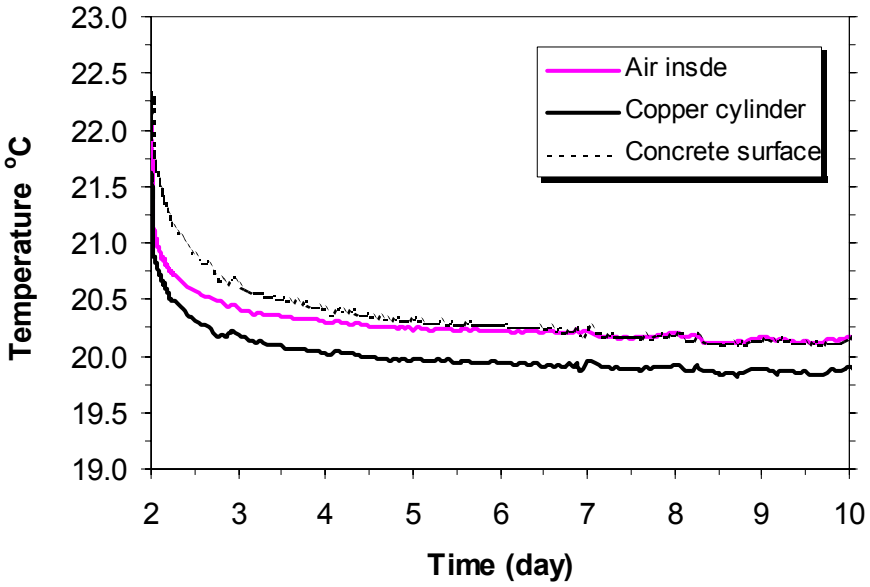

Figure 4.11 Temperature inside the temperature chamber, in a creep test performed at concrete age of 2 days.

4.4.4 Testing Procedure

Immediately after casting, the moulds were stored in a climate room at 20 °C and a relative humidity of about 50%. The moulds were covered to prevent evaporation until demoulding of the specimens and preparation for testing. About 2 hour before testing, the specimens were demoulded and sealed in the foil, one as a dummy for measuring of the load-independent deformations and the other one (active specimen) for measuring of the total deformations under load. During the preparation and throughout the tensile test period the following procedure was followed in the Tensile Creep Rig:

1. The measuring frame fastened to the 200 mm middle part of the specimens. The work was done by slow and careful tightening of the bolts against the young concrete surface.
2. The strain measurement devices (LVDT)s, mounted to the measuring frame, have to be adjusted around zero-position to prevent exceeding the measuring limits.
3. The specimens (active and dummy) were set inside the temperature control chambers.
4. Sealing the specimens in the chambers by putting the covers on the chambers and making them tight.

5. The active specimen was loaded manually as fast as possible to the desired loading level by increasing the loading arm gradually.
6. During the load application and throughout the test, the output of the strain devices was recorded automatically.

Some deviations from this procedure were made due to upgrading and development of the Tensile Creep Rig, and they are described in the next section. It is also worth to mention that the LVDTs were calibrated 3-4 times during the investigation period.

4.4.5 Difficulties During Testing

During the development of the Tensile Creep Rig, many tests were conducted to check the function of the apparatus. Placement of the concrete specimen together with the measuring devices inside the temperature chambers resulted in unsystematic reaction of the strain measurement devices (LVDTs). The reason for such reaction was the change of temperature and the high relative humidity (RH) inside the two chambers, described in the following.

The temperatures of the concrete specimens in the beginning of the creep tests were usually different from the desired one under isothermal conditions (se Figure 4.11). Using the temperature control system, the initial temperature will be forced to change to the desired one. Any temperature change will certainly conduct to contraction/expansion of the specimen. The influence of such temperature change on the stability of LVDTs is investigated.

The two aluminium rings, described earlier and used in the creep tests, were fastened together in parallel, with a three aluminium cubic 100 mm in between. Three LVDT's were mounted to each of the aluminium rings, where the tip of the LVDTs met the opposite aluminium ring. The frame complex was then placed in the temperature chamber and then the chamber was tightened. The initial temperature inside the chamber was 23.2 ^{o}C, and the desired isothermal temperature was 20 ^{o}C. The result of the test for 7 hours is shown in Figure 4.12. The LVDTs 1-3 and 4-6 have been used on the loaded and the unloaded specimens, respectively, in the creep tests during the investigation.

The test result reveals that the temperature is reduced to constant 20.2 ^{o}C after about 4 hours, and the LVDTs show a deformation during this period. Afterwards, the strain maintains nearly constant during the constant temperature. The response of LVDTs to the temperature reduction consists of the contraction of the aluminium cubes and the instability of the LVDTs. All the LVDTs deform in the same direction but with different magnitudes.

Further investigation showed that the relative humidity inside the temperature control chamber increased right after tightening the chamber when the upper cylinder cover was placed on the top. The influence of such change of RH is also investigated, by repeating the same test as above, but with placing a wet concrete specimen inside the chamber together with the frame complex. The results showed that the RH increased very fast from its initial value about 50% to about 95% and the temperature reduced from 21.3 ^{o}C to about 20 ^{o}C. The results of the test are presented in Figure 4.13.

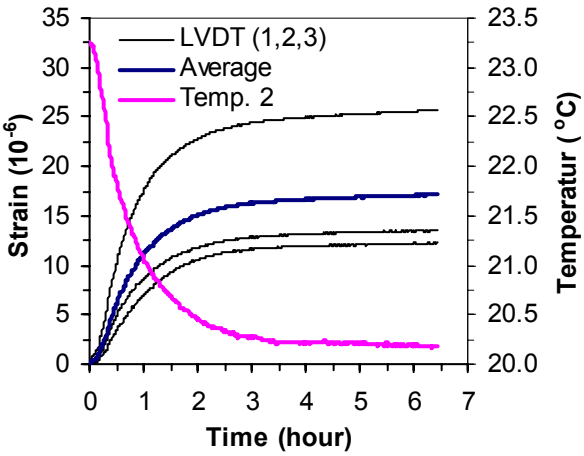

a) LVDTs No.: 1, 2 and 3

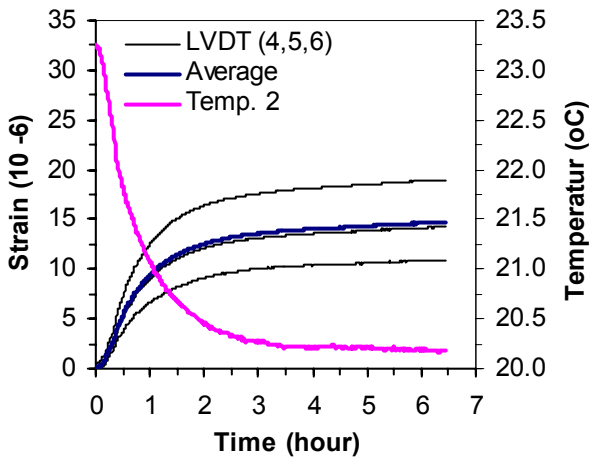

a) LVDTs No.: 4, 5 and 6

Figure 4.12 Influence of temperature on strain measurement devices LVDT's.

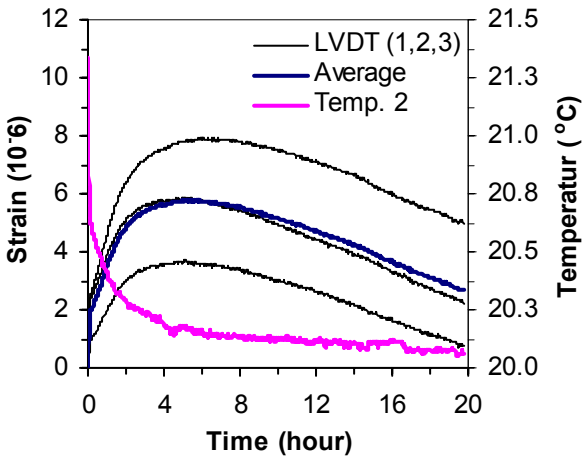

a) LVDTs No.: 1, 2 and 3

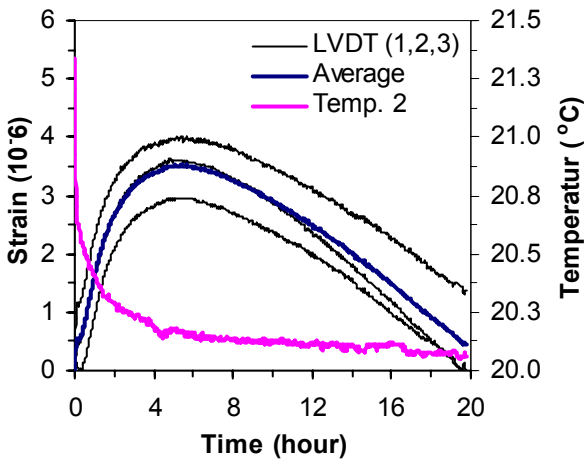

a) LVDTs No.: 4, 5 and 6

Figure 4.13 Influence of temperature and constant high relative humidity (95%) on strain measurement devices LVDT's.

The results reveal that LVDTs contract at high RH, something, which was unexpected and rather surprising. In spite of this undesirable behaviour of the LVDTs under the temperature change and the high RH, the good news is that all of the LVDTs expand or contracts systematically. Thus we assume that any appeared errors in the strain measurement will be

diminished when the strain curves form the loaded and the unloaded are subtracted from each other.

An attempt to solve these problems a climate room was built, with the aim to keep constant RH (about 50%) and constant temperature (about 20 ^{o}C). During the creep tests at isothermal temperature 20 ^{o}C the temperature chamber were left open at the top during the tests, so that the surrounding climate room controlled the RH.

To perform the creep tests under varying temperature the Tensile Creep Rig was upgraded, by moving the LVDTs outside of the chamber, as shown in Figure 4.6b. The Invar steel rod, mounted to the lower aluminium ring, was extended to the outside of the chamber, and another parallel Invar steel rod was mounted to the upper aluminium ring. The relative movement of the two Invar rods was then recorded as the deformation in the 200 mm long concrete specimen.

Compared to the first version of the creep rig, the new rig had two long parallel Invar rods, and thereby more effort was needed to mount the measuring frame and the LVDTs to the specimen body.

Repeating the whole Series I, and comparing the results under the same test conditions documented the function of the new upgraded Tensile Creep Rig. However, due to the instability of the new system and with that uncertainty in the test results, it did not become possible to measure creep during changing temperature - only isothermal tests at different temperatures has been carried out.

Another problem concerning the measuring system is the way measuring frame was fastened to the specimen body by the six bolts. Right under the upper layer of the concrete specimen pores or sand may exists, and one or two bolts may meet them. Tightening of the frame by the bolts less or more than "necessary", may lead to an awkward position of the frame, which again may lead to independent movement of the LVDTs. Due to this problem many creep tests had to be repeated several times.

4.5 Compressive Creep Rig

Five Compressive Creep Rigs were available in the Laboratory at the Department of Civil Engineering, described by Tomaszwicz (1988), and shown in Figure 4.14. Each rig was equipped with a hydraulic jack and spherical bearing plate to ensure uniform distribution of the imposed load over the specimen. The hydraulic pressure in the jacks was individually measured and controlled by a central hydraulic system, which included oil pressure accumulators.

Total deformation of the specimen during the time of loading was measured using a set of three TLM electrical strain gauges (type PL-60-11), glued to each specimen. Shrinkage was measured on he companion specimens using the same type of strain gauges. The electrical strain gauges are inexpensive compared to LVDTs, but if a large number of testes are required to perform it makes them more expensive than LVDTs.

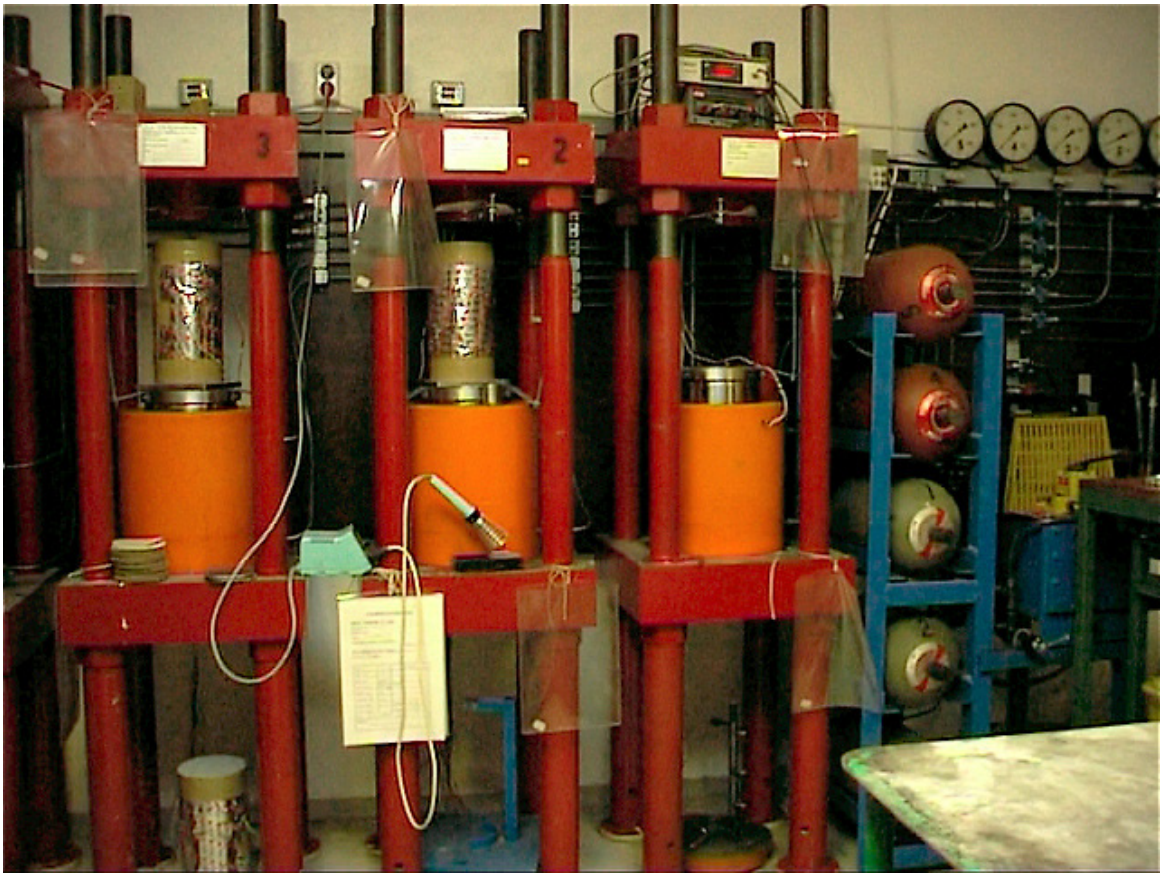

Figure 4.14 Compressive creep rigs equipped with oil pressure accumulators, testing two sealed concrete specimens.

4.3.1 Concrete Specimen

To achieve the same loading level (stress/strength) as in the tensile creep tests a much higher load was necessary to impose on the concrete specimen. Three concrete cylinders ø 150x300 mm were used in each test. Two specimens were loaded to a level corresponding to 40% of concrete strength at loading time, while the third one was used as an unloaded dummy.

The Compression Testing Rigs were placed in the same climate controlled room as the Tensile Creep Rig. The curing conditions and the treatment of the specimens before testing were the same as for the concrete specimens for the tensile creep tests.

4.5.1 Test Procedure

In each creep test two specimens were individually loaded to the same desired load level. The sustained loading level corresponds to initial stress/initial strength ratio of approximately 0.40 based on the known actual compressive cube strength determined separately. To ensure axial loading when placing the test specimens in the loading frame a small preload was applied to note the strain variation around each specimen. During load application the strain gauges readings were recorded and the specimens were then realigned if necessary for greater strain uniformity.

The specimens were loaded gradually to the desired load level at a rate of loading approximately 7-10 MPa per min. The oil pressure in the loading system was adjusted when it deviated from the initial pressure. Logging of the data continued every hour throughout the testing period. The period of sustained loading varied from 3 two 7 days, and in most of the cases, the specimens were unloaded and the creep recovery recorded a few days.

The time of sustained of loading varied from 3 to 10 days. After termination of the tests the specimens where unloaded and the creep recovery was recorded for several of them.

4.6 Stress Rig (TSTM) and Dilation Rig

Bjøntegaard (1999) performed many tests in a special designed Temperature Stress Testing Machine (TSTM), constructed to measure the self-induced stress generation in restrained hardening concrete specimens, and a Dilation Rig, constructed to measure the free deformation of concrete from casting and further on. His test results are analyzed with respect to creep and relaxation in Chapter 6.

Figure 4.15-a shows a principal sketch of the Dilation Rig, Figure 4.15-b a sketch of the TSTM and a cross section of the concrete specimens in the rigs is given in Figure 4.15-c. The horizontal specimens in both rigs are surrounded by a fully temperature controlled mould. Two inductive displacement transducers fastened outside each of the moulds, measure the length change of the specimens in the rigs.

The dimensions of the cross sections are 100 x 100 mm and the total specimen length is 500 mm in the Dilation Rig and 1000 mm in the TSTM. The TSTM can be restrained partially and fully through a feedback system that compensates for any length change over a 700 mm control length.

A detailed description of the rigs, the test procedure and the tests is given in Bjøntegaard (1999). The experimental program, used in this study, is given in Chapter 6.

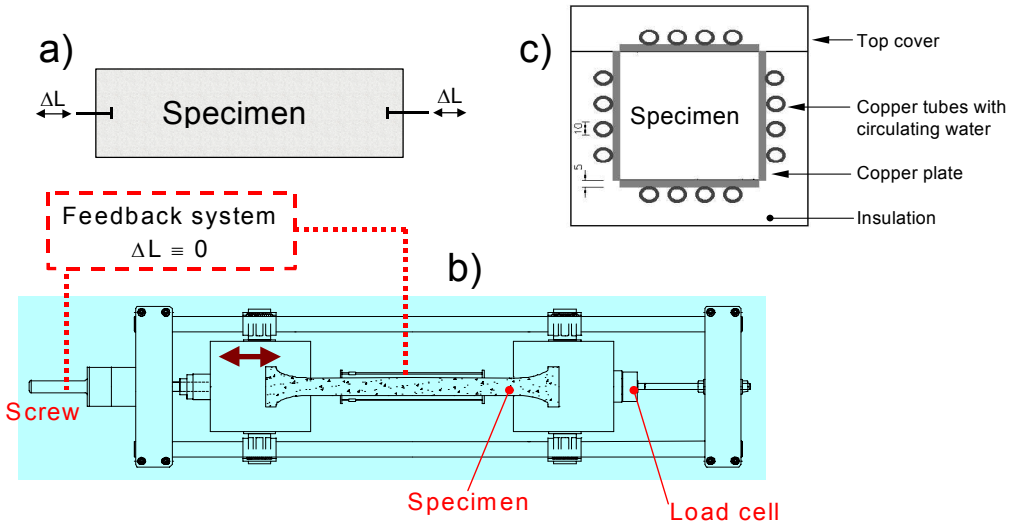

Figure 4.15 Apparatus used in laboratory tests: a) The Dilation Rig (free deformation), b) The Stress Rig (restraint stresses), c) Cross-section of the rigs (showing also the principle of temperature control) [after Bjøntegaard (1999)].

4.7 Concrete Composition

The concrete studied in the present investigation is a typical Norwegian high performance concrete mix for bridges, with w/(c+s) = 0.40. It is called BASE-concrete, contains 0, 5, 10 and 15% silica fume (SF), and are designated as BASE-0, BASE-5, BASE-10 and BASE-15, respectively (see Table 4.1). Crushed stone fractions of 8-16 mm were used as coarse aggregate.

Bjøntegaard (1999) has investigated the same concretes in terms of volume changes, thermal dilatation and autogenous deformation and stress rig tests. A large amount of data is therefore available, which will be used to study the role of creep and relaxation in self-induced stresses in Chapter 6. A detailed description of the concrete can be found in the same reference.

Table 4.1 Mix proportions for the BASE concretes with w/(c+s) = 0.40, and 0, 5, 10 and 15 silica fume (SF).

Materials	**Concrete fractions [Kg/m^3]**			
	BASE-0	**BASE-5**	**BASE-10**	**BASE-15**
Cement CEM I 52, 5 LA (c) (Norcem Anlegg)	389.9	368.1	348.5	330.5
Water (w)	155.9	154.6	153.3	152.0
Elkem silica fume (s)	0	18.4	34.9	49.6
Absorbed water	12.2			
Årdal sand 0-2 mm	149.5			
Årdal sand 0-8 med mer	813.1			
Årdal stone 8-11 mm	589.2			
Årdal stone 11-16 mm	317.8			
Scancem P	2.1	2.0	1.9	1.8
Mighty 150	3.3	3.1	3.5	5.3
w/(c+s) ratio	**0.40**			
Measured values				
Air		*2.3%*		
Density		*2436 kg*		
Slump		*16.6 cm*		
Number of mixes		*18*		
f_{c28} (MPa) [1] (average ± st.dev)	71.5 ± 3.33	81.0 ± 2.94	85.0 ± 4.37	83.7 ±
f_{t28} (MPa) [1] (average ± st.dev)	3.96 ± 0.248	4.60 ± 0.208	4.73 ± 0.286	4.3 ±

[1] According to Kanstad *et al.* (1999)

Another concrete type, called "Maridal" concrete, is also tested for both tensile and compressive creep in the present investigation. Maridal concrete is a high performance concrete with a w/b ratio of 0.42 and 5% silica fume. It was used for the Maridal culvert in Oslo, and has been the subject of comprehensive filed testing as well as laboratory testing within the EU-project IPACS, Heimdal *et al.* (1998).

Table 4.2 Mix proportions for the Maridal concrete with w/(c+s) = 0.42.

Materials	**Concrete fractions [Kg/m^3]**
Cement CEM I 52, 5 LA (c) (Norcem Anlegg)	350.0
Water	154.4
Silica fume	18.0
Absorbed water	21.9
Svelvik sand 0-8 mm	953.2
Svelvik sand 8-14 mm	206.0
Svelvik stone 14-24 mm	658.1
SIKA BV 40	3.0
SIKA AIR 1.0%	0.3
SIKMENT 92, 30%	1.5
w/(c+s) ratio	**0.42**
Measured values	
Air (%)	*4.3*
Density (kg)	*2378*
Slump (cm)	*18.5*
Number of mixes	*1*
f_{c28} (MPa) [1]	69

[1] According to Bjøntegaard (1999)

4.8 Experimental Program

As mentioned previously in Chapter 3 there are many variables that influence creep deformations. The parameters studied in the present investigation are loading age, stress level, silica fume content and temperature on tensile creep. For this purpose a large number of creep tests were carried out. The creep tests were started at 1, 2, 3, 4, 6 and 8 days of curing and the duration of the tests varied from 3 to 10 days. This program covers the most important time period regarding the early age creep prediction.

Four series of creep tests, listed in Table 4.3**,** were carried out to study the above mentioned creep parameters.

Table 4.3 Test series performed on early age concrete.

Series	*Investigation*
I	Comparison between tensile and compressive creep.
II	Non-linearity in tensile creep.
III	Influence of silica fume content in the BASE concrete on tensile creep.
IV	Influence of temperature on tensile creep.

The first three series of tests were conducted under nearly isothermal conditions since both the Tensile Creep Rig and the Compression Creep Rigs were placed in a climate room with a quite stable temperature about 20 ±0.5 °C.

The number of concrete specimen needed for each creep test, their dimensions and the use of the specimens are given in Table 4.4.

Table 4.4 Concrete specimens used in each creep test.

Number	**Dimension**	**Test**		**Use of specimen**
4	150x300 (cylinder)	Compressive creep	2	Loaded (active)
			1	Unloaded (dummy)
			1	Reserve
3	103x425 (cylinder)	Tensile creep	1	Loaded (active)
			1	Unloaded (dummy)
			1	Reserve
3	100x100x100 (cubic)	Compressive strength	3	Testing

The creep properties of the concrete were determined by recording the deformation of cylindrical specimens under constant load in a time domain. Other time-dependent deformations (autogenous shrinkage and thermal dilation) were measured simultaneously on the unloaded companion specimen kept in the same conditions. The creep deformation was determined as the difference between the loaded specimen and the dummy specimen and it is

thus considered as the single effect of the applied stress, which is a convention for reporting creep results.

To determine the compressive strength at loading ages three 100 mm concrete cubes were tested in each creep test. Few tests on the E-modulus were performed on 150 x 300 cylinders, in accordance with Norwegian Standard (NS) 3676 which is based on ISO 6784-1982. The results are discussed in Chapter 5.

Within each series, each single test was repeated at least once. All the tests are given in Appendix A. The letter T and C in each test name characterize whether the test is carried out in tension or in compression.

Series I *(Loading age)*

In the first series, tests on both tensile creep and compressive creep were performed in parallel at 20 ^{o}C. The intention was to evaluate the influence of the concrete age at loading on the viscoelastic behaviour of the concrete, and to compare the viscoelastic behaviour of the concrete in tension and compression.

In general, the applied stress level is about 40% of the strength at initial loading, and the load maintained constant during the test. Due to access to more compressive rigs than tensile rigs more compressive tests were carried out. The tests are carried out on concrete compositions BASE-5 and Maridal. In each parallel test, several concrete specimens were cast from the same batch.

After upgrading the Tensile Creep Rig the series was repeated once to check the new rig and the reproducibility of the test results:

> *Series I-a:*
> Carried out *before* upgrading the Tensile Creep Rig, with *locked* upper cover of the cylinder and *without* climate room.
>
> *Series I-b*:
> Curried out *after* upgrading the Tensile Creep Rig, with *open* upper cover of the cylinder and *with* climate room.

Series II *(Loading level)*

Tensile creep tests in this series were carried out to study the influence of stress level on tensile sealed creep on 3-days old BASE-5 concrete. The applied initial tensile stress levels were 0.2, 0.3, 0.4, 0.6, 0.7 and 0.8 times the tensile strength. One of the series (Series I-B) is conducted on the original Tensile Creep Rig and the two other series (Series II-A and Series II-B) on the upgraded Tensile Creep Rig. The concrete specimen and the test conditions were the same as for forgoing tests. The only variable studied here is the applied loading level. The tensile strength, compressive strength and E-modulus for the 3-days old concrete are 3.7 MPa, 47.8 MPa and 29.3 GPa, respectively.

Series III *(Silica fume)*

This series of tensile creep tests were conducted on concretes with different silica fume contents, to study the effect of silica fume on the viscoelastic behaviour. The concrete mixes are described in Table 4.1, and they are denoted BASE-0, BASE-5, BASE-10 and BASE-15. The numbers represent the percent silica fume in the mixes.

From each concrete batch two tests are conducted: at 1 day and 4 days of loading, and the duration of testes are varied from 3 to 4 days. The tests (at 20 ^{o}C) are repeated once or twice to confirm both the function of the test rig and the test results. Throughout this series of the tests, the applied stress is 40% of the tensile strength at loading age, and its magnitude (but not the stress/strength ratio) maintains constant during the tests.

The total test program involving totally 16 tests is given in Appendix A (Table 4.7). To maintain both the water/cement ratio and the necessary workability, it was necessary to increase dosage of super-plasticizer when silica fume content increased. The amounts of super-plasticizer used in the tests are also indicated in the table.

Series IV *(Temperature)*

Finally, the influence of temperature on sealed creep in tension, at early ages of concrete, is studied and few tests are conducted in Tensile Creep Rig. Tensile creep tests are conducted at different isothermal temperatures (20, 34, 40, 57 and 60 ^{o}C) on BASE-5 concrete. The curing temperature for all the tests is about 21±2 ^{o}C until it is increased to achieve the desired testing temperature.

For the test at 34 ^{o}C the temperature was increased 3 hrs before loading. For the other tests (40, 57 and 60 ^{o}C) the temperature was increased to the desired level one day before loading. The number of specimens and the test procedures are the same as described in earlier series.

Chapter 5
Creep Test Results and Discussion

5.1 Introduction

The results of the comprehensive experimental work conducted on creep of concrete in both tension and compression at early ages are described in this chapter. With regard to various parameters, the analysis of the results is divided into five parts. In the first part, the development of the modulus of elasticity for the different concrete mixes is discussed. The differences between creep behaviour in tension and compression are presented in part two. In the third part, the influence of the stress level on tensile creep for a specific age of concrete is investigated. The influence of silica fume content in concrete mixes on creep is considered in the forth part. In the last part, the effects of isothermal temperature level on creep are studied and some conclusions are made.

The load level in all cases is about 40% of the concrete's cube strength at loading ages (except the part where the effects of different load levels on creep is studied), and the magnitude of the applied load stays nearly constant during the tests. Due to the progress of hydration, the concrete strength increases and the actual applied load level (%) reduces with time. Some researchers adjust the load level during the creep tests, but some do not. The author belongs to the last category. This means that the load ratio decreases to levels lower than 40% with time because the tensile and compressive strength growths during the tests.

When a load is applied to a concrete specimen, it responds by an immediate deformation followed by creep. The magnitude of the instantaneous deformation depends mainly on the modulus of elasticity and the loading rate, but of course the meaning of "instantaneous" must be defined. The dependence of instantaneous deformation on loading rate is discussed in Chapter 4. For the practical reasons the term creep is defined as the elastic plus time-dependent deformation in this Chapter.

As mentioned in Chapter 4, the measured creep under sealed conditions has normally been defined as basic creep. The measured creep of sealed high performance concrete includes, in addition to basic creep, a drying creep component because sealing of the concrete of course does not eliminate the autogenous shrinkage. Thus the term *sealed creep* is used to characterize the creep occurring under sealed condition

5.2 Development of Modulus of Elasticity and Strength

The development of mechanical properties of concrete and particularly the modulus of elasticity is very important when considering the creep behaviour of concrete. Kanstad *et al.* (1999) reports the results of a comprehensive test program on mechanical properties including the modulus of elasticity. The tests were performed on the same concrete mixes which are studied in the present investigation, namely concrete mixes with 0, 5, 10 and 15% silica fume content, designated as BASE-0, BASE-5, BASE-10 and BASE-15, respectively. One of the main conclusions was that there were no significant differences between the E-modulus determined from compressive or tensile tests for the test methods used (see Figure 2.5a). This is in agreement with results reported among others by Pane and Hansen (2001).

Compressive strength tests were performed on 100 mm cubes. Direct *tensile strength* was measured on 100x100x600 mm prisms, in accordance with SINTEF/NTNU internal procedure (KS 70106), where the specimen is loaded, with the strain rate approximately $100x10^{-6}$/min, until failure. The deformation was recorded over 100 mm mid section of the prism by the use of two displacement transducers placed on the opposite sides of the prisms. The *tensile E-modulus* was calculated from the load deformation curves as the secant modulus between 5 and 40% of the ultimate load. The *compressive E-modulus* was measured on 150 x 300 cylinders on the third unloading, in accordance with Norwegian Standard (NS) 3676 which is based on ISO 6784-1982. Tests on compressive E-modulus are also conducted in the present work and they will be discussed later.

Referring to the earlier described expression for modulus of elasticity, Eq. (5. 1), the development of the E-modulus for the relevant concretes are obtained and presented in Figure 5.1. The figure shows that the higher silica fume content is, up to 10%, the higher the E-modulus. On the other hand, it reveals that the E-modulus develops slower the higher silica fume content is. The stiffness is defined to be zero at time $t_{0,}$ and the model parameters for the four concrete mixes are given in Table 5.1.

$$E_c(t_e) = E_{c28} \cdot \left\{ \exp\left[s \cdot \left(1 - \sqrt{\frac{28}{t_e - t_0}} \right) \right] \right\}^{n_E} \qquad (5.\ 1)$$

The developments of compressive and tensile strength are expressed by Eq. (5. 2) and (5. 3), and they are presented in Figure 5.2. In Figure 5.3 the development of all three mechanical properties versus compressive strength development is shown. It is worth noting the role of n_E and n_t in the given expressions, which is to characterize the different time developments, for the three material properties. It shows that the E-modulus develops faster than the tensile strength, which again develops faster than the compressive strength.

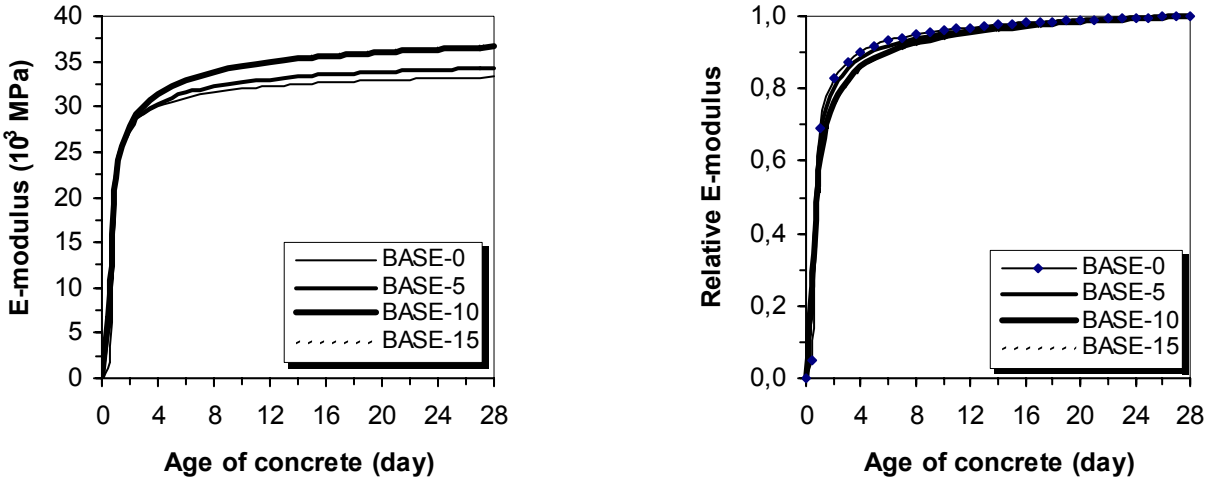

a) E-modulus; *E(t)* b) Relative E-modulus; *E(t)/ E(28)*

Figure 5.1 Development of modulus of elasticity for concretes with different silica fume contains.

Table 5.1 Material and model parameters.

Model parameter	BASE-0	BASE-5	BASE-10	BASE-15	Maridal
f_{c28} (MPa)	71.5	81.0	85.0	78.3	71.5
f_{t28} (MPa) [1]	3.96	4.44	4.75	4.18	4.16
E_{28} (MPa)	33300	34300	36600	36700	42218
s	0.170	0.173	0.211	0.219	0.199
n_E	0.337	0.394	0.339	0.394	0.620
n_t	0.573	0.658	0.621	0.539	0.620
t_0 (hrs)	12	11	10	9	10

[1] Tensile strength at 28 days is determined as 80% of the tensile splitting strength.

Compressive strength:

$$f_c(t_e) = f_{c28} \cdot \left\{ \exp\left[s \cdot \left(1 - \sqrt{\frac{28}{t_e - t_0}} \right) \right] \right\} \tag{5. 2}$$

Tensile strength:

$$f_t(t_e) = f_{t28} \cdot \left\{ \exp\left[s \cdot \left(1 - \sqrt{\frac{28}{t_e - t_0}} \right) \right] \right\}^{nt} \tag{5. 3}$$

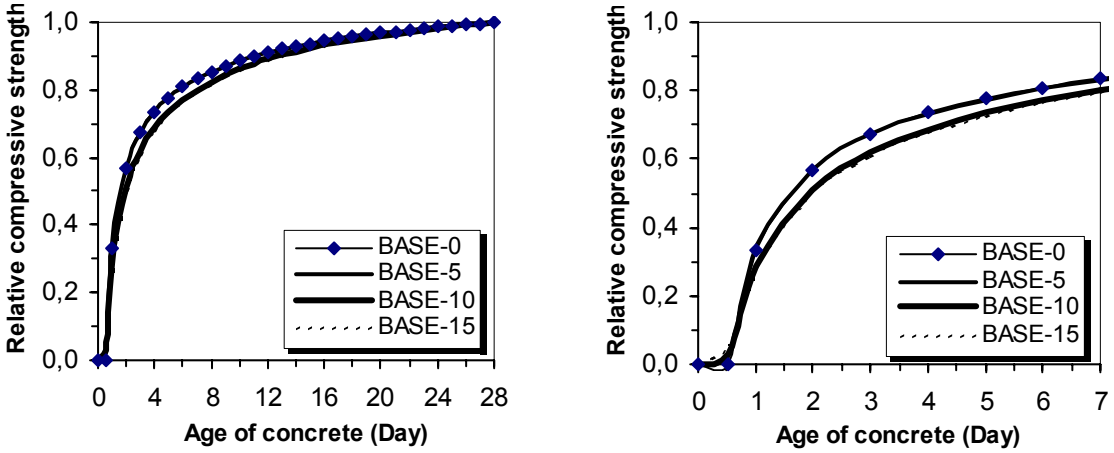

a) Relative compression strength; $f_c(t)/f_c(28)$

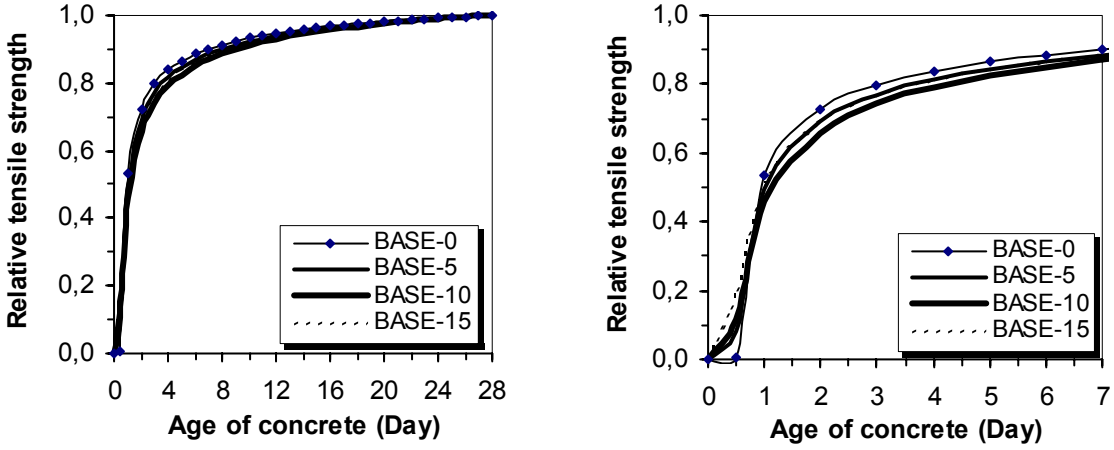

b) Relative tensile strength; $f_t(t)/f_t(28)$

Figure 5.2 Strength development of concretes with different silica fume.

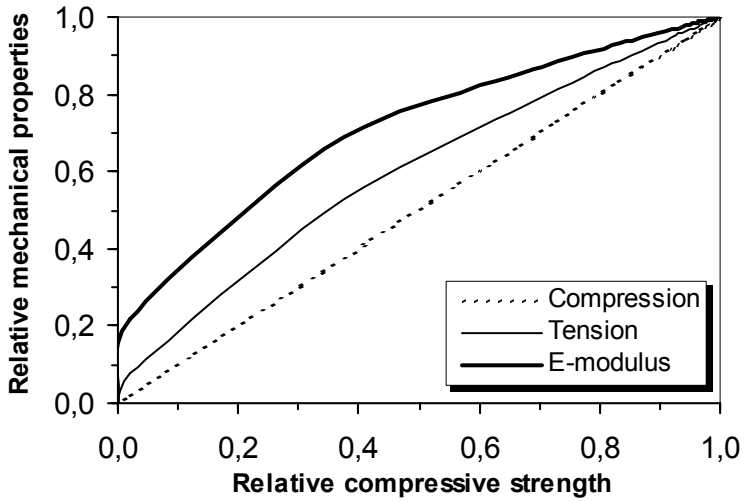

Figure 5.3 Development of mechanical properties versus compressive strength development for BASE-5 concrete, according to Eq. (5. 1) - (5. 3).

As mentioned earlier in Chapter 2, most of the available data in the literature on the modulus of elasticity considers that the modulus of elasticity in equal in tension and compression. There exist also few reported results, which show difference between the modulus of elasticity under the two load conditions.

In the present investigation 6 tests on the modulus of elasticity in compression were carried out following the NS 3676. According to this code the tests include two preloading cycles, in order to reduce irreversible effects and thus the curvature during the final loading. The information about the tests and the testing machine is given in Table 5.2.

The procedure consists of three steps:

1. Loading to 45% of ultimate load. Resting period 90 sec. Unloading followed by a new 90 sec resting period.
2. Loading to 30% of ultimate load. Resting period 60 sec. Unloading followed by a new 60 sec. resting period.
3. Loading to 30% of ultimate load. Rest period 90 sec. Unloading followed by a new 90 sec resting period.

The deformation was measured over the 150 mm mid section, using 3 displacement transducers, placed 120^{o} to each other. Figure 5.4 presents the result of one of the compression tests on 4-days old BASE-5 concrete. According to the NS 3676 the modulus of elasticity in compression is determined from the unloading part of the step 3 (including 90 sec resting period).

Table 5.2 Data on testing of modulus of elasticity in compression for BASE-5.

Testing procedure:	NS 3676
Concrete type:	BASE-5[1]
Specimen dimensions (DxL):	100x200 mm
Weight:	4.058 kg
Compressive strength, f_{cc}:	49.9 MPa
Failure stress:	41500 kpa
Loading rate:	0.8 MPa /sec

[1] The concrete is described in chapter 4.

The compressive E-modulus determined as the static E-modulus, is always influenced by creep to a certain extent. Since the tendency of concrete to creep is greater at an early age, creep influences the E-modulus more at the loading time during this stage. This means that the E-modulus determined from the unloading part of loop 3, denoted E_1, do not represent the compressive stiffness during the loading in the creep tests. The more correct and relevant E-modulus in compression should be that which is determined from the first loading part of the loop 1, denoted E_2. This procedure is exactly one of the two methods, which is followed in Swedish Standard SS 137232. The value of E_2 in the current test in Figure 5.4 is $29.3 \cdot 10^3$ N/mm^2, while $E_1 = 32.0 \cdot 10^3$ N/mm^2.

On the other hand, Kanstad *et al.* (1999) reported that the tensile E-modulus (E_t) is the same as E_1 in compressive E-modulus tests, which probably is due to the linear stress/strain relation in tension and the lower stress level applied in tension, illustrated in Figure 5.5. As mentioned earlier the modulus of elasticity in tension was calculated from the load-deformation curve as the secant modulus between 5 and 40% of the ultimate load.

The ratio between E_1 and E_2 (defined in Figure 5.4) for the concretes with different silica fume contain is shown in Figure 5.6. The diagonal dashed lines represent the ratio $E_1/E_2 = 1$ and the solid regression lines are based on the experimental points. The results reveal that the E_1 is 13% and 17% higher than the E_2 for BASE-0 and BASE-5 respectively, and 10% for both BASE-10 and BASE-15. The general observation is then that E_1 is 10-17 % higher than the E_2 for the four tested concrete mixes, i.e. that the first loading includes large irreversible effects, as is evident in Figure 5.4.

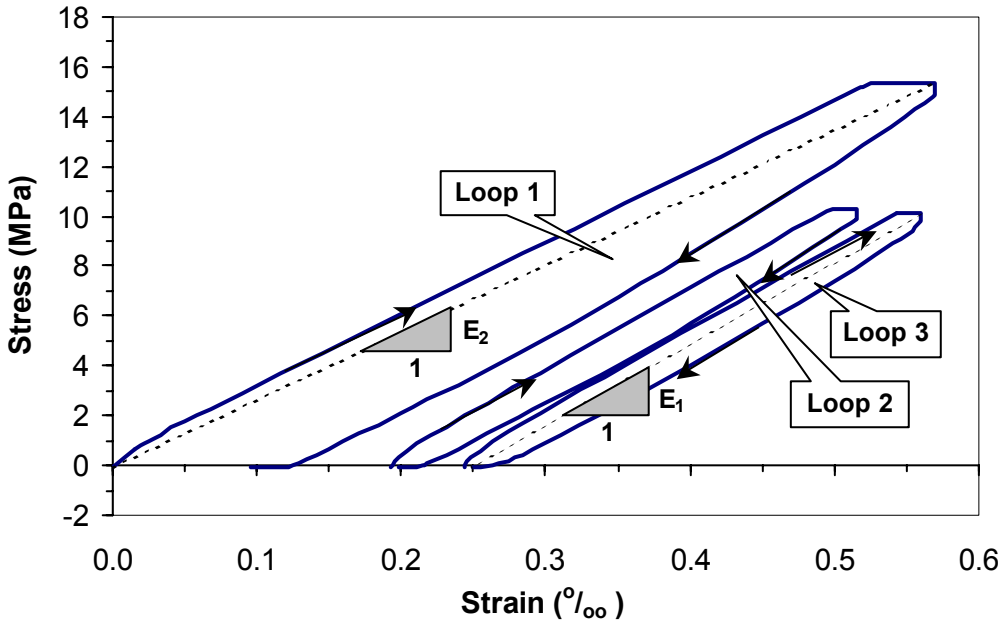

Figure 5.4 Test result for modulus of elasticity, determined according to Norwegian Standard NS 3676. 4-days old BASE-5 concrete, T=20 °C.

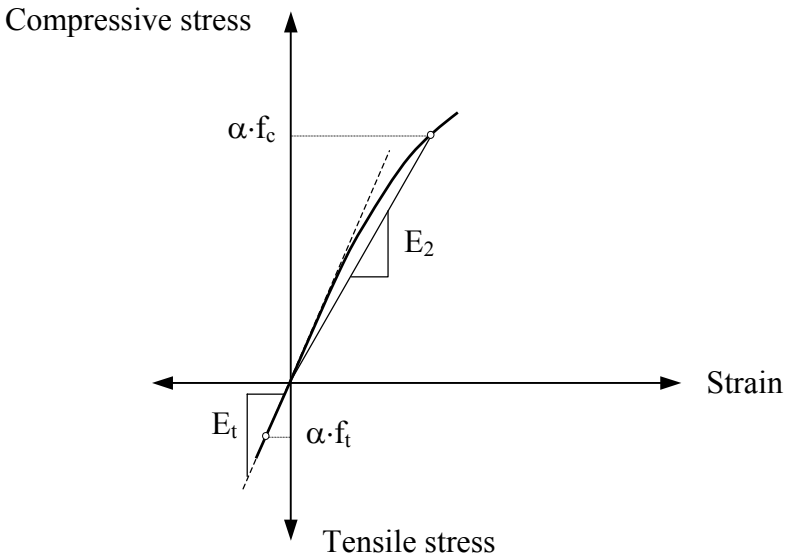

Figure 5.5 Stress-strain relationship in compression and tension (α<1.0).

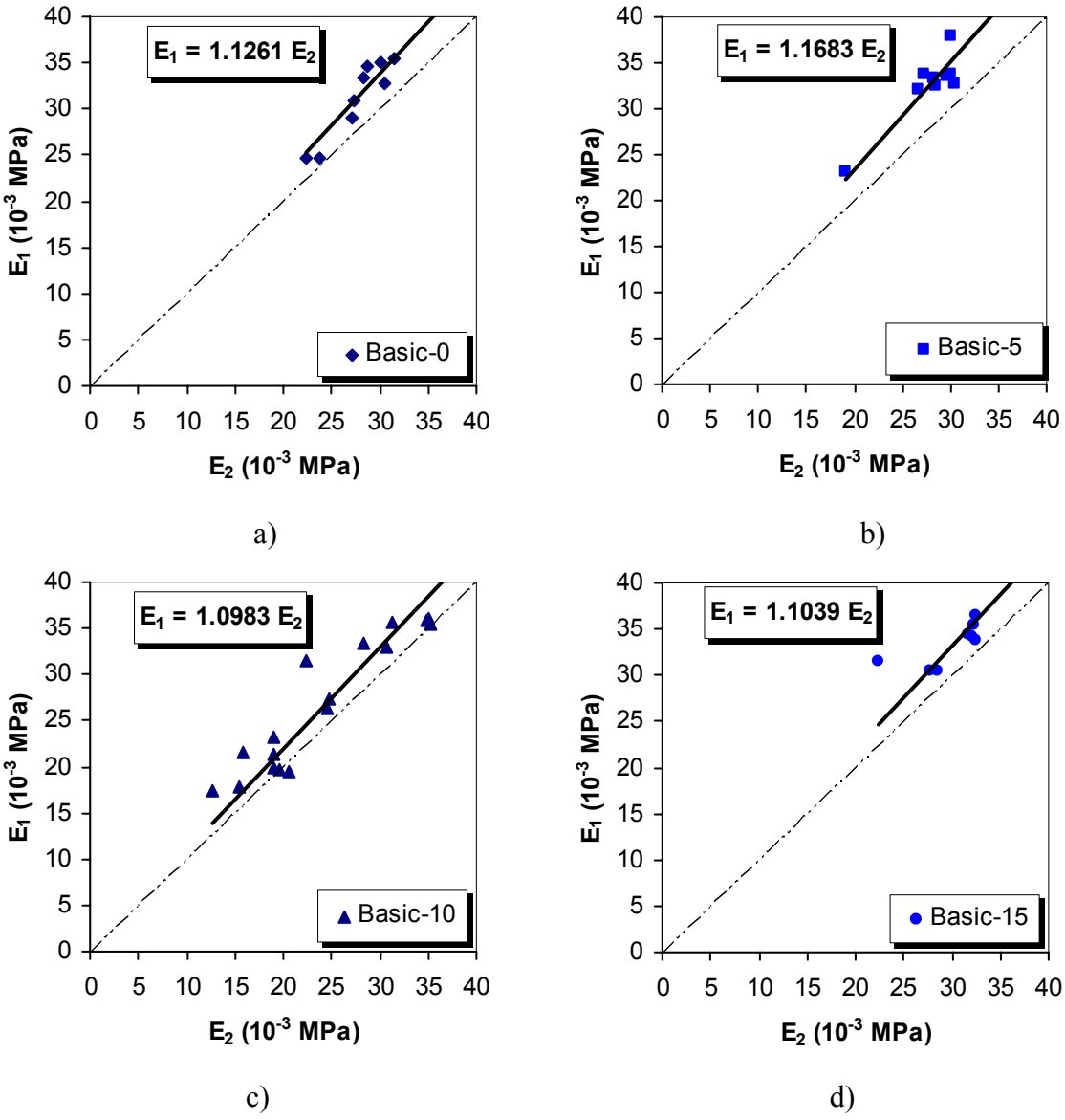

Figure 5.6 Ratio between the modulus of elasticity for BASE-5 concrete during the loading in first cycle (E_2), and during the unloading in third cycle (E_1) in Figure 5.4, T=20 ^{o}C.

All tests with results in both compression and tension are compiled in Figure 5.7. The figure shows that the E-modulus in tension E_t (equal to E_1, determined by following the standard procedure) is about 11% higher than E_2, which represents the compressive E-modulus (E_c) at early ages at first loading. With this result it is reasonable to conclude that the modulus of elasticity in tension is about 11% higher than the modulus of elasticity in compression for the investigated concrete mixes. These results corresponds well to the investigation of Onken and Rostasy (1995) and Hagihara *et al.* (2002), who concluded that the modulus of elasticity

determined in tension is approximately 15% and 7-18% higher than in compression due to less non-linearity in tension, respectively.

The difference between the E-modulus in tension and compression might have several reasons, among others:

- Different σ-ε relation in tension and compression, beyond the initial tangent relation.
- Different load magnitudes imposed to the concrete in the different directions.
- Test procedure.

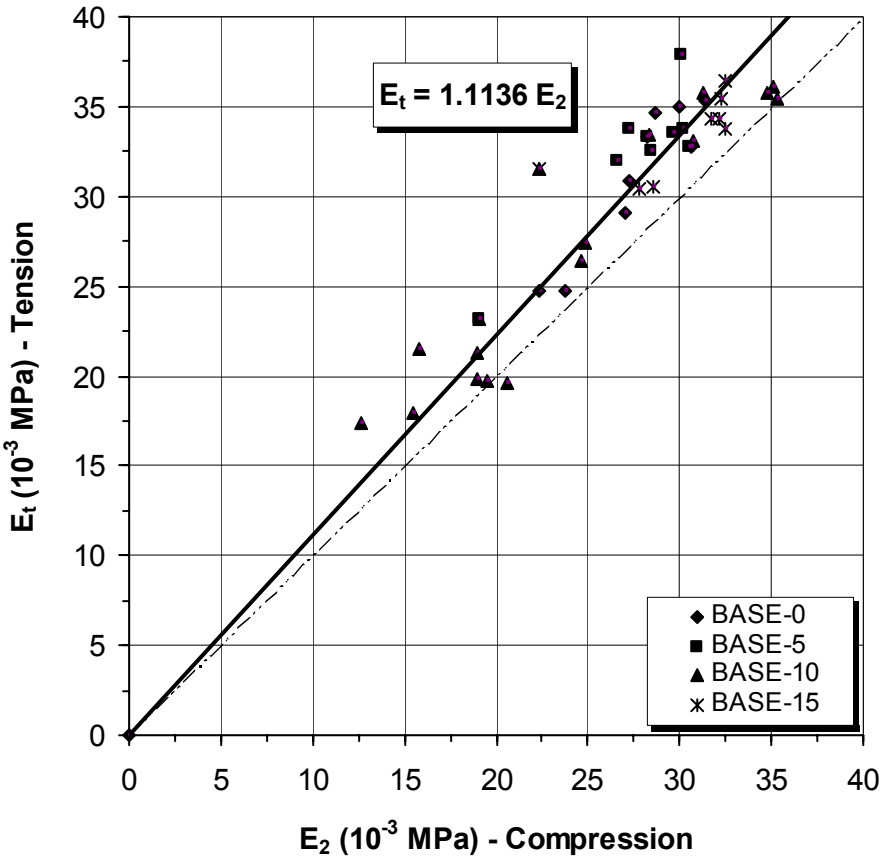

Figure 5.7 Ratio between the modulus of elasticity in tension and in compression, for concretes with silica fume contain 0-15%.

5.3 Comparison Between Creep Properties in Tension and Compression

Due to the reasons mentioned earlier in Chapter 3, in contrast to creep in compression, little attention has been paid to the viscoelastic behaviour of concrete in tension and thus the relation between creep in compression and tension is still not quite clear. From the limited data that are available in the literature on comparative test results on creep, different relation between tensile creep and compressive creep can be found. Thus reliable statements about creep in tension are difficult to find in the literature.

In this section the influence of age at load application on creep is studied, and the results of both tensile and compressive creep tests are presented. Several parallel tests on both tensile creep and compressive creep have been performed under nearly the same conditions. For each single test five cylinders were cast from the same concrete batch, three for compressive creep test and two for tensile creep test. In addition, three (or six) cubes were cast and tested for compressive strength. The evaluation of the test results emphasizes the comparison between the time dependent material behaviour under compression and tension, in terms of magnitude and rate. Tests are conducted on two concrete mixes, the reference concrete BASE-5 and the Maridal concrete. The mix properties are listed in Table 4.1 and Table 4.2.

According to G. Westman (1999) the creep response of early age concrete, during the three days after load application, is the most important part of the creep spectra. Some of the tests performed here are also conducted for only three days.

3.2.4 Creep in compression

Three series of creep tests in compression were conducted in the compressive rigs described earlier in Chapter 4, and presented in Appendix A. Creep in compression has been measured at different ages of loading (1, 2, 3, 4, 6 and 8 days). Totally 18 tests were performed, and their results are summarized in this section and some of them shown in Appendixes B and C. For each test three specimens with dimension of 150x300 mm are used. Two specimens were loaded to measure the total load-dependent deformation and the third one was kept unloaded to measure the load-independent deformation, which represents autogenous shrinkage in this case. A detailed description of the test specimens, measurement devices and testing procedure is given in Chapter 4.

The results of typical tests on compressive creep are presented in Figure 5.8 - Figure 5.15.

Figure 5.8 shows the measured strains as a function of time for a creep test where two specimens were loaded at 48 hrs concrete age, and the third one was left unloaded. In each diagram four nearly parallel curves representing three strain gauge measurements on each specimen and the average of them. The results reveal a good agreement between the measurements of the total strains of the loaded specimens 1 and 2, which confirms the centricity of the loads on the two specimens. The measured total strain is the sum of the elastic and the time-dependent strains in addition to the load-independent strains. The minus sign on the ordinate indicates that the strains are compressive. The load-independent strain in

the figure represents autogenous shrinkage since the specimens are sealed and the test is carried out under isothermal condition.

Figure 5.8a-b show also the loads applied to the two specimens. The specimens were individually loaded in a monotonic way to the their respective loading levels. The breaks in the curves are due to reduction in oil pressure in the loading system, and then the adjustment of the loads to their initial load levels. The applied load is 399 kN, where it reduces to 391 kN and 382 after 4.7 days loading for specimen 1 and 2 respectively. These are the maximum deviations from the initial pressure, and they correspond to about 2.5 to 4% variation in initial stress. For the other compression tests the load variation interval is about 1.5 to 4% depending on the load level and its adjustment time.

The specimens were unloaded after 12 days loading time. As can be seen in the diagrams, there is a good consistent in the measurements of strain recovery in each specimen. A good harmony between the strain measurements in the same specimen and also between the measurements of the two different specimens is apparent.

Development of autogenous shrinkage, measured on specimen number 3, is shown in Figure 5.8c. The magnitude is small compared to the load-dependent deformation, but it is known that the effect of shrinkage on creep is to greatly increase its magnitude. The development of creep strains is estimated by subtracting the autogenous shrinkage from the total measured strains in line with common convention, shown in Figure 5.9. The agreement between the results of the two specimens is very good.

According to Figure 5.6b the compressive E-modulus for BASE-5 concrete E_1 is 17% higher than E_2. Using the material parameters listed in Table 5.1 the theoretical modulus of elasticity $Ec(t)$ in Eq. 5.1 is the same as E_1. To calculate E_2 the E-modulus $E_c(t)$ has to be reduced by 17%. For the actual compressive creep test the calculated elastic strain ($1/E_2$) pr. unit stress is $43 \cdot 10^{-6}$ m/m, shown in Figure 5.10. For the other tests the values of E_2 are summarized in Table 5.3. In addition, the applied stresses on the concrete specimen, the calculated elastic strain at loading age are also listed in the table. Unfortunately, there are not sufficient data in the first minutes of the compressive creep tests, and therefore no comparison to the theoretical elastic strains can be made.

Table 5.3 Theoretical data related to compressive creep tests.

Age of loading	**E-modulus**	**Applied Load**		**Elastic strain**	
	$\mathbf{E_2}$	**P**	$\boldsymbol{\sigma_c}$	$\boldsymbol{\sigma/E_2}$	$\mathbf{1/E_2}$
[day]	$[10^{-6} \cdot \text{MPa}]$ [1]	[kN]	[MPa]	$[10^{-6}]$	$[10^{-6}/\text{MPa}]$
1	19.2	181	10.2	531	52
2	23.5	290	16.4	698	43
3	25.0	403	22.8	911	40
4	25.9	439	24.8	959	39
6	26.9	395	22.4	831	37
8	27.5	523	29.6	1076	36

[1] Calculated values according to Eq. (5. 1) multiplied by 1.17, according to Fig. 5.5b.

a) Specimen No. 1

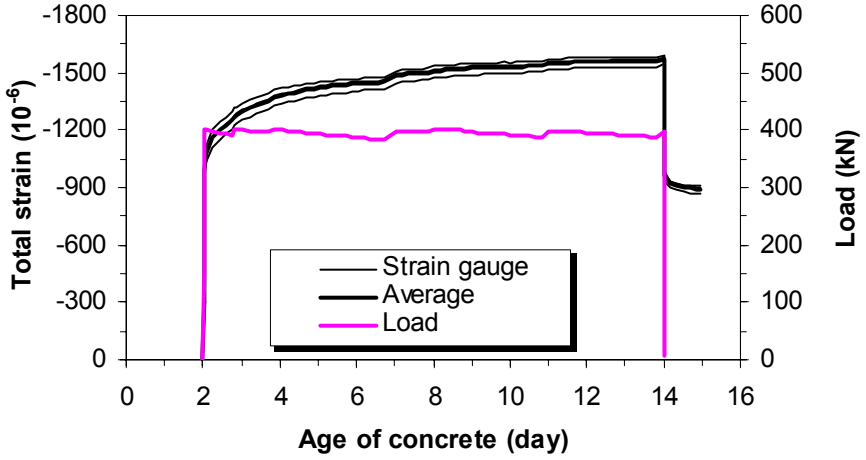

b) Specimen No. 2

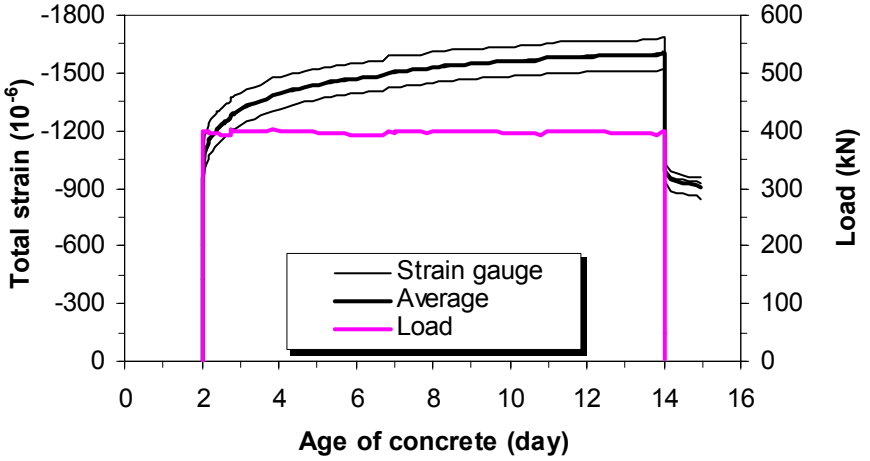

c) Specimen No. 3

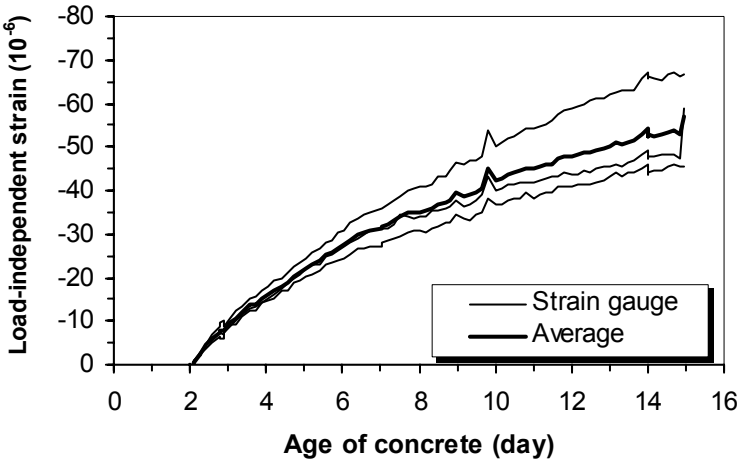

Figure 5.8 Compressive creep measurements on 2-days old concrete specimen under sealed condition (RH=50% and T=20 ^{o}C in room, Test C102).

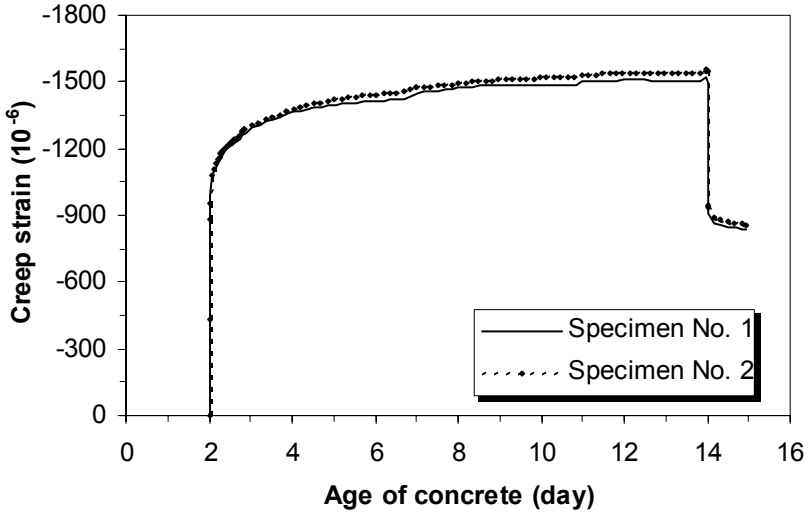

Figure 5.9 Total elastic plus creep strain in each specimen (RH=50% and T=20 ^{o}C in room, Test C102).

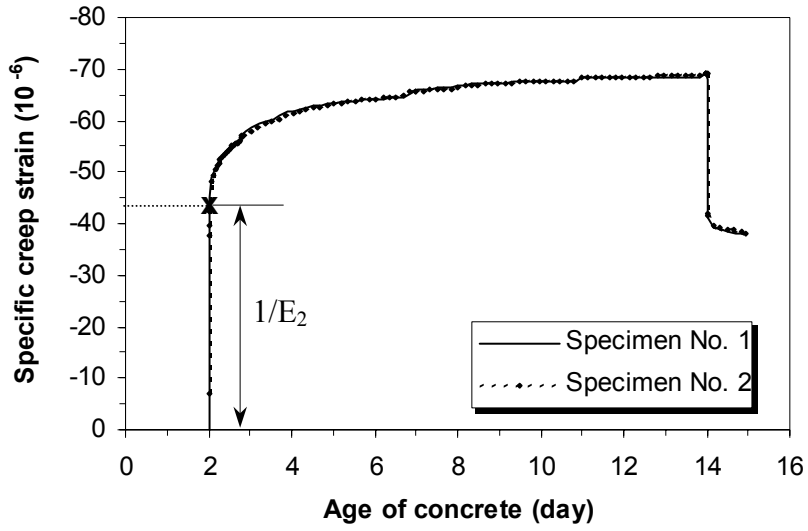

Figure 5.10 Specific creep results from compression creep test for a concrete loded at two-day age (RH=50% and T=20 ^{o}C in room, Test C102).

As stated earlier, the stress applied on the specimen is 40% of the cube strength at the loading age. In the Table 5.3 it is noticeable that the load applied on 6-days age concrete is lower than the load applied on 4-days old concrete. The reason is simply the low compressive strength measured for the concrete after 6 days curing.

The results of several other tests at different loading ages are separately presented in Figure 5.11 and Figure 5.12. The thermal conditions and the relative humidity in the test room are

nearly the same for all the tests. The test duration varies somewhat, but the creep trend is obvious in each single test measurement. The applied load on the specimen for one of the tests at each loading age is also shown in the figures. The load history is almost the same also for the other tests performed at the same loading age, but the duration of loading time might be different for different tests. Performance of several tests at each loading age confirms the reproducibility of the test results, and thus the accuracy of the creep apparatus.

For the three creep tests loaded at 1-day old concrete, the creep rates are quite different the first day, but they approach the same value with time. The same behaviour is also observed in the tests on 2- and 3-days old concrete. On the other hand, creep for the tests at each loading ages of 4, 6 and 8 days have the same rate from the beginning but different elastic strain at 8 days loading age. This observation indicates that concrete's viscoelastic behaviour, is much more sensitive at the ages lower than 2 days than at the older ages. The figures reveal also that the magnitudes of specific creep strains at each loading age are in good accordance with each other.

Some of the specimens at loading ages of 1, 2 and 3 days were unloaded after they have been loaded for few days. Due to the stiffer material at the age of unloading than the age of loading, a lower instantaneous strain is observed. The creep recoveries reveals a good agreement between the tests can be observed.

a) Age at loading is 1 day

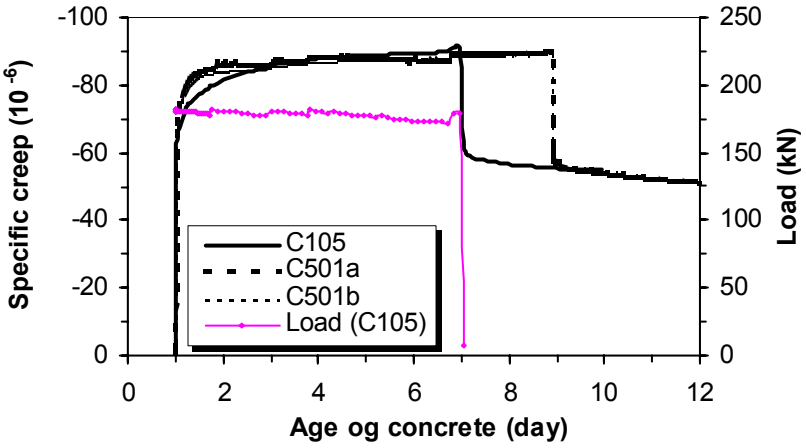

b) Age at loading is 2 day

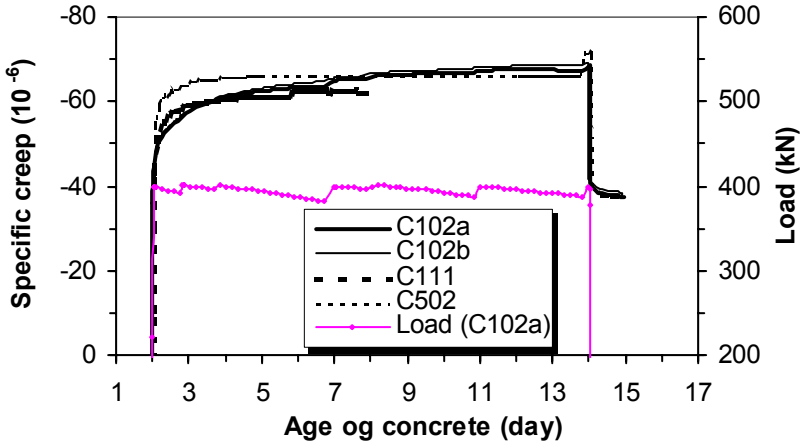

c) Age at loading is 3 day

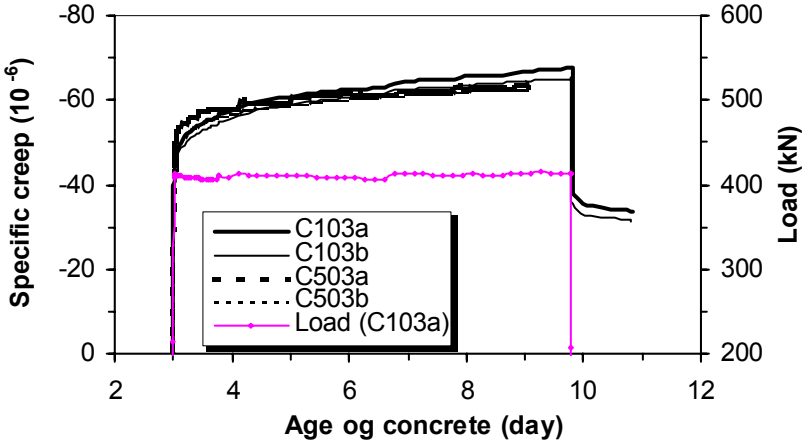

Figure 5.11 Specific creep strains from compression tests for BASE-5, T=20 °C. Applied load is 40% of strength at loading age: a) 10.2 MPa, b) 16.4 MPa and c) 22.8 MPa.

a) Age at loading is 4 days

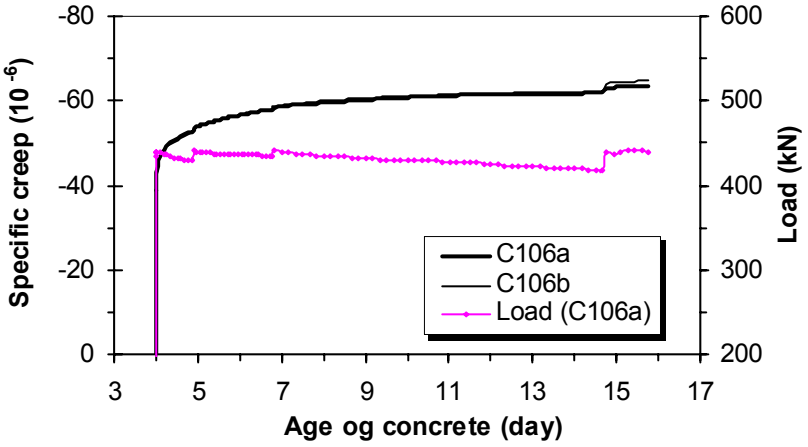

b) Age at loading is 6 days

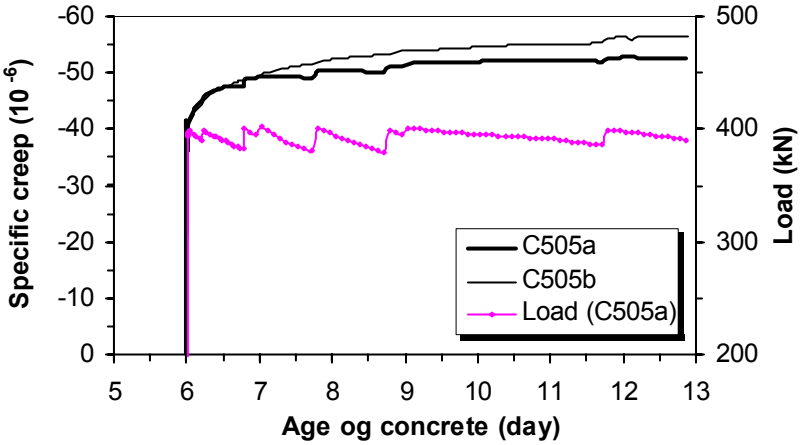

c) Age at loading is 8 days

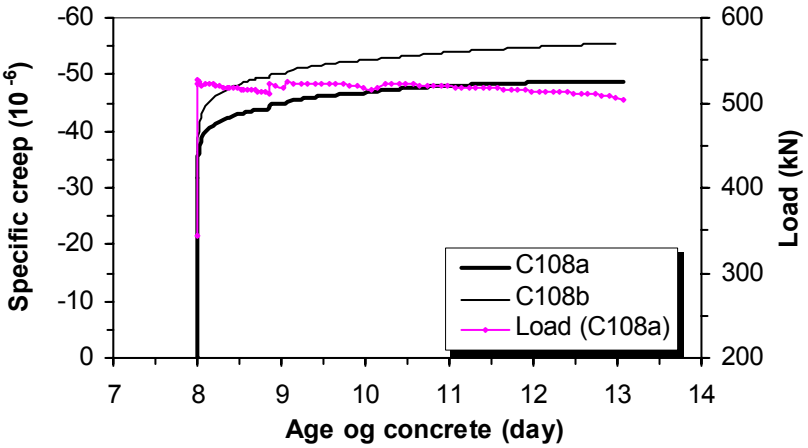

Figure 5.12 Specific creep strains from compression tests for BASE-5, T=20 °C. Applied load is 40% of strength at loading age: a) 24.8 MPa, b) 22.4 MPa and c) 29.6 MPa.

URN:NBN:no-3377

The overall results of these tests are summarized in Figure 5.13, where the development of specific creep with time, for different loading ages, is compared. The calculated elastic deformations ($1/E_2$) are also given, indicated by dots in the figure. It shows a higher measured elastic strain than the calculated one at one-day age concrete - an indication to uncertainty regarding the strains under loading. The figure shows that creep magnitude increase with a decrease in the age at application of load, and that the rate of creep during the first day under load is greater for concrete loaded at an early age than for concrete loaded later. The curves indicate that the creep rate after about 3 days loading (t-t'=3 days) are nearly parallel to each other for the short period of time studied.

A relatively high creep response when concrete is loaded at 24 hrs after casting, and a far stiffer response after 2 days are the two main observations in the tests. These observations are in accordance with earlier finding by Østegaard *et al.* (2001), Bisonette *et al.* (1995) and Umehara *et al.* (1994).

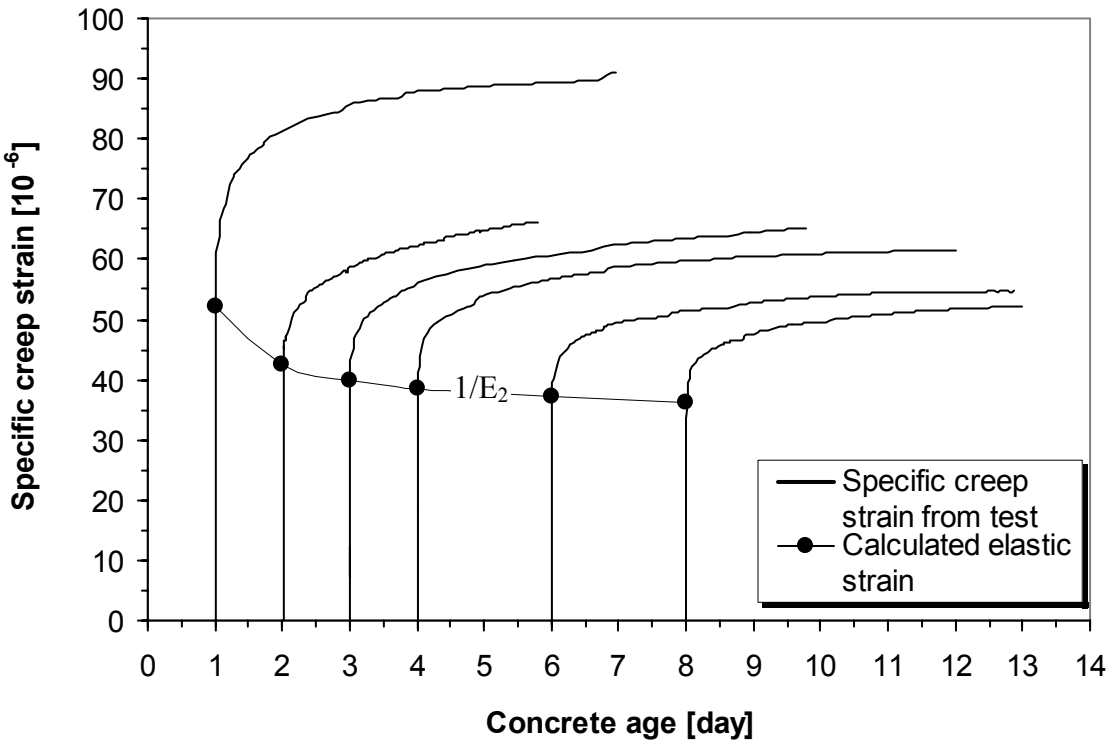

Figure 5.13 Compressive creep development for BASE-5, at different loading ages. T=20 ^{o}C, applied load is 40% of strength at loading age.

The second series of compressive creep tests are performed on Maridal concrete described in Chapter 4. Unlike the case in BASE-5, all the specimens used in the tests were poured from the same concrete batch. The specimens were kept under the same curing conditions (sealed)

before and during the tests. Two creep tests were performed at each concrete age of 2, 3 and 6 days. In addition, two tests on compressive strength and modulus of elasticity for this concrete mix were conducted at the respective loading ages, see Table 5.4. Test No. 2 was performed about one hour after test No. 1. As in BASE-5 concrete, the results show a higher E-modulus (E_1) determined from the unloading part of the step 3 than the E-modulus (E_2) determined from the loading part of the step 1, see Table 5.4. The ratio between E_1 and E_2 varies in the range of 1.14 - 1.32. The table shows that the ratio E_1/E_2 decreases with concrete age, except for the age of 3 days. The reduction demonstrates lower irreversibility with time.

Table 5.4 Testing data on compressive E-modulus for Maridal concrete.

Age [day]	Test No. 1				Test No. 2			
	f_{cc} [MPa]	E_2 [Gpa]	E_1 [Gpa]	E_1/E_2	f_{cc} [MPa]	E_2 [Gpa]	E_1 [Gpa]	E_1/E_2
2	30.24	24.46	29.64	1.21	30.37	24.22	30.64	1.27
3	36,86	26.72	35.29	1.32	35.74	29.22	37.63	1.29
6	42,74	28.56	34.13	1.20	43.37	31.36	35.96	1.15
30	56,99	35.95	41.44	1.15	59.49	37.55	42.99	1.14

f_{cc}: Cylindrical concrete strength.
E_1: E-modulus from the unloading part of the step 3.
E_2: E-modulus from the loading part of the step 1.

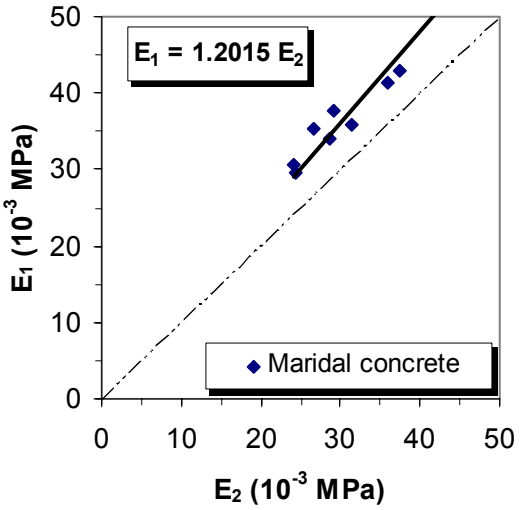

Figure 5.14 Relation between the modulus of elasticities in tension ($E_1 = E_t$) and compression ($E_2 = E_c$) for Maridal concrete at T=20 °C.

The test results are plotted in Figure 5.14, where they give an average E_1/E_2-ratio of about 1.20, which is higher than the ratios observed for BASE concretes which were 1.11 to 1.17.

Figure 5.15 shows results of the tests, two tests at each loading age given by two thin curves and the mean value of the tests represented by a bold curve. It shows a scatter in the test results within the same loading age for all the 3 tests, which might be an indication that at each loading age more than one test are needed to establish the creep behaviour of the current concrete type. The figure reveals also that the same observations on the creep tests on BASE-5 concrete can also be observed in Maridal concrete; a higher creep response at lower loading ages, and a stiffer response as concrete become older. Detailed test results are given in Appendix C.

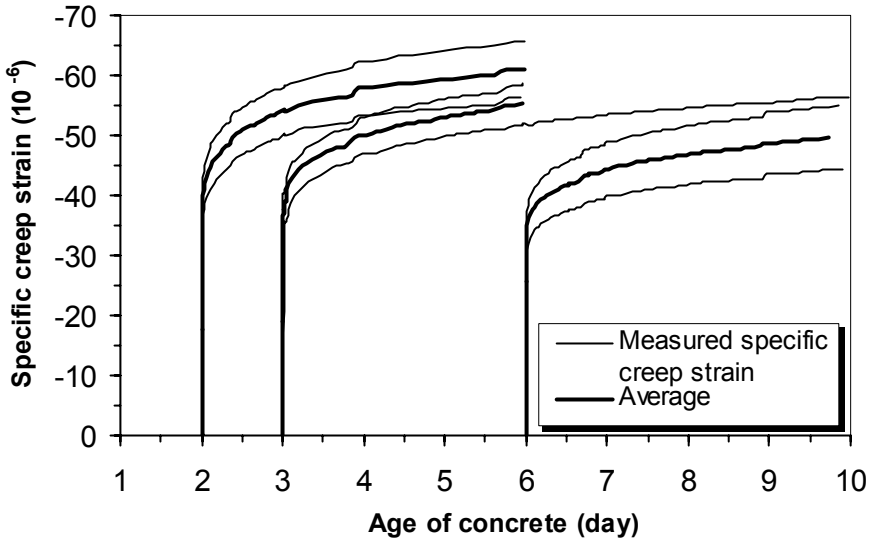

Figure 5.15 Development of creep strains pr. unit stress in compression for Maridal concrete, T=20 °C. Stress/strength ratio at loading age is 40%.

Table 5.5 Data on Maridal concrete.

Age of loading	**E-modulus**	**Applied Load**		**Theoretical elastic strain**	
	$\mathbf{E_1=E_c}$ [1]	**P**	$\boldsymbol{\sigma_c}$	$\boldsymbol{\sigma_c/E_c}$	$\mathbf{1/E_c}$
[day]	[GPa]	[kN]	[MPa]	(10^{-6})	(10^{-6}/MPa)
2	27.8	277	15.7	641	36.0
3	31.3	341	19.3	723	31.9
6	35.9	429	24.3	850	27.8

[1] Calculated values according to Eq. (5. 1).

Table 5.5 shows some of the data related to the theoretical elastic strains for the creep tests. The elastic strain is estimated as the inverse of the relevant modulus of elasticity (E_c) calculated by Eq. (5. 1). Curves for mean creep values, denoted average, together with the curves for both E_1 and E_2 are shown in Figure 5.16. The E-modulus E_2, which in average is calculated to be 20% less than E_1, seems to be in consistent with the measured instantaneous deformation for 2- and 6-days loading ages, but somewhat higher for 1-day loading age. As

known, the E_2 represents exactly the same loading procedure (first loading) as used in the creep tests in Figure 5.16.

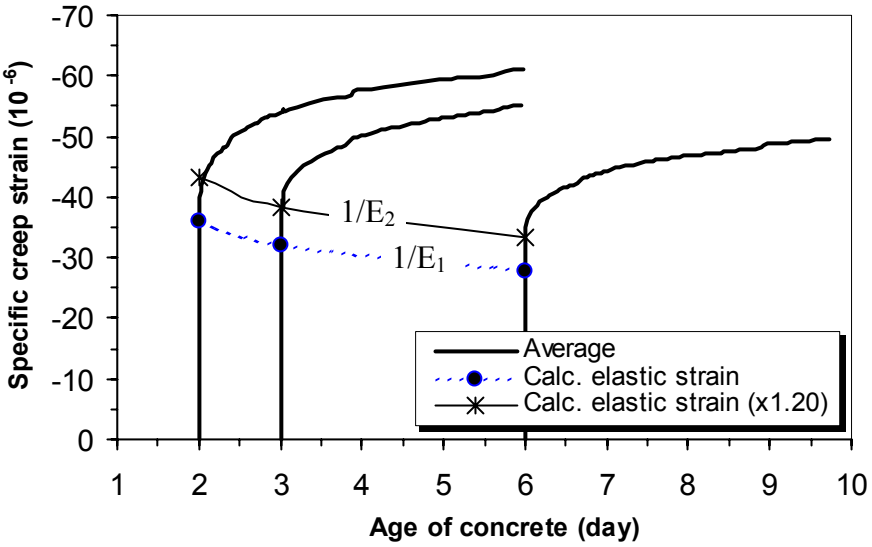

Figure 5.16 Specific creep strains and calculated instantaneous deformations in compression for Maridal concrete, T=20 °C. Stress/strength ratio at loading age is 40%.

3.2.5 Creep in tension

As previously mentioned, 25 parallel concrete tests on tensile creep were performed in the tensile creep rig described earlier in Chapter 4, with the loading age as the only variable. The test results are summarized in this section and fully shown in Appendix D. For each test two sealed specimen with dimension of 103x425 mm were used. One specimen was loaded to measure the total load-dependent deformation and the second one was kept unloaded to measure the load-independent deformation, which represents autogenous shrinkage in this isothermal case. A detailed description of the test specimens, measurement devices and testing procedure is given in Chapter 4.

The results of the tensile creep test on one-day old concrete specimens (BASE-5 concrete) are presented in Figure 5.18. The applied tensile stress level is 1.29 MPa, and it corresponds to a stress level, which is 40% of the uniaxial tensile strength at the loading age. The manual loading process and the concrete response, automatically recorded by three LVDTs, are illustrated in Figure 5.17. The different break-points on the curves indicates different loading actions during the loading process, in which each action takes short time to be performed. As can be seen there is a good correspondence between the applied loads and the deformations. The loading time for the current test was about 3 minutes.

Figure 5.18-a shows simply the automatically recorded results from the loaded specimen, while Figure 5.18-b shows results from the unloaded specimen. The three curves in each

diagram represent the three LVDT measurements on each specimen. In general the agreement is satisfactory. The small deviation between the curves in the figure indicates that the eccentricity of the loading is small.

The total deformations are compensated for the load-independent deformations measured on the dummy specimen, producing the creep strains (initial elastic- plus time-dependent strains) shown in Figure 5.18-c. The corresponding relation in terms of creep compliance (creep strain per unit stress) is shown in Figure 5.18-d. This curve shows that the rate of creep is high in the beginning, and then reduced to a nearly constant rate.

Figure 5.18a shows clearly that soon after instantaneous elongation of the specimen due to the load, the autogenous shrinkage dominates the deformation process and the specimen contracts even under tensile load. As is well known, the phenomena involved in time dependent deformations are not independent of each other, but even so, independence has also been assumed here. In contrast to the compressive creep tests, the load-independent deformations in tensile creep tests are in the same order of magnitude as the load-dependent deformations, and thus the former has always a dominant influence on both the magnitude and the rate of the creep development. The question, which arises here, is whether this approach is valid to determine tensile creep. This is a fundamental question, which is recognized and discussed further later.

The estimated E-modulus by Eq. (5. 1), the elastic strains, the applied load and stresses for the tests at different loading ages are listed in Table 5.6. The E-modulus value at 28-days for the equation is given in Table 5.1.

Table 5.6 Data related to tensile creep tests.

Age of loading	**E-modulus**	**Applied Load**		**Theoretical elastic strain**	
	$\mathbf{E_1=E_c}$ [1]	**P**	$\boldsymbol{\sigma_c}$	$\boldsymbol{\sigma_c/E_c}$	$\mathbf{1/E_c}$
[day]	[MPa]	[kN]	[MPa]	(10^{-6})	(10^{-6}/MPa)
1	22.5	10.7	1.29	57	44
2	27.5	14.1	1.70	62	36
3	29.3	15.4	1.85	63	34
4	30.3	16.2	1.94	64	33
6	31.5	17.1	2.05	65	32
8	32.2	17.6	2.11	66	31

[1] Calculated values according to Eq. (5. 1).

Several creep tests were performed at 1, 2, 3, 4, 6 and 8 days age concrete, and the specific creep for the tests are presented separately in Figure 5.19. For each loading ages 1, 2 and 6 days, the results of 2 tests are shown, and for each loading ages 3, 4 and 8 days the results of respectively 3, 4 and 1 tests are presented. The appearance of some deviations between the repeated test results for each of the loading ages is expected when so many aspects and mechanism are involved in testing, but the creep curves points to the same behaviour. By getting more experience in loading process with time, the loading time was reduced to less than one minute for latest creep tests performed.

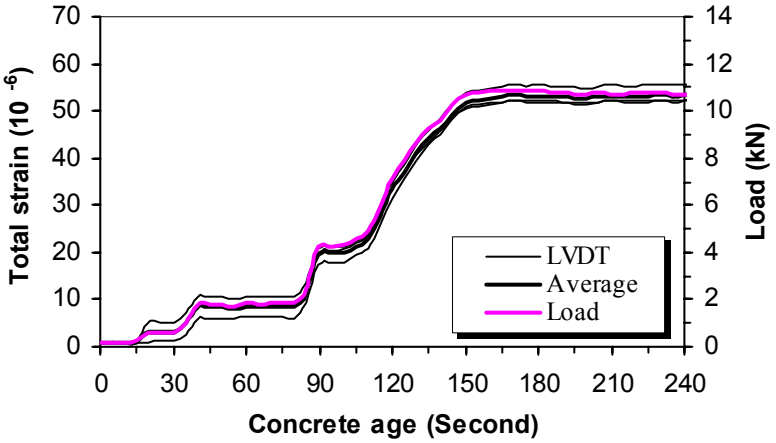

Figure 5.17 Loading and measured strain during a tensile creep test on one-day old BASE-5 concrete, with load level 1.29 MPa and at 20 °C, (T105).

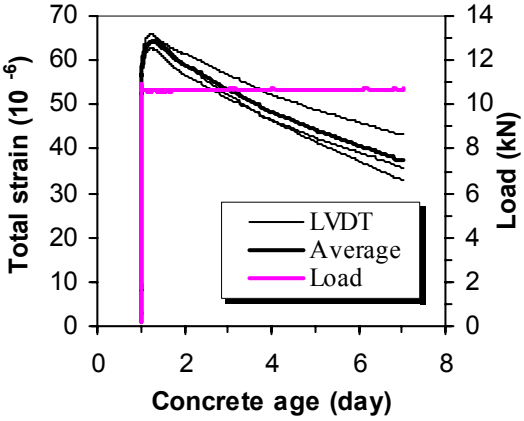

Measured strains and load on loaded specimen

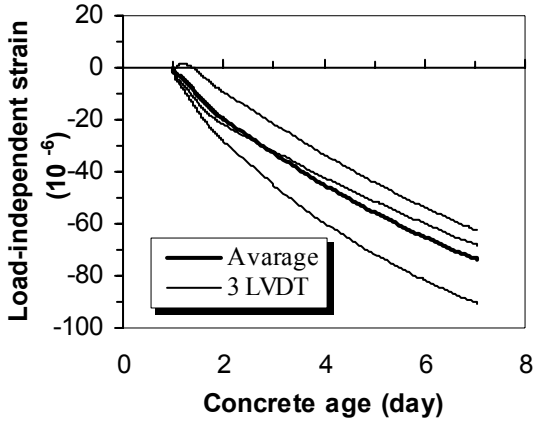

Measured strains on unloaded specimen

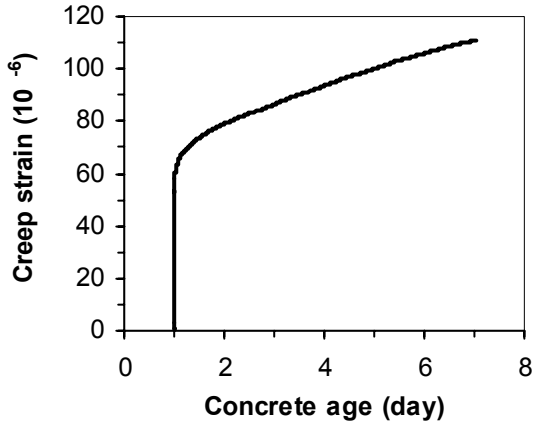

c) Load-dependent strains

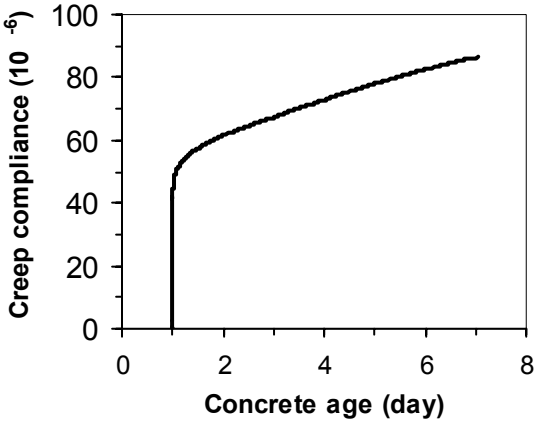

d) Specific creep

Figure 5.18 Measured deformations from tensile creep test on one-day old BASE-5 concrete, with load level 1.29 MPa and at 20 °C, (T105).

URN:NBN:no-3377

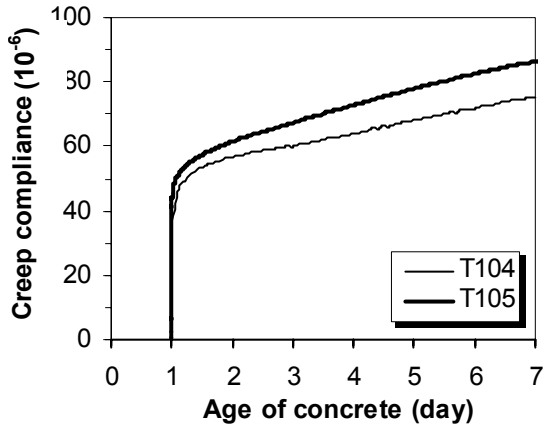

a) Loading at 1-day old, 1.29 MPa.

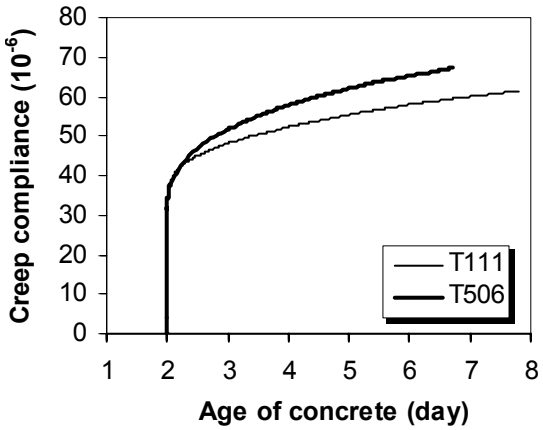

b) Loading at 2-days old, 1.70 MPa.

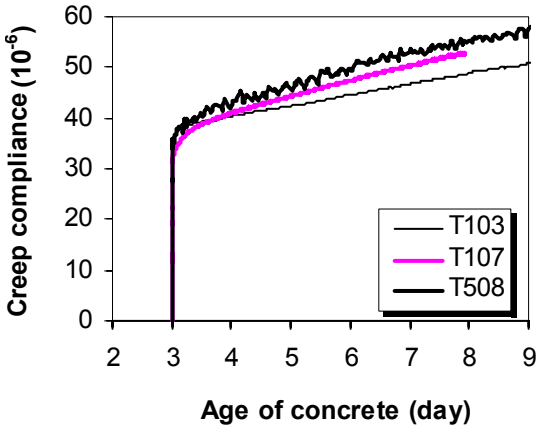

a) Loading at 3-days old, 1.85 MPa.

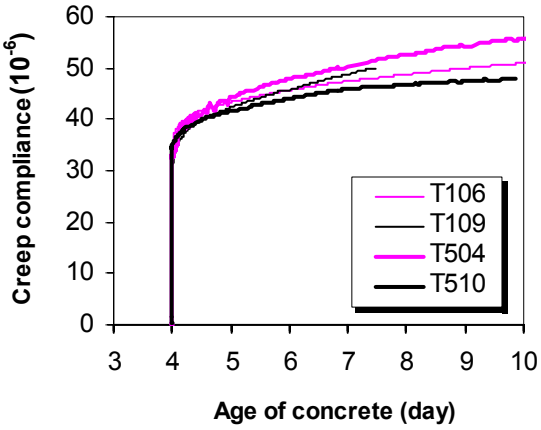

b) Loading at 4-days old, 1.94 MPa.

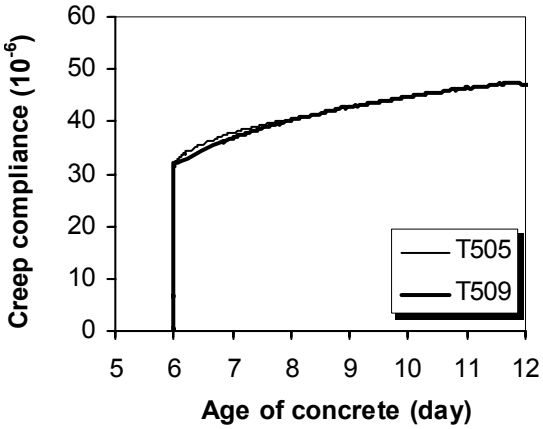

a) Loading at 6-days old, 2.05 MPa.

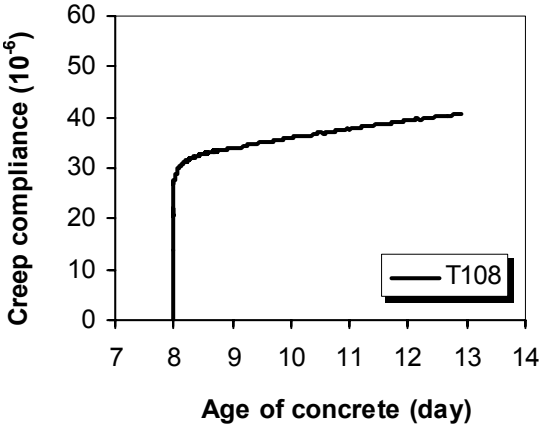

b) Loading at 8-days old, 2.11 MPa.

Figure 5.19 Specific tensile creep deformations due to different loading ages, BASE-5 concrete, at 20 °C.

Taking the mean value of the tests for each loading age, the creep development shown in Figure 5.20 is found. In other words, each curve on the figure represents the average results of several tests. As for creep in compression, the concrete age at application of load obviously has a major influence on the value of the deformation due to tensile creep. The same effect on creep rate is also pronounced in the figure. The calculated elastic strains based on E-modulus (E_1) are also given in the figure. The measured elastic strains are somewhat higher than the calculated one at ages of 6 and 8 days.

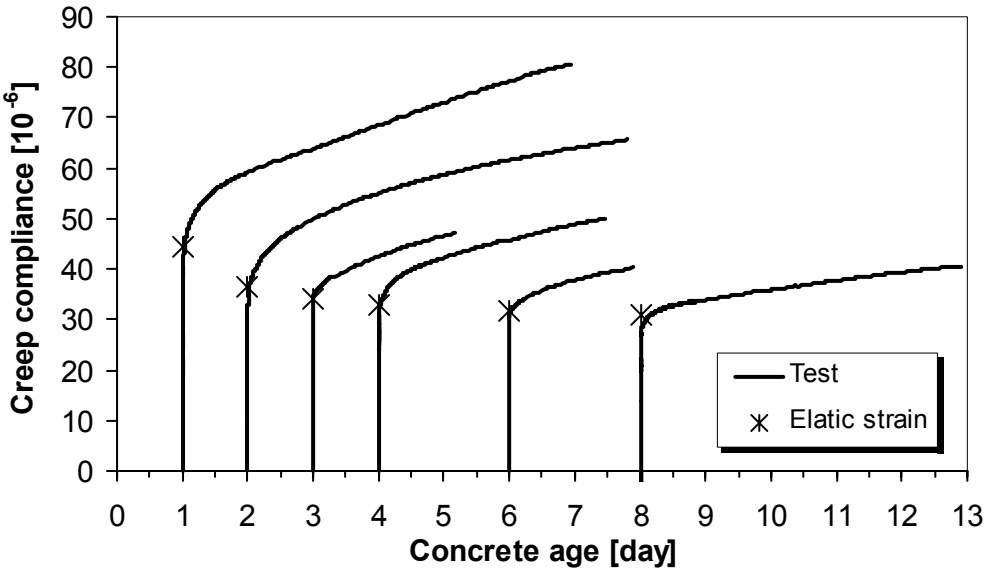

Figure 5.20 Tensile creep strains from tensile tests for BASE-5 concrete, T=20 ^{o}C. Stress/strength ratio is 50% at loading age.

For Maridal concrete only one tensile creep test at age of 2 days was performed, and the results are shown in Figure 5.21 and Figure 5.22. The calculated elastic strain is $36.0 \cdot 10^{-6}$ m/m. The earlier description concerning Figure 5.18 (BASE-5) applies also here, and will not be repeated again.

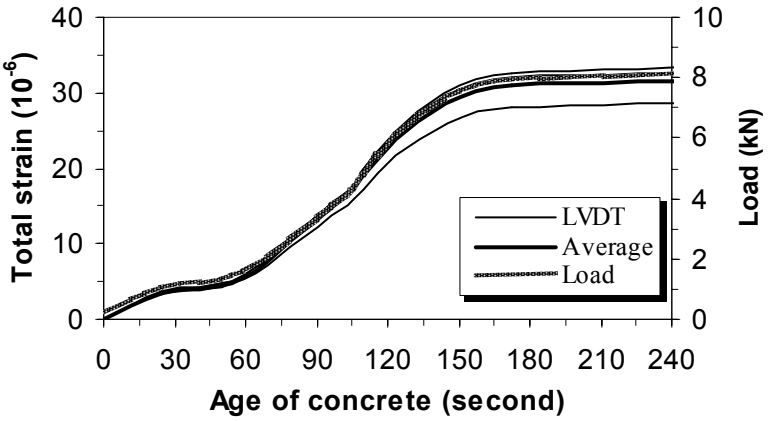

Figure 5.21 Loading and measured strain during a tensile creep test on two-days old Maridal concrete, with load level 1.37 MPa and at 20 °C, (T301).

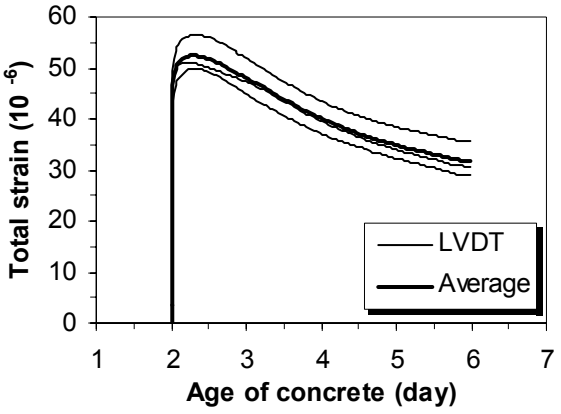

a) Measured strains and load on loaded specimen

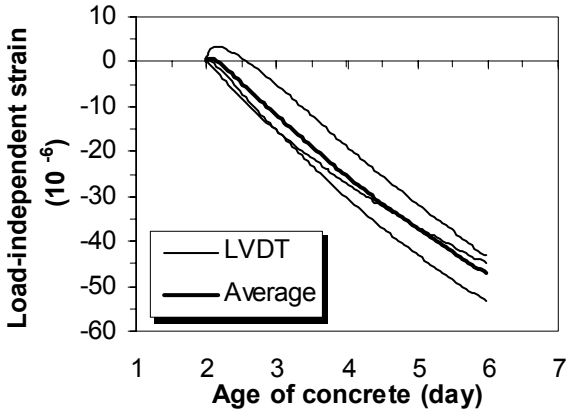

b) Measured strains on unloaded specimen

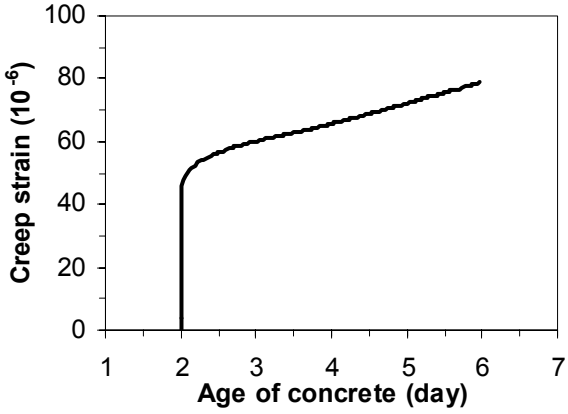

c) Load-dependent strains

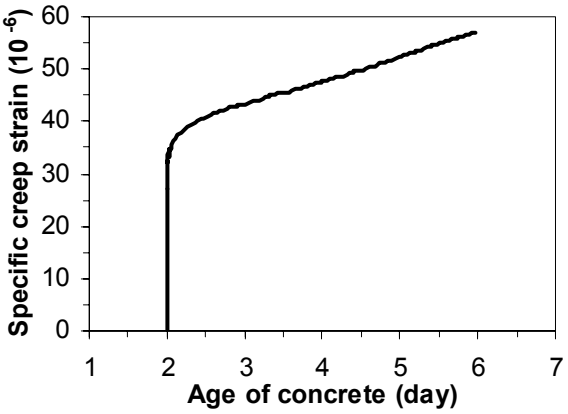

d) Specific creep

Figure 5.22 Time dependent deformations from tensile creep test on two-days old Maridal concrete, with load level 1.37 MPa and at 20 °C, (T301).

3.2.6 Comparison Between Tensile Creep and Compressive Creep

The results of the parallel creep tests in both tension and compression, discussed earlier, are compiled in Figure 5.23 and Figure 5.24 for BASE-5 and Maridal concretes respectively, where creep is presented in term of creep compliance (elastic- plus time-dependent strains, pr. unit stress). Comparing the results of tensile creep tests and compressive creep tests, the following observations can be made:

- *Instantaneous deformation;*
  Immediate response of the concretes to the imposed loads shows that the instantaneous deformation under tension tests is lower than under compression tests. The main reason is the higher E-modulus in tension than in compression, discussed earlier (see Figure 5.6b and Figure 5.14). Strange enough E-modulus in tension corresponds well with E_1 in compression, possibly because the load is much lower in tension tests than in compression, and as shown in Figure 5.4 the response during first load in compression is quite nonlinear initially.

- *Creep rate;*
  Immediate after loading and within approximately the first 24 hrs, the creep rate of compressive creep is higher than the creep rate of tensile creep. Afterwards, the creep rates decreases continually with time, but the decrease in tensile creep is much less pronounced than in compressive creep. This leads to crossing of the curves few days after loading for the current loading ages and, subsequently, a higher tensile creep than compressive creep. For instance, for the case of loading at 2 days the creep in tension becomes equal to the creep in compression after approximately 6 days loading. The experimental results show a similar tendency for other loading ages, but the crossing time becomes longer as the loading age become higher, with exception of the loading age of one day.

- *Creep magnitude;*
  A stiffer response of concrete to the imposed load in tension at loading age implies a lower creep magnitude in tension than in compression in the beginning. The difference between the creep curves reduces by time, and then the ratio between them changes to be opposite. In other words, considering compliance creep *without* instantaneous deformations, it means a higher time-dependent deformation in tension than in compression from the beginning and divergence of the curves. This difference has obvious implications for the stress relaxation in restrained specimens. The topic will be further analyzed in Chapter 6.

The influence of age on tensile creep is observed to be about the same as on compressive creep, namely that the magnitude of creep decreases with concrete age at loading. The same observation has been made in earlier studies, [e.g. Neville (1983) and Pigeon (1999)]. Note that the autogenous shrinkage of course affects tensile creep and compressive creep in opposite directions – for tension they are in opposition while in compression they are additive. Thus the difference between the tensile and compressive creep can partly be a

consequence of the compensation procedure used in Figure 5.18 and Figure 5.22. This is one of the fundamental questions in the comparison.

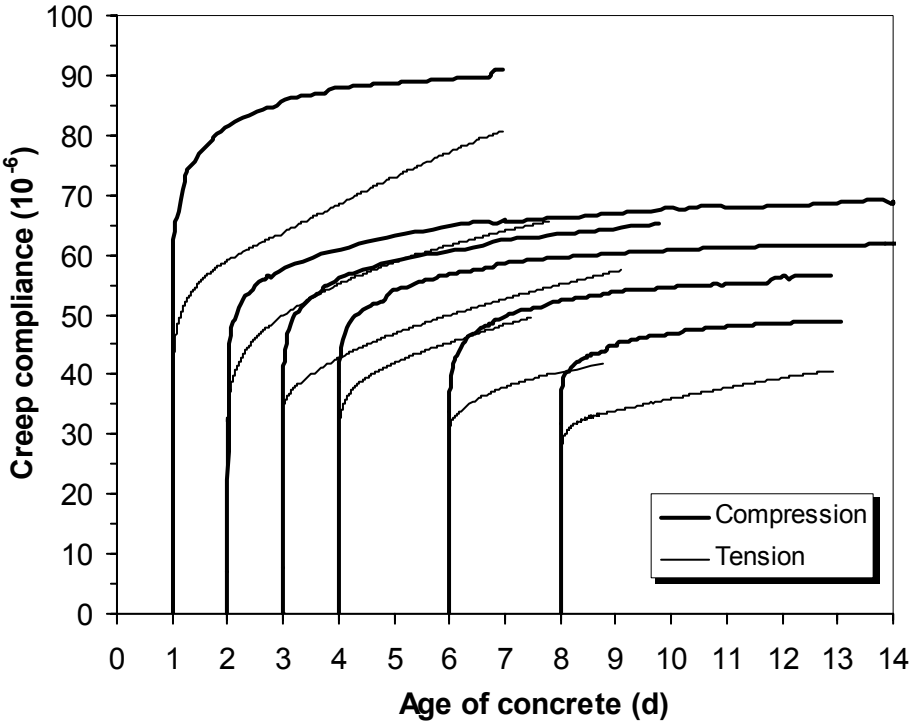

Figure 5.23 Comparison between creep in tension and compression, BASE-5 concrete, stress/strength ratio is 40% at loading age, T=20 ^{o}C.

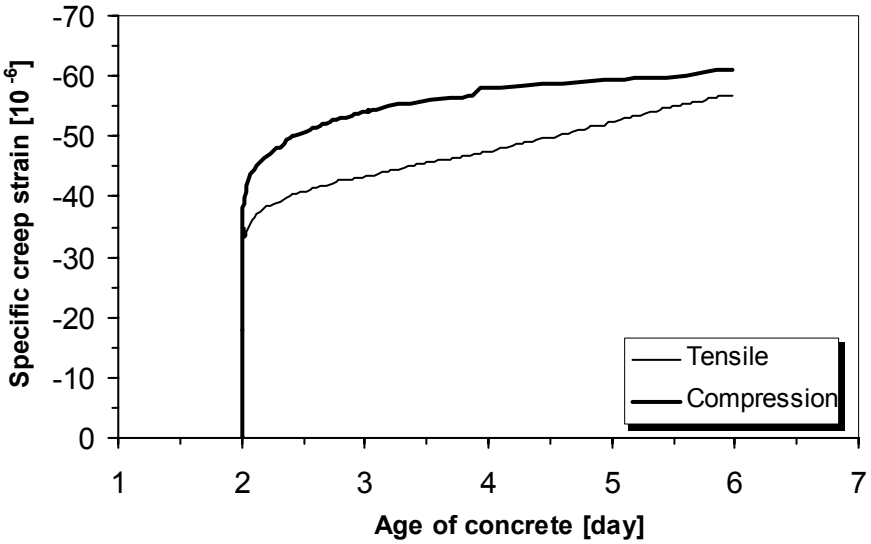

Figure 5.24 Comparison between creep in tension and compression, Maridal concrete, stress/strength ratio is 40% at loading age, T=20 ^{o}C.

Another important concrete property, which may explain, at least, some of the different behaviour in tension and compression is the strength development since creep is a function of the applied load level (normally expressed as stress/strength ratio). Figure 5.25 shows the development of stress/strength ratio (with initial ratio: 40%) under load for creep tests in tension and compression loaded at 1, 3 and 6 days concrete ages. When the applied stress on the test specimens is maintained constant, the stress/strength ratio reduces with time due to development of strength. The figure reveals faster reduction of stress/strength ratio in compression than in tension, particularly at very early ages, which again means a lower strength/stress ratio on compression specimen than in tension one at the same time, i.e. this effect implies lower time-dependent deformation in compression than tension.

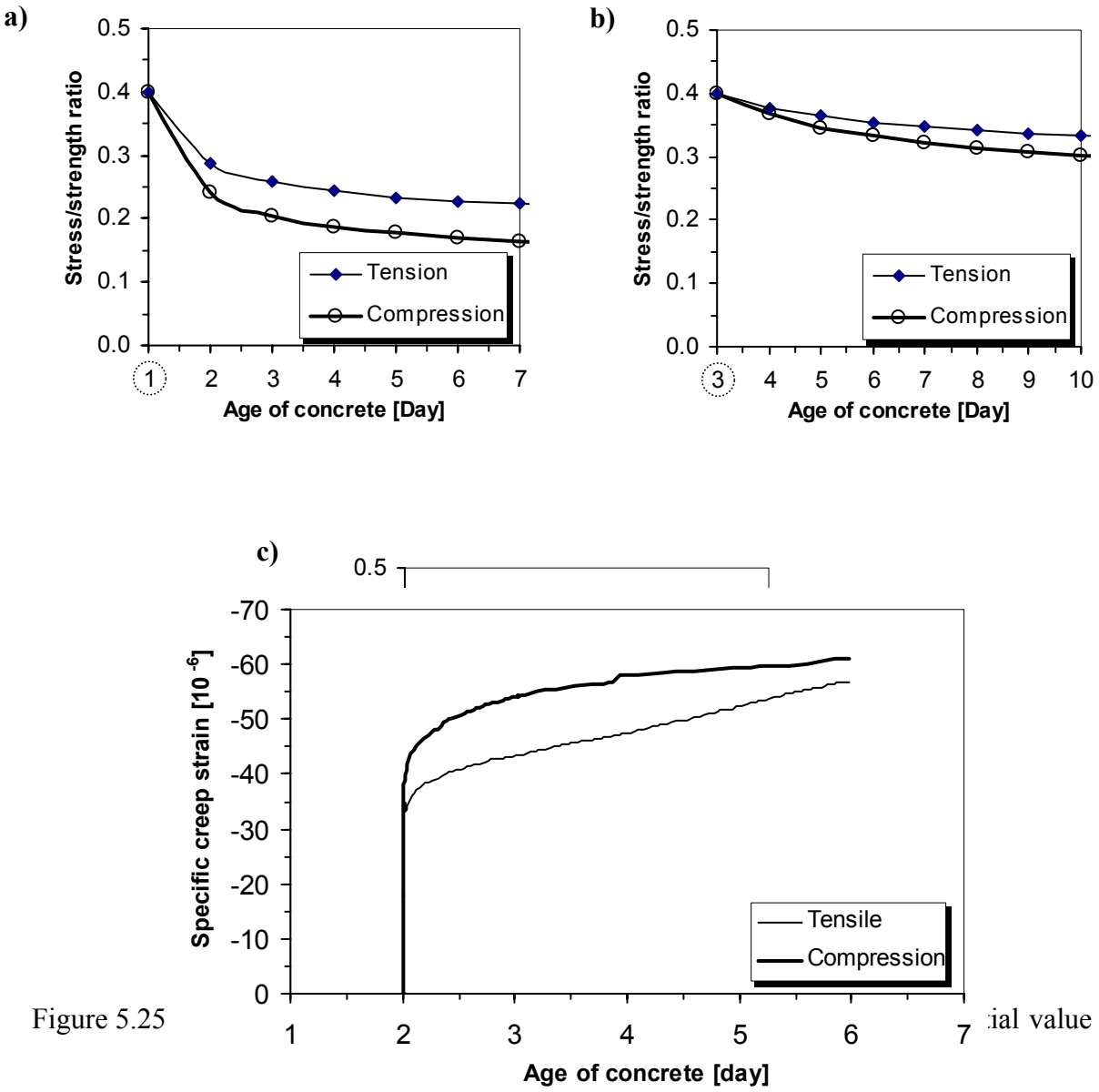

Figure 5.25 ial value

The obtained test results, with significant differences between tensile creep and compressive creep, need more documentation, and such parallel tests should therefore continue in the future. Factors contributing to the differences may be:

- The assumption of independence between autogenous shrinkage and creep strains, which means assumption of equal effect of self-desiccation in tension and compression. This is highly questionable and consequently the use of the superposition principle and indeed the very definition of creep strains are questionable.
- The faster growth of the tensile strength than the compressive strength [Neville *et al.* (1983), Kanstad *et al.* (1999), Hauggaard-Nielsen (1997) and Kasai (1971)], which results in higher stress/strength-ratio in tension than in compression with time (i.e. $\sigma_t(t)/f_t > \sigma_c(t)/f_c$).
- The modulus of elasticity in tension is 17% higher than in compression for the current concretes. The approximately same result was reported by Onken and Rostasy (1995) and Hagihara *et al.* (2002). The compressive creep curves in Figure 5.23 are the results of relative high loads, and thus E_2 is relevant. In stress calculation in Chapter 6 the compressive load level is low (about 2 MPa), i.e. due to nonlinearity (Figure 5.4) the E_2 is higher close to origin and simply equal to E_t (and therefore equal E_1) shown in Figure 5.5. The conclusion in stress calculation is therefore that always E_1 should be used, in both tension and compression.
- Different specimen size used (diameter and length).
- Different measuring length.
- Different measuring devices.
- The temperatures of the concrete specimens in the compression tests were 1–2 °C higher than the temperatures in the tensile creep tests.

5.4 Non-linearity in Tensile Creep

3.2.7 General

Only few researchers have investigated the subject of whether non-linearities appear in tensile creep, and thus it is not clear if the non-linearity in creep observed at high compressive stress levels shown in Figure 3.10 apply for tensile loading too. The figure reveals that for relative loading up to 50% of strength the creep in compression is linear, but a large non-linearity appears at higher loading.

In restrained structure members exposed to volume change the compressive stress/strength ratio is normally well below 50%, and therefore the non-linearity of creep is of less important here. However, the concern of this work is prevention of cracking, so obviously we are concerned with stress prediction up to the tensile strength, and any non-linearity will have a significant influence.

3.2.8 Experimental Procedure

In this section results of three series of tensile creep tests, conducted on the BASE-5 concrete, are presented and discussed. One of the series (Series I-B) is conducted on the original tensile creep rig and the two other series (Series II-A and Series II-B) on the upgraded tensile creep rig. The concrete specimen and the test conditions were the same as for the forgoing tests. The only variable studied here is the applied loading level.

The age at loading is 3 days, and six initial tensile load levels 0.2, 0.3, 0.4, 0.6, 0.7 and 0.8 times the tensile strength, are investigated. The mechanical properties of the BASE-5 concrete developed at the age of 3 days, based on calculated values at 28 days given in Table 5.1 and Equations 5.1 – 5.3 are:

- Tensile strength: 3.7 MPa
- Compressive strength: 47.8 MPa
- E-modulus (E_1): 29.3 GPa.

For each load level tests are repeated at least once. Totally 35 tests are conducted during this investigation, but due to the different technical problems some of the tests failed and the other are presented in Appendix E. Table 5.7 presents data on a few tests performed under stresses 20-80% of the concrete strength at loading age of 3 days. For these concretes, the applied stress, loading time and loading rate varies in ranges 0.74-2.96 MPa, 1.9-2.8 minutes and 0.29-1.16 MPa/minute, respectively.

Table 5.7 Loading data for tests in tensile creep rig, T=20 ^{o}C.

Test No.	Initial stress/strength [%]	Load [MPa]	Loading time [min]	Loading rate [MPa/min]
405	20 %	0.74	2.6	0.29
400	30 %	1.11	1.9	0.58
404	40 %	1.48	2.3	0.63
403	50 %	1.85	2.4	0.79
402	60 %	2.22	2.4	0.93
401	70 %	2.59	2.8	0.92
411	80 %	2.96	2.5	1.16

3.2.9 Results and Discussions

The loading histories applied on the concrete in the tensile creep tests with their respective stress/strength ratios are shown in Figure 5.26a. As mentioned earlier, due to the progress of hydration, the concrete strength develops fast and the actual applied load level reduces with time. The concrete specimens were unloaded at the end of the tests. The corresponding measurements of deformation on the active and the dummy specimens are shown in Figure 5.26b and Figure 5.27, respectively. Each curve represents a mean value of three measurements by LVDTs from one test.

The results on Figure 5.26b, which represents the measured total strains in the sealed loaded specimen, reveal some interesting features about early age tensile creep and the autogenous deformation. First, all the tests show creep deformations immediate after loading with an increasing rate as initial stress/strength level increase. Second, the autogenous shrinkage dominates the deformation process after the initial period in the loaded specimen for initial stress/strength ratios up to 50%, and the specimen actually contract under tensile load. Measurements on the dummy specimen represent autogenous deformation and denoted as load-independent strains in Figure 5.27. The figure reveals significant differences. In some of the curves initial expansion is recorded, which must be disturbances of the measuring devices probably due to unstable environmental conditions around the testing ring. We assume the same initial disturbances (errors) in the loaded specimen when each curve is compensated by its "own" dummy in Figure 5.27.

Figure 5.28 shows the creep deformations (elastic plus time-dependent strains) compensated for load-independent strains, noting that for each creep test its respective curve for autogenous shrinkage is used. The influence of the initial stress/strength ratio on creep compliance is shown in Figure 5.29a. It shows clearly that creep response during the time period 3 to 6 days, is proportional to initial stress/strength level up to about 70%. Higher specific creep is observed when the specimen is loaded to 80% of the tensile strength, and thus non-linearity is a fact. The same observations can be made when only the time dependent strain is shown in Figure 5.29b. The time dependent strain is considered from 1 minute after the loading is applied. i.e. the measured deformations after instantaneous deformation. The instantaneous deformation is defined as the measured deformation due to

loading in a specimen at one minute after the load has reached its intended value. The measured instantaneous deformation is compared to the theoretical values (based on E_I) for different stress/strength ratio in Figure 5.30.

To be more specific, we can say that a little non-linearity is observed already when the applied stress is under 70% of the tensile strength, an observation, which is evident in all three figures for creep.

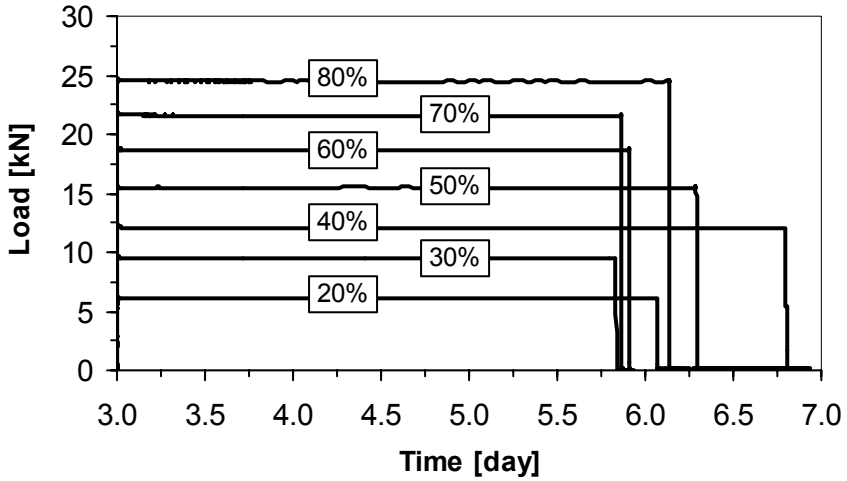

a) Load histories with the stress/strength level

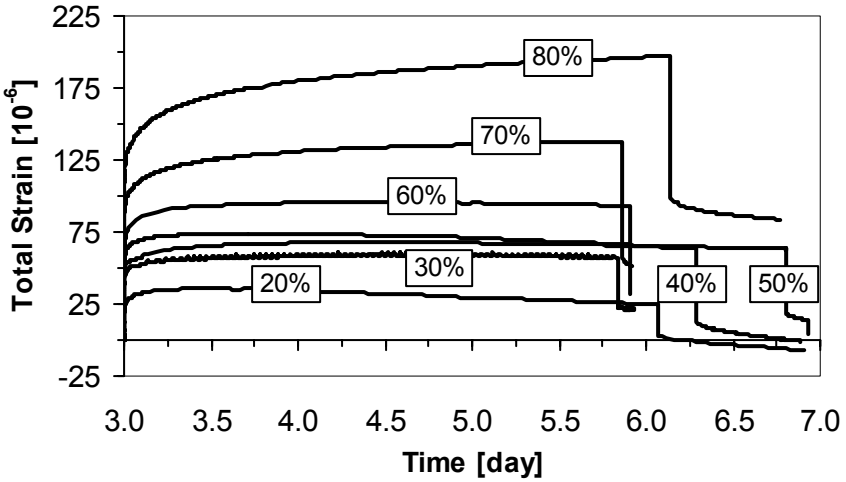

b) Measured strain on loaded specimen (average of 3 LVDT)

Figure 5.26 Load histories and measured strains in the tensile creep tests, with different stress/strength levels, age of loading 3 days, concrete type BASE-5 and T=20 ^{o}C.

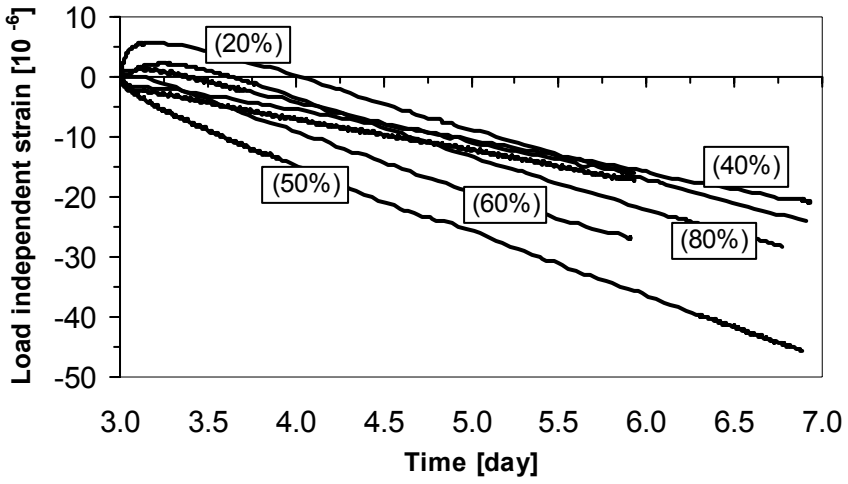

Figure 5.27 Measured strain on unloaded specimen (average of 3 LVDT) in the tensile creep tests from the age of 3 days, concrete type BASE-5 and T=20 °C.

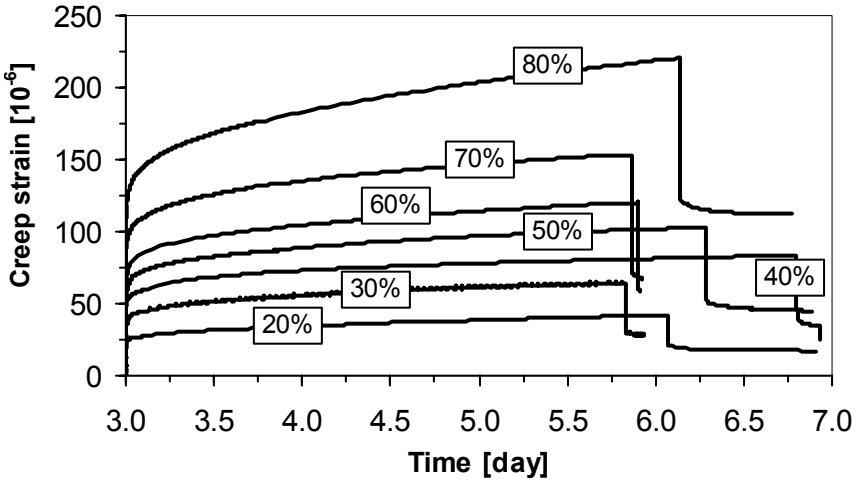

Figure 5.28 Creep strains compensated for measured strains in dummy in the tensile creep tests from the age of 3 days, concrete type BASE-5 and T=20 °C.

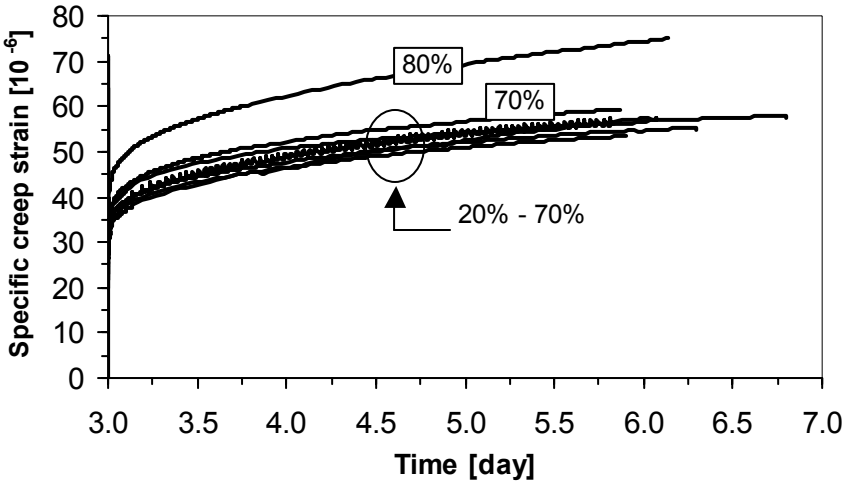

a) Creep strains pr. unit stress

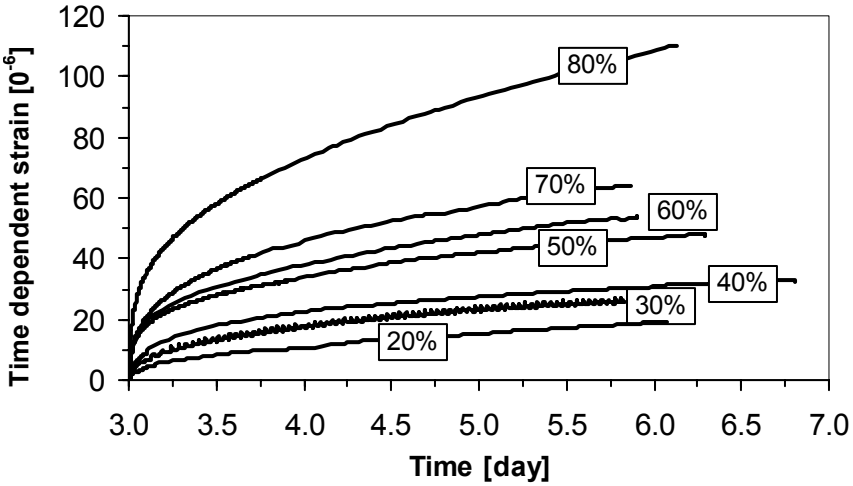

b) Time dependent strain

Figure 5.29 Sealed creep strains under different loading level, age of loading 3 days, concrete type BASE-5 and T=20 ^{o}C.

The relation between amount of time dependent strain and stress/strain ratio, from one minute after loading is applied, after 24 and 48 hrs is shown in Figure 5.31. For relative loadings up to between 60 to 70% the magnitude of creep seems to be linear whereas a non-linear behaviour takes place at higher loading.

Another observation in the figure is that the non-linearity increases with time. For the current case, the ratio between magnitudes of time-dependent strain, when the stress/strength ratio increase from 70 to 80%, at respectively 48 and 24 hrs after loading is 1.97.

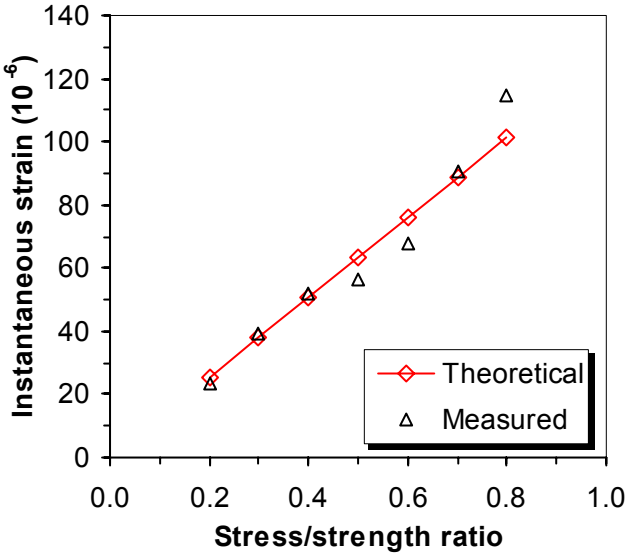

Figure 5.30 Measured instantaneous deformations compared to the theoretical values under different stress/strength ratios at loading age of 3 days, BASE-5 concrete and T=20 °C.

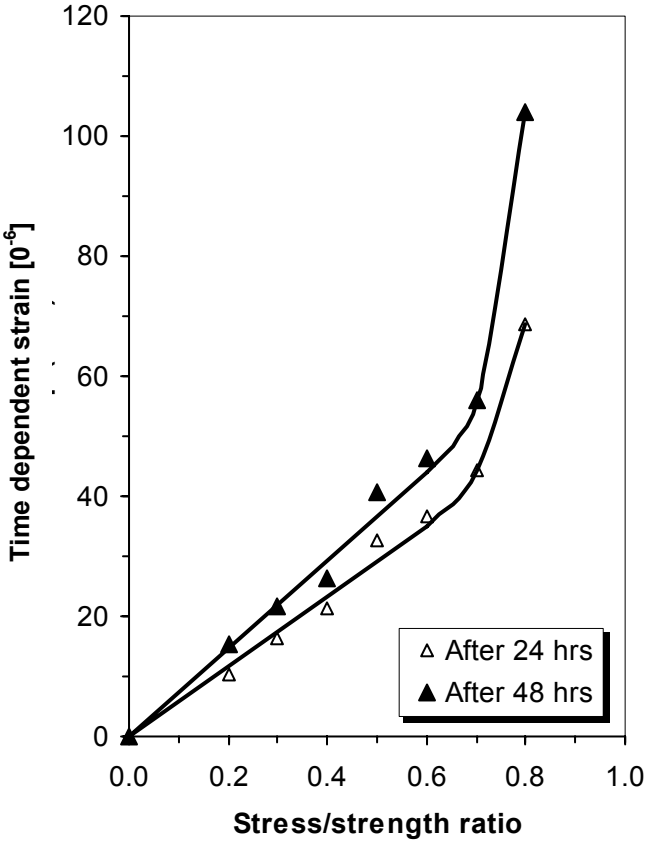

Figure 5.31 None-linearity of sealed creep in tension at loading age of 3 days, BASE-5 concrete and T=20 °C.

Considering the variations shown in Figure 5.26b and Figure 5.27, it is quite astounding that after compensation the net results in Figure 5.28 are very systematic, as are the results when the two components are treated separately; the instantaneous part (Figure 5.30) and the time dependent (Figure 5.29 and Figure 5.31).

This quit good linearity of the deformation components with applied stress is of fundamental importance, since it, at least partly, justifies the compensation procedure of subtracting the unloaded dummy deformation from the loaded one. This is particularly noteworthy considering that the dummy deformations are generally much larger than the time dependent deformations of the loaded ones.

5.5 Influence of Silica Fume on Autogenous Shrinkage and Tensile Creep

The type of cementitious material obviously affects creep so far as it influences the strength and stiffness of the concrete at the time of application of load and the time beyond that. Any comparison of creep in early age concrete made with different type of cementitious material should therefore also take into account the influence of the type of cementitious material on the strength and modulus of elasticity of concrete at the time of application of load. More details on this issue are discussed in Chapter 3.

Generally, the creep of silica fume concrete is smaller than for concrete without silica fume with equal water to binder ratio if the load is applied when the concrete is well matured [Built and Acker (1985)]. Contrary to this effect of silica fume on creep in mature concretes, different trends for early age concrete has been reported [Kanstad *et al.* (2000), Igarashi e*t al.* (2000) and Bissonnette *et al.* (1995)]: The use of silica fume in concrete tends to increase the tensile creep at early ages. This, together with other material properties might be important in evaluating concrete mixes in terms of sensitivity to early cracking. Tests of high performance concrete with varying silica fume contents demonstrated clearly that no single parameter is sufficient for predicting the risk of early age cracking [Bjøntegaard *et al.* (2003)].

There is a good correlation between autogenous shrinkage, pore characteristics and silica fume content. As the silica fume content increase, the pores become smaller, and thus increase the autogenous shrinkage, presumably due to increased capillary tension.

Tests reported in the literature have shown that autogenous shrinkage increases with silica fume when it is recorded from the time when it is measurable, a short time after casting. The most significant increase is observed the first day after casting, when the E-modulus is very low [Tazawa and Miyazawa (1997), Person (1997), Bloom (1995) and Kanstad *et al.* (1995)]. Moreover, study of the test results in the literature shows that silica fume has just a modest influence on autogenous shrinkage for the time period 1 to 4 days. These are valid for isothermal tests 20 ^{o}C, but at other temperatures and varying temperatures the behaviour is much more complicated.

The results of direct tensile creep tests performed on early age concrete, with different silica fume contents and under constant load are presented in this section. For the restrained concrete tests, where the internal stresses, induced by restrained thermal dilation and autogenous shrinkage, results are presented and treated in Chapter 6.

3.2.10 Outline of the tests

A series of tensile creep tests (Series III) were conducted on concretes (at 20 ^{o}C) with different silica fume contents, to study the effect of silica fume on the viscoelastic behaviour. The concrete mixes are described in Chapter 4, and they are denoted: BASE-0, BASE-5, BASE-10 and BASE-15. The numbers represent the per cent silica fume in the mixes.

Similar to the earlier described procedure for tensile creep tests, two specimens are used in each creep test. From each concrete batch two tests are conducted: at 1 day and 4 days of loading, and the duration of testes are varied from 3 to 4 days. Some of the tests are repeated to confirm both the function of the test rig and the test results. Throughout this series of tests, the applied stress is 40% of the tensile strength at loading age, and its magnitude (but not the stress/strength ratio) maintains constant during the tests. The tensile stresses imposed on the specimen at one-day age were 1.05, 1.10, 1.09 and 1.07 MPa for the concrete with 0, 5, 10 and 15% silica contain respectively. At four-days age, the stresses applied were 1.66, 1.81, 1.88 and 1.69 MPa for the concrete specimen with 0, 5, 10 and 15% silica content respectively. The applied stresses are somewhat different because, as was mentioned earlier, tensile strength develops in different rates for different silica fume contents (Figure 5.2b).

The test program involving totally 16 tests is given in Appendix A (Table 7). To maintain both the water/cement ratio and the necessary workability, it was necessary to increase dosage of super-plasticizer (25-50 gr) when silica fume content increased.

Strength tests

Nine 100 mm cubes were cast from each batch, and they were cured sealed under the same condition as the testing cylinders. Results from the compressive strength tests carried out at the age of 1, 4, and 28 days, are summarized in Appendix A (Table 7). Other mechanical properties such as the tensile strength and modulus of elasticity are estimated from 28-day results of Kanstad *et al.* (1999), and the models given in the beginning of this chapter.

3.2.11 Results and discussion

In the following the discussion of the effects of silica fume on tensile creep is divided into two parts; the first part considers the autogenous deformation in sealed specimens and the second part considers the tensile sealed creep.

Free autogenous shrinkage deformation

In parallel with the loaded specimens, free shrinkage tests of sealed specimens were conducted in temperature-controlled system at 20 ^{o}C. The results of tests performed on the four concrete mixes are presented in Figure 5.32 and Figure 5.33, which show development of the autogenous deformations (dummy specimen) and the total deformations (loaded specimen) with time at loading ages 1 and 4 days. For 0, 5 and 10% silica fume concretes at 1-day age loading two tests are performed, where the results show good reproducibility of data in some and less good in other tests.

Figure 5.32 shows that the autogenous shrinkage (at 20 ^{o}C) decreases with silica fume content when it is considered from 1 day. This observation might seem surprising, but note

that the figure is not showing the development of autogenous shrinkage for the first 24 hrs after casting, the period where the development of shrinkage is largest.

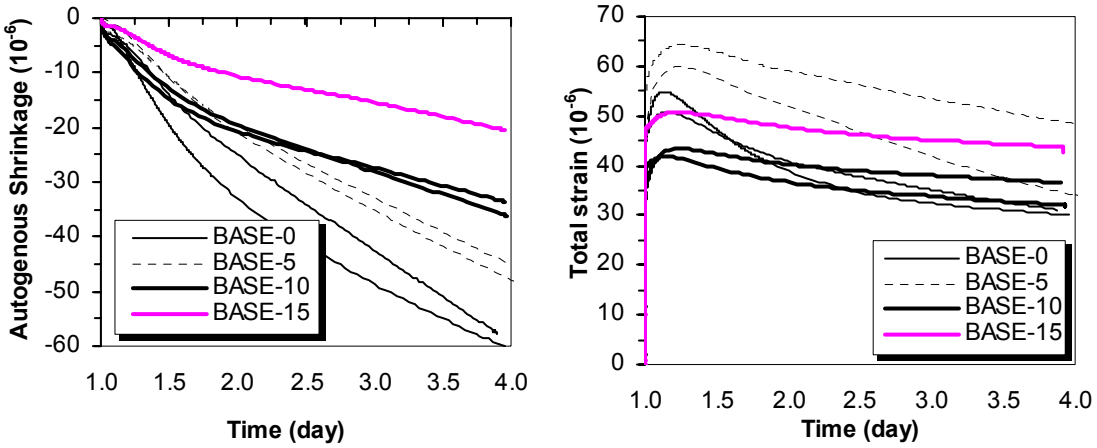

a) Unloaded specimen (dummy) **b)** Loaded specimen (active)

Figure 5.32 Measured strains in creep tests at isothermal conditions (T=20 °C), starting from 24 hrs after casting.

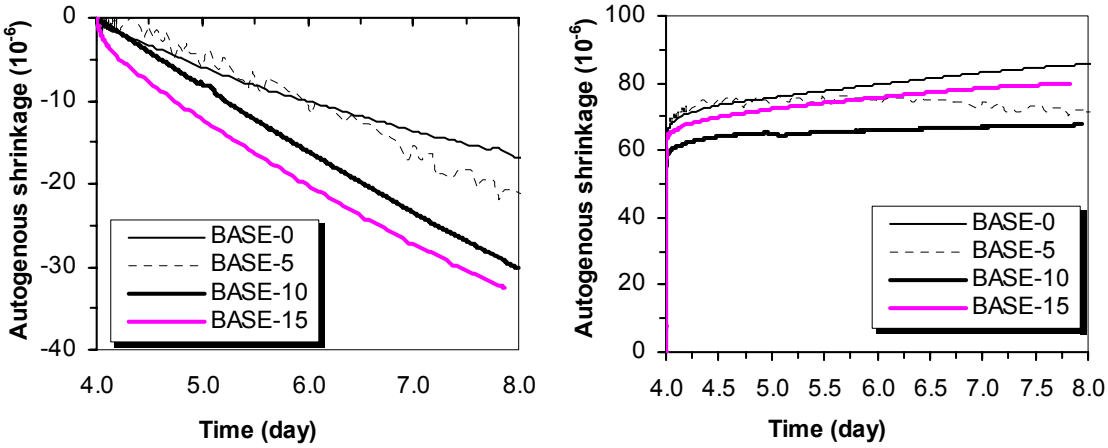

a) Unloaded specimen (dummy) **b)** Loaded specimen (active)

Figure 5.33 Measured autogenous shrinkage at T=20 °C, starting from 4 days after casting.

Figure 5.33 presents the measured deformations from 4-days age. The results here indicate an opposite trend in development of autogenous shrinkage than for one-days age concrete, namely that the higher contents of silica fume the higher autogenous shrinkage is. These observations agree with the test results presented by Bjøntegaard *et al.* (2003) shown in

Chapter 6. The two sets of curves do not appear consistent in that their slopes at 4 days do not match very well. It is surprising that this "inconsistency" also is present in Bjøntegaard *et al.* (2003). However, each of the present curves is the dummy of a loaded specimen and is therefore used to compensate its partner to produce the creep curves in Figure 5.34.

Creep deformations

Figure 5.34 presents the development of the specific creep strains as a function of time for different silica fume concretes. The specific creep curves for each concrete type are in good agreement with each other.

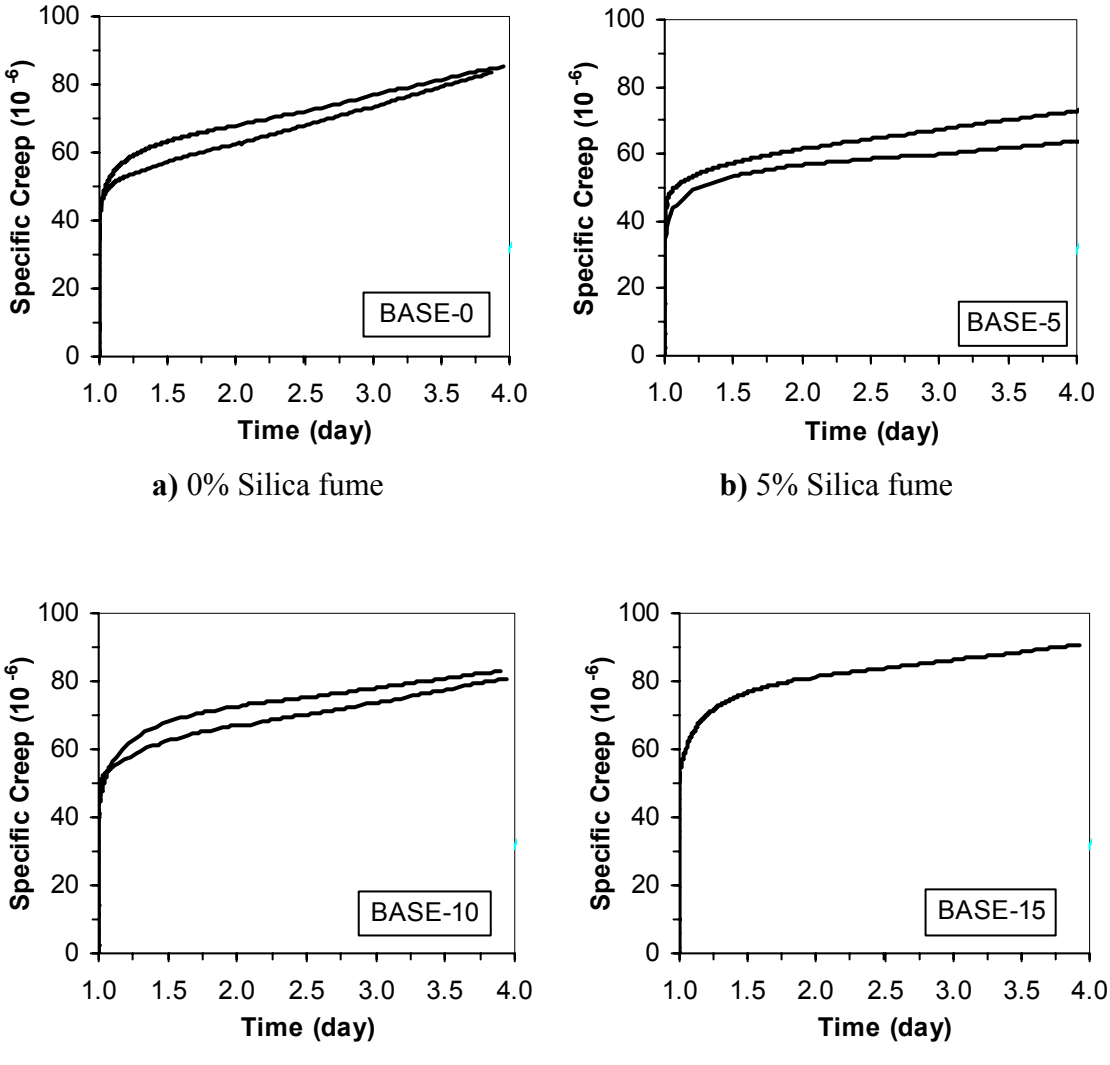

a) 0% Silica fume **b)** 5% Silica fume

c) 10% Silica fume **d)** 15% Silica fume

Figure 5.34 Sealed creep strain for concrete with different silica fume content, loaded on one-day age, at T=20 °C.

The results reveal a relatively high creep rate right after loading as we have shown earlier. A few hours after the loading, the creep rate of all the mixes reduces and the creep proceeds with slowly reducing rate, somewhat different for concrete with or without silica fume content. We also notice that, for the same concrete type, different creep rates are observed. The difference has probably its main source from the different rates of autogenous deformation, which is subtracted from the total measured deformations to find the specific creep.

Comparison between all the results is made in Figure 5.35. There is no significant difference between the 0, 5, 10% silica fume concretes, except for BASE-0 which reveals a pronounced higher creep rate after about 2 days. This trend for BASE-0 concrete may arise from the differences in the E-modulus development of each concrete type. Figure 5.1 shows that E-modulus is lower for the silica fume concretes than for the concrete without silica fume in the first days after casting, and then it develops faster for increasing silica fume content. The concrete with 15% silica fume content exhibits a greater creep rate, and thus higher creep strain than others in the whole time period.

In Figure 5.36 the mean creep curves for each mix is given which gives a more consistent picture. The mean values of the specific creep for the 0, 5, 10 and 15% silica fume concretes, after about 4 days, are 84.6, 75.5, 81.8 and 90.7 μm/m, respectively. However, one should be aware that the scatter in the test results is of the same order as the difference in the creep curves for different silica fume concretes. Ignoring the scatter in the test results one can conclude that higher silica fume content produces more specific creep in the first few days, but the creep rate seems to slow down faster than for the reference mix without silica fume.

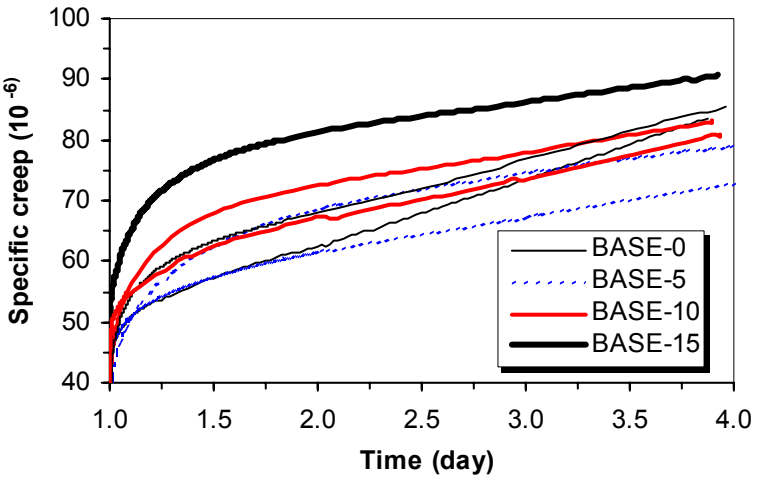

Figure 5.35 Sealed creep strain development for concrete with different silica fume content, loaded at one-day age, T=20 ^{o}C.

Figure 5.37 shows the development of specific creep for the four mixes, when the loading age is 4 days. Only one creep test was performed for each silica fume concrete, and thus no comments on scatter in test results can be mentioned here. As in one-day loading age, the creep rate of the concretes is high right after loading. It decreases slowly with time to different constant rates for the different silica fume concretes, something, which leads to divergence of curves and thus different creep magnitudes. The creep strain after 3 days loading is 51.1, 46.3, 52.4 and 58.8 μm/m for 0, 5, 10 and 15% silica fume concretes, respectively. Assuming no scatter in creep test results in the Figure 5.37, we can conclude that the higher silica fume the higher tensile specific creep, with exception for BASE-0.

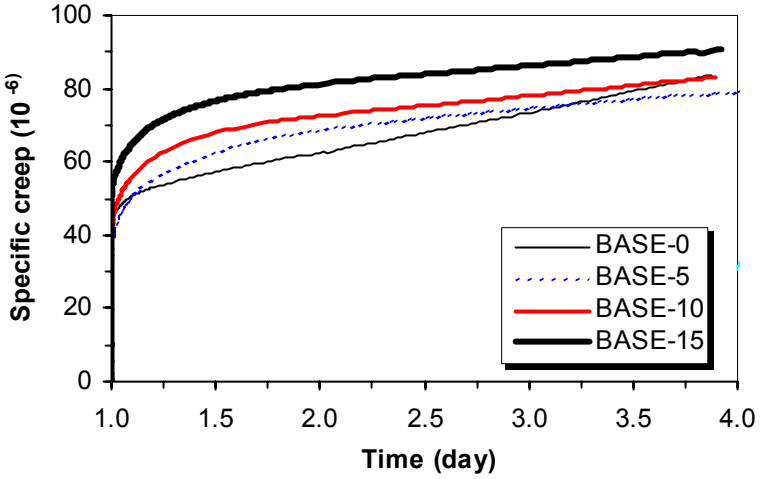

Figure 5.36 Sealed creep strain for concrete (mean values for each mix) with different silica fume content, loaded at one-day age, T=20 °C.

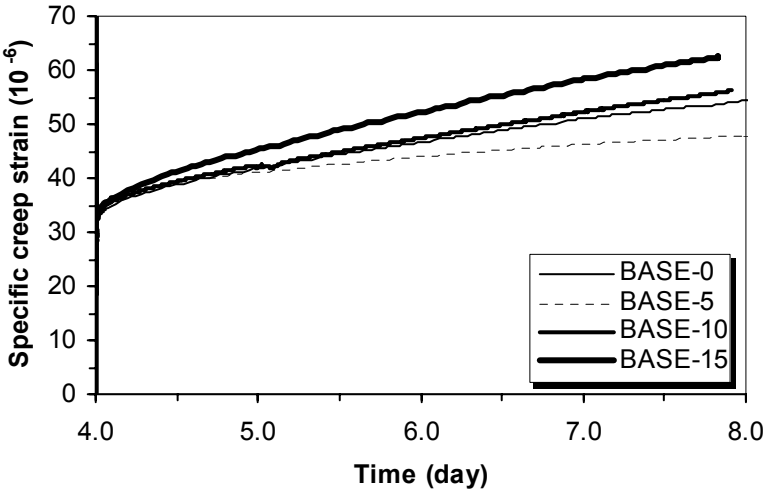

Figure 5.37 Sealed creep strain for concrete with different silica fume content, loaded on four-days age, T=20 °C.

In both Figure 5.36 and Figure 5.37 the concrete without silica fume behaves different than the silica fume concretes. For the silica fume concretes the results are consistent, but assuming similar scatter in test results for both loading ages, we can conclude that there is no significant influence of 5-10% silica fume on tensile sealed creep. 15% silica fume seems to increase the creep.

The effect of loading age on the specific creep is shown in Figure 5.38. From the estimation of E-modulus, the four-days age concrete is about 25-30% stiffer than one-day age concrete, a fact that also is evident in the figures. As expected, the magnitude of the creep strain decreases with increasing loading time. In the case of one-day old concrete, the creep strain varied between 70-90 μm/m after 3 days loading, but in the case of loading of four-days old concrete the creep strain varied between 45-69 μm/m after 3 days.

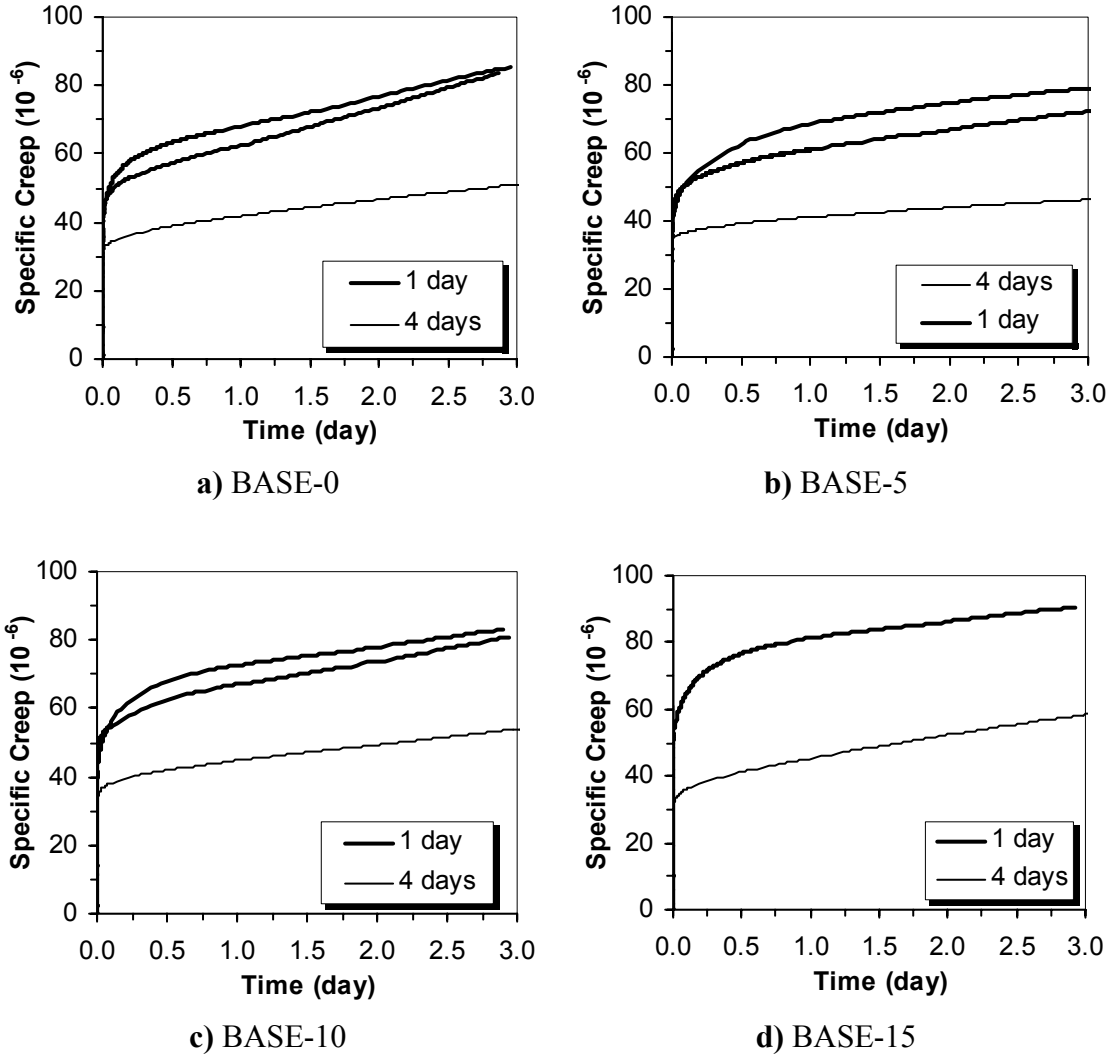

a) BASE-0 **b)** BASE-5

c) BASE-10 **d)** BASE-15

Figure 5.38 Specific creep strain for concrete with different silica fume content, loaded on one-day age and four-days age.

Comprehensive test results on silica fume effects on self-induced stresses and autogenous shrinkage are presented and treated in Chapter 6, and the present creep results are utilized in the analysis and discussion.

5.6 Influence of Temperature Levels on Tensile Creep

Temperature is one of the main environmental factors, which influence the time-dependent deformations, including shrinkage, instantaneous deformation as well as sealed and drying creep. The influence of temperature is larger at early ages than at mature concrete, since any increase of temperature means faster hydration, and thus it is very important in thermal stress analysis.

Generally, creep increases with increasing temperature, but in young concrete the effect is offset by the fact that a temperature increase also accelerates hydration, which in turn reduces creep. Thus, a higher temperature tends to increase the creep rate, but will also indirectly reduce the creep. Dependent on the concrete age, the former effect is usually higher than the latter one.

In this section, the influence of temperature on sealed creep in tension, at early ages of concrete, is studied and few tests are conducted in tensile creep rig.

3.2.12 Outline of the tests

Tensile creep tests are conducted at different isothermal temperatures (20, 34, 40, 57 and 60 ^{o}C) on BASE-5 concrete. The temperature histories of the tests are shown in Figure 5.39. The curing temperature for all the tests is about 21±2 ^{o}C until it is increased to achieve the desired testing temperature. Tests on 20 ^{o}C have already been presented. For the test at 34 ^{o}C the temperature was increased 3 hrs before loading. For the other tests (40, 57 and 60 ^{o}C) the temperature was increased to the desired level one day before loading, see Table 5.8. The table gives also the maturity of each specimen at the time of load application, using activation energy 24420 units [Kanstad *et al.* 1999]. The number of specimens and the test procedures are the same as described in earlier sections.

Table 5.8 Temperature and timetable for the tensile creep tests.

Test [No.]	Temperature [^{o}C]	Installing time of the specimen in the creep rig (t´) [hrs]	At loading		
			Real time (t) [hrs]	Maturity (t_e) [hrs]	Temperature [^{o}C]
800	34	69	72	73	32.2
801	40	48	71	91	41.1
802	60	48	72	124	60.5
803	57	24	43	87	58.0
804	57	24	44	83	58.5

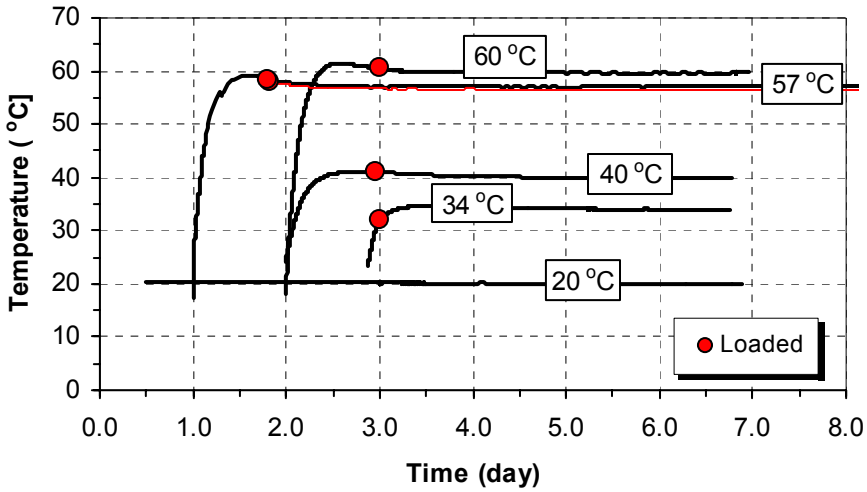

Figure 5.39 Temperature histories for the tensile creep tests on BASE-5 concrete.

3.2.13 Results and discussion

Figure 5.40 shows an example of raw measured data for the test (at 57 °C), and the data for the other four tests are given in Appendix F. Figure (a) shows the measured strains (autogenous deformation) on the unloaded (dummy) specimen. Figure (b) shows the load history and the total strain (included creep) on the loaded (active) specimen, and finally figure (c) shows the calculated specific creep. Some eccentricity in strain measurements are observed, but the average values are used in the calculations.

Temperatures higher than 20 °C accelerate the hydration process in concrete, and in consequence the concrete gain a higher degree of maturity. In the following the creep development at the high temperatures is compared to the available creep data at 20 °C at loading ages of 3 and 4 days, in which it uses the maturity values at loading for the tests at elevated temperatures (Table 5.8).

Figure 5.41 shows the result of a tensile creep test, conducted on 3-days-old concrete at temperature 34 °C. The temperature was increased, starting 3 hrs prior to loading and it was achieved 32 °C at the loading time. This means that the temperature increased further by 2 °C while the concrete was under loading. When concrete undergoes creep deformation under varying temperature no thermal equilibrium is obtained, and thus the creep rate will increase and influence the rate of aging of the concrete. Both features are evident in the figure, where the creep rate at 34 °C, right after loading, is higher than the case at 20 °C and the rate continues to be higher further on. The rapid increase in creep, due to temperature increase, is called transient creep (or transitional thermal creep), and the ageing effect is taken to account by maturity principle. The figure (b) shows the same creep development, but in relation to maturity.

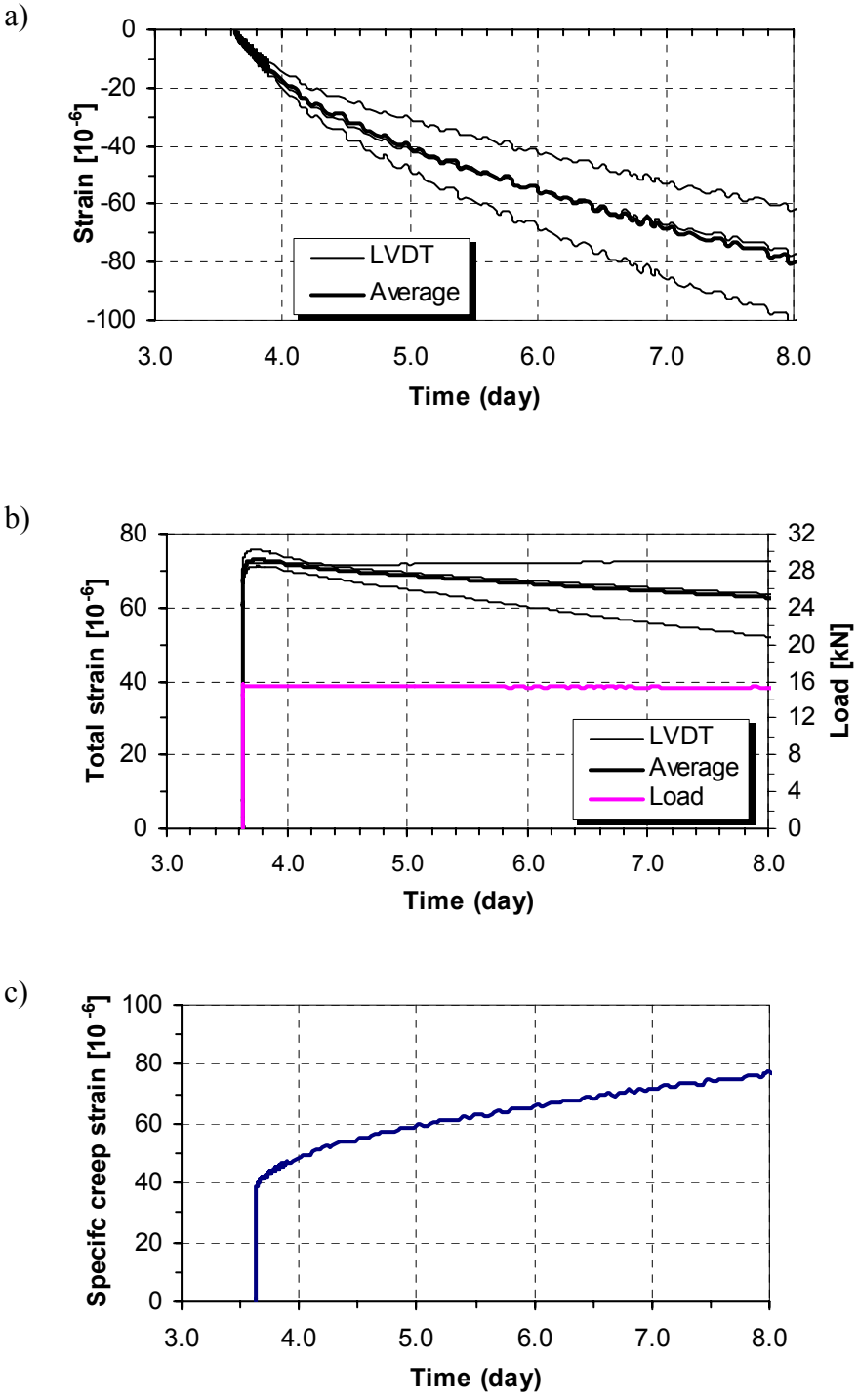

Figure 5.40 Measured strains in the tensile creep tests, age of loading 44 hrs (maturity = 83 hrs), concrete type BASE-5 and **T=57 °C**. a) Unloaded specimen, b) loaded specimen, c) specific creep, (Test No. 803).

URN:NBN:no-3377

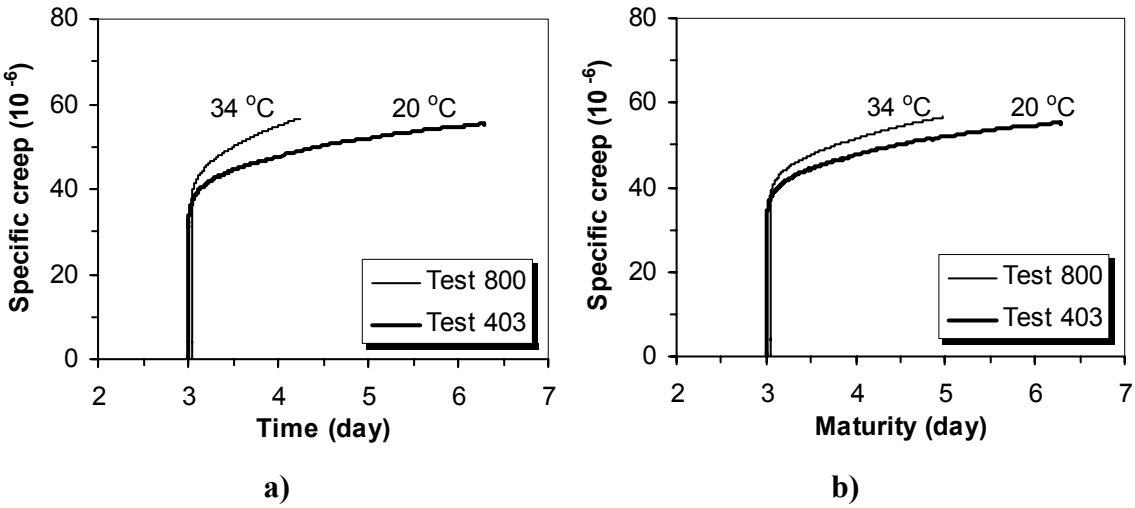

Figure 5.41 Measured tensile sealed creep pr unit stress on BASE-5 concrete, loaded at age of 72 hrs at **T=34 °C**. a) versus real time, b) versus maturity.

Results of creep tests for three other tests at higher temperatures (40 and 57 °C) are shown in Figure 5.42. The temperatures were started increasing to the desired temperature one day prior to the loading, at the ages of 2 days for the test at 40 °C and of 1 day for the two tests at 57 °C. The specific creep in the figures at the left hand and the right hand are plotted as a function of the real time and the maturity, respectively. The loading ages are somewhat less than four days, and the results are compared to the available creep test for 4-days-old concrete at 20 °C. (The results of the test No. 802 at 60 °C are not presented, due to lack of data on creep development at 5-maturity-days old concrete at any other temperature level to be compared with.) The general trend in the figures on the left hand seems to be that the higher the temperature the higher the rate of sealed creep in tension as well as its magnitude is for the current tests. On the other hand, the maturity on the figures at the right hand, takes the aging effect well into account – even better with higher activation energy. The consequence for modelling is that the maturity transformation succeeds in characterizing the creep development quit well, at least from 3 days maturity.

From the limited data that are available, and from the comparative test results reported by Umehara *et al.* (1994), the sealed creep in tension, as in compressive sealed creep, accelerates for temperatures higher than 20 °C under loading, and thus the creep deformation increase significantly with increasing temperature.

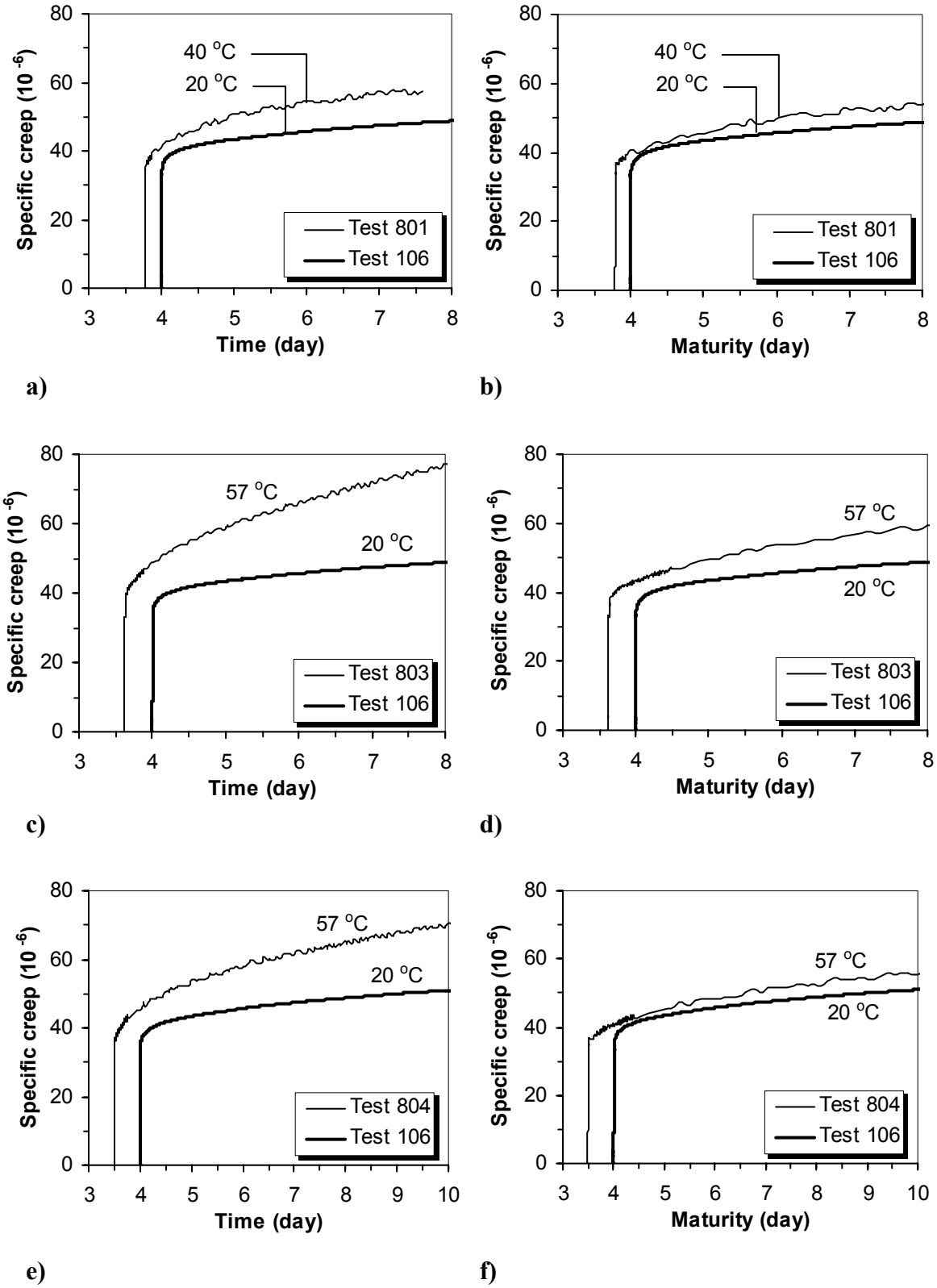

Figure 5.42 Measured tensile sealed creep pr unit stress on BASE-5 concrete, loaded at different ages and temperature histories, versus both the real time and the maturity.

5.7 Summary and Conclusions

The results of the new tests and the earlier available experimental data on the development of mechanical properties of early age BASE-concrete, with 0, 5, 10 and 15% silica fume content, were studied. A few tests were also conducted on Maridal concrete. The modulus of elasticity in tension and compression were particularly discussed. It was found that the E-modulus in tension (E_t=E_1) was greater than the E-modulus in compression (E_2) by 13% and 17% for BASE-0 and BASE-5 concretes respectively, and 10% for both BASE-10 and BASE-15 concretes. The general observation is then that E_1 is 10-17 % higher than the E_2 for the four tested concrete mixes; the observation which corresponds well to the investigation by earlier findings. For Maridal concrete E_1/E_2-ratio was found to be 1.20. The main reason for difference between the E-modulus in tension and compression is the load level, as long as both are determined during the first loading. The E-modulus in compression determined in standard procedure after the 3 unloading is very close to the tension value on first load (E_t=E_1), an observation that can be utilized in calculations.

The rest of this chapter treats the results of the experimental work conducted on creep of concrete in both tension and compression at early ages under sealed conditions. Since the measured creep of sealed high performance concrete includes, in addition to basic creep, a drying creep component, term *sealed creep* is introduced to characterize the creep occurring under sealed condition.

With regard to various parameters, four test series were conducted in the new tensile creep apparatus. In each creep test one or two sealed specimens (2 in compressive creep tests and one in tensile creep tests) were loaded to measure the total load-dependent deformation and one sealed specimen was kept unloaded to measure the load-independent deformation, which represents autogenous shrinkage in this case. The commonly used procedure to define the creep is simply to subtract the measured autogenous shrinkage in an unloaded dummy from the total deformation measured on the loaded. In contrast to the compressive creep tests, the load-independent deformations in tensile creep tests are at least of the same order of magnitude as the load-dependent deformations, and thus the former has always a large influence on both the magnitude and the rate of the creep development. The question, which arises here, is whether this approach is valid to determine tensile creep.

- Series I: A comparative experimental study on the relation between the tensile creep and the compressive creep was made, conducting parallel tests on both, and the influence of age at load application on creep is studied. Tests are conducted at about 20 ^{o}C, on two concrete mixes, the reference concrete BASE-5 and the Maridal concrete. The stress applied on the specimens was 40% of its cube strength at the loading age. Several tests at each loading age were performed and the results confirmed the reproducibility of the test result of BASE-5 concrete, and thus the accuracy of the creep apparatus. On the other hand a larger scatter in the test results of Maridal concrete, within the same loading age for all the tests was observed. The latter should be taken as an indication that at each loading age more than one test are needed to establish the creep behaviour of the any concrete type.

The evaluation of the test results emphasizes the comparison between the time dependent material behaviour under compression and tension, in terms of magnitude and rate. Both similarities and differences between the viscoelatic behaviour of concrete in both cases were observed.

Among the similarities the following observations can be mentioned: The test results showed an increase of creep magnitude with a decrease in the age at application of load, and a high rate of creep within the first day after loading followed by lower rate. They indicated also that the concrete's viscoelastic behaviour in both tension and compression, is much more sensitive at the ages lower than 2 days than at the older ages. A relative high creep response when concrete is loaded at 24 hrs after casting, and a far stiffer response after 2 days are the two main observations in the tests. The creep curves indicates that the creep rates after about 3 days loading are nearly parallel to each other for the short period of time studied.

In addition to the mentioned similarities, differences between creep in tension and compression in both immediate response of concrete to the load, creep rate and creep magnitude were also observed.

- The instantaneous deformation under tension tests is found to be lower than under compression tests. The main reason is that the load level in tension is much lower than in compression.

- Immediate after loading and within approximately the first 24 hrs, the creep rate in compression is higher than the creep rate in tension. Afterwards, the creep rates decreases continually with time, but the decrease in tensile creep is much less pronounced than in compressive creep. This leads to crossing of the curves a few hrs or days after loading for the current loading ages and, subsequently, a higher tensile creep than compressive creep. The crossing time becomes longer as the loading age become higher, with exception of the loading age of one day.

- A stiffer response of concrete to the imposed load in tension at loading age implies a lower creep magnitude in tension than in compression in the beginning. The difference between the creep curves reduces over time, and then the ratio between them changes to be opposite. Considering only the time dependent deformations, due to higher elastic strain pr. unit stress in compression than in tension, the creep curves will cross each other earlier, which means earlier higher tensile creep than compressive creep and earlier divergence of the curves.

Furthermore, because the instantaneous deformation under tension tests is found to be lower than under compression tests, the ratio of time dependent deformation to elastic deformation (creep coefficient) in tension is greater than in compressive creep tests.

A significant feature of the creep tests in both cases is that the autogenous shrinkage compensation of course affects tensile creep and compressive creep in opposite directions – for tension they are in opposition while in compression they are additive. Thus the difference between the tensile and compressive creep can partly be a consequence of the

compensation procedure used in Figure 5.18. This is one of the fundamental questions in the comparison.

Another important point of interest which may explain some of the difference in viscoelastic behaviour of concrete in tension and compression is the relative strength development in tension and compression, since creep is a function of the stress/strength ratio. Figure 5.25 reveals faster reduction of stress/strength ratio in compression than in tension, particularly at early ages. However, in spite of this effect the early age creep in compression is greater than in tension.

- Series II: The influence of stress level on tensile sealed creep on 3-days old BASE-5 concrete was investigated. The applied initial tensile stress levels were 0.2, 0.3, 0.4, 0.6, 0.7 and 0.8 times the tensile strength.

  The test results (Figure 5.27b) showed that the autogenous shrinkage dominates the deformation process after the initial period in the loaded specimen for initial stress/strength ratios up to 60%, i.e. that the specimen contract under tensile load. Due to disturbances of the measuring devices significant differences was observed in measurements of autogenous shrinkage (Figure 5.27c). Assuming the same disturbances (errors) in the loaded specimen, each creep curve was compensated by its "own" dummy, which provided very systematic net result.

  Moreover, the test results (Figure 5.31), from one minute after loads were applied, showed that for relative loadings up to about 60% the magnitude of the time-dependent deformations after 24 and 48 hrs is linear whereas a non-linear behaviour takes place at higher loading. This means that the limit of proportionality was found to be 60% for tensile sealed creep. This quite good linearity of the deformation components with applied stress is of fundamental importance, since it, at least partly, justifies the compensation procedure of subtracting the unloaded dummy deformation from the loaded one. This is particularly noteworthy considering that the dummy deformations are generally much larger than the time dependent deformations of the loaded ones.

  Another observation was that the non-linearity increases with time. For the studied case, the ratio between magnitudes of time-dependent strain, when the stress/strength ratio increase from 70 to 80%, at respectively 48 and 24 hrs after loading is 1.97.

- Series III: This series of tensile creep tests were conducted on concretes with different silica fume contents (0, 5, 10 and 15%), to study the effects of silica fume on the viscoelastic behaviour of early age concrete. Tests were conducted at 1 day and 4 days of ages at 20 ^{o}C, and the duration of testes were varied from 3 to 4 days. The applied stress was 40% of the tensile strength at the loading ages, which means that their magnitudes were somewhat different because tensile strength develops in different rate for different silica fume contents (Figure 5.2b). The total test program involved 16 tests.

Autogenous shrinkage normally increases with silica fume content, where the most significant increase occurs the first day after casting. The test results showed that autogenous shrinkage for the time period 1 to 4 days (at 20 ^{o}C) decreases with silica fume content. On the other hand, the results for the time period 4 to 8 days indicated an opposite trend. The two sets of curves do not appear consistent in that their slopes at 4 days do not match very well. However, each curve is the dummy of a loaded specimen and each is therefore used to compensate its partner to produce the creep curves in Figure 5.34.

Taking the mean values of the creep test results for 1-day age concrete, the concrete with higher silica fume content exhibited a greater creep rate, and thus higher creep strain than concrete with lower silica fume content. BASE-0 concrete was an exception and has a higher creep rate than all other three concretes. This trend for BASE-0 concrete may refers to its faster development of E-modulus in the first days after casting, succeeded by a lower rate. The effect of silica fume is more pronounced for 4-days concretes. Considering the single tests for each of the silica fume concretes, the results showed that silica fume increases the tensile specific creep somewhat.

However, the scatter in creep test results for each silica fume concretes at 1-day loading age is about the same value as the difference between creep magnitudes in the concretes. Assuming the same scatter at 4-days loading the same observation might be made. Considering these variations in results it should be concluded that there is no significant influence of 5-10% silica fume on tensile sealed creep, but 15% silica fume seems to have en increasing effect on the creep.

- Series IV: The influence of isothermal temperatures on tensile specific creep was investigated and few creep tests were conducted at 34, 40, 57 and 60 ^{o}C on BASE-5 concrete. The test specimens were cured at about 21±2 ^{o}C until it is increased to achieve the desired testing temperature. The temperatures were increased few hours or one day before loading. The specimens were loaded between 3 and 4 maturity-days ages, and the creep development at high temperatures was compared to the available creep data at 20 ^{o}C.

  A higher temperature tends to increase the creep rate of mature concrete, but will also indirectly reduce creep in young concrete since hydration is accelerated. The general trend in the current test results, not so unexpected, was that the higher the temperature the higher the rate of sealed creep in tension as well as its magnitude. From these limited data, and from the comparative test results reported by Umehara *et al.* (1994), the sealed creep in tension, as in compressive sealed creep, accelerates for temperatures higher than 20 ^{o}C under loading, and thus the creep deformation increase significantly with increasing temperature.

  An important observation was that the maturity takes the temperature effect well into account. The consequence for modelling is that the maturity is good enough to use for different isothermal temperatures. Note however that the present results are only for loading ages of more than 3 days maturity. At lower ages no data exists, but we know that the maturity concept does not characterize autogenous shrinkage at short times and

elevated temperatures. Since creep in essence is autogenous plus an external load, we do not expect the unloading concept to function for creep data either at such early ages.

Chapter 6

Self-induced Stresses in Hardening Concrete, Experimental Results and Theoretical Modelling of Creep

6.1 Introduction

The chemical reactions that occur during the hydration process in early age concrete is accompanied by significant volume changes in the hardening concrete member. Under restrained conditions, as in massive concrete elements, and when the modulus of elasticity is sufficiently developed, the concrete will generate stresses.

In a hardening concrete member under restrained conditions in a Temperature Stress Testing Machine (TSTM) the stress generation, called self-induced stresses in the present research, can be measured and then the elastic strains can be calculate when the E-modulus is known. Assuming the principle of superposition, the creep strains can be obtained by subtracting the elastic strains from the total free strains.

For investigation of the influence of creep on the stress development in hardening concrete, test results from TSTM are very useful. TSTM is a suitable tool to optimize the concrete mix as to high cracking resistance. The experimental data can also be used as a valuable information for checking theoretical numerical models. In this chapter stress results from the TSTM tests and the Dilation rig tests on early age concrete are analyzed with particular focus on temperature effects on creep and relaxation. The effect of silica fume on the stress developed are also evaluated and considered in conjunction with the creep behaviour of the concrete. Stress simulations are performed using a model based on the theory of linear visco-elasticity, where creep is separated into sealed creep and transient creep (i.e. under changes in temperature).

As mentioned in Chapter 4 a new version of TSTM was developed, many tests were conducted and extensive data was therefore available for different temperature histories, Bjøntegaard (1999). Results from the test program, which originally was designed to separate the effect of thermal and autogenous deformations, are analyzed with respect to creep and relaxation.

Before performing the numerical calculations a short overview on the test apparatus and the test program is necessary. Bjøntegaard (1999) gives full description of the test equipment, test procedure and the total test program.

6.2 Experimental Program

The experimental equipment was described in Chapter 4 (Figure 4.15). The *Free deformation* was measured in a Dilation Rig, and the *self-induced stress development* in a special Stress Rig (TSTM). Both rigs are temperatures controlled. The dimensions of the cross sections of the concrete specimens were 100 x 100 mm and the total specimen length is 500 mm in the Dilation Rig and 1000 mm in the Stress Rig. The Stress Rig was at full (100%) restraint by a feedback system that compensates for any length change over a 700 mm control length.

The same concrete mixes, which are used in the creep tests in Chapter 5 and described in Chapter 4, are used here, namely BASE-0, BASE-5, BASE-10 and BASE-15. The only difference between the four mixes is the amount of silica fume in exchanged with cement on a 1:1 weight basis in each mix.

The total test program covers a range of different temperature histories and was originally designed to separate the effect of thermal and autogenous deformations during the hydration process in the Dilation Rig, Bjøntegaard (1999). The aim was to construct a general model for each of the two mechanisms for use in stress calculation. The Dilation- and the Stress Rig were always run in parallel hence the free deformation and stress development results can be used in conjunction with E-modulus data (measured independently) to calculate the creep/relaxation effect. Examples of imposed temperature histories are shown in Figure 6.1, and the whole test program involving totally 22 tests is given in Table 6.1.

***Isothermal tests*:**

The effect of different constant temperatures on the time-dependent deformations and the stress generation was measured. The concretes were cast at a temperature as close as possible to the desired test temperature. The test temperatures were reached within one hour after casting the concrete in the temperature-controlled rigs, and then the desired temperature is kept constant.

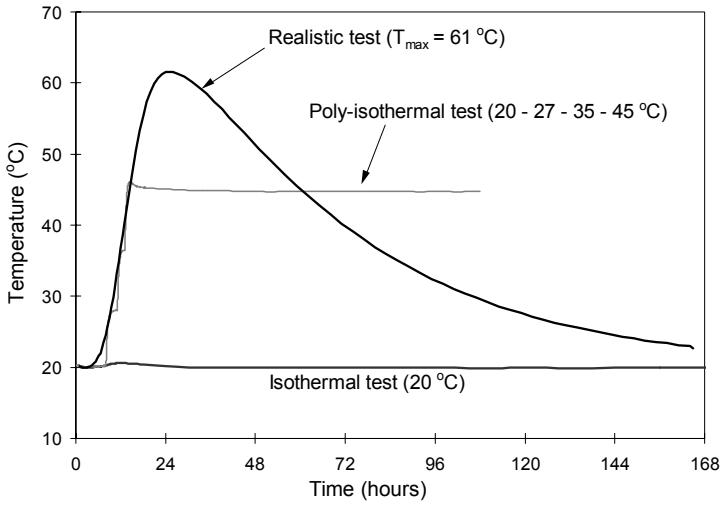

Figure 6.1 Examples of temperature histories used in the Dilation- and Stress Rig tests.

Table 6.1 Survey of temperature histories used in the TSTM and Dilation Rig tests.

Silica Fume	**Isothermal**	**Poly-Isothermal**	**Realistic Temperature (T_{start} = 20 °C)**
0% (BASE-0)	20 °C		T_{max} = 61 °C T_{max} = 61 °C [1] T_{max} = 61 °C [2]
5% (BASE-5)	5 °C 13 °C 20 °C (*Fig. 2*) 45 °C	13 - 20 °C 13 - 20 - 27 - 35 °C 20 - 27 °C 20 - 27 - 35 °C 20 - 27 - 35 - 45 °C (*Fig. 2*) 20 - 60 °C [3]	T_{max} = 29 °C T_{max} = 40 °C T_{max} = 47 °C T_{max} = 61 °C (*Fig. 2*)
10% (BASE-10)	20 °C		T_{max} = 39 °C T_{max} = 61 °C T_{max} = 61 °C [2]
15% (BASE-15)	20 °C		T_{max} = 61 °C [2]

[1] Delayed imposed temperature, [2] Reduced restraint, [3] One large step from 20 °C to 61 °C was imposed

Poly-isothermal tests

Tests with stepwise temperature changes were performed to get a more realistic (practice) way to get up to a desired temperature to study the transient behaviour of the concrete. The concrete was cast with a given starting temperature (20 ^{o}C in Figure 6.1) until 8 hrs when the temperature was increased in steps of 7 - 10 ^{o}C until the desired isothermal temperature was reached. This "final" isothermal level (45 ^{o}C in Figure 6.1) was then maintained until the end of the test. The temperature steps will be used to study the transient behaviour of the concrete in this research.

Realistic temperature histories

Temperature histories relevant for different concrete structure dimensions and different environmental conditions, for instance T_{max}= 61 ^{o}C in Figure 6.1. The temperature histories with its maximum about 60 ^{o}C are relevant to wall structures with thickness of 600 mm. The other temperature histories with lower maximum temperatures are relevant for other structures.

6.3 Experimental Procedure and Self-induced stresses in TSTM

Contraction as well as expansion of concrete was restrained from the beginning of the hardening process, and the restraint stresses were measured continuously in the TSTM. In the fully restrained condition all of the deformations are transformed into stresses. In case where restraint is reduced to prevent cracking of the concrete, only a part of deformations are transformed into stresses.

Figure 6.2 illustrates how tensile stresses build up due to autogenous shrinkage in the TSTM. The curves start from the time where tensile stress develops (t_0). The operation of the system is shortly explained in the following:

The concrete specimen in the equipment (TSTM) with a movable head is shown in Figure 6.2a, where the specimen is partly free to deform (contract) depending on the relative stiffness between the concrete specimen and the steel frame heads. Bjønteggard (1999) estimated this relative stiffness to be about 40% for the used TSTM, meaning that the $\Delta\varepsilon_1$ (shrinkage + creep) is only 60% of the free deformation. Thus, stresses ($\delta\sigma_1$) will be developed during the time period t_0 to t_1. As soon as deformation of the specimen reaches a predefined value $\Delta\varepsilon_1$ (2.0, 0.6 and 0.2 micro-strain used in the current tests), shown in Figure 6.2b, an additional sufficient axial force, $\Delta\sigma_1$, will be applied on the specimen to return it back to its original position, as in Figure 6.2c. This corresponds to the elastic strain denoted by $\Delta\varepsilon_2$ at t_1. By this, the total stress build-up has reached to σ_1. The specimen then left partly free to deform again while the total applied force (σ_1) changes until the predefined strain ($\Delta\varepsilon_1$) once more reached. Again, the force is increased by $\Delta\sigma_2$ in order to return it back to its original position. Such procedures continuous and it makes it possible to determine the stress

build-up in the specimen as a function of time. Note that the strain increments $\Delta\varepsilon_1$ and $\Delta\varepsilon_2$ are equal in magnitude, but they represent different strain components.

A schematic illustration of stress build-up and control of length deformation for the same test above is shown in Figure 6.3. It shows that it takes longer time to gain $\Delta\varepsilon_1$ for each subsequent time interval. This is due to lower strain rate and mature concrete with time. Furthermore, though the figure shows that $\delta\sigma_t$ increases with time within each time interval, but in real situation, due to the relaxation, the stresses might be constant or even decrease. The E-modulus can be calculated at each t_i simply by dividing the applied stress increment $\Delta\sigma_t$ by elastic strain $\Delta\varepsilon_t$.

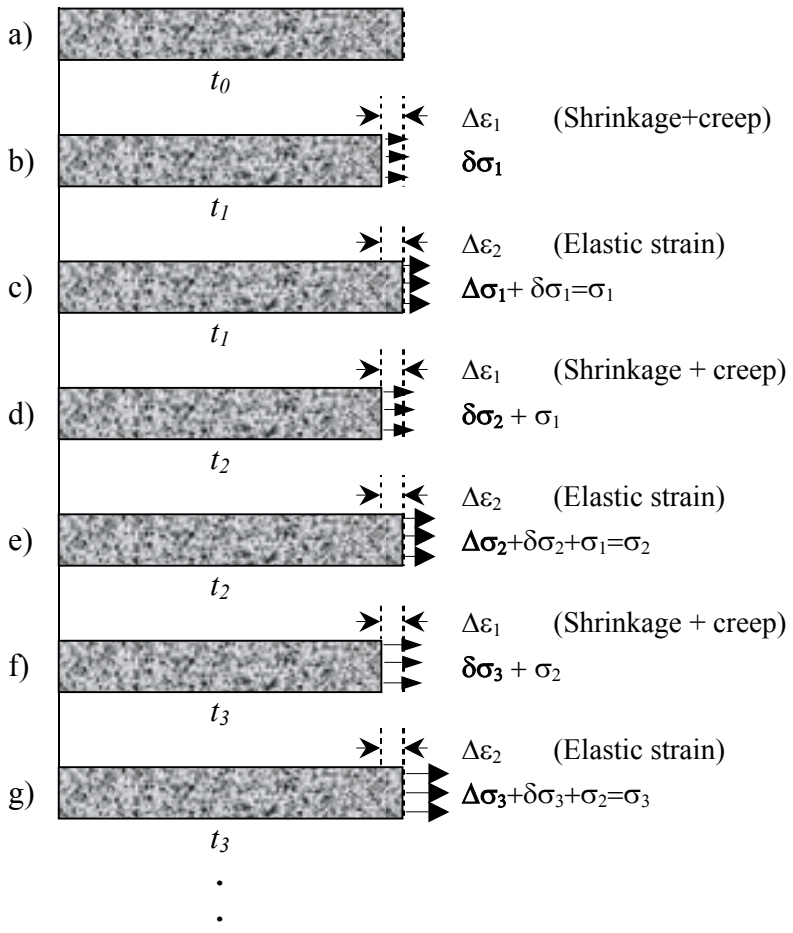

Figure 6.2 Stress build-up in the TSTM, assuming contraction due to autogenous shrinkage. ($\Delta\varepsilon_1 = \Delta\varepsilon_2$)

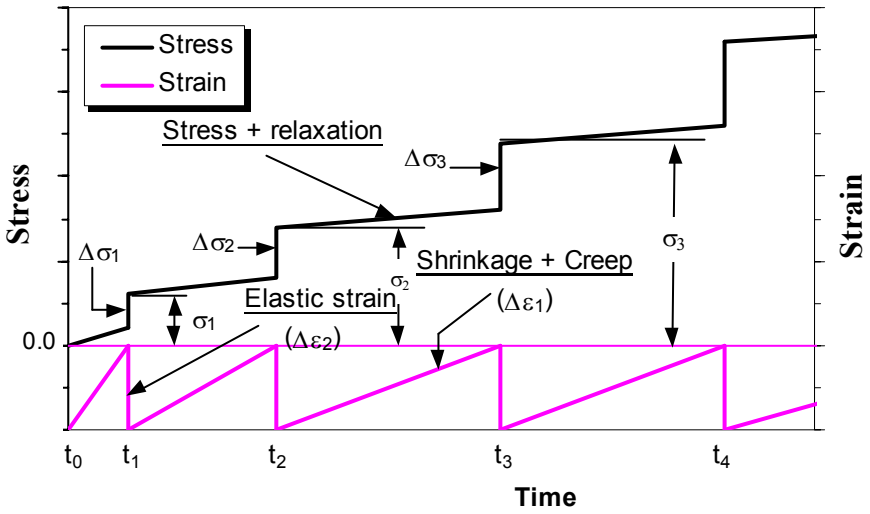

Figure 6.3 Schematic stress build-up and control length deformation during a test in TSTM.

An extract of a TSTM test is shown in Figure 6.4. The figure shows measured deformation, deformation due to screw movement (where the predefined strain value in average is 0.4 mμ here) and the stress increase at each screw movement during the curing age 30-40 hrs. As can be seen, deformations develop due to hydration induced volume changes of the hardening concrete reaching the predefined strain level after about 1 hour, followed by pulling the movable head back to its original position something that produces a small stress increase. It takes about 2 minutes for the screw to move the concrete back to its original length, i.e. to the zero deformation. Detail description on how system is operated is given in Bjøntegaard (1999).

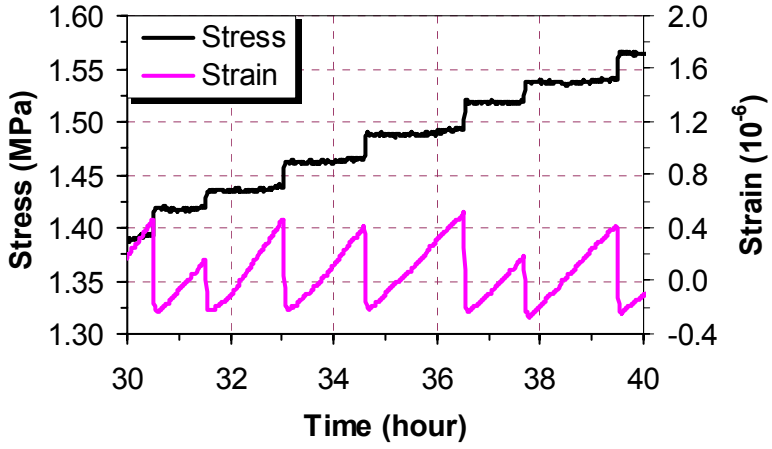

Figure 6.4 Measured stress build-up and control length deformation during a test in TSTM [Bjøntegaard (1999)].

URN:NBN:no-3377

6.4 Theoretical Modelling of Creep

6.4.1 Solution Method for the Numerical Calculations

Calculation of stress from a given strain history and vice versa can be accomplished by various methods described earlier in Chapter 3. For the present analysis an integral type formulation is used. Generally for analysing a structure the use of this method is inefficient due the fact that the entire stress history must be stored for all the integration points in the structure, and there will be need for a large storage capacity. Nevertheless, since only data from the TSTM tests are considered, this formulation is chosen in the present work. In general structural problems, the stress history is unknown in advance, and the desired task is to predict stresses in concrete on the basis of the volume changes and the boundary conditions (restraint).

The expression for total strain using the integral creep law is:

$$\varepsilon(t) = \int_{t_1}^{t} J(t,t')d\sigma(t') + \varepsilon^{o}(t) \qquad (6.\ 1)$$

In which $\varepsilon(t)$ denotes the total strain at time t, t_1 is the concrete age at the first application of stress and $d\sigma(t')$ is the stress increment applied at time t'. $J(t,t')$, usually termed the compliance function, represents the total stress-dependent strain at time t when a stress increment equal to a unity is applied at time t'. Finally, $\varepsilon^{o}(t)$ is the load-independent strain. All the calculations presented in the following sections are based on the hypothesis that the principle of superposition of stress and strain is valid. A short description of this principle is given in Chapter 3. When the analysis is performed based on the superposition principle, the time history has to be subdivided into time intervals, and the integral expression (Eq. 6.1) can then be replaced by:

$$\varepsilon(t_n) = \sum_{j=1}^{n} J(t_n, t_j) \cdot \Delta\sigma_j + \varepsilon^{o}(t_n) \qquad (6.\ 2)$$

Concerning the time discretization, Kanstad (1990) has discussed the importance of the number of time-steps that should be used throughout the entire time history. Dependent on the number of time-steps and an assumption about the time variation of the stresses, different results might be achieved. For the purpose of analysis, the total time is subdivided into a number of time steps whose length depends on how often (or how fast) stress changes were recorded during the test. The data from the tests treated in the present work shows that they were recorded frequently for each hour in the first 24 hrs, and then the time interval increased to 2, 3, 4 etc. hrs during the tests. The number of time increments in the algorithm, for the history of varying stress under restrained condition in the present work, is kept as the same as under recording of the data.

For continuously varying strain, different formulations of the step-by-step methods are available to calculate the stress due to a strain increment (or decrement) $\Delta\varepsilon_j$ occurring during the time Δt_j. Using an algorithm for linear creep called Bažant's second order algorithm, Bažant and Najjar (1973), which is based on approximating the integral in Eq. 6.1 by the trapezoidal rule, a good accuracy can be achieved. In the algorithm, the stress increment $\Delta\sigma_j$ is assumed applied in the middle of the *j*th interval (at time $t_{j-1/2}$). The total strain at the end of the *j*th interval is the sum of the strains due to stress increments, $\Delta\sigma_j$, applied during all the previous increments. The notation used for the superposition numerical analysis is defined in Figure 6.5.

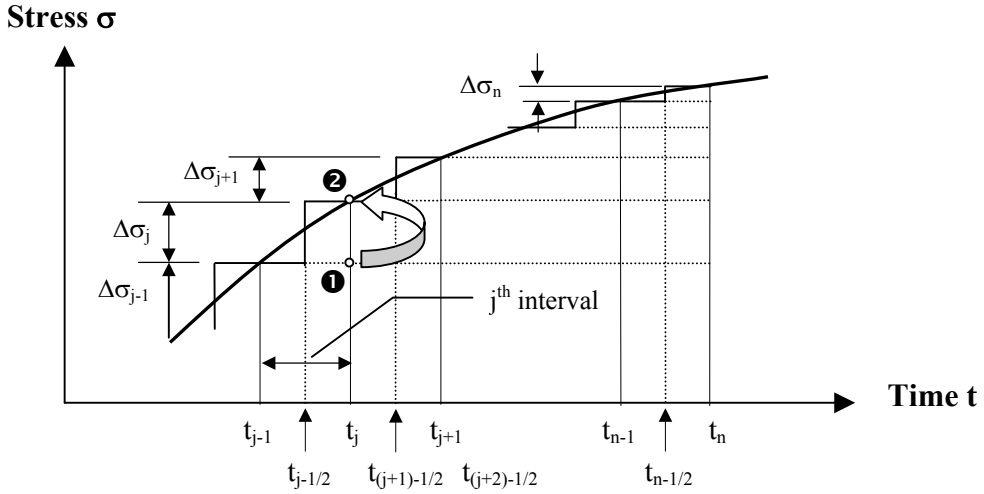

Figure 6.5 Definition of the time interval and stress increments.

The stress increment of the j^{th} time interval, $\Delta\sigma_j$, is assumed and calculated at the time $t_{j-1/2}$ with $E(t_{j-1/2})$, and creep is determined from that time on. At the end of the j^{th} interval at time (t_j) the total creep strain is:

$$\varepsilon(t_j) = \sum_{i=1}^{j-1} J(t_j, t_{i-1/2}) \cdot \Delta\sigma_i \tag{6. 3a}$$

where:

$$J(t_j, t_{i-1/2}) = \frac{1}{E(t_{i-1/2})}\left[1 + \varphi(t_j, t_{i-1/2})\right] \tag{6. 3b}$$

$$t_{i-1/2} = \frac{1}{2}(t_i - t_{i-1}) \tag{6. 3c}$$

In the time steps where load or temperature changes occur, the stress rates are assumed to be constant in the linear time scale. Determination of a stress increment $\Delta\sigma_j$ at a time t_j will be explained step-by-step in the following, and the algorithm used in the numerical solution is given through the expressions 6.3-6.7.

In the description of the constitutive behaviour of young concrete it is assumed that the strain increment $\Delta\varepsilon_j$ in the TSTM at any time t_j may be decomposed into thermal-, autogenous- and creep strains. One should notice that the determined creep strain in (6. 3a) is calculated at point ❶ in the Figure 6.5. The strain compatibility is established at time t_j at point ❷ to determine the stress-induced strain increment.

$$\Delta\varepsilon_j = -(\Delta\varepsilon_{cr} + \Delta\varepsilon_{AD} + \Delta\varepsilon_{TD})_j \tag{6. 4a}$$

The strain component $\Delta\varepsilon_{cr}$ includes creep- and elastic strains. The strain components in the above equilibrium expression are:

$$\Delta\varepsilon_{cr}(t_j) = \varepsilon_{cr}(t_j) - \varepsilon_{cr}(t_{j-1}) \tag{6. 4b}$$

$$\Delta\varepsilon_{AD}(t_j) = \varepsilon_{AD}(t_j) - \varepsilon_{AD}(t_{j-1}) \tag{6. 4c}$$

$$\Delta\varepsilon_{TD}(t_j) = \varepsilon_T(t_j) - \varepsilon_T(t_{j-1}) \tag{6. 4d}$$

$$\Delta_{free}(t_j) = \Delta\varepsilon_{TD}(t_j) + \Delta\varepsilon_{AD}(t_j) \tag{6. 4e}$$

The strain increment in (Eq. 6.4b) may also be written as:

$$\Delta\varepsilon_{cr}(t_j) = \sum_{i=1}^{j}(J(t_j, t_{i-1/2})\cdot\Delta\sigma_i - \sum_{i=1}^{j-1}(J(t_{j-1}, t_{i-1/2})\cdot\Delta\sigma_i \tag{6. 5}$$

where:

- Δ : Represents increments
- ε_{AD} : Autogenous deformation
- ε_{TD} : Thermal dilation
- ε_{free} : Measured free deformation in the Dilation Rig
- ε : Stress-induced strain
- $t_{j-1/2}$: Middle of the time increment

The measured free deformations ε_{free} during the different temperatures are the sum of ε_{TD} and $\varepsilon_{AD.}$ This sum is used directly in the stress calculations. At a time step Δt_j the free strain $\Delta\varepsilon_{free}$ is known and the creep increment can be calculated by using a creep function. The only unknown in Eq. 6.4a is then $\Delta\varepsilon_j$ which is an incremental stress-induced strain that causes stress building in the restraint concrete.

The stress increment at t_j can then be determined as:

$$\Delta\sigma_j = E_{eff} \cdot \Delta\varepsilon_j \qquad \text{or} \qquad \Delta\sigma_j = E_{eff} \cdot (\Delta\varepsilon_{free} - \Delta\varepsilon_{cr})_j \tag{6. 6}$$

In which E_{eff} is defined as the effective modulus of elasticity which take account the creep effect for the time interval, from $t_{j-1/2}$ to t_j. The effective E-modulus can be expressed in terms of compliance function, where it is the inverse of it:

$$E_{eff} = \frac{1}{J(t')} = \frac{E(t')}{1+\varphi(t,t')} \tag{6. 7a}$$

Using a creep function like Double Power Law, the effective E-modulus for the above algorithm can be expressed as:

$$E_{eff}(t_j) = \frac{E(t_{j-1/2})}{1+\varphi_o \cdot t_{j-1/2}^{-d} \cdot (t_j - t_{j-1/2})^p} \tag{6. 7b}$$

The model parameters in the expression are given in the next section. The present algorithm is implemented in a Visual Basic Excel program, given in Appendix G.

6.4.2 Creep Model

The linear sealed creep model Double Power Law (DPL), which expresses the creep function or the compliance function, is used to obtain the stress history in the present work. It is investigated how accurate the model is to simulate the early age behaviour. The model describes the creep of concrete $\varepsilon_{cr}(t)$ as a product of a function dealing with the effect of age (t') at the application of the load and a function dealing with the development of creep with the load duration $(t-t')$, Eq. (6. 8). The creep law expressed by compliance function J(t,t') at reference temperature (20 ^{o}C) is:

$$J(t,t') = \frac{1}{E_c(t')}\left[1 + \varphi_o \cdot t'^{-d}(t-t')^p\right] \tag{6. 8}$$

A brief description of the model, its terms and parameters is given in Chapter 3. The modulus of elasticity $E_c(t')$ is not a curve-fitting parameter as is was proposed in the original equation, but it is determined from separate tests described in Chapter 5.

A standard way to determine the creep model parameters is to use an optimization technique on results from creep tests performed under sustained load applied at different ages. Using this technique, the creep model parameters for the DPL can be determined from either the compressive creep tests or the tensile creep tests presented and discussed in Chapter 4. Since the tensile creep was found to be different from the compressive creep, two sets of creep parameters will be determined. The parameters are determined by minimizing the quadratic sum of the deviation from the test data.

Table 6.2 gives a survey of the model parameters determined from the optimization technique, separately for different *creep tests in compression* with the BASE-5 concrete. The data for the concrete at loading ages 1, 2, 3, 4, 6 and 8 days reveals that the parameters varies in an interval: φ_o varies between 0.71 and 0.81 and p varies between 0.17 and 0.23. The tests at 1, 2 and 3 days were unloaded after few days. The parameter d is set to be 0.20, the value which is found to fit best when all the tests were considered simultaneously.

Table 6.2 Creep model parameters in DPL for different creep tests in compression, BASE-5, 20 ^{o}C isothermal tests (d=20).

Age at loading t_0 (day)	**Creep model parameters**		
	$\varphi_o=(\varphi_{oe}+\varphi_{op})$	**p**	**φ_{oe}**
1	0.78	0.18	0.23
2	0.71	0.21	0.22
3	0.76	0.23	0.08
4	0.81	0.18	-
6	0.79	0.17	-
8	0.80	0.19	-

Compiling all the test results in one diagram and optimizing the model parameters to fit the creep model DPL to all the creep tests simultaneously, the following creep parameters are found:

$$\varphi_o = 0.75, \qquad d = 0.20, \qquad p = 0.21$$

Using these parameters in the creep model good agreement with the test results for the entire loading period is achieved, see Figure 6.6. The elastic strains in the figure are calculated from the E-modulus (defined as E_2 in Chapter 5).

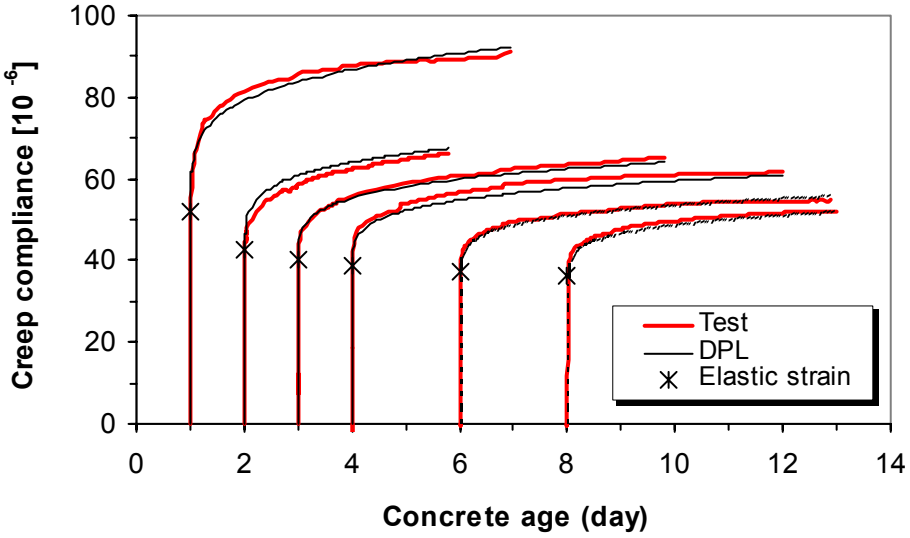

Figure 6.6 Creep strains calculated by the DPL compared to the results from compressive creep tests on BASE-5, 20 °C.

As mentioned, the compressive creep tests at 1, 2 and 3 days of concrete age were performed with sustained load for few days and then the load was totally removed. The results for two of these tests with unloading are shown separately in Figure 6.7. As can be seen, creep for the time under load can be closely predicted by Double Power Law according to Eq. (6. 8), but a considerable deviation appears clearly from the time of unloading. The model greatly overestimates the creep recovery. The recovery creep curves in the figure reveals that a significant part of the deviation is from the instantaneous recovery and the deviation grows very fast in short time after unloading.

According to the conditions of the linear principle of superposition, in which the Double Power Law model follows, a complete removal of load from the concrete exposed to a sustained load will lead to an overestimation of the recovery, i.e. creep of concrete is only partly reversible. This issue is well documented in the literature and it has been discussed earlier in Chapter 3. To overcome the problem it is necessary to adjust the model for the recovery.

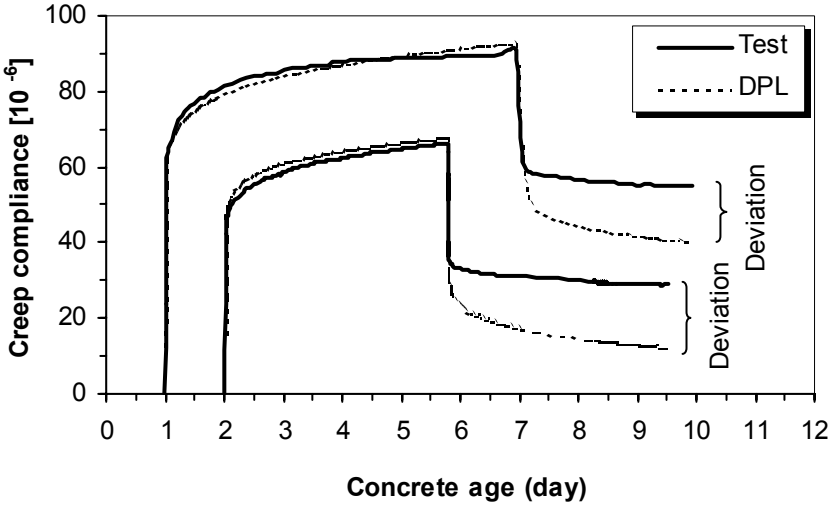

Figure 6.7 Estimated creep strains by the DPL compared to the results from compressive creep tests (loaded and unloaded) on BASE-5, , 20 ^{o}C.

Table 6.3 gives a survey over the second set of the determined model parameters for BASE-5 concrete, determined separately from each of the *tensile creep tests*. As can be seen, test Nr. 108, with loading age 8 days, differ from the other tests. The data for the loading ages 1, 2, 3, 4 and 6 days reveal that the creep parameter varies in a range:

$$\varphi_o: 0.30 - 40 \quad \text{and} \quad p : 0.53 - 0.75$$

Table 6.3 Creep model parameters in DPL for different creep tests in tension (d=0.27).

Test Nr.	**Age at loading t_0 (day)**	**Creep model parameters**	
		φ_o	**p**
105	1	0.30	0.56
111	2	0.40	0.54
508	3	0.34	0.54
109	4	0.40	0.53
505	6	0.30	0.75
108	8	0.15	0.84

The parameter *d* is determined to be 0.27; a value which was found to fit best for all the tests simultaneously. The scatter in the parameters in tensile creep tests is worse than in the compressive creep tests. In the same way as in compressive creep tests, the tensile creep tests were compiled in one diagram and the model parameters were determined, see Figure 6.8. The parameters, which fit best for all the tensile creep tests simultaneously, were found to be:

$$\varphi_o = 0.33, \qquad d = 0.27, \qquad p = 0.56$$

These parameters are very different from those for compressive creep tests. Comparing the creep curves in comparison (Figure 6.6) and tension (Figure 6.8), it is pronounced that the effect of aging seems to be less in tensile creep than in compressive creep (all curves are compiled in Figure 5.23).

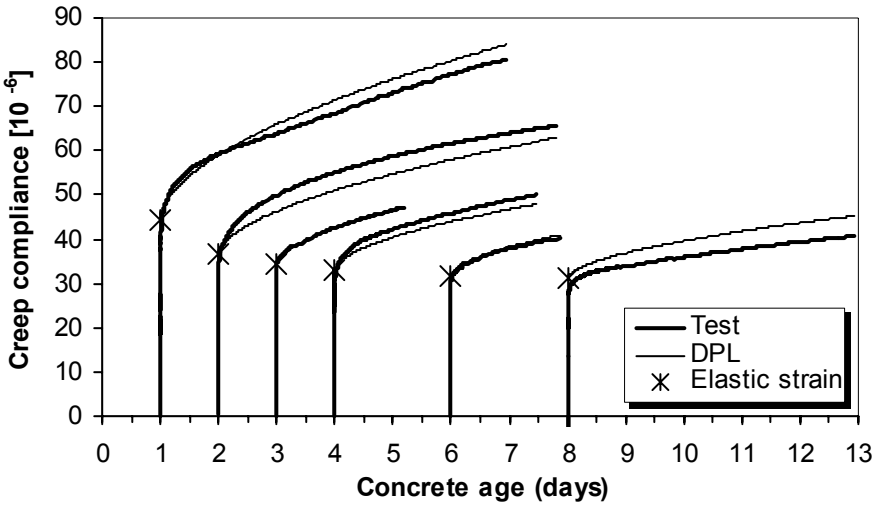

Figure 6.8 Creep strains calculated by the DPL compared to the results from tensile creep tests on BASE-5, 20 °C.

6.4.3 Modified Double Power Law (M-DPL)

To illustrate the recovery effects, we consider stress development in an externally restrained concrete specimen under realistic temperature. Dependent on the type of the stress (compressive or tensile) and on the stress increment the curve is divided into three periods, shown in Figure 6.9:

- Part 1: Increasing compressive stress. Both the compressive strains due to expansion and the modulus of elasticity increase in this period. The concrete material is exposed to higher stresses with time, and creep occurs.

- Part 2: Descending compressive stresses. The compressive strains are reduced due to contraction, but the modulus of elasticity increase. The concrete material is exposed to lower stresses with time, i.e. the concrete is unloaded slowly with time. Creep and the creep recovery occur simultaneously.

- Part 3: Increasing tensile stresses, $\Delta\sigma \geq 0$. Both the tensile strain due to contraction and the modulus of elasticity increase with time. Tensile creep occurs.

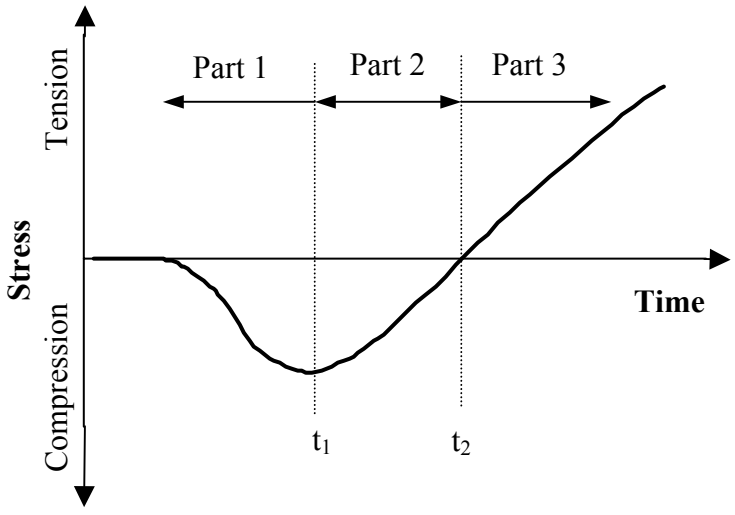

Figure 6.9 Stress development in externally1 full-restrained concrete subdivided into different parts. Maximum temperature is 61.5 ^{o}C.

During the temperature rise in restrained early age concrete the inhibited thermal expansion is transferred into increasing compressive stresses (in Part 1). In this stage a high relaxation reduces the thermal pre-stress. On the other hand, during the subsequent cooling, the thermal contraction and the autogenous shrinkage will cause decreasing of compressive stresses followed by relatively high tensile stresses. The process of increasing (Part 1) to decreasing

of compressive stresses (Part 2) is a loading and an unloading process. When concrete that has been subjected to a sustained stress is unloaded by a stress increment, the recovery of strain occurs. Since the recovery occurs with time it includes both the instantaneous recovery and creep (or time-dependent) recovery.

It is still not clear whether the mechanism of creep and creep recovery are different from one another or whether the creep recovery is simply a negative creep. Using the principle of superposition approach assumes that creep recovery is in essence a negative creep, and is smaller than preceding creep only because of the aging effect. However, since decades it has been known that not all of the creep is recoverable, but this has not been considered in the modelling of creep development. At a given time t between t_1 and t_2 in Part 2, the concrete material undergoes both of the phenomena, creep recovery due to a negative stress increment, $\Delta\sigma$, and creep due to residual stresses. They work simultaneously but in opposite directions, something, which makes the explanation of the mechanism of stress relaxation even more complex.

To take account for the unloading effect and creep recovery the Double Power Law is modified. The modification of the Double Power Law consists simply of a division of the creep model parameter φ_o in Eq. (6.8) into two parts: the viscoelastic part φ_{oe} and the visco-plastic part φ_{op}.

For the stress increments applied in part 1 and 3 in Figure 6.9 the modified Double Power Law (M-DPL) is:

$$J(t,t') = \frac{1}{E(t')}\left[1 + (\varphi_{oe} + \varphi_{op}) \cdot t'^{-d} (t-t')^{p}\right] \tag{6. 9}$$

For the stress increments in part 2 in Figure 6.9:

$$J(t,t'') = \frac{1}{E(t'')}\left[1 + \varphi_{oe} \cdot t''^{-d} (t-t'')^{p}\right] \tag{6. 10}$$

where:

t:	Current concrete age
t':	Concrete age at loading prior to unloading
t'':	Concrete age at unloading
$J(t,t')$, $J(t,t'')$:	Compliance function at time t
$E(t')$:	Modulus of elasticity at loading time t'
$E(t'')$:	Modulus of elasticity at the unloading time t''

For practical use of this model, the principle of superposition also has to be modified. This is illustrated by the load history given in Figure 6.10, where the strain after the time t_2 is predicted as:

$$\varepsilon(t) = \frac{1}{E_c(t_1)}\left[1 + \varphi_o \cdot t_1^{-d}(t-t_1)^p\right]\cdot\sigma_1 + \frac{1}{E_c(t_2)}\left[1 + \varphi_{oe} \cdot t_2^{-d}(t-t_2)^p\right]\cdot\sigma_2 \qquad (6.\ 11)$$

Note that σ_2 is negative.

In which σ_1 represents the loading stress at concrete age t_1, and σ_2 is the unloading stress at age t_2, where the sign of σ_2 is negative. The physical interpretation of the new term in the extended Double Power Law is to adjust creep recovery after partial or complete load removed.

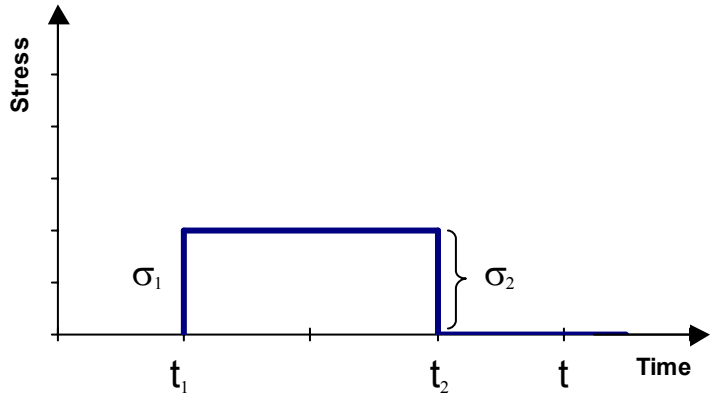

Figure 6.10 Load history for a concrete specimen.

To determine the different components of the creep coefficient φ_o the optimization technique is used again. While the creep model parameters d, p and φ_o, found earlier, were kept constant, the parameter φ_{oe} was determined by minimizing the quadratic sum of the deviation from only the recovery part of the test data. The last column in Table 6.2 gives the determined value of φ_{oe} for each of the three creep curves. Its value varies between 0.08 and 0.23. The determined parameters which fits best to all the creep curves together are:

d = 0.20,
p= 0.21
$\varphi_o = \varphi_{oe} + \varphi_{op} = 0.75$
$\varphi_{oe} = 0.22 \quad \Rightarrow \quad \varphi_{op} = \varphi_o - \varphi_{oe} = 0.53$

It is timely to give some comments on these parameters; We observed that using the parameter φ_o for the entire strain history lead to an overestimation of creep recovery.

Regarding the stress calculation, this will lead to an underestimation of self-induced stresses when the cooling phase has started and the underestimation will increase with time. An increase of the parameter φ_o will result in a slower stress build-up. The creep is not influenced by creep parameter *d* when the loading age is 1 day. For higher loading ages, the lower *d* is the higher creep is generated in the model. The creep parameter *p*, which is the power of loading duration, has a much greater influence on creep development than *d*. The creep coefficient for the recoverable part (φ_{oe}) consists of 28% of the total creep coefficient, φ_o. This means that only 28% of the creep is assumed to be recoverable. The ratio between φ_{op} and φ_{oe} is 2.5. The effect of the new parameter φ_{oe} on the creep recovery in the new M-DPL creep model is shown in Figure 6.11.

For other temperatures than 20 ^oC, the effect of aging in M-DPL is taken into account by maturity dependence of E-modulus, given in Eq. 3.18. Furthermore, the loading age t' and the loading duration is replaced by equivalent age (maturity) t'_e and equivalent load duration (t_e-t'_e):

$$J(t,t') = \frac{1}{E_c(t'_e)}\left[1 + \varphi_o \cdot (t'_e)^{-d}(t_e - t'_e)^p\right] \qquad (6.12)$$

In addition, the transient creep $\Delta\varepsilon_{trcr}$, which takes into account the change in creep rate during changes in temperature, is modeled separately as in Eq. (6.19). It is assumed to be zero for decreasing temperatures.

The Modified Double Power Law, including the effect of variable temperature, is implemented in Visual Basic Excel program, shown in Appendix G, by which the subsequent calculations are carried out.

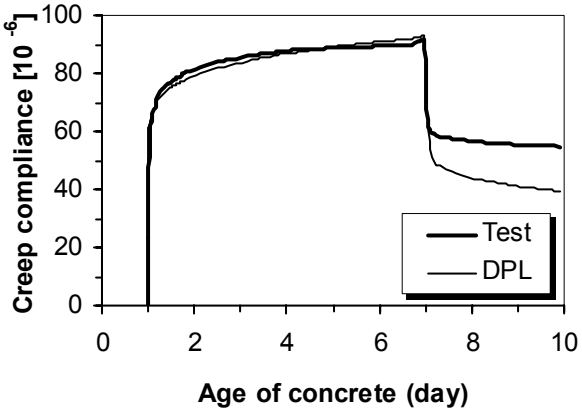

a) DPL. Age of loading, t_0 = 1 day

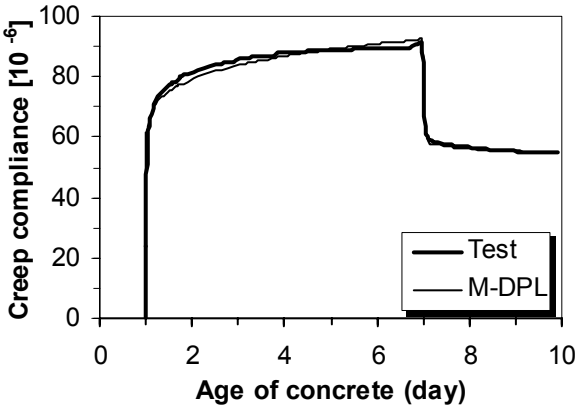

b) M-DPL. Age of loading, t_0 = 1 day

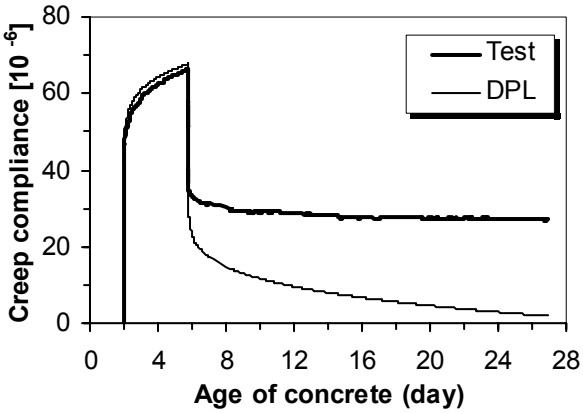

c) DPL. Age of loading, t_0 = 2 days

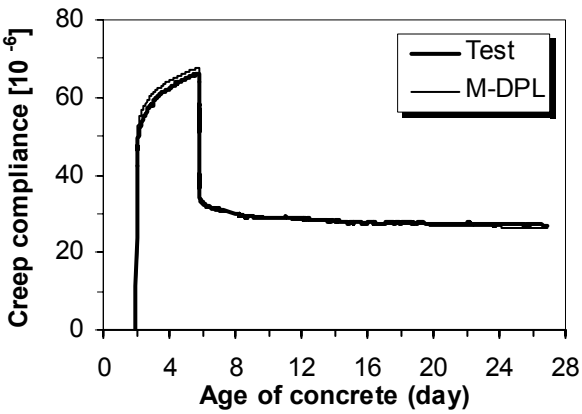

d) M-DPL. Age of loading, t_0 = 2 days

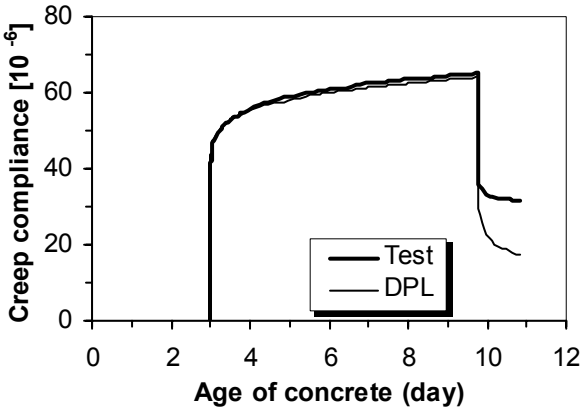

e) DPL. Age of loading, t_0 = 3 days

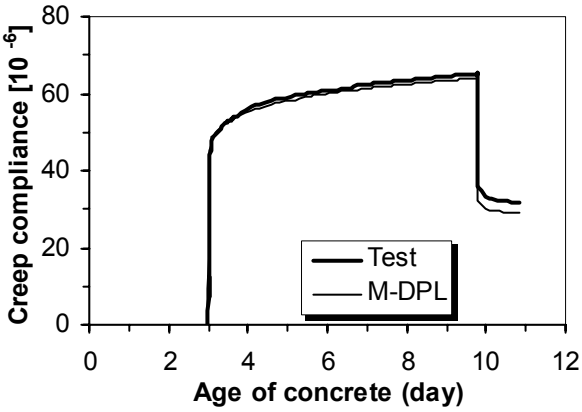

f) M-DPL. Age of loading, t_0 = 3 days

Figure 6.11 Prediction of creep development by DPL and M-DPL, compared to the test results. (BASE-5, T=20 ^{o}C)

6.4.4 Necessary Creep Tests for Estimation of Model Parameters

A question, which often arises when a creep model shall be used is: How many creep tests are necessary to perform to estimate the model parameters. Although the issue is very important regarding time consumption and the test costs, the author did not find any study in the literature on this subject.

In the previous section, the results of six compressive creep tests were used to estimate the three model parameters (φ_o, d and p) of the DPL. Table 6.4 shows an estimation of these model parameters for combination of creep tests at loading ages 1, 2, 3, 4, 6 and 8 days. Each test combination is given by number sequence, which represent the loading age for the actual tests. Totally 56 combinations are made: 15 combinations with two tests, 20 combinations with three tests, 14 combinations with four tests, 6 combinations with five tests and finally 1 combination with all six tests simultaneously. In addition to these, model parameters are found for each creep test separately (six tests). It is important to notice that for the individual tests, the parameter d cannot be estimated only from one loading age. Therefore, d was assumed to be 0.20 (the optimized value for all the tests simultaneously) for all these individual tests. The comparison between the creep tests and the creep curves estimated by DPL for all the combinations are shown in figures in Appendix H.

An analysis of the results of the test combinations were made by comparing the new estimated creep curves to the best-fitted creep curve (test combination 1,2,3,4,6,8), which has the model parameters $\varphi_o=0.75$, $d=0.20$ and $p=0.21$. Deviation (denoted as *Dev*) from the best-fitted creep curve, for the new test combinations is defined by Eq. (6. 13) and the estimated values are presented in Table 6.4. *Dev* is given in percentage.

$$Dev = \left(\frac{S_{new} - S_{old}}{S_{old}} \right) \cdot 100 \qquad \text{, in percent} \tag{6. 13)a}$$

$$S_{new} = \sum_{j=1}^{m} R_j \tag{6. 13)b}$$

$$S_{old} = \sum_{j=1}^{n} R_j \tag{6. 13)c}$$

$$R_j = \sum_{i=1}^{r} \left(\varepsilon_{DPL} - \varepsilon_{test} \right)^2 \tag{6. 13)d}$$

where:

r: Number of recorded strain points on creep curve in each test
m: Number of tests in a combination
n: Number of total tests

R_j: Quadratic sum of creep deviation between model and test for one tests
S_{old}: Sum of R for all the tests (1,2,3,4,6,8)
S_{new}: Sum of R for the tests in a test combination
Dev: Deviation in creep model between using a test combination and all tests

In addition, the standard deviation (STD) between the calculated and the measured results is presented, by (6. 14). The Dev and the STD are 0.0% and 3.45 for the test combination (1, 2, 3, 4, 6 and 8), respectively. The range of Dev in percent and the STD for 2, 3, 4 and 5 test combinations are given in Table 6.5. Test combinations, which give the lower and upper limits of the deviation range, are also given in the table. The table reveals that the more tests the less scattering in the deviation is.

$$STD = \sqrt{\frac{S_{new}}{t}} \qquad (6.\ 14)a$$

$$t = \sum_{i}^{n} r \qquad (6.\ 14)b$$

where:

t: Total number of recorded strain points on creep curve in all tests.

As both the mentioned tables shows, the best combinations include the creep tests at loading ages of 1 and 2 days, which indicates that the creep properties at very young ages (≤ 2 days) are most uncertain, and consequently that they must be included. Four test combinations 1234, 1238, 1246, 1248, each consisting of four creep tests, provide 100% relative accuracy, i.e. a STD equal to 3.45. In addition, the two test combinations 124 and 128 provides 99% relative accuracy, i.e. a STD equal to 3.46. The main characteristic of the worst cases is that the test at loading age of 1 day is not included in the test combinations.

The conclusion from the analysis of the six compressive creep tests is that the creep development at early ages, which has different behaviour than at the later ages, has significant effect in determining the creep parameters. Depending on the desired accuracy level of the calculations, the necessary number of creep tests can be determined. The best results can be achieved when the test combinations cover a large part of the possible loading ages, conditionally including the tests at 1 and 2 days for this particular concrete type.

Table 6.4 Model parameters and STD for DPL from combination of different creep tests.

Parameter	Test Combinations - noted by Loading ages (days)						
	1	**2**	**3**	**4**	**6**	**8**	**12**
ϕ_0	0.78	0.71	0.75	0.80	0.77	0.79	0.77
d	0.20	0.20	0.20	0.20	0.20	0.20	0.32
p	0.18	0.21	0.23	0.18	0.17	0.19	0.20
Dev.% (STD)	*7 (3.57)*	*12 (3.67)*	*5 (3.53)*	*15 (3.70)*	*13 (3.67)*	*8 (3.60)*	*54 (4.28)*
	13	**14**	**16**	**18**	**23**	**24**	**26**
ϕ_0	0.77	0.78	0.78	0.78	0.67	0.67	0.69
d	0.20	0.19	0.21	0.20	0.10	0.10	0.16
p	0.20	0.18	0.18	0.19	0.22	0.21	0.20
Dev.% (STD)	*3 (350.)*	*11 (3.63)*	*8 (3.58)*	*8 (3.58)*	*22 (3.3.81)*	*23 (3.82)*	*14 (3.68)*
	28	**34**	**36**	**38**	**46**	**48**	**68**
ϕ_0	0.68	0.76	0.81	0.75	0.95	0.81	0.64
d	0.14	0.19	0.24	0.19	0.32	0.21	0.10
p	0.21	0.21	0.21	0.22	0.18	0.18	0.18
Dev.% (STD)	*15 (3.70)*	*2 (3.48)*	*10 (3.61)*	*2 (3.49)*	*110 (5.00)*	*17 (3.74)*	*53 (4.26)*
	123	**124**	**126**	**128**	**134**	**136**	**138**
ϕ_0	0.76	0.75	0.75	0.75	0.78	0.78	0.77
d	0.24	0.21	0.22	0.21	0.19	0.21	0.20
p	0.21	0.21	0.21	0.21	0.20	0.19	0.20
Dev.% (STD)	*6 (3.55)*	*1 (3.46)*	*4 (3.51)*	*1 (3.46)*	*5 (3.53)*	*3 (3.50)*	*4 (3.51)*
	146	**148**	**168**	**234**	**236**	**238**	**246**
ϕ_0	0.78	0.78	0.78	0.67	0.70	0.69	0.69
d	0.20	0.19	0.21	0.10	0.16	0.14	0.14
p	0.18	0.19	0.18	0.21	0.21	0.22	0.21
Dev.% (STD)	*7 (3.57)*	*9 (3.68)*	*8 (3.59)*	*22 (3.81)*	*7 (3.57)*	*11 (3.63)*	*12 (3.65)*
	248	**268**	**346**	**348**	**368**	**468**	**1234**
ϕ_0	0.68	0.68	0.82	0.76	0.77	0.85	0.75
d	0.12	0.14	0.25	0.19	0.21	0.24	0.20
p	0.21	0.20	0.20	0.20	0.20	0.18	0.21
Dev.% (STD)	*15 (3.70)*	*16 (3.72)*	*16 (3.71)*	*2 (3.49)*	*2 (3.48)*	*32 (3.97)*	*0 (3.45)*
	1236	**1238**	**1246**	**1248**	**1346**	**1348**	**1368**
ϕ_0	0.75	0.75	0.75	0.75	0.78	0.78	0.78
d	0.22	0.20	0.21	0.19	0.21	0.19	0.21
p	0.21	0.21	0.21	0.21	0.19	0.19	0.19
Dev.% (STD)	*1 (3.47)*	*0 (3.45)*	*0 (3.46)*	*0 (3.45)*	*4 (3.52)*	*5 (3.53)*	*4 (3.51)*
	1468	**2346**	**2348**	**2368**	**2468**	**3468**	**12346**
ϕ_0	0.78	0.70	0.69	0.70	0.69	0.79	0.75
d	0.20	0.15	0.13	0.15	0.14	0.21	0.21
p	0.18	0.21	0.21	0.21	0.20	0.20	0.21
Dev.% (STD)	*8 (3.58)*	*8 (3.59)*	*12 (3.65)*	*9 (3.60)*	*12 (3.65)*	*6 (3.55)*	*0 (3.35)*
	12348	**12368**	**12468**	**13468**	**23468**	**123468**	
ϕ_0	0.75	0.75	0.75	0.78	0.70	**0.75**	
d	0.19	0.20	0.20	0.20	0.15	**0.20**	
p	0.21	0.21	0.21	0.19	0.21	**0.21**	
Dev.% (STD)	*0 (3.45)*	*0 (3.45)*	*0 (3.45)*	*4 (3.52)*	*8 (3.59)*	***0 (3.45)***	

Table 6.5 Creep test combinations with deviation from the best-fitted creep curve, and STD form the measured test data.

Number of Creep Tests	Deviation *Dev* (%)	Standard Deviation (STD)	Test Combination	
			Best Case	Worst Case
2	2 - 110	3.48 - 5.00	(34) (38)	(46)
3	1 - 32	3.46 - 3.97	(124) (128)	(468)
4	0 - 12	3.45 - 3.65	(1234) (1238) (1246) (1248)	(2348) (2468)
5	0 - 8	3.45 - 3.59	(12346) (12348) (12368) (12468)	(23468)
6	0	3.45	(12346.8)	

6.4.5 Prediction of Relaxation from Creep

Using the solution method for the numerical calculation described in section 6.4.1, the relaxation can be predicted from the creep development. The creep compliance, *J(t,t')* is converted to the relaxation funtion, *R(t,t')*, which is then used to calculate the stress. *R(t,t')* is obtained by solving the following integral equation:

$$1 = \int_0^1 J(t,t') \cdot dR(t') \qquad (6.\ 15)$$

The result of such calculations for a creep test performed at loading age of 2 days is illustrated in Figure 6.12. The algorithm used for this purpose is given in Appendix G.

The creep and relaxation values at three concrete ages (72, 120 and 137.5 hrs) are given on the figure. The creep coefficient, denoted by ϕ in the figure represents the ratio between the creep and the instantaneous deformation. The measured instantaneous deformation per unit stress at the loading age for the creep test is $41 \cdot 10^{-6}$, (i.e. measured deformation one minute after the load was applied divided to the load). Both creep and relaxation develop with a high rate in the two first hrs, and then their rates reduce considerably. Comparing their development, relaxation develops more rapid than creep the first few hrs, and then the trend

changes, and the relaxation proceeds with a lower rate than creep. However, the creep as % of elastic deformation is always much larger than the % of the initial elastic stress that is relaxed at any given time, i.e. 47% vs 34% at 72 hrs etc. The same behaviour is illustrated in Figure 6.13 when the development of the associated phenomenon creep and relaxation relative to their values at concrete age 5 days is considered.

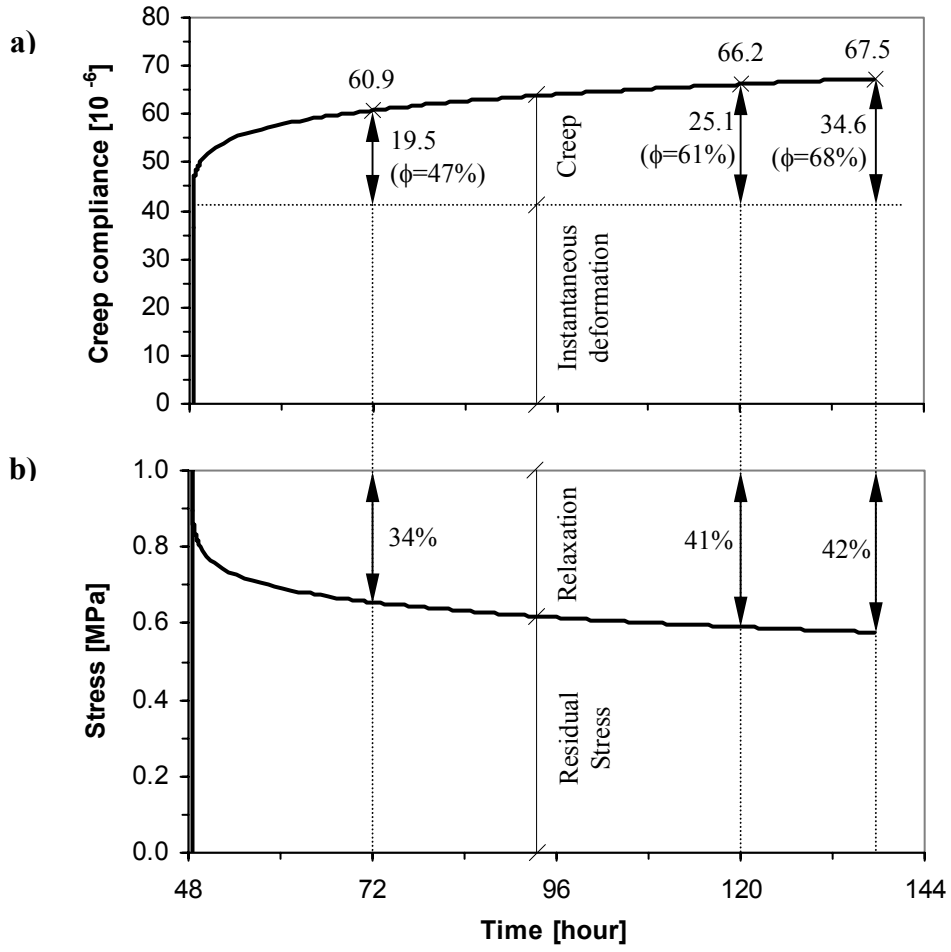

Figure 6.12 Calculation of relaxation from creep. a) Creep development, b) Relaxation development, for BASE-5 at T=20 ^{o}C.

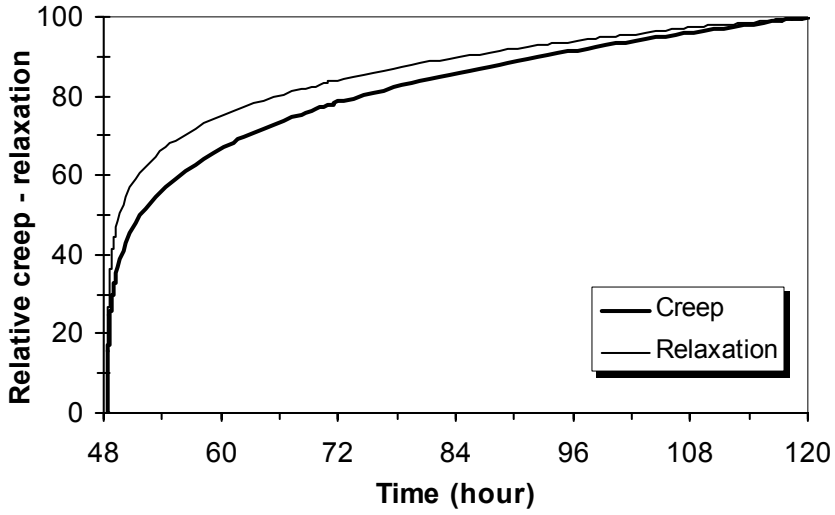

Figure 6.13 Relative creep-relaxation development for BASE-5 at T=20 ^{o}C.

6.5 Test Results From The TSTM

Test results from the TSTM accompanied by parallel results from the dilation rig are evaluated and analyzed in order to deduce creep and relaxation. In the description of the constitutive behaviour of young concrete it is assumed that the strain rate in the TSTM at full restraint may be decomposed as follows:

$$\Delta\varepsilon_{free} + \Delta\varepsilon_{el} + \Delta\varepsilon_{cr} + \Delta\varepsilon_{trcr} = 0 \tag{6. 16}$$

where Δ represent increments, and ε_{free} is the measured deformation in the Diation Rig, ε_{el} the elastic strain, ε_{cr} the creep strain without thermal effect and ε_{trcr} is the transient creep component which takes into account the change in creep rate during changes in temperature. The creep deformation, at any given point in time, can be obtained by subtracting the cumulative sum of the elastic strains in the restrained specimen in the TSTM from the measured free strains in the companion specimen in the Dilation Rig. The constitutive law for each strain component involved in strain compatibility in the TSTM may be defined independently. The sum of the elastic and creep strain in Eq. (6. 16) is replaced by the visco-elastic strain:

$$\varepsilon_{ve}^{'} = \varepsilon_{el} + \varepsilon_{cr} = \int_{t_0}^{t} J(t,t')d\sigma(t) \tag{6. 17}$$

$$\varepsilon_{ve} = \varepsilon_{ve}^{'} + \varepsilon_{trcr} \tag{6. 18}$$

$$\Delta\varepsilon_{trcr} = CTE \cdot \Delta T \cdot \rho \cdot \frac{\sigma_c}{f_t^{'}} \cdot sign\Delta T \tag{6. 19}$$

In which $\boldsymbol{\varepsilon}_{ve'}$ denotes visco-elastic strain *without* transient creep, $\boldsymbol{\varepsilon}_{ve}$ denotes visco-elastic strain *with* transient creep, $\boldsymbol{\varepsilon}_{trcr}$ (or $\boldsymbol{\Delta\varepsilon_{trcr}}$) is transient creep (described in Chapter 3) and *J(t,t')* is the compliance function (or creep function).

Diagrams in this section presents experimental and theoretical results of stress and strain development for some typical tests for each temperature case mentioned before. In addition to the measured free strain and the self-induced stress developed under restrained conditions, various mechanical properties can be computed. In the diagrams σ_{fe} represents stresses in absence of relaxation in the specimen, i.e. simply the integral of the product of the incremental free deformation measured in Dilation rig and the appropriate E-modulus. Similarly, ε_{el} is the integral of the ratio incremental stresses measured in Stress-Rig to

appropriate E-modulus. Note that ε_{free} is used in calculation of σ_{ve}, and σ_{test} is used in calculation of ε_{ve}.

$$\sigma_{fe} = \sum_{i=1}^{n} \Delta\varepsilon_{free}(t)_i \cdot E(t_e^{'})_i \tag{6. 20}$$

$$\varepsilon_{el} = \sum_{i=1}^{n} \frac{\Delta\sigma_{test}(t)_i}{E(t_e^{'})_i} \tag{6. 21}$$

$$R = \frac{\sigma_{fe} - \sigma_{test}}{\sigma_{fe}} \cdot 100 \tag{6. 22}$$

where the different notations in the figures and the above equations represent the following:

σ_{fe} : Fictive elastic stress
ε_{free} : Free deformation in Dilation Rig
ε_{el} : Elastic strain
σ_{test} : Stresses measured in TSTM
R : Relaxation in percent
$\sigma_{ve'}$: Calculated stress *without* transient creep
σ_{ve} : Calculated stress *with* transient creep

Due to different creep behaviour in tension and compression, the calibration of the creep model to the test data resulted in two different sets of model parameters in the previous section, set (C) and set (T) summarized in Table 6.6.

Table 6.6 Model parameters in M-DPL, obtained from compressive- and tensile creep tests (BASE-5, T=20 ^{o}C).

Set	**Model Parameters in M-DPL**				
	φ_o	**d**	**p**	**φ_{oe}**	**φ_{op}**
C (Compressive creep tests)	0.75	0.20	0.21	0.22	0.53
T (Tensile creep tests)	0.33	0.27	0.56	0.09	0.24

Since restrained hardening concrete is exposed to high tensile stresses for a relatively long time, it is expected that the model parameters deduced from tensile creep tests (set T) should fit better to the creep and stress calculations than the model parameters calibrated from the

compressive creep tests (set C). Both sets of parameters will be applied in the calculations in the next section for tests under different temperature conditions; Isothermal, Poly-isothermal and Realistic temperature histories.

6.5.1 Isothermal Tests

The measured self-induced stresses in the TSTM and the measured free deformations in the Dilation rig, for isothermal tests at 5, 13, 20 and 45 ^{o}C, are shown in Figure 6.14. Under isothermal conditions the free deformations caused only by autogenous deformation (AD). A general experience with AD-measurements is observation of an initial expansion right after setting time. Since the major stress-build-up occurs after the expansion period, the measured free deformations are zeroed at time t_0 (defined in Chapter 3), which coincidentally corresponds to the end of the expansion period for most concretes.

Considering the tests at the lower temperatures (5 and 13 ^{o}C) in Figure 6.14, the free deformations seem to be relatively high, i.e. that the temperature has a significant influence on AD, but the effect is unsystematic. The induced stresses are, however, relatively small due to the fact that the modulus of elasticity develops slower under low temperature conditions than under high temperatures. The restrained autogenous shrinkage in the isothermal tests resulted in a relatively high stress, but it did not caused any premature cracking at the first 6 days. For tests at 20 and 45 ^{o}C the self-induced stresses appears as a confirmation of the measured deformations in Dilation Rig, as for instance the relative high rate of deformation during the first 48 hrs causes a rapid build-up of tensile stresses.

Generally, under isothermal conditions the restrained concrete is only exposed to contraction and thus only tensile stresses develop. It is therefore important to notice two things: the first one is that the transient creep has no contribution in building-up the self-induced stresses, i.e. $\Delta\varepsilon_{trcr}$ is zero in Eq. (6. 18). The second one is that, since no unloading occurs under constant temperatures, no creep recovery occurs. This means that the same creep coefficient φ_o is used for the whole time period, and thus the modification of Double Power Law has no influence in determination of self-induced stresses.

Under isothermal conditions the only driving force to generate stresses is AD, and as can be seen in the Figure 6.14 the correspondence between AD and the generated stresses is quite good, but the relationship depends strongly on temperature). At t_0 (which varies from 6 to 20 hrs depending on temperature - equal to 11 maturity hrs), where the stress generation is insignificant (about 0.05 MPa compressive stress), the AD is zeroed. This small compressive stress is probably due to expansion caused by reabsorption of bleed water [Bjøntegaard (1999)].

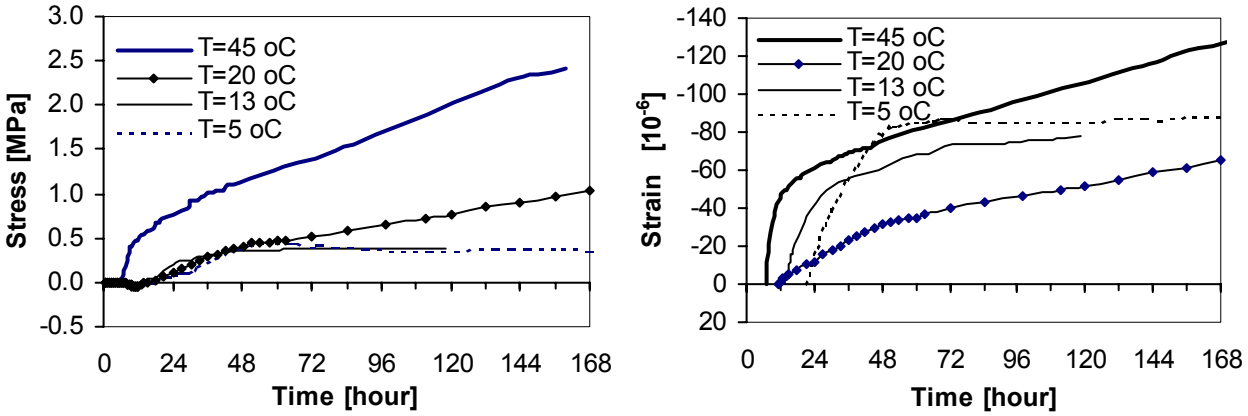

a) Measured stress development

b) Measured strain development

Figure 6.14 Measured stress and strain development in concrete type BASE-5 at different isothermal temperatures.

Figure 6.15a shows measured and calculated self-induced stresses for the isothermal creep test at 20 ^{o}C. The DPL with model parameters calibrated from both the compressive creep tests, and the tensile creep tests, denoted as set (C) and set (T) in Table 6.6 respectively was used. Both curves are in reasonable agreement with the measured results. Using model parameters from (C), a good agreement between the calculated and the measured stresses is observed at the first 4-5 days of concrete age, but some deviation appears after 4 days and it becomes about 14% after 7 days. On the other hand, using model parameters from (T), a high calculated rate of stress-build-up is observed in the first 50 hrs, which leads to a higher predicted than measured stresses. The high stress rate reflects the relative lower creep rate (compared to compressive tensile creep tests) observed in tensile creep tests in the beginning. The stress deviation reduces with time by a lower stress rate, where it becomes about 8% after 7 days. The calculated stress increments $\Delta\sigma$ are also given in the figure to illustrate its values and the time interval when it is applied.

The agreement is quit good for the considered time period at 20 ^{o}C, which gives confidence to experimental results, material models and calculation procedure. It is of course a bit surprising that tensile creep data does not produce a better fit than compressive, since the test specimen is under tension the entire experiment. This will be discussed later.

The corresponding deformations are given in Figure 6.15b. The free deformation, ε_{free}, which corresponds to elastic- and creep deformations (ε_{el} and ε_{cr}) at 100% restrained conditions, and its components are plotted with their respective signs as they appear in the concrete to simplify the comparison. The elastic strains are calculated according to Eq. (6. 21), and the creep strain is the difference between the free deformation and the elastic deformation at a given time.

Relaxation, which is defined by Eq. (6. 22) as the relative difference between the elastic stresses determined by Eq. (6. 21) and the measured self-induced stresses, is illustrated in

Figure 6.16. Because creep is a time dependent phenomenon, the relaxation is low in the beginning and increases to about 40% at a concrete age at 3 days. This means that the ratio between the residual stresses and the total elastic stresses is high in the beginning and decreases to about 60% after about 3 days. This ratio is nearly constant at the rest of the time. In isothermal tests under 100% restraint condition, the ratio between creep and shrinkage can also be used as measure of stress relaxation, as shown in the figure.

The calculation results of the isothermal tests at 5, 13 and 45 ^{o}C (from Figure 6.14) are shown in Figure 6.17. For the test at isothermal temperature 45 ^{o}C in Figure 6.17a, the stresses calculated by the DPL are too low, using both parameter sets (C) and (T). For the case of parameter set (C) the creep model provide a good agreement only in the first 24 hrs, while for the case of parameter set (T), the creep model do not follow the measured stress at all.

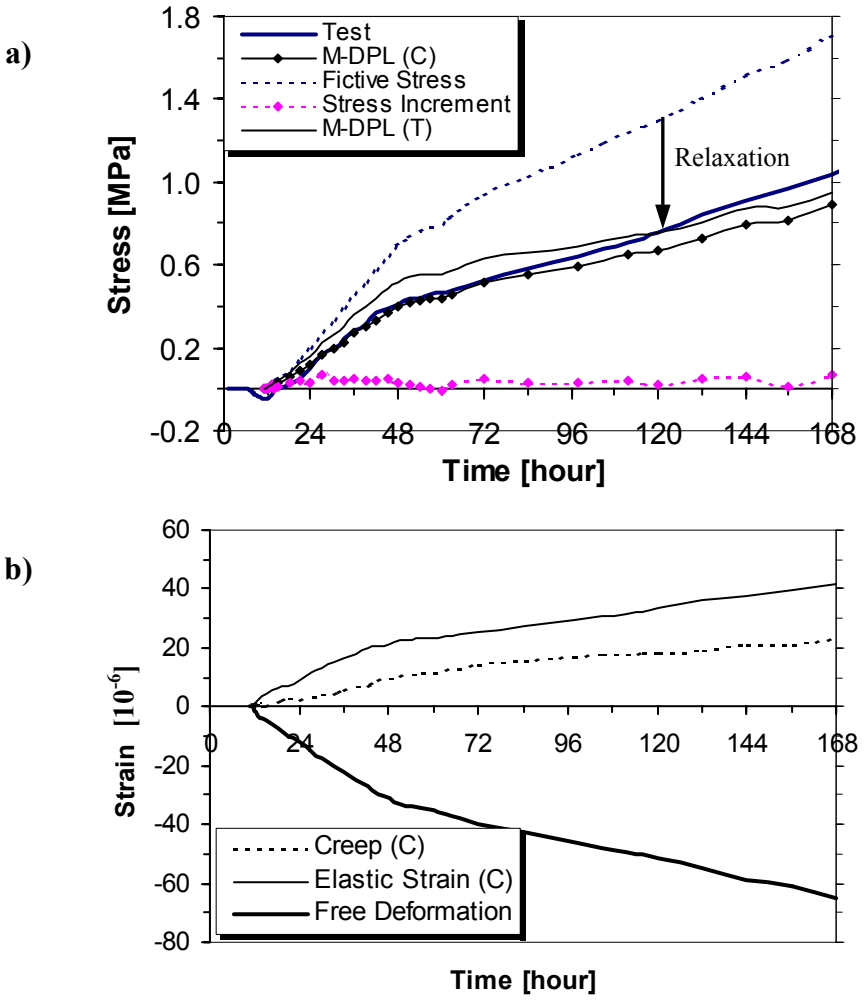

Figure 6.15 Development of stresses and strains in hardening concrete at constant temperature T= 20 ^{o}C. a) Stress components, b) Strain components.

For further discussion of the results of the tests under temperatures lower than 20 °C, we have to clarify some aspects. The model parameters used in estimation of E-modulus, creep and activation energy are all based on the test results conducted for temperatures T ≥ 20 °C, i.e. the activation energy used in estimation of development of mechanical properties is only valid for T ≥ 20 °C, and the creep model can not utilize the same parameters to T ≤ 20 °C. Utilizing the models at 5 °C and 13 °C is therefore an extrapolation of the models into unknown territory.

Figure 6.17b-c shows that the stresses in the tests with 5 and 13 °C start to build-up at 18.0 and 14.5 hrs real time (not at t_0 = 11 hrs), respectively. On the other side, the stress calculations of these tests, using the same activation energy as in tests with 20 and 45 °C, showed that t_0 (11 maturity hrs) were as high as 44.5 and 18.5 hrs real time, demonstrating that this value is wrong at two temperatures. This approach gave very small stresses.

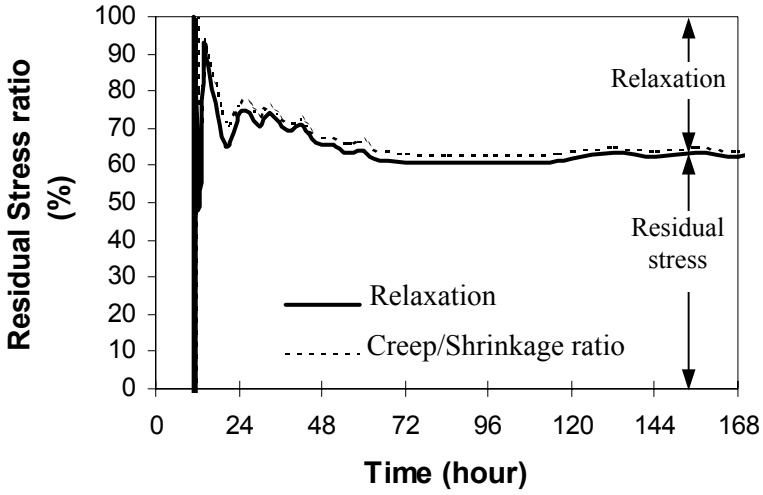

Figure 6.16 Relaxation and residual stresses in concrete (type BASE-5) under isothermal conditions at T = 20 °C.

The discussion above indicates that t_0 is not realistic for 5 and 13 °C, and that it has to be changed to the time where the stresses start initiating. To operationally compensate for the starting error introduced by a wrong t_0 two approaches can be used:

a) Maintain the value of activation energy (A_r = 3000, B_r = 300 in Eq. 3.18), but reduce the maturity time t_0 from 11 hrs to a time that really matches the time where stresses start build up.

b) Keep the maturity time t_0 constant (11 hrs for BASE-5), but reduce the activation energy for the setting period.

Both approaches may produce a t_0 of 18.0 and 14.5 hrs for the tests under isothermal temperatures 5 and 13 °C, respectively. According to Bjøntegaard (2003) the activation

energy is different for the time before and after setting, and therefore two sets of activation energy parameters should be considered: one set for the period before setting and the second one for the time period after setting. However, since only one set of activation energy is behind estimation of the mechanical properties so far, the idea of dividing it into two sets is not considered here.

For the current cases, method (a) is used and the maturity time t_0 at the time where the stresses develop under 5 ^{o}C and 13 ^{o}C is found to be 4.5 and 9.5 hrs, respectively. As can be seen in Figure 6.17, the DPL(C) shows a better agreement with the test results than DPL(T), particularly in the tests with temperature 5 ^{o}C, with an overestimates of the stresses by about 40%.

The influence of the constant temperatures on relaxation is presented in Figure 6.18. The relaxation in the all tests increases rapidly during the first hrs. In the test with temperature 45 ^{o}C, it increases rapidly to about 60%, and then it decreases slowly to about 30% after 6 days. During the period after 48 hrs the relaxation varies between 30-40% for the tests with 20 and 45 ^{o}C.

Figure 6.18d shows the relaxation and the residual stress ratio for all the tests together. As it is seen, the effect of isothermal temperature is not systematic, but comparing the results of the tests with temperature below 20 ^{o}C and the test at 20 ^{o}C, where the stress estimation is best, indicates that the relaxation inversely proportional to temperature. This is not in according to reported findings in the literature.

For the case of temperatures lower than 20 ^{o}C the relaxation is shown to be higher, about 60%, and it increases with time to about 70% at 4 day of age, which is higher than the relaxation at 20 ^{o}C. These results are not in accordance with the reported findings in the literature, but they can be explained by the tests conducted by Bjøntegaard (2003); hydration heat and mechanical properties were measured on specimens cured at 20 ^{o}C isothermal conditions and at semi-adiabatic (realistic) conditions at 30 ^{o}C as initial concrete temperature. It was found that t_0 was not very temperature sensitive, hence the activation energy for the time before t_0 is lower than for the hydration phase (after t_0). This agrees well with the observations made in this section and may explain the trouble introduced regarding t_0 in the stress calculations when using the "old" activation energy values that really are most relevant for the hydration phase in the case where initial concrete temperature is 20 ^{o}C.

The present results at 5 and 13 ^{o}C demonstrate clearly that on extrapolations beyond temperatures where experimental data is available can lead to large errors in calculated stresses. This is a clear warning against using the material models outside its limit of validity. A more thorough investigation on the stiffness development at low temperature includes activation energy, E-modulus and creep is necessary before any further refinement of the models can be conducted. At 45 ^{o}C the situation is different, but we have no clear explanations for the large difference between measured and calculated stresses.

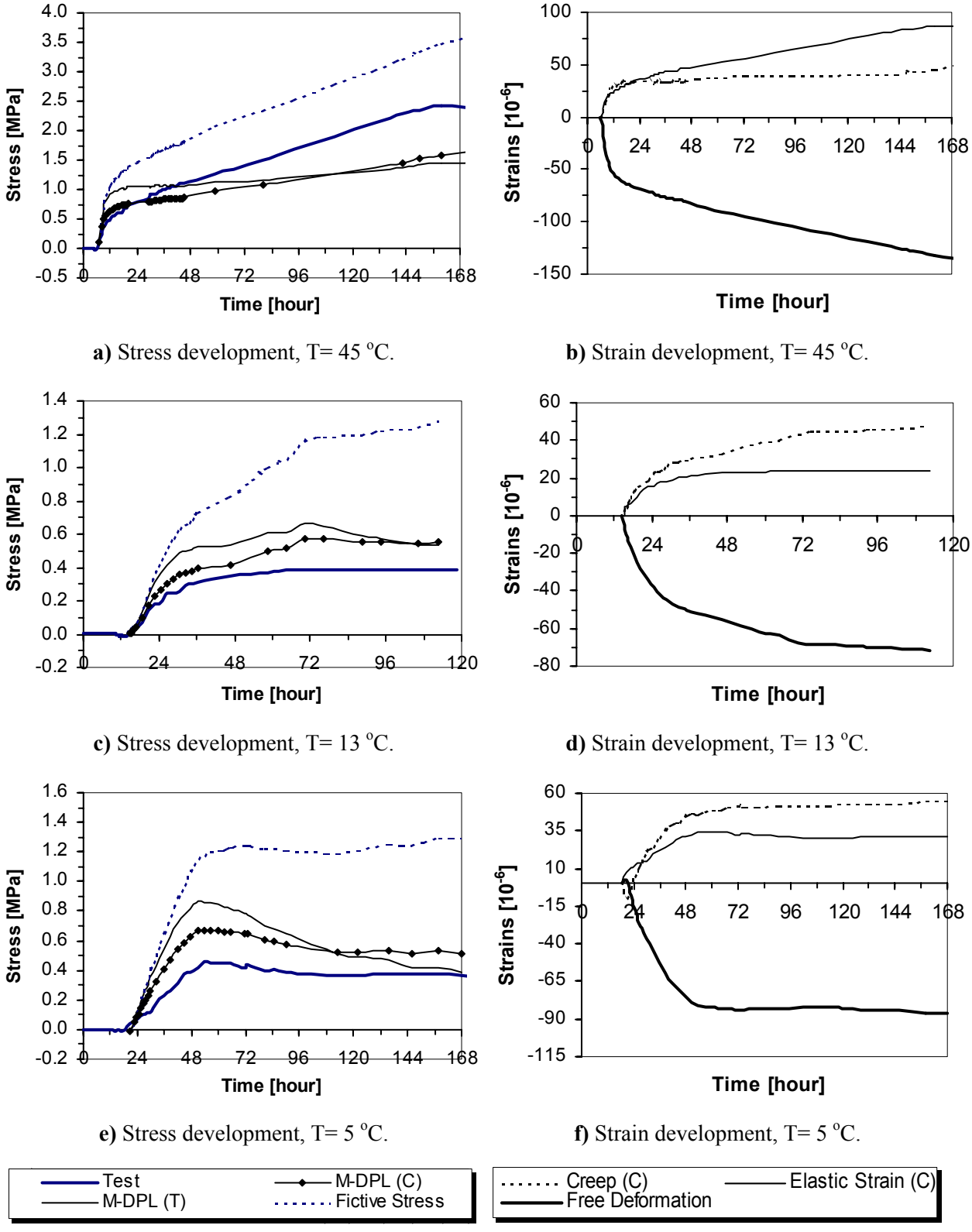

a) Stress development, T= 45 °C.

b) Strain development, T= 45 °C.

c) Stress development, T= 13 °C.

d) Strain development, T= 13 °C.

e) Stress development, T= 5 °C.

f) Strain development, T= 5 °C.

Figure 6.17 Measured stress- and strain development in TSTM and calculated by DPL for isothermal tests: T = 45 °C in a-b), T=13 °C in c-d), and T=5 °C in e-f).

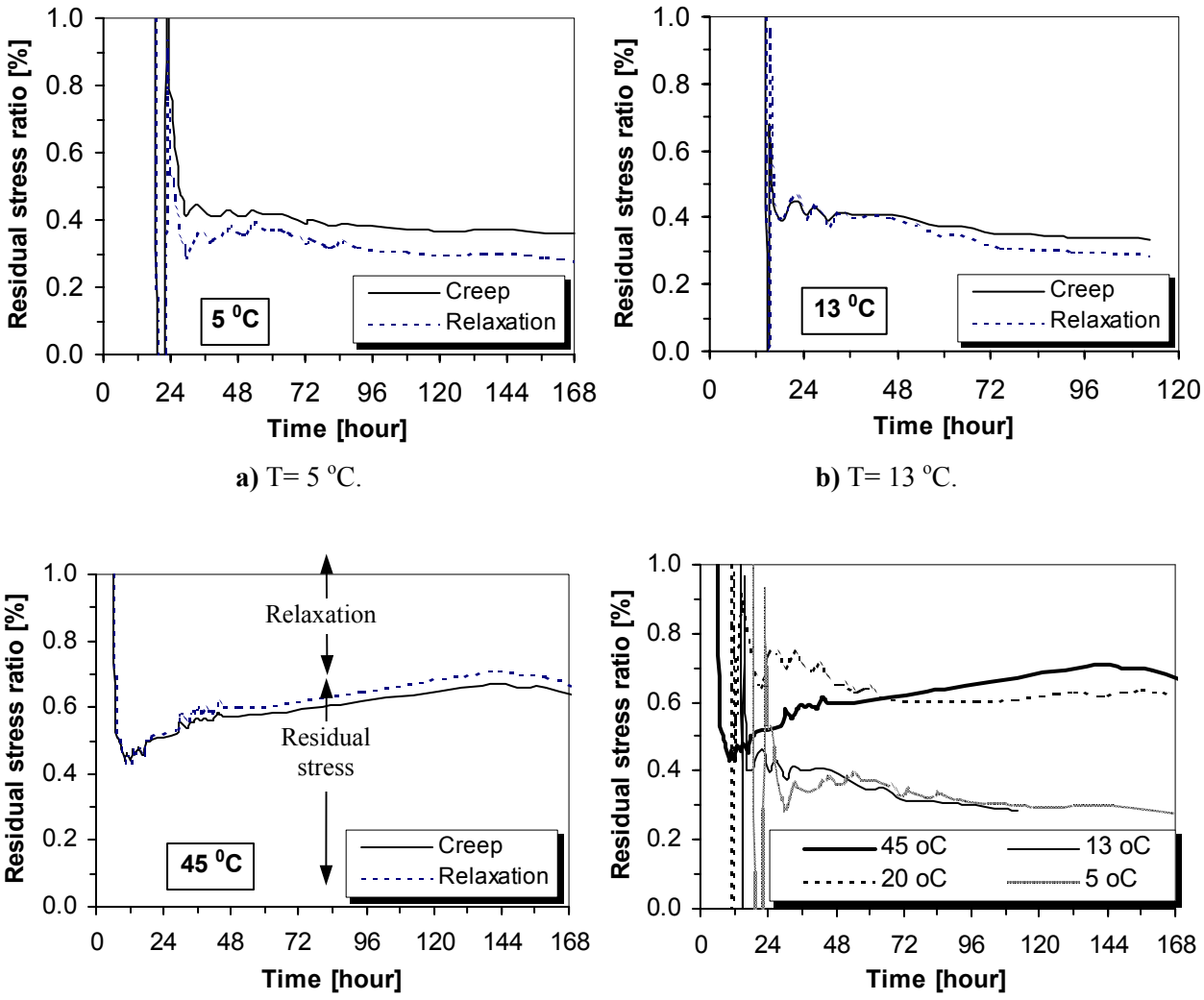

a) T= 5 °C.

b) T= 13 °C.

c) T= 45 °C.

d) T= 5, 13, 20 and 45 °C.

Figure 6.18 Influence of temperature on relaxation in concrete BASE-5, under isothermal conditions.

Case Study for Autogenous Deformations at 20 ^{0}C

For the same concrete under the same testing conditions, the measured free deformation will deviate from a test to another. There are numerous factors that may contribute to this fact, but no systematic investigations have to our knowledge been carried out. The results of such measurements for three isothermal tests (T21, T26 and T48) on concrete BASE-5, under temperature 20 ^{o}C, are shown in Figure 6.19. The test T48 has already been studied, but it is considered here again for comparison. The autogenous deformations are zeroed at t_0 =11 hrs. As can be seen, for test T21 the measured autogenous deformation is about 20x10^{-6} higher than the other two after 6 days. Furthermore, it is interesting to note that the test with higher autogenous deformation produce lower self-induced stresses.

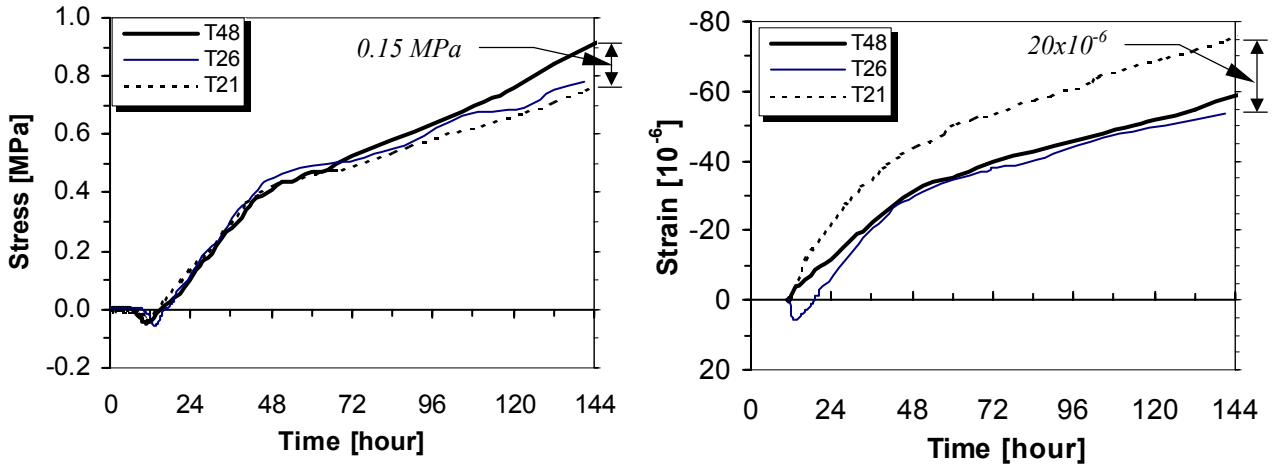

a) Self-induced stresses **b)** Free deformations

Figure 6.19 Measured stress and strain development in concrete type BASE-5 under isothermal temperature 20 ^{o}C.

For each test, the fictive elastic stress and the self-induced stresses are calculated using model parameter form both the tensile creep tests (T) and the compressive creep tests (C), shown in Figure 6.20. Considering the same E-modulus development in stress calculations for all tests, the measured free deformations in concrete will have a significant effect on the magnitude of the fictive elastic stresses and the relaxation. Since the measured free deformation is one of the main input parameters in the calculations, it also affects the stresses calculated using M-DPL.

Figure 6.20a-c shows that the model parameters from compressive creep tests, set (C) gives a better agreement between DPL and the measured stresses than what the tensile creep tests, set (T) gives. Why this is so is still an unsolved problem that needs further investigation. Figure 6.20d-f shows the scatter in the calculated stresses due to scatter in measured autogenous deformations. As can be seen, the scatter in calculated self-induced stresses by the DPL is about 0.15 MPa in both cases, but in calculated fictive elastic stresses it is about 0.37 MPa after 6 days. The scatter in the latter is also a measure for difference in stress relaxation.

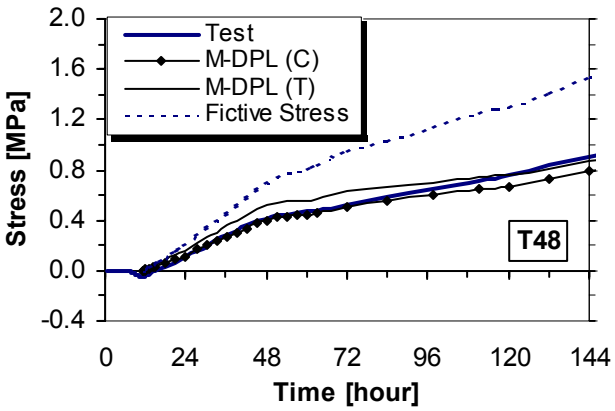

a) Test T48

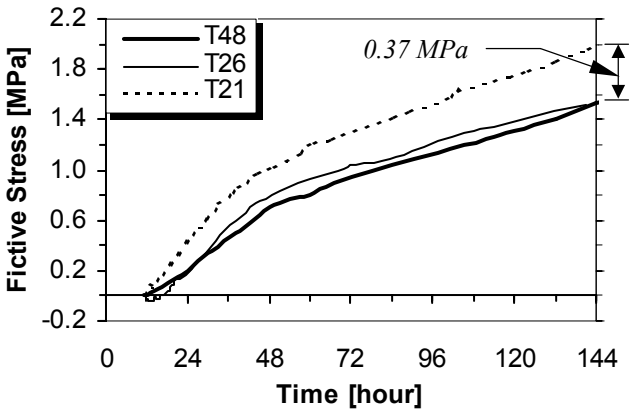

d) Fictive elastic stress

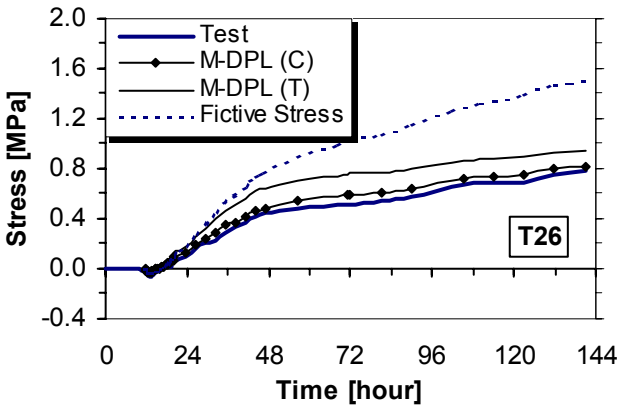

b) Test T26

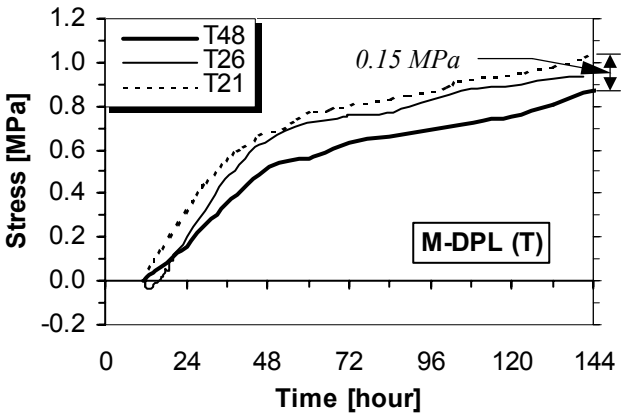

e) Self-induced stresses by M-DPL (T)

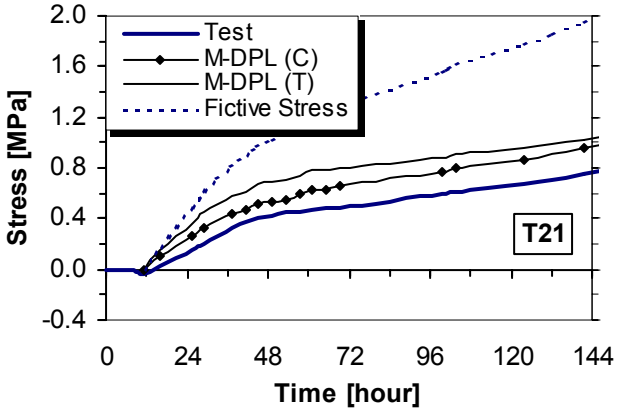

c) Test T21

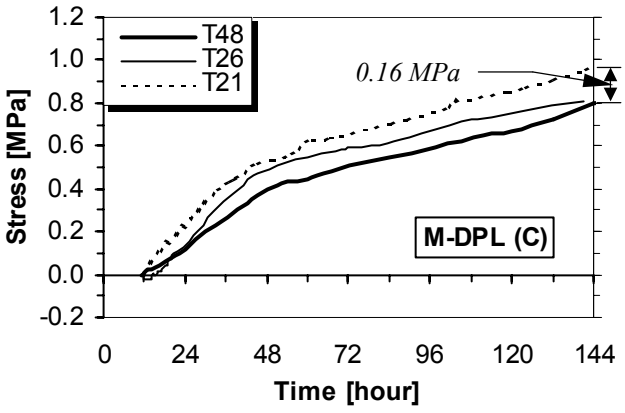

f) Self-induced stresses by M-DPL (C)

Figure 6.20 Calculated stress development in the same concrete type (BASE-5), but different mix batches, during 20 ^{o}C isothermal condition.

URN:NBN:no-3377

The relaxation curves for the tests are shown in Figure 6.21, which shows surprisingly a large scatter. The figure reveals that a change in autogenous deformation leads to different fictive elastic stresses, and then a different stress relaxation magnitude. However, the relaxation after 72 hrs becomes nearly constant in all three tests.

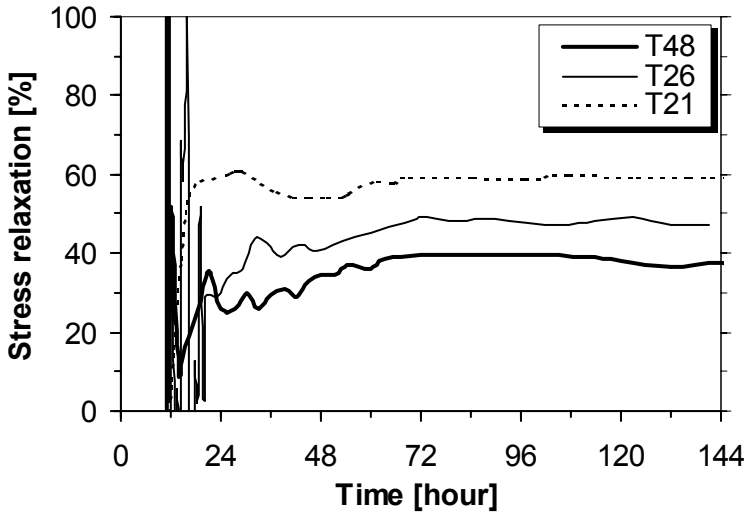

Figure 6.21 Relaxation and residual stresses in concrete (type BASE-5) under isothermal conditions at T = 20 ^{o}C.

6.5.2 Poly-isothermal Tests

Measurements of temperature, deformations and stresses in Poly-isothermal tests, which have "more realistic" early temperature histories than the isothermal ones, are presented in Figure 6.22 - Figure 6.24. Bjøntegaard (1999) performed these series intended to determine the thermal dilation coefficient at each step, using temperature 13 °C or 20 °C the first 8 hrs, and then increasing the temperature in steps to the desired level. The results of isothermal tests at 20 °C and 13 °C are also included as references.

Figure 6.22 shows the imposed temperatures during the first 48 hrs, and they were maintained constant after this time. The temperature steps are given in the figure.

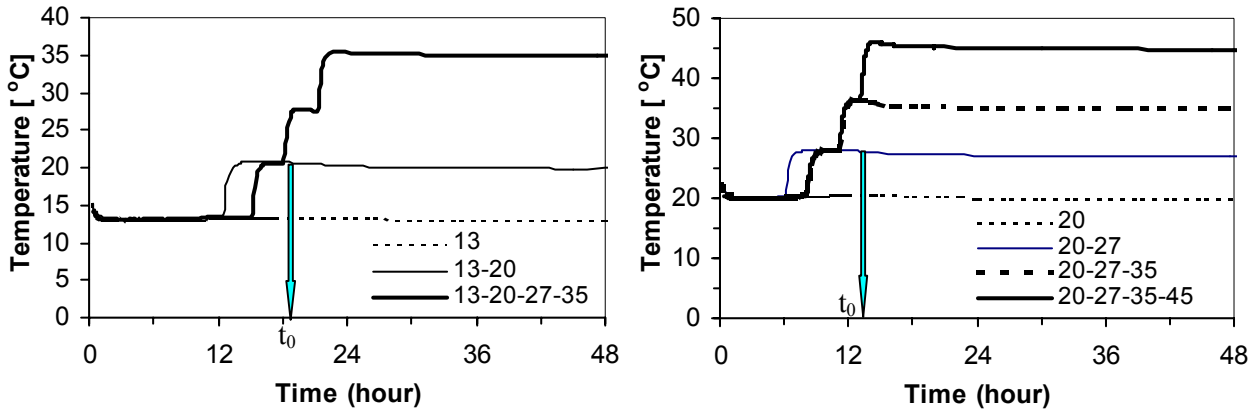

a) Start temperature is 13 °C

b) Start temperature is 20 °C

Figure 6.22 Imposed temperature histories during poly-isothermal tests in TSTM, with different initial temperatures: a) 13 °C and b) 20 °C.

The measured total deformation for the same period is shown in Figure 6.23. The figure shows a significance influence of the temperature steps on the deformations compared to the influence of the autogenous deformations. An interesting observation made by Bjøntegaard was that the thermal dilation coefficient is higher at very early ages since the deformation steps are considerably decreased in size with increasing time and temperature. This is caused by the fact that water has higher coefficient of thermal expansion (CTE) than the solid, and at early age the water phase dominates.

Figure 6.24 shows the results of the parallel TSTM tests confirming a good correspondence to the measured total deformations. Any temperature step causes expansion of the concrete, with a high rate, and thus a "jump" in compressive stress in the figure. These "stress jumps" are followed by stress reductions due to relaxation and autogenous shrinkage during the constant temperatures. These effects are very pronounced during temperature steps 13-20-27-35 °C and 20-27-35-45 °C. One should note that for almost the same size of the temperature

step the size of the stress steps are progressively increased with increasing time. The main reason for that is the evolution of modulus of elasticity and thus stiffer concrete with time, overriding the effect that the strain steps decrease progressively.

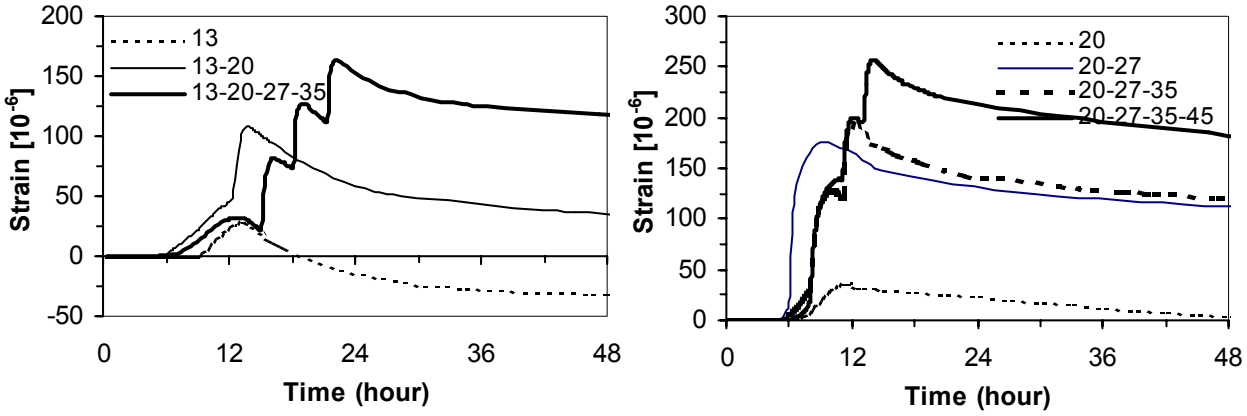

a) Start temperature is 13 °C **b)** Start temperature is 20 °C

Figure 6.23 Measured total deformation during poly-isothermal tests in Dilation Rig, with different initial temperatures: a) 13 °C and b) 20 °C.

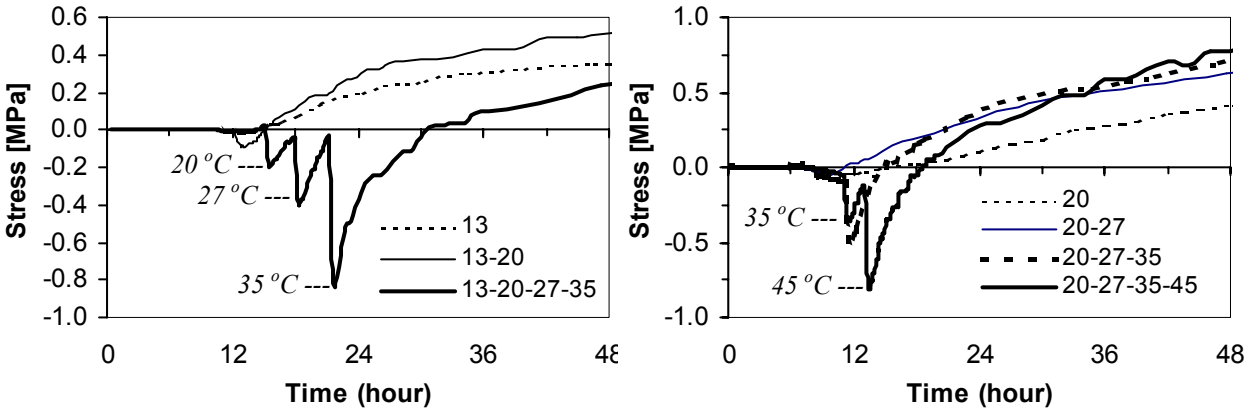

a) Start temperature is 13 °C **b)** Start temperature is 20 °C

Figure 6.24 Measured stress development during poly-isothermal tests in TSTM, with different initial temperatures: a) 13 °C and b) 20 °C.

The stress development in the poly-isothermal tests are estimated by the Double Power Law and presented for each of the tests in the following. Since the stress reduction during the constant temperature causes creep recovery the Modified Double Power Law is also used and the results are compared.

All the results are zeroed at about the end of the initial autogenous expansion, i.e. 11 hrs maturity time. This implies that the start temperature used in estimation of the self-induced stresses may not be the same as 13 ^{o}C and 20 oC. Table 6.7 gives the start temperature and the "real time" where the calculations start.

Table 6.7 Start "real time" and start temperature used in calculations of self-induced stresses and strain components.

Poly-Isothermal tests	"Real time" correspond to t_0 (11 maturity hrs)	Temperature at t_0 [^{o}C]
13 - 20 ^{o}C	15.1	20.8
13 - 20 - 27 - 35 ^{o}C	16.2	20.4
20 - 27 ^{o}C	10.1	28.1
20 - 27 - 35 ^{o}C	10.4	28.0
20 - 27 - 35 - 45 ^{o}C (*Fig. 2*)	10.4	28.0

Figure 6.25 shows the stress- and strain development during the first 6 days of the concrete age for the case with temperature steps 13-20-27-35 ^{o}C. At the concrete age of 11 maturity hrs the temperature is already raised to 20.4 ^{o}C, and only the effects of the last two temperature steps are evident in the figures.

In Figure 6.25-a the stress generation is simulated with and without creep and the effect of the stress relaxation can bee seen. The calculations with creep include also the transient creep. To follow the stress development the first hours, the same figure is repeated in Figure 6.26 for the first 48 hrs. The calculations start from t_0, where the temperature is already reached the temperature level of 20.4 ^{o}C. The maximum compressive stress measured at 35 ^{o}C is 0.74 MPa and the relaxation at this moment is about 35%. When the stress increments change the direction, from compression to tension, it is difficult to present the relaxation. Nevertheless, one can see that the high relaxation during the time period with compressive stresses leads to relatively high tensile stresses.

The stress calculations by DPL(C) in the heating period, i.e. when the compressive stress develops, are in relatively good agreement with the measured stresses as long as it concerns the compressive stress increments higher than zero and until the maximum compressive stresses are gained. When the compressive stresses start reducing, i.e. with negative stress increments at constant temperature, the deviation from the measured stresses starts to appear. Furthermore, the figure reveals that the deviation increases with unloading and with time, and the DPL underestimates the self-induced stresses. The estimated stress by DPL is 27% lower than the measured stress value (which is 1.46 MPa) after 6 days. As it was explained earlier, one possible explanation is that the linear viscoelastic model is not strictly valid here and that there is a need for a non-linear correction term to take into account the effect of unloading. This correction is made in M-DPL by introducing a new creep coefficient, for the time where unloading is occurred, taking into account the creep recovery.

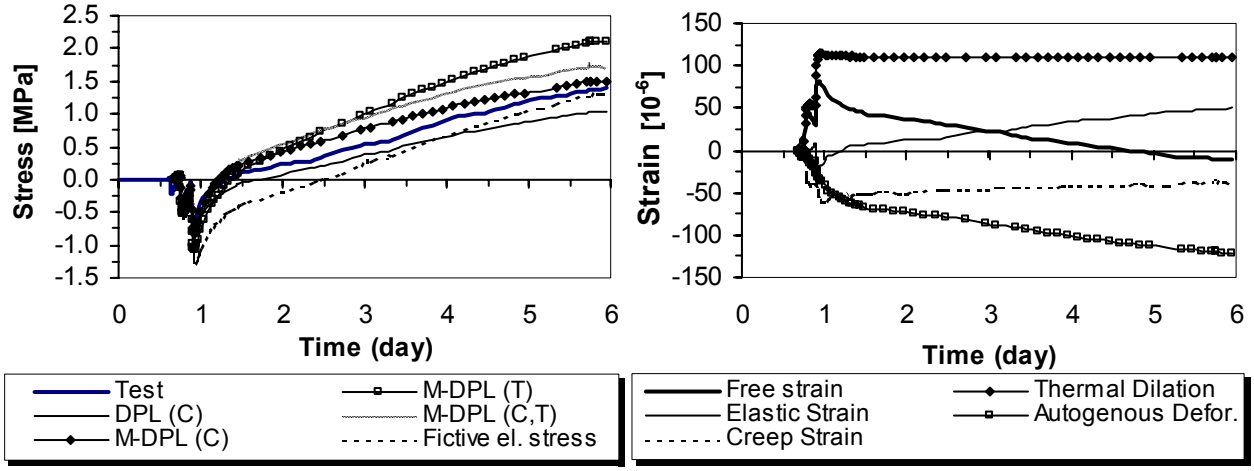

a) Stress development **b)** Strain components

Figure 6.25 Stress and strain development during a poly-isothermal test with initial temperature 13 ^{o}C, and temperature steps 13-20-27-35 ^{o}C. The temperature is 20.4 ^{o}C at t_0.
a) Stress simulation by DPL and M-DPL compared to measurements.
b) Different strain components.

The calculated stresses by M-DPL, shown in the figures, utilized three sets of model parameters:

- Model parameter set (T) noted as M-DPL(T): the results show a high rate of stress development under both compression and tension, which leads to an overestimation of stresses.
- A combination of model parameter set (C) during development of the compressive stresses and model parameter set (T) during the reduction of compressive stresses and the development of tensile stresses, noted as M-DPL(C,T): A good harmony to the measured stresses is achieved during the compressive stress period, but it overestimates the stresses under tensile stresses.
- Model parameter set (C) noted as M-DPL(C): the results reveal the best harmony with the measured stresses, something which clearly proves the importance of a realistic estimate of creep recovery in calculations, in that the creep has a large irrecoverable part.

The different strain components are shown in Figure 6.25-b, where the measured free deformation is separated into autogenous shrinkage, AD, and thermal dilation, TD. The thermal coefficient is used according to Figure 2.4. The concrete response to these deformations is in form of elastic strains, ε_{el}, and creep strains, ε_{cr}. The major part of the total measured strain due to the temperature "jump" (or the thermal dilation) is elastic strain, but a creep strain is also observed in the figure. When the total strain changes the direction, from expansion to contraction the creep rate changes considerably.

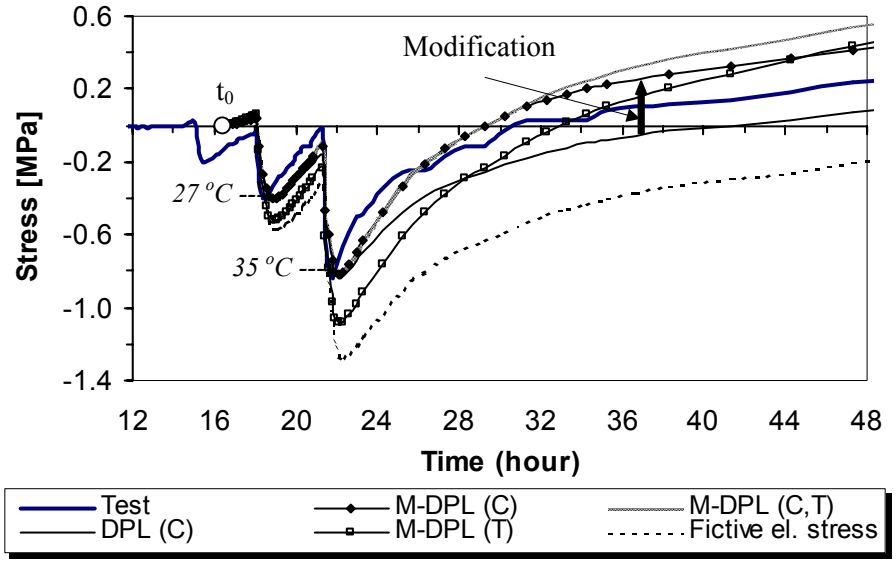

Figure 6.26 Stress simulation by DPL and M-DPL compared to measurements during poly-isothermal test with initial temperature 13 °C, and temperature steps 13-20-27-35 °C.

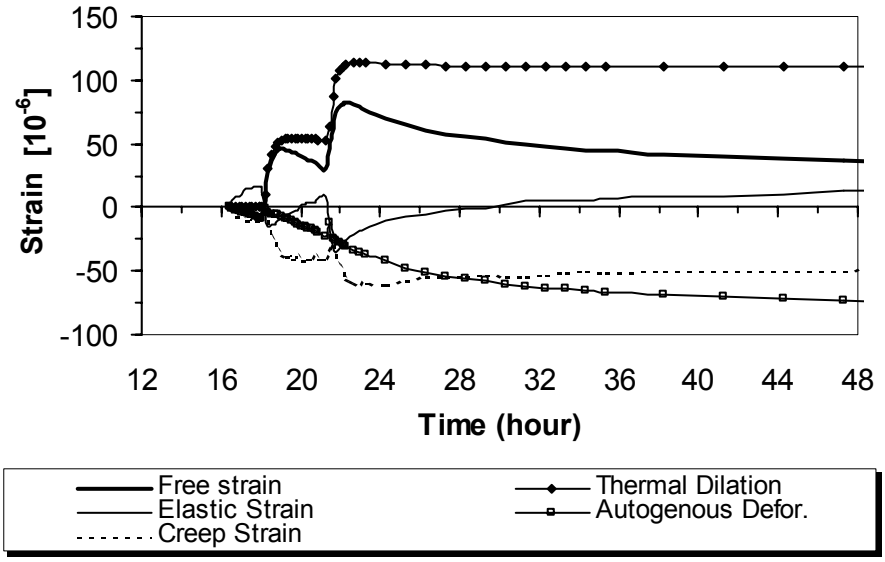

Figure 6.27 Different strain component together with the measured total deformation during poly-isothermal test with initial temperature 13 °C, and temperature steps 13-20-27-35 °C.

The results of the stress- and strain estimations for the test with temperature step 13-20 °C are presented in Figure 6.28. Like the previously discussed test, the temperature is already increased to 20.4 °C when the calculation starts. Thus, the test can be considered as an isothermal test at about 20 °C, with a lower previous temperature. Like the other isothermal tests, the creep coefficient for creep recovery is not utilized here, meaning that the DPL and M-DPL gives the same stresses. The figure reveals that the M-DPL(C) results in a stress development parallel and more consistent with the measured stresses than the M-DPL(T), but both give a good agreement. A little deviation from the measured stresses can be seen in the figure, but it is on the conservative side. The relaxation is very high, about 50% after 24 hrs and it increases to 65% after 6 days – in contrast to the purely isothermal where is become a constant of about 40% after 1.2 days.

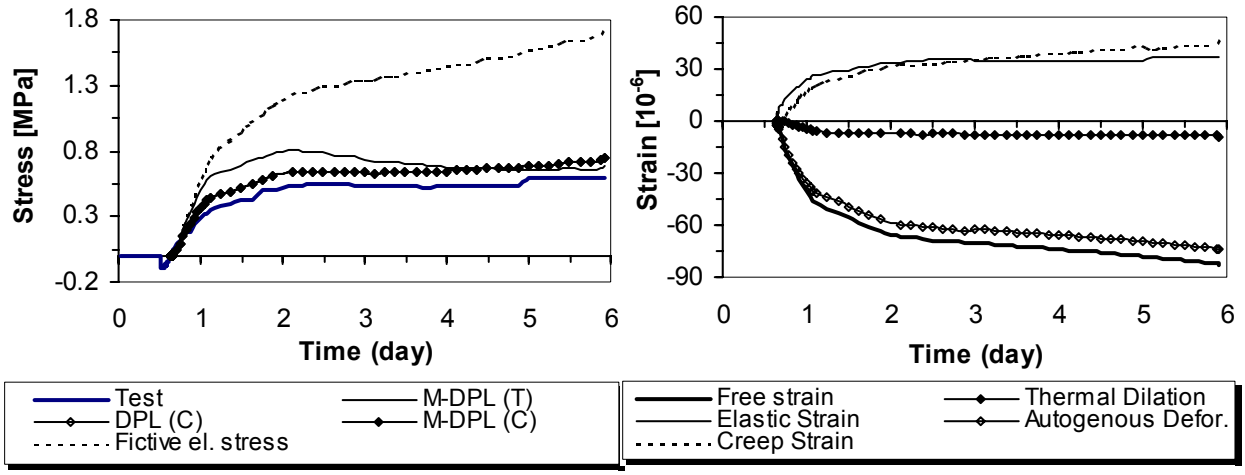

a) Stress development **b)** Strain development

Figure 6.28 Stress and strain development during poly-isothermal test with initial temperature 13 °C, and temperature steps 13-20 °C. The temperature has reached 20 °C at t_0. a) Stress simulation by DPL and M-DPL compared to measurements, b) different strain components.

In Figure 6.29 the measured strain- and stress development of the test with temperature step 13-20 °C and the previous discussed test with constant temperature 20 °C are compared. The increase of temperature to a certain constant value influences the deformations rate and its magnitude, and thus also the rate of stress build-up. The stress rate is higher in the first period, but it reduces to a lower level than in the case with constant 20 °C. This implies that the influence of temperature on relaxation is greater when concrete is heated to gain the desired constant temperature than when it has been at a desired temperature since beginning. Consequently, the isothermal tests are useless as a basis for predicting behaviour under realistic conditions.

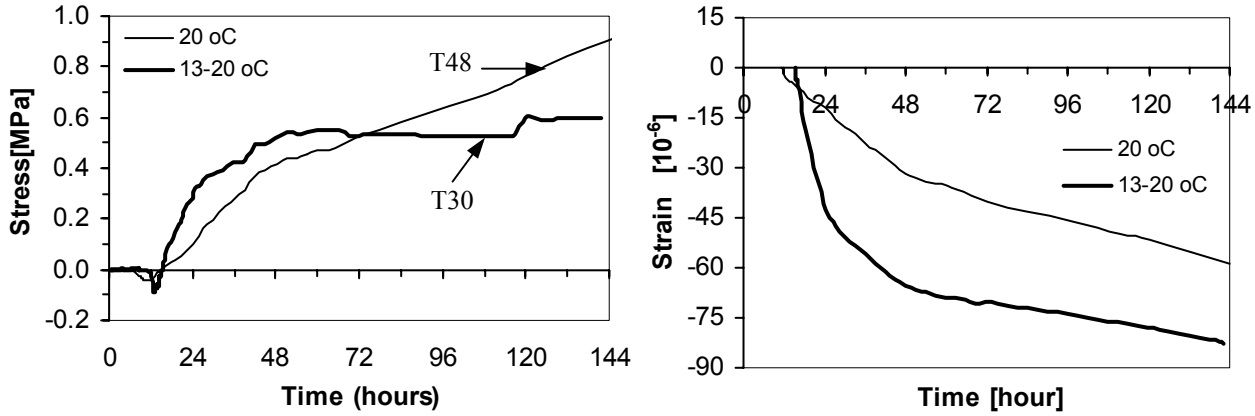

a) Stress development

b) Strain development

Figure 6.29 Comparison of measured stress and strain development during isothermal temperature 20 ^{o}C and poly-isothermal temperature steps 13-20 ^{o}C, shown in Figure 6.22. a) Self-induced stress, b) Total strain.

Estimation of stress development in three other poly-isothermal tests with start temperature 20 ^{o}C are presented in Figure 6.30. As mentioned earlier, the calculations start at maturity time 11 hrs (or at about 10 hrs real time), and the temperature has already reached about 28 ^{o}C. For the test with the temperature steps 20-27-35-45 ^{o}C, i.e. maximum temperature 45 ^{o}C, shown in Figure 6.30a, it is revealed that the DPL underestimating the stresses, while they are predicted well by M-DPL(C). The measured maximum compressive stress is 0.83 MPa, and the relaxation is about 42%.

For the test with temperature steps 20-27-35 ^{o}C, shown in Figure 6.30b, the maximum compressive stress is low, and thus the unloading stress is relatively small. The double power law with and without modification, DPL(C), M-DPL(c) or M-DPL(C,T), can closely predict the results, but not DPL(T) For the last test, which is almost an isothermal test with temperature 28 ^{o}C, little compression develops and the models predict the stress progress very well. Again the M-DPL(T) is least successful.

Figure 6.31 shows the measured total deformation in addition to different strain components.

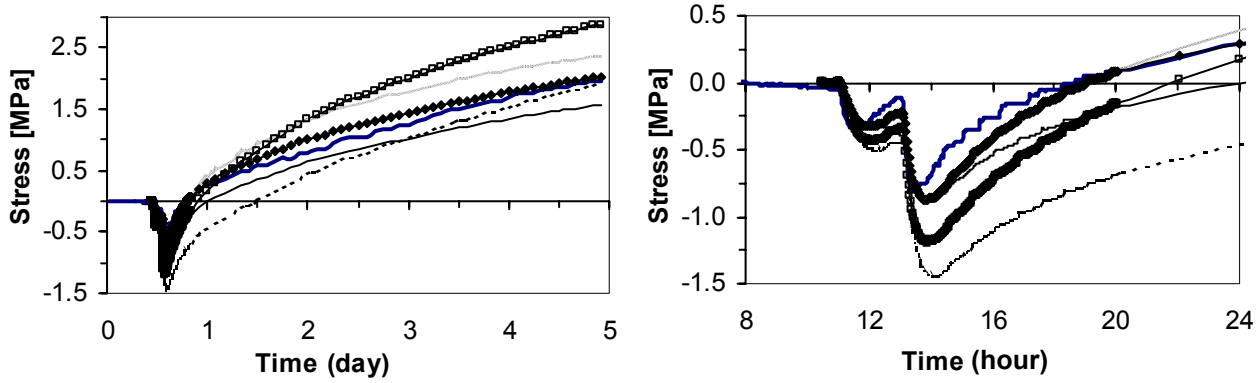

a) Poly-isotherm 20-27-35-45 °C

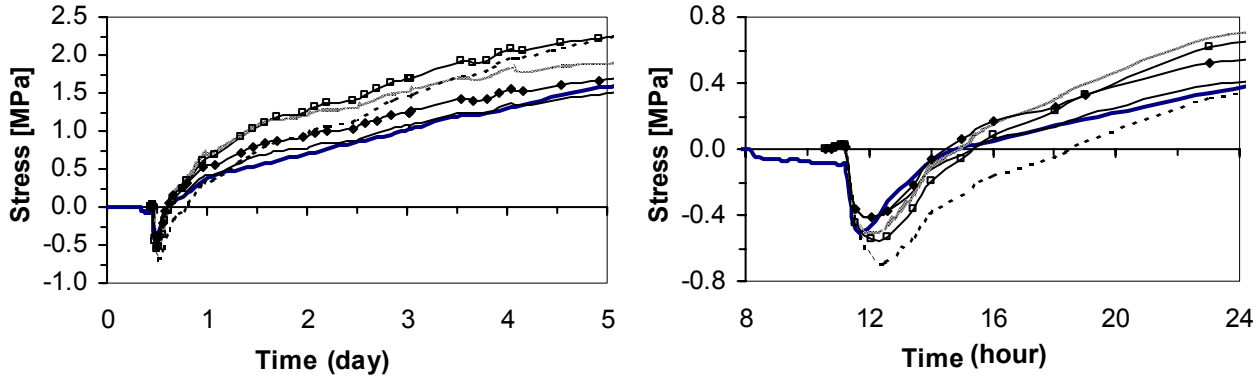

b) Poly-isotherm 20-27-35 °C

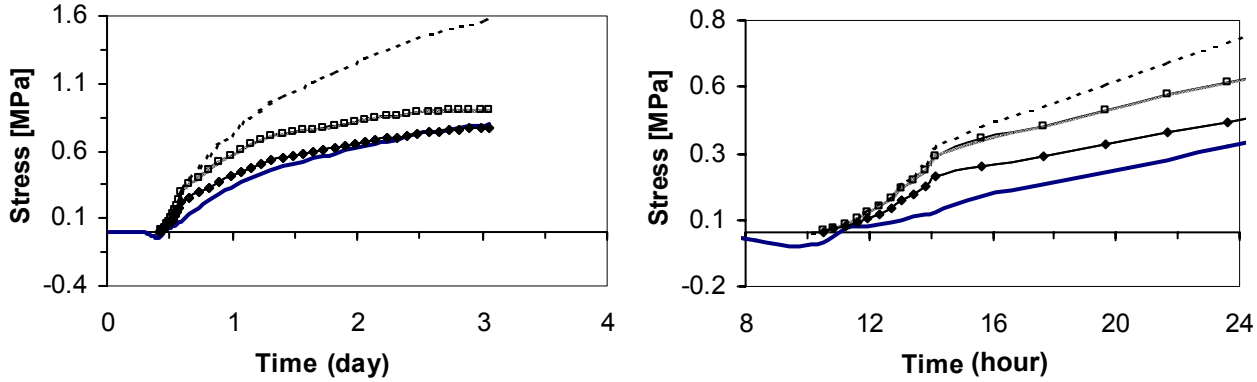

c) Poly-isotherm 20-27 °C

Figure 6.30 Stress simulation by DPL and M-DPL compared to measurements during poly-isothermal test with initial temperature *13 °C*, and different temperature steps: a) 20-27-35-45 °C, b) 20-27-35 °C, c) 20-27 °C. The estimation starts from 10 hrs, where the temperature gained 28 °C.

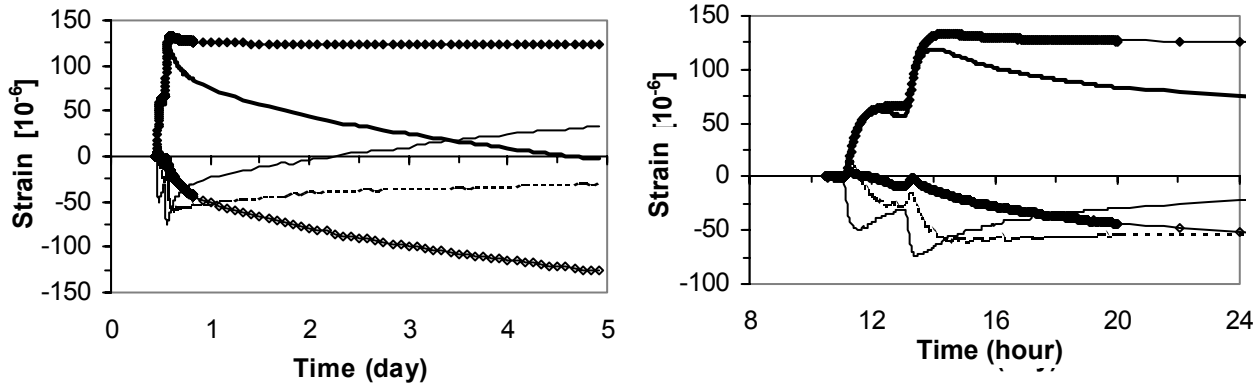

a) Poly-isotherm 20-27-35-45 °C

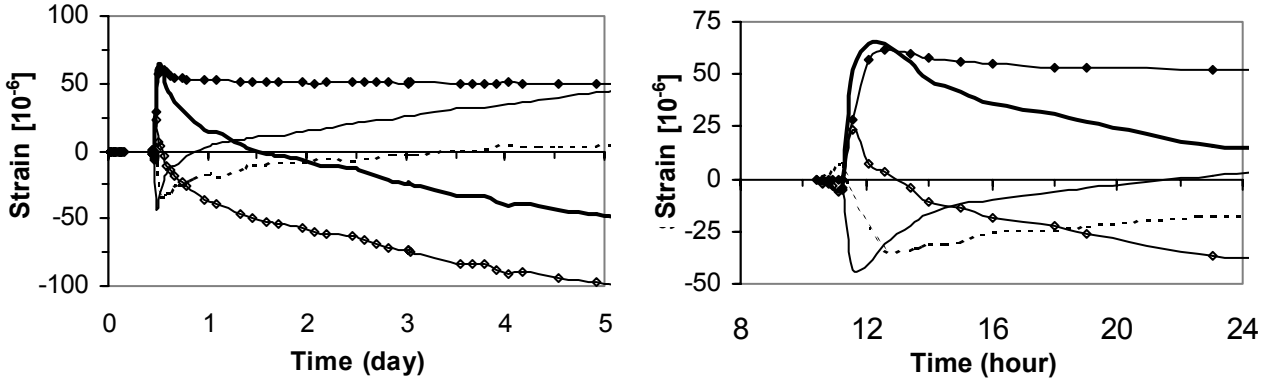

b) Poly-isotherm 20-27-35 °C

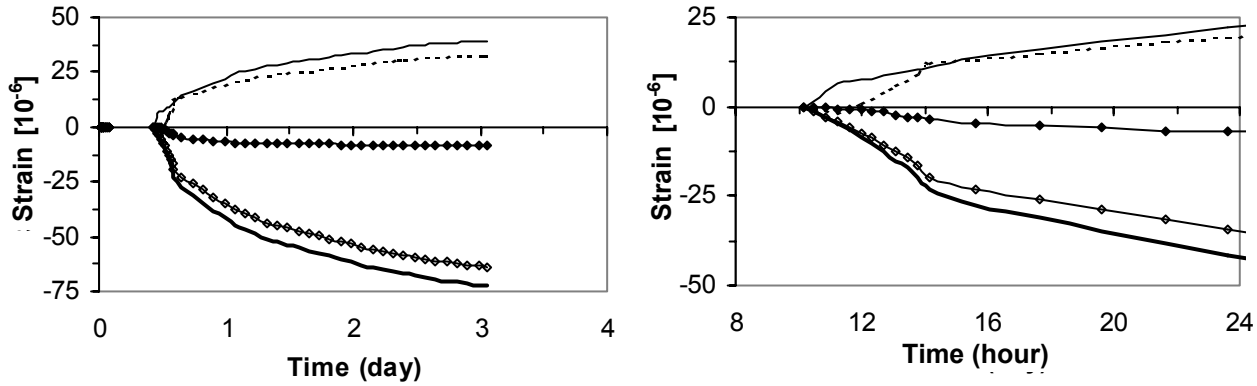

c) Poly-isotherm 20-27 °C

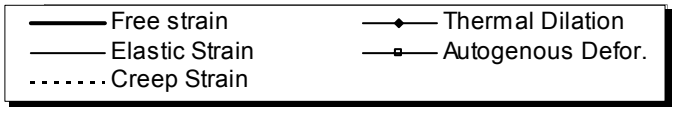

Figure 6.31 Different strain component together with the measured total deformation during poly-isothermal test with initial temperature *13 °C*, and different temperature steps: a) 20-27-35-45 °C, b) 20-27-35 °C, c) 20-27 °C. The estimation starts from 10 hrs, where the temperature gained 28 °C.

6.5.3 Realistic Temperature Tests

Similar to the two previous thermal conditions, calculations have been conducted for tests under realistic temperature histories listed in Table 6.1, and the results are presented in Figure 6.32 - Figure 6.42. The results are shown for concrete with different amounts of silica fume, but the discussion on the influence of silica fume on creep and relaxation is included in the subsequent section 6.5.4. The start curing temperature in all the tests was 20 ^{o}C, but since the calculations start at t_0 (in maturity time), the real time at t_0 and the temperature at that time may be different from 20 ^{o}C. In Table 6.8 their start values are given, and as it is shown the temperature, when the calculations start, is somewhere between 24 ^{o}C and 31 ^{o}C.

Table 6.8 Survey of tests on concrete with different silica fume content, carried out under realistic temperature histories with different maximum temperature in the Dilation rig- and TSTM tests.

Silica fume [%]	Test	T_{max} [^{o}C]	t_0 [hrs]		Temperature at t_0 [^{o}C]
			Real time	Maturity	
0	T37	59.5	12.0	12.6	29.0
	T79 [1]	60.0	11.7	12.2	27.6
	T36 [2]	59.5	12.7	12.7	25.9
5	T33	29.0	10.9	11.2	24.4
	T58	40.0	10.5	11.2	26.2
	T44	61.5	10.5	11.6	31.4
	T70 [1]	60.0	10.2	11.2	30.1
10	T46	39.0	9.5	10.7	26.3
	T47	58.5	9.0	10.3	28.1
	T78 [1]	60.0	9.0	10.4	28.0
15	T86 [1]	60.0	8.7	9.5	24.8

[1] *Reduced restraint*
[2] *Delayed imposed temperature*

As for isothermal and poly-isothermal conditions, the stress calculations carried out using M-DPL(C) is better than the calculations using M-DPL(T) under the realistic temperature histories. Thus, only the calculated stress results using M-DPL(C) are presented in this section. A complete comparison between the creep model using parameter sets (C) and (T) is given in Appendix I.

The measured stress development curves in the TSTM, due to the respective temperature histories in three of the tests (T33, T58, T46), are shown in Figure 6.32. The notations in the figures in this section are the same as used in the previously presented equations. The measured maximum compressive stress for the test with T_{max} = 29 ^{o}C is only 0.05 MPa, something which means that the thermal dilation and the autogenous deformations are nearly equal during the heating period of the hardening concrete. The tensile stresses develop relatively fast to about 1.0 MPa, and then the rate decreases to an approximately constant

value. The stress development in concrete with 5% and 10% silica fume for a realistic temperature history with its maximum about 40 ^{o}C is also shown in the figure. Due to high temperature compressive stresses appear and some of their values are given in Table 6.9. The concrete cracked in both tests; the concrete with 5% silica fume at 2.90 MPa after 192 hrs, and the concrete with 10% silica fume at 3.25 MPa after 125 hrs.

In the right side of Figure 6.32 the measured strains development in Dilation Rig and the various strain components are presented. The strain components are calculated in the same way as previously described for the isothermal and poly-isothermal conditions. Figure 6.32a shows that the hardening concrete contracts and thereby introduces tensile stresses and tensile creep. The tensile creep strains in test T33 (T_{max} =29 ^{o}C), calculated according to Eq (6. 16), increase with increasing stress/time.

Some expansion is observed in both T58 and T56 (T_{max} = 40 & 39 ^{o}C) in the first few hrs of hardening, something which leads to compressive stresses and thus compressive creep. The compressive creep strain increases progressively to 37% of the total deformation at maximum compressive strain 44x10^{-6}. When the cooling phase starts the concrete contracts and thus the compressive stresses decreases, i.e. concrete is unloading with time. During removal of stresses the elastic deformations reduces, but the creep magnitude maintains approximately constant. Thus the creep strain percentage increases further to 64% of the total deformation at the time where the compressive self-induced stresses is removed totally. At the time with zero stress the total free strain is 28x10^{-6}, and the corresponding stress-dependent strain consist of 18x10^{-6} creep strain and 10x10^{-6} unrecoverable elastic strain due to stiffer concrete.

Table 6.9 Stresses at the time where maximum compressive stress appears and at 5 days after casting, under realistic temperature histories.

Test	**T_{max} [^{o}C]**	**Stress [MPa]** ***At max. compressive stress***			**Stress [MPa]** ***After 120 hrs***		
		σ_{test}	**σ_{fe}**	**Relaxation**	**σ_{test}**	**σ_{fe}**	**Relaxation**
T33	29	≈ 0 stress			1,55	3,27	1,72 (53%)
T46	39	-0,56	-0,70	-0,15 (21%)	3,10	5,41	2,35 (43%)
T58	40	-0,49	-0,62	-0,14 (22%)	2,81	4,51	1,70 (38%)

In Figure 6.33 the corresponding self-induced stresses are estimated and compared to measured stress development. Curves for fictive elastic stress development are also given in the figure, where it is shown how high the stresses would become if no creep/relaxation had occurred. Regarding the stress calculations in all the three tests the used creep law gains a good estimation. According to strength estimations the concrete would fail after 4.4 days if stress relaxation had not occurred. The figures at the right side show the same curves for the first 48 hrs. Figure 6.33b shows that the measured stress in the test T58 at t_0 (= 10.5 hrs) is 0.11 MPa, while in the model it is zero. This initial difference between the two continues during built-up of compressive stresses, but it disappears after the cooling phase has started.

The short effect of creep recovery is also evident in the figure starting right after maximum compressive stress.

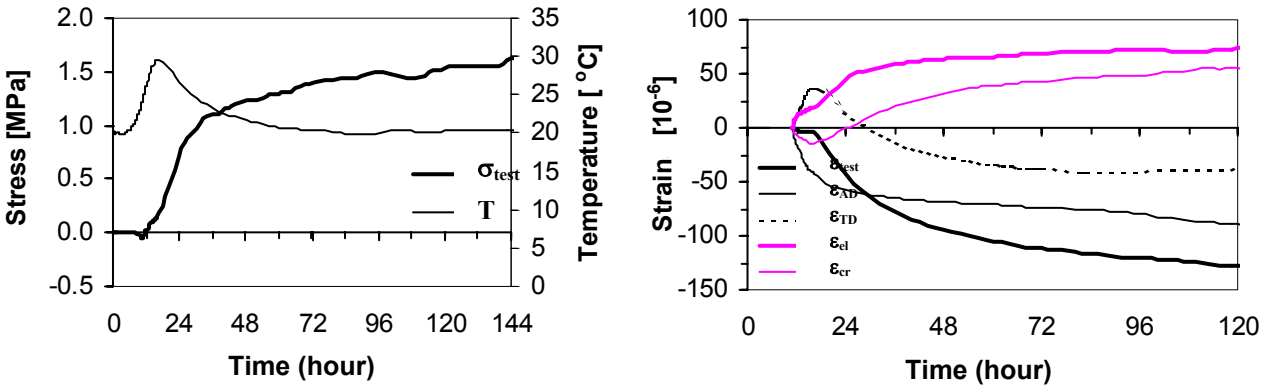

a) T_{max} = 29 °C, 5% silica fume, (T33)

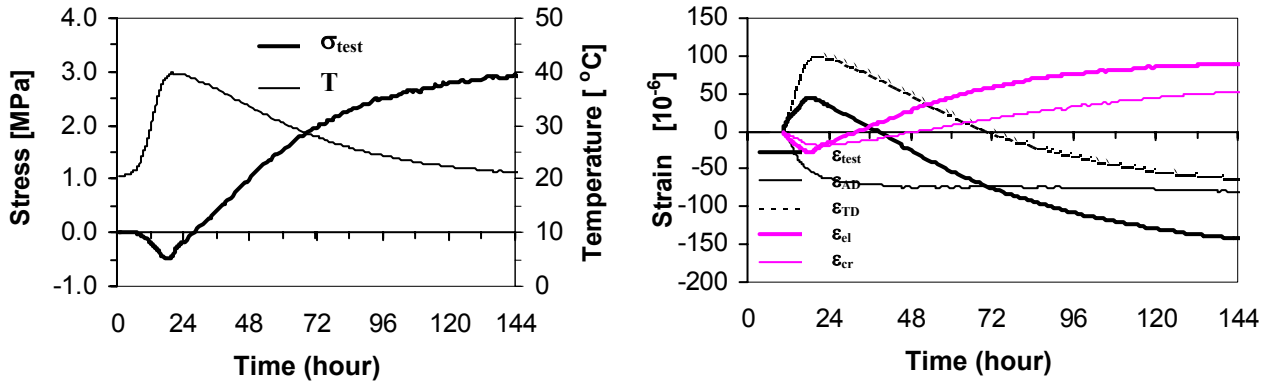

b) T_{max} = 40 °C, 5% silica fume, (T58)

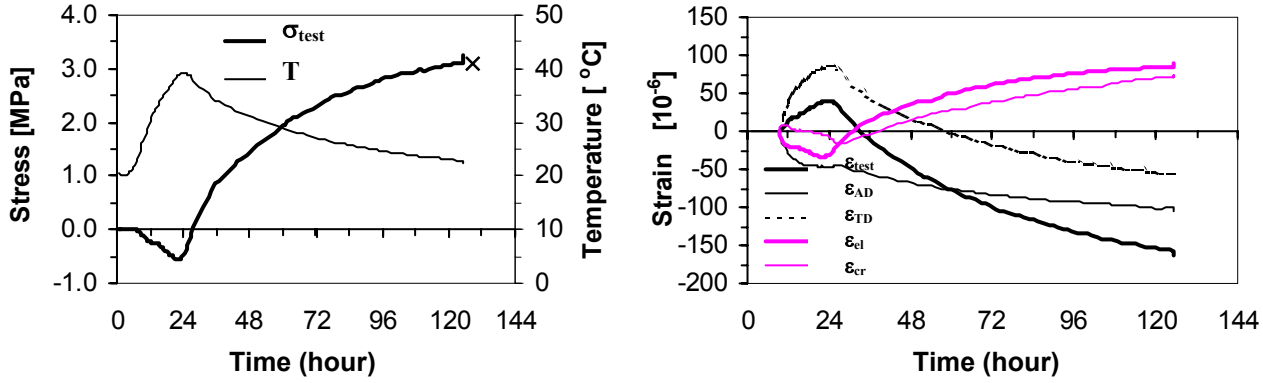

c) T_{max} = 40 °C, 10% silica fume, (T46)

Figure 6.32 Measured stress and strain development in hardening concrete exposed to different realistic temperature histories. Different strain components corresponding to total free deformation are calculated.

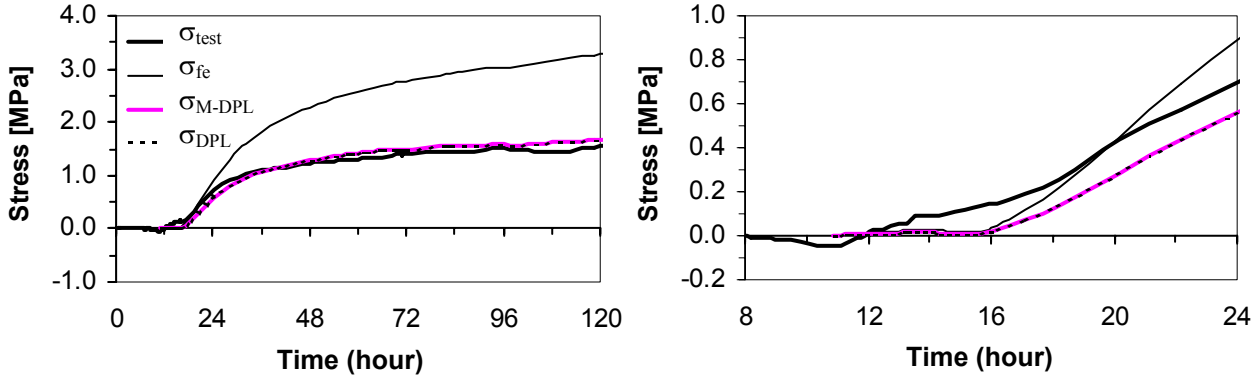

a) T_{max} = 29 °C, 5% silica fume, (T33)

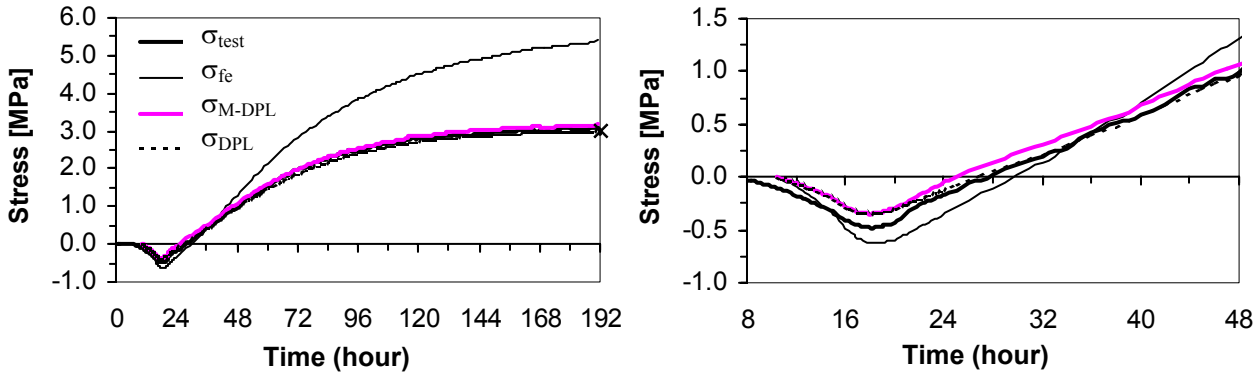

b) T_{max} = 40 °C, 5% silica fume, (T58)

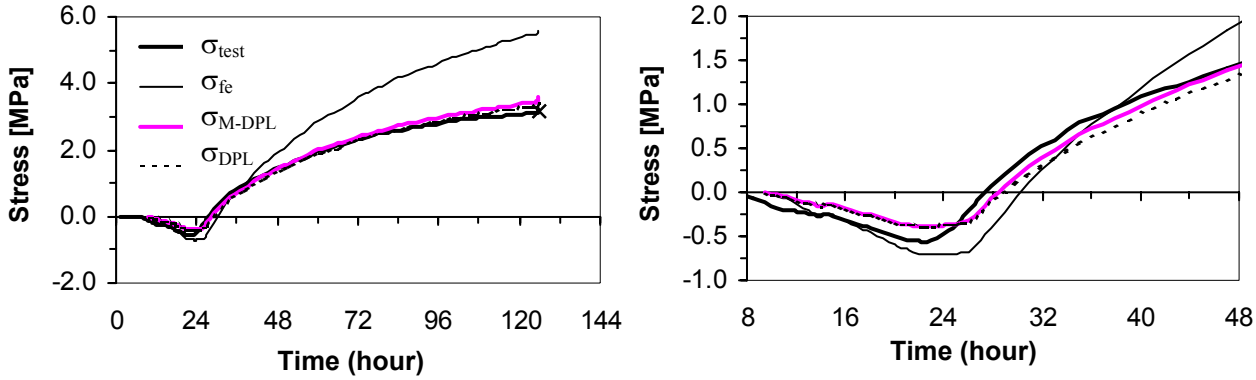

c) T_{max} = 40 °C, 10% silica fume, (T46)

Figure 6.33 Stress development in hardening concrete exposed to different temperature histories, estimated by the DPL and its modified version (both using creep parameters from compressive creep tests).

The main point in the forgoing discussion is that; at these low T_{max}, very good agreement is achieved, either by DPL(C) or M- DPL(C) – but not using (T).

Figure 6.34 shows stress and strain development during realistic temperature history with maximum temperature about 61.5 ^{o}C at 24 hrs. Due to the high temperature a higher compressive stress is gained than in the forgoing tests. The highest compressive stress is achieved after 22 hrs and is 2.0 MPa. The compressive stresses and their corresponding estimated elastic- and creep strains are given in Table 6.10 for two hardening times; at the time where highest compressive stress appears, t_1, and at the time where the compressive stresses have been totally reduced to zero at t_2. At t_1 the creep strain is 79x10^{-6}, which is 45% of the total deformation.

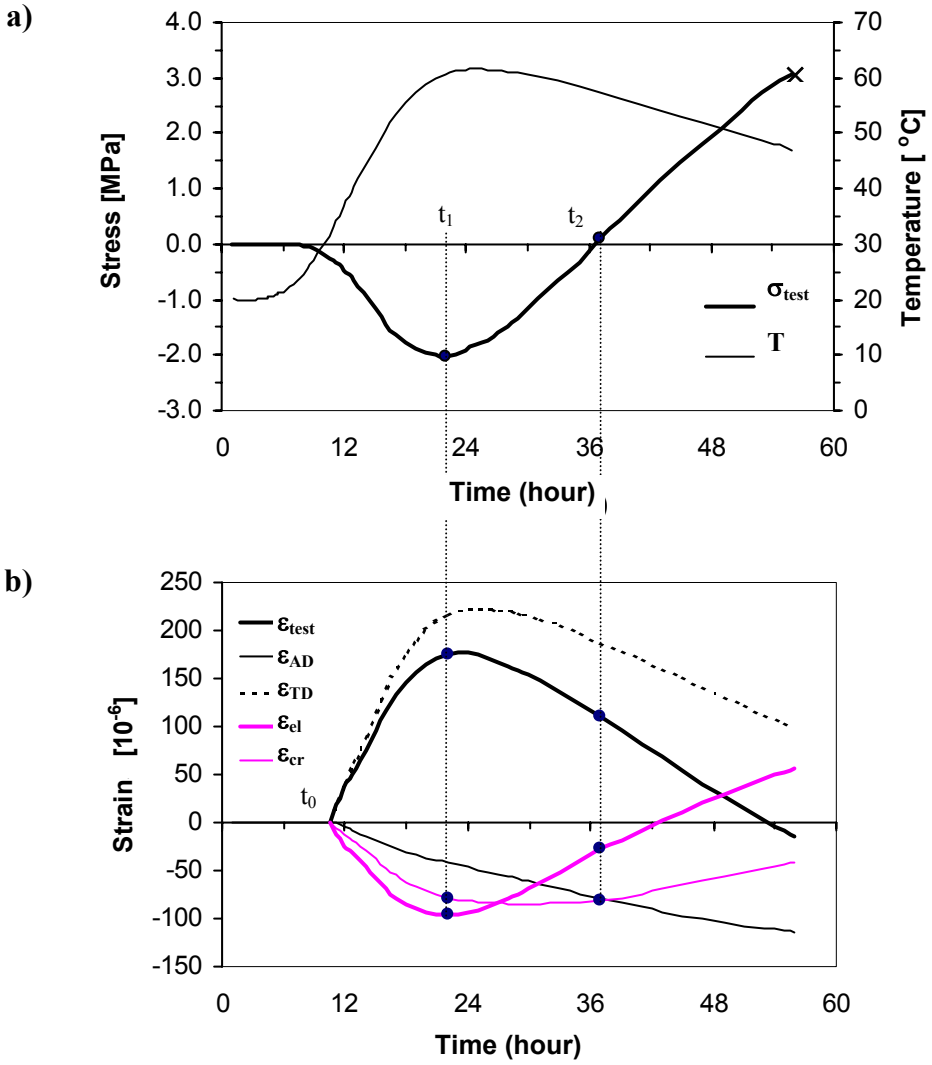

Figure 6.34 Stress and strain development in hardening concrete (T44) exposed to a realistic temperature history with T_{max} = 61.5 ^{o}C. a) Measured stress development, b) Measured free deformation, and different calculated strain components.

When the concrete specimen unloads with time at a certain rate, the elastic strains reduces progressively, and when the stresses are zero at t_2 the concrete will remain with unrecoverable strains. Unloading occurs gradually during 15 hrs between t_1 and t_2, and it results in a reduction of total strain from 175×10^{-6} to 109×10^{-6}, respectively. 75% of the residual strain at t_2 is creep strain, and 25% is elastic strain. During the time period t_1 - t_2 both the creep recovery and the creep will progress. The former is due to the continuous removal of stress increments from the concrete, and the latter is due to the remaining of compressive stresses in the concrete.

Table 6.10 Strains at the time where maximum compressive stress appears, t_1, and when the stresses are reduced to zero, t_2, under realistic temperature histories with maximum temperatures about 60 °C.

Test	SF** [%]	Strain [10^{-6}] At *max.* compressive stress (t_1)			Strain [10^{-6}] At *zero* compressive stress (t_2)		
		ε_{free}	ε_{el}	ε_{cr}	ε_{free}	ε_{el}	ε_{cr}
T36*	0	220	-119	-101 (46%)	162	-52	-110 (68%)
T37	0	191	-104	-87 (46%)	130	-37	-93 (72%)
T44	*5*	*175*	*-96*	*-79 (45%)*	*109*	*-27*	*-82 (75%)*
T47	10	153	-86	-67 (44%)	118	-74	-43 (63%)

* *Delayed temperature history*
** *Silica Fume*

Table 6.11 Stresses at the time where maximum compressive stress appears, t_1, and at the failure point under realistic temperature histories with maximum temperatures about 60 °C.

Test	SF** [%]	Stress [MPa] *At max. compressive stress (t_1)*			Stress [MPa] *At failure point*			
		σ_{test}	σ_{fe}	Relaxation	t [hour]	σ_{test}	σ_{fe}	"Relaxation"
T36*	0	-2,33	-4,77	2,44 (51%)	97	2,78	1,32	-1,46 (-110%)
T37	0	-1,74	-3,75	2,01 (53%)	81	2,99	2,31	-0,68 (-29%)
T44	*5*	*-2,03*	*-3,38*	*1,35 (40%)*	*56*	*3,06*	*2,40*	*-0,66 (-27%)*
T47	10	-1,81	-3,23	1,42 (44%)	45	3,15	2,67	-0,48 (-18%)

* *Delayed temperature history*
** *Silica Fume*

For this test the stress estimation by the creep models is shown in Figure 6.35. As in the test with maximum temperature 40 °C discussed earlier, the calculations start with some difference in initial stress compared to the measured stresses at t_0. The stress difference maintains during the progress of built-up of compressive stresses and then it "disappears". The advantage of using the M-DPL in preference to DPL is clear in the figure, but both models underestimate the stress at failure. The DPL model underestimates the stresses by

23% at failure time, while the M-DPL underestimates it by 6% which is about 1/4th of the error in DPL. One should also note that the M-DPL starts underestimating the stresses later than in DPL, something which means that stresses can be estimated by M-DPL for a longer period of time without any negative consequence than by DPL. Relaxation is about 40% at maximum compression, where this in combination with the high temperature and rapid cooling leads to early cracking (failure) after 56 hrs at 3.02 MPa. The self-induced stresses at 56 hrs would be 2.40 MPa if no relaxation had occurred, meaning that the effect of relaxation in the compression phase is negative.

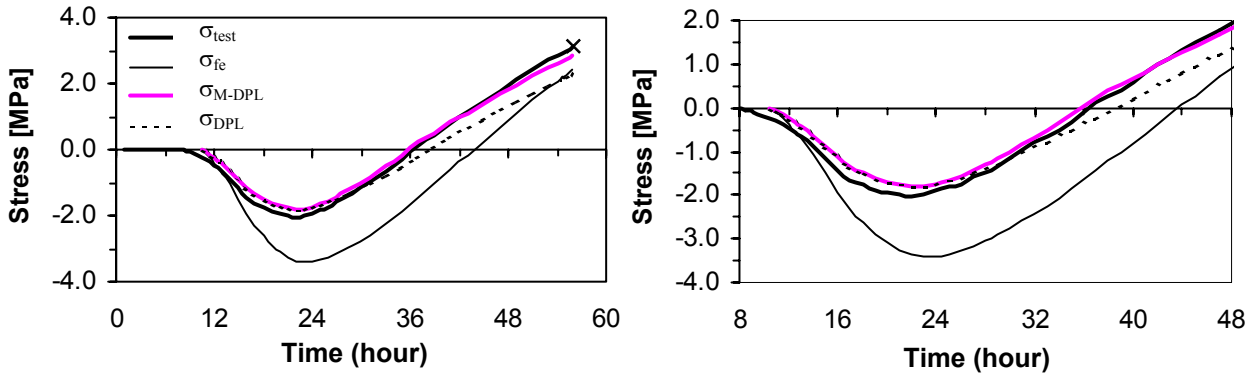

Figure 6.35 Estimated stress development in hardening concrete with 5% silica fume, exposed to realistic temperature history, by DPL and M-DPL. Maximum temperature is 61.5 ^{o}C.

More results are presented in Figure 6.36 and Figure 6.37. The maximum temperature is about 60 ^{o}C in the tests, but the concretes fail at different ages after casting, probably due to different silica fume contents. The results in both figures a) and b) represent the same concrete (with no silica fume content), but the temperature imposed in case of a) is somewhat delayed. The strain components at t_1 and t_2 are given in Table 6.10, and the stresses and the estimated relaxation at t_1 and at the failure time is given in Table 6.11. The previous discussion about stress estimations by DPL and M-DPL in Figure 6.35 is valid also for these three tests. For all the four tests the creep is about 45% of the total strains at maximum compressive stresses.

Comparisons between calculated and measured stresses, at failure time and at 24 hrs prior to failure time are made and presented in Table 6.12. Studying the stress values one can easily see that the stresses estimated by the M-DPL are much closer to the measured values than the values obtained with the DPL model.

The overall picture is that high relaxation during build-up of compressive stresses contributes to higher tensile stresses later and thereby earlier cracking will occur. Bosnjak (2000) made the same conclusion. Taking the creep recovery in consideration in the Modified Double

Power Law using two different creep coefficients leads to much better stress predictions for all the tests than using only one creep coefficient in the Double Power Law.

Table 6.12 Stresses estimated by the DPL and the M-DPL at the time where failure occur and at 24 hrs before that, under realistic temperature histories with maximum temperatures about 60 ^{o}C.

Test	**SF****	**Stress [MPa]** *24 hrs before failure point*				**Stress [MPa]** *At failure point*			
	[%]	**t [hrs]**	σ_{test}	$\sigma_{M\text{-}DPL}$	σ_{DPL}	**t [hrs]**	σ_{test}	$\sigma_{M\text{-}DPL}$	σ_{DPL}
T36*	0	*73*	1,70	1,40	0,74	*97*	2,78	2,71	2,01
T37	0	*57*	1,47	1,45	0,87	*81*	2,99	2,99	2,37
T44	5	*32*	-0,65	-0,51	-0,79	*56*	3,06	2,82	2,30
T47	10	*21*	-0,80	-0,82	-0,81	*45*	3,15	2,91	2,41

* *Delayed temperature history*
** *Silica Fume*

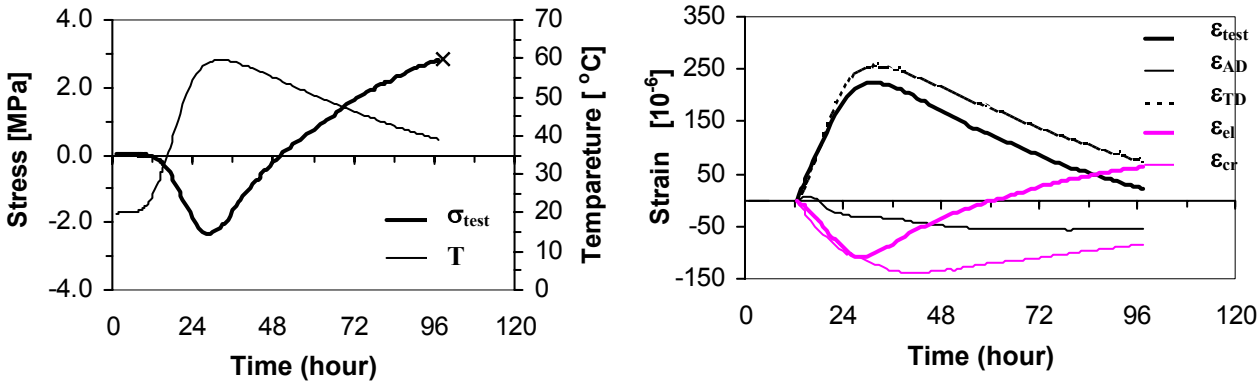

a) 0% silica fume, with "delayed" temperature history, (T36), T_{max} = 59.5 °C

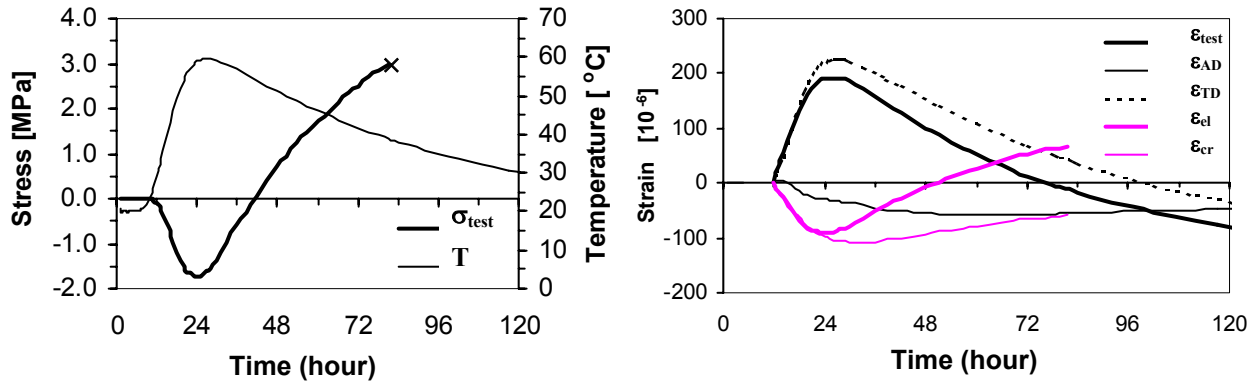

b) 0% silica fume, (T37) , T_{max} = 59.5 °C

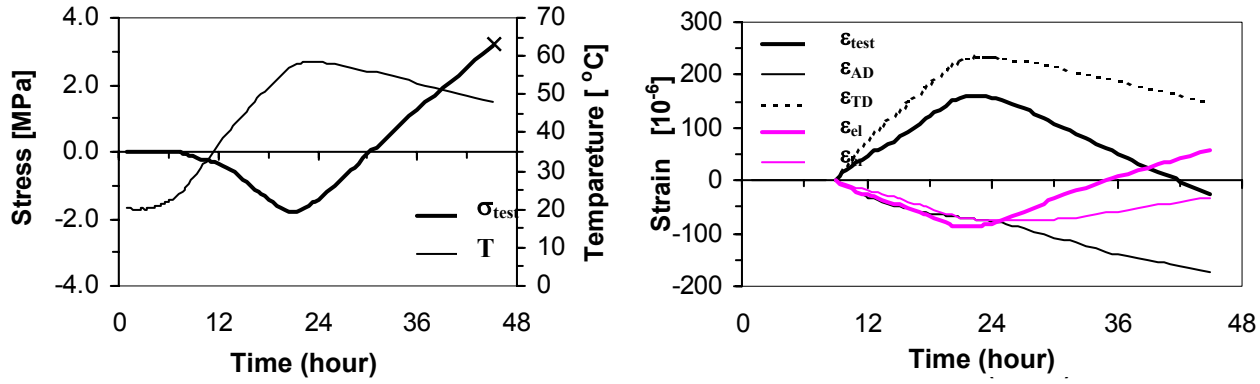

c) 10% silica fume, (T47) , T_{max} = 58.5 °C

Figure 6.36 Measured stress and strain development in hardening concrete exposed to different realistic temperature histories. Different strain components corresponding to total free deformation are calculated. Maximum temperature is about 60 °C.

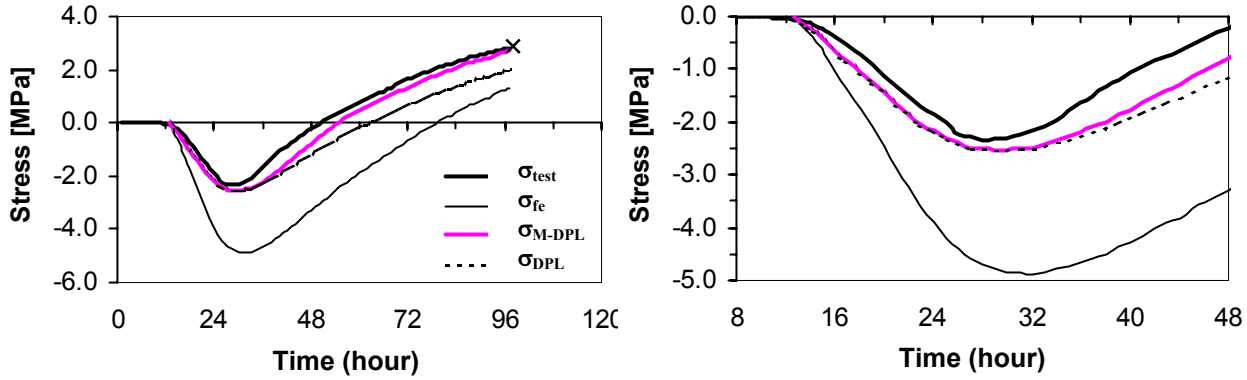

a) 0% silica fume, with "delayed" temperature history, (T36) T_{max} = 59.5 °C

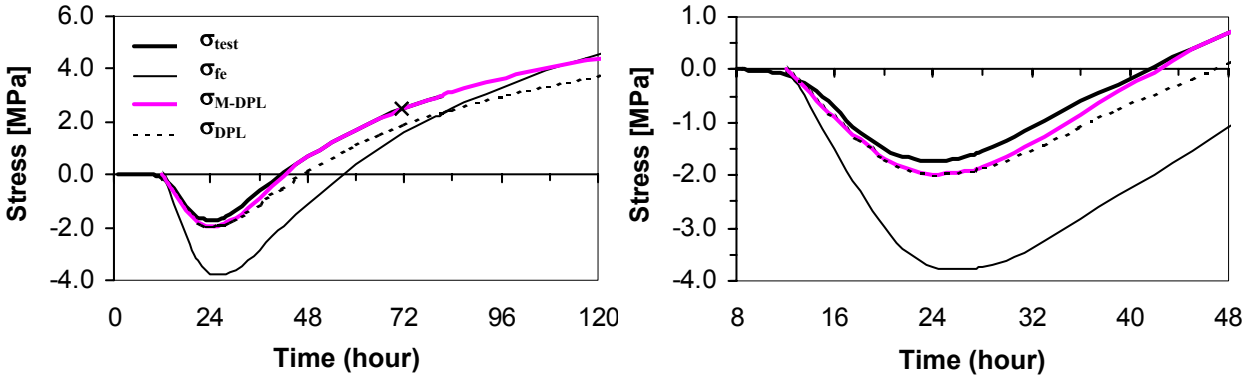

b) 0% silica fume, (T37) T_{max} = 59.5 °C

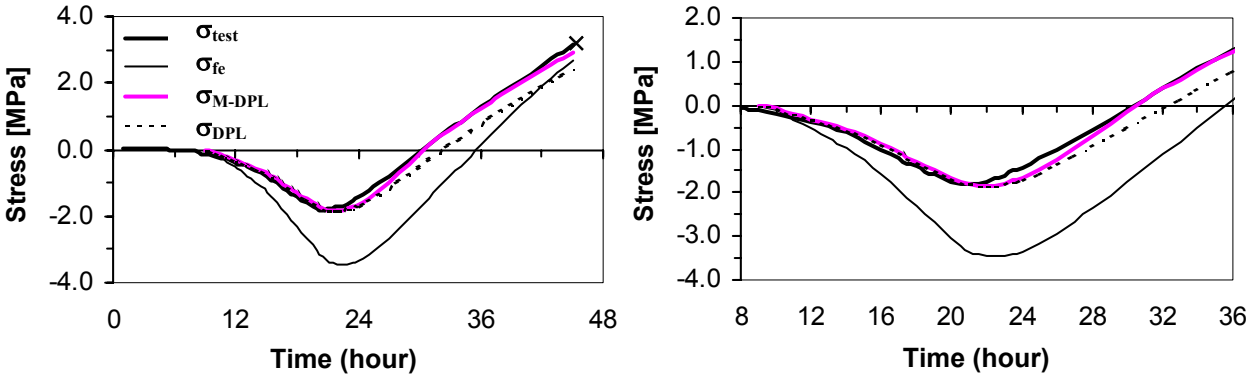

c) 10% silica fume, (T47) T_{max} = 58.5 °C

Figure 6.37 Measured and calculated stress development in hardening concrete exposed to different realistic temperature histories. Maximum temperature is about 60 °C.

The effect of transient creep, described in Chapter 3, is shown in Figure 6.38 for two tests on stress development in TSTM. The material parameter, ρ, used in the equation of transient creep, Eq. (6. 19), is found to be 0.15 for the tests in the present investigation. This was obtained by fitting the stress curves to the measured one. The figure reveals an improvement of the stress predictions by considering the temperature effect on the relaxation, i.e. Transient Creep.

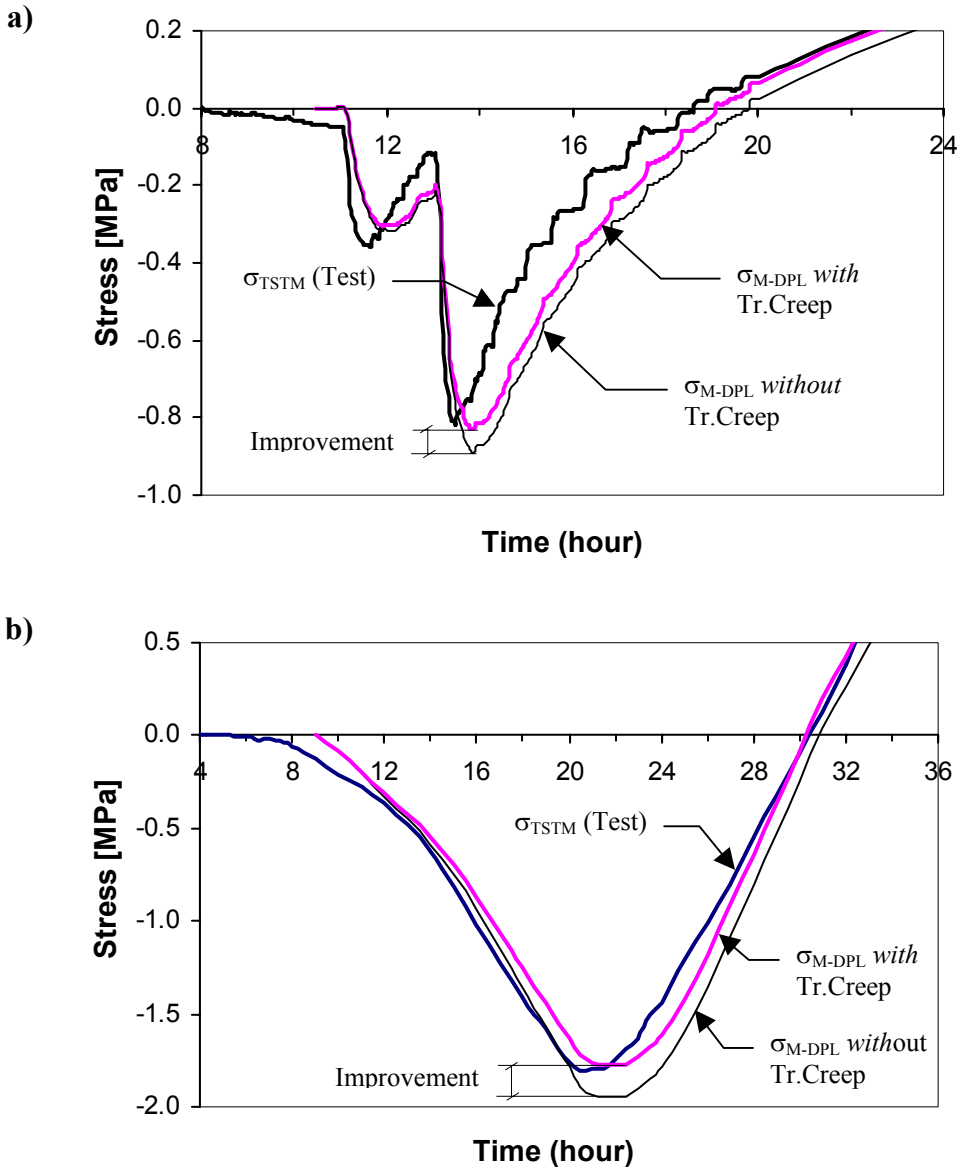

Figure 6.38 Effect of transient creep on calculation of stress development by M-DPL: a) Poly-isothermal test on BASE-5 concrete with temperature steps 20-27-35-45 °C, b) realistic temperature history on BASE-10 with T_{max} = 58.5 °C.

The estimated maximum compressive stress without transient creep appears at 14 hrs and it is 0.88 MPa in the poly-isothermal test, Figure 6.38a. For the test with realistic temperature, Figure 6.38b, it appears after 22 hrs and is 1.97 MPa. The contribution of the transient creep in stress build-up is about 7% and 9% at maximum compressive stresses for the two tests, respectively. The predicted transient creep term is assumed to be irreversible, and thus it remains constant when the temperature is decreasing.

Until now the TSTM tests performed under realistic temperatures and full restraint conditions have shown that the specimen often failed after only a few days. Generally the concrete structures are subjected to a degree of restraint which is lower than 100%, and Bjøntegaard (1999) performed some tests with partial restraint by turning off the feedback system in the TSTM, after the heating phase is over and the cooling phase takes over producing tensile stresses. The results of such tests are presented in Figure 6.39 – 6.42.

Figure 6.39 shows the measured stress in the TSTM, the total free strains in the Dilation Rig and the strains recorded in the partial restrained TSTM from the time of turning off the feedback system. The measured stress development in the system is the result of the difference between the two strain components. The break point in the measured strain and stress curves indicates the time when the feedback system is turned off. In Figure 6.39c the effect of this break on elastic strain is evident, while no direct effect on creep can be observed.

The corresponding stress calculations for the test are shown in Figure 6.40. An improvement in estimation of stresses by the M-DPL during the unloading phase is evident, but it overestimates the stresses after the feedback system was turned off. The overestimation is about 23% of the M-DPL value after 6 days.

The stress relaxation is 48% and 16% at the maximum compressive stress and after 6 days hardening, respectively.

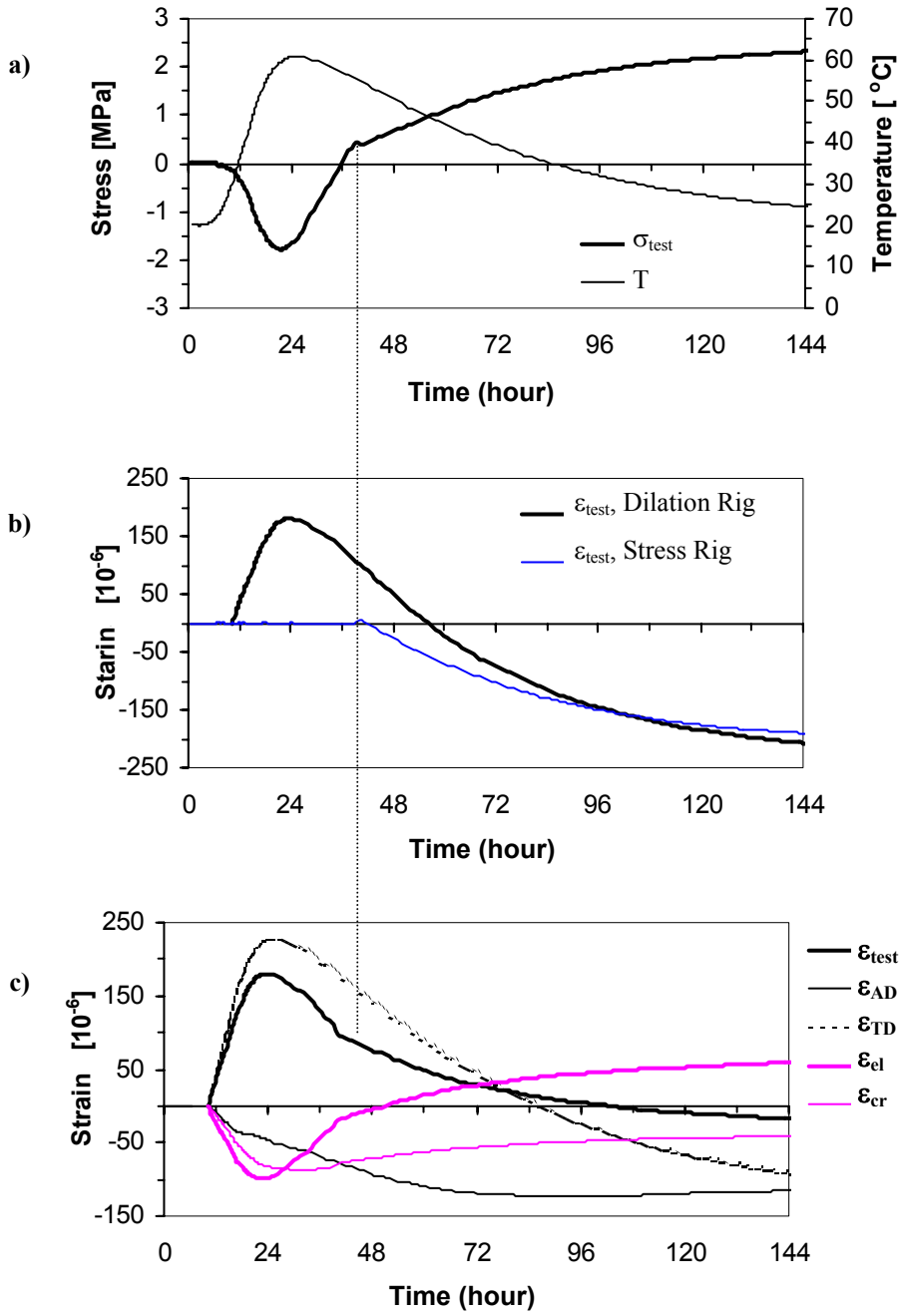

Figure 6.39 Stress and strain development in hardening concrete (BASE-5) exposed to a realistic temperature history and partial restraint. a) Measured stress development, b) Measured free deformation in both the Dilation rig- and the TSTM, and c) Calculated different strain components correspond to the total free deformation. (T70)

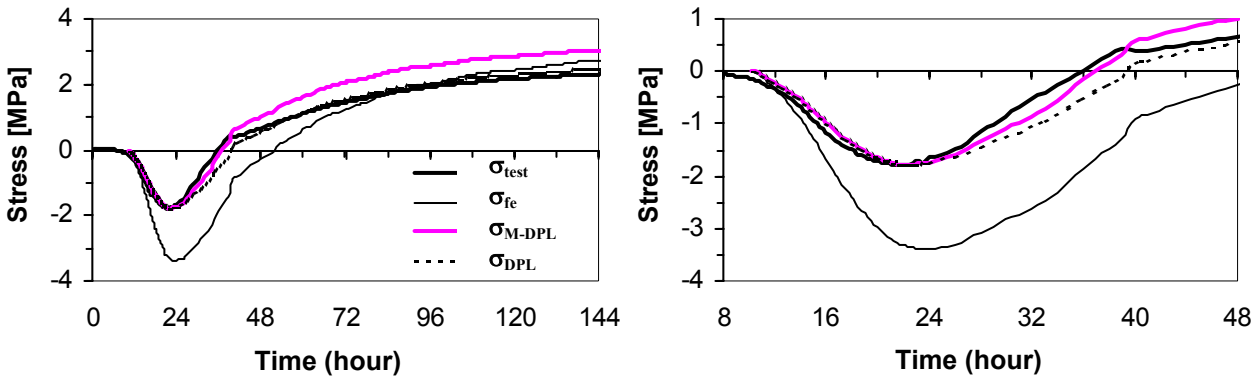

Figure 6.40 Measured and calculated stress development in hardening concrete BASE-5, exposed to different realistic temperature histories (T70).

Other results for concrete mixes with different silica fume content are presented in Figure 6.41 and Figure 6.42. Similar observations to those just discovered can be seen in the results of tests T79 and T78, while the M-DPL is in good agreement with the stress results in T86. Some of the results are given in Table 6.13. The estimated stresses are 14%, 21% and 8% overestimated by M-DPL for the concretes with 0, 10 and 15% silica fume, respectively.

Table 6.13 Stress estimation by DPL and M-DPL at the time where failure occur and at 24 hrs before that, under realistic temperature histories with maximum temperatures about 60 °C.

Test	SF* [%]	Stress [MPa] *At max. compressive stress*				Stress [MPa] *After 144 hrs*			
		σ_{test}	σ_{DPL}	$\sigma_{M\text{-}DPL}$	Relaxation	σ_{test}	σ_{DPL}	$\sigma_{M\text{-}DPL}$	Relaxation
T79	0	-1,63	-2,00	-2,00	63%	2,31	2,04	2,70	- 47%
T70	5	-1,77	-1,79	-1,79	48%	2,32	2,47	3,04	16%
T78	10	-1,88	-1,86	-1,86	46%	2,40	2,40	3,05	10%
T86	15	-1,84	-1,71	-1,71	38%	2,64	2,32	2,88	10%

** Silica Fume*

The overestimation of the stresses obtained by the Modified Double Power Law is on the conservative side, and thus the modified creep law should be regarded as a good model in calculation of self-induced stresses. However, note again that the used M-DPL-parameters are determined from compression tests, not tension. Note also that the relaxation values in the tension phase (Table 6.13 and Figure 6.42) vary greatly over time. They depend strongly on the amount of compressive stress that has been generated under the full restraint, they are therefore not meaningful in given practical application.

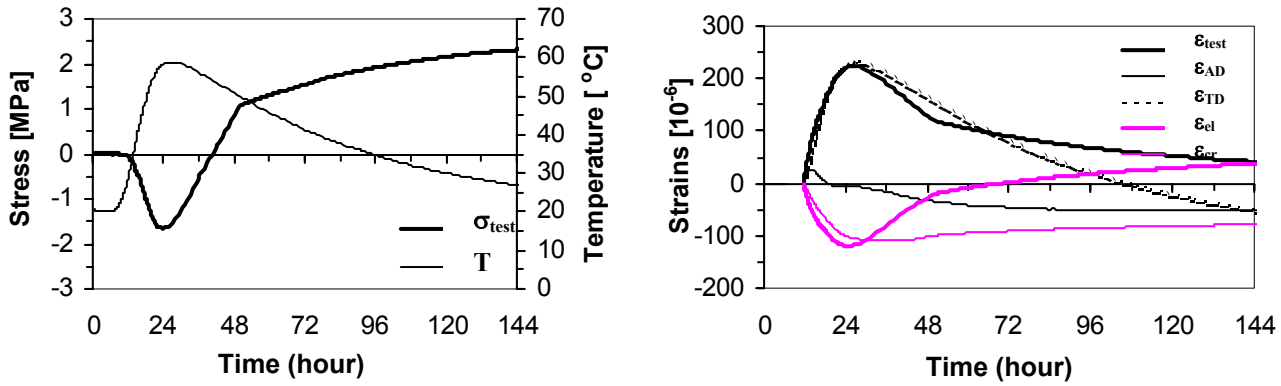

a) 0% silica fume, (T79)

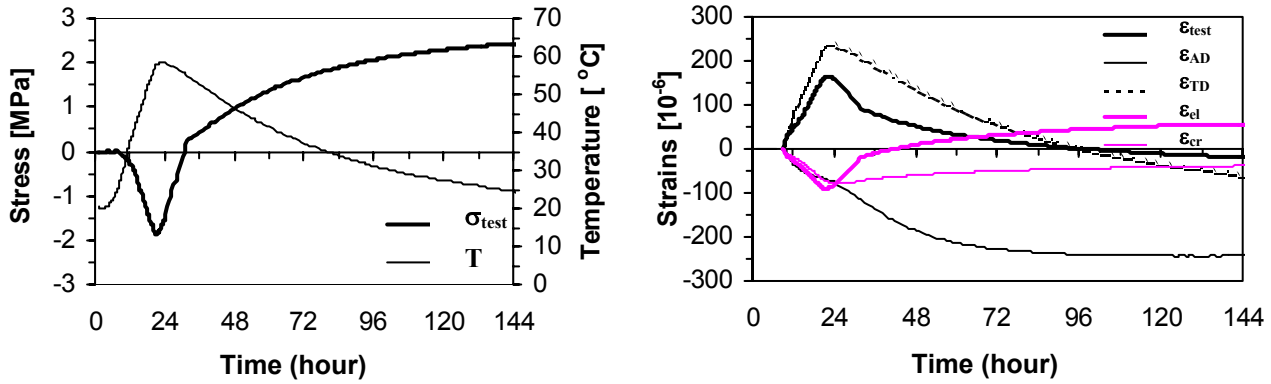

b) 10% silica fume, (T78)

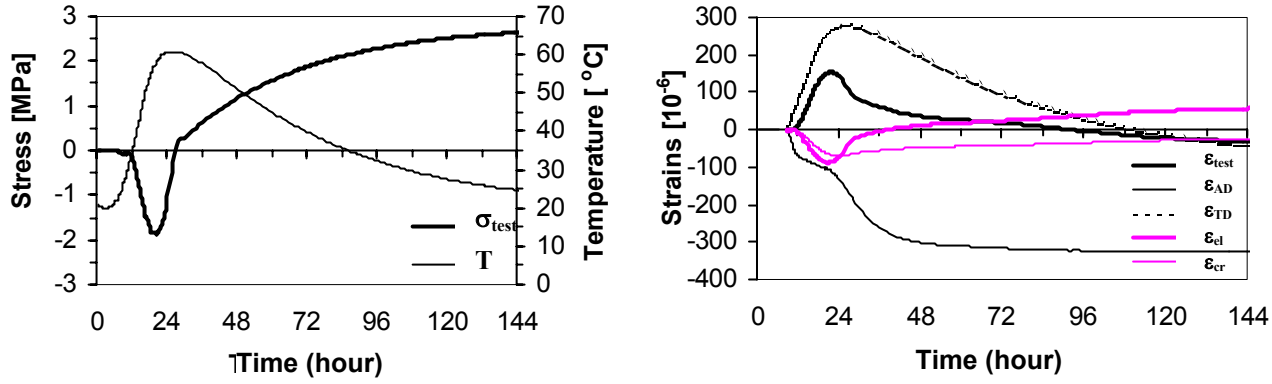

c) 15% silica fume, (T86)

Figure 6.41 Measured stress and strain development in a partially restrained hardening concrete with different silica fume contains exposed to realistic temperature histories with maximum about 60 °C. Different strain components corresponding to total free deformation are calculated.

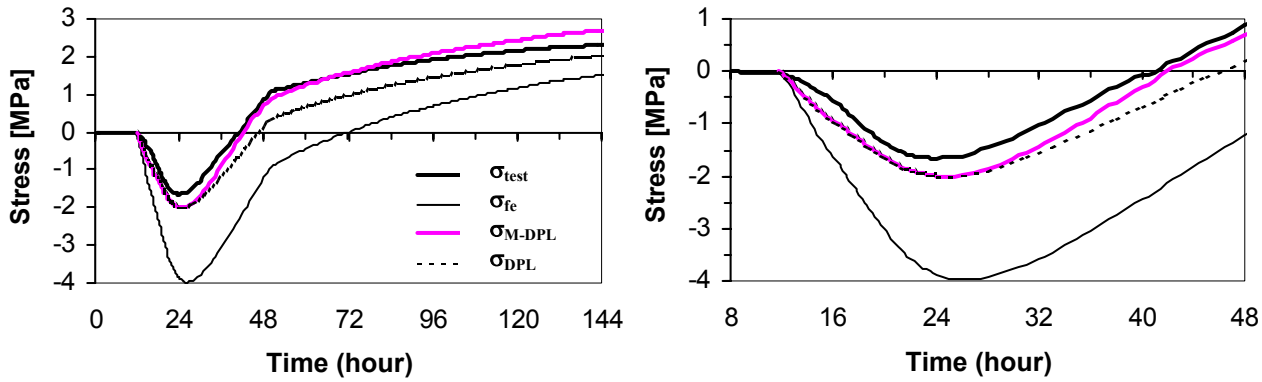

a) 0% silica fume, (T79)

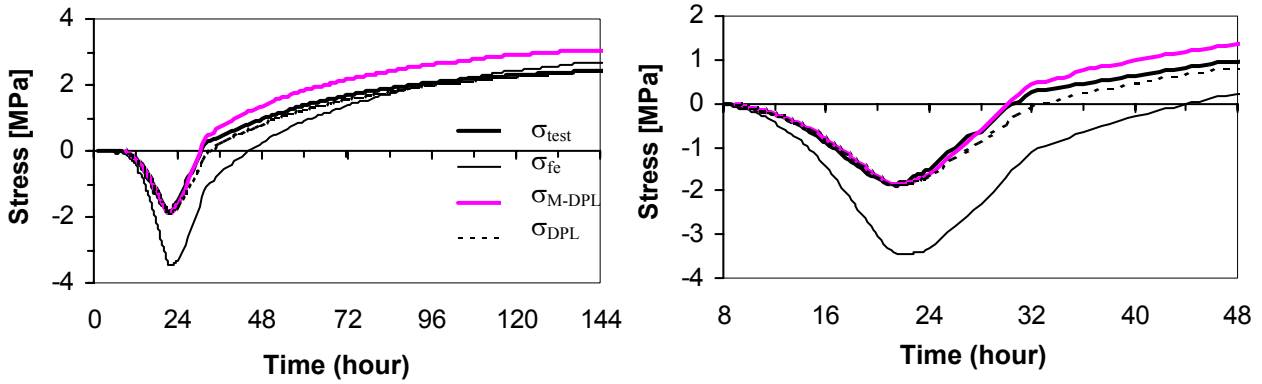

b) 10% silica fume, (T78)

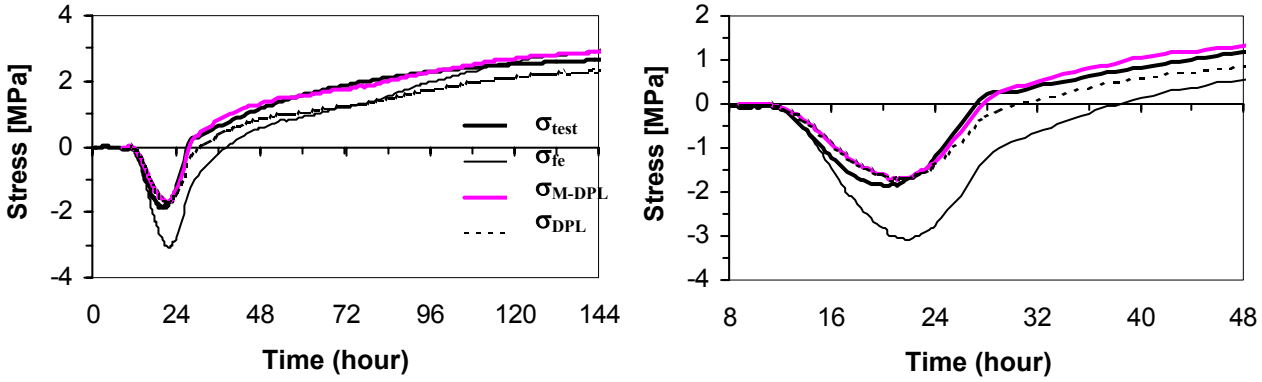

c) 15% silica fume, (T86)

Figure 6.42 Estimated stress in a partially restrained hardening concrete element with different silica fume content, exposed to realistic temperature histories with maximum about 60 ^{o}C.

6.5.4 Influence of Silica Fume Content on Volume Change and Self-Induced Stresses

The effects of silica fume on tensile creep in early age concrete under an *constant load,* was studied in Chapter 5. Further discussion on this issue continues in this section, where the effects of silica fume on the internal stresses induced by restrained thermal dilation and autogenous shrinkage in high performance concrete at early ages is studied. The stresses are evaluated and considered in relation to the creep behaviour of the concrete. In this case of the restrained concrete test, the *stress is continuously changing* at a very slow rate. The tests are fully described by Bjøntegaard in his PhD-thesis (1999).

In the following, comprehensive test results are presented and evaluated.

Mechanical properties

According to the test results, reported by Kanstad *et al.* (1999), on the current mixes, increasing silica fume dosage leads to improved mechanical properties such as tensile strength and E-modulus. The increased tensile strength by addition of silica fume is beneficial in terms of crack risk, while the increased E-modulus is not since restrained thermal dilation and autogenous shrinkage will produce higher stresses.

Total free deformation

The results of two test series, one under isothermal conditions and the other under realistic temperature histories are presented. The free deformations measured at 20 ^{o}C represent autogenous shrinkage, starting from the time t_0, shown in Figure 6.43. The effect of silica fume on autogenous shrinkage is pronounced in the figure, particularly for the mix with high silica fume content BASE-15. At lower silica fume contents, there are small differences between the curves with and without silica fume.

The rate of deformation increased rapidly for the first few hrs of hardening, and then the rate gradually decreases to a nearly constant level. The higher the silica fume dosage the higher the initial rate of deformation, and thus the higher autogenous shrinkage. To compare these results with the earlier observations in Chapter 5 on the same issue, the results for the periods 1-4 days and 4-8 days are shown in Figure 6.43, where autogenous shrinkage is zeroed at 1 and 4 days, respectively. The influence of silica fume content is not very large and the curves show the same somewhat inconsistent trends as the observations in Chapter 5 (Figures 5.30 and 5.31), i.e. that for instance 15% silica fume gives smallest autogenous deformation during from 1 to 4 days, but largest from 4 to 8 days.

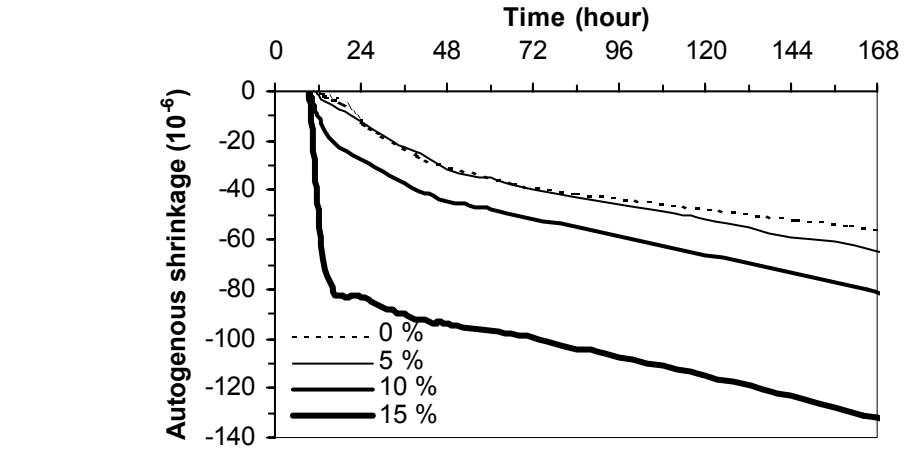

a) From t_0

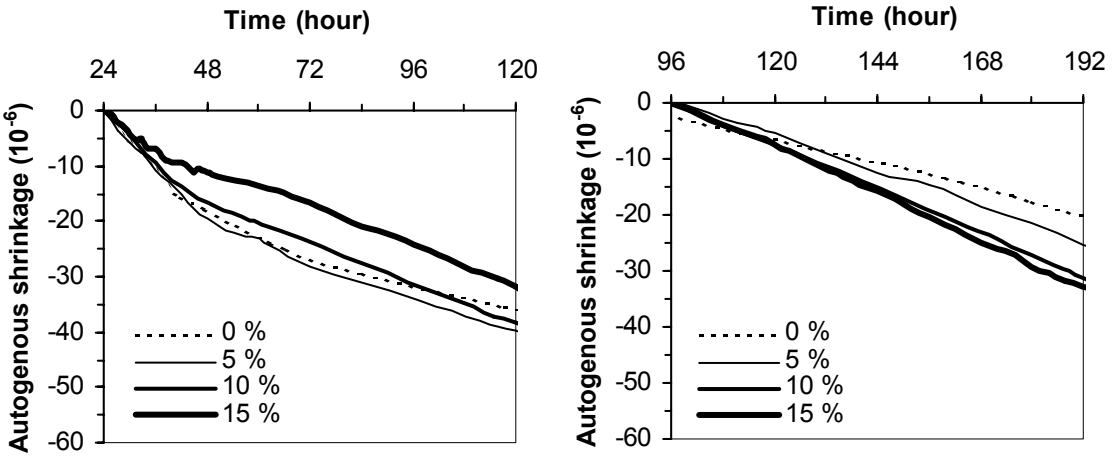

b) From 1 day **c)** From 4 days

Figure 6.43 Development of autogenous shrinkage for concretes with different silica fume contain at isothermal temperature 20 ^{o}C.

Figure 6.44b presents the measured total free deformations under realistic temperatures. The total deformation consists of both thermal dilation and autogenous shrinkage for the realistic temperature histories shown in Figure 6.44a, with maximum temperature 59.5 ^{o}C, 61.5 ^{o}C and 58.5 ^{o}C for concretes with silica fume 0, 5 and 10%, respectively.

The thermal dilation dominance is clear in the first 24 hrs when the temperature is increasing and thus the concrete expands. In the heating phase the autogenous deformation interact with the thermal deformation to produce a reduction of the expansion. The concrete without silica fume exhibits higher expansion than other concretes with silica fume due to less shrinkage. The rate of deformations is nearly equal for all the concretes during the heating phase, but the behaviour is different under cooling. At once the cooling phase starts the deformation trend changes from expansion to contraction. The curves reveal the pronounced difference in the

rate of contraction due to silica fume contents. The free deformation for BASE-0 gains only half of the deformation for the concrete with 5% silica fume after 7 days. This is a good indication of the significant effect of silica fume on the concrete deformation and thus on the stresses this deformation causes under restrained conditions – assuming that CTE for the two concretes are fairly similar. Further analyses are given by Kanstad *et al.* (2001).

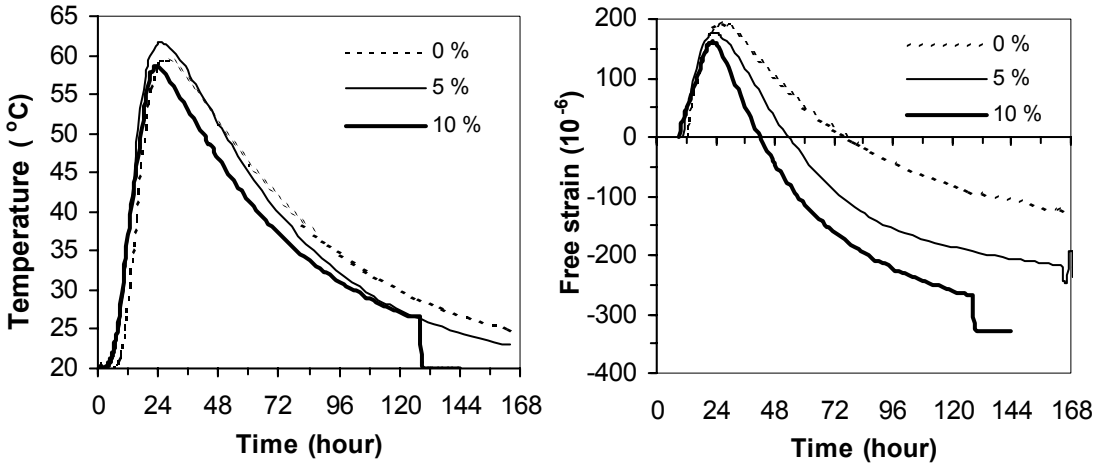

a) Temperature history **b)** Free deformation

Figure 6.44 Measurements in Dilation Rig: a) Realistic temperature histories with T_{max} (0% SF) = 59.5 °C, T_{max} (5% SF) = 61.5 °C, T_{max} (10% SF) = 58.5 °C, b) Total free deformation (AD + TD).

Self-induced stresses and Creep/Relaxation

In parallel with the tests conducted in the Dilation Rig, tests were also performed in the TSTM. The stress built-up under isothermal condition (20 °C) as a function of time is shown in Figure 6.45. All concretes reveal almost the same response to the restrained condition. Up to an age of four days no effect of silica fume on self-induced stresses is observed, and a linear development of stresses continues for the silica fume concretes even beyond that. After 4 days, the BASE-0 behaves somewhat different from other concretes by producing less stresses and its non-linear behaviour is worth to note. For BASE-0 the self-induced stresses are 0.65 and 0.8 MPa after 4 and 7 days respectively, while these values are 0.75 and 1.1 MPa for the same ages for the other three mixes with silica fume.

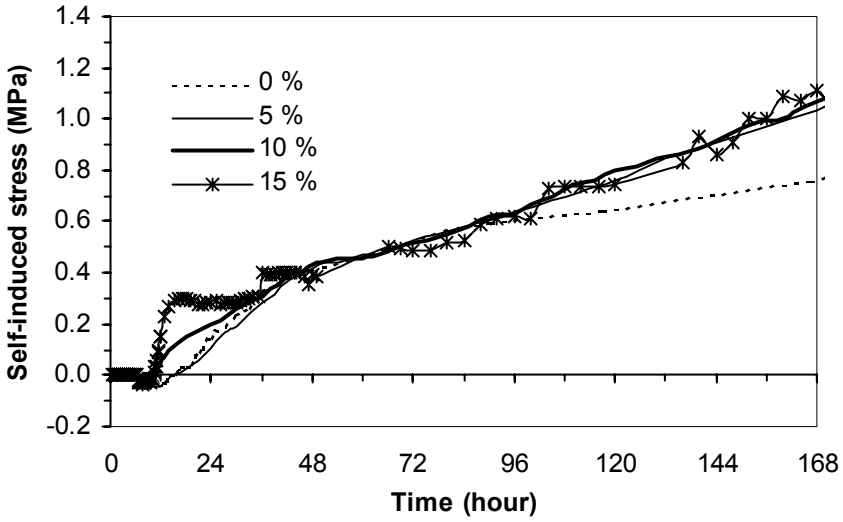

Figure 6.45 Measured self-induced stresses in the TSTM under isothermal temperature histories with different silica fume contents and T≈20 ^{o}C.

The self-induced stresses are not as high as expected from the elastic theory, since considerable relaxation takes place with time. Calculated relaxation due to restraint, defined as in the beginning of this section, is shown in Figure 6.46. Figure a) shows the stress values relaxed with time, where its variation for 0-15% silica fume content is about 0.25 MPa. As can been see, an increase of silica fume from 5% to 10% leads to a higher relaxation, and the effect of further increase of silica fume to 15% is negligible, except the first 72 hrs. The stress relaxation in the concrete with no silica fume is as high as in the concrete with 5% silica fume.

Figure 6.46b demonstrates relaxation and the residual stress in percent of the fictive elastic stress. The figure reveals that the stress relaxation is rapidly increasing during the first hrs of stress build up to almost constant values at approximately 72 hrs. The higher the silica fume content the higher the rate of relaxation for silica fume concretes until its constant value is gained. The relaxation in BASE-5 maintains approximately constant about 40%, and for BASE-0 and BASE-10 it maintains approximately constant about 45%, in the time period between 3 and 8 days. In the concrete with 15% silica fume (BASE-15) the relaxation percentage is reduced during this period, and its value becomes 45% at about 4 days. It should also be noted that the stress relaxation, defined as in Figure 6.46a, develops over a significantly shorter period than for creep. The same observation is made in Morimoto and Koyanagi (1994) and it agrees with linear viscoelasticity. Unlike stress building, the effect of silica fume on stress relaxation under isothermal temperature 20 ^{o}C is scarcely observed after it has gained its ultimate value.

For the given concrete mixes under isothermal conditions one can conclude that the silica fume accelerates the relaxation in the first 24 hrs and it reaches a constant percent after about 72 hrs. Further addition of silica fume has no effect on the ultimate value of the relaxation.

The relaxation in the concrete with no silica fume takes more time to build up than in concrete with silica fume.

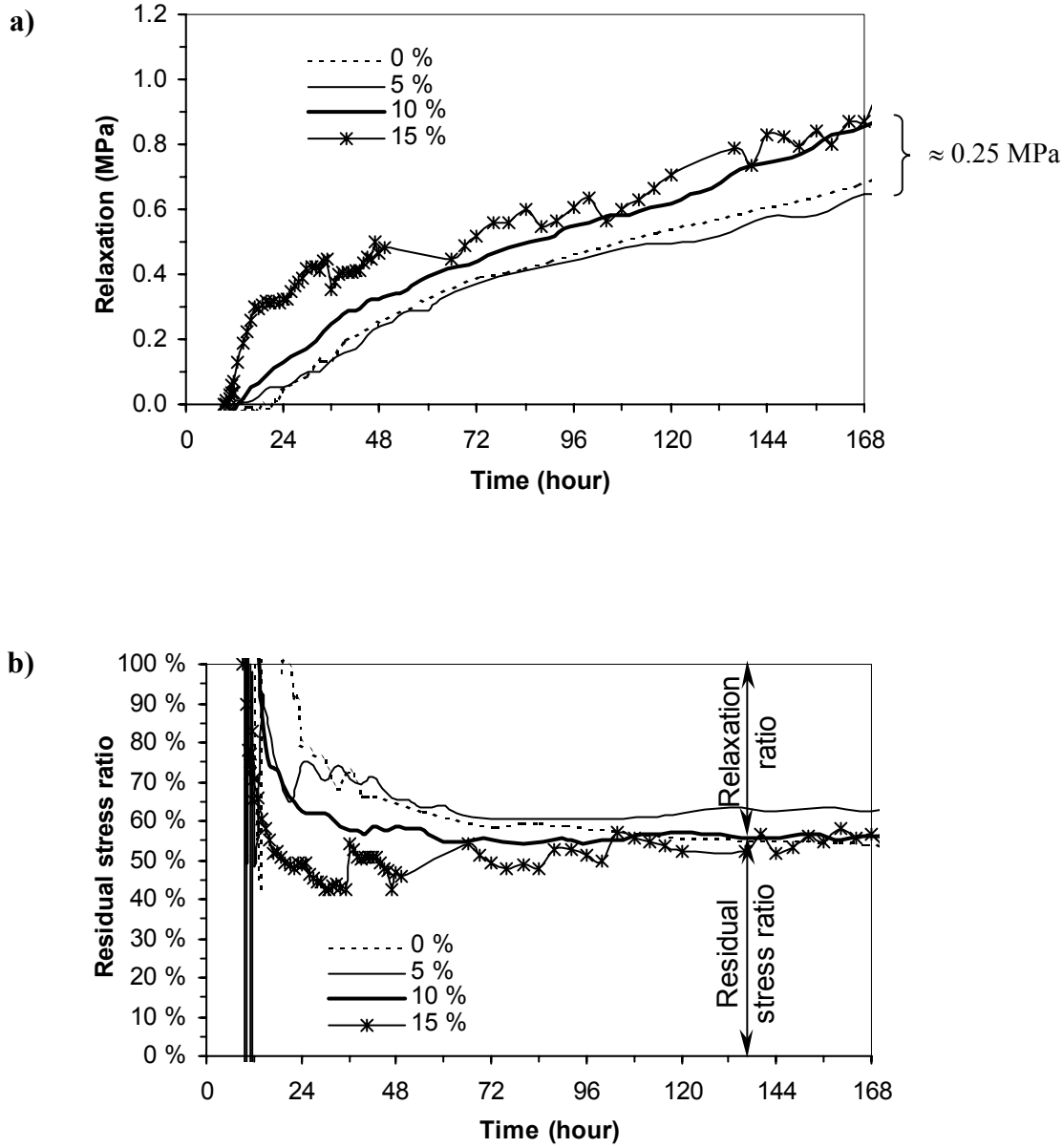

Figure 6.46 Estimated stresses due to viscoelastic behaviour of concretes with 0, 5, 10 and 15% silica fume content. a) Relaxation stresses b) Relaxation and residual stress ratio. (T≈20 °C)

In the case where realistic temperature histories are imposed on the concrete specimens, the test results for the stress development are shown in Figure 6.47. The tests were conducted under uniaxial full restraint conditions for the concretes with 0, 5 and 10% silica fume with the temperature histories shown Figure 6.44. The curves shown in the figure indicate that

increased silica fume content leads to both increased rate and amount of self-induced stresses at early ages. For instance after 42 hrs (when the free strain in 10% silica fume concrete is zero) the concrete stresses are 0.17, 1.20 and 2.65 MPa for 0, 5 and 10% silica fume contain respectively. The increase is mainly due to the high autogenous shrinkage since we expect the thermal contributions to be quit similar. All the concretes fail at a tensile stress of about 3.1 MPa.

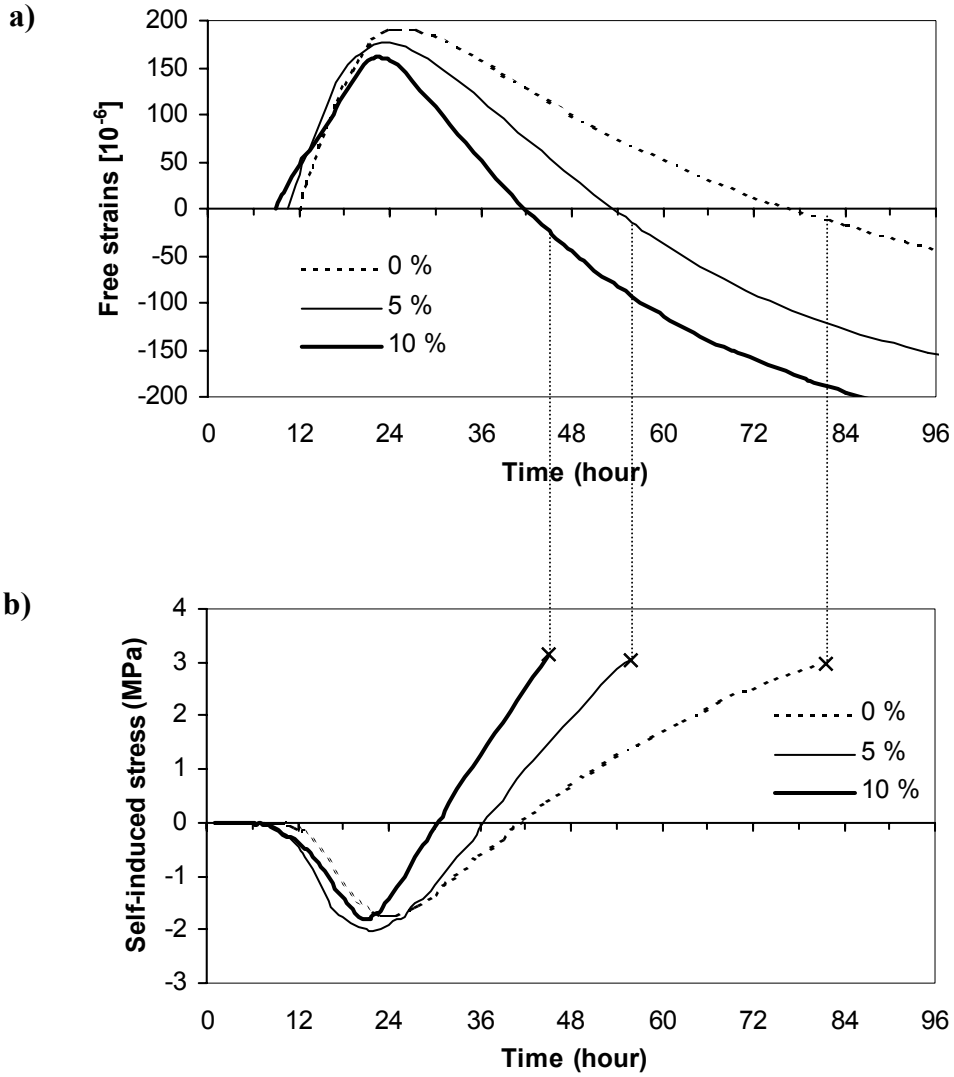

Figure 6.47 Measured strain and self-induced stresses in concretes with different silica fume contain, in TSTM, under full restraint condition and realistic temperature histories shown in Figure 6.44a, with max. temperatures about 60 ^{o}C.

The summary of the results for the different strain components, measured and calculated self-induced stresses and relaxation for the concrete mixes is given in Table 6.10 - Table 6.11. In Table 6.11 the relaxation at maximum compressive stresses and at failure points is given. The

relaxation at maximum compressive stresses in the concrete without silica fume is high (53%), while the relaxation in the concretes BASE-5 and BASE-10 are 40 and 44% respectively. This is about the same relaxation level, as we found for tension in the isothermal tests discussed earlier for the concretes with silica fume. However, the BASE-0 concrete had lowest relaxation in tension, but highest in compression at elevated temperature. For silica fume concretes no major effect of temperature on relaxation is apparent in the 20 to 60 ^{o}C range. Bjøntegaard *et al.* (2003) made the same conclusion for the 20 to 40 ^{o}C range. The negative relaxation in the right column in the same table demonstrates the negative effect of relaxation in the compressive phase on the self-induced stresses in the tensile phase. The lower the negative relaxation values, the higher stress relaxation has occurred in the concrete. This means that the higher silica fume, the higher the stress relaxation is and vice versa.

To avoid very early failure in the concrete partial restraint was imposed on the same concrete mixes, and new tests were conducted. These tests were discussed in the previous section, but because they where performed under different conditions we can not compare their results directly in regard to effect of silica fume on relaxation.

6.6 Summary and Conclusions

The creep model Double Power Law (DPL) is used to calculate the self-induced stresses in early age concrete. The three parameters of the creep model were determined by calibration of the creep model to the creep test data, using an optimization technique on the results of the six creep tests performed under sustained load applied at different ages and at 20 ^{o}C. Due to different creep behaviour in tension and compression, the calibration of the creep model resulted in two different sets of model parameters; set (C) from the compressive creep tests and set (T) form the tensile creep tests. Referring to the model parameter sets (C) and (T) the creep model is noted as DPL(C) and DPL(T), respectively.

Using these two sets of parameters led to an important observation. While the creep model was consistent with the results of the creep tests, the creep recovery tests showed that the DPL used together with the linear superposition principal overestimated creep recovery considerably. This is due to the fact that this approach considers creep recovery identical to creep. Thus, it was necessary to adjust the model to take into account the effect of irrecoverable creep. The modification of DPL consists of division of the creep parameter φ_o in Eq. (6.8) into two parts: the visco-elastic part φ_{oe} and the visco-plastic part φ_{op}. By modification of the linear viscoelastic creep parameter in DPL, the creep model takes irrecoverable creep during decreasing stresses into account. The new creep parameters were found by adaptation of the creep model to the results of the creep recovery tests. The new modified creep model is called M-DPL.

In stress calculations, the modification of the model takes into account the effects of the stress reduction due to temperature decrease in the cooling phase of the hardening, where the linear visco-elasticity is not strictly valid since a large part of the creep is irreversible. The stress reduction is considered as unloading of the concrete. For the time period where self-induced stresses reduce, i.e. recovery occurs a creep parameter φ_{oe} is used. For increasing stresses, both in compression and in tension, the creep parameter for the elastic part is supplemented with the visco-plastic part, φ_{op}, to take account of not recoverable creep.

Both sets of parameters were applied in the calculations for tests under different temperature conditions; isothermal, poly-isothermal and realistic temperature histories.

Stress calculations using linear visco-elasticity with aging and the DPL(C) are in good agreement with the measured stresses for isothermal tests at 20 ^{o}C, which obviously is a necessary condition for also using the DPL parameters outside the conditions where they were determined (i.e. at 20 ^{o}C). The scatter is about 0.15 MPa at 6 days. For other isothermal temperatures than 20 ^{o}C deviations are large. In the case of 45 ^{o}C quite good agreement between DPL and the measured stresses exist in the 30 first hours, while the model underestimates the stresses by 35% after 7 days. For the temperatures lower than 20 ^{o}C, the t_0 is adjusted to fit to the measured results, but still the creep model overestimated the stresses by about 20-30%.

For changing temperature during hardening, the transient creep is taken into account by an additional creep term. The term depends on the state of stress and strength of concrete, and on the model parameter (ρ), which was determined to be 0.15 for the current tests. Its

contribution to stress relaxation was found to be up to10% at maximum temperatures. Transient creep is considered to be irrecoverable during the subsequent temperature decrease.

The DPL(C) performs well for tests under increasing poly-isothermal temperatures, when compressive stresses occurs, but performs not so well in the cooling phase. The same observation is made for the tests performed under realistic temperature histories. The M-DPL(C) reduces the problem, and provides a good agreement with the measured self-induced stresses in TSTM under full restraint conditions, something which clearly proves the significance of including irrecoverable creep in calculations and that it has to be considered correctly. Under partial restraint conditions, the M-DPL(C) overestimates the self-induced stresses by a certain amount, starting from the time where the feedback system is turned off. Nevertheless, the overestimation is on the conservative side, and the new model should be regarded as a reasonably good model in stress calculation. The overestimation after 6 days of hardening is in the range of 8-23% for the concrete mixes with 0, 5, 10 and 15% silica fume content.

Since restrained hardening concrete is exposed to high tensile stresses for a relatively long time period, it was expected that the model parameters calibrated to tensile creep tests (set T) should fit better to the calculations than the model parameters calibrated from the compressive creep tests (set C). Calculations using model parameters from tensile creep tests, ***very surprising***, showed that the M-DPL(C) provides better results than the M-DPL(T) under all temperature conditions (isothermal, poly-isothermal and realistic temperature histories). This conclusion is contrary to our expectation and sounds strange. Comparison between the results of creep tests in compression and tension showed that the rate of tensile creep is relatively low in the first few hours after loading and while it becomes relatively high afterwards. These documented facts result in too high calculated stress development rate in the beginning and a too low stress rate afterwards related to the measured values in the TSTM. However, the discussion of the tensile test results should consider the uncertainties of the method used to separate the creep from the autogenous shrinkage. The procedure is simply to subtract the measured autogenous shrinkage in an unloaded dummy from the total deformation measured on the loaded, selfdesiccating sample. In compression this "correction" is relatively small and the result has been shown to be linear with the applied load. Hence the procedure is generally used even if it is well known (and discussed earlier here) that drying creep by no means is independent of shrinkage. For tension the situation is very different; the compensation is in opposite direction to the load-induced deformation, and may well be greater in magnitude. It is very difficult to demonstrate that the resulting creep is linear with load because of data scatter and sensitivity to this. Thus the whole concept is questionable, but no clear alternatives present themselves. Here, the inconsistency of using compressive instead of tensile creep tests as a basis for calculating relaxation is pointed out as an area for future work, and no more mention is made of the issue.

The effect of relaxation, which is defined as the relative difference between the calculated elastic stresses and the measured self-induced stresses, is found to be relatively large and significant in development of self-induced stresses. Under isothermal temperature 20 ^{o}C, the relaxation increases to about 40% of the fictive elastic stresses after 3 days. For the other isothermal temperatures (5, 13 and 45 ^{o}C) the influence of temperature on relaxation is not consistent. Considering all these results together no conclusion on the effect of temperature on stress relaxation can be made.

URN:NBN:no-3377

An analysis of the six compressive creep tests showed that the creep development at early ages, which has different behaviour than at the later ages, has significant effect in determining the creep model parameters. A study on the number of necessary creep tests to be performed for calibrating the creep model concluded that, depending on the desired accuracy level of the calculations, the necessary number of creep tests can be determined. The best results can be achieved when the test combinations cover a large part of the possible loading ages, but the tests at 1 and 2 days at loading must be included for this particular concrete type.

The results indicate that partial replacement of cement with silica fume increases the magnitude of autogenous shrinkage and self-induced stresses in restrained concrete significantly. The effect of silica fume on relaxation was obvious in both isothermal tests and in the tests with realistic temperature histories. The higher the silica fume content in a concrete mix the higher the stress relaxation is occurred. The same conclusion was made in Chapter 5 in connection to the tensile creep tests on concrete with different silica fume content. Silica fume also increases both E-modulus and tensile strength. Thus, the influence of silica fume on early cracking cannot be stated generally, but must be calculated for each particular case. Such case studies have been carried out [Kanstad et al (2001)], with the conclusion that no significant difference in crack sensitivities existed for equivalent mixes with 0-5-10% silica fume.

Chapter 7

Conclusions and Suggestions for Further Work

7.1 Introduction

Early age concrete undergoes volume changes due to shrinkage and hydration heat development, leading to stress build-up if the concrete is restrained. The time-dependent stiffness properties of the concrete, such as tensile creep and its associated stress relaxation, significantly influence the stress development.

This investigation deals with the time dependent stiffness properties of concrete at early ages, particularly in tension. It focuses on properties such as tensile and compressive creep under sealed conditions, stress relaxation, autogenous deformation, and development of mechanical properties. The summary of the findings and conclusions from this study, based on the experimental and calculated results, are presented below.

7.2 Summary and Conclusions

The study of time-dependent behaviour of high performance concrete presented in this thesis comprises four inter-related phases; Literature survey, Development of a tensile creep test rig, Experimental research program, Theoretical modelling and Evaluation.

The literature survey included; material properties of high performance concrete at early ages, time-dependent deformations and development of self-induced stress. A brief State-of-the-art chapter on tensile creep and relaxation at early ages is included, and some of the existing material models and theories for creep in concrete are explored. Finally, a suitable creep model for early age concrete was chosen and described. On the basis of the survey it can be concluded that the viscoelastic behaviour of early age concrete in tension plays a significant role in the stress development, and thereby also for the crack sensitivity.

The measured creep of sealed high performance concrete includes, in addition to basic creep, a drying creep component because sealing of the concrete of course does not eliminate internal drying and autogenous shrinkage. Therefore, the term *Sealed Creep* is introduced in the present investigation to characterize the creep occurring under sealed conditions.

Models for prediction of self-induced stresses and risk of cracking suffer from serious lack of experimental data about the viscoelastic behaviour of hardening concrete. Although the assessment of cracking involves creep properties in tension, the traditional focus has been almost exclusively limited to creep in compression. The relation between the creep in tension and compression has not been investigated enough, and thus similar creep behaviour in tension and compression is normally assumed in creep models. For this purpose a new experimental equipment (Tensile Creep Rig) for uniaxial tensile creep tests was developed. The tensile Creep Rig fulfils the main requirements suggested by subcommittee RILEM TC 107 for creep tests, namely to; maintain a constant known stress during testing period, ensure uniform stress distribution over the cross-section of the specimen, apply the load very quickly, and operate in a room with controlled temperature and humidity. The used LVDTs have high resolution to capture the small deformations, but they are unstable under temperature change. Since the tensile deformations are relatively small, it is recommended to attach the LVDTs as directly to the concrete samples as possible, without any extension rods, since these tend to introduce uncertainty in the measurements.

The experimental program is subdivided into four series. Each of the series involves one varying parameter, which is relevant to the time-dependent behaviour of early age HPC. Most of the tests are repeated to check the reproducibility of the test results. The reproducibility of the test results for the BASE concretes confirmed that the experimental setup is reliable, and that it can be used to determine tensile creep of concrete at early ages. On the other hand, the scatter in the test results for the Maridal concrete, is an indication that, at each loading age, more than one test is needed to establish the creep behaviour of any concrete type.

This research work puts special emphasis on tensile creep behaviour. Comparing the results of parallel creep tests in tension and compression for two concrete types (BASE-5 and Maridal concretes), both similarities and differences were observed:

> Similarities: The creep magnitude increase strongly with a decrease in the loading age. A high rate of creep within the first day after loading is followed by a lower rate. The time dependent behaviour in both tension and compression is much more sensitive to the loading age, at ages less than 2 days, than later.
>
> Differences: Smaller instantaneous deformation under tension than under compression. Right after load application the creep in compression is high, but it levels off to a progressively lower rate. In contrast, creep in tension is lower than in compression initially, but an almost linear rate is soon established which is much higher than in compression. The consequence is greater creep magnitude and thus greater creep coefficient in tension than in compression.

The modulus of elasticity in tension and compression also differ. It was found in independent tests that the E-modulus in tension (E_t) is greater than the E-modulus in compression (E_c) by

10-17% for the BASE concrete and 20% for the Maridal concrete. This confirms the difference in instantaneous deformations found for tension and compression in the creep rig. The main reason for the difference between the E-modulus in tension and compression is probably the load levels. A significant feature of creep, as commonly defined, is that the autogenous shrinkage compensation affects tensile creep and compressive creep in opposite directions. For tension they are in opposite directions, while for compression they are additive. Therefore, the difference between the tensile and compressive creep can partly be a consequence of the compensation procedure. This is a fundamental question, which should be investigated further.

The proportionality limit between stress and sealed tensile creep strain is found to be about 60% of the tensile strength. This linearity of the deformation components with applied stress is of fundamental importance, since it, at least partly, justifies the compensation procedure of subtracting the unloaded dummy deformation from the loaded one. This is particularly important for tensile creep because the dummy deformations in this case are generally much larger than the stress dependent deformations. Another observation was that the non-linearity becomes more pronounced with time under load. For the studied case, the ratio between the time-dependent strain at stress levels 80 and 70% of the strength is 1.55 after 24 hours while it is 1.81 at 48 hours.

Furthermore, the test results indicate that partial replacement of cement with silica fume (5-15%) increases the sealed tensile creep. However, the reference concrete without silica fume dose not fit to this systematic pattern. Analysing TSTM isothermal test results the higher silica fume content led to higher stress relaxation. Since silica fume also increases both E-modulus and tensile strength, then its influence on early age cracking cannot be stated generally, but must be calculated for each particular case.

From a relatively limited amount of test data on the influence of isothermal temperatures on creep, it can be concluded that sealed tensile creep, accelerates for temperatures higher than 20 ^{o}C, as compressive creep also does. In addition, the maturity principle describes the aging effect reasonably well. The agreement is even better if an activation energy higher than the one determined from compressive strength testing is used. The consequence for material modelling is that the maturity principle is applicable for isothermal temperature histories, at least beyond about 3 maturity days.

The relatively large amount of experimental data, available in this study, has been used to check model equations for creep. Comprehensive test results from the TSTM apparatus are analyzed with respect to creep and relaxation, where the effect of temperature on creep and relaxation is emphasized. Simulations of self-induced stresses are performed using the creep model denoted the Double Power Law (DPL). As solution method, the theory of linear viscoelasticity is being used. A term, denoted transient thermal creep, is included to describe the additional creep, which occurs when the temperature increases while the concrete is loaded. The DPL is chosen mainly due to its simplicity with only three model parameters, which quite easily can be determined by calibration to creep test data. Due to different creep behaviour in tension and compression, the calibration resulted in two different sets of model parameters; set (C) from the compressive creep tests and set (T) form the tensile creep tests. The creep model is then denoted DPL(C) and DPL(T), depending on which parameter set is being used.

Using these two sets of parameters led to an important observation, which is by no means new, but not often considered in modelling. While the creep model was consistent with the results of the creep tests, the creep recovery tests showed that the DPL used together with the linear superposition principle overestimated creep recovery considerably. This is due to the fact that this approach considers creep recovery identical to creep. Consequently, the model was adjusted to take into account the effect of irrecoverable creep; dividing the creep parameter φ_o into a visco-elastic part φ_{oe} and a visco-plastic part φ_{op}. The new creep parameters were found by adaptation of the creep model to the results of the creep recovery tests. The resulting modified creep model (M-DPL) considers the stress reduction due to the temperature decrease in the cooling phase of the hardening period, where linear viscoelasticity is not valid since a large part of the creep is irreversible.

Stress calculations using linear viscoelasticity with aging and the DPL(C), are in good agreement with the measured stresses for isothermal tests at 20 ^{o}C, which obviously is a necessary condition for also using the DPL parameters outside the temperature range where they were determined.

For increasing temperatures during the hardening phase, the transient creep (takes place during heating) is taken into account by an additional creep term. Its contribution to stress relaxation was found to be up to 10% at maximum temperatures. This transient creep term is considered to be irrecoverable during the subsequent temperature decrease.

The DPL(C) performs also well for tests with stepwise increasing temperatures, when compressive stresses occurs at each step, but performs not so well in the cooling phase. The same observation is made for the tests performed under realistic temperature histories. The M-DPL(C) improves the modelling, and provides good agreement with the measured self-induced stresses in TSTM under full restraint conditions. This clearly proves the significance of including irrecoverable creep. In other words, the DPL(C) fits well when the stresses, either tensile or compressive, increase. However, when unloading occurs, the M-DPL(C) fits best. The modified model captures the various characteristics of sealed creep and describes the tensile behaviour at early ages reasonably accurate.

Since restrained hardening concrete is exposed to high tensile stresses for a relatively long time period, it was expected that the model parameters calibrated to the tensile creep tests (set T), should provide a better fit to the experimental TSTM-data, than the model parameters calibrated from the compressive creep tests (set C). But, ***very surprisingly***, the M-DPL(C) provided better agreement with the test results than the M-DPL(T), under all temperature conditions (isothermal, poly-isothermal and realistic temperature histories). This conclusion is in contradiction to our expectation and sounds strange. All aspects of the tensile test and modelling procedures should therefore be reconsidered, and in particular the method used to separate the creep from the autogenous shrinkage.

The effect of stress relaxation, which is defined as the relative difference between the calculated elastic stresses and the measured self-induced stresses, is found to be relatively large and significant in the development of self-induced stresses. Under isothermal temperature of 20 ^{o}C, the relaxation increases to about 40% of the fictive elastic stresses after 3 days and remains about constant after that. For the other isothermal temperatures (5, 13 and 45 ^{o}C) the influence of temperature on relaxation is not consistent. Presentation of relaxation

under realistic temperature histories is even more complicated, because the stresses changes from compression to tension. Considering all these results together, no conclusion on the effect of temperature on stress relaxation can be made.

Early age creep is normally beneficial in reducing stresses, but it might also lead to increased stresses. Under realistic temperature histories it might have negative effect on the cracking risk in externally restrained structures; because compressive creep reduces compressive stresses, but increases the subsequent tensile stresses. Underestimation of creep in this early period will lead to underestimation of the cracking risk.

Creep at very early ages has a significant effect in determination of the creep model parameters. After an evaluation of the necessary number of creep tests that should be performed for calibration of the creep model, it was concluded that, depending on the desired accuracy level of the calculations, the necessary number of creep tests could be determined. The most optimal test programmes should include combinations which cover a large part of the possible loading ages, but the tests at ages of 1 and 2 days at loading must be included.

The experimental results indicate that partial replacement of cement with silica fume increases the magnitude of autogenous shrinkage and self-induced stresses in restrained concrete significantly. The effect of silica fume on relaxation was clear in both isothermal tests and in the tests with realistic temperature histories: Higher silica fume content led to higher stress relaxation. Silica fume also increases both E-modulus and tensile strength. Thus, the influence of silica fume on early age cracking cannot be determined generally, but must be calculated for each particular case.

7.3 Recommendations for Further Research

Based on the results and the limitations of the present work, some recommendations for more research and further improvement of the material modelling of concrete at early ages are given:

- The inconsistency of using compressive instead of tensile creep test data as a basis for calculating tensile relaxation has to be pointed out as a major topic for future work.

- The commonly used procedure to define creep is simply to subtract the measured autogenous shrinkage of an unloaded dummy specimen from the total deformation measured on the loaded specimen. In contrast to the compressive creep tests, the load-independent deformations in the tensile creep tests are at least of the same order of magnitude as the load-dependent deformations. Consequently the load independent strains always have a large influence on both the magnitude and the rate of the creep development in tensile tests. Although the observed linearity of the deformation components up to 60% of the strength may partly justify the compensation procedure, the question whether this approach is valid for determination of tensile creep has to be documented more.

- While it is quite simple to present the development of relaxation under isothermal temperatures, it is difficult to do the same for realistic temperature histories. There is a need for a procedure to characterize the relaxation behaviour under different temperature conditions in a simple manner.

- Further tensile creep testing under different isothermal temperatures, and under other temperature histories, should be performed as basis for further improvement of the material modelling and understanding of the topic.

References

ACI Committee No. 207, (1973): *"Effect of restraint, volume changes and reinforcement on cracking of massive concrete"*, ACI Journal, pp. 445-470.

ACI Committee No. 209 (1992): *"Prediction of Creep, Shrinkage and Temperature Effects in Concrete Structures"*, Report No. ACI 209R-92.

Acker, P. (1993): *"Creep Tests of Concrete: Why and How? - Invited Lecture";* Proc. of the 5th RILIM International Conference on: Creep and Shrinkage of Concrete, E & FN SPON, Spain, pp. 3-14.

Ali, I., and Kesler, C.E. (1964): *"Mechanisms of creep in Concrete*", Symp. on 'Creep of concrete', ACI special publication No. 9, pp 35-57.

Altoubat, S. A. (2000): *"Early Age Stresses and Creep-Shrinkage Interaction of Restrained Concrete",* Doctoral thesis, Dept. of Civil Engineering, University of Illinois, Urbana-Champaign.

Altoubat, S. A. and Lange, D. A., (2001): *"The Pickett Effect in Early Age Concrete Under Restrained Conditions*". RILIM International Conference on Early Age Cracking in Cementitious Systems (EAC'01), Haifa, pp. 133-144.

Arthanari, S. and Yu, C. W. (1967): "*Creep of Concrete Under Unixial and Biaxial Stresses at Elevated Temperatures",* Magazine of Concrete Research, Vol. 19. No. 60, pp. 149-156.

Atrushi, D., Bjontegaard, O., Bosnjak, D., Kanstad, T. and Sellevold, E. J., (2001): "*Creep deformations due to self-stresses in hardening concrete, effect of temperature"* - "Creep, Shrinkage and Durability Mechanics of Concrete and Other Quasi-Brittle Materials", in Proc., 6th International Conference, CONCREEP-6, August, 20-22, M.I.T., Cambridge, USA, pp. 613-618.

Atrushi, D., Bosnjak, D., Kanstad, T. and Sellevold, E. J., (2000): "*Tensile Creep of Young High Performance Concrete*", International PhD Symposium in Civil Engineering, Vienna.

Bäckström, S. (1956): *"Creep and Creeo Recovery in Cement Mortar",* Preliminary Report of the Fifth Congress of the International Association of Bridge and Structural Engineering, Lisbon, pp 77-83.

Bažant, Z. P. (1975): *"Theory of Creep and Shrinkage in Concrete Structures: A Précis of Resent Development"*. Mechanics Today, Vol. 2, pp 1-93, Pergamon Press.

Bažant, Z. P. (1977): *"Viscoelasticity of Solidifying Porous Material - Concrete"*. Swedish Cement and Concrete Research Institute, Fo 5:77, Stockholm.

Bažant, Z. P. and Baweja, S., (1995): "*Creep and Shrinkage Prediction Model for Analysis and Design of Concrete Structures – B3*", Materials and Structures, Vol. 28.

Bažant, Z. P. and Chern, J.C. (1985a), "*Concrete Creep at variable humidity*", Journal of Engineering Mechanics, 18(103).

Bažant, Z. P. and Kim, S.S. (1979): "*Nonlinear Creep of Concrete – Adaption and Flow*", J. Eng. Mech. Div. (ASCE), 105, pp. 419-446.

Bažant, Z. P. and Osman, E. (1975): "*Double Power Law for Basic Creep of Concrete*", Materials and Structures, (RILEM, Paris) Vol. 9, No. 49, pp. 3-11.

Bažant, Z. P. and Wittman, F.H. (1982): "*Creep and Shrinkage in Concrete Structures*", Wiley & Sons, New York.

Bažant, Z. P., and Najjar, L. T. (1973): *"Comparison of Approximate Linear Methods for Concrete Creep*". Journal Strut. Div. ASCE, 99, No. ST9, pp. 1851-74.

Bažant, Z. P., Baweja, S., and Carol, I., (1993): *"Preliminary guidelines and recommendation for characterizing creep and shrinkage in structural design codes";* Proc. of the 5th RILIM International Conference on: Creep and Shrinkage of Concrete, E & FN SPON, Spain, pp. 805-829.

Bažant, Z. P., Chern, J.C. (1985b): "*Concrete creep at variable humidity: constitutive law and mechanism"*, Materials and Structures (RILEM), Vol.18.

Bažant, Z. P., Panula, L. (1978a): "*Simplified Prediction of Concrete Creep and Shrinkage From Strength and Mix"*, Structural Engineering Report, No. 78-10/6403, Department of Civil Engineering, Technological Institute, Northwestern University, Illinios, pp. 24.

Bažant, Z. P., Panula, L. (1978b): "*Practical prediction of time dependent deformations of concrete*", Materials and Structures, Part I and II: Vol. 11, No. 65, pp. 307-328.

Bellander, U. (1976): *"Hållfasthet i Ferdig Konstruktion, Del 1. Førstørande Metoder, Rimeliga Kravsnivåer (Strength in Completed Structures, Part 1, in Swedish)*, Swedish

Cement. and Concrete. Research Institute, Research 13:76, Stockholm (quoted from Byfors 1980).

Bennet, E. W. and Loat, D. R. (1970): *"Shrinkage and Creep of Concrete as Affected by The Fineness of Portland Cement*". Mag. Concr. Res., 22, No. 71, pp. 69-78.

Bentur, A. (2002): "*Overview of Early Age Cracking"*, Chapter 1.5 in the State-of-the-art, RILEM-publication: 'Early Age Shrinkage and Cracking of Cementitious Systems', Ed. by Bentur, A..

Bentur, A. net, E. W. and Loat, D. R. (1970): *"Shrinkage and Creep of Concrete as Affected by The Fineness of Portland Cement*". Mag. Concr. Res., 22, No. 71, pp. 69-78.

Bentur, A., (2001): "*Comprehensive Approach to Prediction and Control of Early-Age Cracking in Cementous Materials"*, in Proc. of the 6th International RILEM Conference on 'Creep, Shrinkage & Durability Mechanics of Concrete and other Quasi-Brittle Materials' (Concreep6), Cambridge, USA, Aug. 2001, (Elsevier Science Ltd., Oxford 2001), pp. 589-598.

Bentur, A., Igarashi, S. and Kovler, K., (1999): "*Control of autogenous shrinkage stresses and cracking in high strength concretes*" in 'Utilization of High Strength/High Performance Concrete', I. Holand and E.J.Sellevold, editors, Proc. 5th Int. Symp. Sandefjord, Norway1017-1026.

Bentur, A., Igarashi, S., and Kovler, K. (2001): "*Internal curing of high strength concrete to prevent autogenous shrinkage and internal stresses by use of wet lightweight aggregates*"' *Cement and Concrete Research*, 31 1587-1591.

Bernander, S., (1998): *"Practical Measures to Avoiding Early Age Thermal Cracking in Concrete Structures"*, in 'Prevention of Thermal Cracking in Concrete at Early Ages', R. Springenschmid, editor, E&FN SPON, pp. 355-314.

Bernander, S., and Emborg, M. (1994): *"Risk of Cracking in Massiv Concrete Structures - New Development and Experiences"*"; Thermal Cracking in Concrete at Early Ages, Proc. of the RILEM International Symposium, Edited by R. Springenschmid, E & FN Spon, London, pp. 385-392.

Bissonnette, B., Pigeon, M. (1995): "Tensile creep at early age of ordinary silica fume and fibre reinforced concretes". Cement and Concrete Research 25. Pp. 1075-85.

Bjøntegaard Ø. and Sellevold E.J., (2000): "*Interaction Between Thermal Dilation and Autogenous Deformation in High Performance Concrete*", In the International RILEM Workshop on Shrinkage of Concrete - Shrinkage 2000, Ed. V. Baroghel-Bouny and P.C. Aitcin, Paris 16 – 17.

Bjøntegaard, Ø. (1999): "*Thermal Dilation and Autogenous Deformation as Driving Forces to Self-induced Stresses in High Performance Concrete*", Doctoral thesis, NTNU, Dept. of Structural Eng., ISBN 82-7984-002-8.

Bjøntegaard, Ø. and Sellevold E. J. (2002): "*Effect of Silica Fume and Temperature on Autogenous Deformation of High Performance Concrete"* ACI Fall, to be published in an ACI - Special Publication.

Bjøntegaard, Ø., (to be published in 2003): "*Young high performance concrete with w/b=0.40 and varying silica fume content during hot weather conditions: Experimental tests on cracking risk related properties and 1D stress calculations*", NOR-CRACK report, DP-3 Parameter studies.

Bjøntegaard, Ø., Kanstad, T. Sellevold E., Hammer, T.A., (1999): *"Stress-inducing deformation and mechanical properties of concrete at very early ages*", in 'Utilization of High-Strength/High Performance Concrete Technology', Proc 5th Int. Symposium, Sandefjord, Norway, pp. 1027-1040.

Bloom, R., Bentur, A. (1995): *"Free and restrained shrinkage of normal and high-strength concrete"*, ACI Material Journal, 92, pp. 211-217.

Bosnjak, D. (2001): *"Self-induced Cracking Problems in Hardening Concrete Structures"*, Doctoral thesis, NTNU, Dept. of Structural Eng., ISBN 82-7984-151-2.

Bosnjak, D. and Kanstad, T. (1997): *"Analysis of Hardening High Performance Concrete Structures"*, Finite Elements in Engineering ad Science, edited by Hendriks, Jonedijk, Rots and van Spanje, Published by Balkema, Rotterdam, ISBN 90 5410 8835, pp 45-54.

Breitenbucher, R. (1989): "*Zwangsspannungen und Ri⇓bildung infolge Hydratationsv™rme",* Dissertation, TU Munchen, 206 pp.

Brooks, J.J., and Neville, A.M., (1977): "*A Comparison of Creep, Elasticity and Strength of Concrete in Tension and in Compression*", Magazine of Concrete Research, V.29, No. 100, pp. 131-141.

Brooks, J. J., Wainwright, P. J. and Al-Kaisi, A. F., (1991): "*Compressive and Tensile Creep of Heat-cured Ordinary Portland and Slag Cement Concretes*", Magazine of Concrete Research, V. 43, pp. 1-12.

Buil, M. and Acker (1985): *"Creep of Silica Fume of Concrete*". Cement and Concrete Research, 18, No. 5, pp. 463-7.

Byfors, J., (1980): "*plain concrete at early ages"*. Swedish Cement and Concrete Institute. Fo 3:80, Stockholm.

CEB Design Manual (1984): *"Structural effects of time-dependent behaviour of concrete"*, CEB Bulletin D'information No. 142.

CEB-FIB (1990): *"High Strength Concrete - State-of-the-Art report",* CEB Bulletin D'information No. 197, 61 pp.

CEB-FIP (1970): "*International Recommendations for the Design and Construction of Concrete Structures - Principles and Recommendations",* Comité Euro-International - Federation Internationale de la Précontrainte, London, 80 pp.

CEB-FIP Model Code 1990 (1993): "*Comité Euro-International du Beton"*, Bulletin D'information No. 213/214, Tomas Telford, London, 473 pp.

Cook, D. J., (1972): "*Some Aspects of the Mechanism of Tensile Creep in Concrete*", ACI Journal, Proc., V.69, No. 10, pp. 645-649.

Dahlblom, O., (1992): *"HACON-S-A Program for Simulation of Stress in Hardening Concrete*", Vattenfall Hydro Poer Genetion, Vällingby, 77 pp.

Davies, R.E., Davies, H.E., and BHamilton, J.S. (1934): *"Plastic flow of concrete under sustained stress*", ASTM Proc. 34, Part 2, 1934, pp 354-386.

de Borst, R. and van den Boogard, A. H., (1994): "*Finite element modelling of deformation and cracking in early-age concrete"*, Journal of Structural Engineering, ASCE.

De Schutter, G. (2001): *"Modelling of Early Age Thermal Cracking in Hardening Concrete, Including and softening Behaviour*". RILIM International Conference on Early Age Cracking in Cementitious Systems (EAC'01), Haifa, pp. 31-38.

De Schutter, G. and Taerwe, L., (1996): "*Degree of hydration-based description of mechanical properties of early age concrete"*, Materials and Structures, 29, pp. 335-344.

De Schutter, G. and Taerwe, L., (1997): *"Towards a more fundamental non-linear basic creep model for early age concrete"*, Magazine of Concrete Research, 49 (180), pp. 195-200.

Digler, W. H. (1982): "*Methods of Structural Creep analysis"*, in 'Creep and Shrinkage in Concrete Structures', (edited by Bažant, Z. P. and Wittman, F.H.) Wiley & Sons, New York, pp. 305-339.

Emborg M., (1989): "*Thermal Stresses in Concrete Structures at Early Ages"*, Doctoral thesis, Lulea Univ. of Technology, Division of Structural Engineering, 280 pp, (Referred by Bjøntegaard, O., (1999)).

Emborg, M. and Bernander, S. (1994): *"Avoidance of Early age thermal Cracking in Concrete Structures - Predesign, Measures, Follow-up*"; in 'Thermal Cracking in Concrete at Early

Ages', Proc. of the RILEM International Symposium, Edited by R. Springenschmid, E & FN Spon, London, pp. 409-416.

Emborg, M., (1998): *"Development of mechanical behaviour at early ages"*, in 'Prevention of Thermal Cracking in Concrete at Early Ages', R. Springenschmid, editor, E&FN SPON, pp. 77-148.

England, G. L., and Illston, J. M. (1965): *"Methods of Computing Stress in Concrete From a History of Measured Strain"*, Civil Engineering, London.

Eurocode 2 (1991): *"Design of Concrete Structures – Part 1-1, General Rules and Rules for Buildings"*, ENV 1992-1-1:1991.

fib Bulletin N^{o} 1, (1999): *"Structural Concrete, Textbook on Behaviour, Design and Performance, Updated Knowledge of the CEB/FIP Model Code 1990"*, Manual - Vol. 1.

fip-Report (1998): *"Condenced Silica Fume in Concrete"*, Stat-of-the-Art by Telford, T., FIP Commission on Concrete, London, 37 pp.

Geymayer, H. G., (1972): *"Effect of Temperature on Creep of Concrete; A Literature Review"* Concrete for Nuclear Reactors, Vol. I, ACI Special Publication SP-34, American Concrete Institute, Detroit, pp 565-589.

Glanville, W. H., (1933): *"Creep of Concrete Under Load"*, The Structural Engineer, 11, No. 2, pp. 54-73.

Gutsch, A. (2001): *"Properties of Early Age Concrete - Experiments and Modelling*". RILIM International Conference on 'Early Age Cracking in Cementitious Systems' (EAC'01), Haifa, pp. 11-18.

Gutsch, A., (1998): *"Stoffeugenschaften Jungen Beton – Versuche und Modelle"*, Doctoral Thesis, TU Braunschweig.

Gutsch, A., Rostásy, F. S., (1994): *"Young Concrete Under High Tensile Stresses - Creep, Relaxation and Cracking*", Thermal Cracking in Concrete at Early Ages, Proc. of the RILEM International Symposium, Edited by R. Springenschmid, E & FN Spon, London, pp. 111-118.

Hagihara, S., Masuda, Y. and Nakamura, S. (2002): *"Creep Behaviour of High-Strength Concrete in Early Age"*, 6th International Symposium on High Strength/High Performance Concrete.

Hansen, P. L., (1956): "*Physical Properties of Concrete at Early Ages*". School of Mines and Metallurgy of the University of Missouri, 140 pp.

Hansen, T. C. (1960): "*Creep and Stress Relaxation of Concrete* ". Proc. No. 31, Swedish Cement and Concrete Research Institute, Stockholm, pp. 112.

Hansen, T. C. and Mttock A. H. (1966): "*The Influence of Size and Shape of Member on The Shrinkage and Creep of Concrete*". Journal of American Concrete Institute, 63, pp. 267-90.

Hansen, W. (2002): "*Early Age Creep and Stress Relaxation Tests"*, Chapter 6.6 in the State-of-the-art RILEM-publication: Early age shrinkage and cracking of cementitious systems, Ed. by Bentur, A..

Hansen, W. and Almudaiheem, J. A. (1960): *"Ultimate drying shrinkage of concrete – Influence of major parameters"*.

Hauggaard-Nielsen, A. B., Damkilde, L., Hansen, P. F., Hansen, H. J., Nielsen, A., Christensen, S. L., (1997b): "*Control of Early Age Cracking in Concrete",* HETEK Report No. 111, The Danish Road Directorate, Denmark.

Hauggaard-Nielsen, A. B., Damkilde, L., Hansen, P. F., Pedersen, E. S., Nielsen, A., (1997c): "*Material Modelling - Continuum Approach",* HETEK Report No. 113, The Danish Road Directorate, Denmark.

Hauggaard-Nielsen, A.B.*,* (1997a): *"Mathematical Modelling and Experimental Analysis of Early Age Concrete",* Doctoral Thesis, Technical University of Denmark, Series R, No. 34.

Hauggaard-Nielsen, A.B., Berrig, A., Fredriksen, J. O., (1993): "*Curing Technology - A 2 Dimensional Simulation Program",* Proc. from the Nordic Concrete Research Meeting, Gotheburg, The Nordic Concr. Fed., Oslo, pp. 222-224.

Hedlund, H. (1996): "*Stresses in High Performance Concrete due to Temperature and Moisture Variations at Early Age",* Licentiate thesis, Division of Structural Engineering, Luleå University of Technology, Sweden.

Heimdal E., Kanstad T. and Kompen R. (1998): *"Maridal Culvert"*. IPACS Report, Task 5 - Field tests.

Hellman (1969): *"Beziehungen Zwischen Zug- und Druckfestigkeit des Betons."*, Beton, No. 2, pp. 68-70 (quoted from Byfors 1980).

Hilsdorf, H. K. and Müller, H. (1999): *"Material",* Chapter 3 in ***fib*** Bulletin N^{o} 1 [ref. 46], Vol. 1, pp. 21-35.

Igarashi, S. I. and Kawamura, M. (2002): "*Effect of microstructure on Restrained Autogenous Shrinkage behaviour in High Strength Concrete at Early Ages*". Materials and Structures, Vol. 35, March, pp. 80-84.

Igarashi, S. I., Bentur, A. and Kovler, K. (1999): "*Stress and Creep Relaxation Induced in Restrained Autogenous Shrinkage of High-Strength Pastes and Concretes* ". Advances in Cement Research, 11, No. 4, Oct., pp. 169-177.

Igarashi, S. I., Bentur, A. and Kovler, K., (2000): "*Autogenous shrinkage and induced restraining stresses in high-strength concretes*". Cement and Concrete Research 30. pp. 1701-7.

Illston, J. M, (1965): "*The Creep of Concrete under Uniaxial Tension*", Magazine of Concrete Research, V.17, No. 51, pp. 77-84.

Illston, J.M. and sanders, P. D., (1973): "*The effect of temperature change upon the creep of mortar under torsional loading*", Magazine of Concrete Research, V. 25, No. 84, pp. 136-44.

Jonasson, J. E., (1985): "*Early Strength Growth in Concrete – Preliminary Test Results Concerning Hardening at Elevated Temperatures"*, International Symposium on Winter Concreting (RILEM)), Espoo, Technical Research Center of Finland (VTT), pp. 249-254, (quoted from Emborg (1998)).

Jonasson, J. E., (1994a): "*Modelling of Temperature Moisture and Stresses in Young Concrete*", Doctoral thesis, Division of Structural Engineering, Luleå University of Technology, Sweden, 1994:153D, 225 pp.

Jonasson, J.P., Groth, P. and Hellund, H., (1994b): *"Modelling of temperature and moisture field in concrete to study early age movements as a basis of stress analysis",* in 'Thermal Cracking in Concrete at Early Ages', Proc. of the RILEM International Symposium, Edited by R. Springenschmid, E & FN Spon, London, pp. 45-52.

Jones, P.G., and Richart, F.E. (1936): *"The effect of testing speed on strength and elastic properties of concrete*", ASTM Proc. 36, part 2, pp 380-391.

Kanstad T., Bjøntegaard Ø., Sellevold E.J., Hammer T.A. and Fidjestøl P. (2001): *"Effects of Silica Fume on Crack Sensitivity*", Concrete International, vol. 23, 12, pp. 53-59.

Kanstad T., Hammer T.A., Bjøntegaard Ø. and Sellevold E.J. (2002a): *"Mechanical Properties of Young Concrete: Part I - Experimental Results related to Test Methods and Temperature Effects"*, Accepted for publication in Materials and Structures.

Kanstad T., Hammer T.A., Bjøntegaard Ø. and Sellevold E.J. (2002b): *"Mechanical Properties of Young Concrete: Part II - Determination of Model Parameters and Test Programme Proposals"*, Accepted for publication in Materials and Structures.

Kanstad T., Hammer, T. A., Bjøntegård, Ø. and Sellevold, E. J. (1999): *"Mechanical properties of young concrete: Evaluation of test methods for tensile strength and modulus of elasticity. Determination of model parameters*", NOR-IPACS report STF22 A99762. ISBN

82-14-01062-4.

Kanstad, K., Bjøntegaard, O., Sellevold, E.J., Hammer, T.A. and Fidjestol, P., (2000): *"Effect of silica fume on early age cracking sensitivity of high performance concrete*", in 'Shrinkage of Concrete – Shrinkage 2000', V.Baroghel-Bouny and P.-C.Aitcin, editors, Paris, (RILEM PRO 17 2000) 101-114.

Kanstad, T. (1990): *"Nonlinear Analysis Considering Time-dependent Deformation and Capacity of Reinforced and Prestressed Concrete"*, Doctoral thesis, NTH, Trondheim, Norway.

Kanstad, T., Bjøntegaard, Ø., Sellevold. E. J., Hammer, T.A., Figjestøl, P. (1995): *"Effects of silica fume on crack sensitivity"*. Concrete International. Vol. 23. No. 12. pp. 53-9.

Kanstad, T., de Borst, d., van den Boogaard, A.H. (1994): *"Early Age Behaviour of Concrete and Reinforced Concrete Structures"*, In Bell, K., editor, NSCM VII, Seventh Nordic Seminar on Computational Mechanics, Department of Structural Engineering, Norwegian Institute of Technology, Trondheim, Norway.

Kasai, Y. (1961): "*Initial Strength of Concrete*". Japan Cement Engineering Association, 15th General meeting, pp. 188-189.

Kasai, Y., Yokoyama, K. and Matsui, I. (1971): *"Tensile Properties of Early Age Concrete",* Proc. of the International Conference on 'Mechanical Behaviour of Materials', Vol. IV, pp. 288-299.

Kasai, Y., Yokoyama, K., Matsui, I., and Tobinai, K., (1974): "*Tensile properties of early age concrete*", in 'Mechanical Behaviour of Materials', The Society of Materials Science, Japan, 2**,** pp. 433-441.

Khan, A. A., Cok, W. D., and Mittchell, D., (1996): "*Tensile strength of low medium and high-strength concretes at early ages"*, ACI Materials Journal 93 (5), pp. 487-493.

Khoury, G. A., Grainger, B. N. and Sullivan, P. J. (1985): *"Transient Thermal Strain of Concrete: Literature Review, Condition Within Specimen and Behaviour of Individual Constituents"*, Magazine of Concrete Research, 37 (123), (quoted from Bosnjak 2000).

Kovler, K., Igarashi, S. and Bentur, A., (1999): *"Tensile creep behaviour of high strength concretes at early ages"*, Materials and Structures, 32, pp. 383-387.

Krauss M., Hariri K. and Rostasy F. (2001): *"Non-Destructive Assessment of Mechanical Properties of Concrete at Very Early Age"* by US Techniques - Methods, Results and Modelling, IPACS-report BE96-3843/2001:12-5.

Lange, D. A. and Altoubat, S., (2002): "*Early Age Concrete"*, Chapter 3.7 in the State-of-the-art RILEM-publication: 'Early age shrinkage and cracking of cementitious systems', Ed. by Bentur, A., to be published in 2002.

LaPlante, P., and Boulay C. (1994): "*Evolution du coefficient de dilation thermique du beton en fonction de sa maturite aux tout premiers ages"*, *Materials and Structures* 2 (1994) 596-605 (in French).

Laube, M. (1990): *"Werkstoffmodel zur Berechnung von Temparaturspanungen in Massigen Betonbauteilen im jungen Alter",* Doctoral Thesis, Universität Braunschweig, [quoted from Emborg (1998)].

Lindgaard, J., Sellevold, E. J., (1993): "*Is High-Strength Concrete more Robust against Elevated Curing Temperature*', in Proc. of the third International Symposium on Utilization of High Strength Concrete, Lillehammer, Norway, June20-23, Vol. 2, pp. 810-821.

Løfquist, B (1946): *"Temperatureffekter i hårdnande betong" (Temperatur effects in hardening concrete)*", In Swedish, dissertation, Kungliga Vattenfallsstyrelsen, Teknisk meddelande No 22, Stockholm 1946, 195 pp.

Lorman, W. R., (1973): "*The theory of concrete creep*", Proc. ASTM, 40, pp. 1082-1102, (from Neville 1983).

Lura, P., Van Breugel, K., Maruyama, I., (2000): *"Effect of Curing Temperature and Type of Cement on Early-Age Shrinkage of High Performance Concrete"*, Submitted to Cement Concrete Research Special issue, Proc. of Symposium 'Materials Science of High Performance Concrete', Boston.

Maatjes, E., Schillings, J. M. and de Jong, R. (1994): "*Experience in Controlled Concrete Behaviour*"; in 'Thermal Cracking in Concrete at Early Ages', Proc. of the RILEM International Symposium, Edited by R. Springenschmid, E & FN Spon, London, pp. 247-254.

Mangold, M., (1998): *"Methods for Experimental Determination of Thermal Stresses and Crack Sensitivity in the Laboratory"*, in 'Prevention of Thermal Cracking in Concrete at Early Ages', R. Springenschmid, editor, E&FN SPON, pp. 26-36.

Marchal, J.C. (1972): *"Variation in the Modulus of Elasticity and Poisson's Ratio with Temperature",* Concrete for Nuclear Reactors, Vol. I, ACI Special Publication SP-34, American Concrete Institute, Detroit, pp 495-503

Maslov, G. N. (1940): *"Thermal Stress State in Concrete Mass With Account to Creep of Concrete"*, Izvestia Nauchno-Issledovatelskogo Instituta VNII Gidrotekhniki, Gosenergoizdat, USSR, 28, pp. 175-88, (quoted from Neville 1983).

Matsui, K., Nishida., N., Dobashi., Y. and Ushioda., K. (1994): "S*ensitivity Analysis and Reliability Evaluation of Thermal Cracking in Mass Concrete*"; in 'Thermal Cracking in Concrete at Early Ages', Proc. of the RILEM International Symposium, Edited by R. Springenschmid, E & FN Spon, London, pp. 305-312.

McHenry, D. (1943): *"A New Aspect of Creep in Concrete and its Application to Design"*. Proc. ASTM., 43, pp. 1069-84.

Miao, B., Chaallal, O., Perraton, D., and Aitcin, P. C., (1993): "*On-site early age monitoring of high performance concrete columns*", ACI Materials Journal, No. 90, 415-420.

Mitchell, D., Khan, A. A., and Cook, W. D., (1998): "*Early age properties for thermal and stress analyses during hydration*", In Material Science of Concrete V, Jan Skalny and Sidney Mindess, editors, The American Ceramic Society, pp. 265-305.

Morimoto H., Koyangi W. (1994): *"Estimation of stress relaxation in concrete at early ages"*, Proceeding of the RILEM International Symposium on 'Thermal Cracking in Concrete at Early Ages', edited by R. Springenschmid E & FN Spon, London, pp. 95-120.

Müller, H. S. and Rübner, K. (1996): *"Creep of High-Performance Concrete - Characteristics and Code-Type Prediction Model"*. 4th International Symposium on 'Utilization of High-Performance Concrete', Paris, pp. 377-385.

Müller, H.S. and Rübner, K. (1995): *"High Strength Concrete - Microstructural Characteristics and Related Durability Aspects. Durability of High-Performance Concrete"*. Ed. H. Sommer, RILEM, Cachan, France, pp. 23-37.

Nagy, A. and Thelandersson, S. (1994): "*Material Characterization of Young Concrete to Predict Thermal Stresses*"; in 'Thermal Cracking in Concrete at Early Ages', Proc. of the RILEM International Symposium, Edited by R. Springenschmid, E & FN Spon, London, pp. 161-169.

Neville, A. M. (1996): *"Properties of concrete"*, 4rd edition, John Wiley & Sons, Inc. New York, USA.

Neville, A. M., Dilger, W. H., Brooks, J.J., (1983): "*Creep of Plan and Structural Concrete",* Construction Press, Logman Group Limited, London and New York.

Neville, A. M., Stautun, M. M. and Bonn, G. M. (1966): *"A Study of The Relation Between Creep and The Gain of Strength of Concrete*". Symposium on Structure of Portland Cement Past and Concrete, Highw. Res. Bd, Special Report No. 90, pp. 186-203.

Onken, P. and Rostásy, F. S. (1994): "*A Practical Planning Tool for the Simulation of Thermal Stresses and for the Prediction of Early Thermal Cracks In Massive Concrete Structures*"; Thermal Cracking in Concrete at Early Ages, Proc. of the RILEM International Symposium, Edited by R. Springenschmid, E & FN Spon, London, pp. 289-296.

Onken, P., Rostasy, F., (1995): "*Wirsame Betongzugfestighur im Bauwerk bei fruh einsetzendem Temperaturzwang"*. Deulscher Auschuss fur stuklbeton, Heft 449, Berlin.

Østergaard, L., Lange, D.A., Altoubat, S.A., Stang, H., (2001): *"Tensile Basic Creep of Early-age Concrete Under Constant Load*". Cement and Concrete Research, 31, pp. 1895-99.

Paillèere, A.M., et Serrano, J.J., (1976): "*Appareil d'étude de la fissuration du béton",* Bull. Liaison Labo. P. et Ch., 83, mai-juni, pp. 29-38.

Paillère, M., Buil, M., Serrano, J. J. (1989): *"Effect of Fiber Addition on the Autogenous Shrinkage of Silica Fume Concrete"*. ACI Materials Journal, V. 86, No. 2, pp. 139-144.

Pane, I. and Hansen, W. (2001): *"Early Age Creep and Stress Relaxation of Concrete Containing Blended Cements*". RILIM International Conference on 'Early Age Cracking in Cementitious Systems' (EAC'01), Haifa, pp. 279-290.

Pane, I. and Hansen, W. (2002): "*Early Age Creep and Stress Relaxation of Concrete Containing Blended cement",* Material and Structures, 35, pp. 92-96.

Pane, I., and Hansen, W., (2001): "*Early age tensile creep and stress relaxation in Portland cement concrete – effects of cement replacement with mineral additives*", in Proc. of the 6th International RILEM Conference on 'Creep, Shrinkage & Durability Mechanics of Concrete and other Quasi-Brittle Materials' (Concreep6), Cambridge, USA, Aug. 2001, (Elsevier Science Ltd., Oxford 2001), pp. 605-611.

Parrott, L. (1978): *"Effect of loading at early age upon creep and relaxation of concrete*". RILEM Committee 42-CEA, International report, UK5.

Paulini, P. and Bilewicz, D. (1994): "*Temperature Field and Concrete Stresses in a Foundation Plate*"; in 'Thermal Cracking in Concrete at Early Ages', Proc. of the RILEM International Symposium, Edited by R. Springenschmid, E & FN Spon, London, pp. 227-344.

Pedersen, E. S. (1994): "*Prediction of Temperature and Stress Development in Concrete Structures*"; Thermal Cracking in Concrete at Early Ages, Proc. of the RILEM International Symposium, Edited by R. Springenschmid, E & FN Spon, London, pp. 297-304.

Pedersen, F-H (1997): "*Måleinstrument til Kontroll av Betons Herding"*, Nordisk Betong, No. 1, Stockholm, pp. 21-25.

Persson, B. (1997): "*Self-desiccation and its Importance in Concrete Technology",* Material and Structures, 30, No. 199, pp. 293-305.

Pigeon, M. and Bissonnette, B. (1999): "*Tensile Creep & Cracking Potential",* Concrete International, November 1999, pp. 31-35.

Plank, A. (1971): "*Ube das verformungsverhalten jungen Zement-mortels bei Druckbeansprunchung*". Betonstein-Zeitung, 37:12, pp. 741-751.

Polivka, M., Pirtz, D. and Adams, R. F. (1964): *"Studies f Creep in Mass Concrete",* Symposium on 'Mass Concrete', ACI, Special Publication, NO. 6, pp 257-83.

Roelfstra, P. E., Salet , T. M., Kuiks, J. E. (1994): *"Defining and application of Stress-Analysis-Based Temperature Difference Limits to Prevent Early-Age Cracking in Concrete Structures*"; Thermal Cracking in Concrete at Early Ages, Proc. of the RILEM International Symposium, Edited by R. Springenschmid, E & FN Spon, London, pp. 273-280.

Ross, A. D. (1958): *"Concrete of Concrete Under Variable Stress",* ACI Journal, 55, pp 739-57.

Rostásy, F. S., Gutsch, A. and Laube, M. (1993): *"Creep and relaxation of concrete at early ages – experiments and mathematical modelling*", in 'Creep and shrinkage of concrete*', Z.* Bazant and C. Carol, E&FN Spon, London, pp. 453-458.

Samadi, M.M., Slate, F.O. and Nison, A.H. (1987): *"Shrinkage and Creep of High-, Medium- and Low-Strength Concrete, Including Overloads"*. ACI Material Journal, May-June, pp 224-234.

Schöppel, K., Springenschmid, R. (1994): "*The effect of thermal deformation, chemical shrinkage and swelling on restraint stresses in concrete at early ages*". Ingenierburo, Munich, Germany. Thermal Cracking in concrete at Early ages. R. Springenschmid.

Schrage, I. (1994): "Versuche über das Kriechen Hochfesten Betons", Abschluβbericht zum Forschungsvorhaben AIF-Nr. 8798, DBV-Nr. 148, Technical University of Munich (quoted from Müller and Rübner 1995).

Schrage, I. And Summer, Th. (1994): "*Factors Influencing Early Cracking of High Strength Concrete"*, in 'Thermal Cracking in Concrete at Early Ages', R. Springenschmid, editor, RILEM proceeding 25, Munich, 237-244.

Sellevold, E. J., Bjøntegaard, O. Justins, H. and Dahl, P. A., (1994): *"High performance concrete: early volume change and cracking tendency",* Proceeding on 'Thermal Cracking in

Concrete at Early Ages', R. Springenschmid, editor, E&FN SPON, pp. 229-236.

Sellevold. E. J. (1969): "*Inelastic Behaviour of Hardened Portland Cement Past*". Department of Civil Engineering, Stanford University, Doctoral Thesis, Technical Report No. 113.

Sellevold. E. J., Bager, D. H., Klitgaard, J. E., Kundsen, T., (1982): "*Silica fume cement pastes: Hydration and pore structure*". Report BML 82.610, The Norwegian Institute of Technology, Trondheim, Norway.

Šerda, Z. and Křístek, V. (1988): *"Creep and Shrinkage of Concrete Elements and Structures*". Developments in Civil Engineering, 21, Czechoslovakia.

Shkoukani H., and Walraven, J.C. (1993): *"Creep and relaxation of concrete subjected to imposed thermal deformations*", in 'Creep and Shrinkage of Concrete', Proc. of the 5th International RILEM Symposium, Barcelona, E.& FN Spon, London.

Skudra, A. M. (1956): *"Résistance á longterme du béton á la traction*". Academy of Sciences of Latvian, SSR, Riga.

Smadi, M. M. and Slate, F. O., (1989): *"Microcracking of high and normal strength concretes under short- and long- term loading"*. ACI Material Journal, 86, No. 2, pp. 117-27.

Springenschmid, R., editor (1994): *"Thermal Cracking in concrete at Early ages"*, Proceeding of the International RILEM Symposium.

Springenschmid, R., Gierlinger, E., Kiernozycki, W. (1985): "*Thermal Stress in Mass Concrete: A New Testing Method and the Influence of Different Cements*", 5th Int. Conf., Larg Dams (ICOLD), Lausanne Q. 57-R. 4, pp. 57-72.

Springenschmid, R., Nicher, P. (1973): "*Untersuchungen ⁄ber die Ursache von Querrissen im jungen Beton",* Beton- und Stahlbetonbau, 68, pp. 221-226.

Takács, P. F., (2002): *"Deformations in Concrete Cantilever Bridges: Observations and Theoretical Modelling"*, Doctoral thesis, NTNU, Dept. of Structural Eng., ISBN 82-471-5415-3.

Tazawa E., Matsuoka Y, Miyazawa S., Okamoto S., (1994): "*Effect of autogenous shrinkage on self stress in hardening concrete"*, in 'Thermal Cracking in Concrete at Early Ages', R. Springenschmid, editor, RILEM proceeding 25, Munich, 221-228.

Tazawa, E., Miyazawa, S. (1995): "*Influence of Cement and admixture on Autogenous Shrinkage of Cement Paste*", Cement and Concrete Research, 25, No. 2, pp. 281-287.

Tazawa, E., Miyazawa, S. (1997): "*Influence of consistent and composition on autogenous shrinkage of cementitious materials*". Magazine of Concrete Research. 49. No. 178. Pp. 15-22.

Thelanderson, S. (1987): *"Modelling of Combined Thermal and Mechanical Action in Concrete"*, Journal of Engineering Mechanics, 113 (6), (quoted from Bosnjak 2000).

Theuer, A. U., (1937): "*Effect of Temperature on the Stress Deformation of Concrete"*, Journal of Research, National Bureau of Standards: Washington, DC, 18, No. 2, pp. 195-204.

Tomaszwicz, A., (1988): "*High Strength Concrete Subjected to Long-Term, Sustained Loads",* SINTEF Report 1.4, Norway.

Torrenti, J. M., Larrard, F., Guerrier, F., Acker, P. and Grenier, G. (1994): *"Numerical Simulation of Temperature and Stresses in Concrete at Early Ages - The French Experience"*; in 'Thermal Cracking in Concrete at Early Ages', Proc. of the RILEM International Symposium, Edited by R. Springenschmid, E & FN Spon, London, pp. 281-288.

Umehara, H., Uehara, T, Iisaka, T and Sugiyama, A. (1994): "*Effect of Creep in Concrete at Early Age on Thermal Stresses*", Thermal Cracking in Concrete at Early Ages, Proc. of the RILEM International Symposium, Edited by R. Springenschmid, E & FN Spon, London, pp. 79-86.

van Breugel, K. (1991): *"Simulation of Hydration and Formation of Structure in Hardening Cement-based Material*". PhD Thesis, Technical University of Delft, 295 pp.

van Breugel, K. (1992): *"Numerical Simulation of Hydration and Microstructural development in Hardening Cement-Based Material*". HERON, 37(2).

van Breugel, K. (1995): *"Numerical Simulation of the Effect of Curing Temperature on the Maximum Strength of Cement-based Material*", in 'Thermal Cracking in Concrete at Early ages', Proc. Of the RILEM International Symposium, Edited by R. Springenschmid, E & FN Spon, London, pp. 127-134.

van Breugel, K. and Lokhorst, S. J. (2001): *"The Role of Microstructural Development on Creep and Relaxation on Hardening Concrete*". RILIM International Conference on Early Age Cracking in Cementitious Systems (EAC'01), Haifa, pp. 3-10.

van Breugel, K., Ouwerkerk, H. and de Vries, J., (2000): "*Effect of mixture composition and size effect on shrinkage of high strength concrete*", in 'Shrinkage of Concrete –Shrinkage 2000', V.Baroghel-Bouny and P.-C.Aitcin, editors, RILEM Publications PRO 17, 161-178.

Visschedijk, M. (1995): *"Creep in Aging Concrete"*, TNO.

Wallo, E. M., Yuan, R. L., ott, J. L. and Kesler, C. E. (1965): "*Prediction of Creep in Structural Concrete From Short-term Tests*". Six progress report, T. and A. M. Report, No. 658, University of Illinois, pp 26.

Walraven, J.C., and Shen J-H. (1993): *"Non-linear creep: A general constitutive model",* in 'Creep and Shrinkage of Concrete', Proc. of the 5th International RILEM Symposium, Barcelona, E.& FN Spon, London.

Ward, M.A, and Cook, D.J., (1969): "*The Mechanism of Tensile Creep in Concrete*", Magazine of Concrete Research, V.21, No. 68, pp. 151-158.

Weiss, W. J. and Shah, S. P. (2002): "*Restrained Shrinkage Cracking: The Role of The Shrinkage Reducing Admixtures and Specimen Geometry*", Material and Structures, V. 35, pp. 85-91.

Westman. G., (1999): "*Concrete Creep and Thermal Stresses",* Doctoral Thesis, Luleå University of Technology, Sweden. 1999:10.

Wittmann F. and Lukas J. (1974): *"Experimental study of thermal expansion of hardened cement paste"*, Materials and Structures No. 40, 247-252.

Zhutovsky, S., Kovler, K. and Bentur, A. (2002): "*Efficiency of Lightweight Aggregates for Internal Curing of High Strength Concrete to Eliminate Autogenous Shrinkage*". Materials and Structures, Vol. 35, pp. 97-101.

APPENDIX A

Test Series on Tensile- and Compressive Creep on Concrete Under Different Conditions

Four test series on creep are performed on early age concrete, where the influence of different factors on creep is studied. Within each series, each single test is repeated at least once. For each test the compressive strength at loading age is determined on three 100 mm concrete cubes. All the tests are listed in tables in this Appendix. The letter T and C characterize whether the test is carried out in tension or in compression.

Factors, which are studied, are:

Series I: Loading age
Series II: Loading level
Series III: Silica fume content
Series IV: Temperature

SERIES I-A:

Table 1 Parallel creep tests in tension (T) and compression (C) at ***different loading ages***, load level 50% of the initial strength, temperature 20.5 ± 1 ^{o}C, on concrete BASE-5.

Test No.	Concrete Casting				Concrete Age [days]	Test Type		Compressive Strength [MPa]
	Date	Slump [cm]	Air [%]	Density [kg]		T	C	
101	17.12.99	14.5	1.8	2462	3	x	x	55.5
102	24.01.00	-	-	-	2	x	x	52.2
103	07.02.00	-	-	-	3	x	x	54.7
104	23.02.00	18.5	4.3	2378	1	x	x	23.4
105	03.04.00	18.0	2.1	2458	1	x	x	24.0
106	10.04.00	14.0	1.6	2444	4	x	x	58.5
107	16.05.00	16.0	1.9	2454	3	x	x	54.1
108					8	x	x	69.7
109	25.05.00	16.5	2.3	2413	4	x	-	-
110	06.06.00	19.5	-	-	2	x	-	41.6
111	12.09.00	18.5	2.0	2396	2	x	x	38.6
112					8	x	x	61.8
SUM:		**16.9**	**2.3 %**	**2429**				

SERIES I-B:

Table 2 Parallel creep tests in tension (T) and compression (C) at ***different loading ages***, load level 50% of the initial strength, temperature 20 ± 1 °C, on concrete BASE-5.

Test No.	Concrete Casting				Concrete Age [days]	Test Type		Compressive Strength [MPa]
	Date	Slump [cm]	Air [%]	Density [kg]		T	C	
501	19.03.01	13.0	2.1	2455	1	x	x	25.9
502	03.04.01	17.5	2.3	2447	2	x	x	39.9
503	17.04.01	16.0	2.3	2447	3	x	x	48.8
504	23.04.01	14.0	2.2	2428	4	x	x	47.6
505	02.05.01	18.0	2.4	2432	6	x	x	52.6
506	14.05.01	17.0	2.3	2450	2	x	-	36.6
507	22.05.01	16.0	2.5	2440	1	x	-	23.0
508	29.05.01	13.0	2.0	2441	3	x	-	46.5
509	06.06.01	19.0	1.8	2439	6	x	-	-
510	15.06.01	18.0	1.9	2450	4	x	-	50.9
SUM:		**16.2**	**2.2%**	**2443**				

SERIES I-C:

Table 3 Parallel creep tests in tension (T) and compression (C) at ***different loading ages***, load level 50% of the initial strength, temperature 20.5 ± 1 °C, on concrete Maridal Concrete.

Test No.	Concrete Casting				Concrete Age [days]	Test Type		Compressive Strength [MPa]
	Date	Slump [cm]	Air [%]	Density [kg]		T	C	
301	14.03.00	18.5	4.3	2378	2	x	x	36.9
302					3	-	x	45.4
303					6	x	x	57.2

SERIES II-A:

Table 4 Parallel creep tests in tension (T) and compression (C) at loading age of 3 days with ***different loading level*** and temperature 20.5 ± 1 °C, on concrete BASE-5.

Test No.	Concrete casting				Load level [%]	Test type		Compressive Strength [MPa]
	Date	Slump [cm]	Air [%]	Density [kg]		T	C	
201	30.05.00	16.0	2.4	2410	30	x	x	47.6
202	26.06.00	15.0	-	-	30	x	-	51.9
203	04.07.00	9.0	-	-	40	x	-	53.2
204	10.07.00	16.0	-	-	60	x	-	50.8
205	17.07.00	11.0	-	-	70	x	-	49.5
206	24.07.00	11.0	-	-	80	x	-	48.9
207	14.08.00	18.0	2.0	2427	30	x	x	46.1
208	21.08.00	15.0	-	-	70	x	x	53.7
209	04.09.00	14.0	2.3	-	30	x	x	*45.7*
SUM:		**13.9**	**2.2 %**	**1418**				

SERIES II-B:

Table 5 Tensile creep tests (T) at loading age of 3 days with ***different loading level*** and temperature 20.5 ± 1 °C on concrete BASE-5.

Test No.	Concrete Casting				Load Level [%]	Compressive Strength [MPa]
	Date	Slump [cm]	Air [%]	Density [kg]		
200	22.06.01	15.5	2.4	2427	20	45.2
201	26.06.01	17.0	1.9	2443	40	47.1
202	29.06.01	18.5	1.9	2434	50	46.5

203	03.07.01	17.5	2.0	2455	60	46.8
204	06.07.01	18.5	-	-	70	47.7
205	10.07.01	19.5	-	-	73	43.9
206	13.07.01	17.5	2.0	-	60	47.3
SUM:		**17.1**	**2.1 %**	**2440**		

SERIES II-C:

Table 6 Tensile creep tests (T) at loading age of 3 days with ***different loading level*** and temperature 20.5 ± 1 ^{o}C on concrete BASE-5.

Test No.	Concrete Casting				Load Level [%]	Compressive Strength [MPa]
	Date	Slump [cm]	Air [%]	Density [kg]		
400	04.09.01	17.5	2.3	2424	30	48.2
401	07.09.01	15.0	2.7	2433	70	48.3
402	11.09.01	15.0	2.7	2444	60	50.5
403	14.09.01	18.0	2.4	2426	50	48.3
404	18.09.01	17.0	2.3	2423	40	47.1
405	21.09.01	16.5	2.3	2432	20	48.2
406	25.09.01	19.0	2.3	2417	80	46.2
407	28.09.01	20.0	1.8	2447	40	48.4
408	02.10.01	16.0	2.0	2424	40	45.3
409	09.10.01	18.0	1.8	2450	80	47.8
410	12.10.01	17.5	1.6	2475	50	47.8
411	16.11.01	16.5	1.8	2439	80	-
412	23.11.01	18.5	1.9	2440	20	46.5
413	30.11.01	18.0	2.1	2430	30	49.1
SUM:		**17.3**	**2.1%**	**2435**		**47.8**

SERIES III:

Table 7 Tensile creep tests (T) on concretes with ***different silica fume contains*** at loading ages 1 and 4 days. Load level 40% of the initial strength and temperature 20.5 ± 1 °C.

Concrete Mix	Test No.	Concrete Casting				Concrete Age [days]	Compressive Strength [MPa]
		Date	Slump [cm]	Air [%]	Density [kg]		
BASIC-0	1001	17.12.01	19.5	1.8	2451	1	23.2
	1002					4	59.7
	1003	07.01.02	19.5	2.2	2423	1	14.4
	1004					4	45.6
BASIC-10	1001	14.01.02	18.3	2.3	2430	1	18.8
	1002					4	43.0
	1003	21.01.02	17.5	2.4	2408	1	16.4
	1004					4	47.8
BASIC-15	1001	28.01.02	19.0	2.0	2413	1	19.6
	1002					4	50.1
	1003	04.02.02	-	-	-	1	17.6
	1004					4	47.0
SUM:			**18.8**	**2.1**	**2425**		

SERIES IV:

Table 8 Tensile creep tests (T) at loading age of 3 days with ***different temperature levels*** and. BASE-5.

Test No.	Concrete Casting				MAX. Temperature [^{o}C]	Concrete Age [day]	Compressive Strength [MPa]
	Date	Slump [cm]	Air [%]	Density [kg]			
800	23.10.01	18.5	2.0	14096	35	3	44.6
801	05.11.01	14.0	2.1	14122	40	3	48.5
802	12.11.01	18.0	2.2	14045	60	3	-
803	11.03.02	17.5	2.2	14045	60	2	64.4[1]
804	19.03.02	18.0	2.2	13970	60	2	38.7
SUM:		17.2	2.1%				

[1] Compressive strength after 11 days.

APPENDIX B

Compressive Creep Tests on BASE-5 Concrete at Different Concrete Ages

In the first series, tests on compressive creep were performed on 1-8 days old BASE-5 concrete at about 20 ^{o}C and 50% RH. The intention was to evaluate the influence of the concrete age at loading on the viscoelastic behaviour of the concrete, and to compare the viscoelastic behaviour of the concrete in tension and compression.

The applied stress level is about 40% of the strength at initial loading and the load maintained constant during the test.

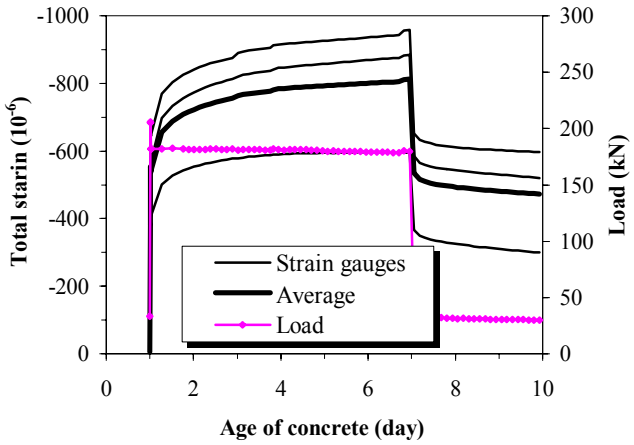

a) Load and total strain (Loaded specimen No. 1)

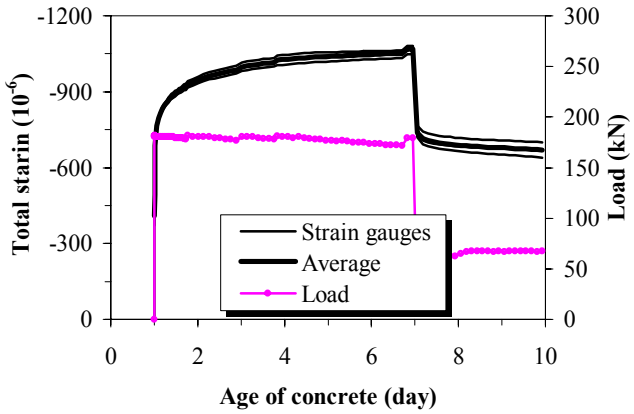

b) Load and total strain (Loaded specimen No. 2)

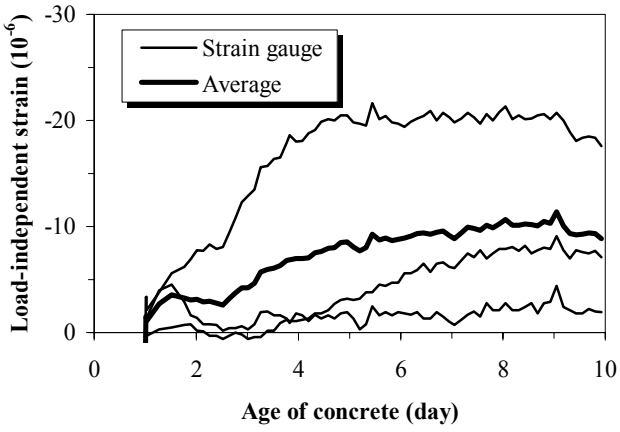

c) Load-independent strain (Dummy specimen)

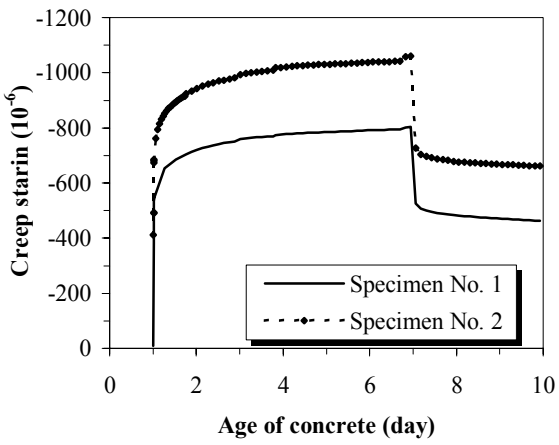

d) Load-dependent strains

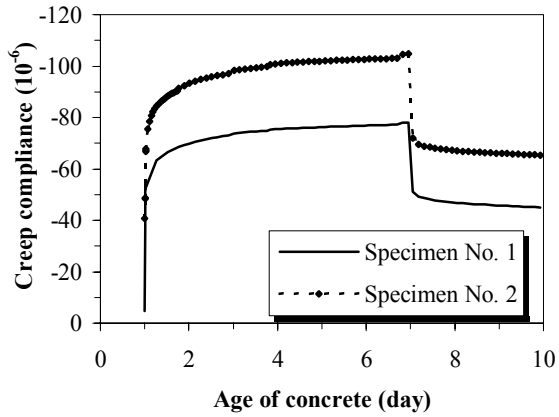

e) Creep complience (strain pr. unit stress)

Compressive creep test on 1-day old BASE-5 concrete - Test No. 105

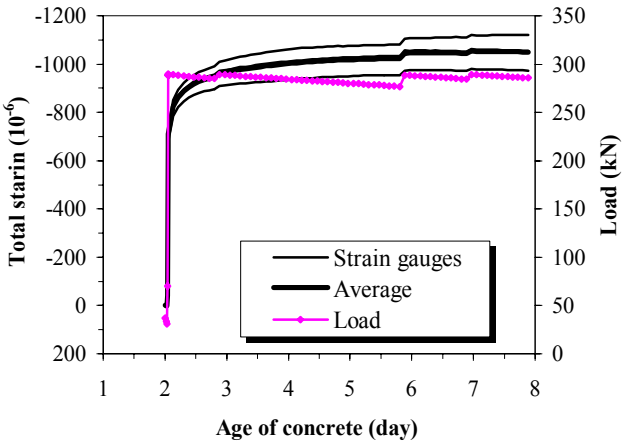

a) Load and total strain (Loaded specimen No. 1)

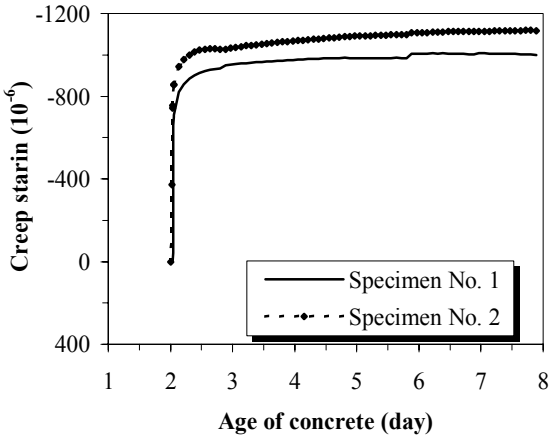

d) Load-dependent strains

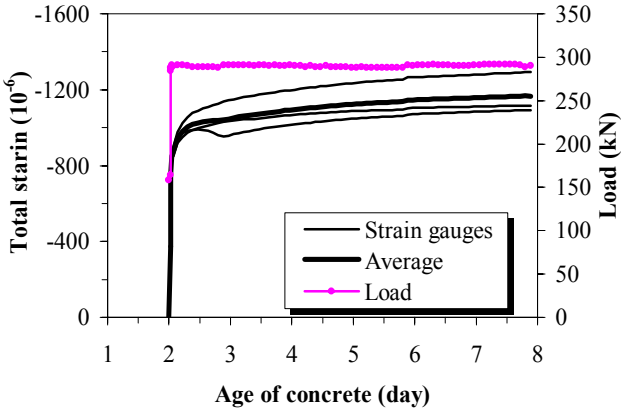

b) Load and total strain (Loaded specimen No. 2)

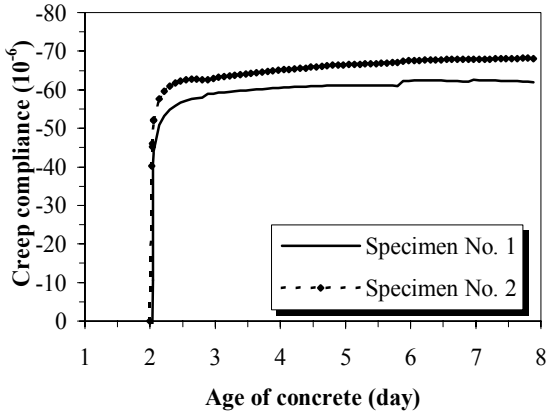

e) Creep complience (strain pr. unit stress)

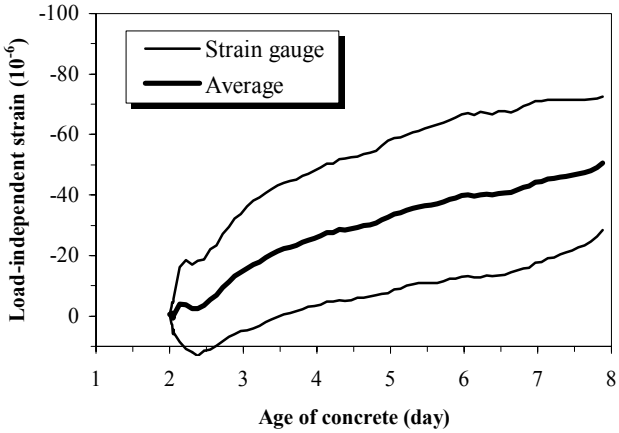

c) Load-independent strain (Dummy specimen)

Compressive creep test on 2-day old BASE-5 concrete - Test No. 111

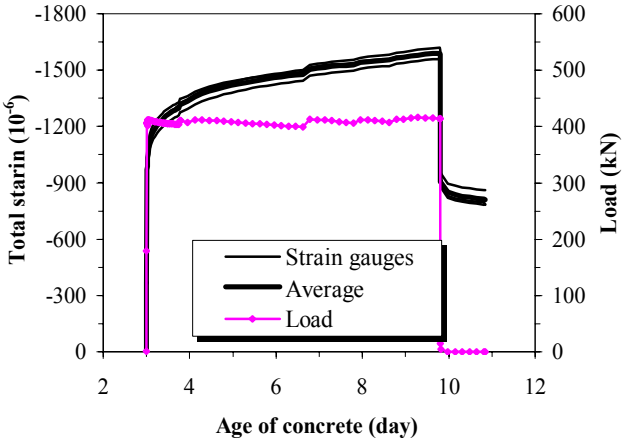

a) Load and total strain (Loaded specimen No. 1)

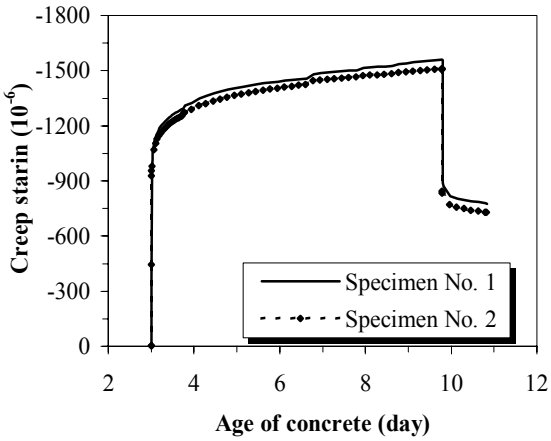

d) Load-dependent strains

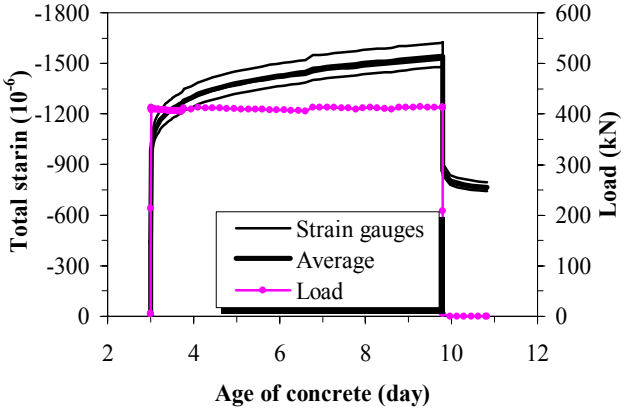

b) Load and total strain (Loaded specimen No. 2)

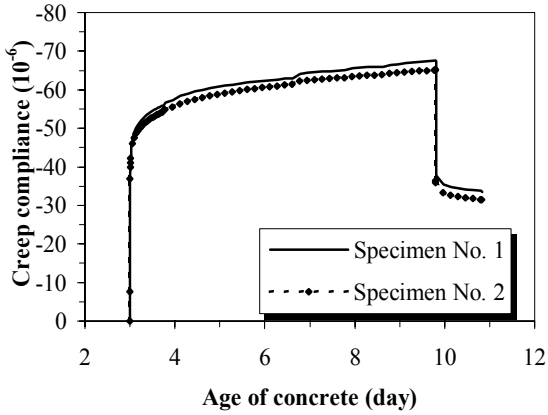

e) Creep complience (strain pr. unit stress)

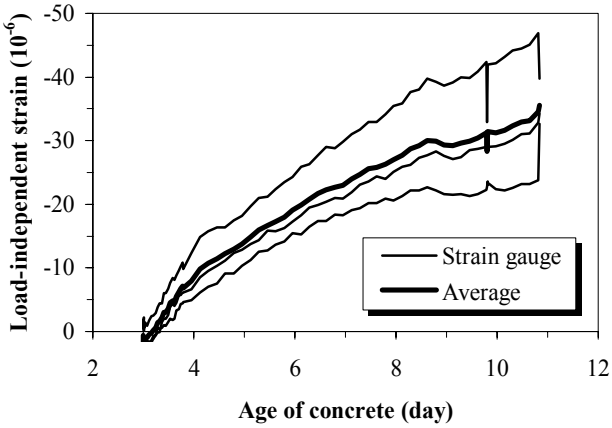

c) Load-independent strain (Dummy specimen)

Compressive creep test on 3-day old BASE-5 concrete - Test No. 103

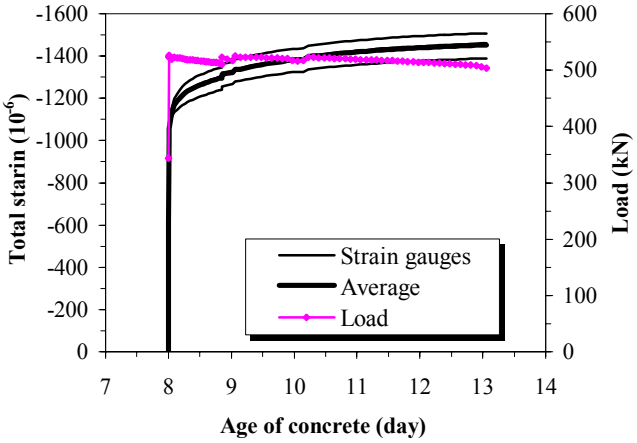

a) Load and total strain (Loaded specimen No. 1)

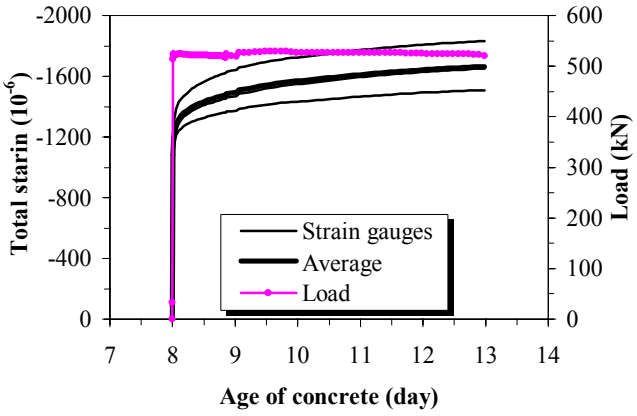

b) Load and total strain (Loaded specimen No. 2)

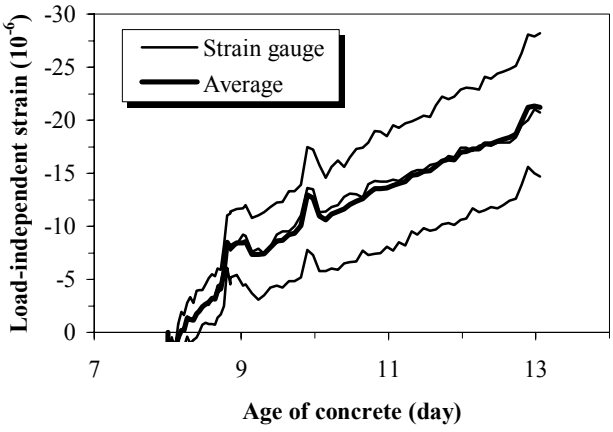

c) Load-independent strain (Dummy specimen)

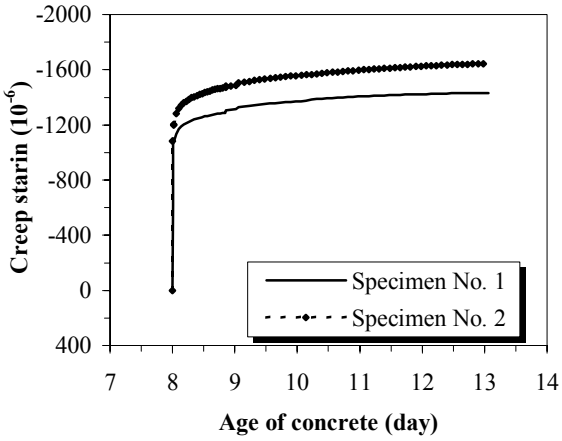

d) Load-dependent strains

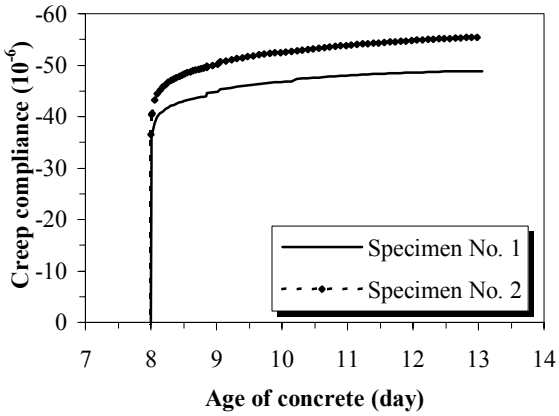

e) Creep complience (strain pr. unit stress)

Compressive creep test on 8-day old BASE-5 concrete - Test No. 108

APPENDIX C

Compressive Creep Tests on Maridal Concrete at Different Concrete Ages

Tests on compressive creep were performed on 1, 3 and 8-days old Maridal concrete at about 20 ^{o}C and 50% RH. The intention was to evaluate the influence of the concrete age at loading on the viscoelastic behaviour of the concrete, and to compare the viscoelastic behaviour of the concrete in tension and compression.

The applied stress level is about 40% of the strength at initial loading, and the load maintained constant during the test.

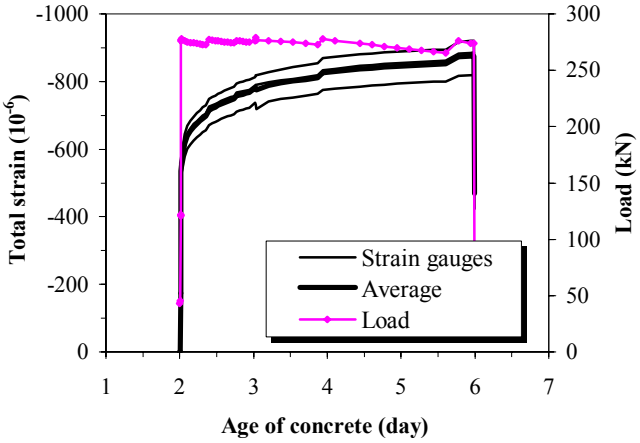

a) Load and total strain (Loaded specimen No. 1)

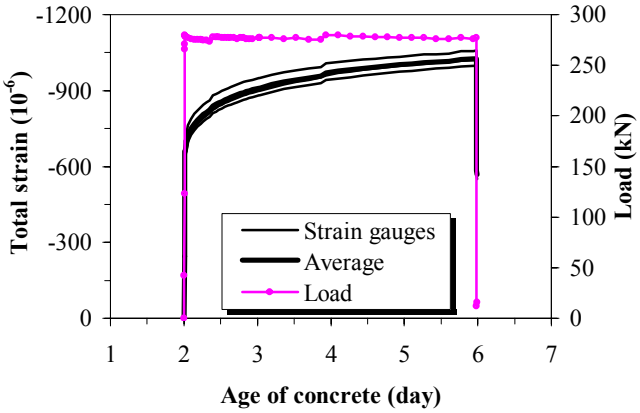

b) Load and total strain (Loaded specimen No. 2)

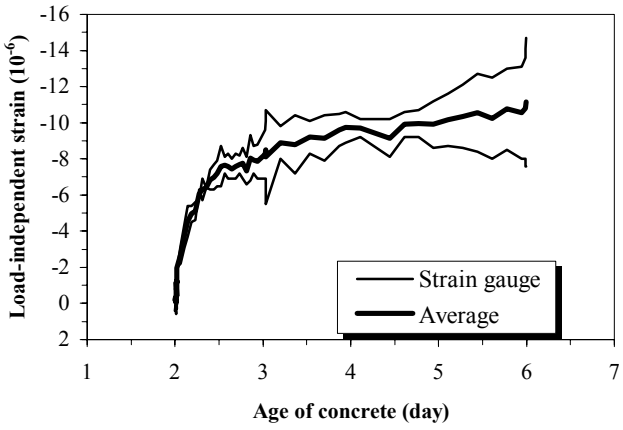

c) Load-independent strain (Dummy specimen)

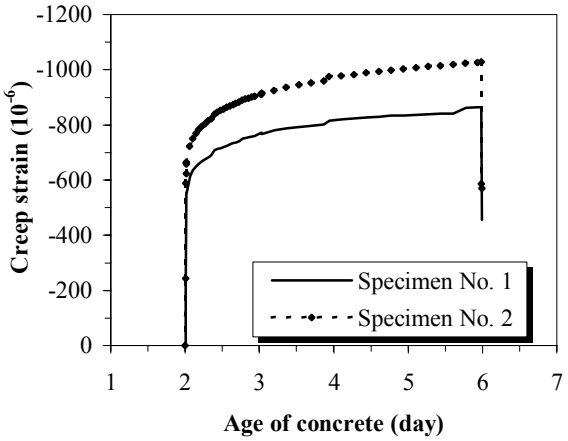

d) Load-dependent strains

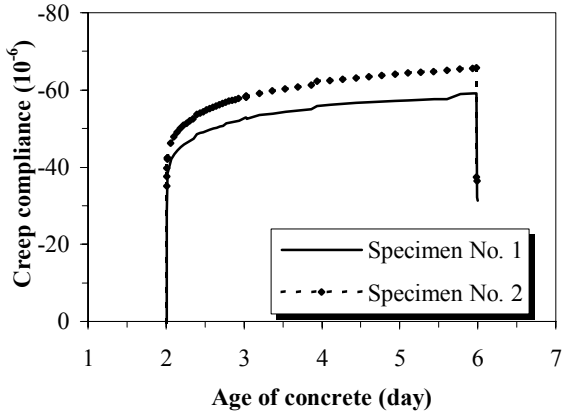

e) Creep compliance (strain pr. unit stress)

Compressive creep test on Maridal concrete - Test No. 301

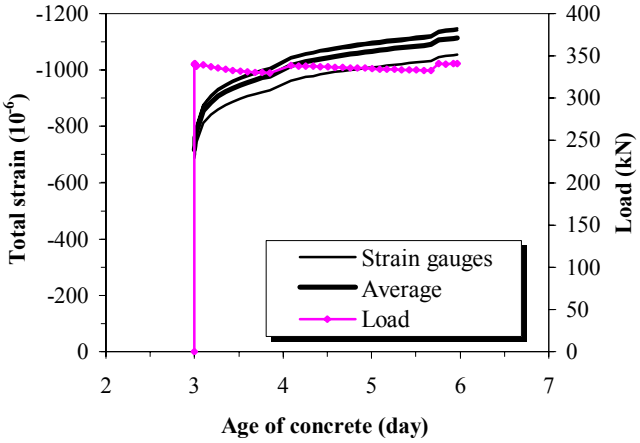

a) Load and total strain (Loaded specimen No. 1)

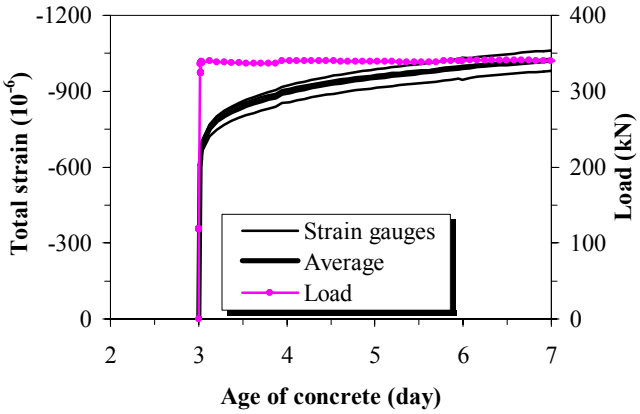

b) Load and total strain (Loaded specimen No. 2)

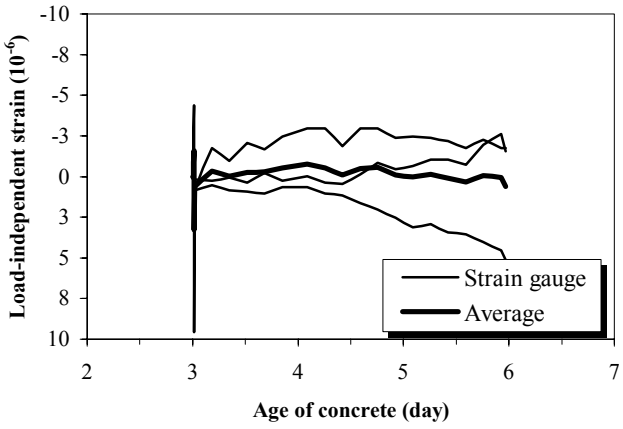

c) Load-independent strain (Dummy specimen)

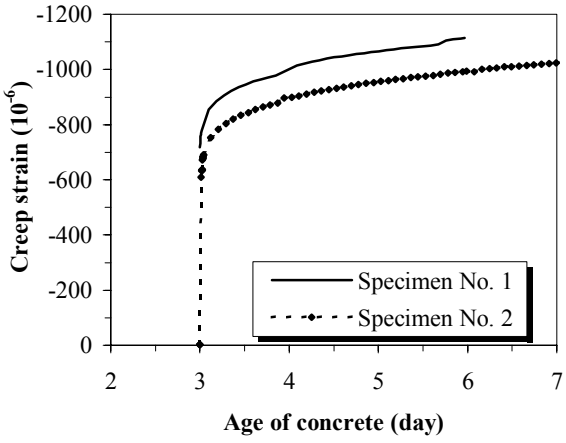

d) Load-dependent strains

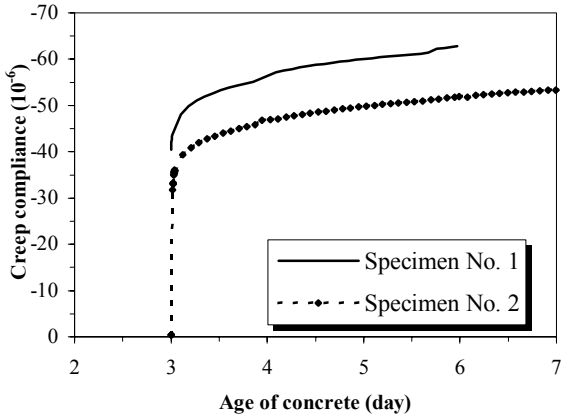

e) Creep compliance (strain pr. unit stress)

Compressive creep test on Maridal concrete - Test No. 302

URN:NBN:no-3377

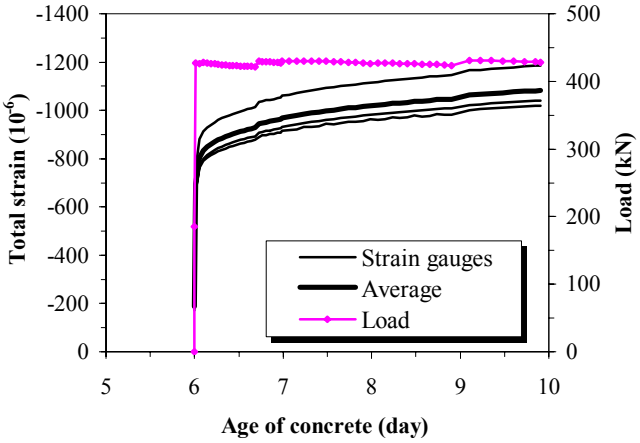

a) Load and total strain (Loaded specimen No. 1)

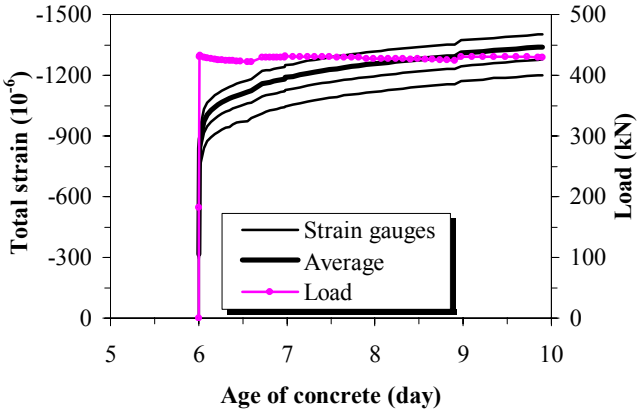

b) Load and total strain (Loaded specimen No. 2)

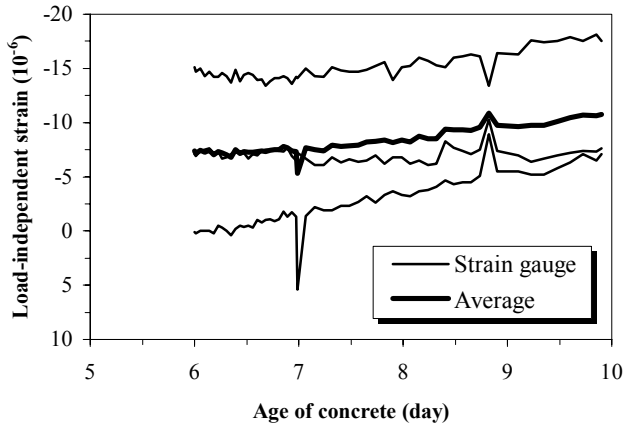

c) Load-independent strain (Dummy specimen)

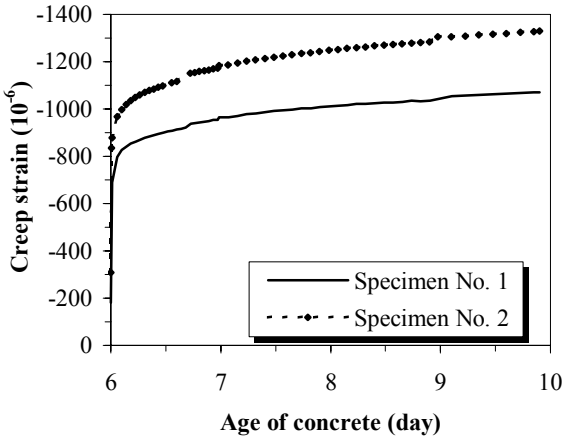

d) Load-dependent strains

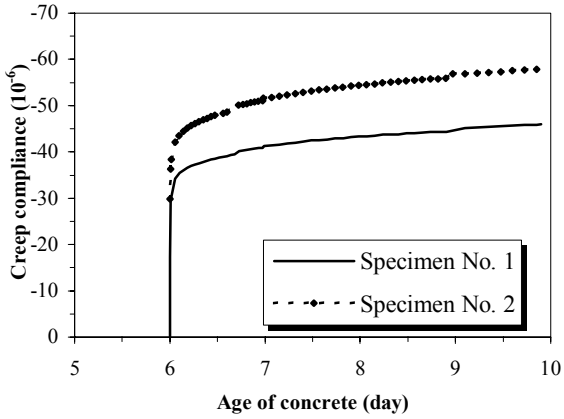

e) Creep compliance (strain pr. unit stress)

Compressive creep test on Maridal concrete - Test No. 303

URN:NBN:no-3377

APPENDIX D

Tensile Creep Tests on BASE-5 Concrete at Different Concrete Ages

Tensile creep tests were performed on 1, 2, 3, 4, 6 and 8-days old BASE-5 concrete at about 20 ^{o}C and 50% RH. The intention was to evaluate the influence of the concrete age at loading on the viscoelastic behaviour of the concrete in tention, and to compare the viscoelastic behaviour of the concrete in tension and compression.

The applied stress level is about 40% of the strength at initial loading, and the load maintained constant during the test.

The diagrams present:

a) Applied load and measured strains during loading.
b) Measured total strains on the loaded specimen.
c) Measured load-independent strains (autogenous shrinkage) on dummy specimen.
d) Calculated creep strain (sum of the measured strains in loaded and dummy specimens).
e) Calculated creep compliance (strains pr. stress unit).

Note that the data was recorded only few times during the loading in test No. T104.

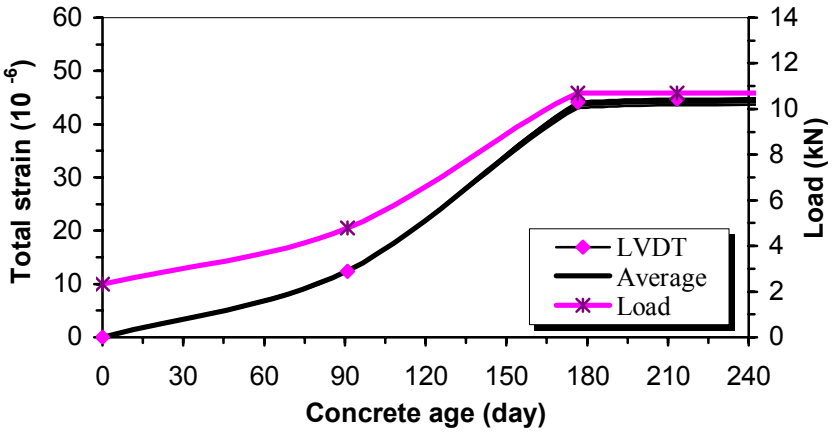

a)

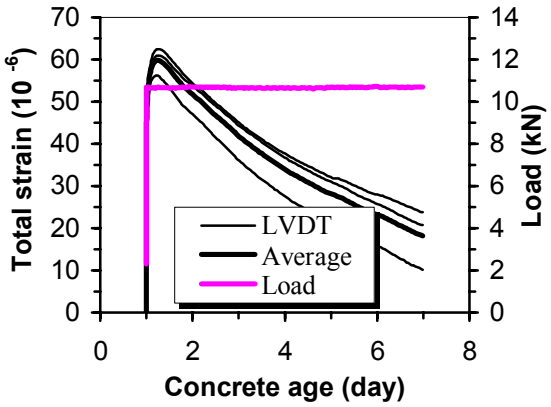

b)

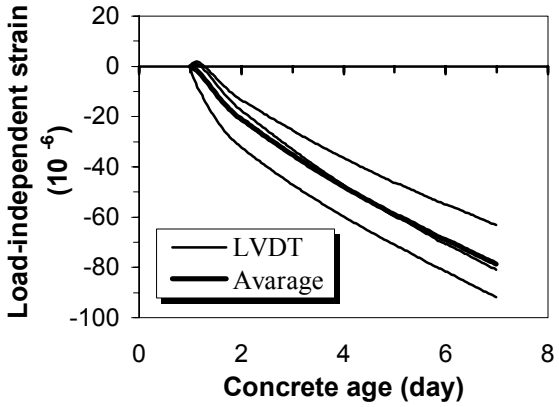

c)

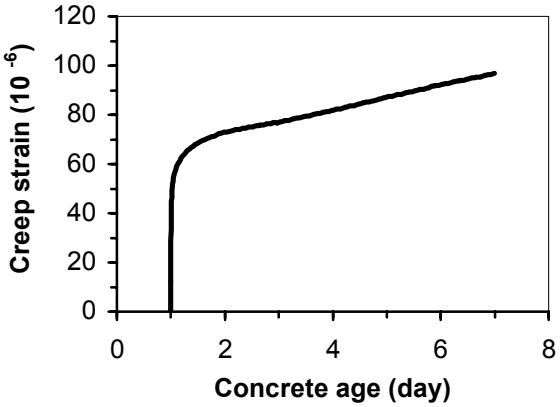

d)

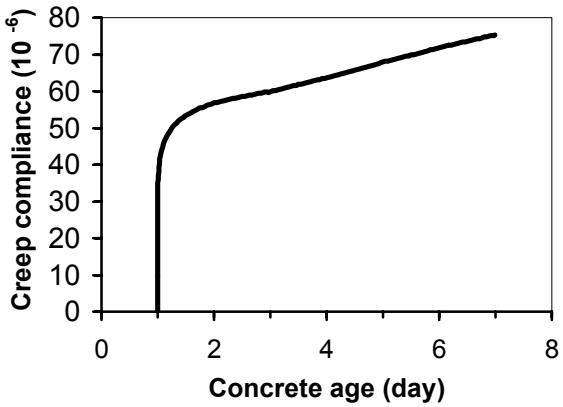

e)

Tensile creep test on 1-day old BASE-5 concrete - test No. T104
Stress = 1.29 MPa and T= 20 °C

URN:NBN:no-3377

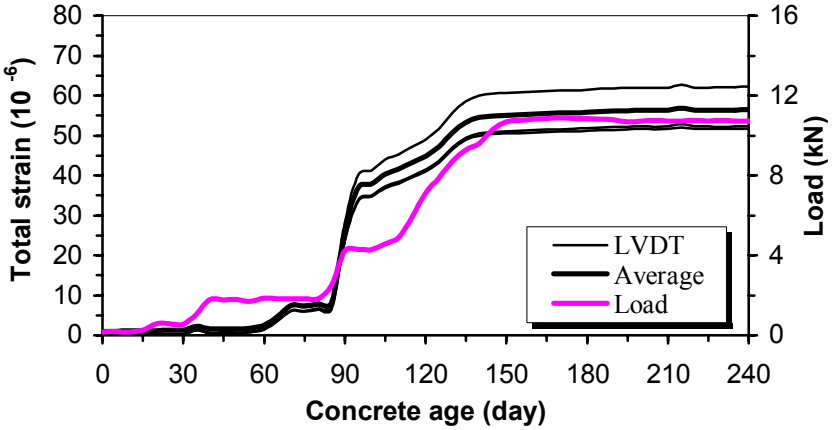

a)

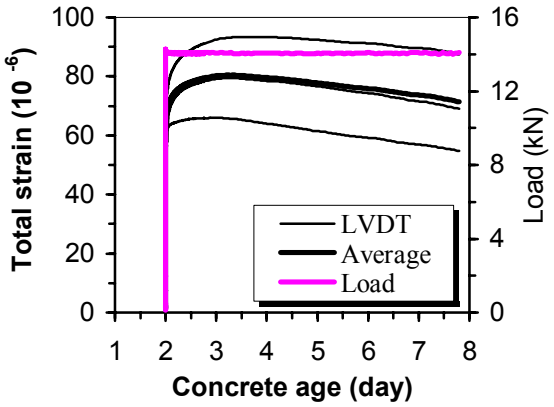

b)

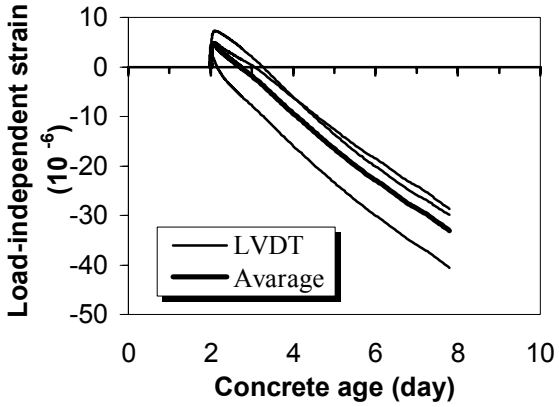

c)

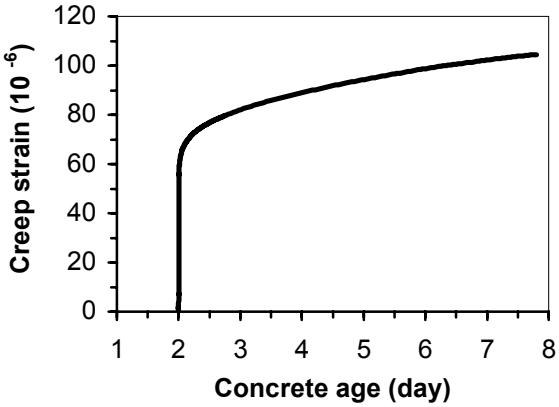

d)

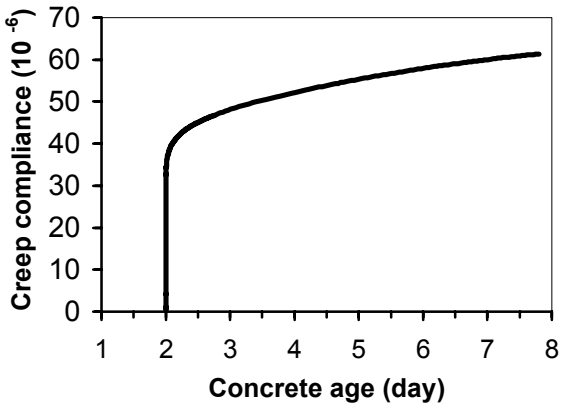

e)

Tensile creep test on 2-days old BASE-5 concrete - test No. T111
Stress = 1.70 MPa and T= 20 ^{o}C

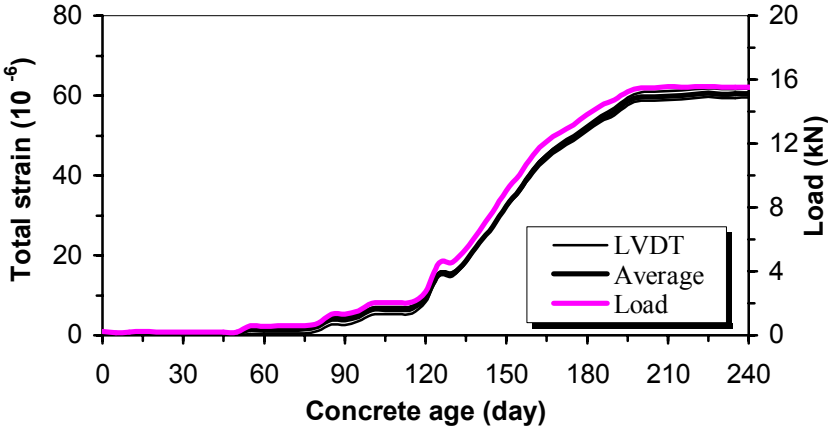

a)

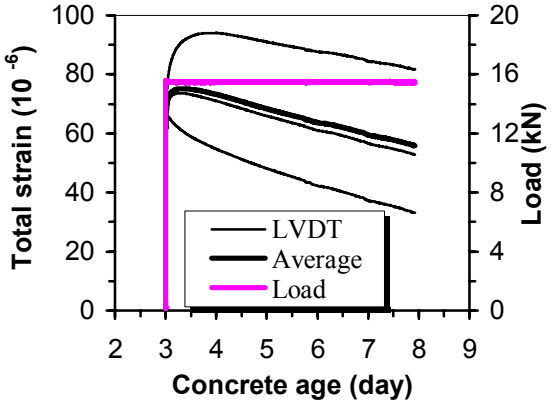

b)

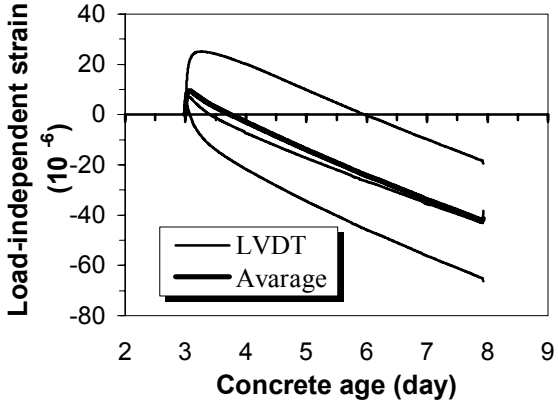

c)

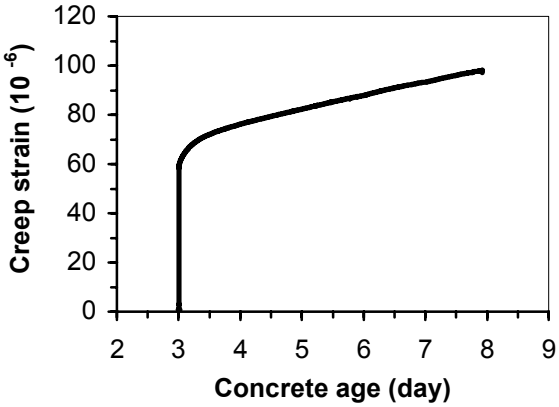

d)

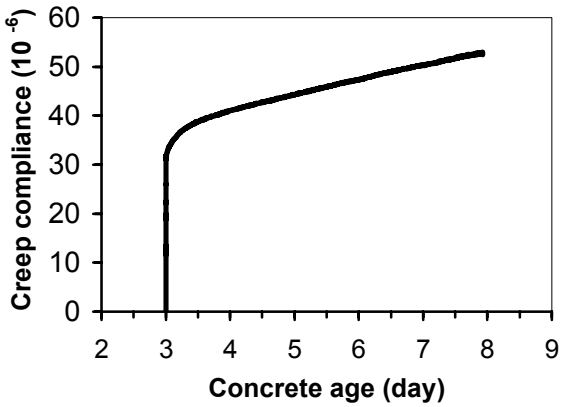

e)

Tensile creep test on 3-days old BASE-5 concrete - Test No. T107
Stress = 1.85 MPa and T= 20 ^{o}C

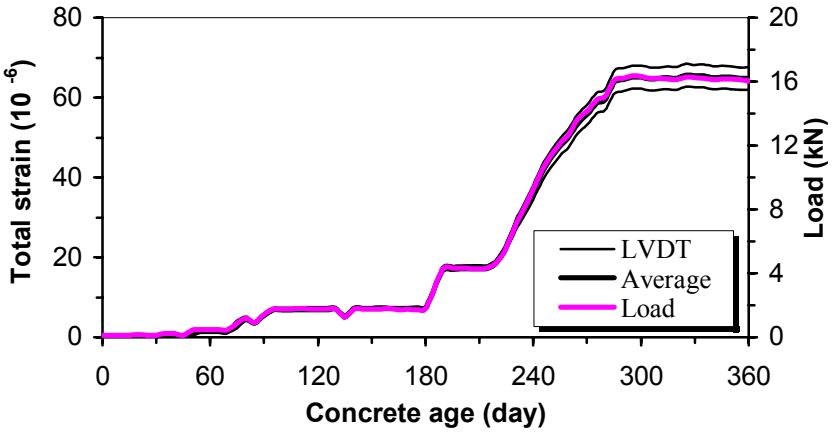

a)

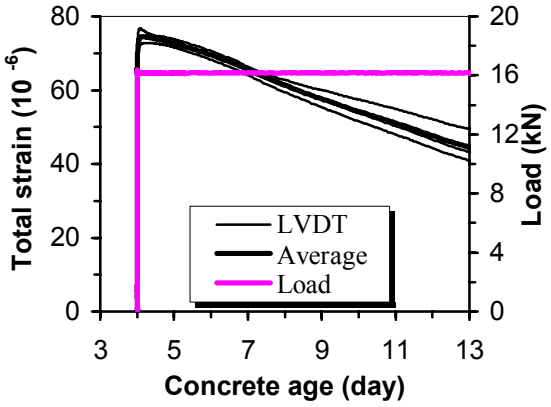

b)

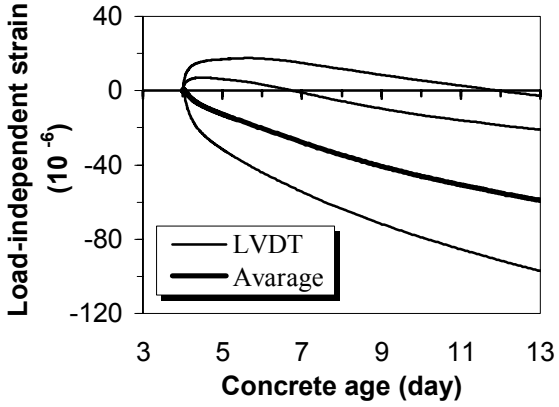

c)

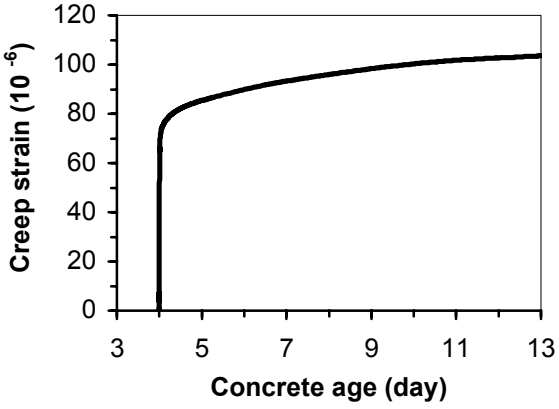

d)

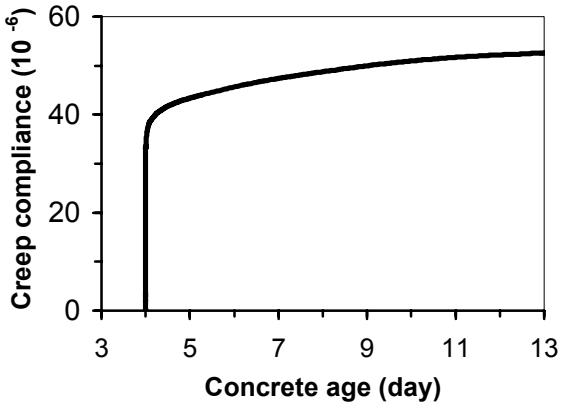

e)

Tensile creep test on 4-days old BASE-5 concrete - test No. T106
Stress = 1.94 MPa and T= 20 ^{o}C

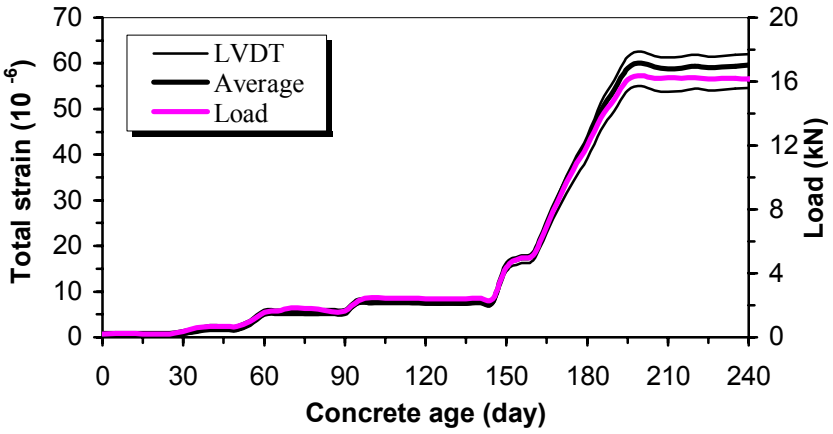

a)

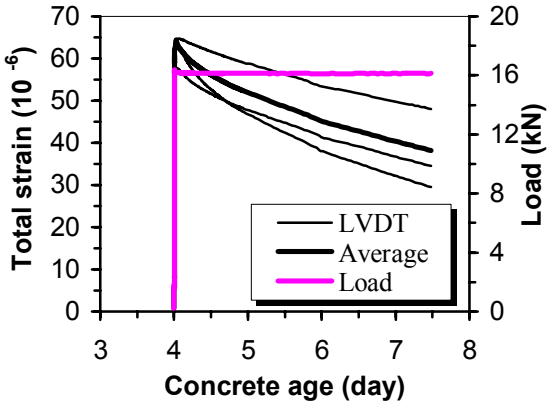

b)

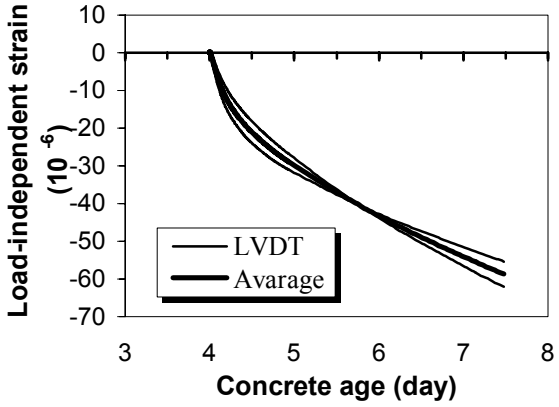

c)

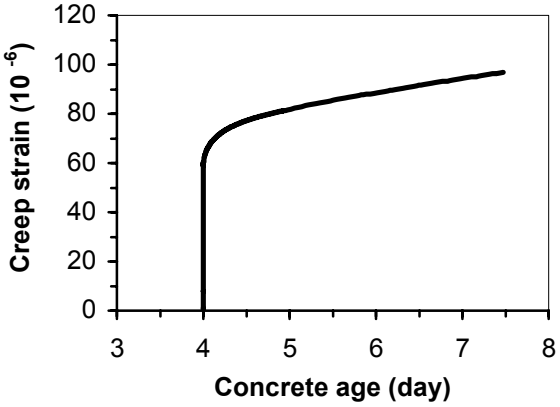

d)

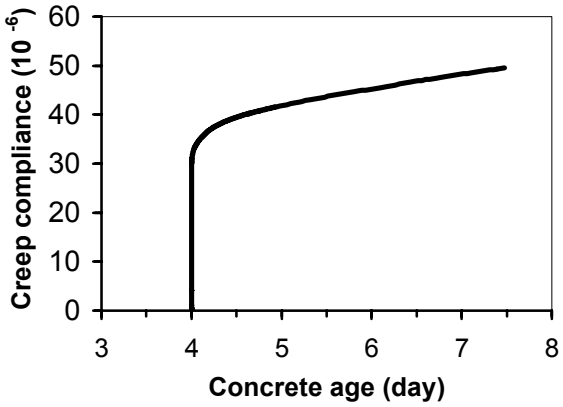

e)

Tensile creep test on 4-days old BASE-5 concrete - test No. T109
Stress = 1.94 MPa and T= 20 ^{o}C

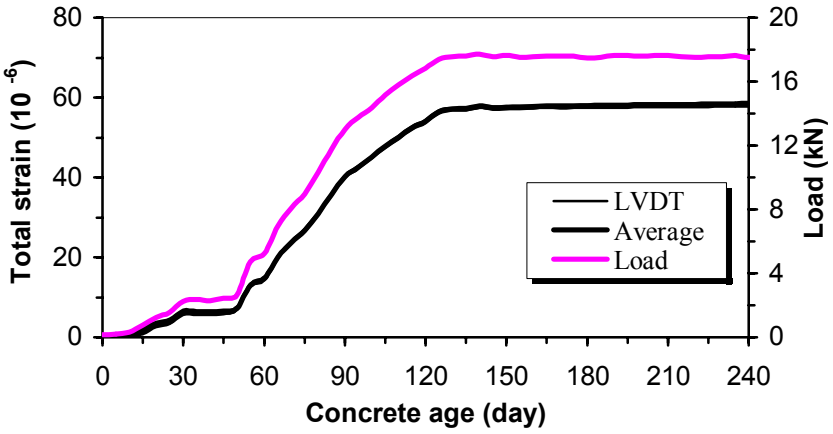

a)

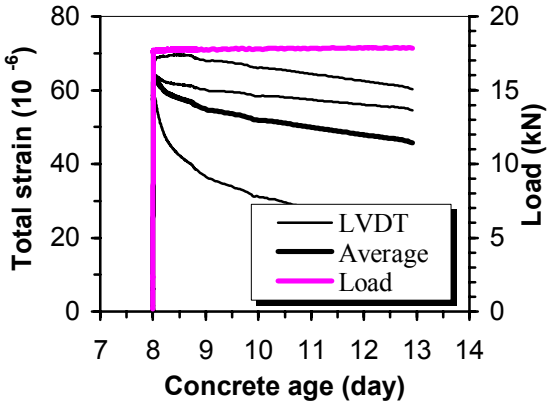

b)

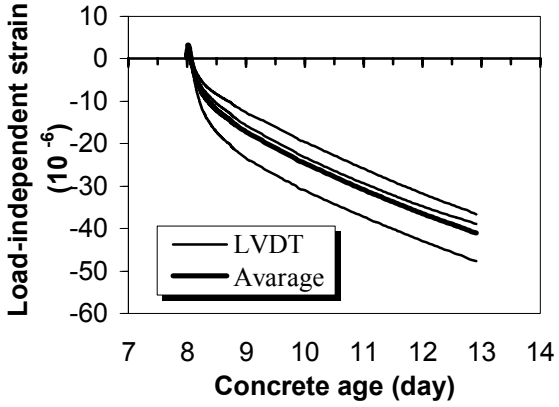

c)

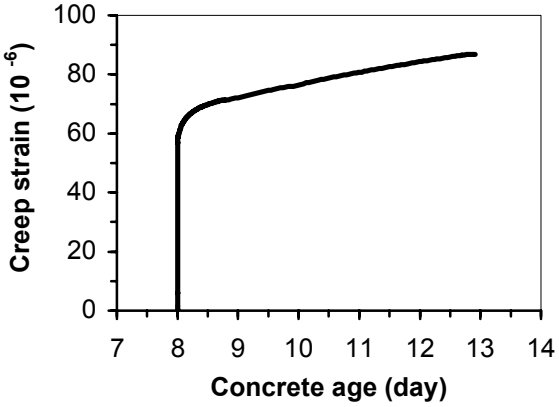

d)

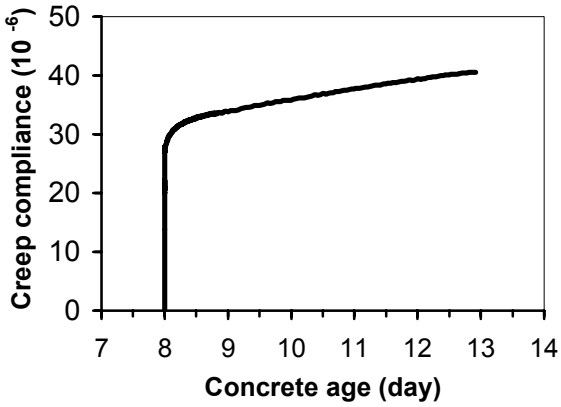

e)

Tensile creep test on 8-days old BASE-5 concrete - test No. T108
Stress = 2.11 MPa and T= 20 °C

URN:NBN:no-3377

APPENDIX E

Tensile Creep Tests on BASE-5 Concrete With Different Stress/Strength-Ratio

Tensile creep tests in this series were carried out on 3-days old BASE-5 concrete to study the creep none-linearity in concrete. The applied initial tensile stress levels were 0.2, 0.3, 0.4, 0.6, 0.7 and 0.8 times the tensile strength. The tensile strength, compressive strength and E-modulus for the 3-days old concrete are 3.7 MPa, 47.8 MPa and 29.3 GPa, respectively.

The diagrams present:

a) Applied load and measured total strain during loading.
b) Stress-strain relationship during the loading.
c) Measured total strain on the loaded specimen.
d) Load-independent strain (autogenous shrinkage) on the dummy specimen.
e) Creep strain (sum of the measured strains in loaded and dummy specimens).
f) Creep compliance (strains pr. stress unit)

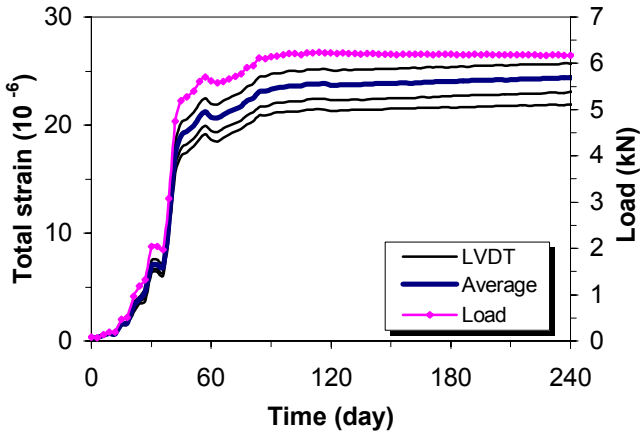

a)

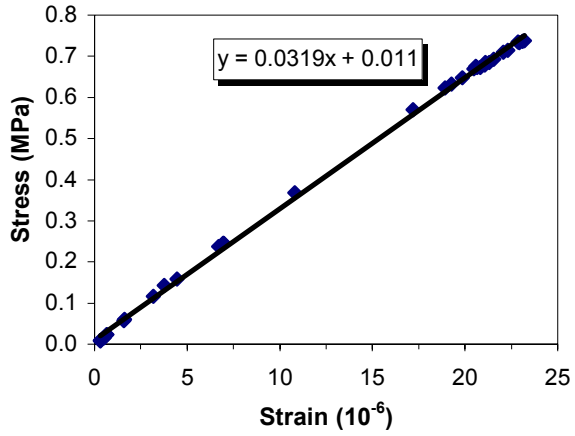

b)

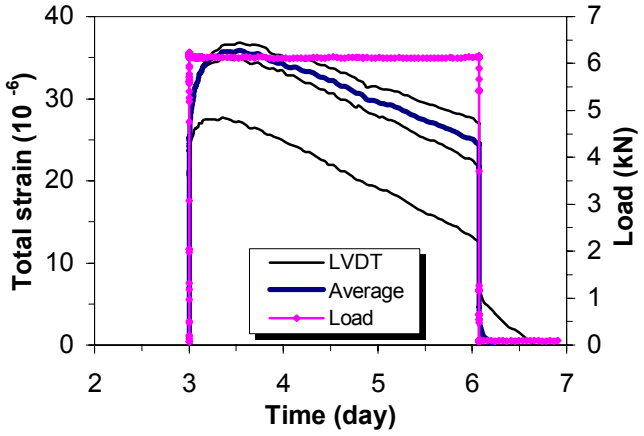

c)

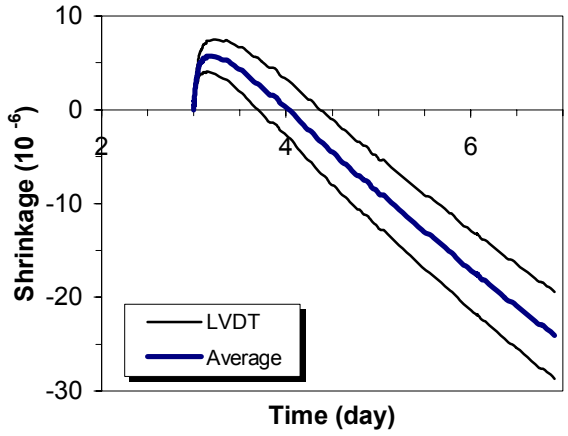

d)

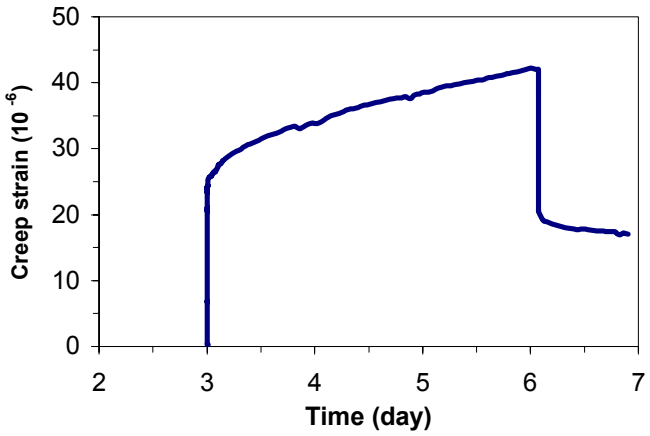

e)

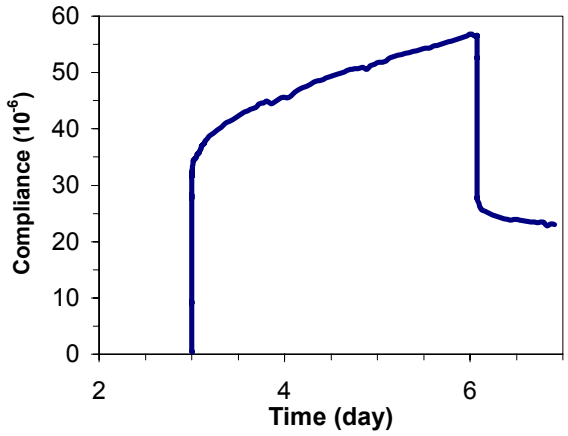

f)

Tensile creep test with stress/strength-ratio 20%

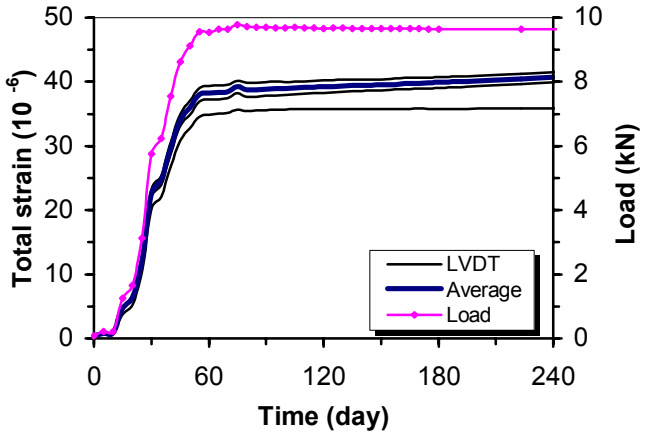

a)

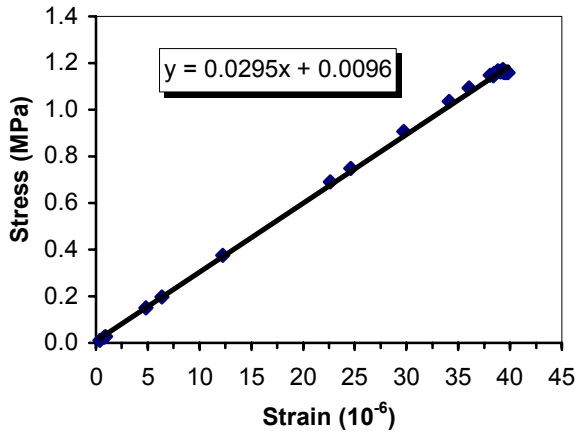

b)

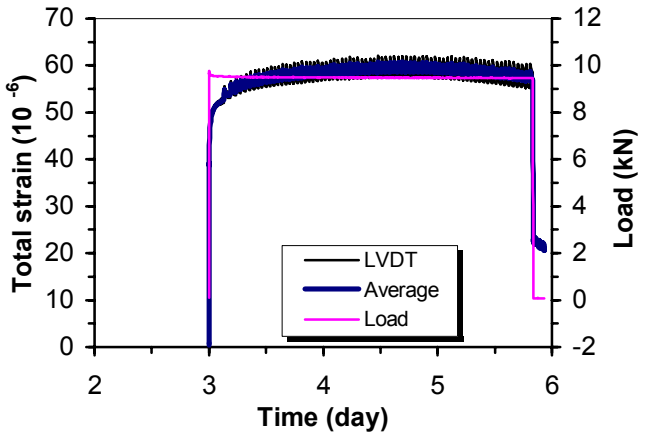

c)

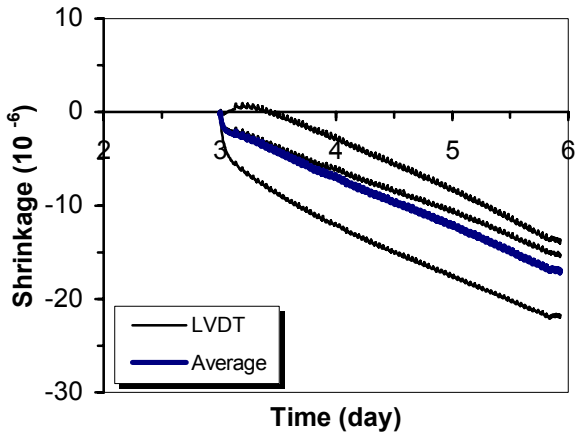

d)

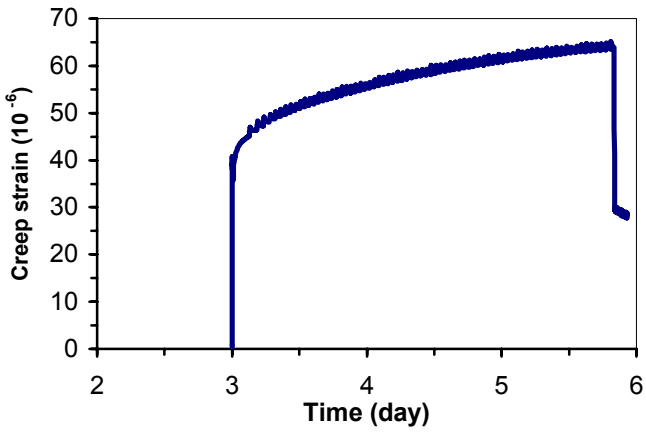

e)

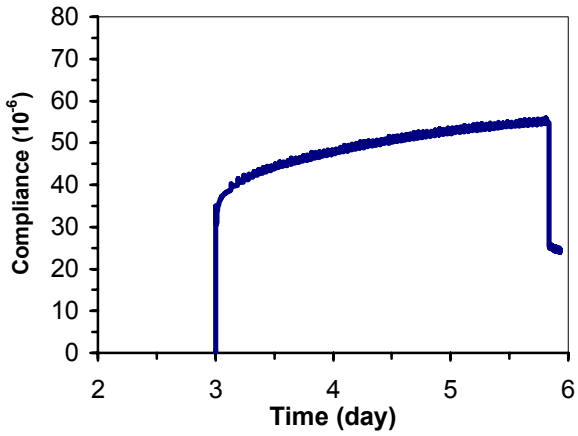

f)

Tensile creep test with stress/strength-ratio 30%

URN:NBN:no-3377

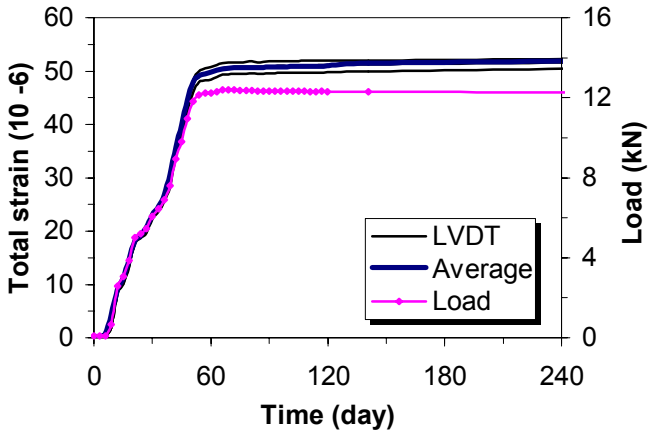

a)

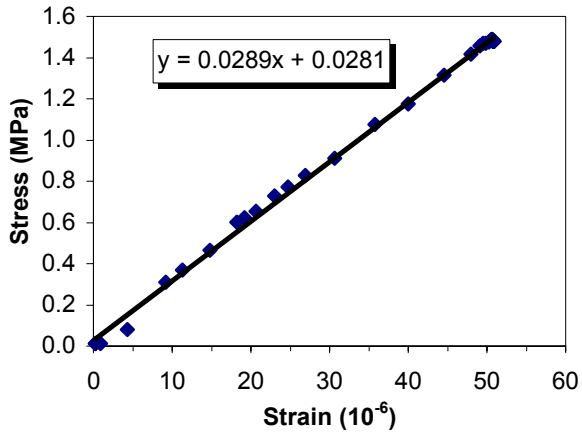

b)

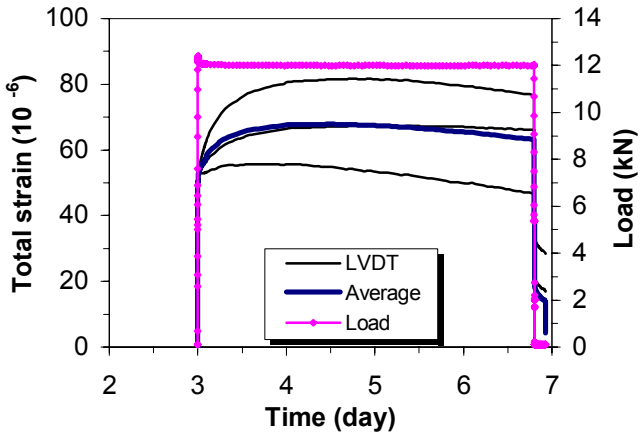

c)

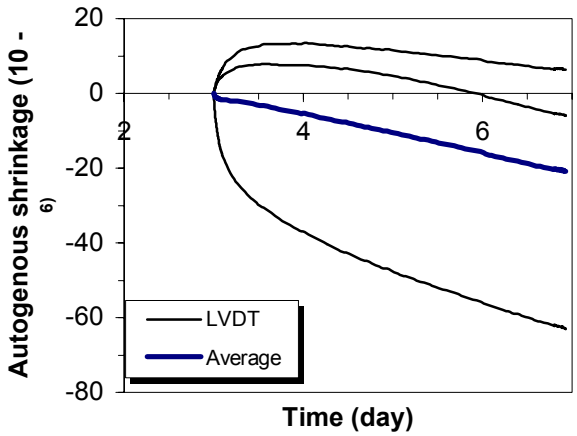

d)

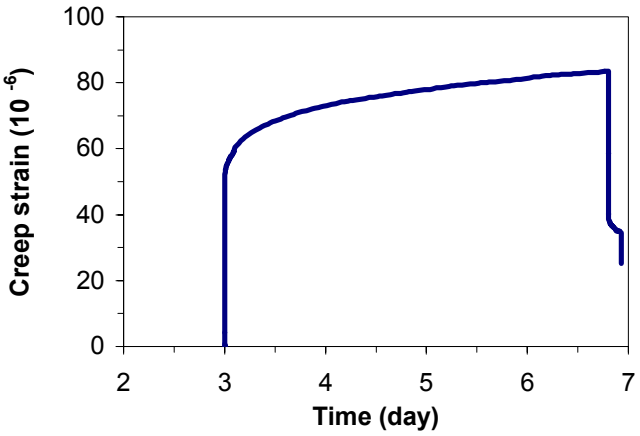

e)

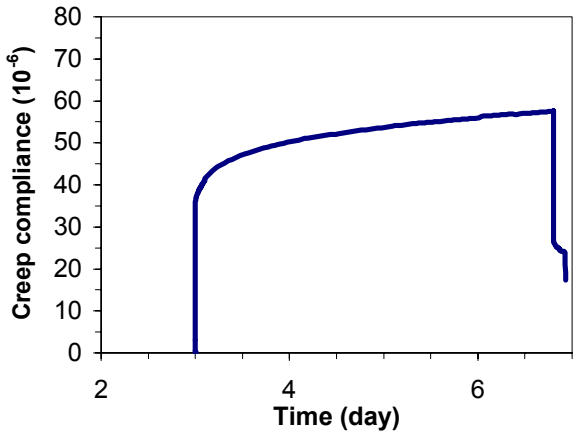

f)

Tensile creep test with stress/strength-ratio 40%

URN:NBN:no-3377

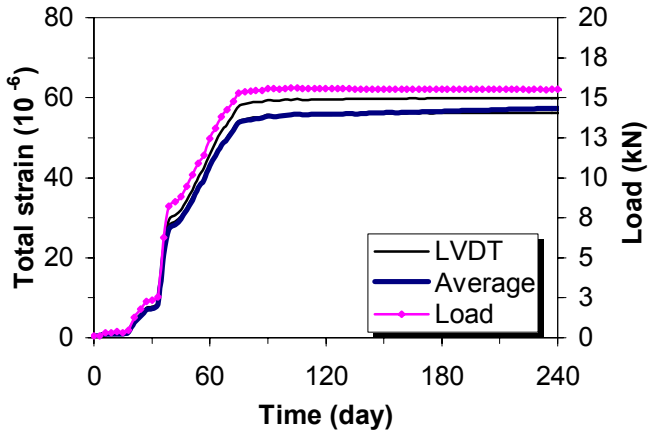

a)

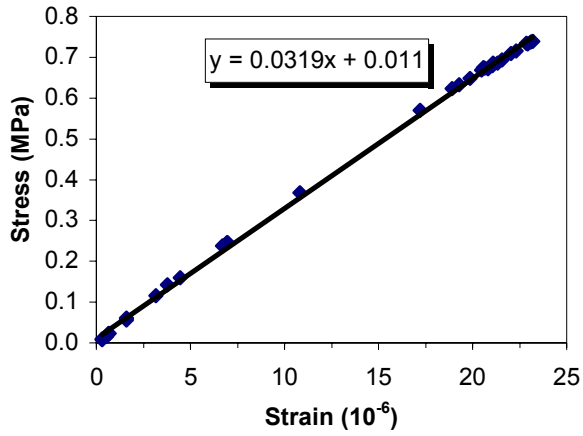

b)

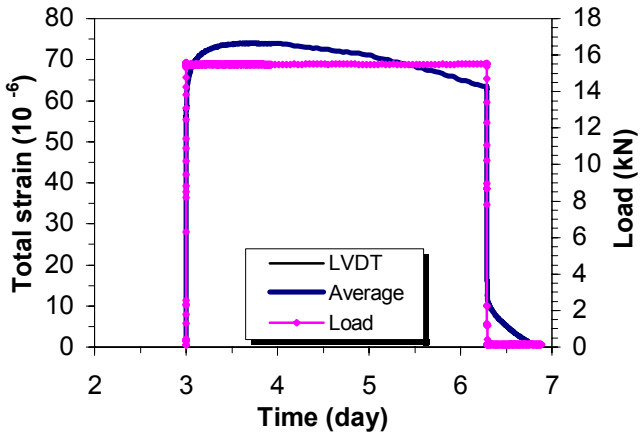

c)

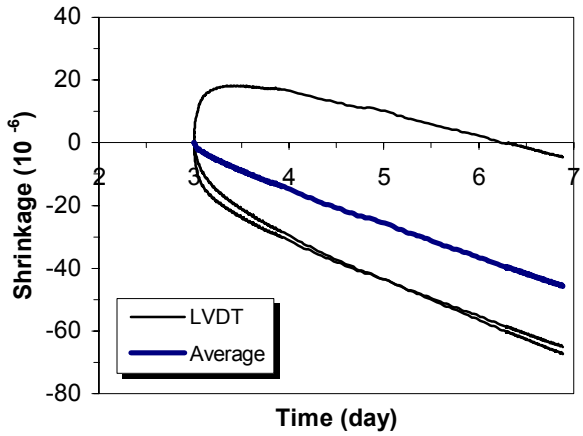

d)

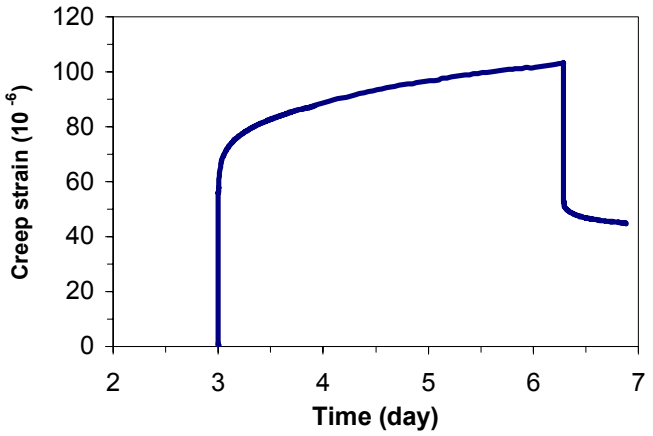

e)

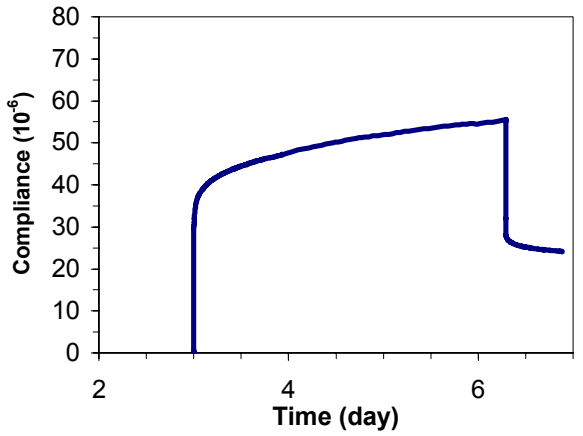

f)

Tensile creep test with stress/strength-ratio 50%

URN:NBN:no-3377

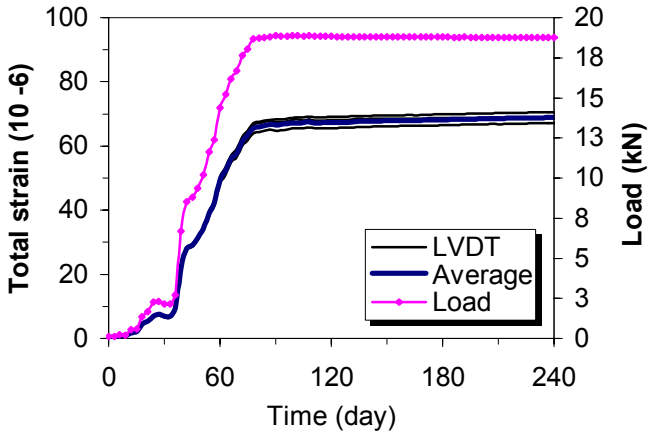

a)

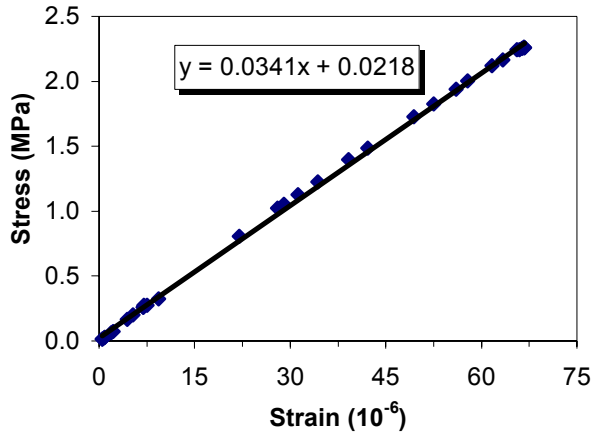

b)

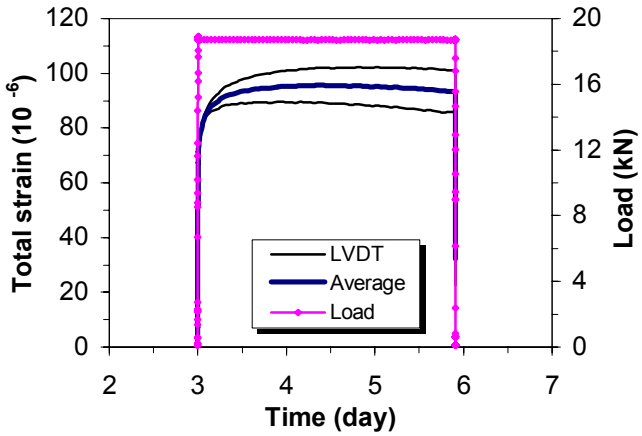

c)

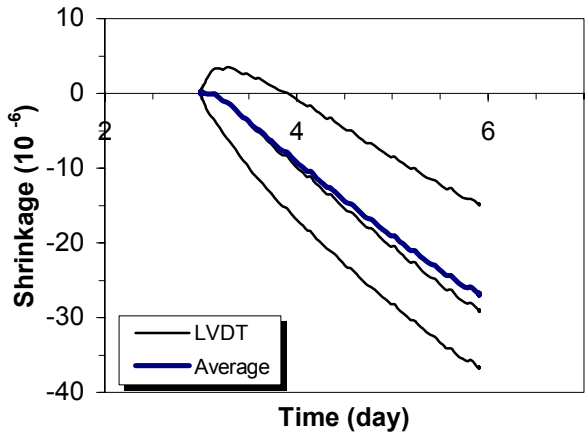

d)

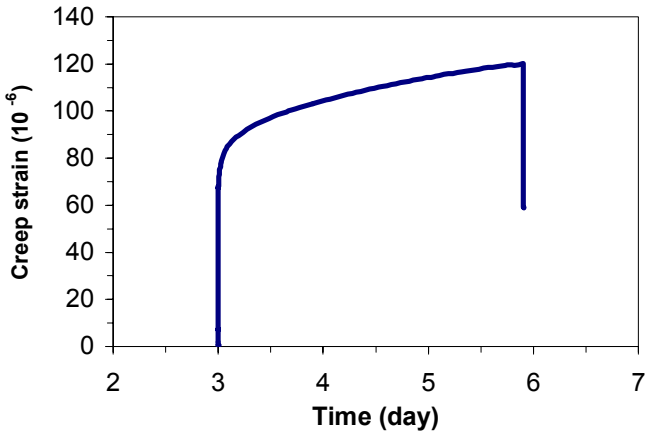

e)

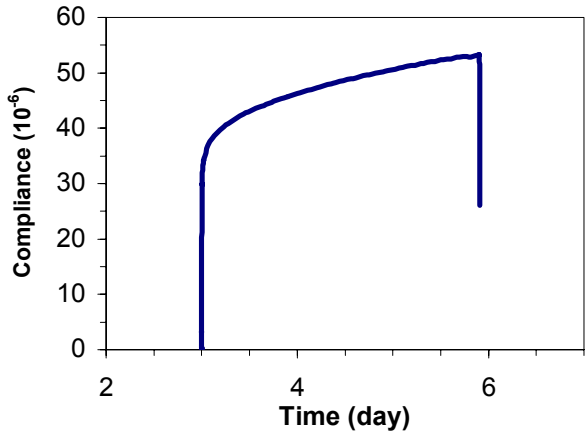

f)

Tensile creep test with stress/strength-ratio 60%

URN:NBN:no-3377

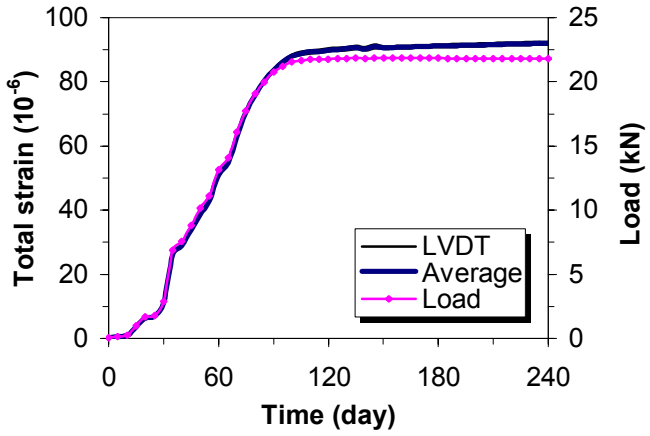

a)

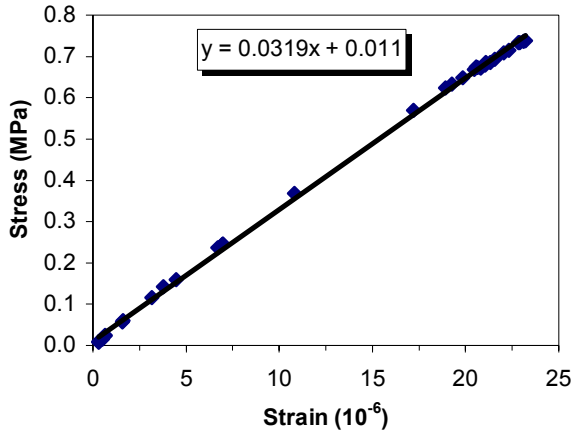

b)

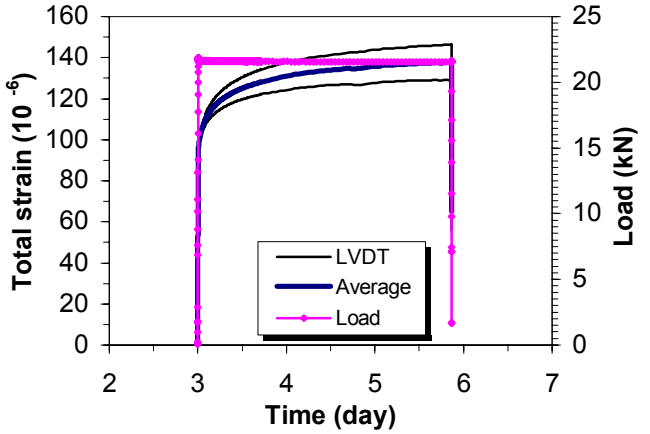

c)

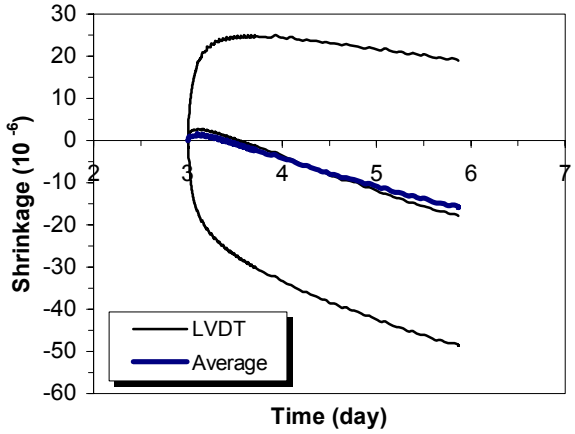

d)

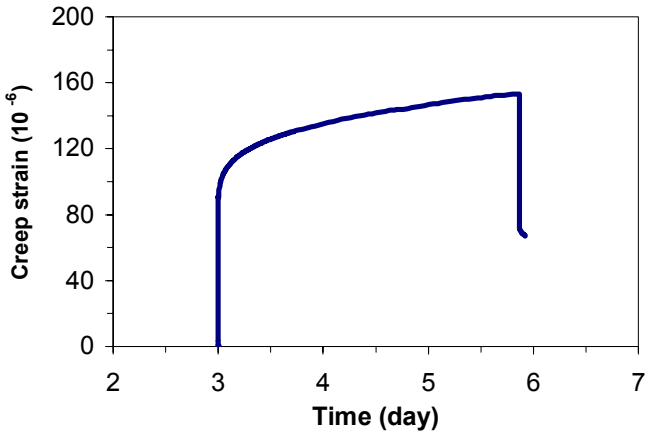

e)

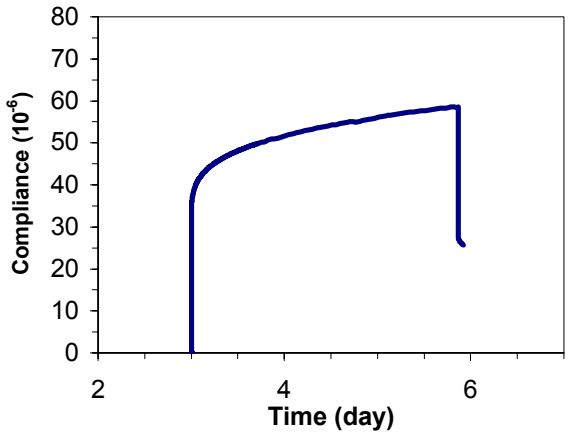

f)

Tensile creep test with stress/strength-ratio 70%

URN:NBN:no-3377

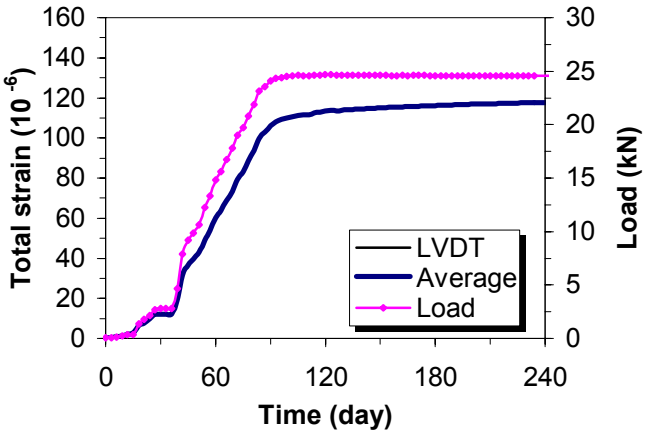

a)

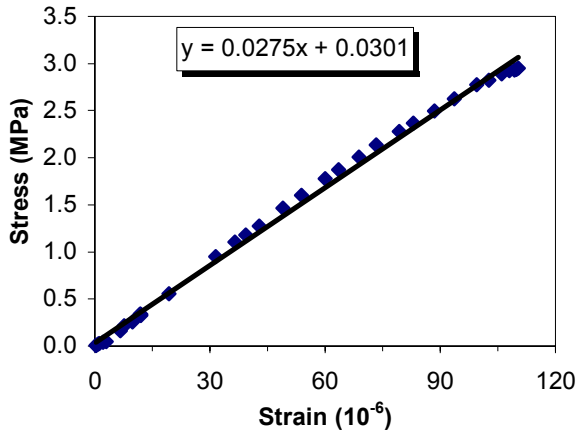

b)

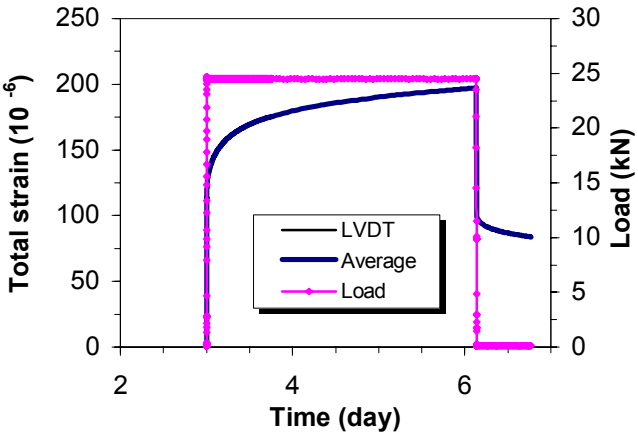

c)

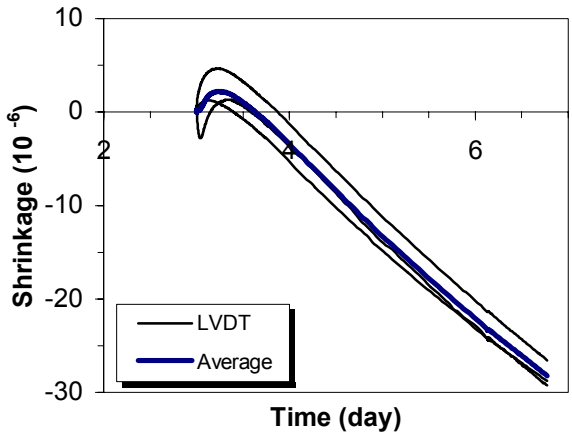

d)

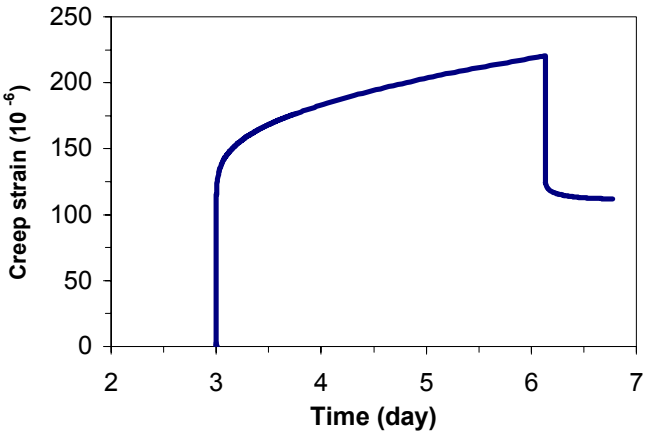

e)

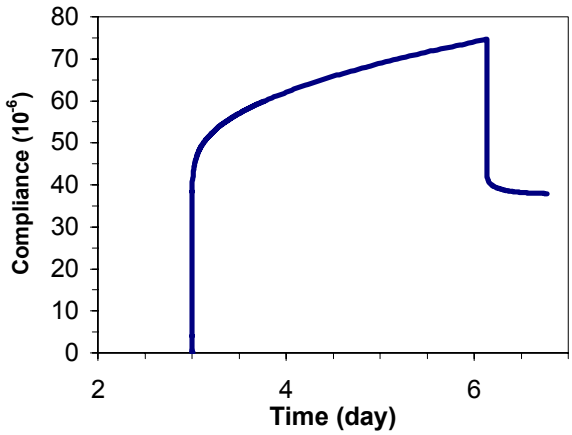

f)

Tensile creep test with stress/strength-ratio 80%

APPENDIX F

Tensile Creep Tests on BASE-5 Concrete under Different Constant Temperatures

Influence of temperature on sealed creep in tension at early ages of concrete is investigated. Tensile creep tests are conducted at different isothermal temperatures (20, 34, 40, 57 and 60 ^{o}C) on BASE-5 concrete. The curing temperature for all the tests is about 21±2 ^{o}C until it is increased to achieve the desired testing temperature.

For the test at 34 ^{o}C the temperature was increased only 3 hrs before loading. For the other tests (40, 57 and 60 ^{o}C) the temperature was increased to the desired level one day before loading.

The diagrams present:

a) Temperature history for the creep test and the measured strains (autogenous deformation and thermal dilation) on the unloaded (dummy) specimen.
b) Load history and the total strain (included creep) on the loaded (active) specimen.
c) Calculated sealed creep pr. unit stress.

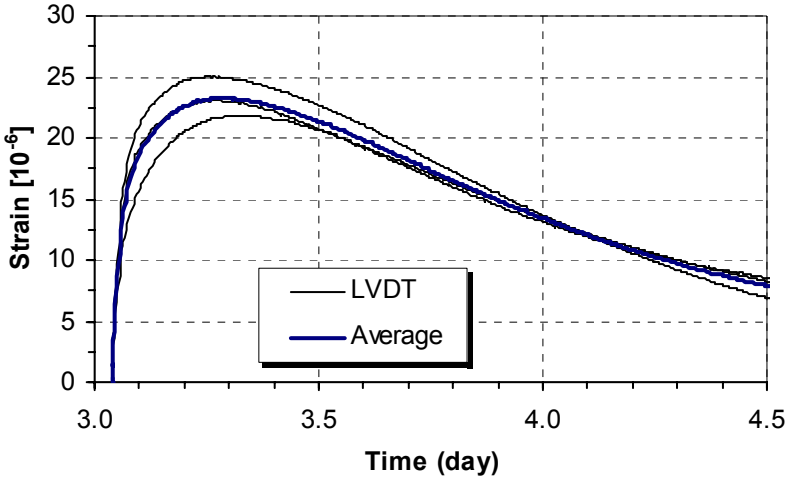

a) Unloaded specimen

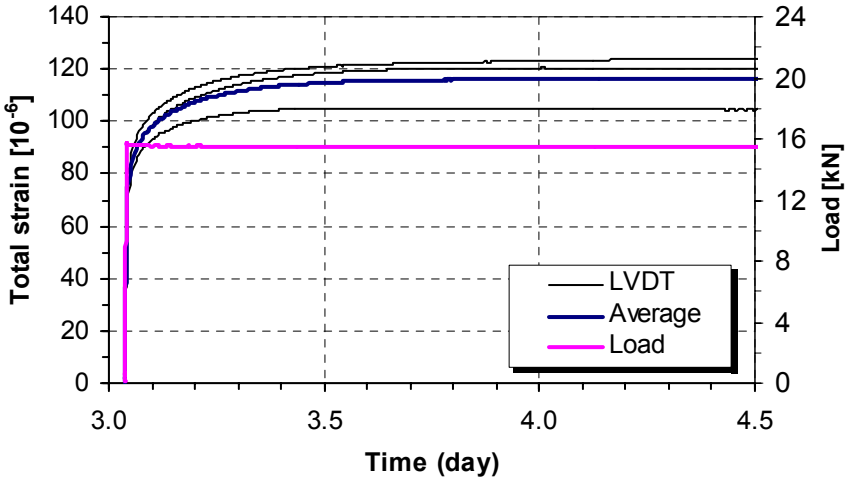

b) Loaded specimen

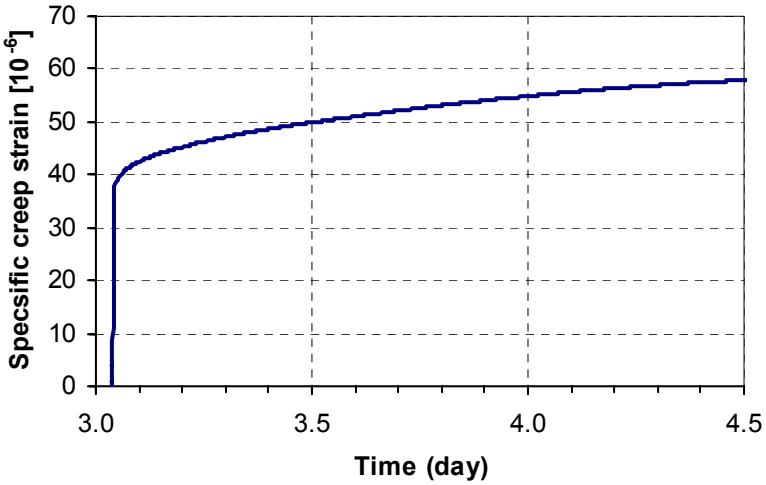

c) Specific creep

Measured strains in the tensile creep tests, age of loading 72 hrs (maturity = 73 hrs), concrete type BASE-5 and T=34 ^{o}C. (Test No. 800).

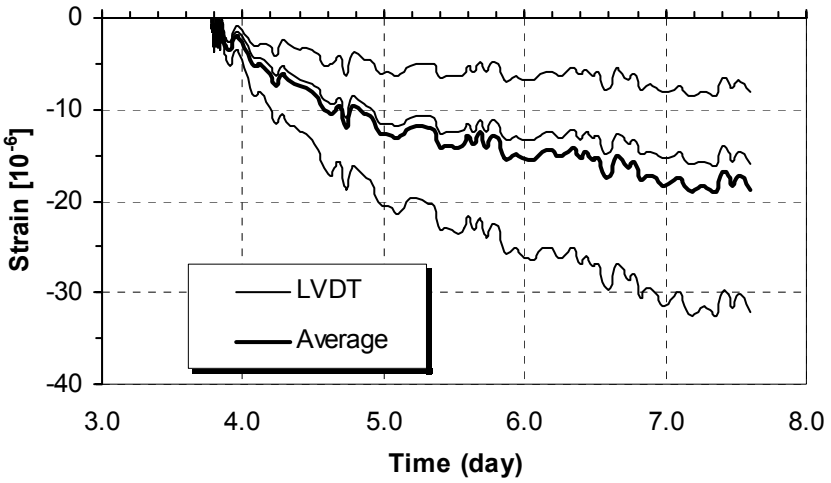

a) Unloaded specimen

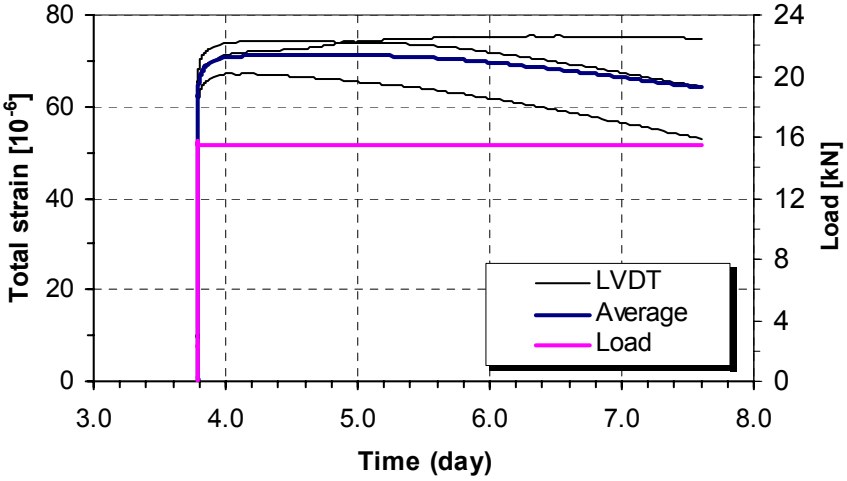

b) Loaded specimen

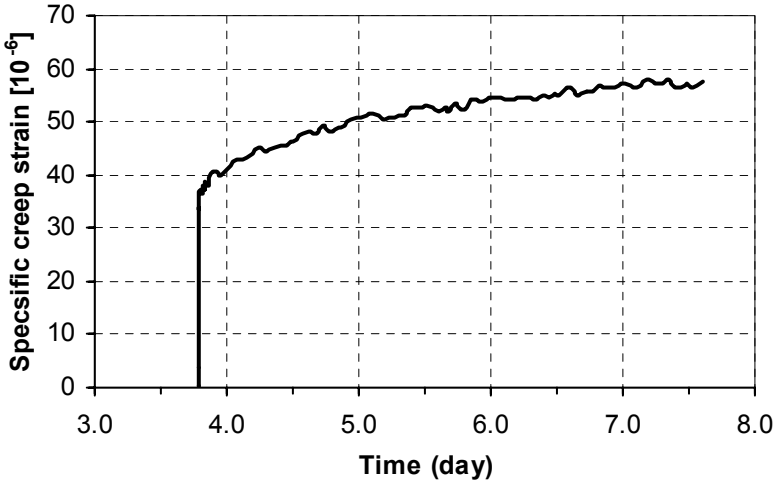

c) Specific creep

Measured strains in the tensile creep tests, age of loading 71 hrs (maturity = 91 hrs), concrete type BASE-5 and T=40 ^{o}C. (Test No. 801).

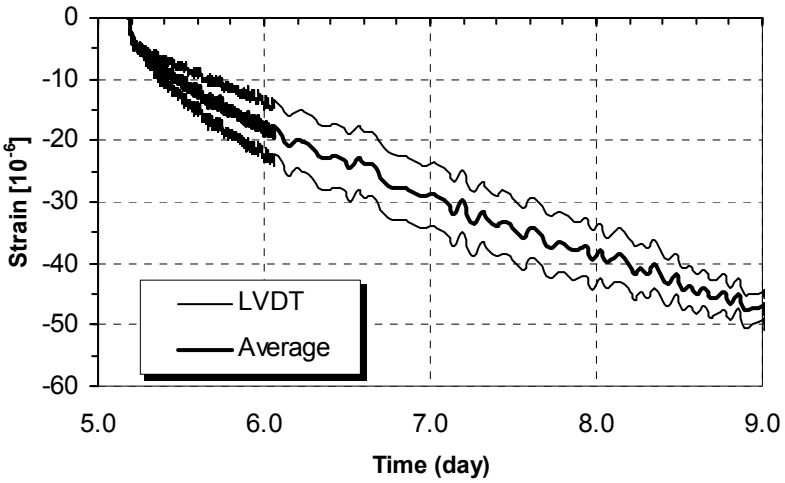

a) Unloaded specimen

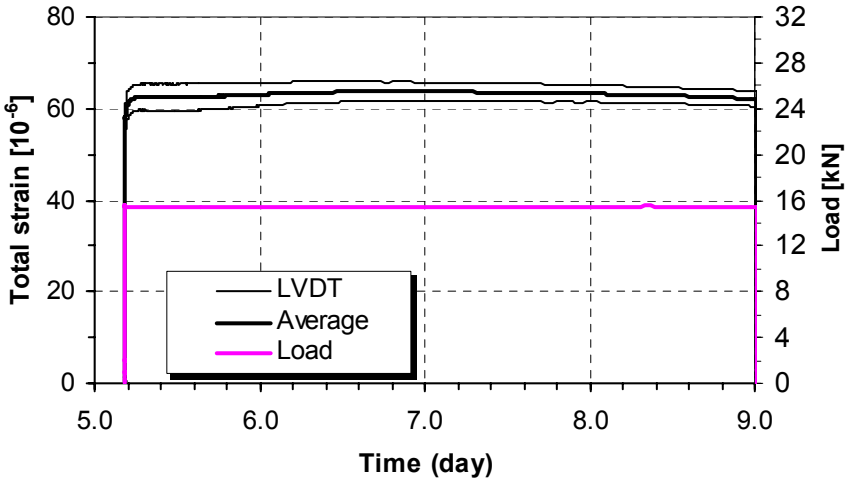

b) Loaded specimen

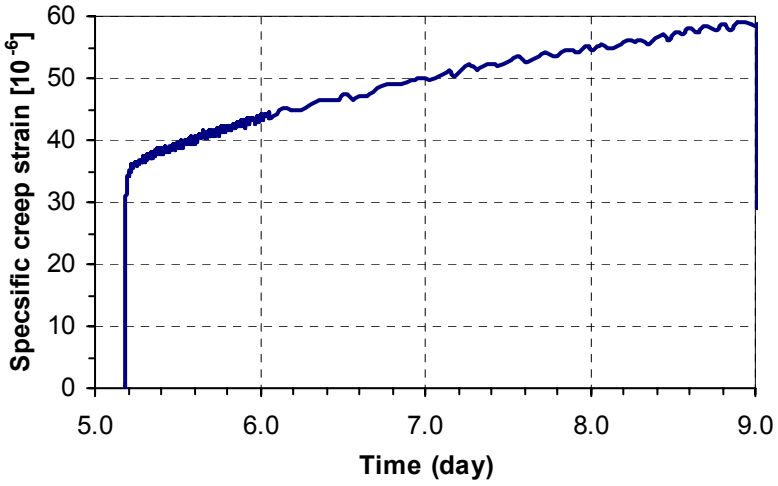

c) Specific creep

Measured strains in the tensile creep tests, age of loading 72 hrs (maturity = 124 hrs), concrete type BASE-5 and T=60 ^{o}C (Test No. 802).

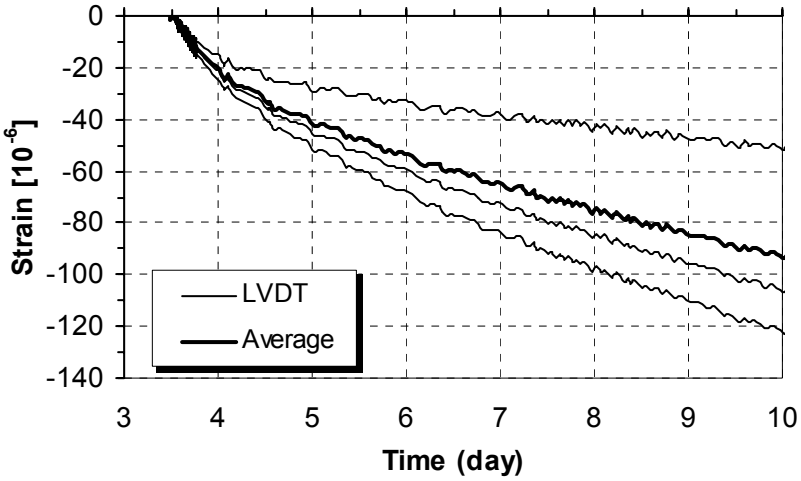

a) Unloaded specimen

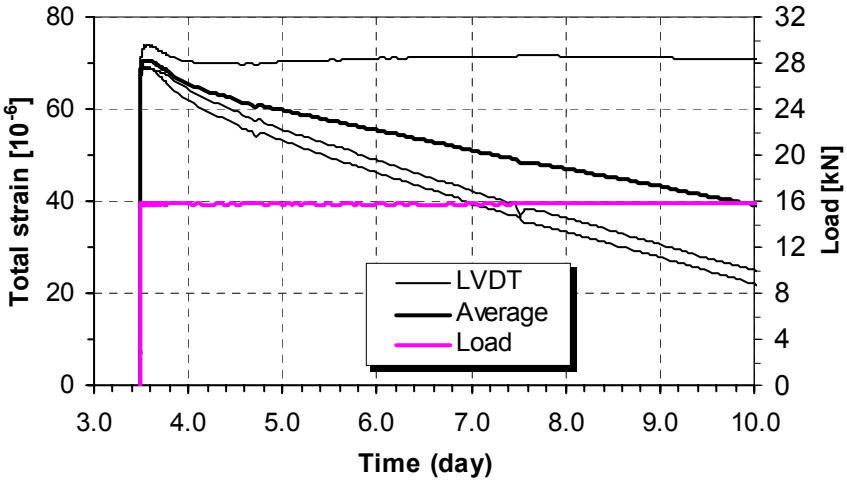

b) Loaded specimen

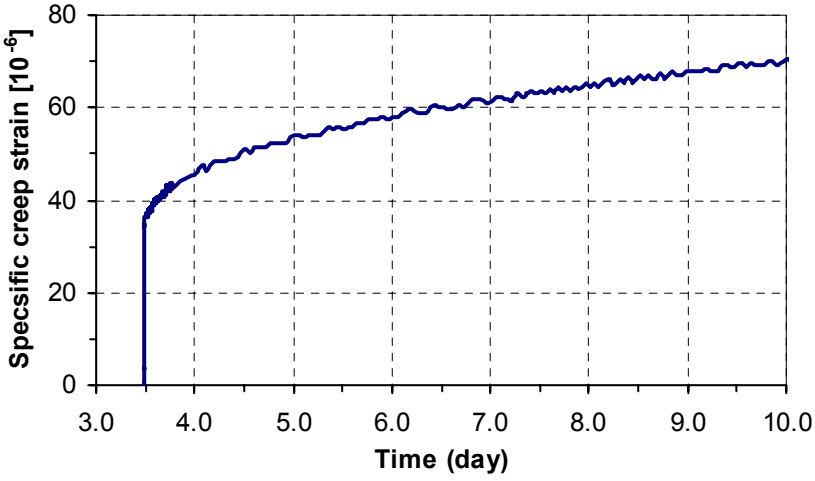

c) Specific creep

Measured strains in the tensile creep tests, age of loading 44 hrs (maturity = 83 hrs), concrete type BASE-5 and T=57 ^{o}C. (Test No. 804).

APPENDIX G

Algorithm for Double Power Law in Visual Basic Excel Program

Simulations of creep and self-induced stresses in the thesis are performed using the creep model denoted the Double Power Law (DPL). These calculations are implemented in a Visual Basic Excel program made for this purpose. The program is divided into different subroutines; four of them are shown in this appendix:

Sub *Curve1*: Calculates stresses not including creep

Sub *Curve2*: Calculates stresses not including transient creep

Sub *Curve3*: Calculates stresses including creep

Sub *Curve4*: Calculates stresses including creep by a Modified Model, M-DPL(C), using creep parameters calibrated against *compressive* creep tests.

Curve1 – Curve4 are the arbitrary names of the subroutines. Other subroutines are also used using creep parameters calibrated against *tensile* creep tests, and the combinations of both.

```
Sub Curve1()
' Algorithm to calculate creep development
' Calculate: Stresses NOT including creep
'
   Fi = 0
   d = Range("a1:a9").Cells(3, 2)
   p = Range("a1:a9").Cells(4, 2)
'
' Loop for creep at different "tn"
   For n = 1 To 225
      tn = Range("a20:a121").Cells(n + 1, 2)
'
' Loop for creep at one "tn"
      Creepj = 0
      For j = 1 To n
         tj = Range("a20:a121").Cells(j, 3)
         Ej = Range("a20:a121").Cells(j, 7)
         DeltaStress = Range("a20:a130").Cells(j, 12)
         DeltaCreepI = 1000000 * (1 + Fi * (tj ^ (-d)) * ((tn - tj) ^ p)) / Ej * DeltaStress
         Creepj = DeltaCreepI + Creepj
      Next j
'
' Calculation of DeltaStrain
         tn = Range("a20:a121").Cells(n, 2)
         tj = Range("a20:a121").Cells(n, 3)
         Ej = Range("a20:a121").Cells(n, 7)
         DeltaStress = Range("a20:a130").Cells(n, 12)
         Stress = Range("a20:a130").Cells(n, 13)
         DeltaCreepJ = 1000000 * (1 + Fi * (tj ^ (-d)) * ((tn - tj) ^ p)) / Ej * DeltaStress
 '
         CreepPrevious = Range("a20:a121").Cells(n, 8)
         DeltaFreeStrain = Range("a20:a121").Cells(n + 1, 5)
         DeltaCreep = Creepj - (CreepPrevious + DeltaCreepJ)
         DeltaStrain = -(DeltaFreeStrain + DeltaCreep)
'
' Calculation of Effective E-modulus
         tn = Range("a20:a121").Cells(n + 1, 2)
         tj = Range("a20:a121").Cells(n + 1, 3)
         Ej = Range("a20:a121").Cells(n + 1, 7)
         EfectiveEj = Ej / (1 + Fi * (tj ^ (-d)) * ((tn - tj) ^ p))
'
' Calculation of Stress increment
         DeltaStress = DeltaStrain * EfectiveEj * 0.000001
'
' Putting the calculated values in the right positions in the Excel sheet.
          Range("a20").Select
          ActiveCell.Offset(n, 7).Value = Creepj
```

```
            ActiveCell.Offset(n, 8).Value = DeltaCreep
            ActiveCell.Offset(n, 9).Value = DeltaStrain
            ActiveCell.Offset(n, 10).Value = EfectiveEj
            ActiveCell.Offset(n, 11).Value = DeltaStress
            SumStress = Range("a20:a121").Cells(n, 13)
            ActiveCell.Offset(n - 1, 13).Value = SumStress
    Next n
    Range("a20").Select
End Sub
```

Sub Curve2()

```
' Algorithm to calculate creep development
' Calculate: Stresses NOT Including Transient Creep
'
    Fi = Range("a1:a9").Cells(2, 2)
    d = Range("a1:a9").Cells(3, 2)
    p = Range("a1:a9").Cells(4, 2)
'
' Loop for creep at different "tn"
    For n = 1 To 225
        tn = Range("a20:a121").Cells(n + 1, 2)
'
' Loop for creep at one "tn"
        Creepj = 0
        For j = 1 To n
            tj = Range("a20:a121").Cells(j, 3)
            Ej = Range("a20:a121").Cells(j, 7)
            DeltaStress = Range("a20:a130").Cells(j, 12)
            DeltaCreepI = 1000000 * (1 + Fi * (tj ^ (-d)) * ((tn - tj) ^ p)) / Ej * DeltaStress
            Creepj = DeltaCreepI + Creepj
        Next j
'
' Calculation of DeltaStrain
            tn = Range("a20:a121").Cells(n, 2)
            tj = Range("a20:a121").Cells(n, 3)
            Ej = Range("a20:a121").Cells(n, 7)
            DeltaStress = Range("a20:a130").Cells(n, 12)
            Stress = Range("a20:a130").Cells(n, 13)
'
            CreepPrevious = Range("a20:a121").Cells(n, 8)
            DeltaFreeStrain = Range("a20:a121").Cells(n + 1, 5)
            DeltaCreep = Creepj - (CreepPrevious + DeltaCreepJ)
            DeltaStrain = -(DeltaFreeStrain + DeltaCreep)
'
' Calculation of Effective E-modulus
```

```
        tn = Range("a20:a121").Cells(n + 1, 2)
        tj = Range("a20:a121").Cells(n + 1, 3)
        Ej = Range("a20:a121").Cells(n + 1, 7)
        EfectiveEj = Ej / (1 + Fi * (tj ^ (-d)) * ((tn - tj) ^ p))
'
' Calculation of Stress increment
        DeltaStress = DeltaStrain * EfectiveEj * 0.000001
'
' Putting the calculeted values in the right positions in the Exel sheet.
         Range("a20").Select
         ActiveCell.Offset(n, 7).Value = Creepj
         ActiveCell.Offset(n, 8).Value = DeltaCreep
         ActiveCell.Offset(n, 9).Value = DeltaStrain
         ActiveCell.Offset(n, 10).Value = EfectiveEj
         ActiveCell.Offset(n, 11).Value = DeltaStress
         SumStress = Range("a20:a121").Cells(n, 13)
         ActiveCell.Offset(n - 1, 14).Value = SumStress
   Next n
   Range("a20").Select
End Sub
```

Sub Curve3()

```
' Algorithm to calculate creep development
' Calculate: Stresses Including Transient Creep
'
   Fi = Range("a1:a9").Cells(2, 2)
   d = Range("a1:a9").Cells(3, 2)
   p = Range("a1:a9").Cells(4, 2)
'
   Alfa1 = Range("a1:a9").Cells(5, 2)
   Ro = Range("a1:a9").Cells(6, 2)
'
' Loop for creep at different "tn"
   For n = 1 To 225
      tn = Range("a20:a121").Cells(n + 1, 2)
'
' Loop for creep at one "tn"
      Creepj = 0
      For j = 1 To n
         tj = Range("a20:a121").Cells(j, 3)
         Ej = Range("a20:a121").Cells(j, 7)
         DeltaStress = Range("a20:a130").Cells(j, 12)
         DeltaCreepI = 1000000 * (1 + Fi * (tj ^ (-d)) * ((tn - tj) ^ p)) / Ej * DeltaStress
         Creepj = DeltaCreepI + Creepj
      Next j
```

```
'
' Calculation of DeltaStrain
        tn = Range("a20:a121").Cells(n, 2)
        tj = Range("a20:a121").Cells(n, 3)
        Ej = Range("a20:a121").Cells(n, 7)
        DeltaStress = Range("a20:a130").Cells(n, 12)
        TotStress = Range("a20:a130").Cells(n, 13)
        DeltaCreepJ = 1000000 * (1 + Fi * (tj ^ (-d)) * ((tn - tj) ^ p)) / Ej * DeltaStress
 '
 ' Calculation of Transient Creep
        DeltaT = Range("a20:a121").Cells(n + 1, 18)
        TensileStrength = Range("a20:a121").Cells(n + 1, 19)
 '
        If DeltaT >= 0 Then
           DeltaCreepT0 = Alfa1 * Abs(DeltaT) * Ro * TotStress / TensileStrength
        End If
           DeltaCreepT = DeltaCreepT0
 '
        CreepPrevious = Range("a20:a121").Cells(n, 8)
        DeltaFreeStrain = Range("a20:a121").Cells(n + 1, 5)
        DeltaCreep = Creepj + DeltaCreepT - (CreepPrevious + DeltaCreepJ)
        DeltaStrain = -(DeltaFreeStrain + DeltaCreep)
'
' Calculation of Effective E-modulus
        tn = Range("a20:a121").Cells(n + 1, 2)
        tj = Range("a20:a121").Cells(n + 1, 3)
        Ej = Range("a20:a121").Cells(n + 1, 7)
        EfectiveEj = Ej / (1 + Fi * (tj ^ (-d)) * ((tn - tj) ^ p))
'
' Calculation of Stress increment
        DeltaStress = DeltaStrain * EfectiveEj * 0.000001
'
' Putting the calculeted values in the right positions in the Exel sheet.
         Range("a20").Select
         ActiveCell.Offset(n, 7).Value = Creepj
         ActiveCell.Offset(n, 8).Value = DeltaCreep
         ActiveCell.Offset(n, 9).Value = DeltaStrain
         ActiveCell.Offset(n, 10).Value = EfectiveEj
         ActiveCell.Offset(n, 11).Value = DeltaStress
         ActiveCell.Offset(n, 19).Value = DeltaCreepT
         SumStress = Range("a20:a121").Cells(n, 13)
         ActiveCell.Offset(n - 1, 16).Value = SumStress
   Next n
   Range("a20").Select
End Sub
```

```
Sub Curve4()
' Algorithm to calculate creep development
' Calculate: Stresses by a Modified Model, M-DPL(C), using creep parameters
' calibrated against compressive creep tests.
'
   Fi = Range("a1:a9").Cells(2, 2)
   d = Range("a1:a9").Cells(3, 2)
   p = Range("a1:a9").Cells(4, 2)
   Fi0e = Range("a1:a9").Cells(2, 3)
'
   Alfa1 = Range("a1:a9").Cells(5, 2)
   Ro = Range("a1:a9").Cells(6, 2)
'
' Loop for creep at different "tn"
   For n = 1 To 225
      tn = Range("a20:a121").Cells(n + 1, 2)
'
' Loop for creep at one "tn"
      Creepj = 0
      For j = 1 To n
         tj = Range("a20:a121").Cells(j, 3)
         Ej = Range("a20:a121").Cells(j, 7)
         DeltaStress = Range("a20:a130").Cells(j, 12)
         TotStress = Range("a20:a130").Cells(j, 13)
'
' Different terms for diffirenet parts of the loadings
         If TotStress <= 0 And DeltaStress <= 0 Then
            DeltaCreepI = 1000000 * (1 + Fi * (tj ^ (-d)) * ((tn - tj) ^ p)) / Ej * DeltaStress
         ElseIf TotStress < 0 And DeltaStress > 0 Then
            DeltaCreepI = 1000000 * (1 + Fi0e * (tj ^ (-d)) * ((tn - tj) ^ p)) / Ej * DeltaStress
         'ElseIf TotStress >= 0 Then
         Else
            DeltaCreepI = 1000000 * (1 + Fi * (tj ^ (-d)) * ((tn - tj) ^ p)) / Ej * DeltaStress
         End If
'
         Creepj = DeltaCreepI + Creepj
      Next j
'
' Calculation of DeltaStrain
         tn = Range("a20:a121").Cells(n, 2)
         tj = Range("a20:a121").Cells(n, 3)
         Ej = Range("a20:a121").Cells(n, 7)
         DeltaStressI = Range("a20:a130").Cells(n, 12)
         TotStressI = Range("a20:a130").Cells(n, 13)
'
' Different terms for diffirenet parts of the loadings
```

```
        If TotStressI <= 0 And DeltaStressI <= 0 Then
           DeltaCreepII = 1000000 * (1 + Fi * (tj ^ (-d)) * ((tn - tj) ^ p)) / Ej * DeltaStressI
        ElseIf TotStressI < 0 And DeltaStressI > 0 Then
           DeltaCreepII = 1000000 * (1 + Fi0e * (tj ^ (-d)) * ((tn - tj) ^ p)) / Ej * DeltaStressI
        'ElseIf TotStress >= 0 Then
        Else
           DeltaCreepII = 1000000 * (1 + Fi * (tj ^ (-d)) * ((tn - tj) ^ p)) / Ej * DeltaStressI
        End If
        DeltaCreepIII = DeltaCreepII
'
' Calculation of Transient Creep
        DeltaT = Range("a20:a121").Cells(n + 1, 18)
        TotStressII = Range("a20:a130").Cells(n, 13)
        TensileStrength = Range("a20:a121").Cells(n + 1, 19)
'
        If DeltaT >= 0 Then
           DeltaCreepT0 = Alfa1 * Abs(DeltaT) * Ro * TotStressII / TensileStrength
        End If
           DeltaCreepT = DeltaCreepT0
'
        CreepPrevious = Range("a20:a121").Cells(n, 8)
        DeltaFreeStrain = Range("a20:a121").Cells(n + 1, 5)
        DeltaCreep = Creepj + DeltaCreepT - (CreepPrevious + DeltaCreepIII)
        DeltaStrain = -(DeltaFreeStrain + DeltaCreep)
'
' Calculation of Effective E-modulus
        tn = Range("a20:a121").Cells(n + 1, 2)
        tj = Range("a20:a121").Cells(n + 1, 3)
        Ej = Range("a20:a121").Cells(n + 1, 7)
'
' Different terms for diffirenet parts of the loadings
        If TotStressI <= 0 And DeltaStressI <= 0 Then
           EfectEjI = Ej / (1 + Fi * (tj ^ (-d)) * ((tn - tj) ^ p))
        ElseIf TotStressI < 0 And DeltaStressI > 0 Then
           EfectEjI = Ej / (1 + Fi0e * (tj ^ (-d)) * ((tn - tj) ^ p))
        ElseIf TotStressI >= 0 Then
        'Else
           EfectEjI = Ej / (1 + Fi * (tj ^ (-d)) * ((tn - tj) ^ p))
        End If
        EfectEj = EfectEjI
'
' Calculation of Stress increment
        DeltaStress = DeltaStrain * EfectEj * 0.000001
'
' Putting the calculeted values in the right positions in the Exel sheet.
         Range("a20").Select
         ActiveCell.Offset(n, 7).Value = Creepj
```

```
        ActiveCell.Offset(n, 8).Value = DeltaCreep
        ActiveCell.Offset(n, 9).Value = DeltaStrain
        ActiveCell.Offset(n, 10).Value = EfectEj
        ActiveCell.Offset(n, 11).Value = DeltaStress
        ActiveCell.Offset(n, 19).Value = DeltaCreepT
        SumStress = Range("a20:a121").Cells(n, 13)
        ActiveCell.Offset(n - 1, 35).Value = SumStress
    Next n
    Range("a20").Select
End Sub
```

APPENDIX H

Fitting the DPL to the Compressive Creep Tests Using Different Model Parameters

An evaluation of the necessary number of creep tests that should be performed for calibration of a creep model, can be made.

The results of six compressive creep tests are used to estimate the three model parameters (φ_0, d and p) of the Double Power Law (DPL). This appendix shows an estimation of these model parameters for combination of creep tests at loading ages 1, 2, 3, 4, 6 and 8 days. Totally 56 combinations of creep tests at different loading ages are made: 15 combinations with two tests, 20 combinations with three tests, 14 combinations with four tests, 6 combinations with five tests and finally 1 combination with all six tests simultaneously. In addition to these, model parameters are found for each creep test separately (six tests). Parameter d is assumed to be 0.20 (the optimized value for all the tests simultaneously) for the latter individual tests.

The comparison between the creep tests and the creep curves estimated by DPL for all the combinations are shown in the figures.

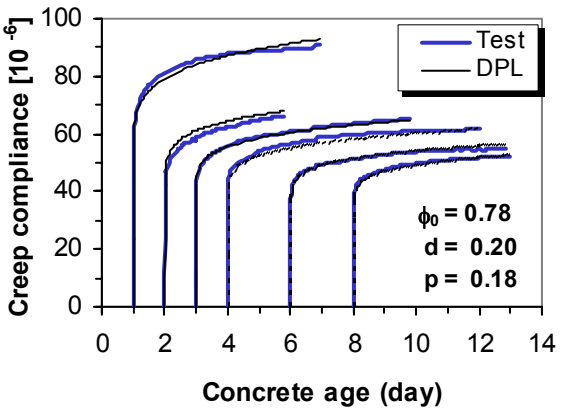

a) Creep parameters referred to creep tests at loading age: **1 day.**

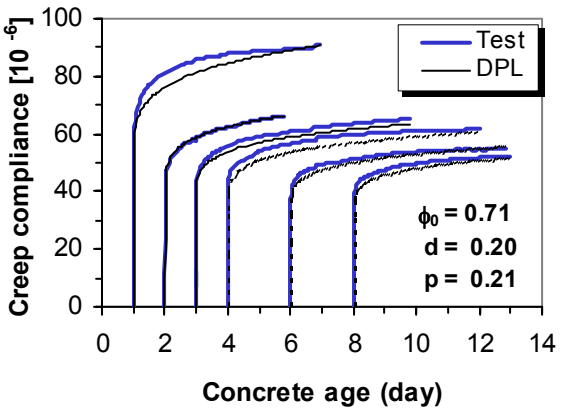

b) Creep parameters referred to creep tests at loading ages: **2 days**

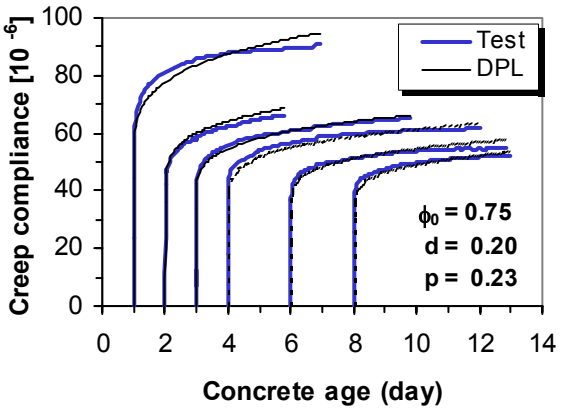

c) Creep parameters referred to creep tests at loading age: **3 days**

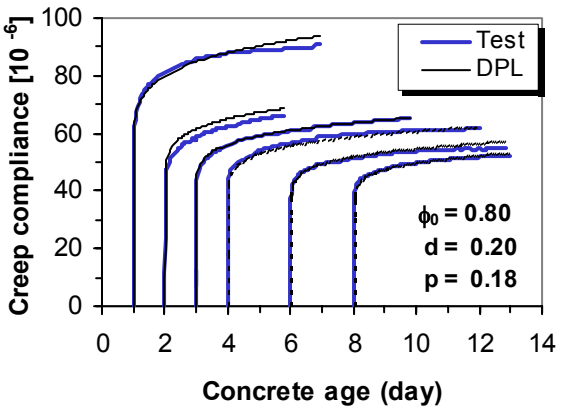

d) Creep parameters referred to creep tests at loading age: **4 days**

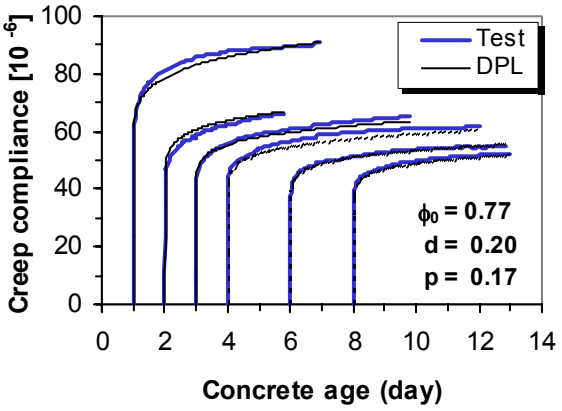

e) Creep parameters referred to creep tests at loading age: **6 days**

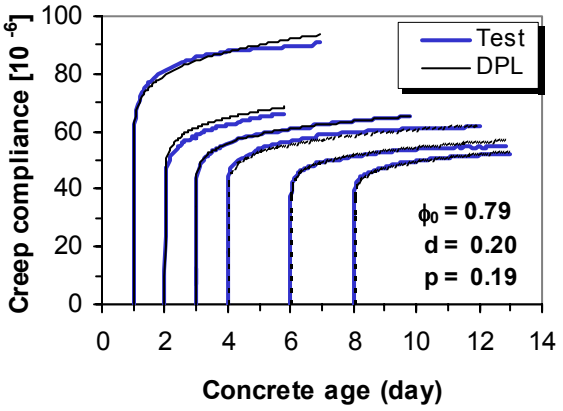

f) Creep parameters referred to creep tests at loading age: **8 days**

URN:NBN:no-3377

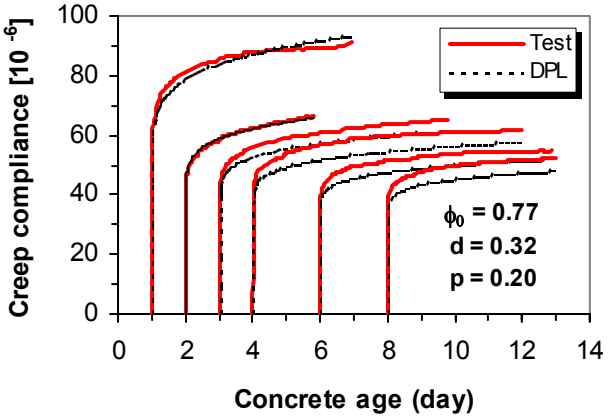

g) Creep parameters referred to creep tests at loading age: **1 & 2 days**

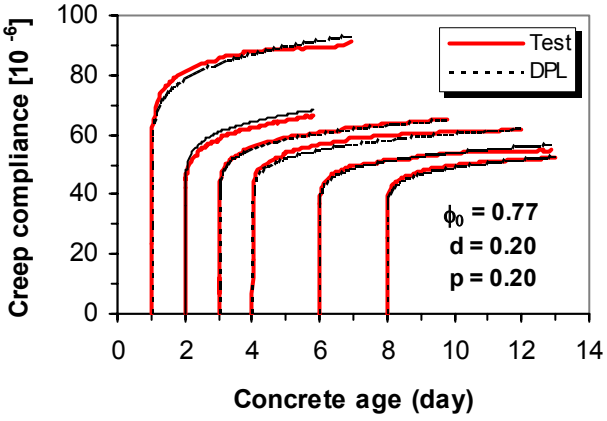

h) Creep parameters referred to creep tests at loading ages: **1 & 3 days**

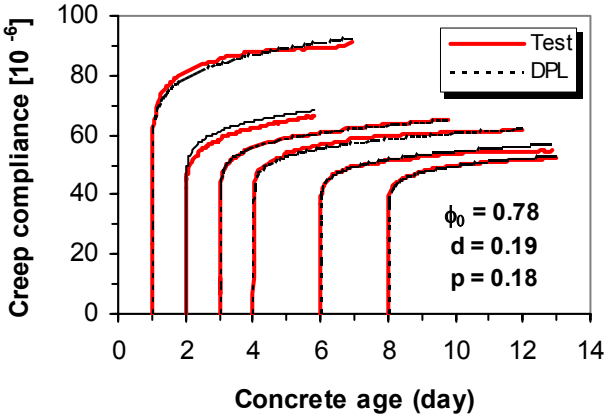

i) Creep parameters referred to creep tests at loading age: **1 & 4 days**

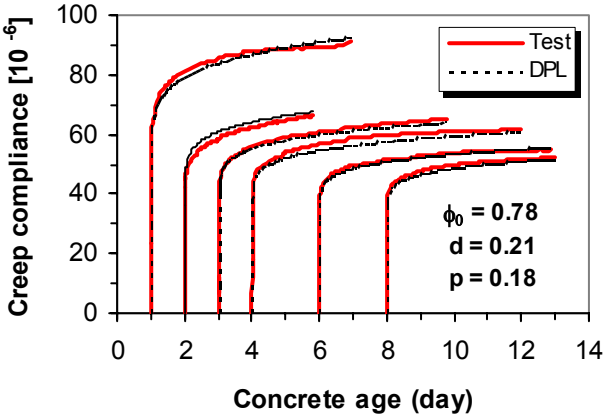

j) Creep parameters referred to creep tests at loading age: **1 & 6 days**

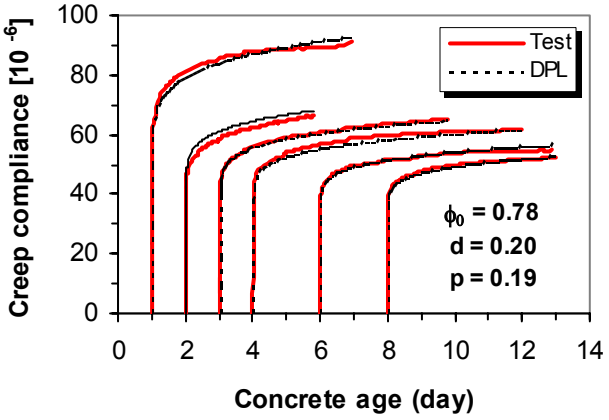

k) Creep parameters referred to creep tests at loading age: **1 & 8 days**

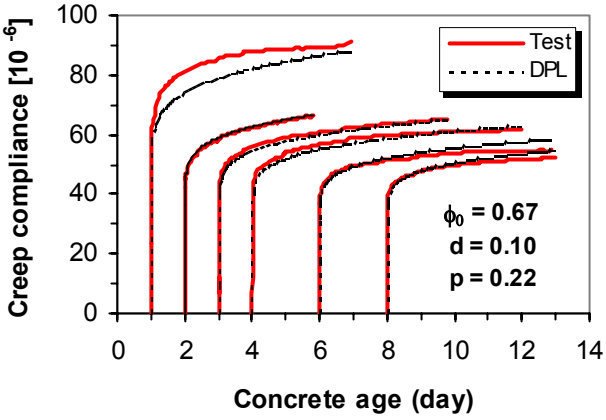

l) Creep parameters referred to creep tests at loading age: **2 & 3 days**

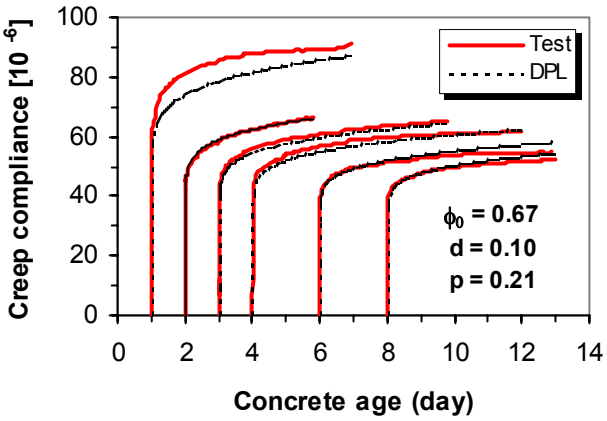

m) Creep parameters referred to creep tests at loading age: **2 & 4 days**

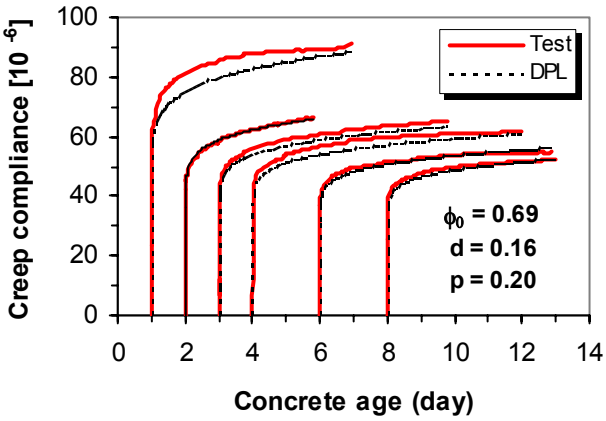

n) Creep parameters referred to creep tests at loading ages: **2 & 6 days**

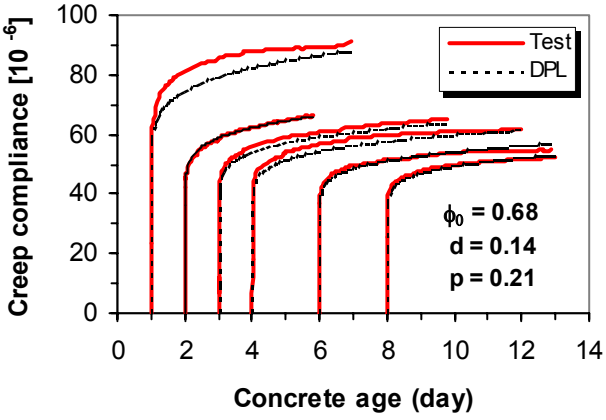

o) Creep parameters referred to creep tests at loading age: **2 & 8 days**

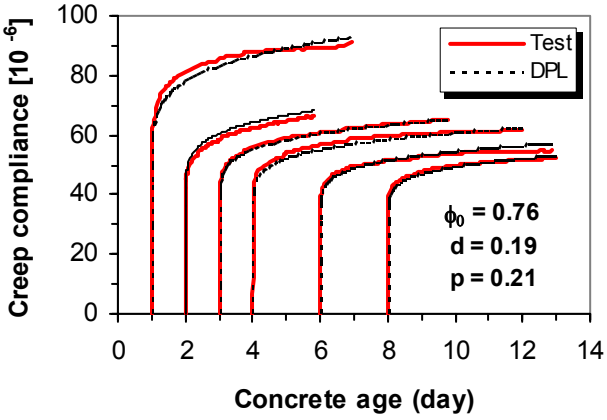

p) Creep parameters referred to creep tests at loading age: **3 & 4 days**

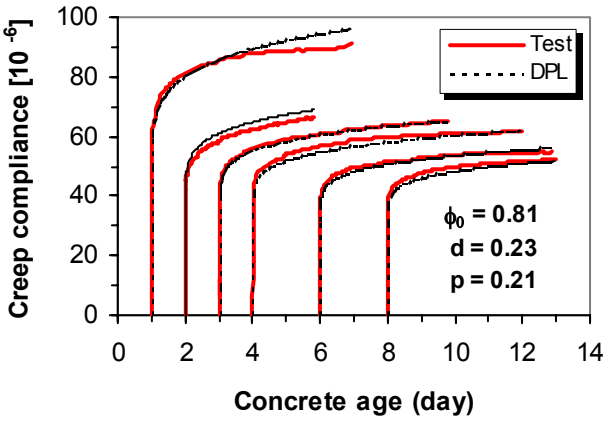

q) Creep parameters referred to creep tests at loading age: **3 & 6 days**

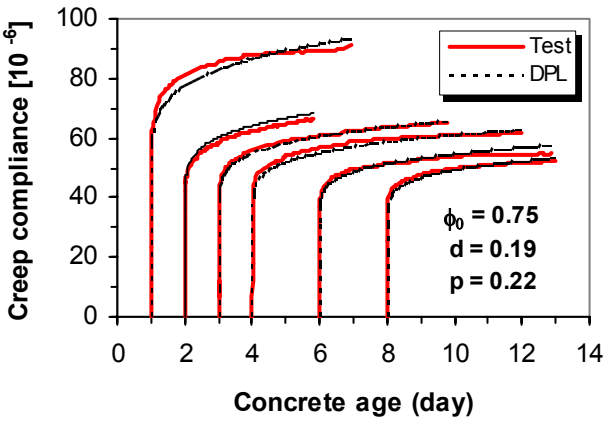

r) Creep parameters referred to creep tests at loading ages: **3 & 8 days**

URN:NBN:no-3377

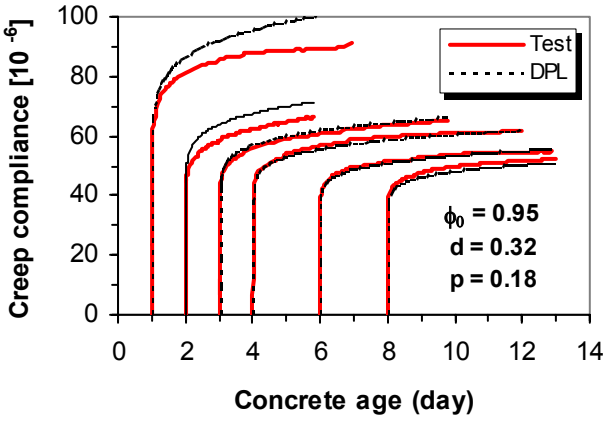

s) Creep parameters referred to creep tests at loading age: **4 & 6 days**

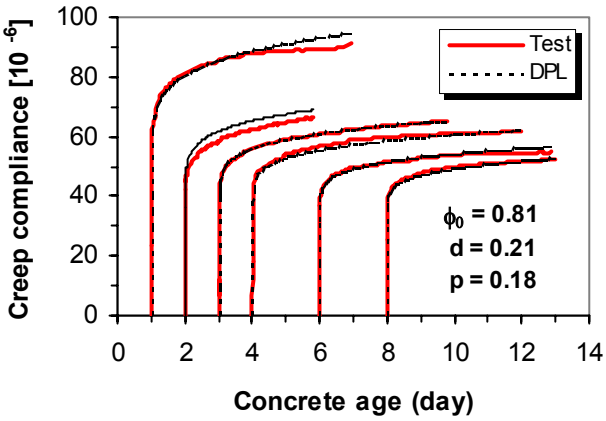

t) Creep parameters referred to creep tests at loading age: **4 & 8 days**

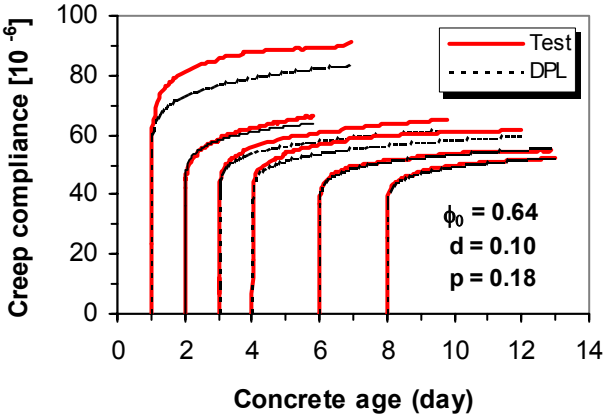

u) Creep parameters referred to creep tests at loading age: **6, & 8 days**

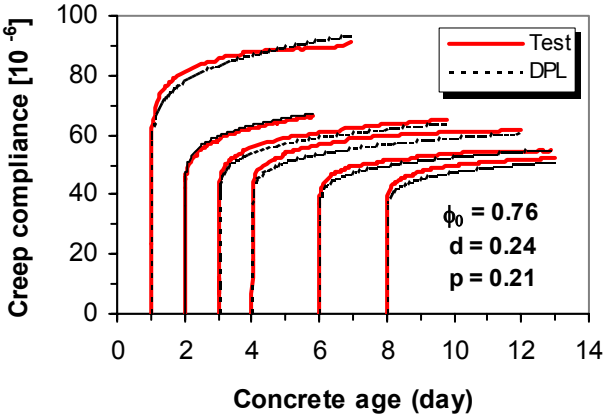

v) Creep parameters referred to creep tests at loading age: **1, 2 & 3 days**

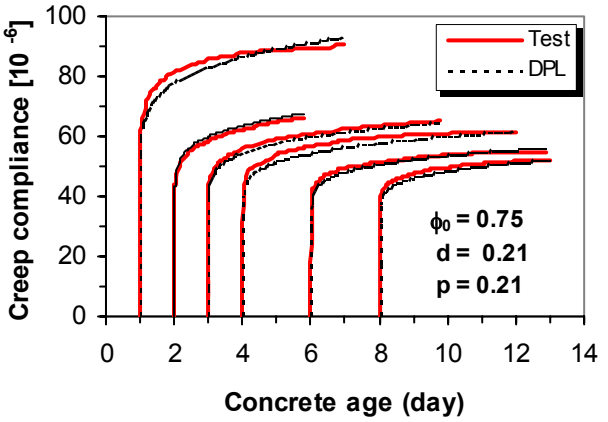

w) Creep parameters referred to creep tests at loading age: **1, 2 & 4 days**

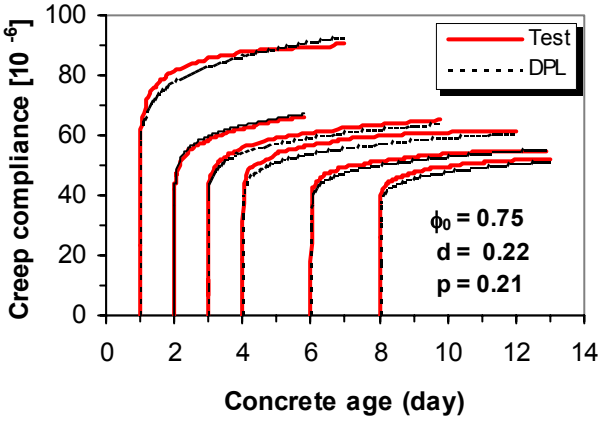

x) Creep parameters referred to creep tests at loading ages: **1, 2 & 6 days**

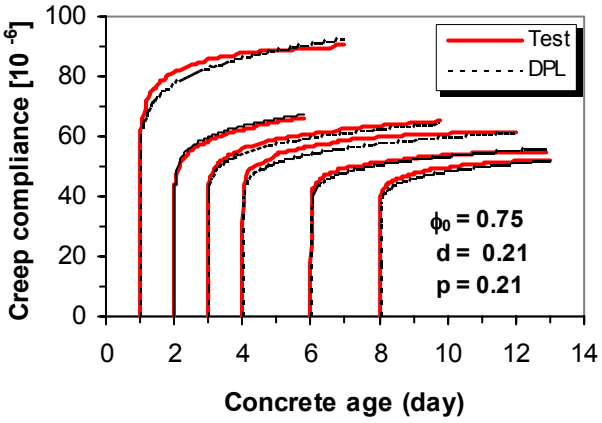

y) Creep parameters referred to creep tests at loading age: **1, 2 & 8 days**

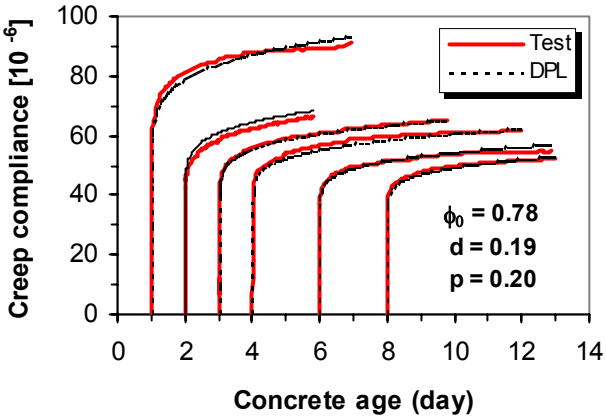

z) Creep parameters referred to creep tests at loading age: **1, 3 & 4 days**

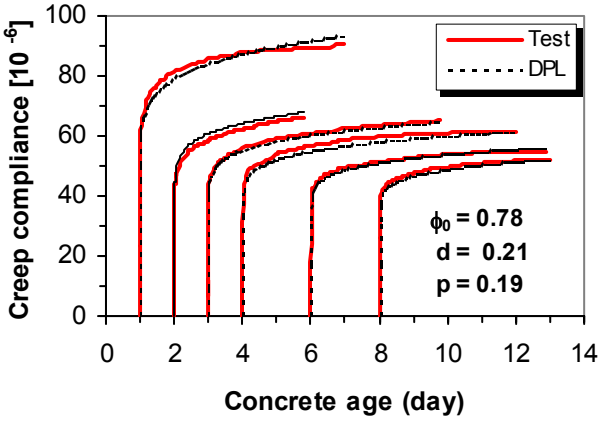

aa) Creep parameters referred to creep tests at loading age: **1, 3 & 6 days**

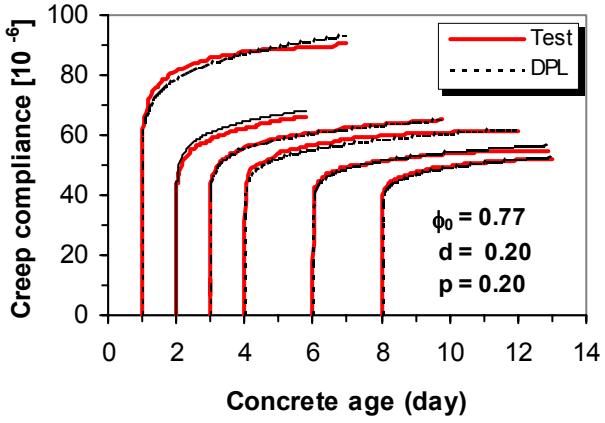

bb) Creep parameters referred to creep tests at loading age: **1, 3 & 8 days**

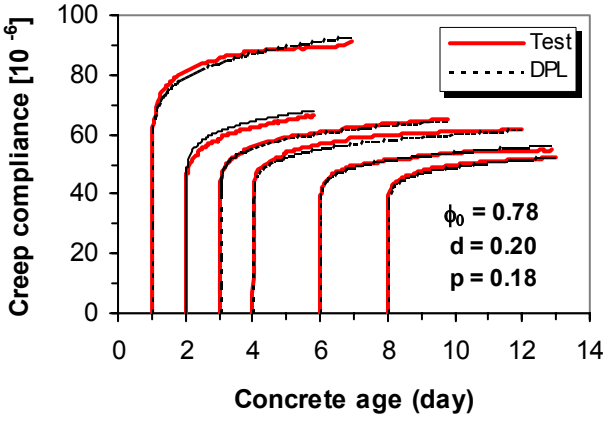

cc) Creep parameters referred to creep tests at loading age: **1, 4 & 6 days**

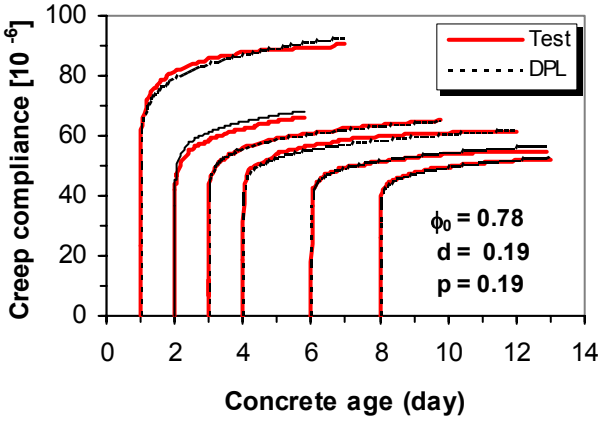

dd) Creep parameters referred to creep tests at loading ages: **1, 4 & 8 days**

URN:NBN:no-3377

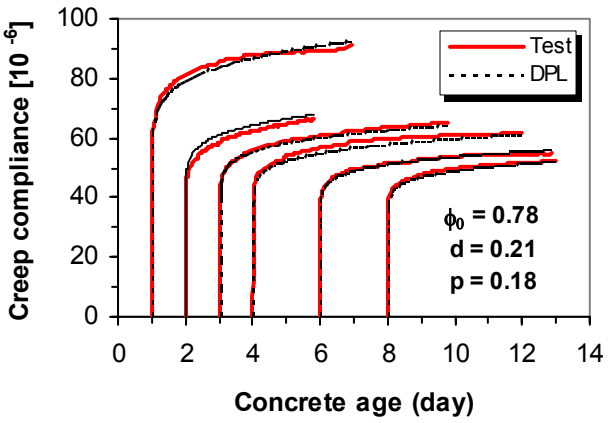

ee) Creep parameters referred to creep tests at loading age: **1, 6 & 8 days**

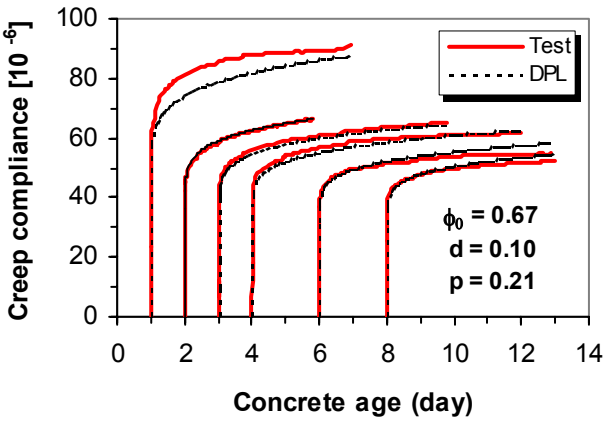

ff) Creep parameters referred to creep tests at loading age: **2, 3 & 4 days**

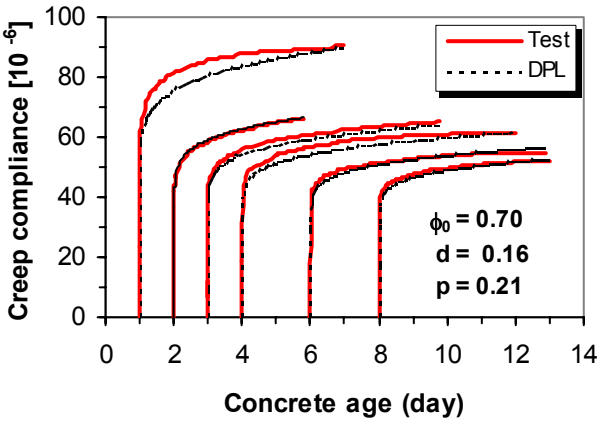

gg) Creep parameters referred to creep tests at loading age: **2, 3 & 6 days**

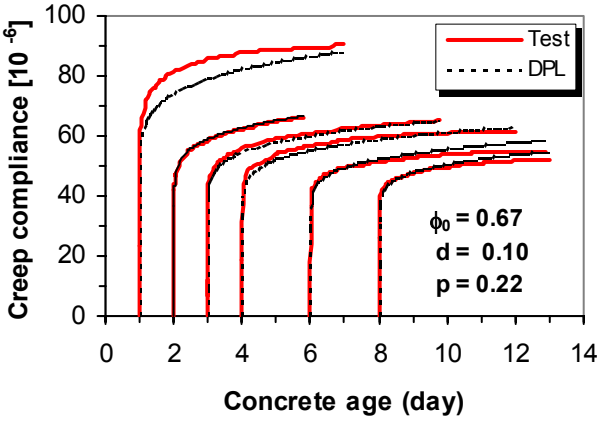

hh) Creep parameters referred to creep tests at loading age: **2, 3 & 8 days**

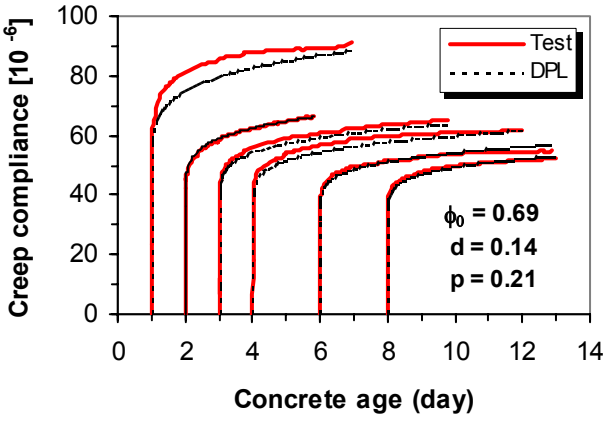

ii) Creep parameters referred to creep tests at loading age: **2, 4 & 6 days**

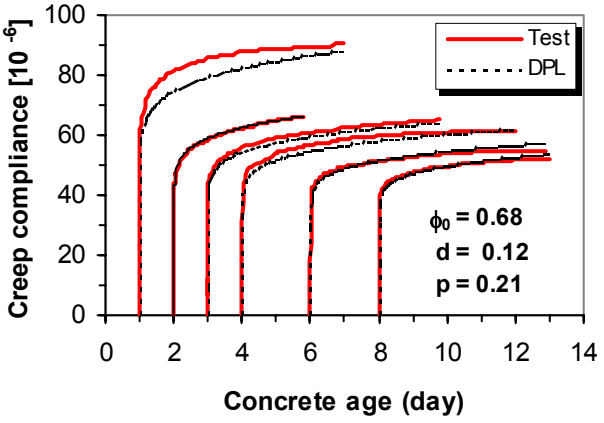

jj) Creep parameters referred to creep tests at loading age: **2, 4 & 8 days**

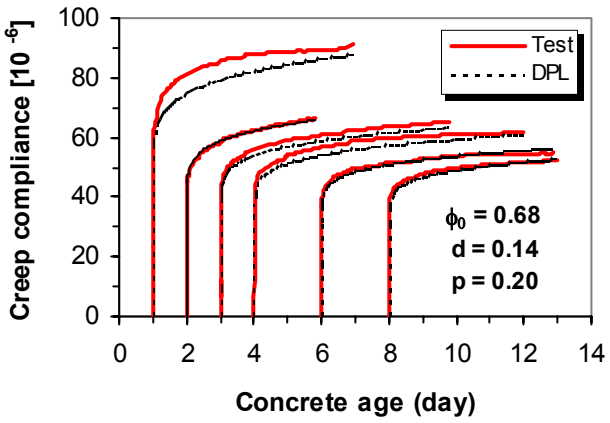

kk) Creep parameters referred to creep tests at loading age: **2, 6 & 8 days**

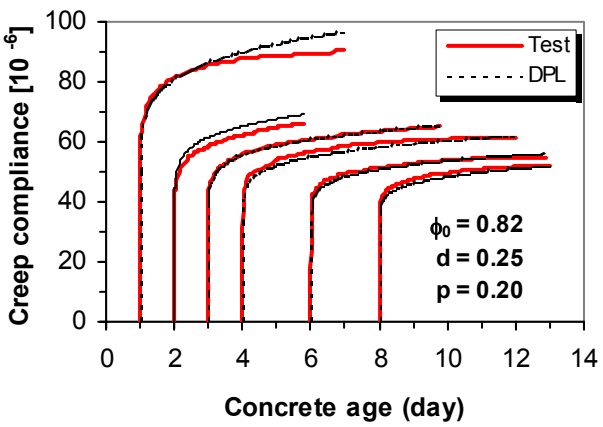

ll) Creep parameters referred to creep tests at loading ages: **3, 4 & 6 days**

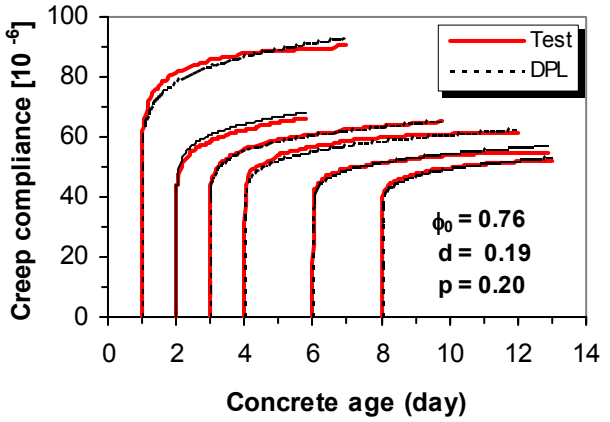

mm) Creep parameters referred to creep tests at loading age: **3, 4 & 8 days**

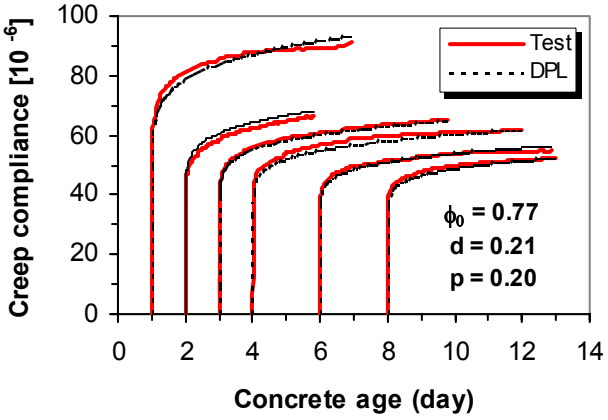

nn) Creep parameters referred to creep tests at loading age: **3, 6 & 8 days**

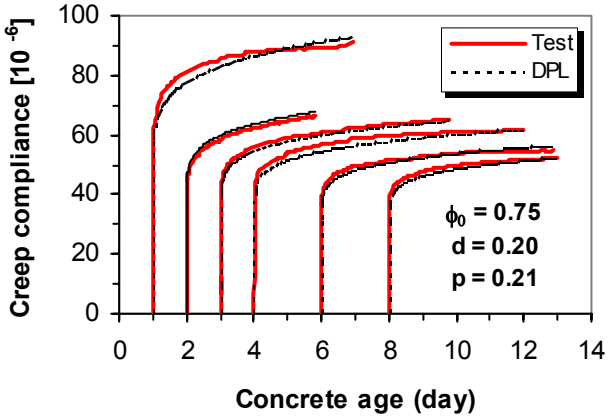

oo) Creep parameters referred to creep tests at loading age: **1, 2, 3 & 4 days**

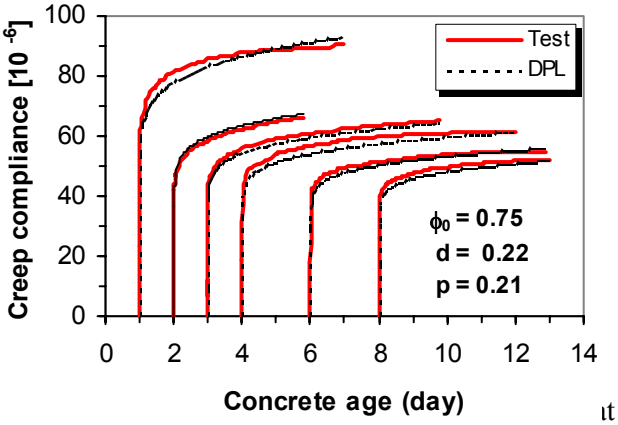

ıt loading age: **1, 2, 3 & 6 days**

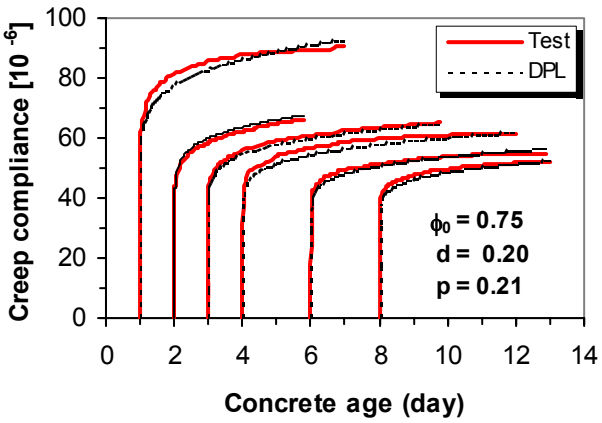

qq) Creep parameters referred to creep tests at loading age: **1, 2, 3 & 8 days**

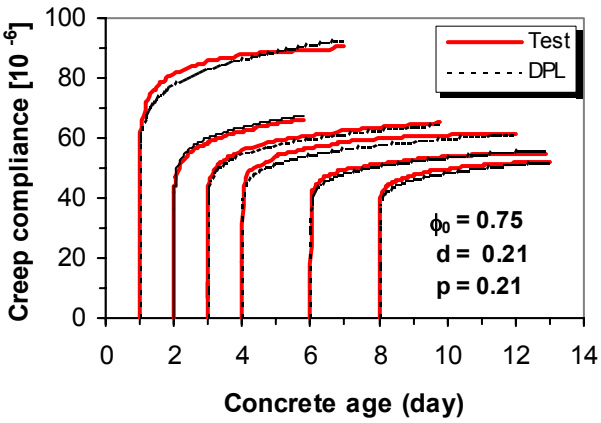

rr) Creep parameters referred to creep tests at loading age: **1, 2, 4 & 6 days**

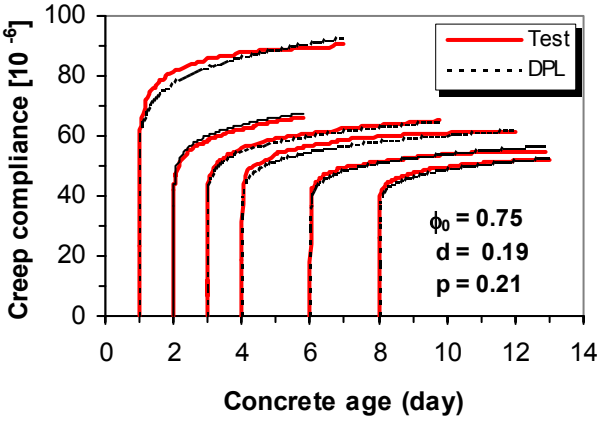

ss) Creep parameters referred to creep tests at loading age: **1, 2, 4 & 8 days**

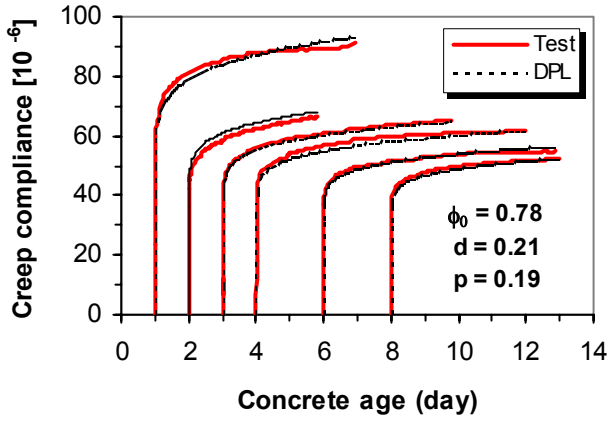

tt) Creep parameters referred to creep tests at loading age: **1, 3, 4 & 6 days**

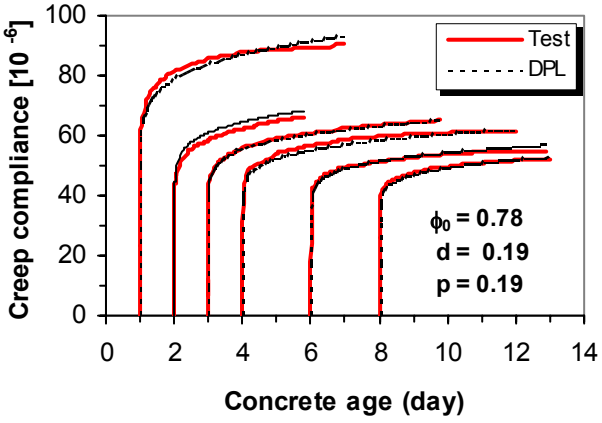

uu) Creep parameters referred to creep tests at loading age: **1, 3, 4 & 8 days**

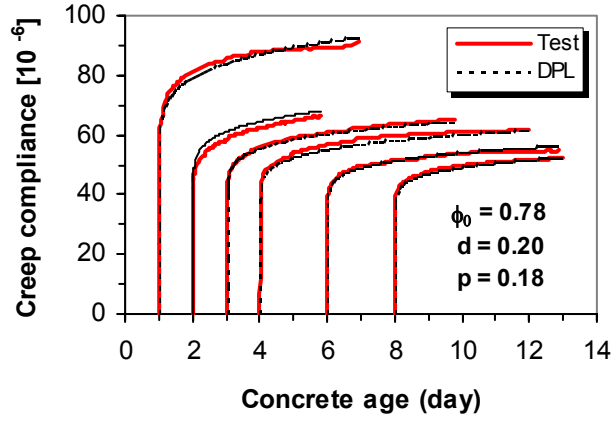

vv) Creep parameters referred to creep tests at loading age: **1, 4, 6 & 8 days**

URN:NBN:no-3377

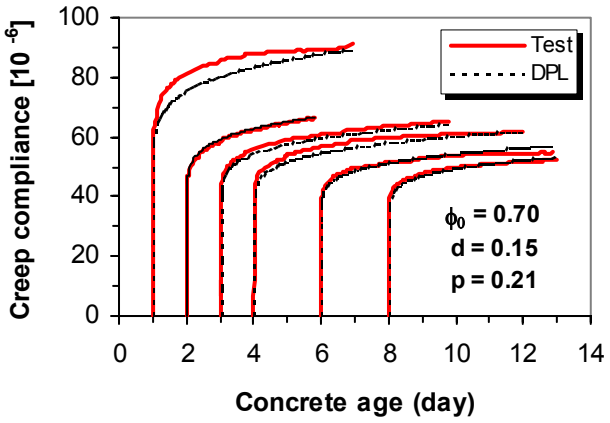

ww) Creep parameters referred to creep tests at loading age: **2, 3, 4 & 6 days**

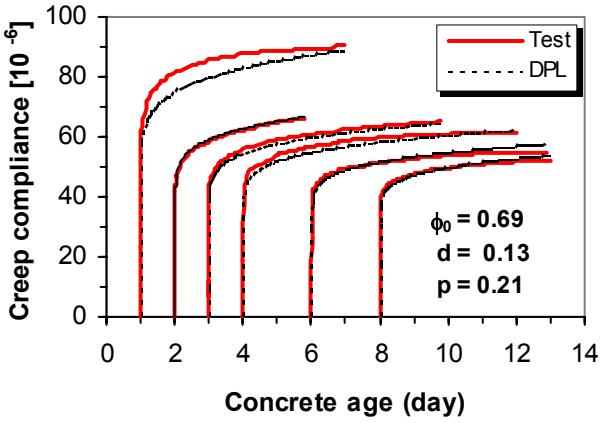

xx) Creep parameters referred to creep tests at loading age: **2, 3, 4 & 8 days**

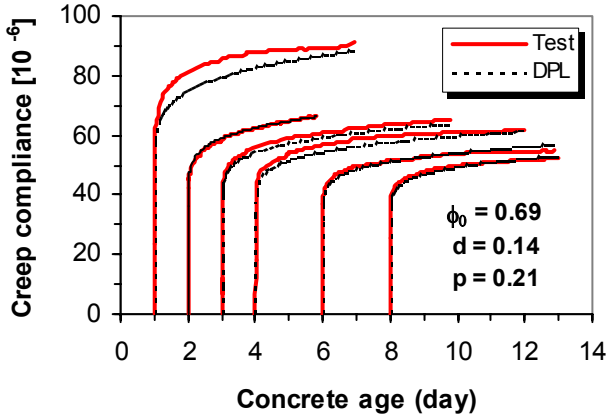

yy) Creep parameters referred to creep tests at loading age: **2, 4, 6 & 8 days**

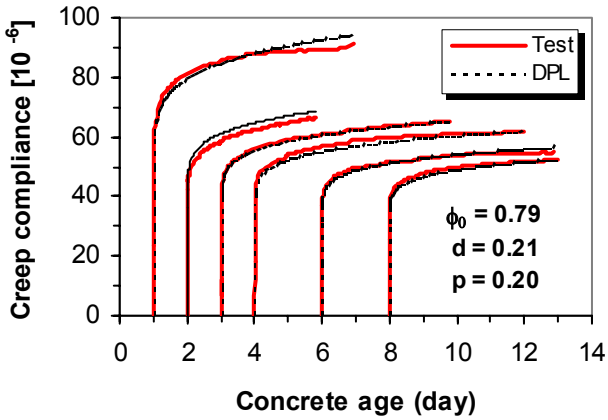

zz) Creep parameters referred to creep tests at loading age: **3, 4, 6 & 8 days**

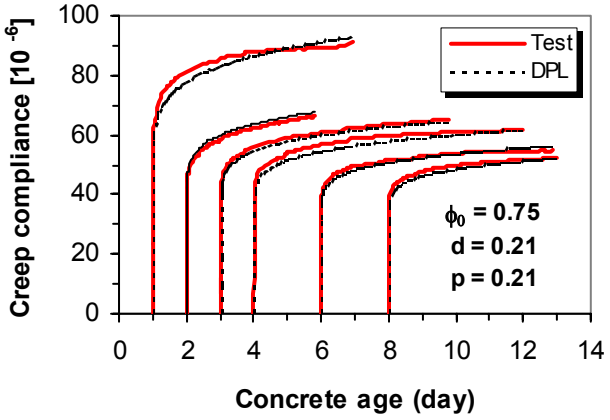

aaa) Creep parameters referred to creep tests at loading age: **1, 2, 3, 4 & 6 days**

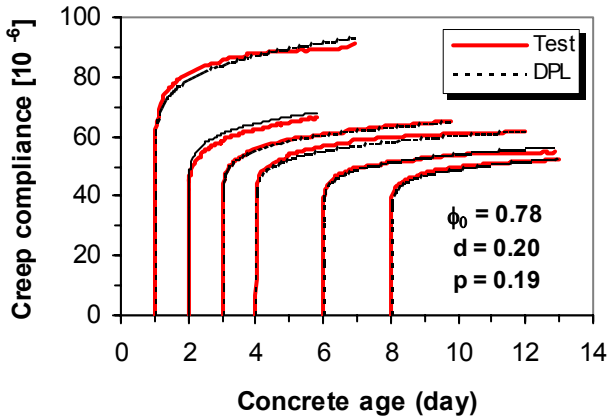

bbb) Creep parameters referred to creep tests at loading age: **1, 3, 4, 6 & 8 days**

URN:NBN:no-3377

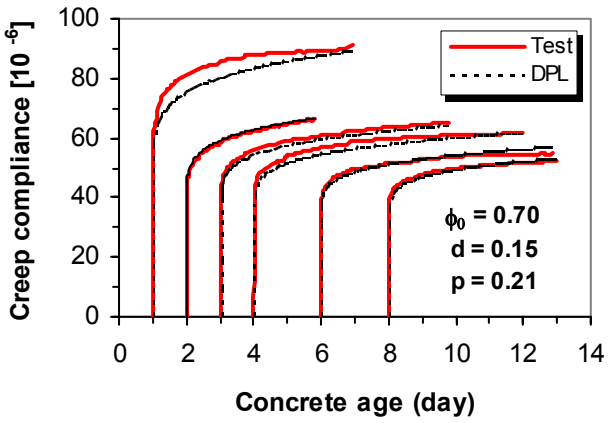

ccc) Creep parameters referred to creep tests at loading age: **2, 3, 4, 6 & 8 days**

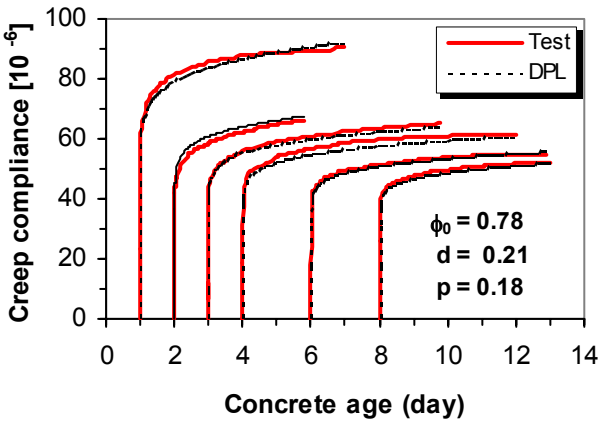

ddd) Creep parameters referred to creep tests at loading age: **1, 2, 3, 4, 6 & 8 days**

URN:NBN:no-3377

DEPARTMENT OF STRUCTURAL ENGINEERING
NORWEGIAN UNIVERSITY OF SCIENCE AND TECHNOLOGY

N–7491 TRONDHEIM, NORWAY
Telephone: +47 73 59 47 00 Telefax: +47 73 59 47 01

"Reliability Analysis of Structural Systems using Nonlinear Finite Element Methods",
C. A. Holm, 1990:23, ISBN 82-7119-178-0.

"Uniform Stratified Flow Interaction with a Submerged Horizontal Cylinder",
Ø. Arntsen, 1990:32, ISBN 82-7119-188-8.

"Large Displacement Analysis of Flexible and Rigid Systems Considering Displacement-Dependent Loads and Nonlinear Constraints", K. M. Mathisen, 1990:33, ISBN 82-7119-189-6.

"Solid Mechanics and Material Models including Large Deformations",
E. Levold, 1990:56, ISBN 82-7119-214-0, ISSN 0802-3271.

"Inelastic Deformation Capacity of Flexurally-Loaded Aluminium Alloy Structures",
T. Welo, 1990:62, ISBN 82-7119-220-5, ISSN 0802-3271.

"Visualization of Results from Mechanical Engineering Analysis",
K. Aamnes, 1990:63, ISBN 82-7119-221-3, ISSN 0802-3271.

"Object-Oriented Product Modeling for Structural Design",
S. I. Dale, 1991:6, ISBN 82-7119-258-2, ISSN 0802-3271.

"Parallel Techniques for Solving Finite Element Problems on Transputer Networks",
T. H. Hansen, 1991:19, ISBN 82-7119-273-6, ISSN 0802-3271.

"Statistical Description and Estimation of Ocean Drift Ice Environments",
R. Korsnes, 1991:24, ISBN 82-7119-278-7, ISSN 0802-3271.

“Properties of concrete related to fatigue damage: with emphasis on high strength concrete”,
G. Petkovic, 1991:35, ISBN 82-7119-290-6, ISSN 0802-3271.

"Turbidity Current Modelling",
B. Brørs, 1991:38, ISBN 82-7119-293-0, ISSN 0802-3271.

"Zero-Slump Concrete: Rheology, Degree of Compaction and Strength. Effects of Fillers as Part Cement-Replacement",
C. Sørensen, 1992:8, ISBN 82-7119-357-0, ISSN 0802-3271.

"Nonlinear Analysis of Reinforced Concrete Structures Exposed to Transient Loading",
K. V. Høiseth, 1992:15, ISBN 82-7119-364-3, ISSN 0802-3271.

"Finite Element Formulations and Solution Algorithms for Buckling and Collapse Analysis of Thin Shells", R. O. Bjærum, 1992:30, ISBN 82-7119-380-5, ISSN 0802-3271.

"Response Statistics of Nonlinear Dynamic Systems",
J. M. Johnsen, 1992:42, ISBN 82-7119-393-7, ISSN 0802-3271.

"Digital Models in Engineering. A Study on why and how engineers build and operate digital models for decisison support", J. Høyte, 1992:75, ISBN 82-7119-429-1, ISSN 0802-3271.

"Sparse Solution of Finite Element Equations",
A. C. Damhaug, 1992:76, ISBN 82-7119-430-5, ISSN 0802-3271.

"Some Aspects of Floating Ice Related to Sea Surface Operations in the Barents Sea",
S. Løset, 1992:95, ISBN 82-7119-452-6, ISSN 0802-3271.

"Modelling of Cyclic Plasticity with Application to Steel and Aluminium Structures",
O. S. Hopperstad, 1993:7, ISBN 82-7119-461-5, ISSN 0802-3271.

"The Free Formulation: Linear Theory and Extensions with Applications to Tetrahedral Elements with Rotational Freedoms", G. Skeie, 1993:17, ISBN 82-7119-472-0, ISSN 0802-3271.

"Høyfast betongs motstand mot piggdekkslitasje. Analyse av resultater fra prøving i Veisliter'n",
T. Tveter, 1993:62, ISBN 82-7119-522-0, ISSN 0802-3271.

"A Nonlinear Finite Element Based on Free Formulation Theory for Analysis of Sandwich Structures", O. Aamlid, 1993:72, ISBN 82-7119-534-4, ISSN 0802-3271.

"The Effect of Curing Temperature and Silica Fume on Chloride Migration and Pore Structure of High Strength Concrete", C. J. Hauck, 1993:90, ISBN 82-7119-553-0, ISSN 0802-3271.

"Failure of Concrete under Compressive Strain Gradients",
G. Markeset, 1993:110, ISBN 82-7119-575-1, ISSN 0802-3271.

"An experimental study of internal tidal amphidromes in Vestfjorden",
J. H. Nilsen, 1994:39, ISBN 82-7119-640-5, ISSN 0802-3271.

"Structural analysis of oil wells with emphasis on conductor design",
H. Larsen, 1994:46, ISBN 82-7119-648-0, ISSN 0802-3271.

"Adaptive methods for non-linear finite element analysis of shell structures",
K. M. Okstad, 1994:66, ISBN 82-7119-670-7, ISSN 0802-3271.

"On constitutive modelling in nonlinear analysis of concrete structures",
O. Fyrileiv, 1994:115, ISBN 82-7119-725-8, ISSN 0802-3271.

"Fluctuating wind load and response of a line-like engineering structure with emphasis on motion-induced wind forces",
J. Bogunovic Jakobsen, 1995:62, ISBN 82-7119-809-2, ISSN 0802-3271.

"An experimental study of beam-columns subjected to combined torsion, bending and axial actions",
A. Aalberg, 1995:66, ISBN 82-7119-813-0, ISSN 0802-3271.

"Scaling and cracking in unsealed freeze/thaw testing of Portland cement and silica fume concretes",
S. Jacobsen, 1995:101, ISBN 82-7119-851-3, ISSN 0802-3271.

"Damping of water waves by submerged vegetation. A case study of laminaria hyperborea",
A. M. Dubi, 1995:108, ISBN 82-7119-859-9, ISSN 0802-3271.

"The dynamics of a slope current in the Barents Sea",
Sheng Li, 1995:109, ISBN 82-7119-860-2, ISSN 0802-3271.

"Modellering av delmaterialenes betydning for betongens konsistens",
Ernst Mørtsell, 1996:12, ISBN 82-7119-894-7, ISSN 0802-3271.

"Bending of thin-walled aluminium extrusions",
Birgit Søvik Opheim, 1996:60, ISBN 82-7119-947-1, ISSN 0802-3271.

"Material modelling of aluminium for crashworthiness analysis",
Torodd Berstad, 1996:89, ISBN 82-7119-980-3, ISSN 0802-3271.

"Estimation of structural parameters from response measurements on submerged floating tunnels",
Rolf Magne Larssen, 1996:119, ISBN 82-471-0014-2, ISSN 0802-3271.

“Numerical modelling of plain and reinforced concrete by damage mechanics”,
Mario A. Polanco-Loria, 1997:20, ISBN 82-471-0049-5, ISSN 0802-3271.

“Nonlinear random vibrations - numerical analysis by path integration methods”,
Vibeke Moe, 1997:26, ISBN 82-471-0056-8, ISSN 0802-3271.

“Numerical prediction of vortex-induced vibration by the finite element method”,
Joar Martin Dalheim, 1997:63, ISBN 82-471-0096-7, ISSN 0802-3271.

“Time domain calculations of buffeting response for wind sensitive structures”,
Ketil Aas-Jakobsen, 1997:148, ISBN 82-471-0189-0, ISSN 0802-3271.

"A numerical study of flow about fixed and flexibly mounted circular cylinders",
Trond Stokka Meling, 1998:48, ISBN 82-471-0244-7, ISSN 0802-3271.

“Estimation of chloride penetration into concrete bridges in coastal areas”,
Per Egil Steen, 1998:89, ISBN 82-471-0290-0, ISSN 0802-3271.

“Stress-resultant material models for reinforced concrete plates and shells”,
Jan Arve Øverli, 1998:95, ISBN 82-471-0297-8, ISSN 0802-3271.

“Chloride binding in concrete. Effect of surrounding environment and concrete composition”,
Claus Kenneth Larsen, 1998:101, ISBN 82-471-0337-0, ISSN 0802-3271.

“Rotational capacity of aluminium alloy beams”,
Lars A. Moen, 1999:1, ISBN 82-471-0365-6, ISSN 0802-3271.

“Stretch Bending of Aluminium Extrusions”,
Arild H. Clausen, 1999:29, ISBN 82-471-0396-6, ISSN 0802-3271.

“Aluminium and Steel Beams under Concentrated Loading”,

Tore Tryland, 1999:30, ISBN 82-471-0397-4, ISSN 0802-3271.

"Engineering Models of Elastoplasticity and Fracture for Aluminium Alloys",
Odd-Geir Lademo, 1999:39, ISBN 82-471-0406-7, ISSN 0802-3271.

"Kapasitet og duktilitet av dybelforbindelser i trekonstruksjoner",
Jan Siem, 1999:46, ISBN 82-471-0414-8, ISSN 0802-3271.

“Etablering av distribuert ingeniørarbeid; Teknologiske og organisatoriske erfaringer fra en norsk ingeniørbedrift”, Lars Line, 1999:52, ISBN 82-471-0420-2, ISSN 0802-3271.

“Estimation of Earthquake-Induced Response”,
Símon Ólafsson, 1999:73, ISBN 82-471-0443-1, ISSN 0802-3271.

“Coastal Concrete Bridges: Moisture State, Chloride Permeability and Aging Effects”
Ragnhild Holen Relling, 1999:74, ISBN 82-471-0445-8, ISSN 0802-3271.

”Capacity Assessment of Titanium Pipes Subjected to Bending and External Pressure”,
Arve Bjørset, 1999:100, ISBN 82-471-0473-3, ISSN 0802-3271.

“Validation of Numerical Collapse Behaviour of Thin-Walled Corrugated Panels”,
Håvar Ilstad, 1999:101, ISBN 82-471-0474-1, ISSN 0802-3271.

“Strength and Ductility of Welded Structures in Aluminium Alloys”,
Miroslaw Matusiak, 1999:113, ISBN 82-471-0487-3, ISSN 0802-3271.

“Thermal Dilation and Autogenous Deformation as Driving Forces to Self-Induced Stresses in High Performance Concrete”,
Øyvind Bjøntegaard, 1999:121, ISBN 82-7984-002-8, ISSN 0802-3271.

“Some Aspects of Ski Base Sliding Friction and Ski Base Structure”,
Dag Anders Moldestad, 1999:137, ISBN 82-7984-019-2, ISSN 0802-3271.

"Electrode reactions and corrosion resistance for steel in mortar and concrete",
Roy Antonsen, 2000:10, ISBN 82-7984-030-3, ISSN 0802-3271.

"Hydro-Physical Conditions in Kelp Forests and the Effect on Wave Damping and Dune Erosion. A case study on Laminaria Hyperborea",
Stig Magnar Løvås, 2000:28, ISBN 82-7984-050-8, ISSN 0802-3271.

"Random Vibration and the Path Integral Method",
Christian Skaug, 2000:39, ISBN 82-7984-061-3, ISSN 0802-3271.

"Buckling and geometrical nonlinear beam-type analyses of timber structures",
Trond Even Eggen, 2000:56, ISBN 82-7984-081-8, ISSN 0802-3271.

”Structural Crashworthiness of Aluminium Foam-Based Components”,
Arve Grønsund Hanssen, 2000:76, ISBN 82-7984-102-4, ISSN 0809-103X.

“Measurements and simulations of the consolidation in first-year sea ice ridges, and some aspects of mechanical behaviour”, Knut V. Høyland, 2000:94, ISBN 82-7984-121-0, ISSN 0809-103X.

”Kinematics in Regular and Irregular Waves based on a Lagrangian Formulation”,
Svein Helge Gjøsund, 2000-86, ISBN 82-7984-112-1, ISSN 0809-103X.

”Self-Induced Cracking Problems in Hardening Concrete Structures”,
Daniela Bosnjak, 2000-121, ISBN 82-7984-151-2, ISSN 0809-103X.

"Ballistic Penetration and Perforation of Steel Plates",
Tore Børvik, 2000:124, ISBN 82-7984-154-7, ISSN 0809-103X.

"Freeze-Thaw resistance of Concrete. Effect of: Curing Conditions, Moisture Exchange and Materials", Terje Finnerup Rønning, 2001:14, ISBN 82-7984-165-2, ISSN 0809-103X

Structural behaviour of post tensioned concrete structures. Flat slab. Slabs on ground",
Steinar Trygstad, 2001:52, ISBN 82-471-5314-9, ISSN 0809-103X.

"Slipforming of Vertical Concrete Structures. Friction between concrete and slipform panel",
Kjell Tore Fosså, 2001:61, ISBN 82-471-5325-4, ISSN 0809-103X.

"Some numerical methods for the simulation of laminar and turbulent incompressible flows",
Jens Holmen, 2002:6, ISBN 82-471-5396-3, ISSN 0809-103X.

“Improved Fatigue Performance of Threaded Drillstring Connections by Cold Rolling”,
Steinar Kristoffersen, 2002:11, ISBN: 82-421-5402-1, ISSN 0809-103X.

"Deformations in Concrete Cantilever Bridges: Observations and Theoretical Modelling",
Peter F. Takâcs, 2002:23, ISBN 82-471-5415-3, ISSN 0809-103X.

"Stiffened aluminium plates subjected to impact loading",
Hilde Giæver Hildrum, 2002:69, ISBN 82-471-5467-6, ISSN 0809-103X.

"Full- and model scale study of wind effects on a medium-rise building in a built up area",
Jónas Thór Snæbjørnsson, 2002:95, ISBN82-471-5495-1, ISSN 0809-103X.

“Evaluation of Concepts for Loading of Hydrocarbons in Ice-infested water”,
Arnor Jensen, 2002:114, ISBN 82-417-5506-0, ISSN 0809-103X.

”Numerical and Physical Modelling of Oil Spreading in Broken Ice”,
Janne K. Økland Gjøsteen, 2002:130, ISBN 82-471-5523-0, ISSN 0809-103X.

”Diagnosis and protection of corroding steel in concrete”,
Franz Pruckner, 20002:140, ISBN 82-471-5555-4, ISSN 0809-103X.